

**Structural Tolerance of Reverse Turn: A Case
Study with Ant-Pro Turns**

A THESIS TO BE SUBMITTED TO THE

UNIVERSITY OF PUNE

FOR THE DEGREE OF

DOCTOR OF PHILOSOPHY

(IN CHEMISTRY)

By

Tukaram S. Ingole

Research Supervisor

Dr. G. J. SANJAYAN

**DIVISION OF ORGANIC CHEMISTRY
NATIONAL CHEMICAL LABORATORY
PUNE 411008
INDIA**

JANUARY 2016

DECLARATION

I hereby declare that the thesis entitled “**Structural Tolerance of Reverse Turn: A Case Study with Ant-Pro Turns**”, submitted for the Degree of Doctor of Philosophy in Chemistry to the University of Pune, has not been submitted by me to any other university or institution. This work has been carried out at Division of Organic Chemistry, National Chemical Laboratory, Pune under the supervision of Dr. G. J. Sanjayan (Research guide).

Date:
Division of Organic Chemistry
National Chemical Laboratory
Pune

Tukaram S. Ingole
(Research student)



राष्ट्रीय रासायनिक प्रयोगशाला
(वैज्ञानिक तथा औद्योगिक अनुसंधान परिषद)
डॉ. होमी भाभा रोड, पुणे - 411 008. भारत
NATIONAL CHEMICAL LABORATORY
(Council of Scientific & Industrial Research)
Dr. Homi Bhabha Road, Pune - 411008. India



CERTIFICATE

Certified that the work incorporated in the thesis entitled “**Structural Tolerance of Reverse Turn: A Case Study with Ant-Pro Turns**”, submitted by **Mr. Tukaram S. Ingole** for the degree of **Doctor of Philosophy** was carried out by the candidate under my supervision in Organic Chemistry Division, National Chemical Laboratory, Pune, India. Materials obtained from other sources have been duly acknowledged in the thesis.

Date:
Place: Pune

Dr. G. J. Sanjayan
(Research Guide)

Communications Channels
+91 20 25902000
+91 20 25893300
+91 20 25893400

Fax +91 20 25902601 (Director)
+91 20 25902660 (Admin.)
+91 20 25902639 (Business Development)

URL : www.ncl-india.org

Dedicated to my family



Acknowledgement

*First and foremost I want to thank my research supervisor **Dr. G. J. Sanjayan** for his guidance, support, timely advice and encouragement during the course of my Ph.D. work. He helped me to face the challenges during the reaction chemistry with his valuable suggestions and taught the power of imagination, creation of novel ideas, and requirement of doing quality work.*

I am grateful to Dr. P. R. Rajamohanan for his help during the 2D NMR studies which are highly requisite for the completion of my thesis work.

I thank Dr. A. T. Biju and Dr. Santosh Babu for their guidance, timely advice and support in all matters. Special thanks to Prof. Wadgaonkar, Prof. Chavan, and Dr. Kalkote for their encouraging talks, kind help and thoughtful suggestions.

I owe my sincere gratitude to Dr. P. K. Tripathi, Head of the Organic Chemistry Division and Dr. Sourav Pal, Director, NCL for providing the infrastructure to work in this prestigious research institute.

I am deeply indebted to Dr. Rajesh Gonnade and Dr. Vedavati. G. Puranik for crystal structure studies of my compounds. Special thanks to Rupesh for his valuable suggestions for obtaining good quality crystals and his efforts in solving data. I also thank Deba, Shridhar and Samir for their help in solving crystal structures.

I take this opportunity to express my heartfelt gratitude to my teachers Prof. B. P. Bandgar, Prof. S. P. Vartale, Prof. Sagar and Prof. V. Kamble who helped me to learn the basics of Chemistry during my post-graduation studies. Their encouragement and suggestions made me ambitious in life. I am deeply indebted to them more than they know.

I would like to thank my senior labmates Amol, Panchami, Pranjali, Sreenivas, Ajay Kale, Pinak, Arup, Sangram, Gowri, Ramesh, Roshna and Vijaydas for their valuable help and guidance. I also thank my labmates Vijay, Sachin, Amol, Sanjeev, R. Suresh, Shivakumar, M. Suresh, Krishnaprasad, Ganesh, and newly joined Krishnachaitanya and Mahendra for their cheerful company and for maintaining the playful atmosphere in lab.

I thank Amol and Shrikant from NMR facility to help me in the NMR analyses.

Special thanks to my hostel friends Sachin, Shivaji (mama), Rupesh, Anil, Dipesh (kaka), Majid, Kiran, Deepak bhau, Deepak, and Indra for helping me in every sense and making the stay joyful.

I would like to thank my NCL colony friends Kaushal, Digambar, Manas, Santosh, Shashi, Dr. Jayshri Thote, Manoj, Nagesh, Ramesh, Kailash, Amit, Mohsin and their families for their wonderful company which I really enjoyed during the stay at NCL SA quarters. I would like to thank my post-graduate friends Chinmay, Digambar, Hemant, Ram Ganapure, V. Adaskar, Vaijnath, Vijay K., Pankaj M., Arvind, Santosh K., Tanaji, and Nitin for being with them and sharing the good times at SRTMU hostel. I also want to thank my seniors Dr. Amol, Dr. Abasaheb, Dr. Manmath, Dr. Ankush Biradar, Dr. Bharat, Dr. Nagendra, Dr. Ankush, Dr. Bavikar, Dr. Namdev, Dr. Pandurang, Dr. Abhijeet, Dr. Asif, Dr. Dhanaraj, Dr. Mangesh and Dr. Sutar for their constant support, assistance and constructive advices.

I owe my deepest gratitude to my family members for their constant encouragement, support and timely advice during my studies. Special thanks to my beloved mother, dear Advait and wife (Vandana) for their faith, unconditional love, and support at every stage of my studies.

I thank UGC, New Delhi, for financial support.

Finally, I would like to thank each and everyone who have helped and supported during a stay at NCL.

Tukaram S. Ingole

Table of Contents

Abbreviations	I
Abstract.....	II
General remarks	VIII
List of publications	IX

Chapter 1

Part A

Influence of N-terminal modification on robustness of Ant-Pro pseudo β -turn motif

1.1 Introduction	2
1.2 Classification of peptidomimetics based on backbone modification	4
1.2.1 Peptidomimetics based on backbone extension	4
1.2.2 Peptidomimetics based on isosteric/isoelectronic exchange	10
1.3 Reverse turn mimetics	14
1.3.1 γ -turns	14
1.3.2 β -turns	14
1.3.3 α -turns	15
1.3.4 π -turns	15
1.3.5 β -turn mimetics and their applications	15
1.4 Objective and design strategy	20
1.5 Synthesis	21
1.6 Conformational analyses	23
1.6.1 Single crystal X-ray diffraction analysis	23
1.6.2 NMR studies	24
1.6.3 Circular dichroism studies	26
1.7 Conclusion	27

Part B

The conformational analysis of oligomers containing 3- aminothiophenecarboxylic acid (3-Atc) an aromatic β -amino acid

1.8 Introduction	28
1.9 Objective of the work and design strategy	29
1.10 Synthesis	30

1.11 Conformational analyses	31
1.11.1 X-ray diffraction study of 15a	31
1.11.2 NMR studies of 15a	32
1.11.3 NMR studies of 16	33
1.11.4 NMR studies of 19	34
1.11.5 Theoretical studies of 19	34
1.11.6 Circular dichroism studies	35
1.12 Conclusion	36
1.13 Experimental section (Part A)	37
1.14 Experimental section (Part B)	65
1.15 References and notes	93

Chapter 2

Conformational preference of ^SAnt-Pro reverse turn scaffold over native β -turn elements – a competition experiment

2.1 Introduction	105
2.2 Objective and design strategy	106
2.3 Results and Discussion	108
2.3.1 Synthesis	108
2.3.2 Conformational analyses by crystal structure and NMR studies	110
2.3.3 Conformational analysis by FT-IR studies	116
2.3.4 Structural elucidation of 2 and 3 by nOe-based MD simulation	117
2.4 Conclusion	118
2.5 Experimental section	119
2.6 References and notes	184

Chapter 3

Part A

H-X-H three-centered hydrogen bonding promoted nonpeptidic robust reverse turn mimetics

3.1 Introduction	188
3.2 Objective and design strategy	190

3.3 Results and discussion	191
3.3.1 Synthesis	191
3.3.2 NMR studies	192
3.3.3 Crystal structure analysis	195
3.4 Conclusion	196

Part B

Synthesis and characterization of novel urea - (^δAnt-Pro) peptide conjugates for potential biomedical applications

3.5 Introduction	197
3.6 Objective of the work and design strategy	198
3.7 Results and discussion	200
3.7.1 Synthesis	200
3.7.2 Conformational analysis	201
3.8 Conclusion	201

Part C

Vesicular self-assembly of urea-tethered α , β -hybrid foldamer as a hydrophobic cargo carrier

3.9 Introduction	202
3.10 Objective of the work and design strategy	204
3.11 Results and discussion	205
3.11.1 Synthesis	205
3.11.2 Microscopic analysis	206
3.11.3 Encapsulation study	209
3.12 Conclusion	210
3.13 Experimental section (Part A)	212
3.14 Experimental section (Part B)	249
3.15 Experimental section (Part C)	266
3.16 References and notes	271

Abbreviations

A		HSQC	Hetero Nuclear Single Quantum Coherence
Å	Ångström	Hz	Hertz
AA	Amino acid	HRMS	High-resolution Mass Spectrometry
Ac	Acyl		
Ala	Alanine		
Aib	Amino isobutyric acid		
Ant	Anthranilic acid	L	
AFM	Atomic Force Microscopy	LCMS	Liquid chromatography– mass spectrometry
B		M	
Boc	tert.- Butyloxycarbonyl	m	Multiplet (NMR)
Bn	Benzyl	MS	Mass Spectrometry
		MS	Molecular Sieves
		Me	Methyl
C		N	
CDCl ₃	Chloroform-d	NOESY	Nuclear Overhauser and Exchange Spectroscopy
COSY	Correlated spectroscopy		
D		P	
d	doublet (NMR)	Ph	Phenyl
δ	Chemical shift (NMR)	Pro	Proline
DCC	<i>N, N'</i> -dicyclohexyl- carbodiimide	Pd/C	palladium 10 % on activated carbon
DCM	Dichloromethane	PLM	Polarized light microscopy
DMF	Dimethyl formamide		
DIEA	Diisopropyl ethylamine	S	
DMSO	Dimethylsulfoxide	s	Singlet (NMR)
DMAP	4-dimethyl aminopyridine	^s Ant	2-aminobenzenesulfonic acid
E		SEM	Scanning Electron Microscopy
EDC	1-Ethyl-3-(3- dimethylaminopropyl) carbodiimide	T	
ESI	Electron spray ionization	TEM	Transmission electron microscopy
Et	Ethyl	TFA	Trifluoroacetic acid
EtOAc	Ethyl acetate	HBTU	O-benzotriazol-1-yl- <i>N, N,</i> <i>N', N'</i> -tetramethyluronium tetrafluoroborate
G		TEA	Triethyl amine
Gly	Glycine	THF	Tetrahydrofuran
H		TBAB	Tetrabutyl ammonium bromide
H-bond	Hydrogen bond	t	Triplet (NMR)
HMBC	Hetero Multiple Bond Correlation		
HBTU	O-benzotriazol-1-yl- <i>N, N,</i> <i>N', N'</i> -tetramethyluronium hexafluorophosphate		
HOBt	1-hydroxybenzotriazole		

ABSTRACT

Name of the Candidate	Tukaram S. Ingole
Name of the Research Guide	Dr. G. J. Sanjayan
Title of the Ph. D. thesis	Structural Tolerance of Reverse Turn: A Case Study with Ant-Pro Turns.

Preamble: Reverse turns are one of the most common structural features found in globular proteins and peptides, involving three (γ -turn) or four (β -turn) or five (α -turn) or six (π -turn) consecutive amino acid residues, characterized by peptide chain reversal. Studies in reverse turns have attracted considerable attention owing to their applications in the interdisciplinary fields such as protein design, organocatalysis, material chemistry and medicinal chemistry.

Chapter 1: The section A of this chapter describes the conformational characterization of short oligomers having extensive modification at N-terminus of Ant-Pro reverse turn (Fig. 1). Extensive conformational studies suggest that all short oligomers exhibited folded *pseudo* β -turn conformation, involving just two residues displaying a closed nine-membered-ring hydrogen-bonded network, formed in the forward direction (1 \rightarrow 2), which is in stark contrast to the native β -turns that involve four residues to form hydrogen-bonded network featuring backward 1 \leftarrow 4 amino acid interactions.

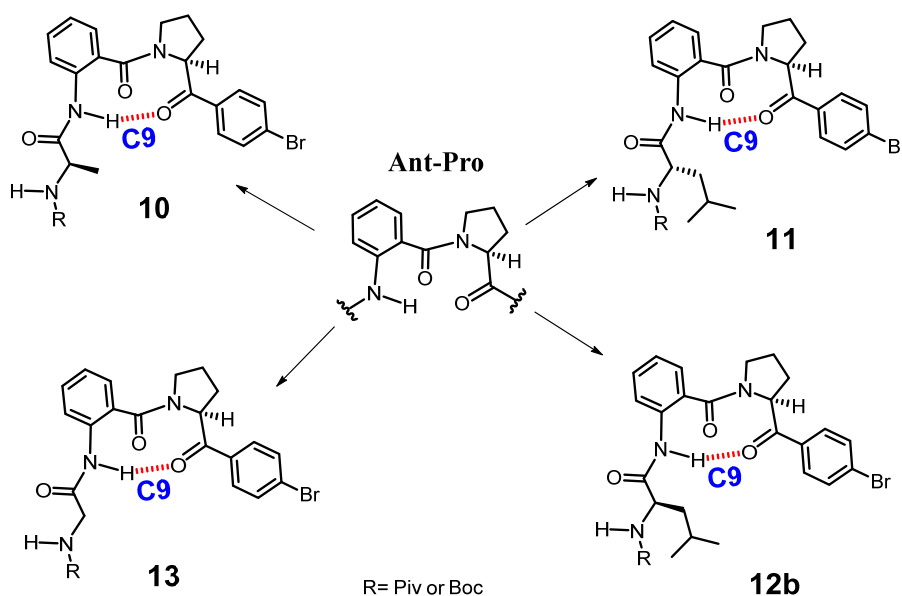


Fig. 1 Molecular structures of N-terminal modified Ant-Pro-based short oligomers featuring C9 hydrogen bonding.

[The Ant-Pro reverse-turn motif. Structural features and conformational characteristics.

V. H. Thorat, **T. S. Ingole**, K. N. Vijayadas, R. V. Nair, S. S. Kale, V. V. E. Ramesh, H. C. Davis, P. Prabhakaran, R. G. Gonnade, R. L. Gawade, V. G. Puranik, P. R. Rajamohan and G. J. Sanjayan, *Eur. J. Org. Chem.*, 2013, 3529.]

The section B of this chapter describes the design, synthesis and conformational analysis of oligomers containing 3-aminothiophenecarboxylic acid (3-Atc); an aromatic β -amino acid (Fig. 2). We have designed α,β,α -hybrid peptide sequence: Gly-3-Atc-Pro-Gly-3-Atc-Pro-Gly, featuring 3-Atc and Pro-Gly motifs. The conformational investigation by crystal structure and 2D NMR studies suggested that the synergistic effect of dihedral parameters of individual amino acids and intra-residual hydrogen bonding within 3-Atc resulted in the formation of helical folding in (Gly-3-Atc-Pro) oligomers, despite the absence of inter-residual hydrogen bonding, which is commonly observed in native polypeptides.

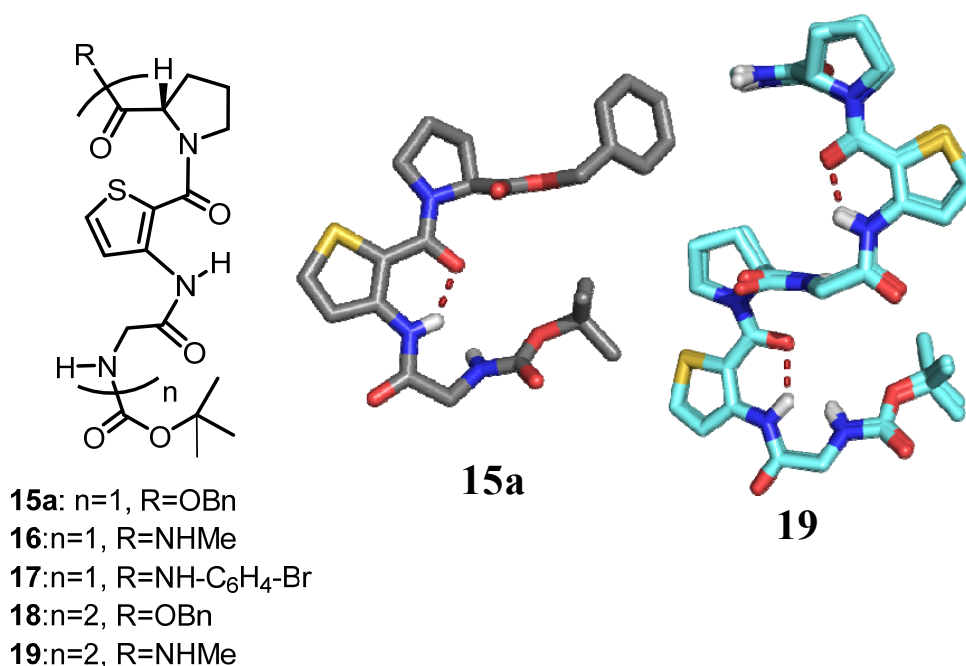


Fig. 2 Molecular structures of (Gly-3-Atc-Pro) oligomers and crystal structure of **15a** and nOe-restrained energy minimized structures of **19**.

[3-Aminothiophenecarboxylic acid (3-Atc)-induced folding in peptides: some observations.

T. S. Ingole, A. S. Kotmale, R. L. Gawade, R. G. Gonnade, P. R. Rajamohan and G. J. Sanjayan (*Manuscript under preparation*).]

Chapter 2: This chapter describes the design, synthesis and conformational studies of oligomers comprising a *pseudo* β -turn S Ant-Pro (orthanilic acid-proline)

attached to different native β -turn forming turn elements (Fig. 3). The peptide sequences having two turn elements can result in multiple hydrogen bonding networks and it is often very difficult to predict which hydrogen bonding network will prevail and hence the outcome of the folding competition. The results of extensive conformational investigation by crystal structure and 2D NMR studies showed that **1** adopts a C9 H-bonding, while **2**, **3** and **4** adopt a C14 H-bonding conformation accompanied by C6 H-bonding. Intriguingly, formation of native β -turn was not observed in any of the peptides.

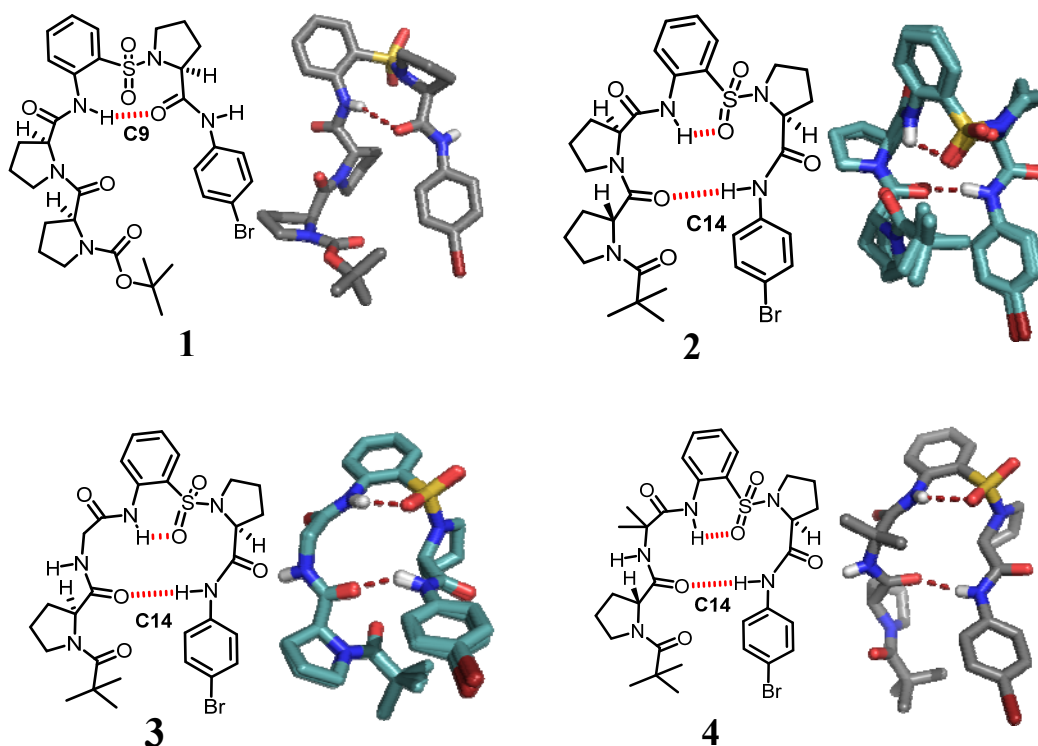


Fig. 3 Molecular structures of peptides showing observed hydrogen bonding pattern and their corresponding crystal structures (**1** and **4**) or nOe-based MD simulated 20 superimposed energy minimized structures (**2** and **3**).

[Disruption of native β -turns: consequence of folding competition between native and orthonilic acid-proline-based *pseudo* β -turn.

T. S. Ingole, K. N. Vijayadas, K. N. Chaitanya, A. S. Kotmale, R. L. Gawade, R. G. Gonnade, P. R. Rajamohanam and G. J. Sanjayan, *Eur. J. Org. Chem.*, 2016 (*Just Accepted*, DOI: 10.1002/ejoc.201501558).]

Chapter 3: The section A of this chapter describes the design, synthesis and conformational characterization of urea-based H-X-H three-centered hydrogen bonding-stabilized reverse turn scaffold containing a ^SAnt-Pro reverse turn and a urea moiety at the N-terminus of the turn motif (Fig. 4). We anticipated that the

urea NHs would form intramolecular dual hydrogen bonding with C=O of proline. In the present study, trichloroacetamide derivative was used as a common intermediate to generate the unsymmetrical urea analogues *via* coupling with various amines. The conformational investigation of designed unsymmetrical urea derivatives in the solid and solution-state by single crystal X-ray crystallography and detailed 2D NMR studies, respectively, revealed that these scaffolds adopt well-defined conformation featuring robust urea-based H-X-H three-centered hydrogen bonding. Interestingly, an interaction between ^SAnt-NH and Pro-N was found to be an augmenting force for the stabilization of dual H-bonded reverse turn scaffold. This nonpeptidic reverse turn scaffold can be attached to peptide strands through N-terminus connection, thus it can serve as a template to promote parallel β -sheet structures.

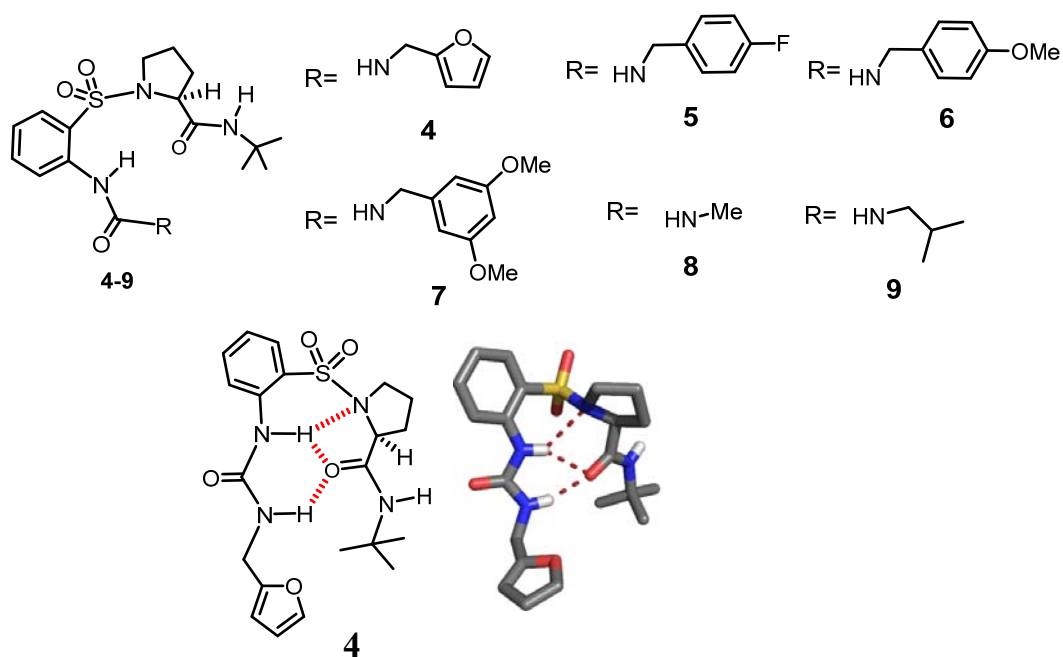


Fig. 4 Molecular structures of various designed unsymmetrical urea analogues and molecular structure and PyMOL-rendered crystal structure of **4** showing robust urea-based H-X-H three centered hydrogen bonding.

[Design and synthesis of H-X-H three-centered H-bonding stabilized nonpeptidic reverse turn scaffold to promote parallel β -sheet structure.

T. S. Ingole, A. S. Kotmale, R. L. Gawade, R. G. Gonnade, P. R. Rajamohan and G. J. Sanjayan (*Manuscript under preparation*).

The section B of this chapter describes the design and synthesis of novel [1,4]-diazepane urea-^SAnt-Pro peptide conjugates (Fig. 5). [1,4]-diazepane moiety is found in many drugs; e.g. orexin receptor antagonists, CXCR3 antagonists,

cannabinoid receptor 2 agonists and factor Xa inhibitors for anticoagulation. We have designed a series of hybrid analogues featuring [1,4]-diazepane moiety or cyclic secondary amines linked to ^SAnt-Pro reverse turn scaffold through the urea linkage. ¹H NMR analysis revealed that these compounds show the characteristics of 9-membered hydrogen-bonded folded conformation.

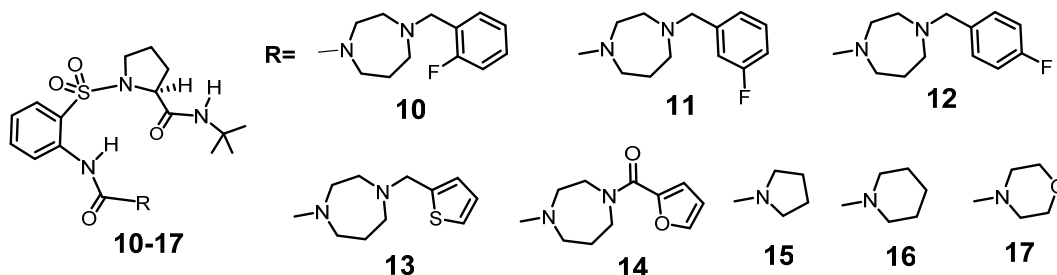


Fig. 5 Molecular structures of various urea-(^SAnt-Pro) peptide conjugates.

The section C of this chapter describes the design and synthesis of urea-appended α,β -hybrid octapeptide which undergoes self-assembly to form vesicular morphology (Fig. 6). Because of properties like intrinsic folding, self-organization, biocompatibility, versatility, and ease of synthetic modification, peptide molecules have been considered as an attractive new choice of materials for developing supramolecular materials using molecular self-assembly process. Earlier, our group reported that iodo-substituted Ant-Pro oligomers adopt helical structures. We envisioned that substitution of iodo group by functional group like urea would induce the intermolecular interactions between molecules. In the present study, a urea moiety was chosen, which was installed on phenyl group through an alkyne spacer using Sonogashira reaction. Microscopic analyses confirmed that the urea-appended octapeptide **21** undergoes self-assembly through the urea-mediated intermolecular interactions forming vesicular structures from methanolic solution. Up on decreasing the concentration of methanol from the binary solvent mixture, octapeptide **21** forms hollow pot-like self-assembled vesicular structures. These vesicles are able to encapsulate the hydrophobic drug like curcumin efficiently which was confirmed by bright green fluorescence in the vesicles under fluorescence microscope.

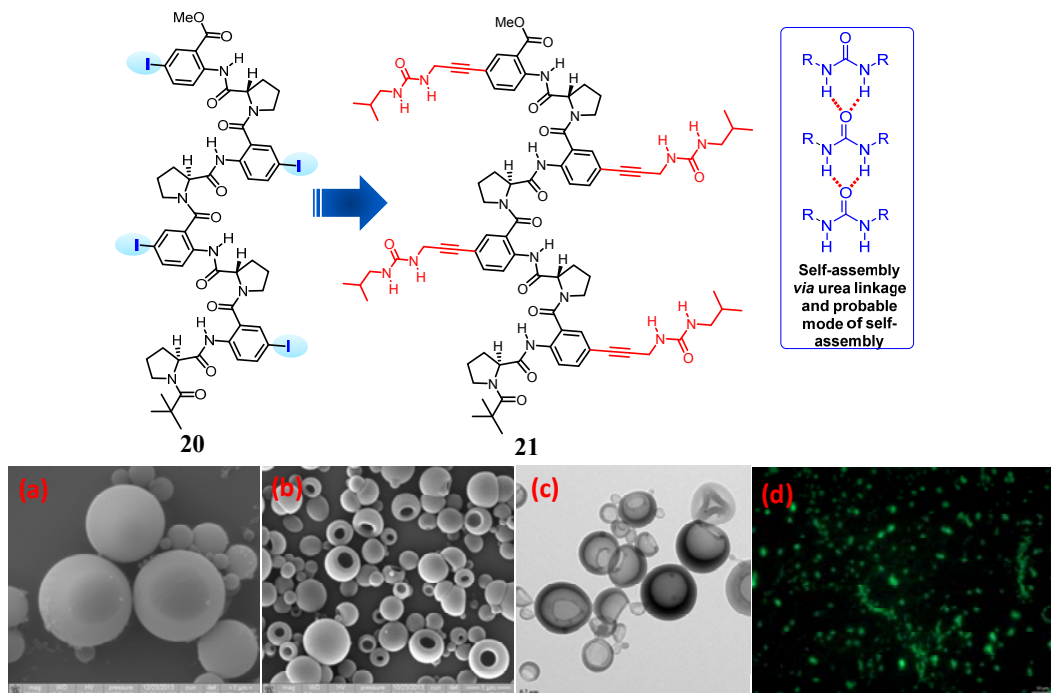


Fig. 6 Design of urea-tethered Ant-Pro octapeptide **21** and schematic presentation of probable mode of urea-mediated self-assembly. Microscopic analyses of self-assembly of octapeptide **21**. SEM images (1 mg/0.5 mL): (a) methanol and (b) 9:1 methanol-toluene. TEM image (1 mg/mL, c). Fluorescence microscopic image (d) showing bright green fluorescence of curcumin encapsulated vesicles.

[Vesicular self-assembly of urea-tethered α,β -hybrid foldamer as a hydrophobic cargo carrier.

T. S. Ingole, P. R. Rajamohanam, S. S. Babu and G. J. Sanjayan (*Manuscript under preparation*).]

General Remarks

- Unless otherwise stated, all chemicals and reagents were obtained commercially.
- Required dry solvents and reagents were prepared using the standard procedures.
- All the reactions were monitored by thin layer chromatography (TLC) on precoated silica gel plates (kieselgel 60F₂₅₄, Merck) with UV, I₂ or ninhydrin solution as the developing reagents in the concerned cases.
- Column chromatographic purifications were done with 100-200 Mesh Silica gel or with Flash silica gel (230-400) mesh in special cases.
- Melting points were determined on a Buchi Melting Point B-540 and are uncorrected.
- IR spectra were recorded in nujol or CHCl₃ using Shimadzu FTIR-8400 spectrophotometer.
- NMR spectra were recorded on Ac 200 MHz, AV 400 MHz or DRX-500 MHz or AV 700 MHz Bruker NMR spectrometers. All chemical shifts are reported in δ ppm downfield to TMS and peak multiplicities as singlet (s), doublet (d), quartet (q), broad (br), broad singlet (bs) and multiplet (m).
- Elemental analyses were performed on a Elementar-Vario- EL.
- Electron scattered ionization (ESI) mass spectrometric measurements were done with API QSTAR Pulsar mass Spectrometer and high-resolution mass spectrometric analyses (HRMS) were carried out using a Thermo Scientific Q-Exactive, Accela 1250 pump mass spectrometer.
- nOe-restrained molecular modeling studies were carried out using MacroModel, version 10.7 program from Schrödinger.
- Single crystal X-ray data were collected on a *Bruker SMART APEX* CCD Area diffractometer.

List of Publications

- (1) The Ant-Pro reverse-turn motif. Structural features and conformational characteristics.
V. H. Thorat, **T. S. Ingole**, K. N. Vijayadas, R. V. Nair, S. S. Kale, V. V. E. Ramesh, H. C. Davis, P. Prabhakaran, R. G. Gonnade, R. L. Gawade, V. G. Puranik, P. R. Rajamohanan and G. J. Sanjayan, *Eur. J. Org. Chem.*, 2013, 3529.
- (2) Synthetic turn mimetics and hairpin nucleators: quo vadimus?
R. V. Nair, S. B. Baravkar, **T. S. Ingole** and G. J. Sanjayan, *Chem. Commun.*, 2014, **50**, 13874 (*Front cover page*).
- (3) Disruption of native β -turns: consequence of folding competition between native and orthanilic acid-proline-based *pseudo* β -turn.
T. S. Ingole, K. N. Vijayadas, K. N. Chaitanya, A. S. Kotmale, R. L. Gawade, R. G. Gonnade, P. R. Rajamohanan and G. J. Sanjayan, *Eur. J. Org. Chem.*, 2016, (*Just Accepted*, DOI: 10.1002/ejoc.201501558)
- (4) 3-Aminothiophenecarboxylic acid (3-Atc)-induced folding in peptides: some observations.
T. S. Ingole, A. S. Kotmale, R. L. Gawade, R. G. Gonnade, P. R. Rajamohanan and G. J. Sanjayan (*Manuscript under preparation*).
- (5) Design and synthesis of H-X-H three-centered H-bonding stabilized nonopeptidic reverse turn scaffold to promote parallel β -sheet structure.
T. S. Ingole, A. S. Kotmale, R. L. Gawade, R. G. Gonnade, P. R. Rajamohanan and G. J. Sanjayan (*Manuscript under preparation*).
- (6) Vesicular self-assembly of urea-tethered α,β -hybrid foldamer as a hydrophobic cargo carrier.
T. S. Ingole, P. R. Rajamohanan, S. S. Babu and G. J. Sanjayan (*Manuscript under preparation*).

CHAPTER 1

PART A

Influence of N-terminal modification on robustness of Ant-Pro pseudo β -turn motif

PART B

The conformational analysis of oligomers containing 3-aminothiophenecarboxylic acid (3-Atc); an aromatic β -amino acid

Influence of N-terminal modification on robustness of Ant-Pro pseudo β -turn motif

1.1 Introduction

Proteins are one of the important classes of biopolymers (ribonucleic acids and polysaccharides), since they are involved in the physiological processes such as molecular recognition, catalysis, cellular communication, information storage, and molecular transportation. In order to perform these functions, protein has to undergo chain of processes called protein folding.¹ Through the protein folding process, protein adopts specific spatial conformation or globular shape which is responsible for the biochemical reactions. The noncovalent forces such as: electrostatic interactions (ionic, hydrogen bonding), van der Waals forces and hydrophobic packing *etc.* are mainly responsible for the stabilization of a protein structure.²

There are four stages of protein folding such as primary, secondary, tertiary and quaternary stage by which a protein attains the native conformation (Fig. 1.1). In the primary stage, the amino acids are covalently bonded together by an amide bond to form a peptide chain which is present in an extended form. The protein utilizes 20 α -amino acids and few unusual amino acids to generate the peptide chains. The sequence of amino acids present in the peptide backbone is important for determining the three dimensional structure and function of a protein. Specifically, intrinsic properties of R-group or side chain of each amino acid determine the property and in turn the function of a protein. The secondary stage involves interactions between adjacent amino acids through hydrogen bonding leading to the formation of ordered structures (α -helix, β -pleated sheets, β -turns or bends and super secondary structures).³ The tertiary stage involves

further folding and super coiling of polypeptide chains. The tertiary structure is governed by the interactions like hydrophobic, hydrogen bonds, salt bridges and disulfide bonds between the R-groups or side chains of amino acids. In this level, secondary structures like helices, β -pleated sheets and turns are arranged spatially in order to assume compact globular shape. The quaternary stage involves the arrangement of multiple protein subunits in a specific manner in order to perform specific functions.

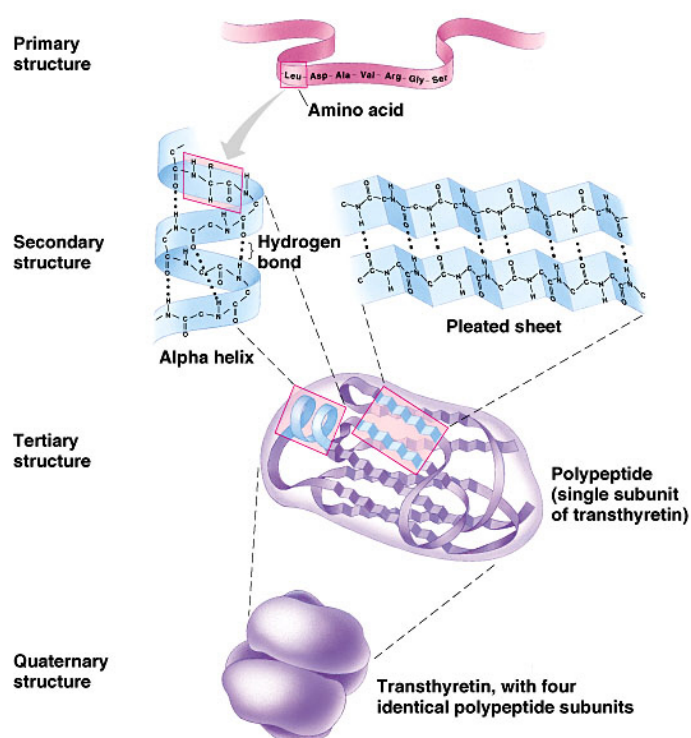


Fig. 1.1 Four levels of protein structure: primary structure (amino acids sequence in extended form), secondary structure (polypeptide linkage folds into helices or sheets), tertiary structure (packing of secondary structures into globular domain) and quaternary structure (protein subunits self assemble to form compact structure) (Image source: internet).

The noncovalent interactions play a crucial role in the transformation of primary to quaternary structure. With just 20 proteinogenic α -amino acids Nature had created diverse structural architectures by making use of noncovalent interactions. Inspired from the Nature, chemists and biochemists have successfully

prepared synthetic oligomers (foldamers) containing non-natural moieties which possess protein-like well-defined conformation.^{4,5,6} In recent years, the synthetic oligomers gained a lot of attention due to the features like easy synthesis, easy backbone modification and predictability of conformations. Moreover, owing to the non-natural content of these oligomers, foldamers exhibit improved proteolytic stability than the native peptides.

1.2 Classification of peptidomimetics based on backbone modification

Modifications in the peptide backbone have been shown to be a promising approach for the generation of peptidomimetics (Fig. 1.2). The approach of peptide backbone modification involves insertion of extra units (β -peptides, γ -peptides and δ -peptides) or the exchange of isosteric or isoelectronic atoms (oligoureas, aminoxy peptides, azapeptides and peptoids).

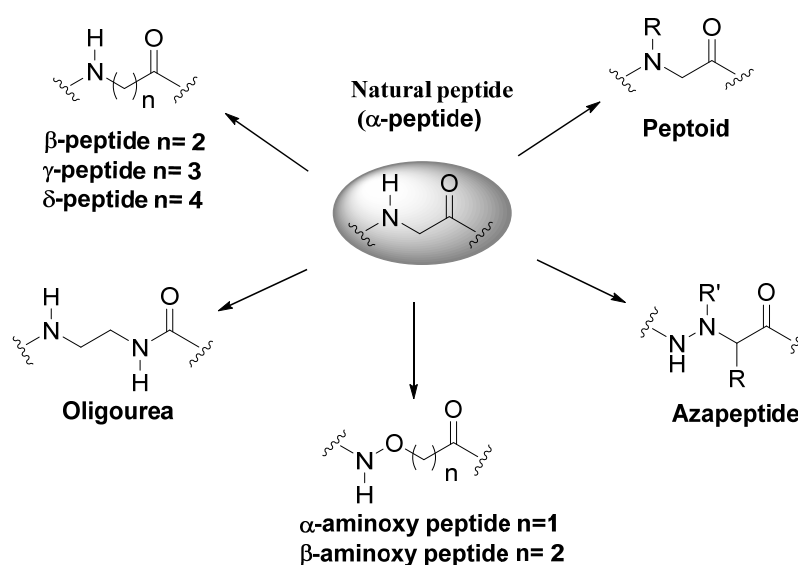


Fig 1.2 Backbone modified peptidomimetics.

1.2.1 Peptidomimetics based on backbone extension

β -peptides

With the intensive research carried out from last few years, researchers have shown that backbone modification such as insertion of extra carbon or other

heteroatoms between amine and carboxylic acid functional groups resulted in the generation of a myriad of structures.^{5,6} β -amino acids (Fig. 1.3a) are the mostly explored building blocks for the creation of peptidomimetics since β -amino acid-containing oligomers have been shown improved proteolytic resistance.⁷ β -amino acids have three torsional variables (ϕ , θ , ψ) compared to α -amino acids and as a result they show increased conformational space. Seebach and Gellman independently established the work on conformational preferences of β -peptides. Gellman group has shown that the use of cyclic β -amino acids such as *trans*-2-aminocyclopentanecarboxylic acid (*trans*-ACPC, Fig. 1.3b)⁸ and *trans*-2-aminocyclohexanecarboxylic acid (*trans*-ACHC, Fig. 1.3c)⁹ can provide conformational rigidity to the peptide backbone. Homo-oligomers of *trans*-ACHC form 14-helix (C_{14} , 3_{14} , 3_{14} -helix),¹⁰ while homo-oligomers of *trans*-ACPC form 12-helix.¹¹ Gellman group has further shown that the variation in the constitutional ratio of α - and β -amino acids in the oligomers drastically affect the hydrogen bonding pattern.¹² Aitken group reported the homo-oligomers of *trans*-2-aminocyclobutanecarboxylic acid (*t*ACBC) adopt a 12-helix (Fig. 1.3d).¹³ Aitken group has further shown that the attachment of primer like N-aminoazetidine-2-carboxylic acid (AAzC) to the N-terminus of *t*ACBC-based homo-oligomer resulted in hydrogen bonding tunable helical foldamers.¹⁴ Balaram group independently explored the conformational features of oligomers containing C^β -substituted acyclic β -amino acids and their hybrid oligomers with α -amino acids.^{6b} Similarly, Reiser group used *cis*- β -aminocyclopropanecarboxylic acid (*cis*- β -ACCs, Fig. 1.3e) in conjunction with α -amino acid like L-alanine to obtain stable 13-helix.¹⁵ Another example of hybrid strategy was demonstrated by our group in which α,β -hybrid peptide containing repeating dipeptide sequence

anthranilic acid-proline (Ant-Pro) adopts right-handed helical architecture stabilized by unusual 9-membered hydrogen bonding in the forward direction (1→2), as shown in Fig. 1.3g.¹⁶ Additionally, oligomers containing conformationally constrained aromatic β -amino acid such as orthanilic acid (^SAnt) have been shown to adopt helical folding (Fig. 1.3f).¹⁷

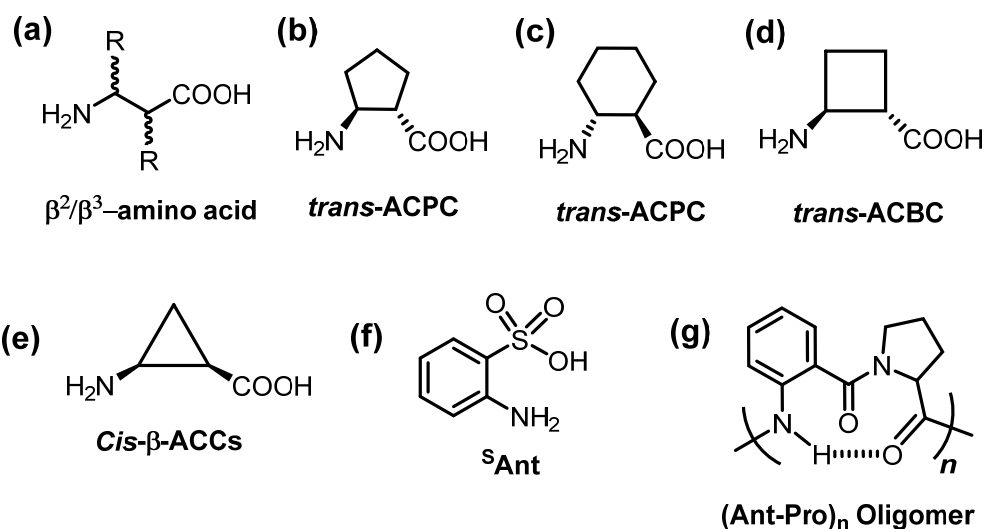


Fig. 1.3 General backbone of substituted β -amino acid residue (a), representative examples of β -amino acids (b-f) and helical Ant-Pro oligomer featuring 9-membered hydrogen bonding (g).

While working on the peptidomimetics research field, several researchers have shown that synthetic oligomers can adopt protein-like well-defined quaternary structure. In this regard, Gellman group has shown that synthetic oligomers having repeating sequence α,α,β display tetrameric quaternary structure in the crystalline-state.¹⁸ Independently, Schepartz group has shown that oligomers made of C2-substituted acyclic β -amino acids assume octameric helix bundle quaternary structural architecture.¹⁹

γ -amino acid

Rapid progress in the conformational studies on the β -peptides has stimulated the use of higher order homologated amino acids such as γ - and δ -

amino acids as building blocks for *de novo* design of folded synthetic oligomers. Hanessian²⁰ and Seebach²¹ research groups independently have shown that insertion of one more carbon atom into β -amino acid backbone (γ -amino acid, Fig. 1.4a) increases the number of degrees of freedom. Moreover, the content of higher order homologated amino acids in the peptide backbone enhances the helical stability as well as proteolytic stability.²² The substitution pattern on the residue backbone and stereochemistry of amino acid residue are the determining factors for the helical handedness and orientation of hydrogen bonds.²³ Seebach reported that homo-oligomers of monosubstituted γ -amino acids assume 14-helix conformation.^{21b} Similarly, Hanessian utilized the homogeneous strategy for the preparation of helical γ -peptides.²¹ Sharma and coworkers have shown that γ -peptides containing C-linked carbo- γ^4 -amino acid and γ -aminobutyric acid (GABA) in alternate fashion adopt 9-helix (Fig. 1.4b).²⁴ Balaram group utilized disubstituted γ -amino acid like gabapentin (Gpn, Fig. 1.4c) to prepare its homo-oligomers, which form 9-helix.²⁵ Additionally, a variety of disubstituted γ -amino acids have been explored for the preparation of γ -peptides library.^{20b,26} Seebach group also explored tri-substituted γ -amino acids to obtain helical oligomers stabilized by 14-membered hydrogen bonding.^{21c,d} Royo, Albericio and coworkers investigated the conformation of synthetic oligomers containing conformationally constrained γ -amino acid like *cis*- γ -amino-L-proline (Fig. 1.4d) by NMR and CD studies which suggested that these oligomers adopt ribbon-like conformation stabilized by the 9-membered hydrogen bonding.²⁷ Recently, Ortuno group prepared γ,γ -peptides utilizing 3-amino-2,2-dimethylcyclobutane-1-carboxylic acid and *cis*- γ -amino-L-proline.²⁸ Similarly, Edwards group used sugar-based γ -

amino acid as a building block for the preparation of γ -peptides (Fig. 1.4e).²⁹ Smith group has shown that C-7 bend-ribbon-like conformation can be achieved using tartrate-based γ -amino acids (Fig. 1.4f).³⁰ Seebach group reported that halogen or hydroxyl group-substituted γ -amino acids can be successfully utilized as building blocks to obtain helical structures.³¹ Interestingly, Schreiber group found that oligomers containing unsubstituted vinylogous γ -amino acids adopt parallel β -sheet structure, while oligomers containing 2-alkyl substituted γ -amino acids adopt antiparallel sheet structure.³² Gellman group utilized *trans*-3-aminocyclopentanecarboxylic acid (*trans*-3-ACPC) for the construction of parallel sheet structures.³⁴ Subsequently, Smith group described the bifurcated hydrogen bonding-stabilized parallel sheet models using cyclopropane-based γ -amino acid (Fig. 1.4g).^{34,35}

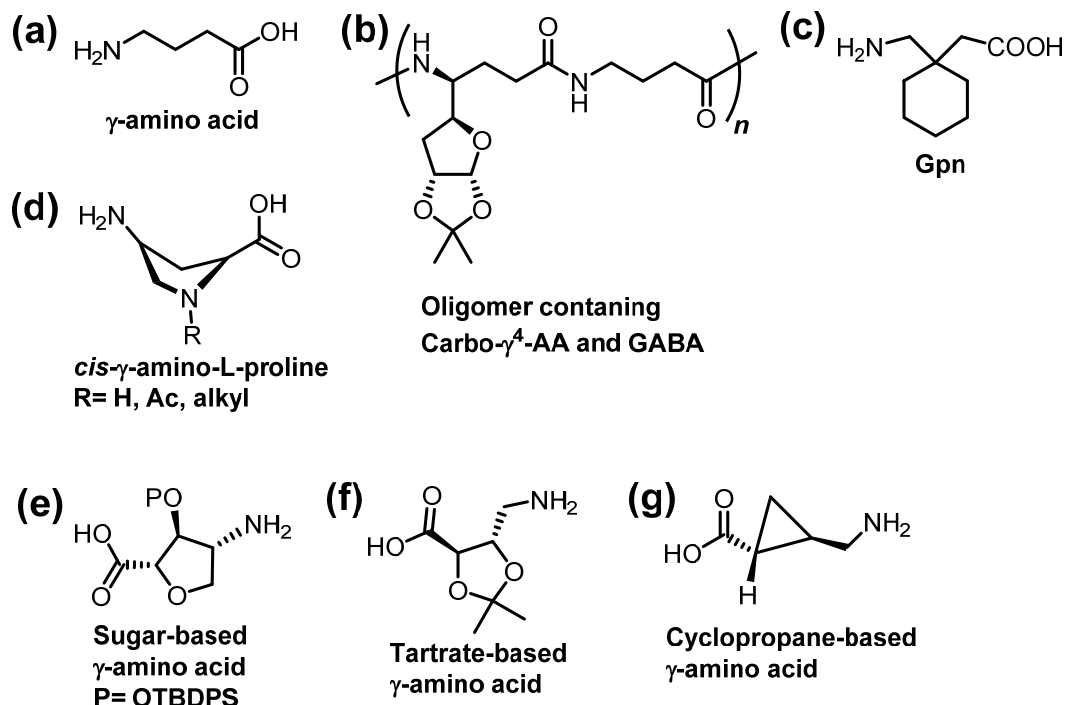


Fig. 1.4 General backbone of γ -AA (a), representative examples of γ -AA (a and c-g) and helical oligomer featuring carbo- γ^4 -AA and γ -aminobutyric acid (b).

Researchers have also shown that hybrid strategy by mixing γ -amino acids with the α - and β -amino acids in appropriate ratio can be a useful strategy to achieve novel hydrogen-bonded structures. The stability of helical γ -peptides is shown to be improved by introducing cyclic constraints on the C^α - C^β or C^β - C^γ bonds.³⁷ In this regard, Gellman group utilized γ -amino acids such as (1*R*,2*R*)-2-aminomethyl-1-cyclopentane carboxylic acid (AMCP)³⁸ or (1*R*,2*R*,3*S*)-2-(1-aminopropyl)-cyclohexanecarboxylic acid (APCH)³⁹ having cyclic constraints on the C^α - C^β bond.

δ -amino acids

Sugar-based δ -amino acids are the prominent class of δ -amino acids and can be considered as isosteric replacements α -dipeptide segment (Fig. 1.5a). The substitution pattern and stereochemistry modulation on the carbohydrate-derived tetrahydrofuran ring can lead to the formation of a variety of secondary structures such as reverse turns or helical structures.⁴⁰ δ -amino acids containing moieties such as tetrahydropyran (THP), tetrahydrofuran (THF) and oxetane have been explored for the preparation of peptidomimetics (Fig. 1.5b-d). Carbopeptoids and sugar amino acids-peptide hybrids have been shown to exhibit potential biomedical applications such as inhibition of protein-protein interaction and enzyme catalysis.⁴¹ Ivan group developed various interesting foldameric structures using versatile building block such as 8-amino-2-quinolinecarboxylic acid: δ -amino acid (Fig. 1.5e). In this connection, they have shown that water-soluble homo-oligomers based on 8-amino-2-quinoline carboxylic acid adopt helical structures.⁴² Furthermore, water-solubility of these oligomers has been increased by introducing different water-soluble groups on the δ -amino acid residue

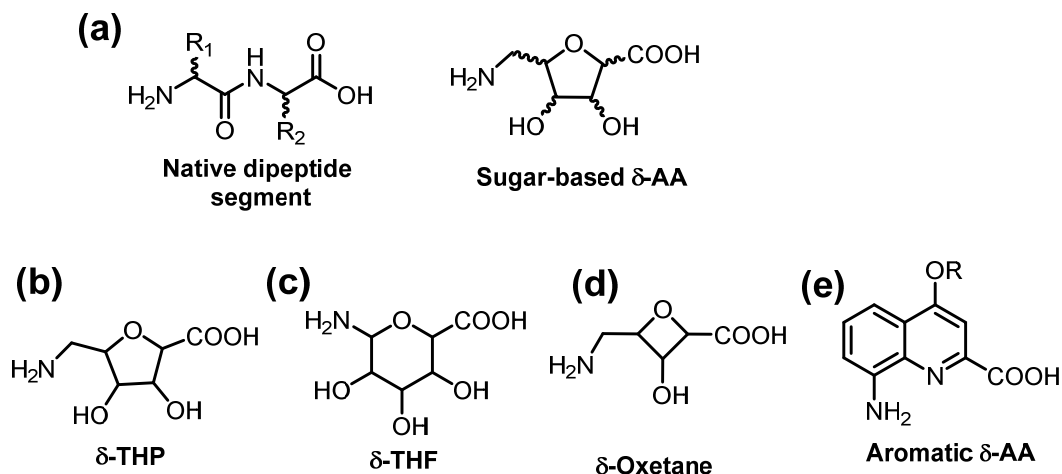


Fig. 1.5 Similarity between native dipeptide segment and sugar-based δ -AA (a) and representative examples of δ -AA building blocks (b-e).

backbone and synthetically modified oligomers have been shown to possess cell penetration abilities, low toxicity and complete proteolytic stability.⁴³ Ivan group prepared heterogeneous helical oligomers as well, by incorporating α -amino acids into oligomeric chain of aromatic δ -amino acids in 1:2 ratio.⁴⁴ Additionally, Ivan group developed synthetic oligomers containing δ -amino acids, ω -amino acids and nonpeptidic scaffolds, which selectively encapsulate fructose moiety among various monosaccharides.⁴⁵

1.2.2 Peptidomimetics based on exchange of isosteric or isoelectronic atoms

Oligoureas

The urea moiety has drawn considerable attention owing to their desirable properties such as planarity, polarity, rigidity and hydrogen bonding capacity. Oligoureas are mimetics of γ -peptides and can be obtained by replacing α -carbon of γ -amino acid backbone by heteroatom like nitrogen (Fig. 1.6a). The general backbone of N,N' -linked oligoureas can be represented as $-\text{[NH-CH(R)-CH}_2\text{-NH-CO-]}_n-$.⁴⁶ Guichard group reported urea oligomers bearing various side chains that adopt 12/14-helical conformation (Fig. 1.6b).⁴⁷ Guichard group developed

synthetic oligomers containing amide and urea groups as well possessing properties such as biomolecular recognition and antibacterial activity.⁴⁸ Recently, amphipathic oligourea bearing histidine units has been shown to exhibit cell penetration ability, assembly with pDNA and efficient delivery of nucleic acids to the cell.⁴⁹ Moreover, Guichard group has shown that urea oligomers adopt helix bundles quaternary structure.⁵⁰

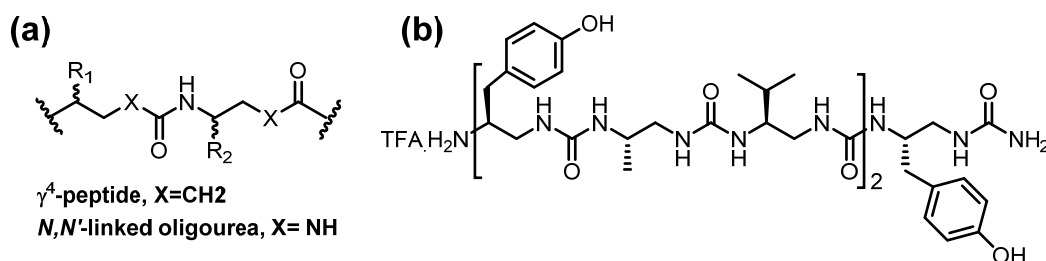


Fig. 1.6 General backbone representation of C3 substituted γ -AA and *N,N'*-linked oligourea (a) and helical oligourea featuring various side chains on the backbone (b).⁴⁷

Aminoxy acids

As a result of repulsion between the lone pair of electrons on the oxygen atom of carbonyl and oxygen atom of the backbone, aminoxy acids exhibit unusual torsional parameters compared to native amino acids. These unusual torsional characteristics imparted enhanced conformational rigidity to the backbone of aminoxy acids. α - and β -aminoxy acids (Fig. 1.7a) have been shown to be versatile building blocks for the generation of various secondary structures.⁵¹ The oligomers containing α -aminoxy acids display 8-membered hydrogen bonding while β -aminoxy acids-based oligomers display 9-membered hydrogen bonding (N-O turn, Fig. 1.7b,c). β -Aminoxy acids allow the variation in the substitution pattern due to the presence of extra carbon atom in the backbone and hence can lead to conformational diversity.⁵²

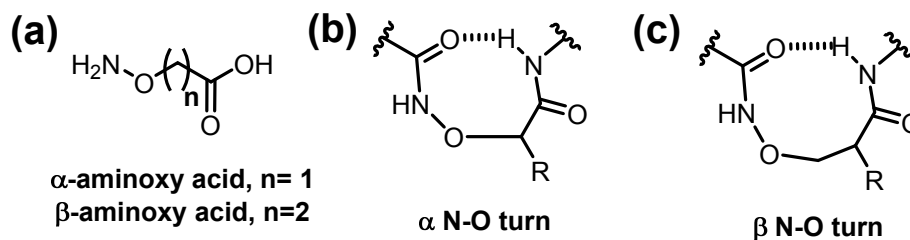


Fig. 1.7 α - and β -Aminoxy acids, a general backbone (a) and short range hydrogen-bonded α - and β -N-O turn (b and c).^{51,52}

Azapeptides

Azapeptides can be obtained by replacement of β^3 -carbon of β -amino acid with the trivalent nitrogen atom (Fig. 1.8a). Similar to aminoxy peptides, azapeptides exhibit short range hydrogen bonding pattern. Homo-oligomers of azapeptides stabilized by bifurcated hydrogen bonding are termed as hydrazinoturn (Fig. 1.8b).⁵³ Grel and coworkers investigated the conformation of aza- β^3 -peptide in solid and solution-state. Conformational studies revealed that peptide backbone was stabilized by consecutive 8-membered hydrogen bonding (Fig. 1.8c).⁵⁴

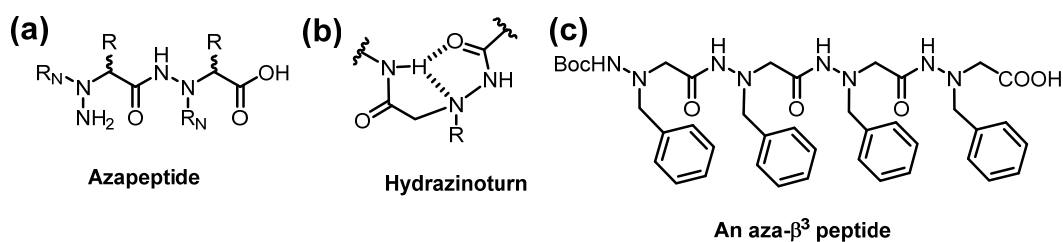


Fig. 1.8 General backbone of an azapeptide (a), hydrazinoturn (b)⁵³ and aza- β^3 -peptide.⁵⁴

Peptoids

Peptoids, also called N-substituted glycines, are considered to be mimics of α -peptides wherein nitrogen atom bears the side chain instead of α -carbon (Fig. 1.9a). Pioneering work in the peptoid field was carried out by Bartlett and coworkers.⁵⁵ The peptoid oligomers have been considered choice of materials for

potential biomedical applications owing to their significant properties such as straightforward synthetic protocol, ease in backbone modification (variation in substitution pattern),⁵⁶ enhanced resistance towards proteases⁵⁷ and cell permeabilities⁵⁸ compared to α -peptides. Taillefumier, Edwards and coworkers reported the synthesis and structural investigations of a linear and cyclic hybrid peptoid oligomer containing α - and β -peptoid residues arranged in alternating fashion.⁵⁹ The major issue associated with peptoid molecules is the *cis/trans* isomerism which leads to conformational heterogeneity.^{56b,c} In this regard, Kirshenbaum group has shown that the issue of *cis-trans* isomerism and structural instability can be successfully circumvented by putting N-aryl group substitution. The N-aryl substituted peptoid oligomers have been shown to adopt helical structures akin to polyproline-II helix (Fig. 1.9b).⁶⁰ Recently, Olsen group reported the conformational investigation of β -peptoid oligomers bearing N-(*S*)-1-(1-naphthyl)ethyl side chains in the solid and solution-state and the results suggested that these oligomers adopt stable helical structures (Fig. 1.9c).⁶¹

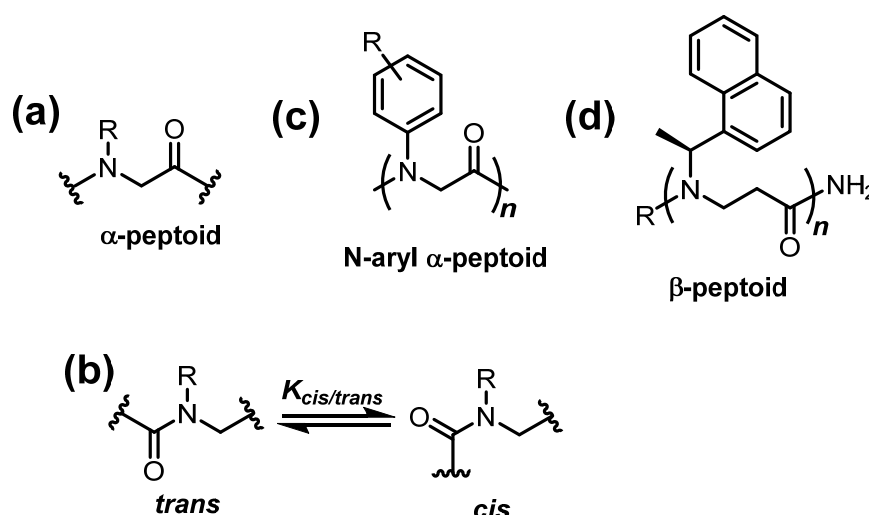


Fig. 1.9 General structure of peptoid (a), *cis-trans* isomerism in peptoids (b), N-aryl α -peptoid oligomers (c),⁶⁰ and helical β -peptoid oligomers (d).⁶¹

1.3 Reverse turn mimetics

Turns are regions in peptide chain where a chain reversal occurs.^{6b,62}

Depending up on the hydrogen bonding pattern, reverse turns can be classified into γ , β , α and π as depicted in Fig. 1.10.⁶³

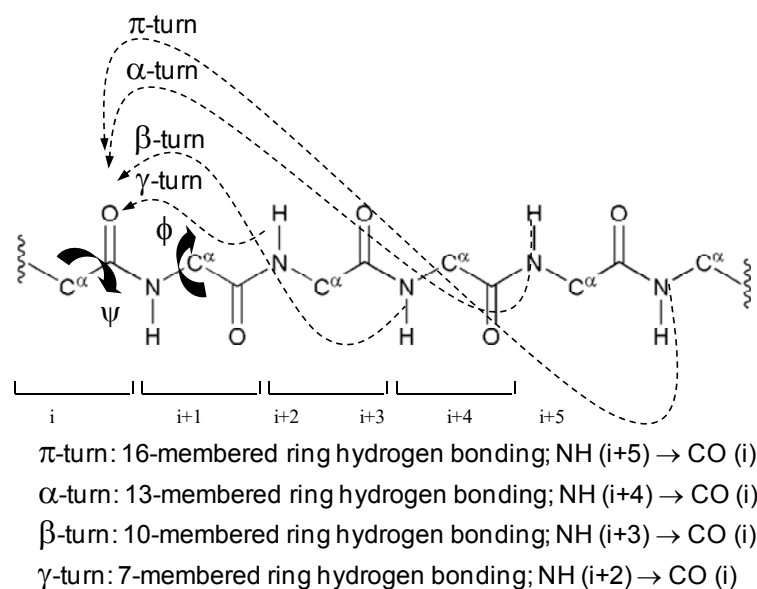


Fig. 1.10 Schematic representation of various types of turns.

1.3.1 γ -turns

γ -Turn is a 7-membered ring hydrogen bonding network formed between NH of third amino acid residue and CO of the first amino acid residue.⁶⁴ It is less prevalent in polypeptides compared to β -turns

1.3.2 β -turns

It is a 10-membered ring hydrogen bonding network formed between NH of fourth amino acid residue and CO of the first amino acid residue.⁶⁵ β -turn is the most common turn scaffold found in proteins and polypeptides. The reverse turns can be further classified into type-I, type-II, type I' and type II' *etc*, on the basis of torsional angle parameters adopted by the amino acids involved in the turn as shown in Table 1.1.¹¹⁰

Table 1.1 β -turn subtypes and torsional angle parameters.¹¹⁰

Types of β -turn	ϕ_{i+1}	ψ_{i+1}	ϕ_{i+2}	ψ_{i+2}
I	-60	-30	-90	0
I'	60	30	90	0
II	-60	120	80	0
II'	60	-120	-80	0
IV	-61	10	-53	17

1.3.3 α -turns

It is a 13-membered hydrogen bonding network formed between NH of fifth amino acid residue and CO of the first amino acid residue.⁶⁶ α -turns play a crucial role in the molecular recognition events, since they are present at protein surfaces.⁶⁷

1.3.4 π -turns

It is a 16-membered hydrogen bonding network formed between NH of sixth amino acid residue and CO of the first amino acid residue.

1.3.5 β -turn mimetics and their applications

β -turns are the most common secondary structural motif found in proteins and polypeptides and have been viewed as potential target for the rational design of therapeutics, since most often they are present at protein surfaces. They play a crucial role in the nucleation of protein folding process and thus help a protein to attain globular shape, which is a prerequisite to accomplish essential biological functions.⁶⁸ Most often, β -turns are stabilized by hydrogen bonding between CO of amino acid residue ' i ' and NH of amino acid residue ' $i+3$ ' in the backward direction ($4\leftarrow 1$). Studies in reverse turns have gained considerable attention since it provides insights into understanding protein topology, protein-protein interactions which facilitate protein design in order to carry out potential biological functions.⁶⁹ Incorporation of synthetic turn motifs (peptidomimetics) in

polypeptide chains provides an opportunity for the generation of an array of well-defined secondary structures^{35,45,70-73} with novel hydrogen bonding networks.^{16,17,73} In recent years, considerable efforts have been made in mimicking reverse turn scaffolds owing to their significant role in the biological processes such as protein-protein interactions and bio-catalysis.

In order to understand the structure and activity relationship and interaction of small molecules with targets such as receptors or enzymes, several synthetically modified peptide scaffolds-incorporated small molecules have been developed.^{71f} In this connection, a myriad of peptidic and nonpeptidic-based reverse turn scaffolds with intriguing structural features and potential biomedical applications have been reported. Freidinger reported nonpeptidic lactam-based scaffold which adopts *trans*-conformation (Fig. 1.11a).⁷⁴ Subsequently, Feigel developed a reverse turn mimic based on the 2,8-dimethyl-4-(carboxymethyl)-6-(aminomethyl)phenoxathiin S-dioxide moiety, which can be further used for the preparation of hairpin models (Fig. 1.11b).⁷⁵ Kelly group has shown that the dibenzofuran-based amino acid can be utilized for the nucleation of sheet structures (Fig. 1.11c).⁷⁶ Robinson reported a spirocyclic γ -lactam-based turn mimic which found an application in the medicinal chemistry (Fig. 1.11d).⁷⁷ Kemp reported a diphenylacetylene-based sheet nucleating turn mimic (Fig. 1.11e).⁷⁸ Nowick group introduced a β -sheet template based on the triurea derivatives of diethylenetriamine (Fig. 1.11f).⁷⁹ Gellman group reported the tetrasubstituted alkene (Fig. 1.11g)⁸⁰ and a dinipeptotic acid scaffold (Fig. 1.11h)⁸¹ as a β -turn mimetics which can be further used in nucleating hairpin models. Hoornaert group described a conformationally restricted dipeptide analogue which shows β -turn characteristics (Fig. 1.11i).^{82a} Tomasini group constructed β -turn

mimetics utilizing pseudoproline such as *trans*-(4*R*,5*S*)-4-carboxy-5-methyloxazolidin-2-one (D-Oxd, Fig. 1.11j).^{82b,103c-e} Overhand group replaced the native β -turn scaffold in the cyclic peptide antibiotic gramicidin S by a new reverse turn such as furanoid sugar amino acid (Fig. 1.11k).⁸³ Lubell group reported an azabicycloalkane amino acid as a β -turn inducer (Fig. 1.11l).⁸⁴ Sacchetti, Silvani and coworkers reported a diazspiropicyclic lactam-based β -turn mimetics (Fig. 1.11m).⁸⁵ Amblard group reported (S)-aminobicyclo[2.2.2]octane-2-carboxylic acid ((S)-ABOC) - a trisubstituted cyclic β -amino acid acting as a potential β -turn inducer (Fig. 1.11n).⁸⁶ Brimble group reported a spiroketal-based amino acid as a β -turn mimic (Fig. 1.11o).^{72a}

In addition to these nonpeptidic reverse turn mimetics, some representative examples of peptide-based β -turn mimetics are explained below. Balaram group used proline-2-aminoisobutyric acid (Pro-Aib) dipeptide segment as a hairpin nucleator (Fig. 1.11p).⁸⁷ Gellman group has shown that an isosteric replacement of amide bond by ester can stabilize the β -turn structures (Fig. 1.11q).⁸⁸ Moreover, Gellman group introduced scaffold containing proline and an acyclic 1,2-dimamine linker to nucleate the parallel sheet structures (Fig. 1.11r).⁸⁹ Similarly, Lee group prepared reverse turn mimetics containing proline and 1,2-diaminocyclohexane linker stabilized by urea-based dual hydrogen bonding (Fig. 1.11s).⁹⁰ Our group developed novel β -turn inducers such as anthranilic acid-proline (Ant-Pro, Fig. 1.11t)^{16,91} and orthanilic acid-proline (^SAnt-Pro, Fig. 1.11u).⁹²

Replacement of native β -turn scaffolds in the bioactive peptides by synthetically modified reverse turn scaffolds resulted into novel peptides with improved therapeutic profile. Seebach group developed somatostatin binding

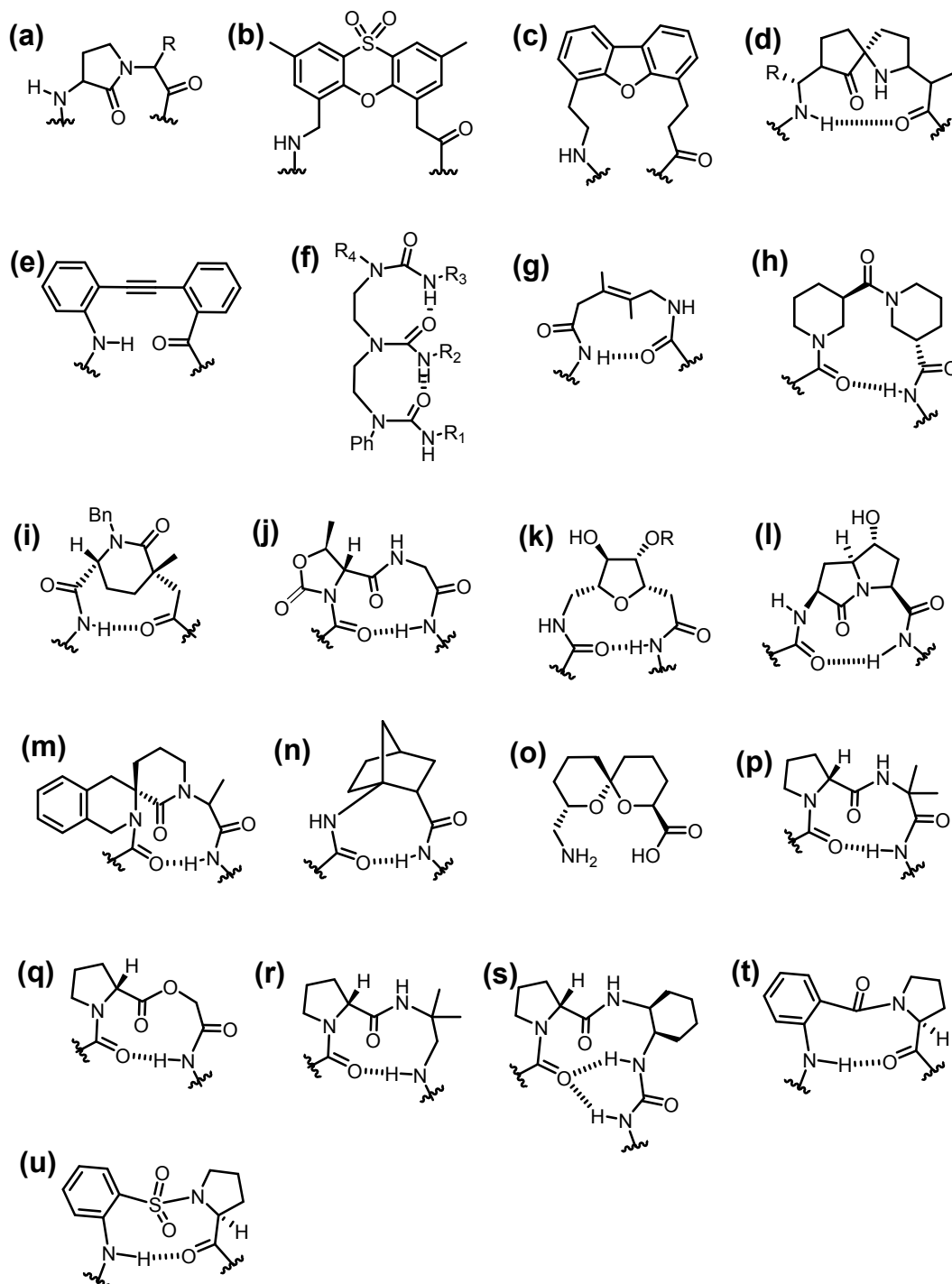


Fig. 1.11 Representative examples of β -turn mimetics: nonpeptidic (a-n) and peptidic reverse turn scaffolds (o-t).

receptor by replacing linear tetrapeptide sequence by a cyclic constrained β -tetrapeptide.⁹³ Muniz and coworkers replaced α -MeTrp residue with a conformationally constrained dipeptoid scaffold containing hexahydroindolizino[8,7-b]indole (Fig. 1.12a) and found enhanced binding

efficiency and selectivity for CCK-A receptors.⁹⁴ Angiotensin II (Ang II) analogues comprising a benzodiazepine-based β -turn mimetic have been shown to possess increased AT₂ receptor binding affinity than Ang II (Fig. 1.12b).⁹⁵ Overhand group used a sugar-based β -turn mimetic to design an antibiotic gramicidin S (GS) analogue (Fig. 1.11k, *vide supra*).⁸³ Mailard and coworkers designed GS analogues by incorporating β -turn mimetics such as thiazole-based γ -amino acids (Fig. 1.12c).⁹⁶

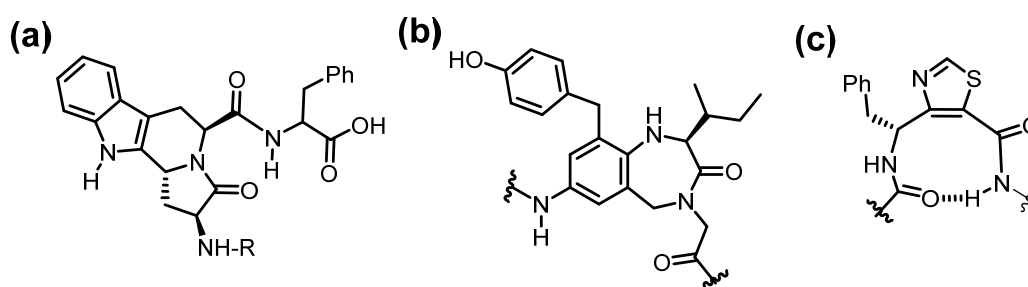


Fig. 1.12 Selective examples of synthetically modified reverse turn scaffolds incorporated into bioactive peptides with a view to improve their therapeutic profile: conformationally rigid dipeptide segment for CCK-A receptor (a), β -turn mimic incorporated into Ang-II (b) and Thiazole-based β -turn mimic incorporated into gramicidin S (c).

It has been well established that reverse turns mediate catalytic processes because of their exterior position in the protein. The research area on development of peptide-based catalysts has attained considerable attention due to their prominent features such as binding capability, conformational rigidity, broad substrate scope and high chemoselectivity.⁹⁷ In this regard, Miller and coworkers developed histidine-containing peptides for functional group transformation reactions.^{97a,b} DeGrado and coworkers have designed peptides which exhibit efficient esterase activity in the presence of zinc ions.^{97c} Wennemer's group introduced Pro-Pro dipeptide-containing oligomers which efficiently carry out asymmetric 1,4-addition reaction of aldehydes to nitroalkenes.^{97d}

1.4 Objective and design strategy: Robustness of Ant-Pro reverse turn

It has been demonstrated that conformationally ordered α,β -hybrid oligomers comprising anthranilic acid (Ant) and L-proline (Pro) building blocks in alternative fashion adopt a compact, right-handed helical architecture featuring an unusual periodic *pseudo* β -turn network of 9-membered hydrogen-bonded rings (C9) formed in the forward direction (1 \rightarrow 2) which is in stark contrast to the native 10-membered hydrogen-bonded β -turns (Fig. 1.13). The helical conformation was investigated by extensive X-ray crystallography and solution-state NMR studies. In the present work, the structural features/stability of Ant-Pro a *pseudo* β -turn has been carried out by structural modifications at the N-terminus reverse turn motif. Our aim was to investigate the effect of structural modulation around the turn segment on the robustness of reverse turn scaffold. In this regard, we introduced various amino acids having different side chains and chirality at the N-terminus of Ant-Pro scaffold. The structural elucidation of short oligomers was carried out by single crystal X-ray diffraction (solid-state) and NMR solution-state studies. The results revealed that Ant-Pro scaffold adopt folded conformation stabilized by

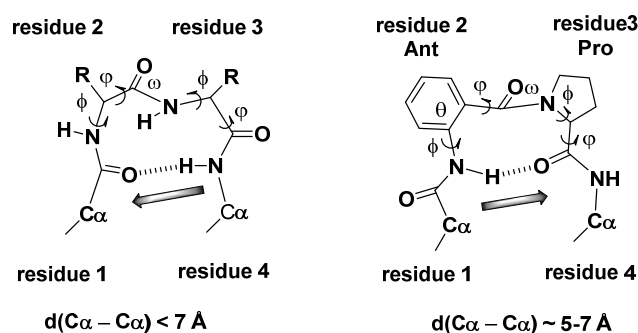


Fig. 1.13 Comparison of a β -turn - C10 structure involving four residues (left) with the Ant-Pro turn - C9 structure involving two-residue (right). The contrasting hydrogen-bonding orientations in the ideal β -turn and Ant-Pro turn are highlighted with shaded arrows. *Note:* $\text{C}\alpha_{i-1}$ - $\text{C}\alpha_{i+2}$ distance range shown for the Ant-Pro reverse turn (right) is calculated from crystal structures studied in the present study.

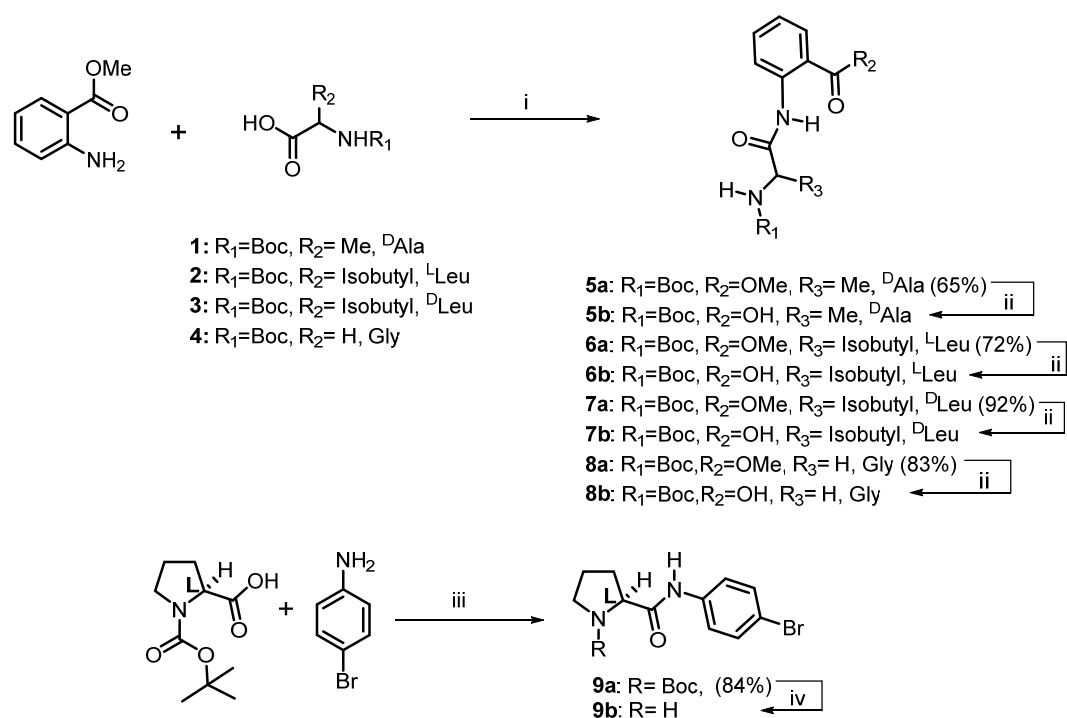
robust 9-membered ring hydrogen bonding despite the diverse structural modulation at the N-terminus of turn scaffold. Hamilton group reported that homo-oligomers of Ant exhibit well-defined secondary structure stabilized by 6-membered hydrogen bonding present in the Ant unit.⁹⁸ However, when Pro - a conformationally constrained amino acid was incorporated into homo-oligomer of Ant in alternative fashion, the hetero-oligomer formed 9-membered hydrogen bonding with an *antiperiplanar* arrangement of Ant and Pro rings. In the present study, all the short oligomers show an *antiperiplanar* orientation of Ant and Pro rings even after diverse structural modification carried out around turn scaffold. Moreover, hydrogen bonding direction was found to be in a reverse direction which is in stark contrast to the hydrogen bonding observed in the native reverse turns. The reversal of hydrogen bonding may impart proteolytic stability.⁹⁹

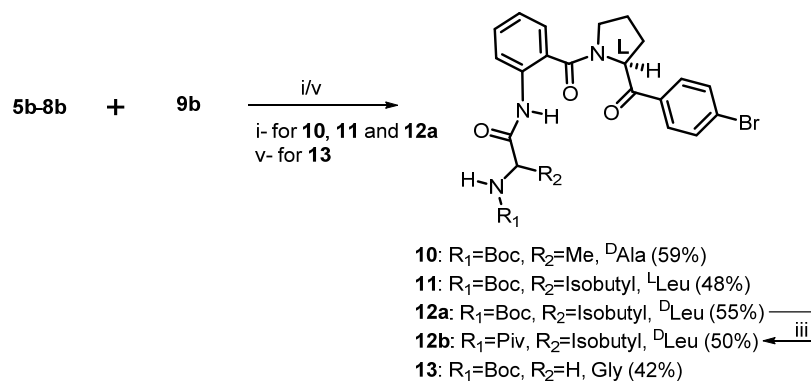
1.5 Synthesis of N-terminal modified Ant-Pro-based short oligomers

The short oligomers featuring Xaa-Ant-^LPro-NH-Ph(4-Br) (where, Xaa stand for various N-terminal protected amino acids) required for the present study were synthesized by direct coupling of Xaa-Ant-OH with H-^LPro-NH-Ph(4-Br) unit using coupling reagents, as shown in Scheme 1.1. C-terminus of all the short oligomers were functionalized with 4(Br)-anilide in order to induce crystallization in peptides, since compounds with heavy atoms such as bromine easily crystallize and also help in X-ray diffraction studies.^{64c,100} The synthesis of short oligomers was started by coupling of methylanilide with different Boc protected amino acids such as chiral ^DAla, ^{D/L}Leu, and achiral Gly in the presence of HBTU as a coupling reagent, HOBt (cat. amount), and DIEA as a base to obtain dipeptide segments. The dipeptide esters were subjected to hydrolysis under basic condition using aqueous LiOH to furnish respective carboxylic acids. The short oligomers

10, **11** and **12a** containing D Ala, L Leu and D Leu respectively, were obtained by coupling of corresponding dipeptide carboxylic acids with H- L Pro-NH-Ph(4-Br) in the presence of HBTU as a coupling reagent, HOBT (cat. amount), and DIEA as a base, while oligomer **13** containing Gly was obtained by coupling of corresponding dipeptide carboxylic acid with H- L Pro-NH-Ph(4-Br) in the presence of DCC as a coupling reagent and DMAP as an additive. The short oligomer **12a** exhibited rotamer formation (slow rotation of bond between N-terminus nitrogen and Boc carbonyl group), which can be effectively arrested by replacing Boc group by Piv group.¹⁶ Thus, **12a** was converted to its Piv derivative **12b** by deprotecting **12a** using trifluoroacetic acid and followed by reacting amine counterpart with Piv-Cl in the presence of triethylamine.

Scheme 1.1 Synthesis of short oligomers.





Reagents and conditions: (i) HBTU, HOBt, DIEA, MeCN, rt, 12 h; (ii) aq. LiOH, MeOH, 4 h; (iii) EDC.HCl, HOBt, DMAP, rt, 12 h; (iv) (a) TFA, DCM, rt, 2 h, then (b) Piv-Cl, Et₃N, DCM, rt, 4 h; (v) DCC, DMAP, DCM, rt, 12 h.

1.6 Conformational analysis

1.6.1 Single crystal X-diffraction analysis

To get an insight into the solid-state conformation of short oligomers, we tried crystallization using different binary solvent mixtures, which resulted in the crystal formation of oligomers **10** and **13**. Investigation of the crystal structures of **10** and **13** revealed that the 9-membered-ring hydrogen bonding in Ant-Pro dipeptide segment remains unaffected even after diverse structural changes made around the turn scaffold. Moreover, crystal structures unambiguously revealed that the Ant and the Pro rings preserve an *antiperiplanar* orientation throughout, which suggested that an *antiperiplanar* arrangement play a crucial role in the formation of folded conformation and 9-membered ring hydrogen bonding, which is completely contradictory to homo-oligomers of anthranilic acid which displayed 6-membered hydrogen bonding due to *coplanar* arrangement. The steric clash between the Ant and the Pro forced the two rings in an *antiperiplanar* fashion which in turn favored the formation of unusual 9-membered ring hydrogen bonding between NH of Ant and carbonyl oxygen of Pro residue; instead of 6-membered hydrogen bonding within the Ant unit.¹⁶ The hydrogen

bonding distance and torsional parameters of crystal structures of **10** and **13** are shown in Table 1.2. Notably, distance between hydrogen bonding sites Ant-NH and carbonyl oxygen of succeeding Pro residue was found to be around 2.34 Å, suggesting strong intramolecular hydrogen bonding.

Table 1.2 Backbone torsional and hydrogen bonding parameters in oligomers **10** and **13**.

Compound No.	Torsion (deg.)						Hydrogen Bonding Parameters		
	Ant			Pro			Distances (Å)		
	ϕ	θ	ψ	ϕ	ψ	NH...O=C	$d(C\alpha_{i-1}-C\alpha_{i+3})$	O...H	N...O
10 (DL)	-172.23	2.93	-86.56	-54.39	159.98	161.20	5.472	2.109	2.956
13 (L)	179.39	6.63	-85.77	-65.01	162.76	-174.99	5.786	2.344	3.193

1.6.2 NMR studies

In order to investigate the conformation of oligomers in the solution-state, we carried out NMR studies of a representative compound **10** in CDCl₃. The unambiguous signal assignments were carried out *via* combination of 2D COSY, NOESY and TOCSY experiments. ¹H NMR spectrum of compound **12a** revealed rotamer formation which was caused due to slow rotation at the N-terminus and Boc carbonyl group. The rotamerism can be effectively arrested by capping N-terminal with Piv group which helps to restrict the free rotation of C-N bond.¹⁶ Previous reports from our group revealed that the Ant-Pro oligomers adopt right-handed helical structure, stabilized by repetitive 9-membered hydrogen bonding. The robustness of this *pseudo* β-turn investigated by DMSO-*d*₆ titration ($\Delta\delta$ NH < 0.1 ppm), CDCl₃ dilution ($\Delta\delta$ NH < 0.15 ppm) and variable temperature [$\Delta\delta/\Delta T(\text{NH}) = -0.1$ ppb/k] studies, suggested strong intramolecular 9-membered hydrogen bonding network between NH of the Ant and the carbonyl oxygen of succeeding Pro residue.¹⁶ Careful analysis of ¹H NMR spectra of short oligomers

synthesized in the present study revealed that chemical shift of NH of the Ant residue appeared in the range of 9-9.5 ppm, suggesting its involvement in the 9-membered hydrogen bonding. The existence of 9-membered hydrogen bonding indicates an *antiperiplanar* orientation of the Ant and the Pro rings. In contrast, amide NH groups of the homo-oligomers of Ant, which are involved in the 6-membered hydrogen bonding, have been shown to appear in the chemical shift range of 10-13 ppm. The *coplanar* arrangement of Ant residues resulted into 6-membered hydrogen bonding.⁹⁸ The evidence of an *antiperiplanar* orientation of the Ant and the Pro residues was provided by the presence diagnostic long-range nOes between the Ant-NH2 and δ -protons of succeeding Pro residue (Fig 1.14). Other characteristic nOes have been observed as well, indicating the folded structure of short oligomers such as: NH3 vs Pro- δ H and Boc-CH₃ vs C21H (4-bromoanilide ring protons).

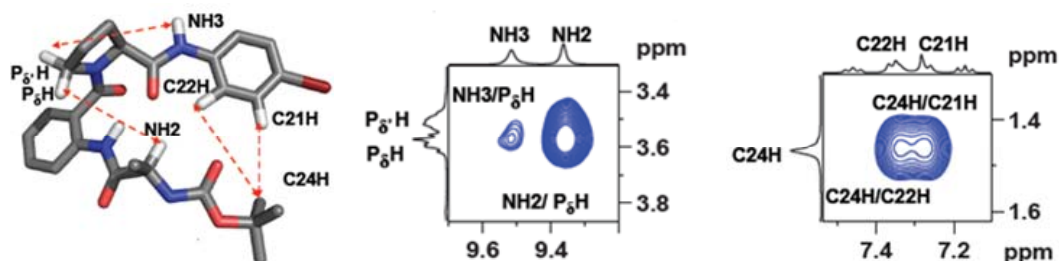


Fig. 1.14 2D nOe extracts of **10** (400 MHz, CDCl₃).

In order to investigate the strength of intramolecular hydrogen bonding, we carried out DMSO-*d*₆ titration study of **10** in CDCl₃. We observed that NH2 shows negligible chemical shift up on gradual addition of DMSO-*d*₆ ($\Delta\delta$ NH = 0.12 ppm) suggesting its involvement in strong intramolecular hydrogen bonding (Fig. 1.15).

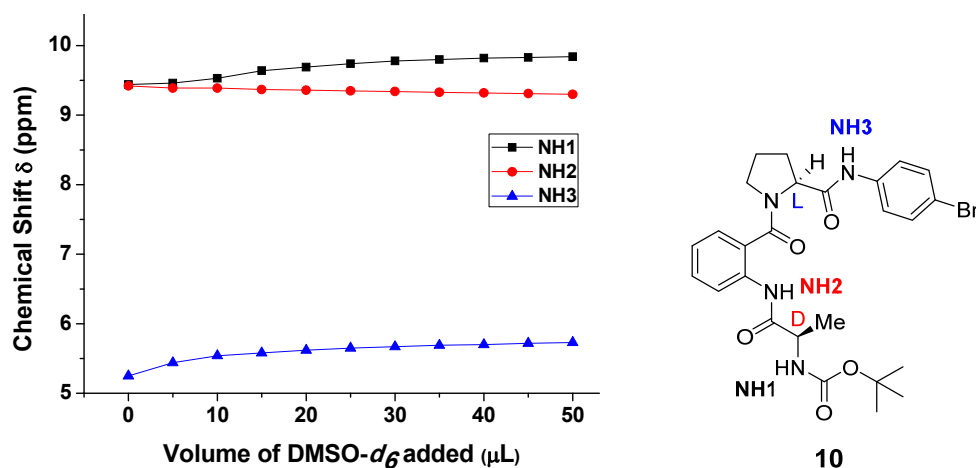


Fig. 1.15 DMSO-*d*₆ titration study of peptide **10**. The initial concentration of samples in CDCl₃ was 2 mM and 5 μL volume of DMSO-*d*₆ used at each addition.

1.6.3 Circular dichroism studies

Furthermore, secondary structural features of these Ant-Pro-based short oligomers have also been investigated by circular dichroism (CD) studies. CD spectra of all the oligomers were recorded in 2,2,2-trifluoroethanol at room temperature (Fig. 1.16). The CD spectra were recorded at the concentration of 0.2 mM. The CD spectra of oligomers **10**, **11**, **12b** and **13** displayed maxima at around 195 nm, zero crossing at 200 nm and minima at 209 nm. Additionally, in all the oligomers second minima around 240 nm was also observed due to the aromatic groups/aromatic electronic transitions in the peptide backbone.¹⁰¹

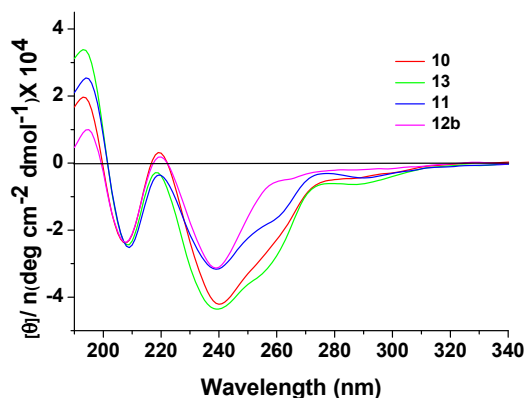


Fig. 1.16 CD spectra of the Ant-Pro-based short oligomers **10**, **11**, **12b** and **13** recorded in trifluoroethanol at 0.2 mM concentration.

1.7 Conclusion

The conformational investigation of short oligomers comprising Ant-Pro scaffold revealed that these oligomers adopt folded conformation featuring *pseudo* β -turn structure. Notably, reverse turn scaffold involves just two residues forming 9-membered *pseudo* β -turn in the forward direction (1 \rightarrow 2), which is in contrast to the native β -turns, wherein 10-membered hydrogen bonding involves four residues and hydrogen bonding is in backward direction (1 \leftarrow 4) as shown in Fig. 1.13. The structural modulations at the N-terminus of turn scaffold do not affect the robustness of intramolecular 9-membered hydrogen bonding. An *antiperiplanar* orientation of the Ant and the Pro residues plays an important role in enforcing the hydrogen bonding sites such as Ant-NH and carbonyl oxygen of succeeding Pro residue to close proximity in order to form a 9-membered hydrogen-bonded network.

The conformational analysis of oligomers containing 3-aminothiophenecarboxylic acid (3-Atc); an aromatic β -amino acid**1.8 Introduction**

Approach of mimicking structures and functions of protein subunits such as helices and sheets has gained considerable attention in recent years. Intensive research using mimicking approach led to novel folded structures (foldamers) with potential biomedical applications.¹⁰² In this context, several strategies have been effectively implemented for the creation of helical architectures including introduction homologated and non-natural residues. Aliphatic β -, γ -, and δ -amino acid residues are shown to be versatile building blocks for the *de novo* design of secondary structures/peptidomimetics.^{5,6} The detailed account on peptidomimetics involving β -, γ -, and δ -amino acid residues have already been discussed in the introduction part of section A, chapter 1. In addition to utilization of homologated amino acids as building blocks, nonpeptidic moieties such as urea,⁴⁶⁻⁵⁰ aminoxy acids^{51,52} hydrazino acids,^{53,54} peptoids,⁵⁵⁻⁶¹ and pseudoproline (ψ Pro)¹⁰³ have also been utilized in developing diverse helical structures with novel hydrogen bonding and enhanced backbone rigidity. An attachment of helix inducing elements to the C or N-terminus of peptide backbone is one of the strategies to generate the helical structures.¹⁰⁴ The non-natural content in the peptide backbone enabled tuning of conformational features and proteolytic stability.^{7,22,43} Although most of the unnatural amino acids belong to the aliphatic family, the relatively small class of unnatural amino acids: the aromatic amino acids are gaining special attention owing to their predictable conformational features for the *de novo* design of folded structures (Fig. 1.17).^{42-45,105}

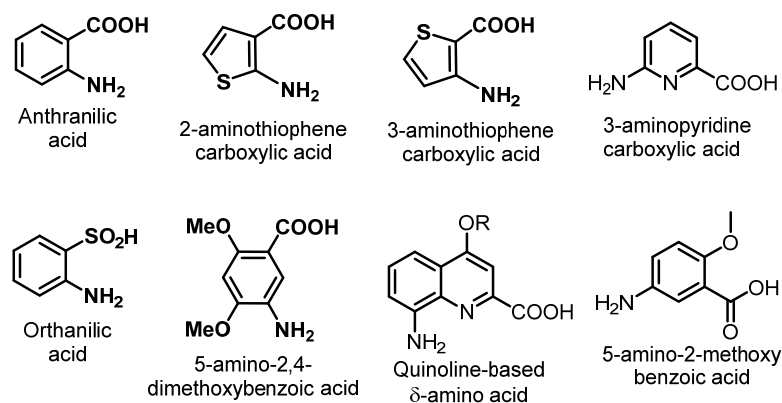


Fig. 1.17 Selected examples of unnatural aromatic amino acids used for development of various peptidomimetic structures.

1.9 Objective of the work and design strategy

We have previously demonstrated that steric clash between anthranilic acid (Ant) and proline (Pro) in their helical α,β Pro-Ant hybrid peptide plays an important role in the formation of an *antiperiplanar* orientation of two rings which in turn brings two hydrogen bonding sites to close proximity to form robust nine-membered hydrogen-bonded network.¹⁶ Although inter-residual hydrogen bonding has been commonly utilized to stabilize the helical architectures, the backbone rigidity and dihedral constraints of individual amino acids have also been shown to play a crucial role in stabilizing the helical structures devoid of inter-residual hydrogen bonding.¹⁰⁶ This was demonstrated by an example, wherein Ant of (Pro-Ant)_n helical oligomer was replaced with Atc (2 or 3-aminothiophenecarboxylic acids) which do not impart significant steric clash to proline in α,β hybrid peptide (Pro-Atc)_n; although the oligomer adopted helical folding lacking inter-residual hydrogen bonding.^{106c} Pro-Gly scaffold is well-known to form β -turn structure (C10 hydrogen bonding),¹⁰⁷ while 3-Atc unit in helical Pro-Atc oligomer displays six-membered hydrogen bonding. In this context, in order to further explore the conformational preferences of 3-Atc, we

have designed the α,β,α -hybrid peptide sequence: Gly-3-Atc-Pro-Gly-3-Atc-Pro-Gly, featuring 3-Atc and Pro-Gly motifs. In the present study, our aim was to investigate the consequences of incorporating conformationally rigid aromatic β -amino acid 3-Atc into peptide sequences comprising turn-forming Pro-Gly motif and its effect on secondary structure of peptide (Fig. 1.18).

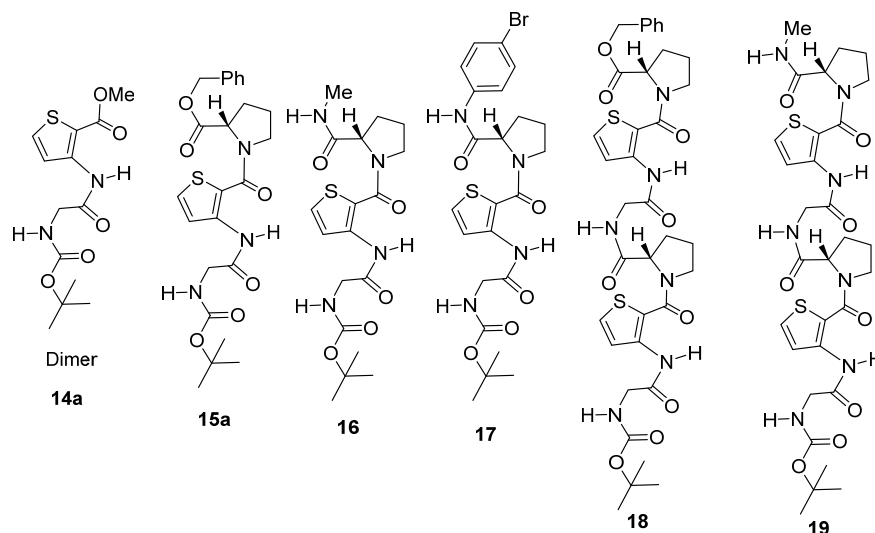


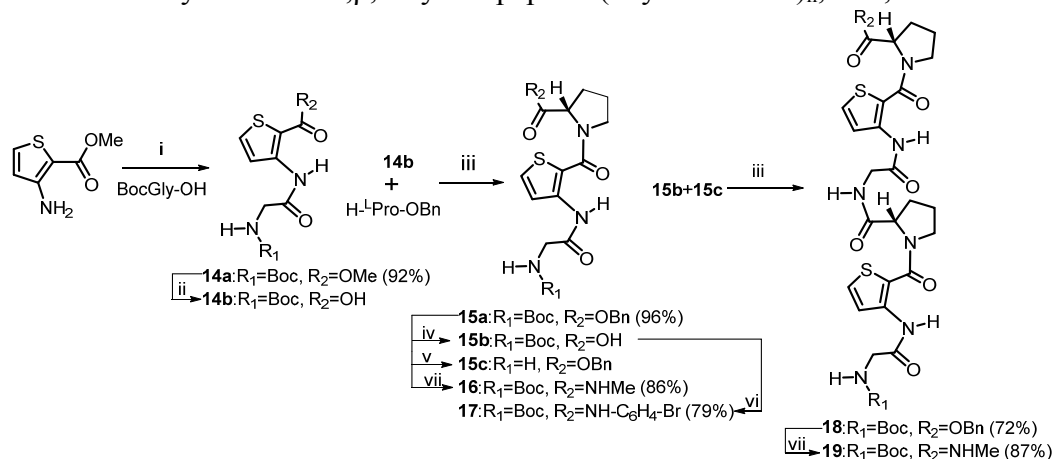
Fig. 1.18 Designed α,β,α heterofoldamer featuring conformationally restricted β -amino acid 3-Atc (3-aminothiophenecarboxylic acid).

1.10 Synthesis

Oligomers required for the present study were prepared by iterative synthetic protocol employing conventional solution phase, as depicted in scheme 1.2. The building block required for synthesis of higher oligomer was obtained from coupling of 3-aminothiophenemethyl carboxylate (3-Atc) with Boc-Gly-OH using DCC as a coupling reagent and HOBT as an additive in catalytic amount, followed by ester hydrolysis of dipeptide **14a** using aq. LiOH to obtain dipeptide acid **14b**, which was further coupled with Pro-OBn in the presence of EDC.HCl as a coupling reagent and HOBT as an additive in catalytic amount to obtain tripeptide building block **15a**. The trimer acid **15b** and amine **15c** counterparts were generated by hydrogenolysis using Pd(OH)₂/C and TFA-mediated removal

of Boc group of **15a**, respectively, and further reacted in the presence of EDC.HCl and HOBt (cat.) to produce hexapeptide **18**. The benzyl ester **18** was further amidated using sat. solution of methanolic methylamide to furnish **19**.

Scheme 1.2 Synthesis of α,β,α -hybrid peptide (Gly-3-Atc-Pro)_n, n=1, 2.



Reagents and conditions: (i) DCC, HOBt, DCM, rt, 12 h; (ii) LiOH, MeOH, rt, 2 h; (iii) EDC.HCl, HOBt, DCM, rt, 12 h; (iv) H₂, Pd(OH)₂/C, MeOH, 70 psi, 24 h; (v) TFA, DCM, 2 h; (vi) H₂N-C₆H₄-Br, EDC.HCl, HOBt, DCM, rt, 12 h; (vii) methanolic MeNH₂, rt, 12 h.

1.11 Conformational analyses

1.11.1 X-ray diffraction study of **15a**

Extensive efforts for crystallization resulted in the formation of crystals of **15a**, suitable for X-ray diffraction (Fig. 1.19). Careful analysis of crystal structure of **15a** revealed that folding was induced at the tripeptide stage, which is apparently due to dihedral constraints of five-membered rigid aromatic β -amino acid 3-Atc imposed on peptide backbone and intra-residual six-membered hydrogen bonding within the 3-Atc unit. The hydrogen bonding distance [$d(\text{N-H}\cdots\text{O}=\text{C})$] was found to be 1.94 Å, which is very strong. The existence of two rings (3-Atc and Pro) nearly in *coplanar* fashion enforces the occurrence of strong six-membered hydrogen bonding within the 3-Atc unit. Moreover, onset of helix formation can be seen from the glimpse of crystal structure at the tripeptide stage itself.

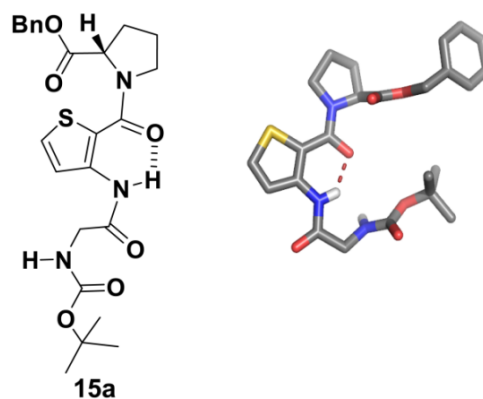


Fig. 1.19 Molecular structure of tripeptide **15a** displaying observed hydrogen bonding and its crystal structure.

1.11.2 NMR studies of **15a**

To gain insight into solution-state conformation of tripeptide **15a**, we undertook detailed 2D NMR studies in CDCl_3 solution. Signal assignments were carried out unambiguously using 2D NMR experiments (COSY, TOCSY, HSQC, HMBC and NOESY). The results obtained from the solution-state NMR studies are indeed in good agreement with the solid-state (crystal) studies of **15a**. The characteristic long range nOes observed such as: Boc- CH_3 /C19H, Boc- CH_3 /C9H, NH2/Boc- CH_3 and NH2/NH1 are indicative interactions for folded structure adopted by **15a** (Fig. 1.20).

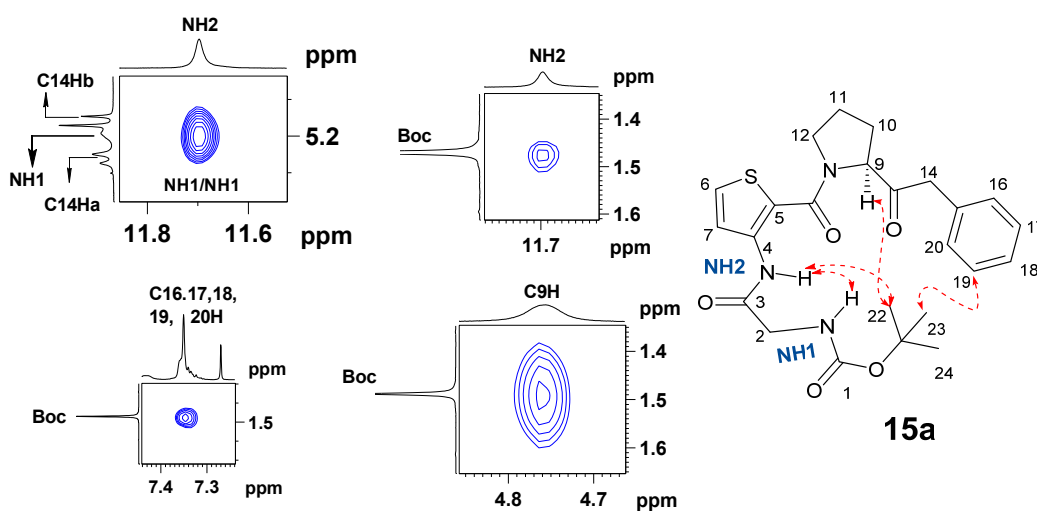


Fig. 1.20 2D NOESY excerpts of **15a** (25 mM, 500 MHz, CDCl_3 , 298 K).

The negligible chemical shift [$\Delta\delta(\text{NH}_2) = 0.11$ ppm] and low temperature coefficient [$(\Delta\delta/\Delta T)\text{NH}_2 = -2.9$ ppb/K] of NH₂ group in **15a**, observed during DMSO-*d*₆ titration (Fig. 1.21) and variable temperature studies, respectively, are suggestive of strong intramolecular hydrogen bonding.

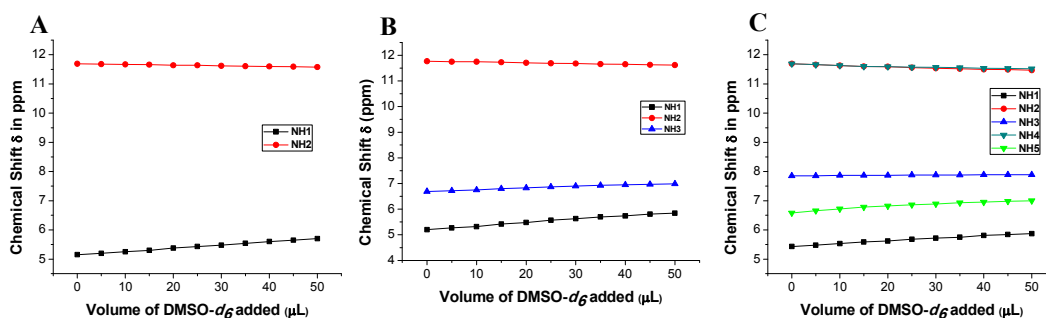


Fig. 1.21 DMSO-*d*₆ NMR titration studies of oligomers (5 mM, 400 MHz). DMSO-*d*₆ titration plots of **15a** (A), **16** (B) and **19** (C). *Note:* The amide NH groups are assigned from N-terminus of the peptides (molecular structures are given in Fig. 1.18, *vide supra*). During titration studies, DMSO-*d*₆ (5 μL) was used at each addition to the 5 mM solution of peptide in CDCl₃.

1.11.3 NMR studies of **16**

Additionally, solution-state conformation of **16** (a methylamide analogue of **15a**) in CDCl₃ solution was investigated. Diagnostic nOes were observed for **16**, such as: Boc-CH₃/C₁₄H, Boc-CH₃/C₉H and NH₂/NH₁ (Fig. 1.22), suggesting that its conformational features are akin to **15a**.

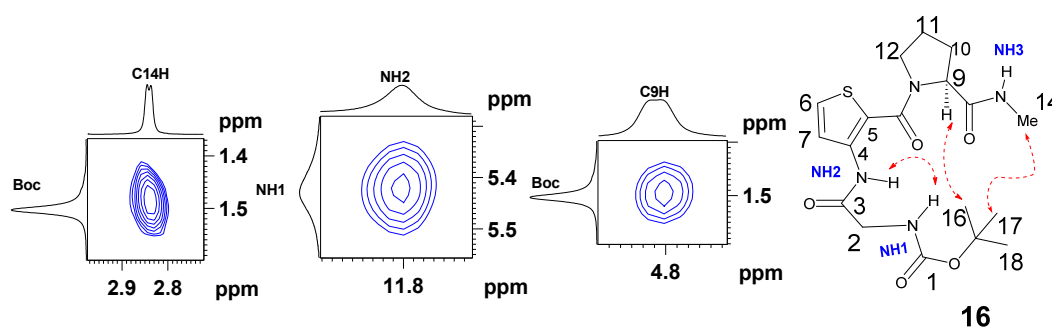


Fig. 1.22 2D NOESY excerpts of **16** (25 mM, 500 MHz, CDCl₃, 298 K).

The negligible chemical shift [$\Delta\delta(\text{NH}_2) = 0.15$ ppm] and low temperature coefficient [$(\Delta\delta/\Delta T)\text{NH}_2 = -3.4$ ppb/K] of NH₂ group in **16**, found during DMSO-

d_6 titration (Fig. 1.21, *vide supra*) and variable temperature studies, respectively, suggested the involvement of NH₂ group in strong intramolecular hydrogen bonding.

1.11.4 NMR studies of 19

The diagnostic nOes observed for hexapeptide **19** are: NH₂/NH₁, NH₄/NH₃, NH₄/C₁₄H and NH₂/C₂H (Fig. 1.23). The solvent shielding nature of NH₂ and NH₄ groups in hexapeptide **19** was confirmed with the DMSO- d_6 titration [$\Delta\delta(\text{NH}_2) = 0.22$ ppm and $\Delta\delta(\text{NH}_4) = 0.17$ ppm] (Fig. 1.21, *vide supra*) and variable temperature studies [$(\Delta\delta/\Delta T)_{\text{NH}_2} = -2.9$ ppb/K and $(\Delta\delta/\Delta T)_{\text{NH}_4} = -4.1$ ppb/K].

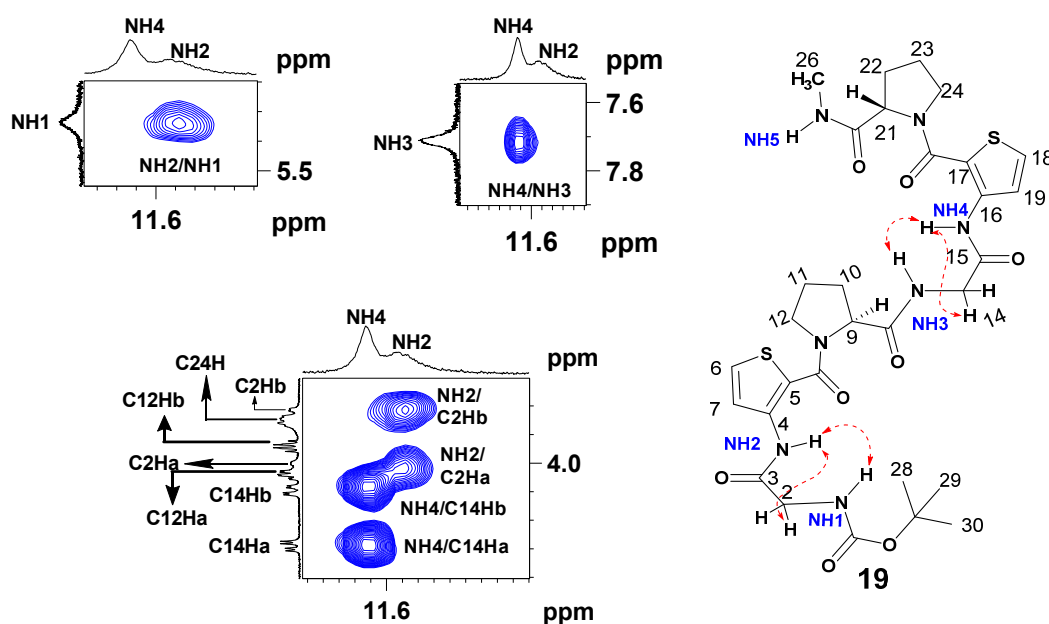


Fig. 1.23 2D NOESY excerpts of **19** (6 mM, 700 MHz, CDCl₃, 328 K). *Note:* In case of hexapeptide **19**, ¹H NMR at 298 K showed signal merging of amide NH and aromatic CH, thus NOESY experiment was carried out at 328 K where resolved set of signals were observed.

1.11.5 Structural elucidation of 19 by nOe-restrained MD simulation

The hexapeptide **19** was highly resistant toward the crystal formation, which prompted us to undertake its structural elucidation in solution-state by nOe-restrained molecular dynamics studies. The 20 energy minimized structures of

hexapeptide **19** were generated by MacroModel, version 10.7 program from Schrödinger¹⁰⁸ and superimposed (Fig. 1.24). The dynamic ensembled structures of **19** revealed that it adopts helical structure featuring six-membered hydrogen bonding in 3-Atc residue. This observation was supported by NMR studies such as DMSO-*d*₆ titration and variable temperature studies.

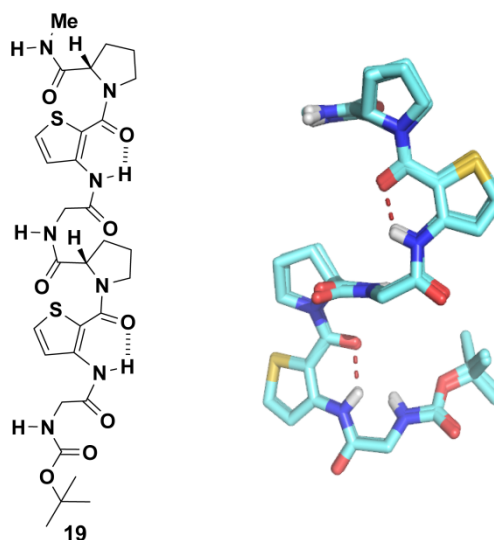


Fig. 1.24 Molecular structure of hexapeptide **19** displaying observed hydrogen bonding (left) and its 20 superimposed energy minimized structures generated by nOe-restrained MD simulation (right).

1.11.6 Circular dichroism studies of oligomers **15a**, **16** and **19**

In order to further assess the helical folding nature of peptides **15a**, **16** and **19**, the circular dichroism experiment was carried out in TFE (trifluoroethanol), since it is known as a good solvent to promote helical folding in peptides.¹⁰⁹ CD spectra of peptides **15a**, **16** and **19** exhibited minima around 202 nm and 236 nm, which suggested the characteristic CD signature of helical folding.¹¹⁰ Additionally, absorbance peak around 290 nm accounted for aromatic groups or aromatic electronic transitions present in the peptide backbone (Fig. 1.25). CD spectra of **16** and **19** revealed that they are nearly superimposable and there is

increase in the ellipticity moving from tripeptide **16** to hexapeptide **19** suggesting ordered secondary structure.

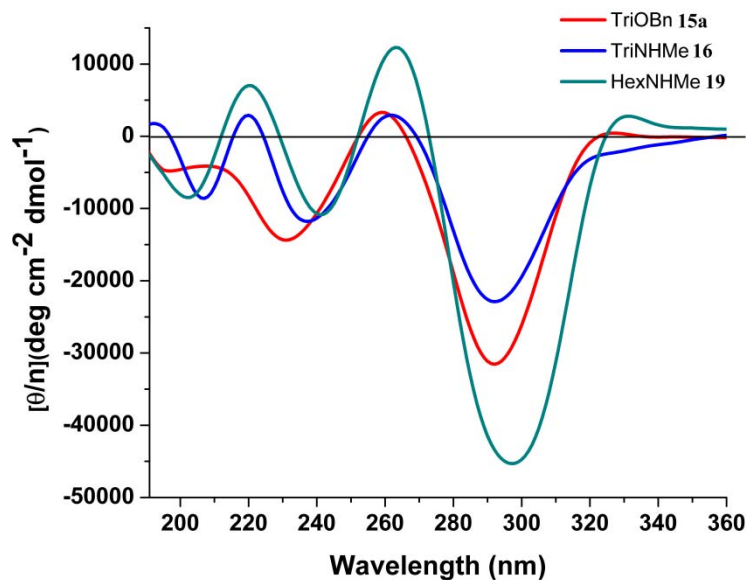


Fig. 1.25 CD spectra of oligomers; tripeptides **15a**, **16** and hexapeptide **19** at concentration of 0.1 mM. All CD spectra were recorded in trifluoroethanol at 298 K.

1.12 Conclusion

Synergistic effect of dihedral parameters of individual amino acids and intra-residual hydrogen bonding within 3-Atc resulted in the formation of helical folding in (Gly-3-Atc-Pro) oligomers, despite the absence of inter-residual hydrogen bonding, which is commonly observed in native polypeptides.¹⁰⁶ This work demonstrates the utility of aromatic amino acids such as aminothiophenecarboxylic acid (Atc) in promoting helical conformation in peptides – even without having inter-residual hydrogen bonding.

1.13 Experimental section (Part A)

Crystal Data for 10:

Single crystals of **10** were grown by slow evaporation of the solution in acetone and pet ether. Colorless needle type crystal of approximate size 0.21 x 0.09 x 0.07 mm³, was used for data collection, Hemisphere data acquisition. Total scans = 3, total frames = 1271, θ range = 1.53 to S22 25.00°, completeness to θ of 25.00° is 99.7 %, C₂₆H₃₁Br N₄O₅, $M = 559.46$. Crystals belong to Monoclinic, space group P2₁, $a = 12.3366(10)$, $b = 8.5383(7)$, $c = 13.9536(11)$ Å, $V = 1403.9(2)$ Å³, $Z = 2$, $D_c = 1.323$ g/cc, μ (Mo-K α) = 1.504 mm⁻¹, 7152 reflections measured, 4447 unique [$I > 2\sigma(I)$], R value 0.0505, wR₂ = 0.1135, largest diff. peak and hole 0.478 and -0.230 e. Å⁻³.

Crystal data for 13:

Single crystals of **13** were grown by slow evaporation of the solution in methanol. Colorless needle type crystal of approximate size 0.21 x 0.20 x 0.17 mm³, was used for data collection, Hemisphere data acquisition. Total scans = 3, total frames = 1271, θ range = 2.31 to 24.99°, completeness to θ of 24.99° is 99.8 %, C₂₅H₂₉BrN₄O₅, $M = 544.42$. Crystals belong to Orthorhombic, space group P2₁2₁2₁, $a = 10.7202(7)$, $b = 15.5510(9)$, $c = 15.4320(10)$ Å, $V = 2572.7(3)$ Å³, $Z = 4$, $D_c = 1.406$ g/cc, μ (Mo-K α) = 1.640 mm⁻¹, 13022 reflections measured, 4517 unique [$I > 2\sigma(I)$], R value 0.0410, wR₂ = 0.1001. Largest diff. peak and hole 0.549 and -0.313 e. Å⁻³.

General procedure for the synthesis of 5a-8a.

(R)-methyl2-(2-(tert-butoxycarbonylamino)propanamido) benzoate 5a:

To an ice cold solution of Boc-^DAla-OH (4.5 g, 23.8 mmol) and Ant-OMe (3 g, 19.8 mmol) in dry MeCN (30 mL), HBTU (9.03 g, 23.8 mmol), HOBt (cat.

amount) and DIEA (4.40 mL, 25.7 mmol) were added. The reaction mixture was allowed to stir at 0 °C for 10 min and at room temperature for 12 h. After removal of solvent under reduced pressure, the residue was dissolved in EtOAc (40 mL) and washed sequentially with sat. NaHCO₃ solution followed by sat. KHSO₄ solution and water. The organic layer was dried over anhydrous Na₂SO₄ and the crude product was subjected to column purification (20:80 EtOAc/pet ether, R_f 0.5) to afford **5a** as a white solid (4.15 g, 65%); mp: 118-120 °C; [α]_D²⁵: 79.91° (c 1, MeOH); IR (CHCl₃) ν (cm⁻¹): 3304, 1722, 1693, 1681, 1604, 1587, 1537, 1519, 1454, 1269, 1165; ¹H NMR (500 MHz, CDCl₃) δ : 11.53 (s, 1H), 8.70-8.68 (d, *J* = 8.53 Hz, 1H), 7.99-7.97 (m, 1H), 7.51-7.48 (t, *J* = 7.70 Hz, 1H), 7.06-7.03 (t, *J* = 7.50 Hz, 1H), 5.29 (bs, 1H), 4.37-4.34 (t, *J* = 6.60 Hz, 1H), 3.88 (s, 3H), 1.48-1.46 (m, 12H); ¹³C NMR (125 MHz, CDCl₃) δ : 171.8, 168.2, 155.1, 140.9, 134.4, 130.7, 122.5, 120.1, 115.1, 52.1, 51.5, 28.2, 18.6; ESI-MS: 323.8735 (M+H)⁺; 345.9242 (M+Na)⁺; 361.9238 (M+K)⁺; Elemental analysis calculated for C₁₆H₂₂N₂O₅: C, 59.61; H, 6.88; N, 8.69. Found: C, 59.70; H, 6.72; N, 8.54.

(S)-methyl2-(2-(tert-butoxycarbonylamino)-4-methyl-pentamido) benzoate 6a:

Compound **6a** was prepared by following the procedure for the synthesis of **5a**. The product **6a** was obtained as a white solid (72%); mp: 118-119 °C; [α]_D²⁵: -41.46° (c 1.01, MeOH); IR (CHCl₃) ν (cm⁻¹): 3310, 1756, 1698, 1651, 1604, 1587, 1537, 1519, 1405, 1272, 1123; ¹H NMR (200 MHz, CDCl₃) δ : 11.56 (s, 1H), 8.73-8.69 (d, *J* = 8.46 Hz, 1H), 8.01-7.98 (d, *J* = 7.70 Hz, 1H), 7.55-7.47 (t, *J* = 7.70 Hz, 1H), 7.10-7.02 (t, *J* = 7.60 Hz, 1H), 5.13-5.09 (m, 1H), 4.31-4.26 (m, 1H), 3.89 (s, 3H), 1.81-1.51 (m, 2H), 1.62-1.51 (m, 1H), 1.45 (s, 9H), 0.98-0.95 (m, 6H); ¹³C NMR (50 MHz, CDCl₃) δ : 171.8, 168.2, 155.3, 140.9, 134.4, 130.7,

122.5, 120.2, 115.2, 54.6, 52.1, 41.7, 28.2, 24.8, 22.8, 22.9, 21.6; ESI-MS: 365.6184 (M+H)⁺; 387.6166 (M+Na)⁺; 403.6037 (M+K)⁺; Elemental analysis calculated for C₁₉H₂₈N₂O₅: C, 62.62; H, 7.74; N, 7.69. Found: C, 62.51; H, 7.55; N, 7.80.

(R)-Methyl-2-(2-(tert-butoxycarbonylamino)-4-methyl pentanamido)benzoate 7a:

Compound **7a** was prepared by following the procedure for the synthesis of **5a**. The product **7a** was obtained as solid (92%); mp: 123-125 °C; [α]_D²⁵: 9.30° (c 1.04, MeOH); IR (CHCl₃) ν (cm⁻¹): 3342, 3020, 2956, 1714, 1666, 1519, 1504, 1276, 1166, 1091; ¹H NMR (400 MHz, CDCl₃) δ : 11.56 (s, 1H), 8.74-8.71 (d, *J* = 8.26 Hz, 1H), 8.03-8.01 (d, *J* = 8.25 Hz, 1H), 7.55-7.51 (t, *J* = 7.02, 1H), 7.10-7.06 (t, *J* = 7.25 Hz, 1H), 5.07-5.06 (m, 1H), 4.32 (m, 1H), 3.91 (m, 3H), 1.81-1.76 (m, 2H), 1.61-1.55 (m, 1H), 1.47 (s, 9H), 1.00-0.97 (m, 6H); ¹³C NMR (100 MHz, CDCl₃) δ : 171.9, 168.3, 155.4, 141.0, 134.5, 130.7, 122.6, 120.6, 115.2, 54.6, 52.6, 52.2, 41.7, 28.2, 24.8, 22.9, 21.7; ESI-MS: 365.3166 (M+H)⁺; 387.3058 (M+Na)⁺; 403.2866 (M+K)⁺; Elemental analysis calculated for C₁₉H₂₈N₂O₅: C, 62.62; H, 7.74; N, 7.69. Found: C, 62.78; H, 7.61; N, 7.52.

Methyl-2-(2-(tert-butoxycarbonylamino)acetamido)benzoate 8a:

Compound **8a** was prepared by following the procedure for the synthesis of **5a**. The product **8a** was obtained as white solid (83%); mp: 117-118 °C; IR (CHCl₃) ν (cm⁻¹): 3313, 2978, 1712, 1693, 1681, 1589, 1504, 1454, 1269, 1165, 756; ¹H NMR (200 MHz, CDCl₃) δ : 11.53 (s, 1H), 8.67-8.63 (d, *J* = 8.22 Hz, 1H), 7.97-7.92 (m, 1H), 7.51-7.43 (m, 1H), 7.07-6.99 (t, *J* = 7.58 Hz, 1H), 5.50-5.48 (m, 1H), 3.99-3.96 (d, *J* = 6.07 Hz, 2H), 3.86 (s, 3H), 1.47 (s, 9H); ¹³C NMR (50 MHz, CDCl₃) δ : 168.7, 168.2, 155.7, 140.6, 134.3, 130.6, 122.6, 120.0, 115.0,

52.1, 45.3, 28.1; ESI-MS: 309.4865 (M+H)⁺; 331.4735 (M+Na)⁺; 347.4612 (M+K)⁺; Elemental analysis calculated for C₁₅H₂₀N₂O₅: C, 58.43; H, 6.54; N, 9.09. Found: C, 58.29; H, 6.43; N, 9.24.

General method for methyl ester hydrolysis:

To a solution of ester (**5a**, **6a**, **7a** and **8a**) (10 mmol) in methanol, LiOH·H₂O (40 mmol) was added in water (12 mL) and the reaction mixture was stirred at room temperature for 4 h. After the complete consumption of the starting material, the solvent was evaporated under reduced pressure. The free carboxylic acid was liberated by treating with sat. KHSO₄ solution and extracted with DCM (2 X 25 mL). The corresponding crude carboxylic acids (**5b**, **6b**, **7b** and **8b**) obtained after evaporation of the solvent under reduced pressure were carried forward for the next reaction, without further purification.

Boc group cleavage of 9a:

A solution containing **9a** (4 g, 10.8 mmol) was subjected to deprotection using TFA:DCM (50%, 10 mL) at 0°C. After completion of the reaction (2 h), the solvent was removed under reduced pressure. The reaction mixture was neutralized with sat. NaHCO₃ solution and repeatedly extracted into DCM (3 x 10 mL). The organic layer was dried over anhydrous Na₂SO₄. The crude product **9b**, obtained after evaporating the solvent under reduced pressure, was used for the next step without further purification.

General procedure for the preparation of 10, 11 and 12a.

Tert-butyl ((2R)-1-((2-(2-((4-bromophenyl) carbamoyl) pyrrolidine-1-carbonyl) phenyl) amino)-1-oxopropan-2-yl) carbamate 10:

To an ice cold solution of **5b** (0.93 g, 3.08 mmol) and **9b** (0.89 g, 3.31 mmol) in dry MeCN (20 mL), HBTU (1.37 g, 3.62 mmol), HOBt (cat. amount) and DIEA (0.67 mL, 3.92 mmol) were added and the reaction mixture was stirred at 0 °C for

10 min and then at room temperature for 12 h. After removal of the solvent under reduced pressure, the reaction mixture was dissolved in EtOAc (30 mL) and washed sequentially with sat. NaHCO₃ solution, sat. KHSO₄ solution, water and brine. The organic layer was dried over anhydrous Na₂SO₄ and the crude product was subjected to column purification (30:70 acetone/pet ether, R_f 0.5) to furnish **10** as a white solid (0.997 g, 59%); mp: 208-210 °C; [α]²⁵_D: -126.95° (c 1, MeOH); IR (nujol) ν (cm⁻¹): 3425, 2955, 2854, 1714, 1681, 1593, 1454, 1377, 1155, 1045; ¹H NMR (500 MHz, CDCl₃) δ : 9.45 (s, 1H), 9.35 (s, 1H), 8.33-8.32 (d, J = 6.71 Hz, 1H), 7.46-7.43 (t, J = 7.63 Hz, 1H), 7.35-7.34 (m, 3H), 7.28-7.26 (m, 2H), 7.17-7.14 (t, J = 7.45 Hz, 1H), 5.57-5.55 (d, J = 6.11 Hz, 1H), 4.95 (bs, 1H), 4.49 (bs, 1H), 3.60-3.55 (m, 1H), 3.51-3.50 (m, 1H), 2.38-2.31 (m, 2H), 2.12-2.07 (m, 1H), 1.96-1.90 (m, 1H), 1.46-1.44 (m, 12H); ¹³C NMR (125 MHz, CDCl₃) δ : 172.1, 169.8, 169.6, 155.2, 136.9, 135.4, 131.6, 131.1, 126.8, 125.5, 123.7, 122.0, 121.2, 116.8, 51.2, 50.1, 29.6, 28.6, 28.3, 25.2, 18.8; ESI-MS: 581.3935 (M+Na)⁺; 597.3860 (M+K)⁺; Elemental analysis calculated for C₂₆H₃₁BrN₄O₅: C, 55.82; H, 5.59; N, 10.01. Found: C, 55.88; H, 5.47; N, 10.22.

Tert-butyl (1-((2-((S)-2-((4-bromophenyl) carbamoyl) pyrrolidine-1-carbonyl) phenyl) amino)-4-methyl-1-oxopentan-2-yl) carbamate 11:

Compound **11** was prepared by following the procedure for the synthesis of **10**. The product **11** was obtained as white solid (48%); mp: 118-120 °C; [α]²⁵_D: -66.88° (c 1.02, MeOH); IR (CHCl₃) ν (cm⁻¹): 3306, 3271, 2958, 1693, 1537, 1454, 1301, 1163, 1045, 756; ¹H NMR (200 MHz, CDCl₃) δ : 9.58 (s, 1H), 9.48 (s, 1H), 8.30-8.26 (d, J = 7.83 Hz, 1H), 7.47-7.31 (m, 4H), 7.23-7.12 (m, 3H), 5.31-5.27 (m, 1H), 4.93-4.90 (m, 1H), 4.52-4.29 (m, 1H), 3.59-3.98 (m, 2H), 2.42-2.27 (m, 2H), 2.10-1.83 (m, 2H), 1.76-1.70 (m, 3H), 1.38 (s, 9H), 1.06-1.00 (m,

6H); ^{13}C NMR (50 MHz, CDCl_3) δ : 172.8, 170.1, 168.8, 155.4, 137.0, 134.8, 131.3, 130.7, 126.5, 124.0, 122.3, 121.2, 116.4, 79.5, 61.1, 53.8, 41.5, 29.5, 28.2, 24.8, 23.1, 21.8; ESI-MS: 623.4253 ($\text{M}+\text{Na}$) $^+$; 639.3826 ($\text{M}+\text{K}$) $^+$; Elemental analysis calculated for $\text{C}_{29}\text{H}_{37}\text{BrN}_4\text{O}_5$: C, 57.90; H, 6.20; N, 9.31. Found: C, 57.78; H, 6.32; N, 9.45.

Tert-butyl ((R)-1-((2-((S)-2-((4-bromophenyl) carbamoyl) pyrrolidine-1-carbonyl) phenyl) amino)-4-methyl-1-oxopentan-2-yl) carbamate 12a:

Compound **12a** was prepared by following the procedure for the synthesis of **10**.

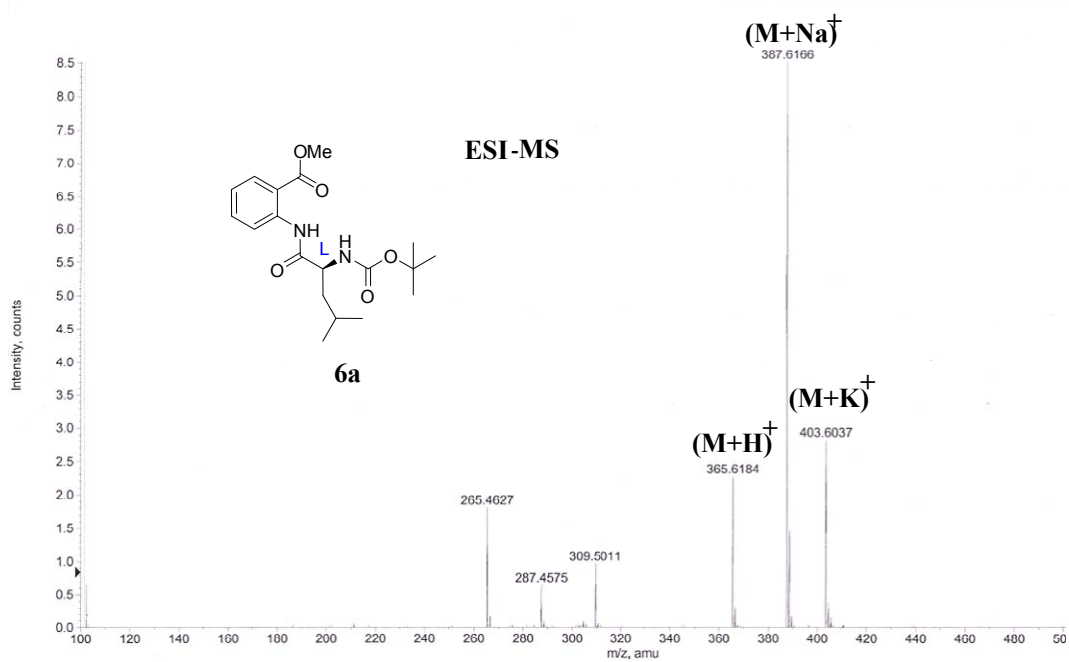
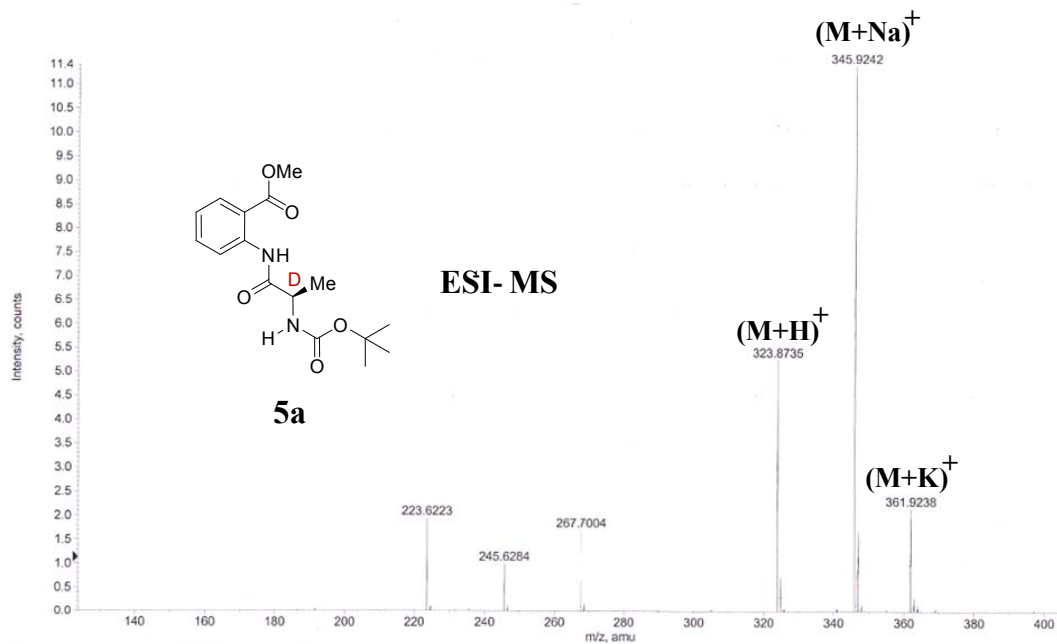
The product **12a** was obtained as a white solid (0.285 g, 55 %); mp: 115-116 °C; $[\alpha]_{\text{D}}^{25}$: -151.58° (c 1, MeOH) ; IR (CHCl_3) ν (cm^{-1}): 3311, 3020, 1675, 1622, 1541, 1427, 1398, 1303, 1216, 1045, 758; ^1H NMR (400 MHz, CDCl_3) δ : 9.83_{rotamer} (1H), 9.80_{rotamer} (0.17H), 9.57-9.51_{rotamer} (0.20H), 9.20_{rotamer} (0.1H), 8.58_{rotamer} (0.20H), 8.46-8.44_{rotamer} (d, $J = 8.10$ Hz, 1H), 8.31_{rotamer} (0.10H), 7.47-7.43_{rotamer} (t, $J = 8.10$ Hz, 1H), 7.34-7.32 (m, 1H), 7.27-7.25 (m, 1H), 7.18-7.14 (m, 4H), 5.99-5.97 (d, $J = 8.99$ Hz, 1H), 4.99-4.96 (m, 1H), 4.53-4.50_{rotamer} (1H), 4.23_{rotamer} (0.25H), 3.57-3.46 (m, 2H), 2.54-2.36 (m, 2H), 2.27-2.22 (m, 1H), 2.09-1.96 (m, 1H), 1.77-1.64 (m, 2H), 1.42_{rotamer} (9H), 1.38_{rotamer} (1H), 0.99-0.95 (m, 6H); ^{13}C NMR (100 MHz, CDCl_3) δ : 173.2, 172.6, 170.7, 170.4, 168.8, 168.4, 155.3, 136.9, 136.0, 131.3, 131.0, 130.8, 126.5, 125.5, 125.4, 123.7, 121.4, 120.9, 116.6, 116.4, 79.6, 61.2, 61.0, 54.7, 49.6, 49.4, 41.3, 40.3, 29.9, 29.6, 28.3, 28.2, 25.3, 24.9, 23.1, 21.5, 21.0; ESI-MS: 601.3143 ($\text{M}+\text{H}$) $^+$; 623.3112 ($\text{M}+\text{Na}$) $^+$; 639.2879 ($\text{M}+\text{K}$) $^+$; Elemental analysis calculated for $\text{C}_{29}\text{H}_{37}\text{BrN}_4\text{O}_5$: C, 57.90; H, 6.20; N, 9.31. Found: C, 57.98; H, 6.32; N, 9.40.

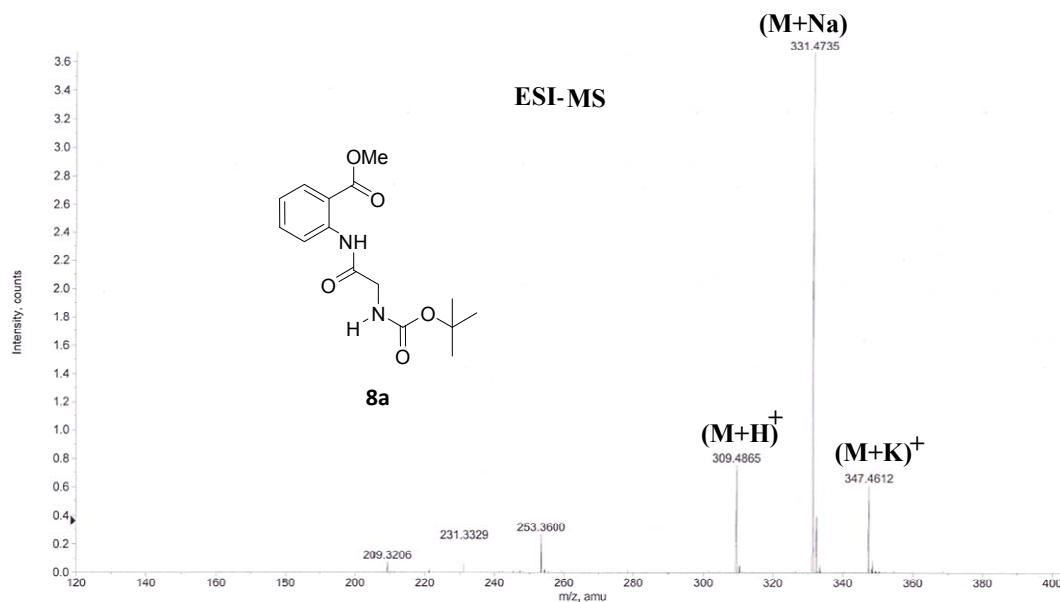
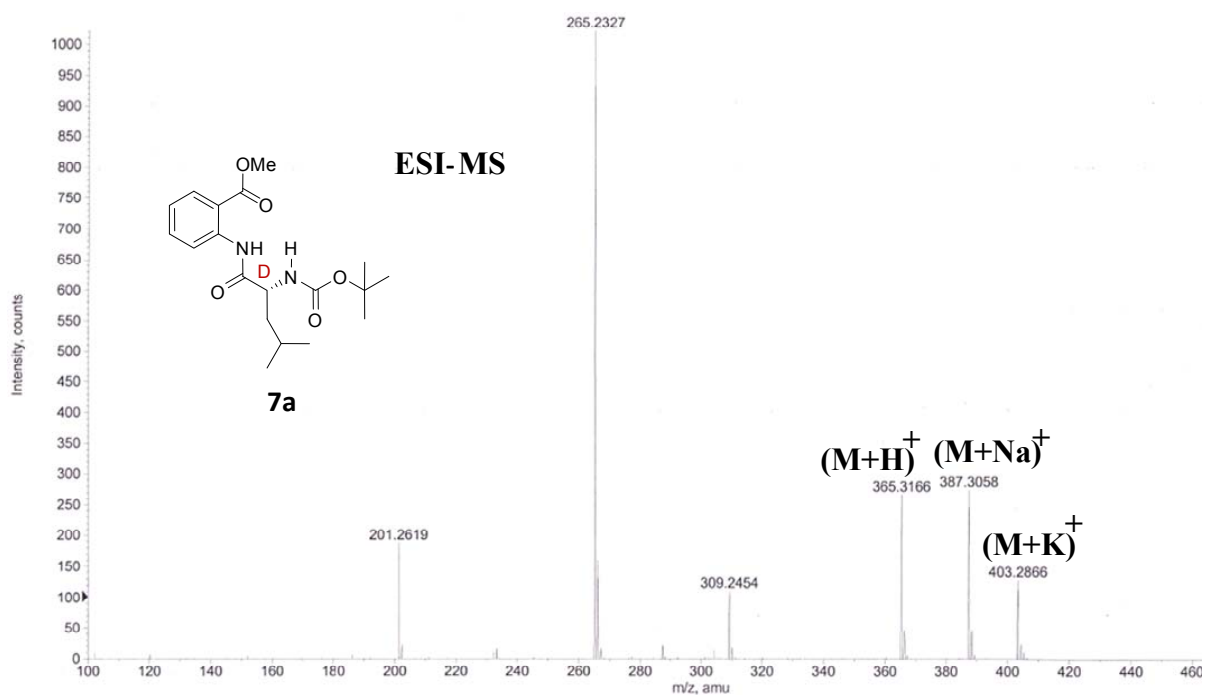
Tert-butyl ((R)-1-((2-((S)-2-((4-bromophenyl) carbamoyl) pyrrolidine-1-carbonyl) phenyl) amino)-4-methyl-1-oxopentan-2-yl) carbamate 12b:

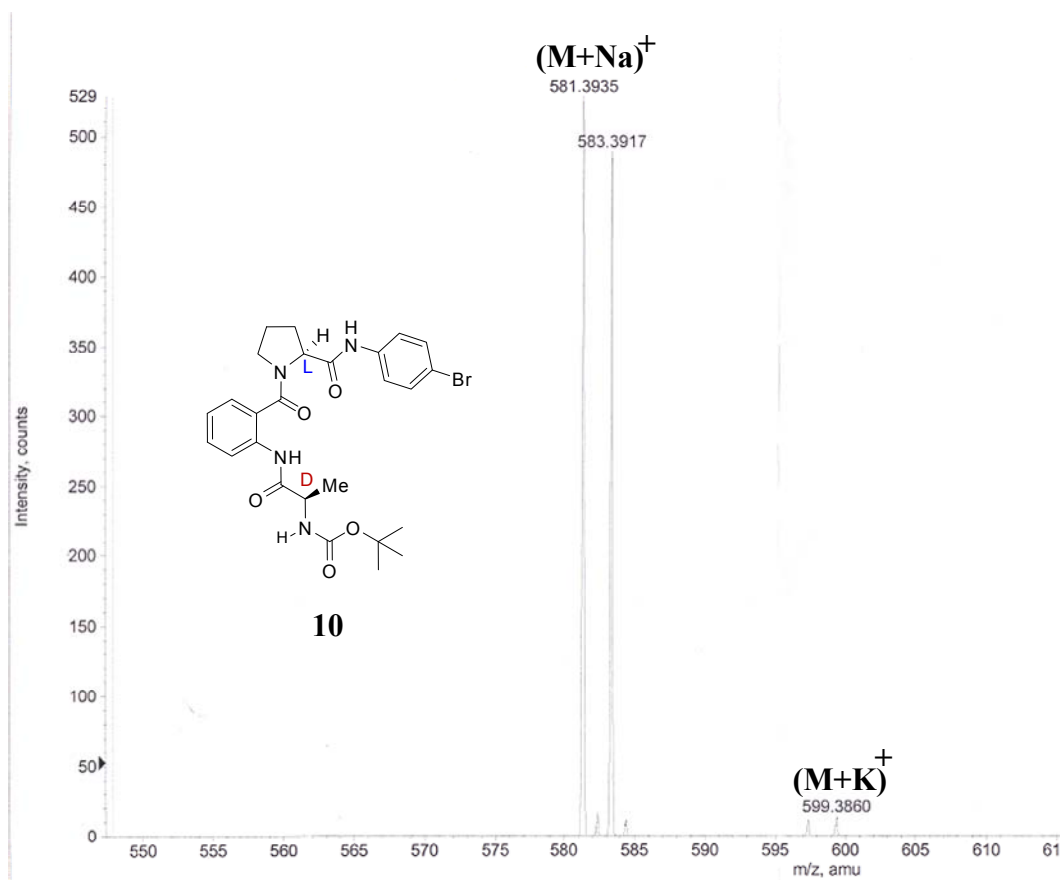
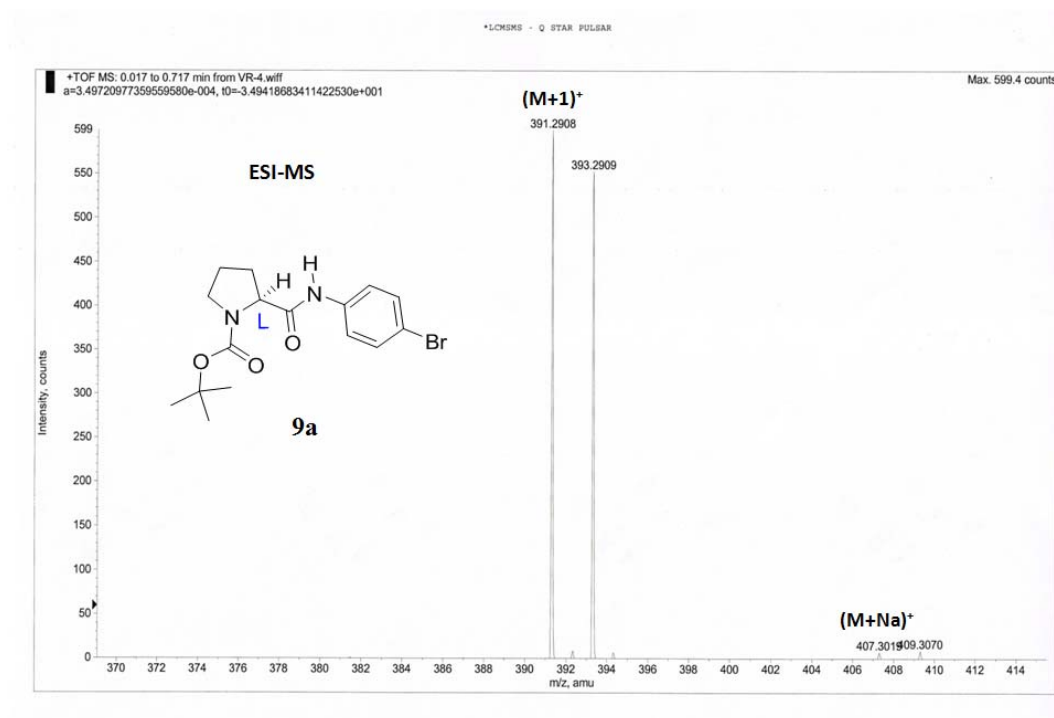
The Boc group of **12a** (0.1 g, 0.2 mmol) was removed using TFA:DCM (2 mL, 1:1). After completion of reaction, the volatiles were removed and the residue was neutralized with sat. NaHCO₃ and extracted with DCM repeatedly. The organic layer was dried over anhydrous Na₂SO₄, evaporated and the residue obtained was taken in dry DCM (10 mL). The reaction mixture was cooled to 0 °C, then pivaloyl chloride (0.07 mL, 0.6 mmol) and Et₃N (0.11 mL, 0.8 mmol) were added and the reaction mixture was stirred at room temperature for 4 h. The reaction mixture was diluted with DCM (10 mL) and washed sequentially with sat. NaHCO₃ solution, sat. KHSO₄ solution, water and brine. The organic layer was dried over anhydrous Na₂SO₄ and the crude product was subjected to column purification (30:70 acetone/pet ether, R_f 0.4) to furnish **12b** as a white solid (0.058 g, 50%); mp: 117-118 °C; [α]_D²⁵: -152.15° (c 1.01, MeOH); IR (CHCl₃) ν (cm⁻¹): 3310, 3020, 2400, 1676, 1591, 1523, 1421, 1046, 928, 755; ¹H NMR (400 MHz, CDCl₃) δ : 9.75 (s, 1H), 9.54 (s, 1H), 9.28-9.26 (d, *J* = 8.48 Hz, 1H), 7.44-7.41 (m, 3H), 7.36-7.34 (m, 1H), 7.28-7.25 (m, 2H), 7.18-7.14 (t, *J* = 7.51 Hz, 1H), 6.51-6.49 (d, *J* = 8.06 Hz, 1H), 4.96-4.93 (m, 1H), 4.84-4.79 (m, 1H), 3.56-3.44 (m, 2H), 2.55 (bs, 1H), 2.34-2.23 (m, 2H), 2.05-1.99 (m, 1H), 1.91-1.84 (m, 1H), 1.71-1.67 (m, 2H), 1.22 (s, 9H), 0.94-0.93 (m, 6H); ¹³C NMR (100 MHz, CDCl₃) δ : 178.5, 171.8, 169.9, 169.2, 137.0, 135.1, 131.6, 130.7, 126.6, 125.9, 123.8, 122.1, 121.2, 116.6, 60.7, 52.7, 50.1, 41.5, 38.7, 28.9, 27.4, 24.9, 23.0, 22.0; ESI-MS: 585.2769 (M+H)⁺; 609.2656 (M+Na)⁺; 625.2522 (M+K)⁺; Elemental analysis calculated for C₂₉H₃₇BrN₄O₄: C, 59.49; H, 6.37; N, 9.57. Found: C, 59.62; H, 6.20; N, 9.64.

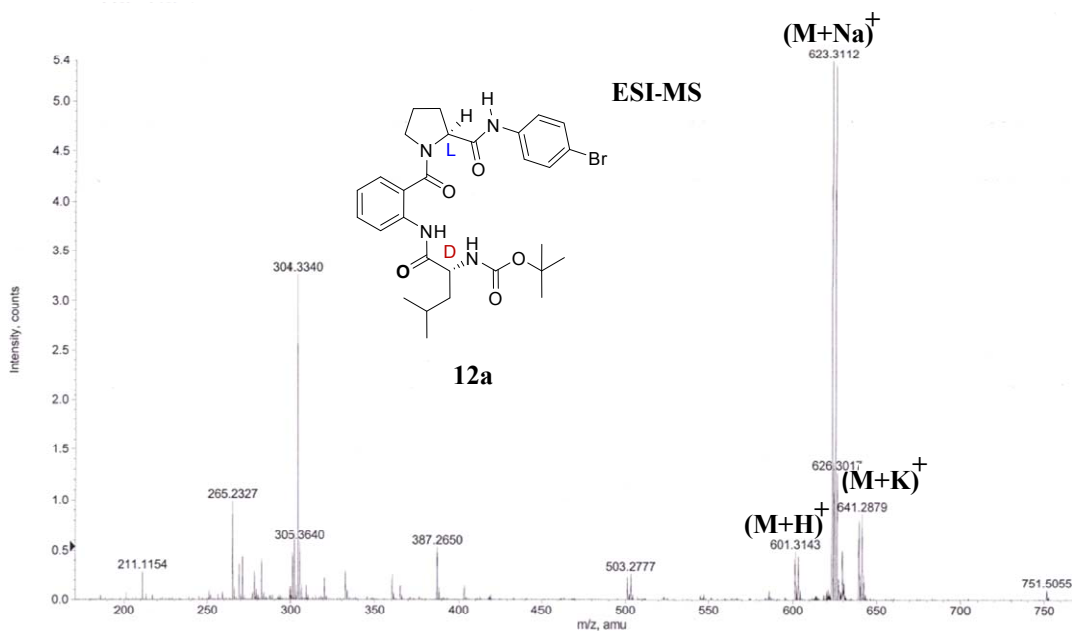
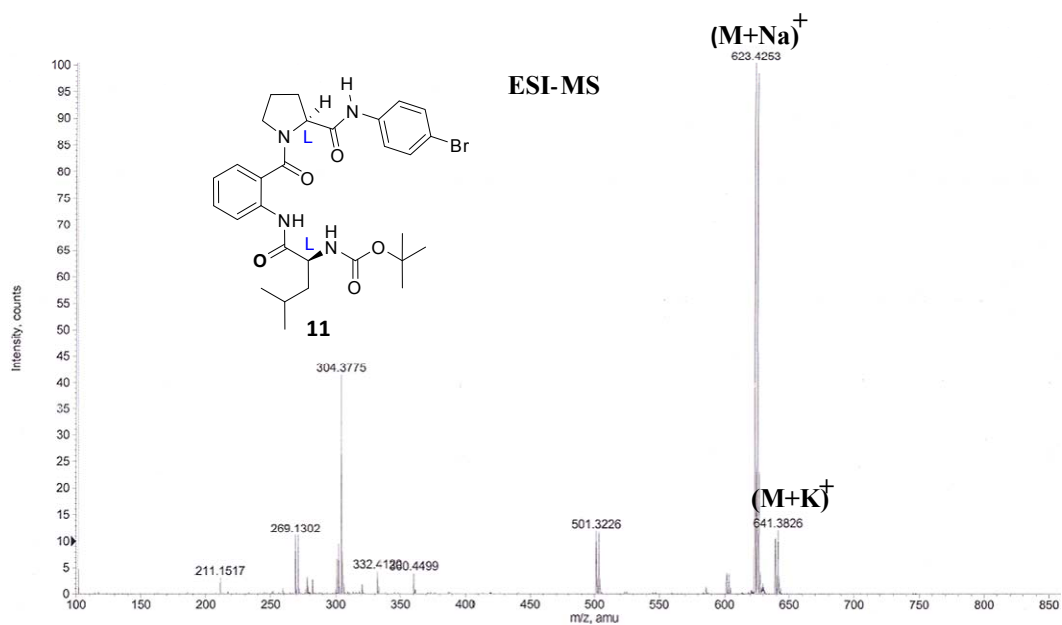
Tert-butyl (S)-(2-((2-(2-((4-bromophenyl) carbamoyl) pyrrolidine-1-carbonyl) phenyl) amino)-2-oxoethyl) carbamate 13:

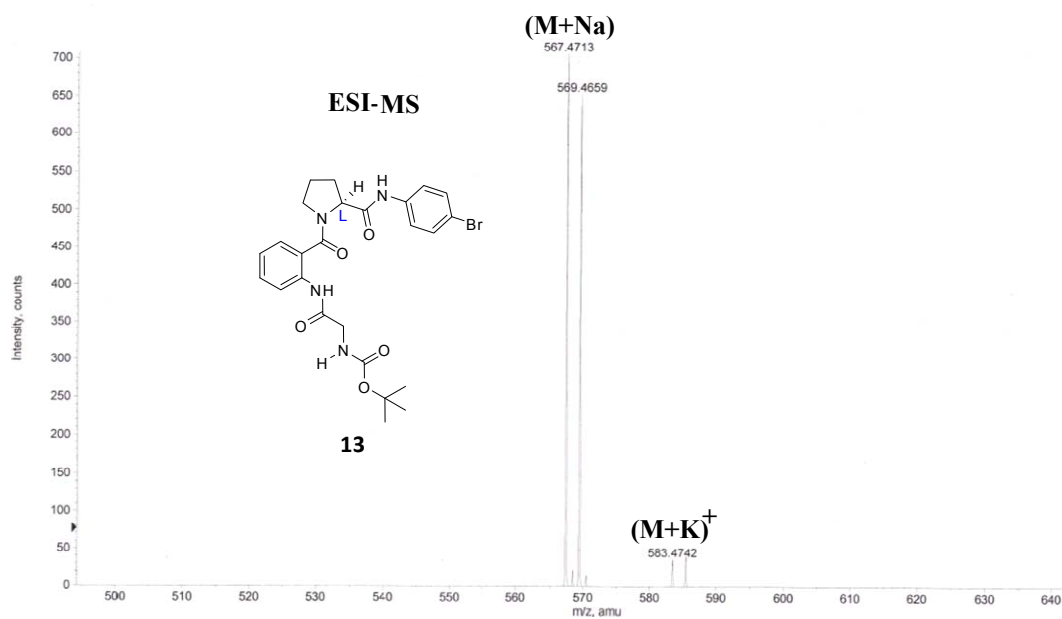
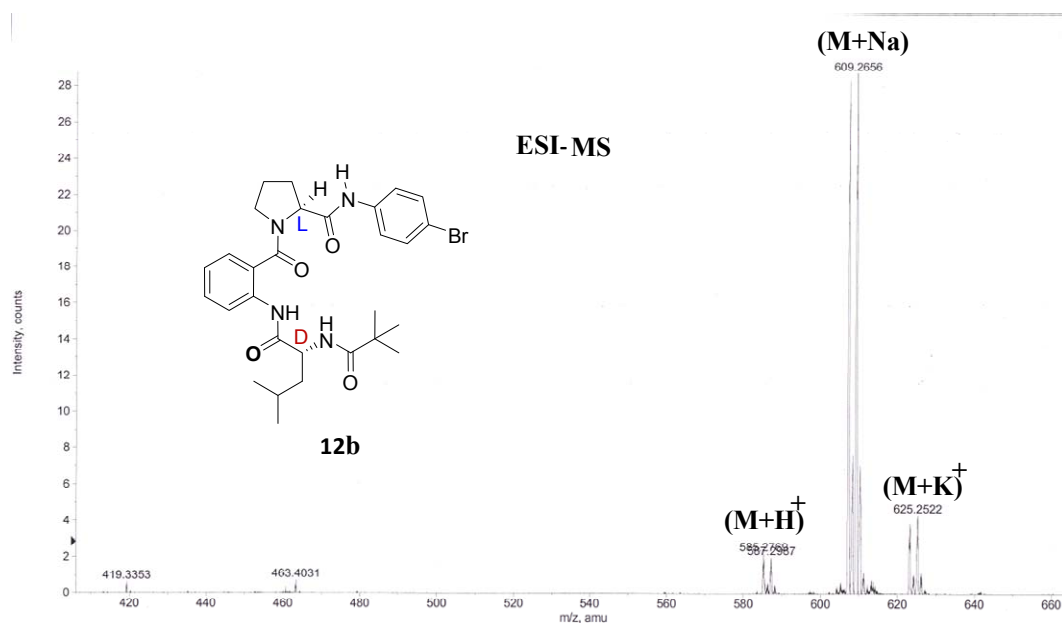
To a solution of **8b** (0.457 g, 1.55 mmol) and **9b** (0.5 g, 1.86 mmol) in dry DCM (20 mL), DCC (0.320 g, 1.55 mmol) and DMAP (cat. amount) were added. The reaction mixture was stirred overnight at room temperature. The reaction mixture was filtered through a celite bed in order to remove dicyclohexyl urea and the filtrate was washed with an ice cold DCM (5 mL). The reaction mixture was diluted with DCM (20 mL) and washed sequentially with sat. NaHCO₃ solution, sat. KHSO₄ solution, water and brine. The organic layer was dried over anhydrous Na₂SO₄ and the crude product was subjected to column purification (30:70 acetone/pet ether, R_f 0.5) to yield **13** as a white solid (0.35 g, 42%); mp: 228-230 °C; $[\alpha]_D^{25}$: -136.73° (c 0.65, MeOH); IR (nujol) ν (cm⁻¹): 2964, 2852, 1712, 1681, 1633, 1491, 1454, 1377, 1169, 1051; ¹H NMR (200 MHz, CDCl₃) δ : 9.53 (s, 1H), 9.41 (s, 1H), 8.22-8.18 (d, *J* = 8.15 Hz, 1H), 7.46-7.28 (m, 5H), 7.24-7.13 (m, 2H), 5.57 (bs, 1H), 4.90 (bs, 1H), 4.16-3.94 (m, 2H), 3.58-3.44 (m, 2H), 2.49-2.21 (m, 2H), 2.07-1.78 (m, 2H), 1.44 (s, 9H); ¹³C NMR (50 MHz, CDCl₃) δ : 170.3, 168.8, 134.7, 131.6, 130.8, 126.4, 126.3, 124.1, 121.1, 116.7, 60.9, 49.9, 30.8, 29.4, 28.2, 25.0; ESI-MS: 567.4713 (M+Na)⁺; 583.4742 (M+K)⁺; Elemental analysis calculated for C₂₅H₂₉BrN₄O₅: C, 55.05; H, 5.36; N, 10.27. Found: C, 55.30; H, 5.28; N, 10.12.

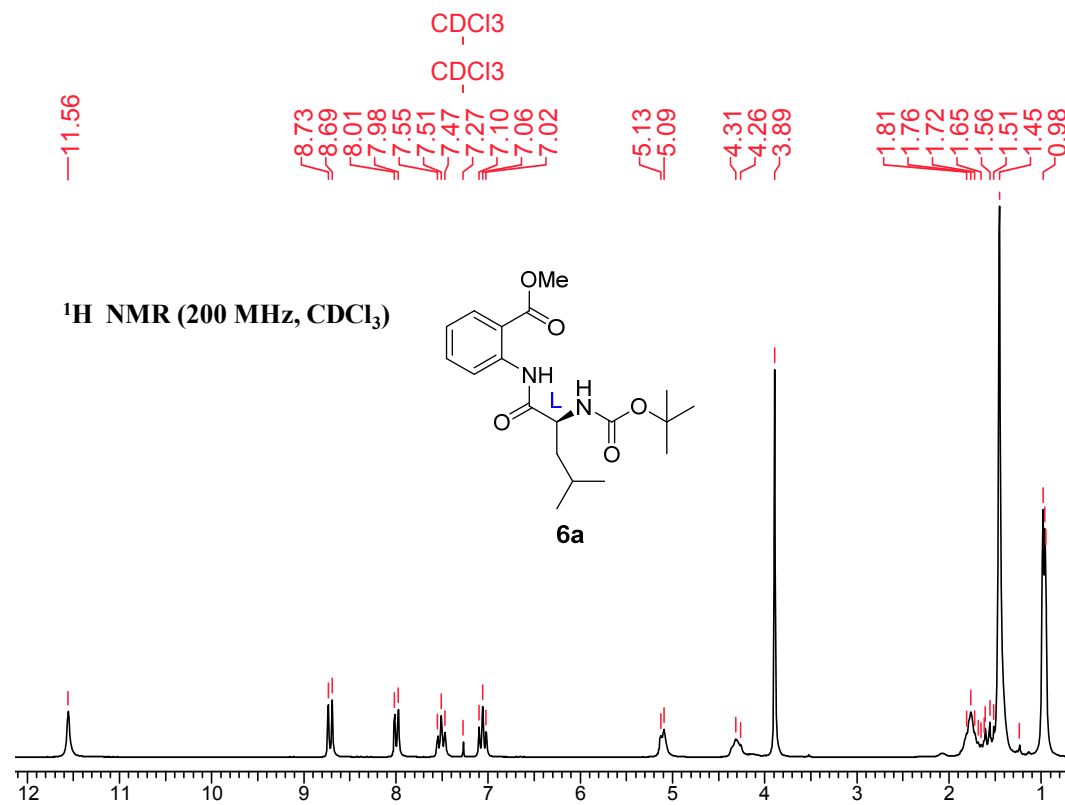
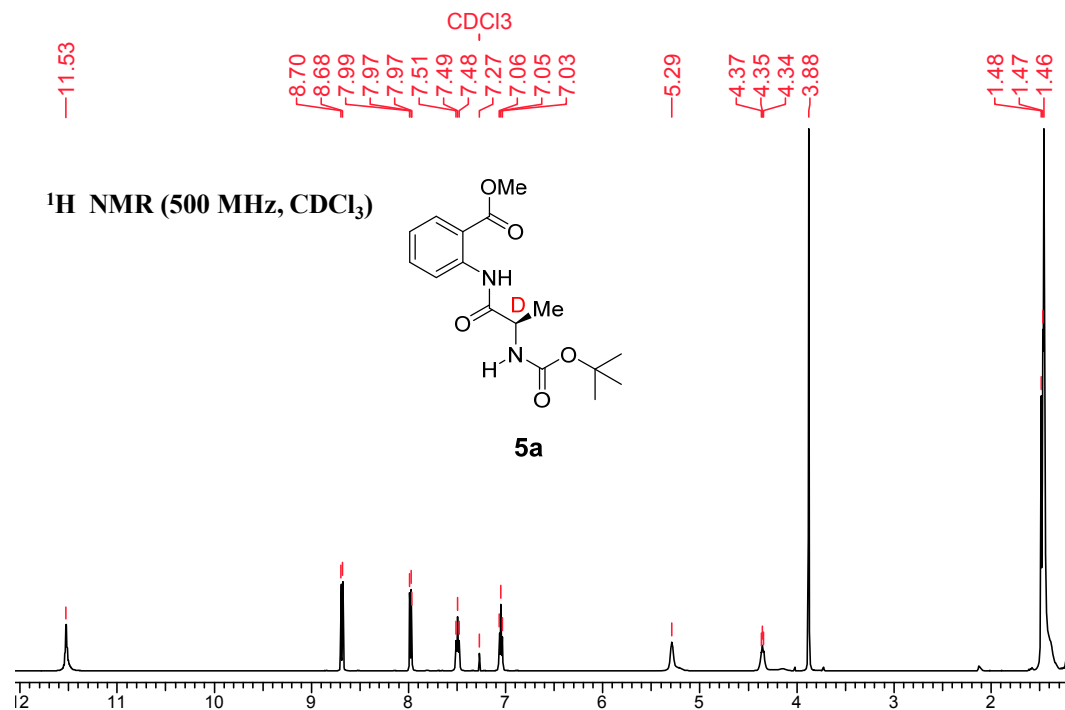


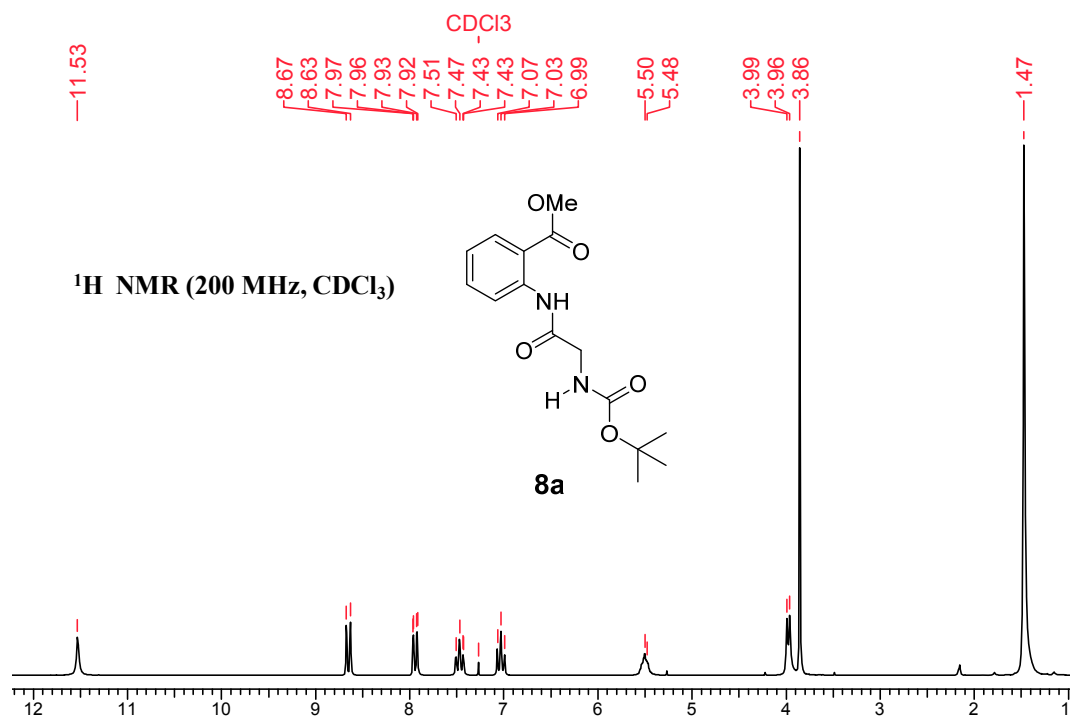
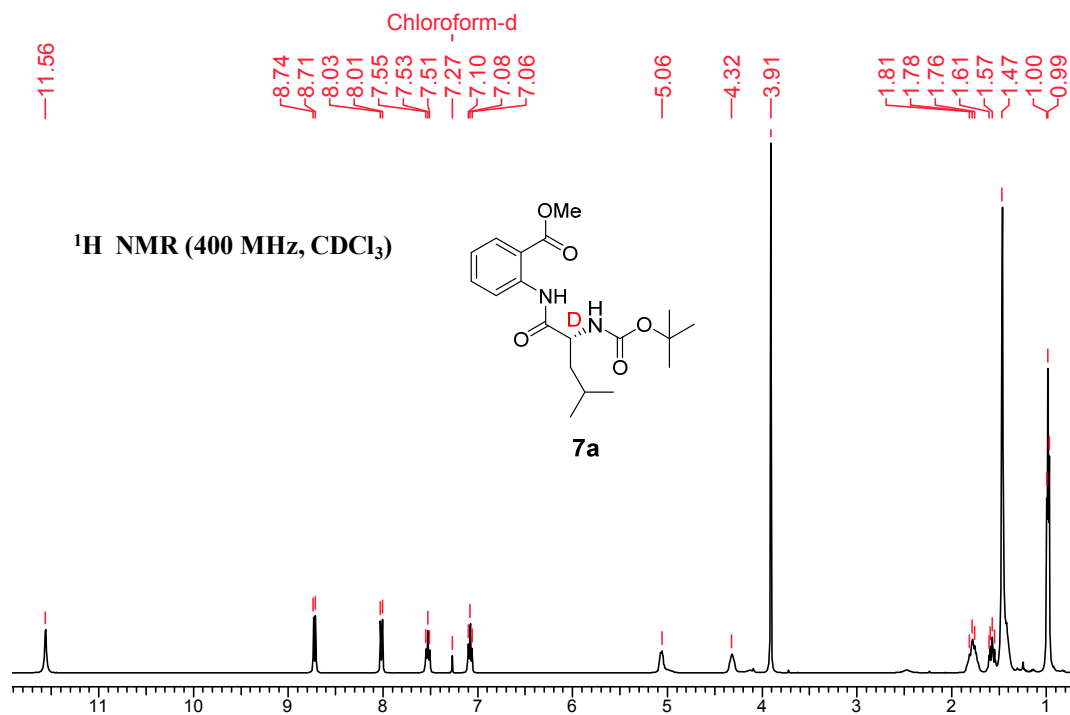


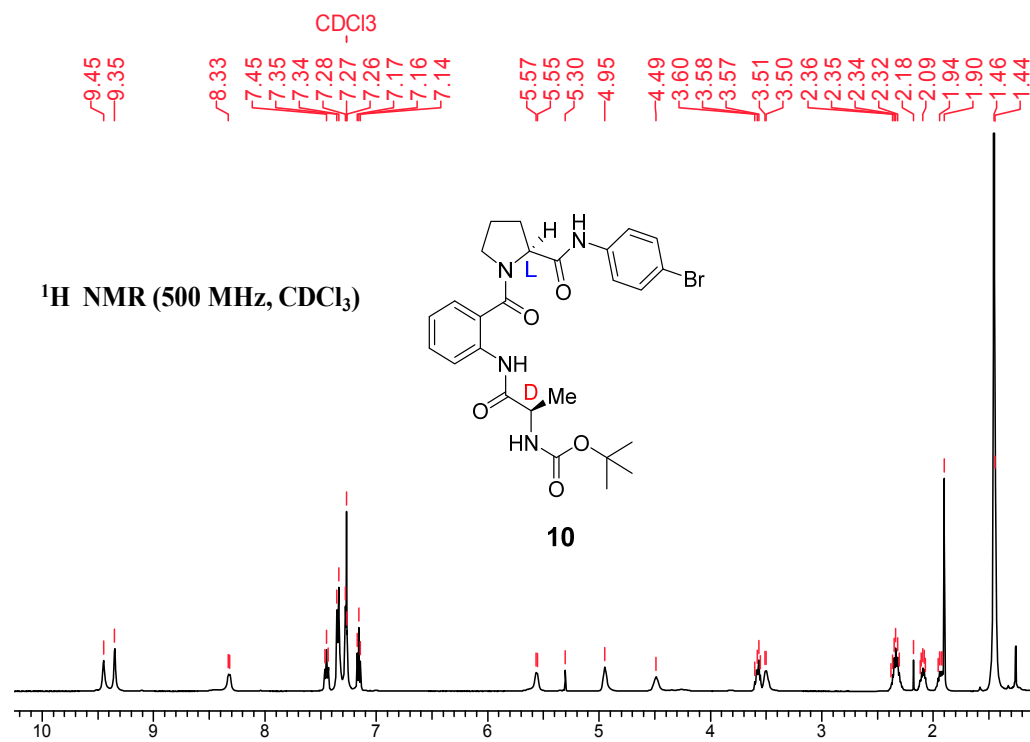
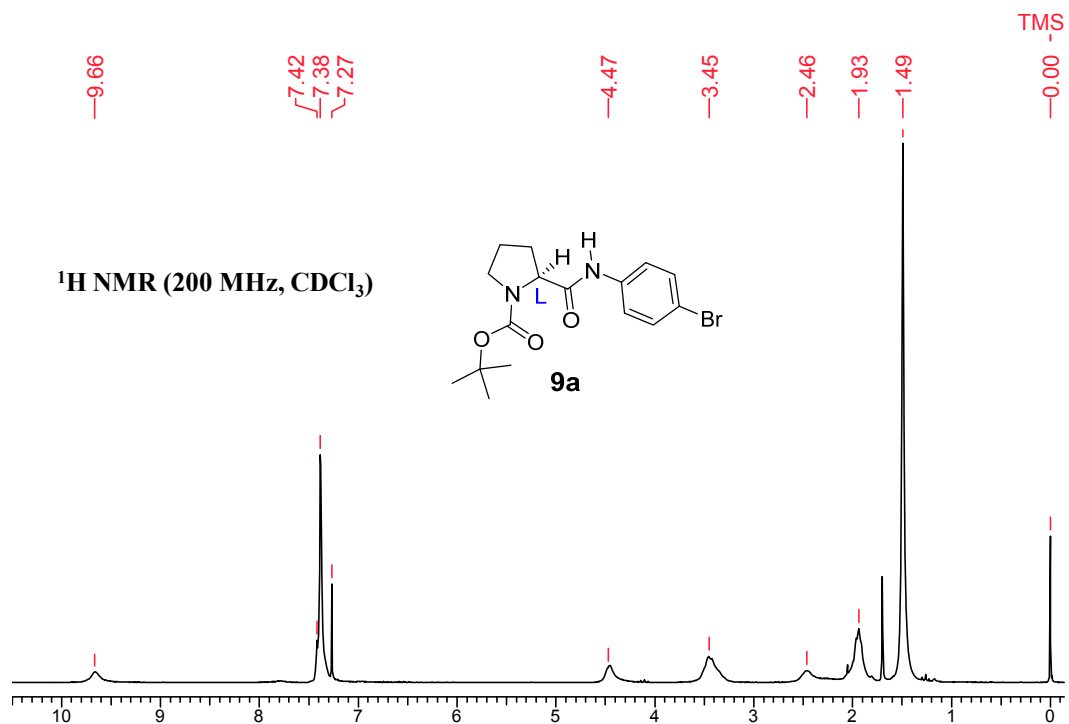


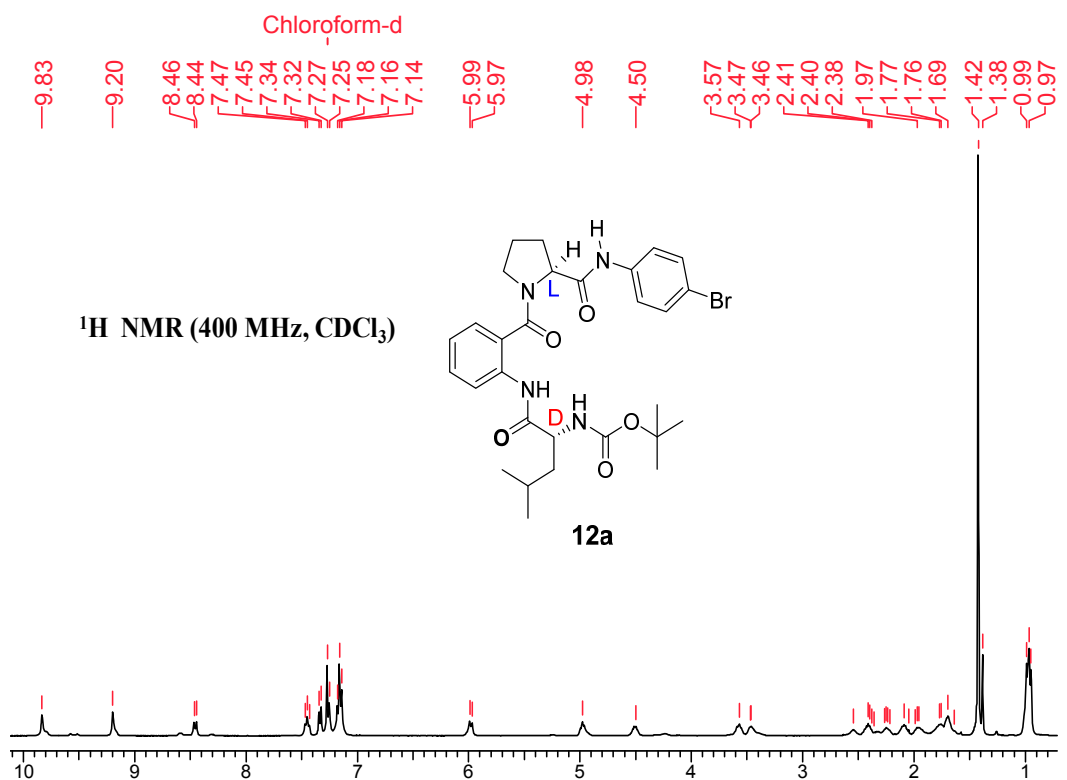
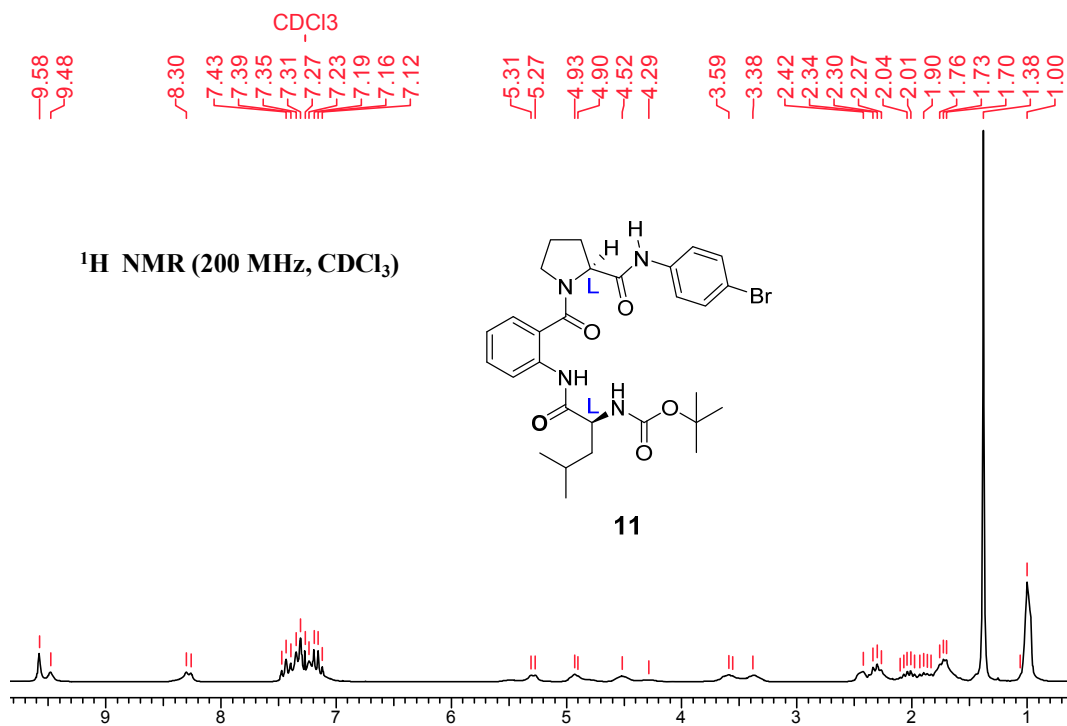


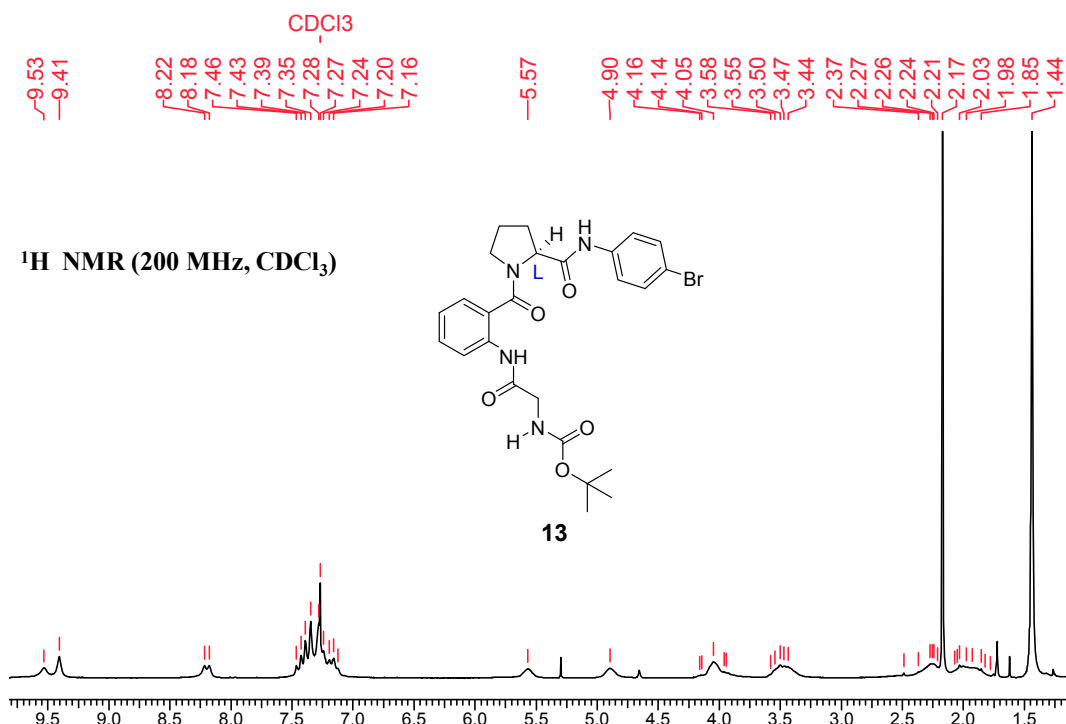
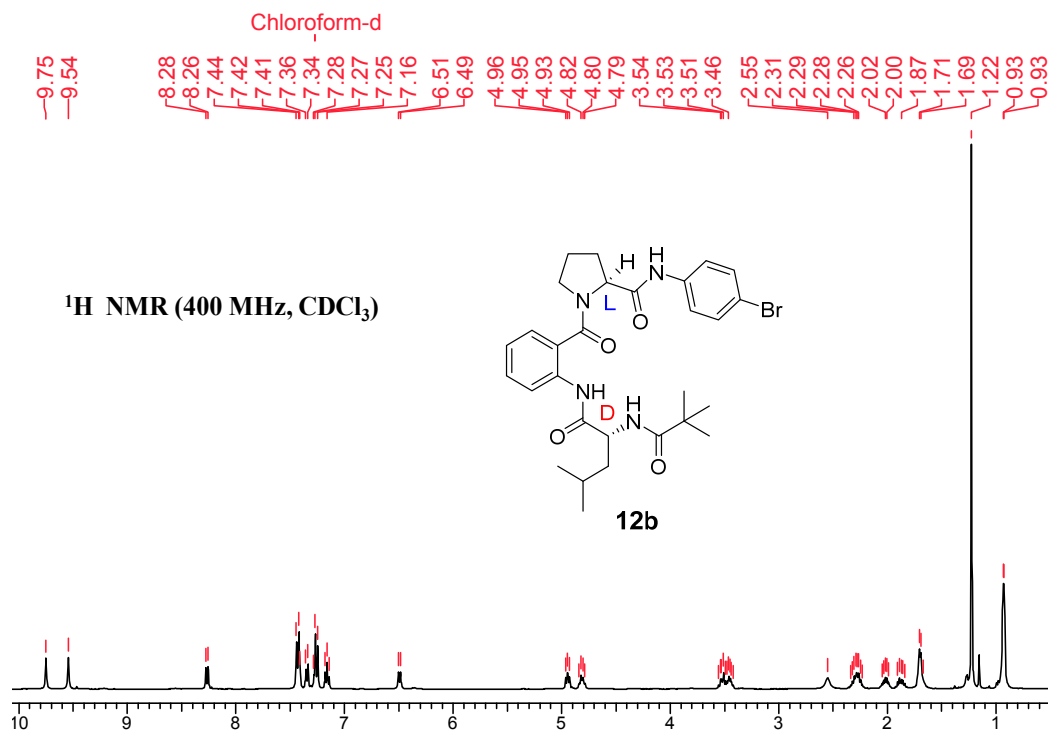


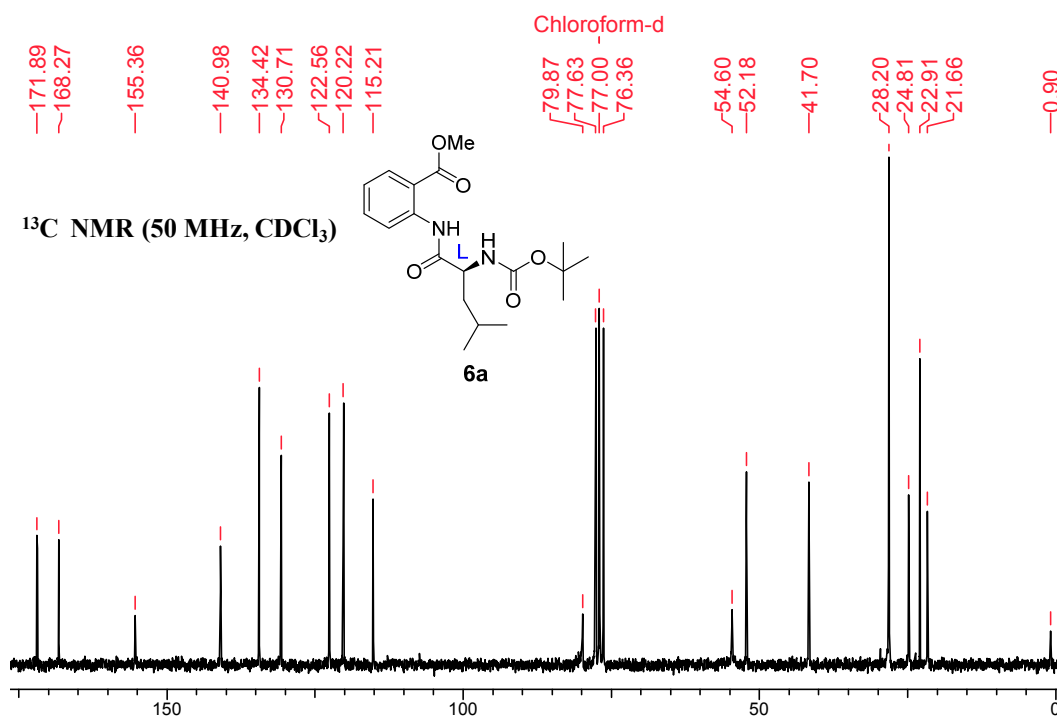
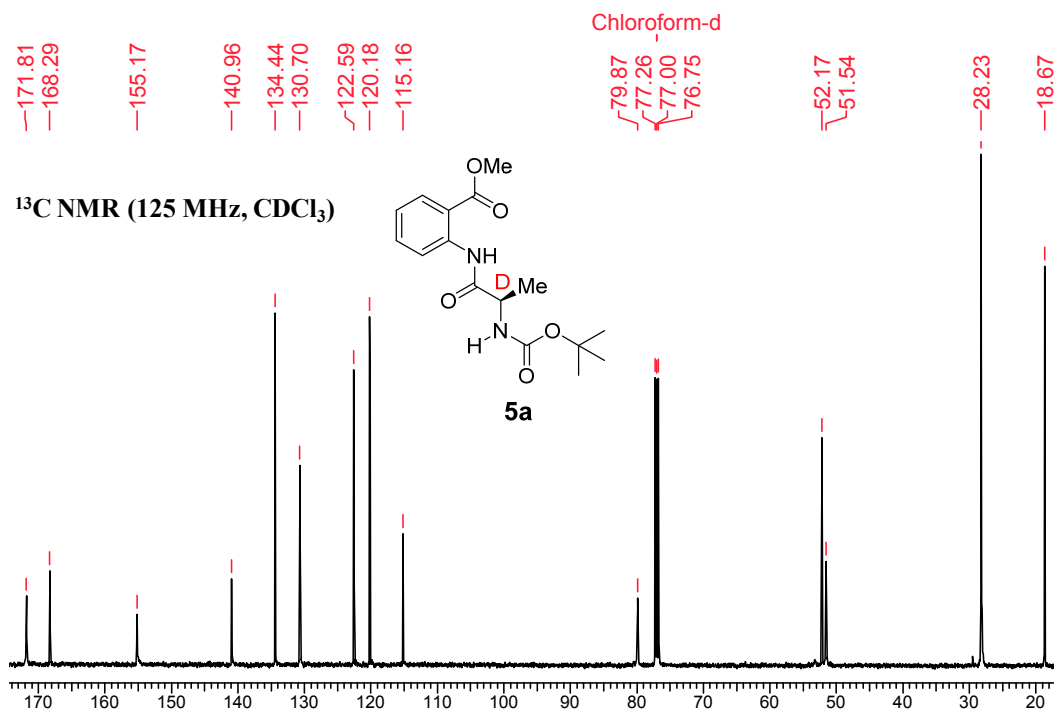


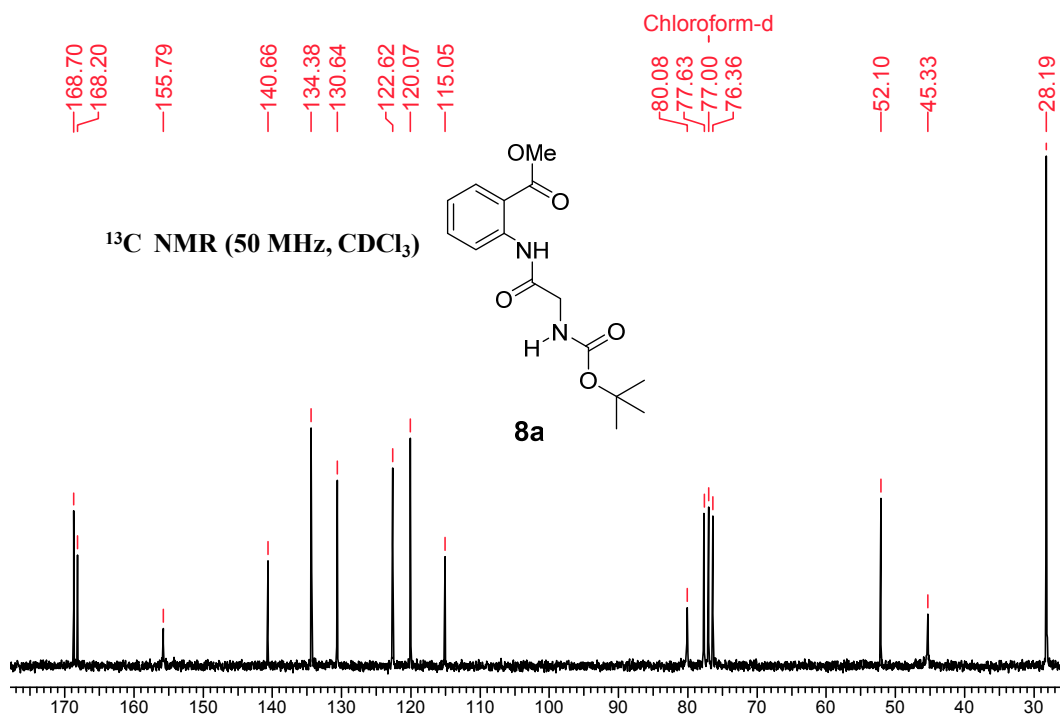
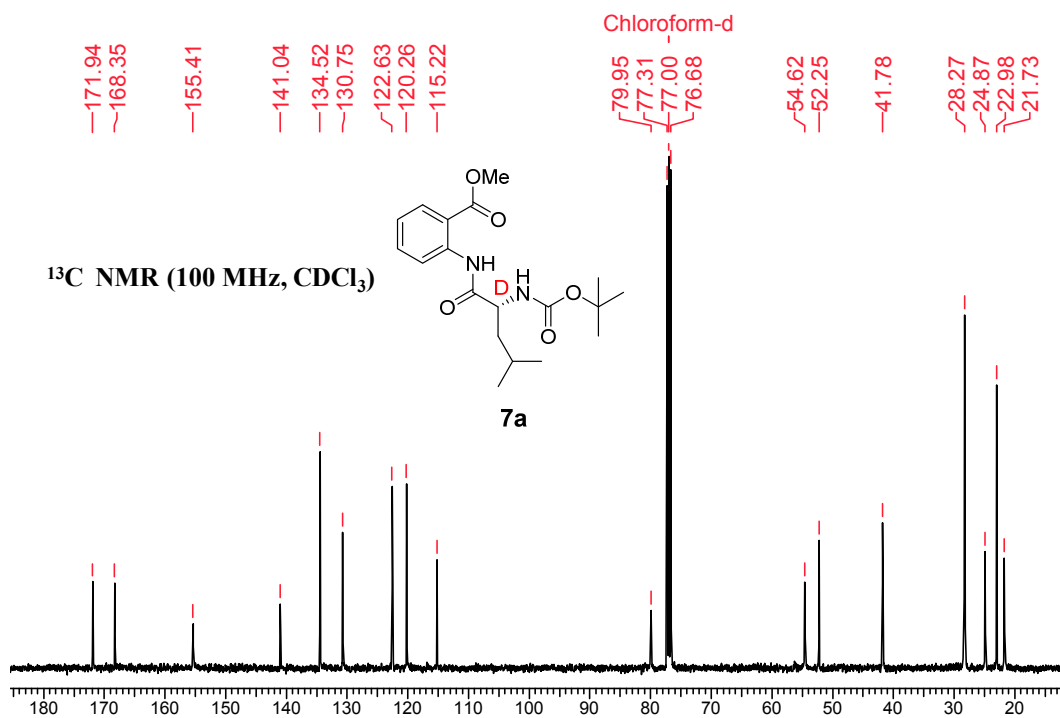


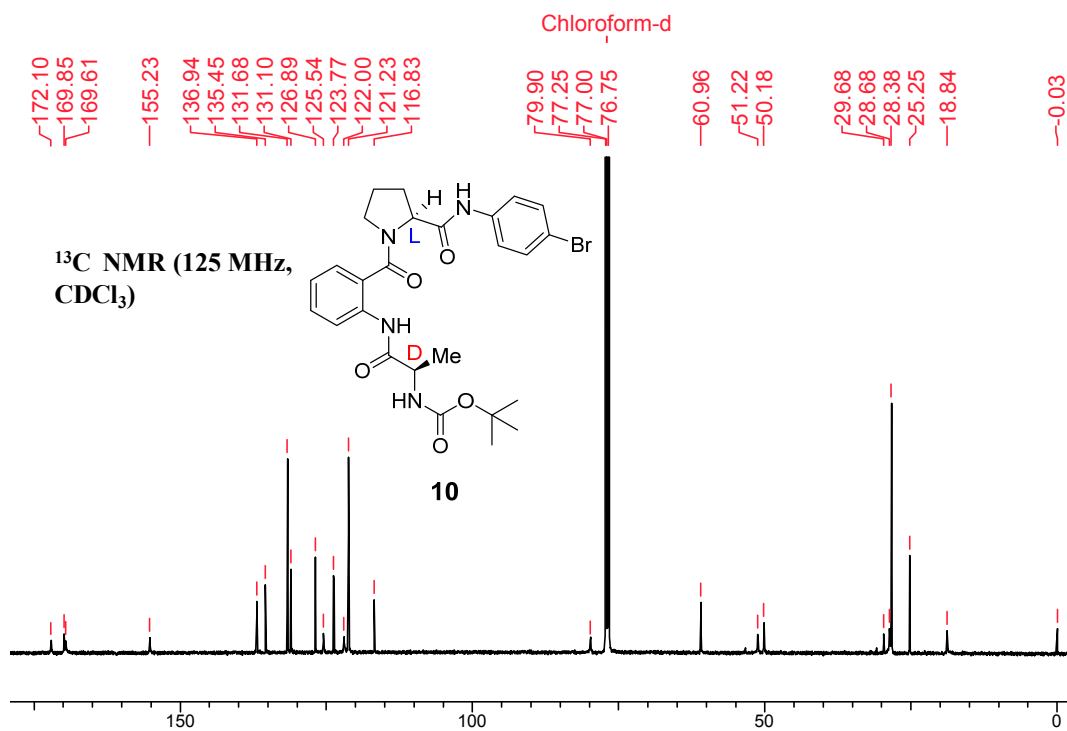
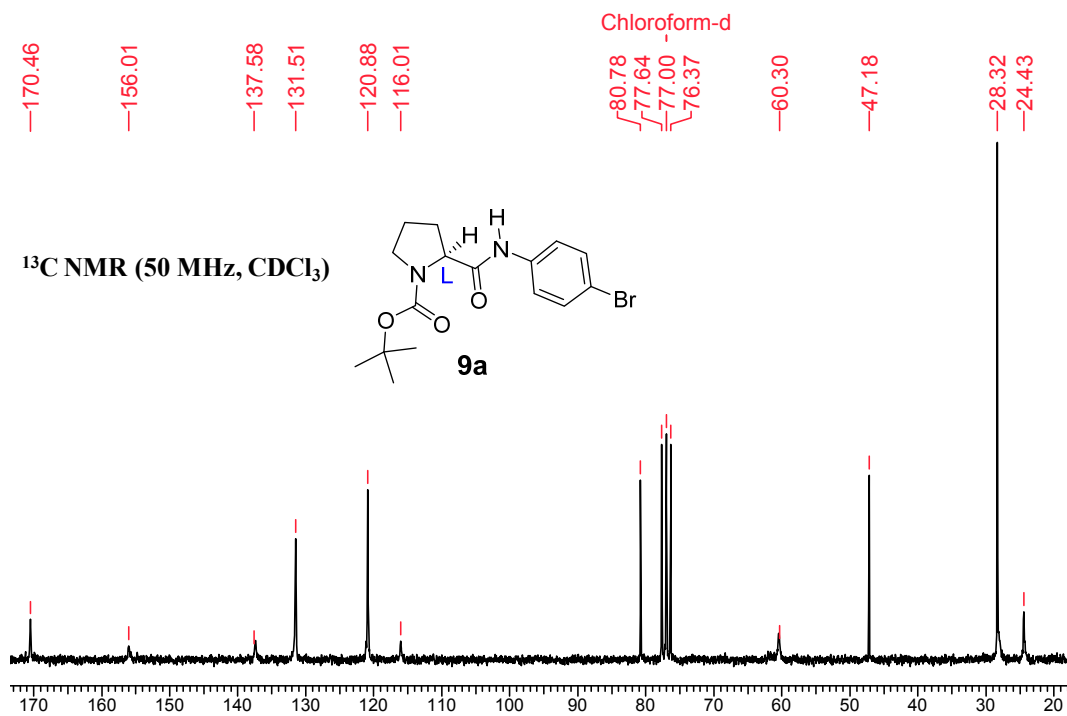


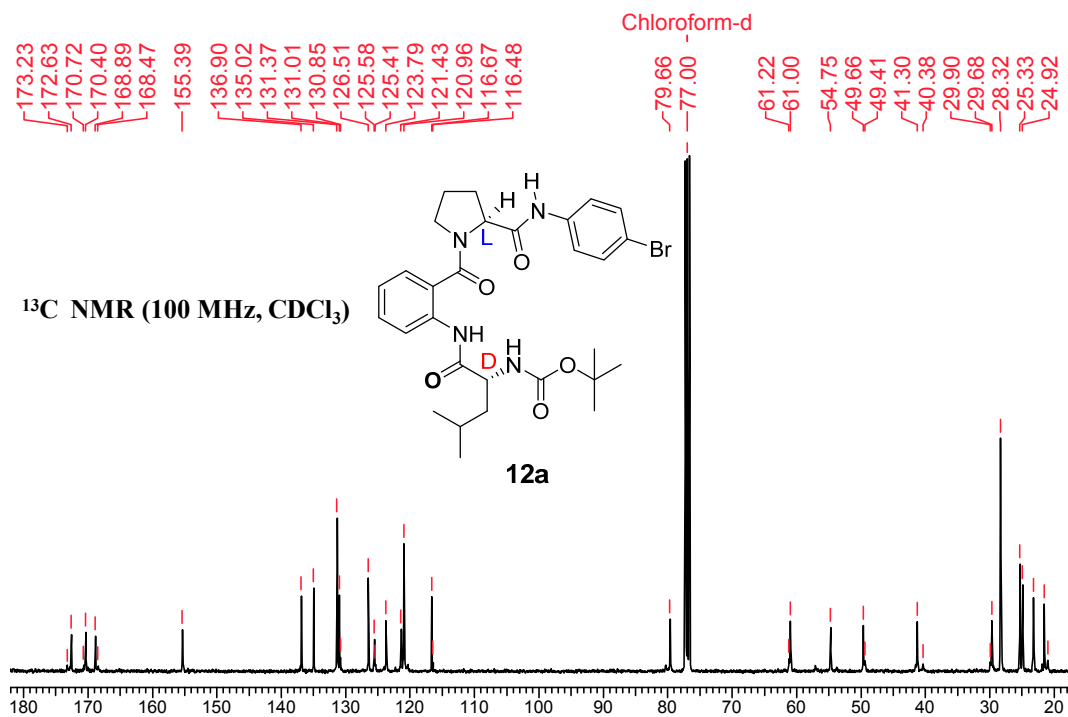
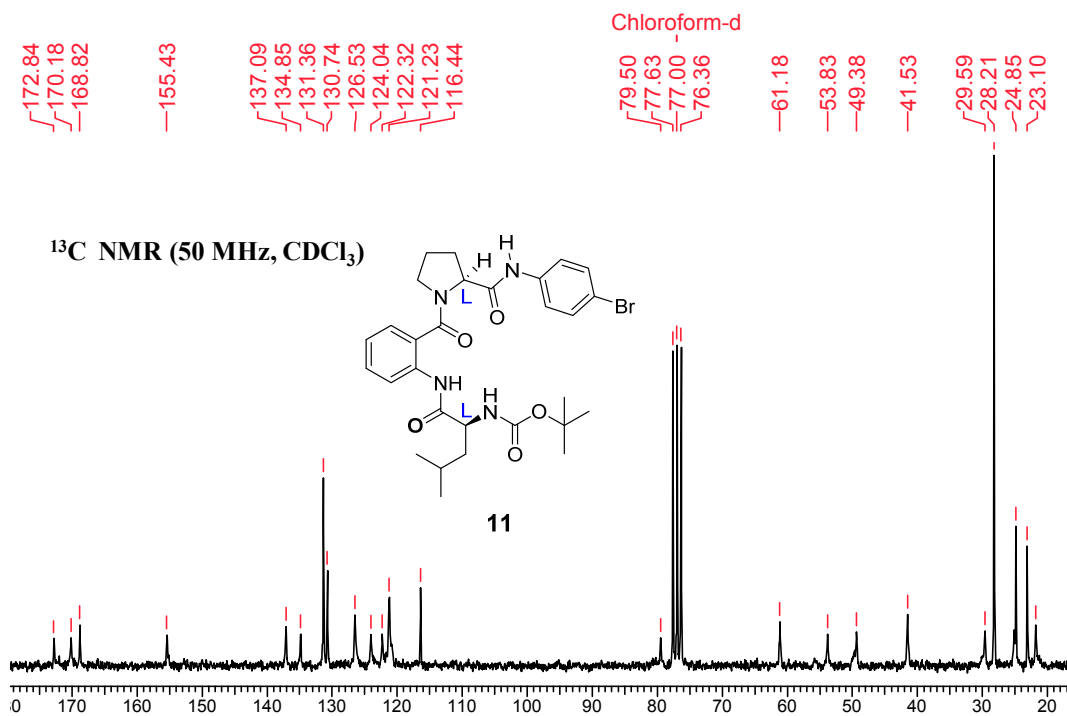












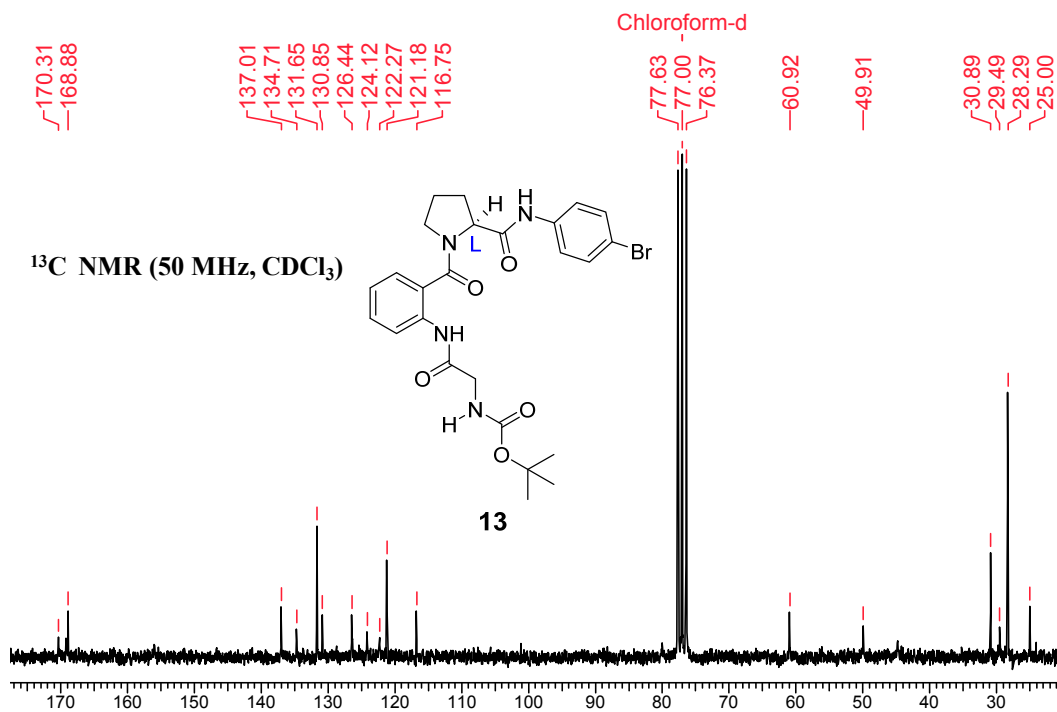
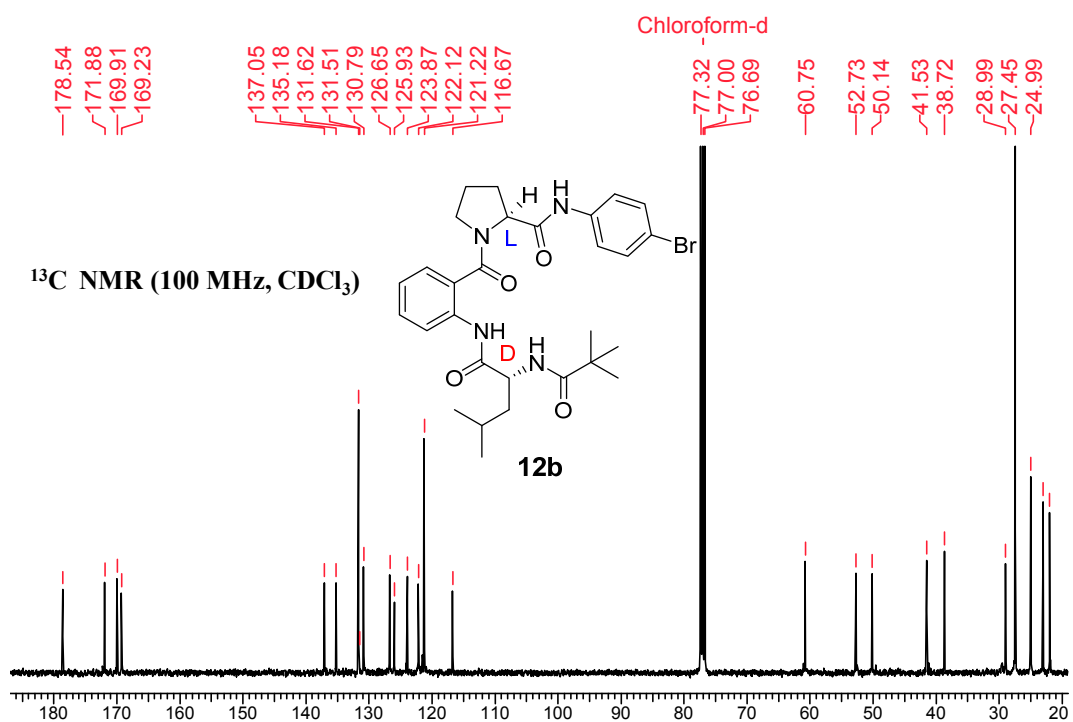


Table 1.3 Titration study of **10** in CDCl_3 (2 mM, 400 MHz) with $\text{DMSO-}d_6$ (Volume of $\text{DMSO-}d_6$ added at each addition = 5 μL)

No	Volume of $\text{DMSO-}d_6$ (μL)	Chemical Shift δ (ppm)		
		NH3	NH2	NH1
1	0	9.44	9.42	5.25
2	5	9.46	9.39	5.44
3	10	9.53	9.39	5.54
4	15	9.64	9.37	5.58
5	20	9.69	9.36	5.62
6	25	9.74	9.35	5.65
7	30	9.78	9.34	5.67
8	35	9.80	9.33	5.69
9	40	9.82	9.32	5.70
10	45	9.83	9.31	5.72
11	50	9.84	9.30	5.73

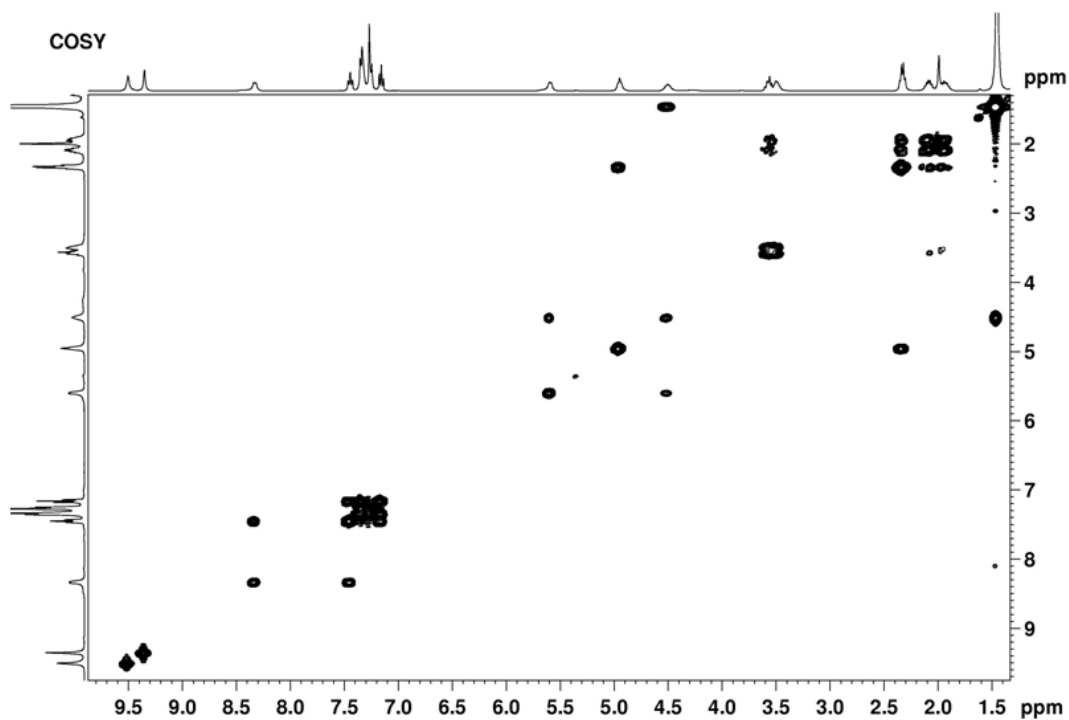
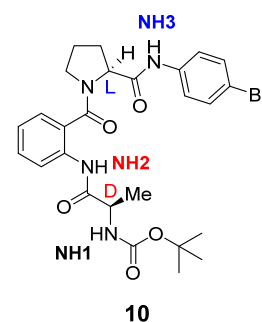


Fig. 1.26 Full COSY spectrum of **10** (400 MHz, CDCl_3).

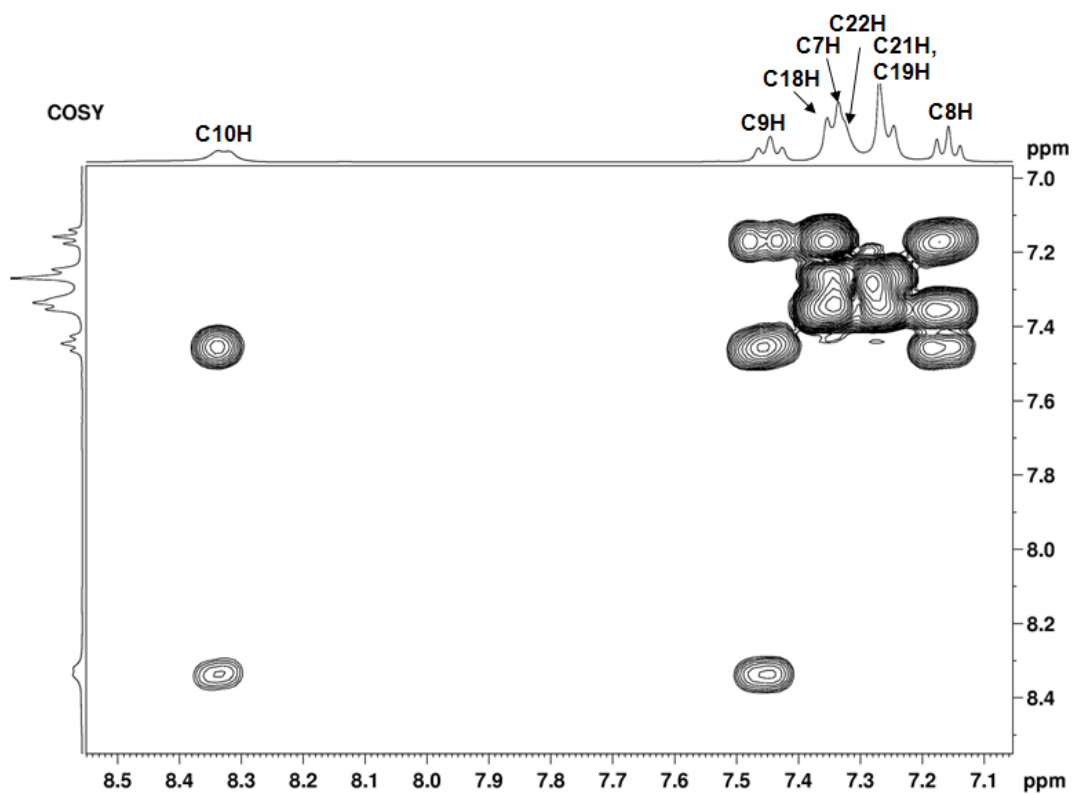


Fig. 1.27 Partial COSY spectrum (aromatic region) of **10** (400 MHz, CDCl₃).

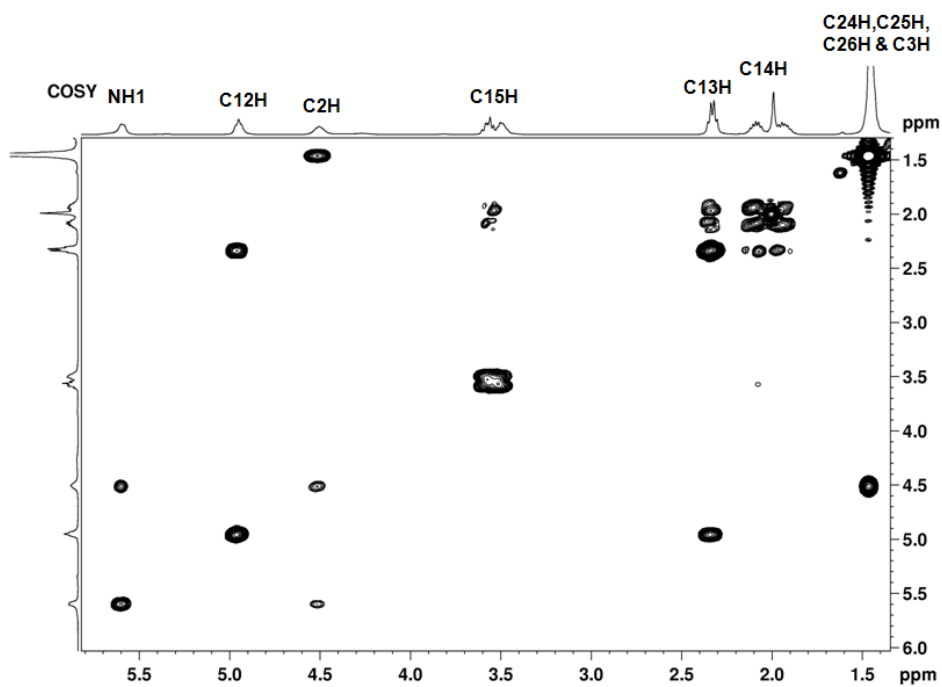


Fig. 1.28 Partial COSY spectrum (aliphatic region) of **10** (400 MHz, CDCl₃).

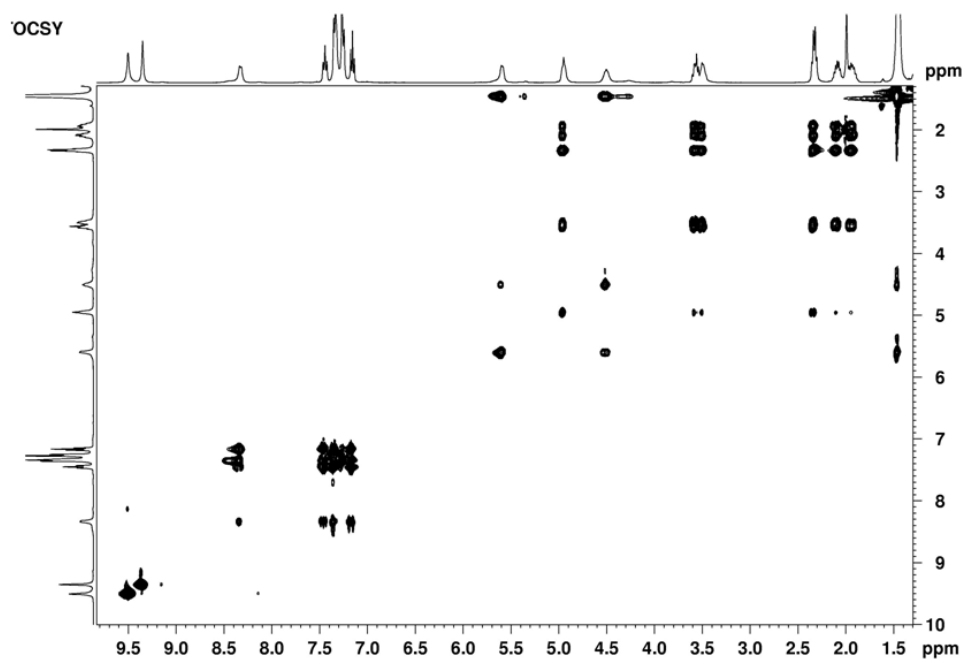


Fig. 1.29 Full TOCSY spectrum of **10** (400 MHz, CDCl₃).

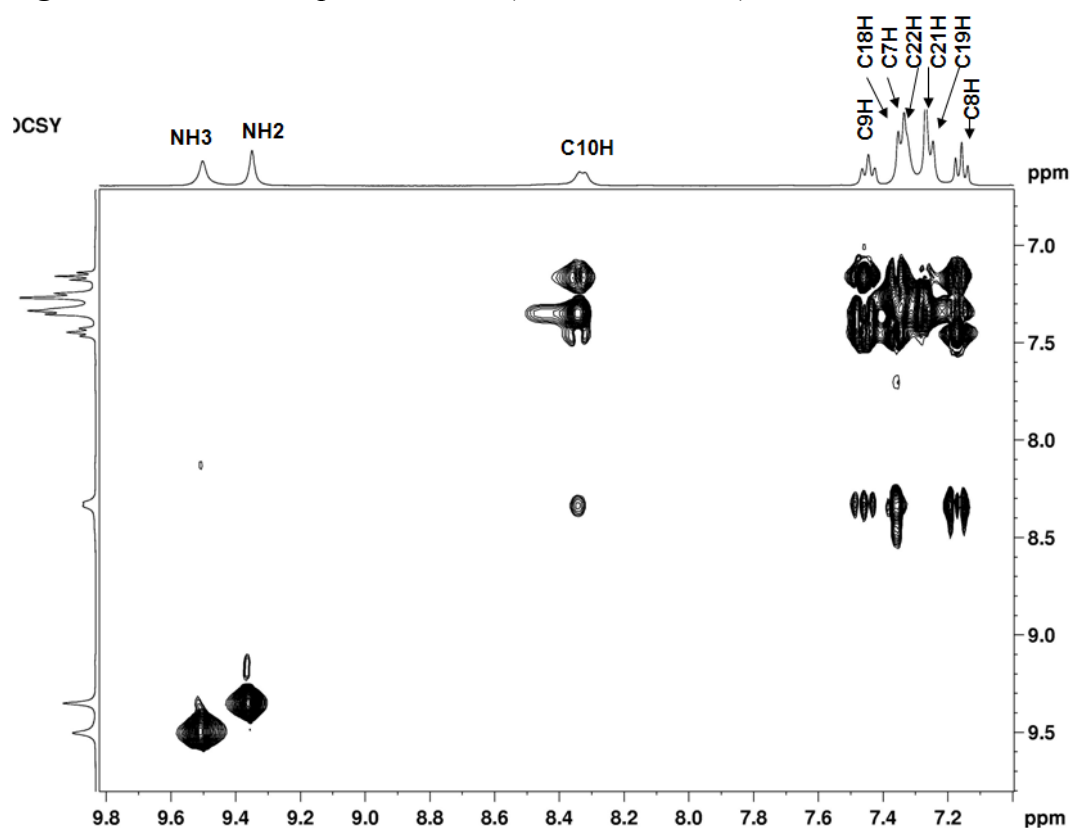


Fig. 1.30 Partial TOCSY spectrum (aromatic region) of **10** (400 MHz, CDCl₃).

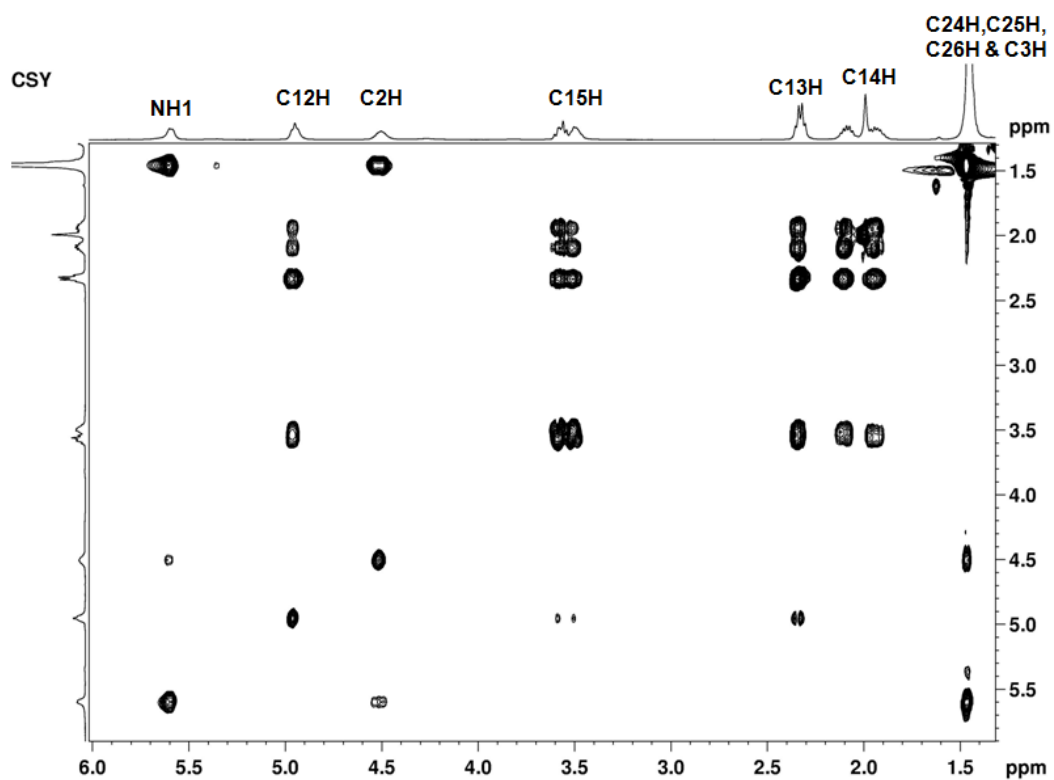


Fig. 1.31 Partial TOCSY spectrum (aliphatic region) of **10** (400 MHz, CDCl₃).

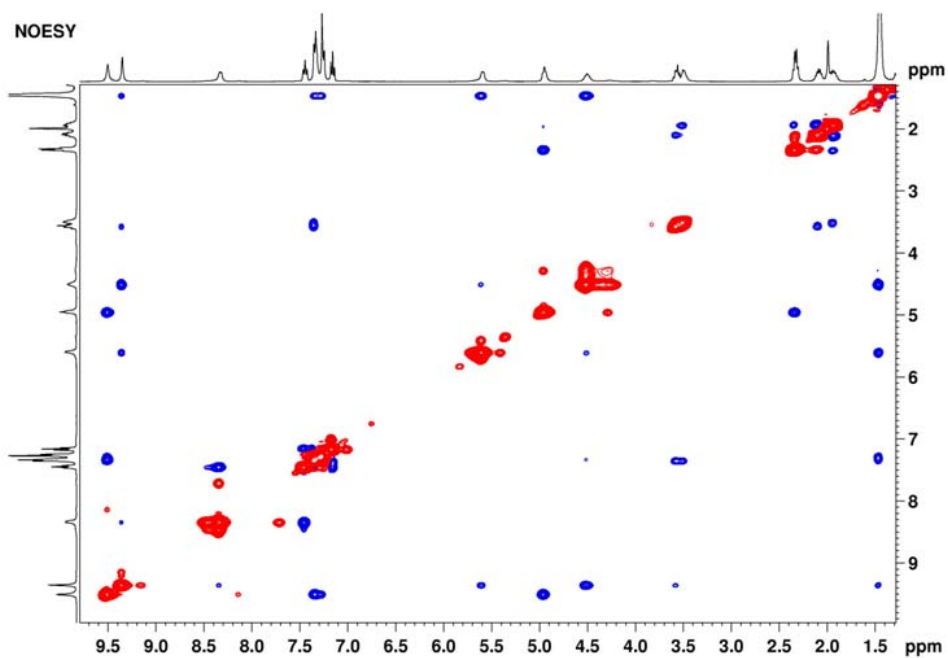


Fig. 1.32 Full NOESY spectrum of **10** (400 MHz, CDCl₃).

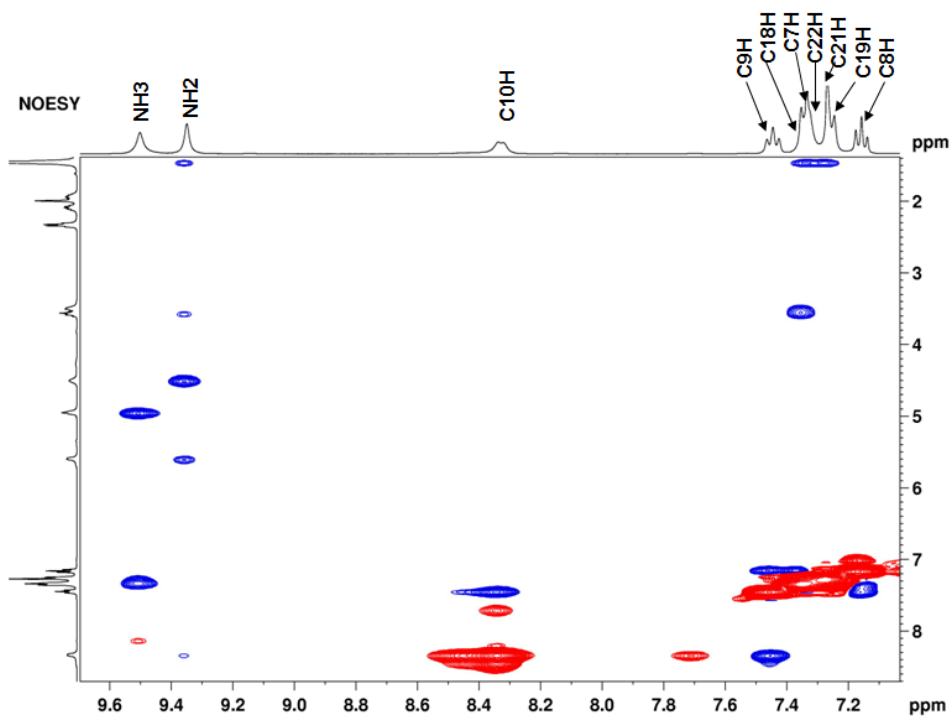


Fig. 1.33 Partial NOESY spectrum (aromatic region) of **10** (400 MHz, CDCl₃).

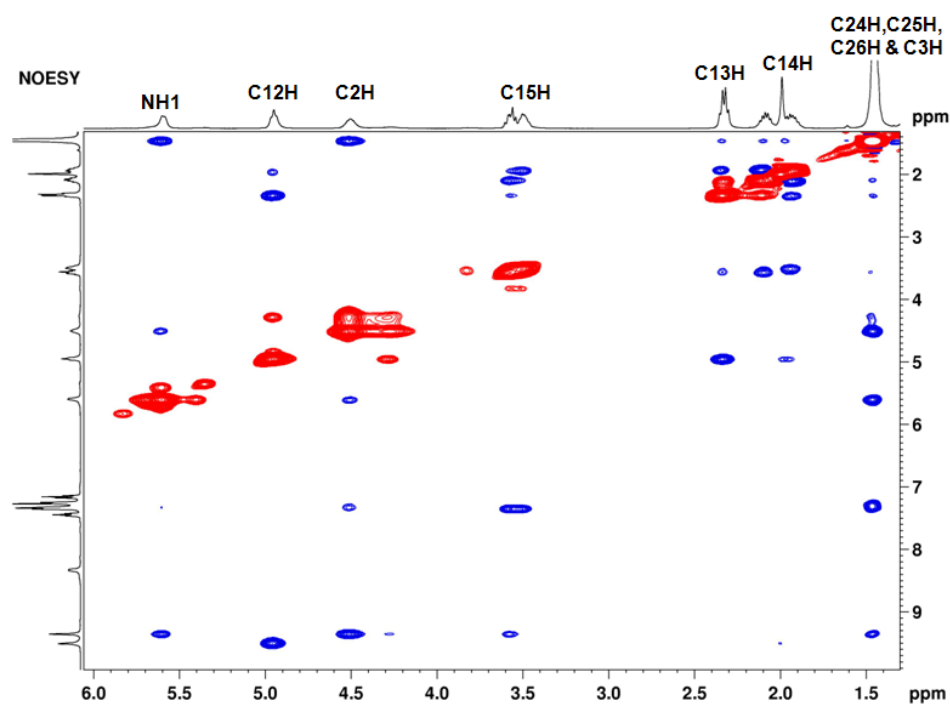


Fig. 1.34 Partial NOESY spectrum (aliphatic region) of **10** (400 MHz, CDCl₃).

1.14 Experimental section (Part B)

Crystal Data for 15a:

Table 1.4 X-ray crystallographic data of trimer 15a.

Crystal Data	15a
Formula	C ₂₄ H ₂₉ N ₃ O ₆ S
M _r	487.56
Crystal Size, mm	0.32×0.25×0.10
Temp. (K)	150(2)
Crystallizing solvent	Ethyl acetate-petroleum ether
Crystal Syst.	Orthorhombic
Space Group	<i>P</i> 2 ₁ 2 ₁ 2 ₁
<i>a</i> /Å	8.8665(3)
<i>b</i> /Å	12.6487(5)
<i>c</i> /Å	21.9234(9)
α°	90
β°	90
γ°	90
<i>V</i> /Å ³	2458.70(16)
<i>Z</i>	4
<i>D</i> _{calc} /g cm ⁻³	1.317
μ /mm ⁻¹	0.176
<i>F</i> (000)	1032
<i>Ab. Correct.</i>	multi-scan
2 θ_{max}	50
Total reflns.	41420
unique reflns.	4322
<i>h, k, l</i> (min, max)	(-10,10),(-15,15),(-23,26)
R _{int}	0.0292
No. of para	311
<i>RI</i> [<i>I</i> > 2 σ (<i>I</i>)]	0.0315
<i>wR2</i> [<i>I</i> > 2 σ (<i>I</i>)]	0.0793
<i>RI</i> [all data]	0.0330
<i>wR2</i> [all data]	0.0801
goodness-of-fit	1.067
$\Delta\rho_{max}, \Delta\rho_{min}$ (eÅ ⁻³)	0.218,-0.177
CCDC no.	1435889

Methyl 3-(2-((tert-butoxycarbonyl) amino) acetamido) thiophene-2-carboxylate 14a:

To a stirred solution of methyl 3-aminothiophene-2-carboxylate (5 g, 31.8 mmol) and Boc-Gly-OH (6.13 g, 35 mmol) in dry DCM (200 mL), DCC (7.88 g, 38.2 mmol) and HOBt (4.29 g, 31.8 mmol) were added under N₂ and the reaction mixture was stirred overnight at room temperature. The reaction mixture was filtered to remove dicyclohexylurea and the filtrate was diluted with DCM (40 mL). The organic layer was washed with sat. NaHCO₃, water, sat. KHSO₄ and then with brine. The organic layer was dried over anhydrous Na₂SO₄ and concentrated under reduced pressure. The crude compound was purified by column chromatography (25:75 EtOAc/pet ether, R_f 0.3) to afford **14a** as a white solid (9.2 g, 92%); mp:113-115 °C; IR (CHCl₃) ν (cm⁻¹): 3309, 2974, 2929, 1978, 1575, 1281, 1254, 1164, 1089, 780; ¹H NMR (400 MHz, CDCl₃) δ : 10.68 (s, 1H), 8.11-8.09 (d, *J* = 5.4 Hz, 1H), 7.47-7.45 (d, *J* = 5.4 Hz, 1H), 5.36 (s, 1H), 4.01-4.00 (d, *J* = 5.1 Hz, 2H), 3.88 (s, 3H), 1.50 (s, 9H); ¹³C NMR (100 MHz, CDCl₃) δ : 167.36, 164.44, 155.82, 143.79, 131.57, 122.10, 110.78, 80.50, 51.89, 44.88, 28.24; HRMS: C₁₃H₁₉O₅N₂S, Calcd: 315.1009 Found: 315.1013; C₁₃H₁₈O₅N₂NaS, calcd: 337.0829 Found: 337.0829.

3-(2-((tert-butoxycarbonyl) amino) acetamido) thiophene-2-carboxylic acid 14b:

To a stirred solution of **14a** (9 g, 28.6 mmol) in methanol (10 mL), aqueous solution of LiOH (4.81 g, 114.6 mmol) was added and the reaction mixture was stirred at room temperature for 2 h. The solvent was stripped off and acidified with sat. KHSO₄, and extracted with DCM (40 mL \times 3). The organic extracts were dried over Na₂SO₄ and concentrated to obtain the crude product **14b**, which was used for the next step without purification.

Benzyl (3-(2-((tert-butoxycarbonyl) amino) acetamido) thiophene-2-carbonyl) prolinatate 15a:

To a solution of dimer acid **14b** (3 g, 10 mmol) and HN-^LPro-OBn (2.46 g, 12 mmol) in DCM (50 mL), EDC.HCl (2.3 g, 12 mmol) and HOBt (0.135 g, 1 mmol) were added and the reaction mixture was stirred overnight at room temperature. The reaction mixture was diluted with DCM (20 mL) and organic layer was washed with sat. NaHCO₃, sat. KHSO₄, and brine. The organic layer was dried over Na₂SO₄. The solvent was evaporated under reduced pressure and the residue was purified by column chromatography (40:60 EtOAc/pet ether, R_f 0.3) to obtain **2** as a white solid (4.67 g, 96%); mp: 153-154 °C; $[\alpha]_D^{25}$: -80.36° (c 0.11, CHCl₃); IR (CHCl₃) ν (cm⁻¹): 3323, 2925, 2850, 1624, 1578, 1431, 1244, 1088, 640; ¹H NMR (500 MHz, CDCl₃) δ : 11.71 (s, 1H), 8.20-8.19 (d, *J* = 5.2 Hz, 1H), 7.42 (s, 1H), 7.35 (s, 5H), 5.28-5.23 (m, 2H), 5.18-5.13 (m, 1H), 4.73 (s, 1H), 4.01-3.90 (m, 4H), 2.25-2.03 (m, 4H), 1.47 (s, 9H); ¹³C NMR (125 MHz, CDCl₃) δ : 171.75, 167.20, 163.95, 155.72, 144.40, 135.57, 128.75, 128.49, 128.23, 128.03, 122.31, 112.05, 79.95, 66.80, 60.56, 48.51, 44.70, 28.26, 25.38; HRMS: C₂₄H₃₀O₆N₃S, Calcd: 488.1850 Found: 488.1849; C₂₄H₂₉O₆N₃NaS, calcd: 510.1669 Found: 510.1669.

Tert-butyl (S)-(2-((2-(2-(methylcarbamoyl) pyrrolidine-1-carbonyl) thiophen-3-yl) amino)-2-oxoethyl) carbamate 16:

To a solution of **15a** (0.4 g, 0.82 mmol) in MeOH (5 mL), sat. solution of methanolic MeNH₂ (10 mL) was added and the reaction mixture was stirred overnight at room temperature. The solvent was evaporated under reduced pressure and the crude compound was purified by column chromatography (90:10 EtOAc/pet ether, R_f 0.3) to yield **3** as a white solid (0.290 g, 86%); mp: 93-95 °C; $[\alpha]_D^{25}$: -168.10° (c 0.17, CHCl₃); IR (CHCl₃) ν (cm⁻¹): 3360, 3125, 2920, 1674,

1560, 1402, 1279, 1163, 771; ^1H NMR (500 MHz, CDCl_3) δ : 11.80 (s, 1H), 8.14 (s, 1H), 7.43 (s, 1H), 6.83 (s, 1H), 5.43 (s, 1H), 4.80 (s, 1H), 4.01–3.85 (m, 4H), 2.85–2.84 (d, $J = 4.0$ Hz, 3H), 2.40 (bs, 1H), 2.18–2.03 (m, 3H), 1.50 (s, 9H); ^{13}C NMR (125 MHz, CDCl_3) δ : 171.69, 167.65, 165.01, 155.84, 144.41, 129.19, 122.00, 111.84, 80.22, 61.69, 48.90, 44.97, 28.30, 26.31; HRMS: $\text{C}_{18}\text{H}_{27}\text{O}_5\text{N}_4\text{S}$: Calcd: 411.1697 Found: 411.1691; $\text{C}_{18}\text{H}_{26}\text{O}_5\text{N}_4\text{NaS}$: Calcd: 433.1516 Found: 433.1512.

Tripeptide acid 15b:

To a solution of ester **15a** (1 g, 2.03 mmol) in MeOH (30 ml), 20% $\text{Pd}(\text{OH})_2/\text{C}$ (0.250 g) was added and the reaction mixture was subjected for hydrogenolysis (70-psi H_2 atmosphere) for 24 h. The reaction mixture was filtered through a celite bed and the solvent was evaporated to afford crude acid **15b**, which was further used for next step without purification.

Tripeptide amine 15c:

To a stirred solution of **15a** (1 g, 2.03 mmol) in DCM (20 mL), TFA (10 mL) was added and the reaction mixture was stirred at room temperature for 2 h. The excess TFA was evaporated under reduced pressure and the reaction mixture was basified with sat. NaHCO_3 . The aqueous layer was extracted with DCM (3 \times 20 mL) and organic extracts were dried over Na_2SO_4 . The organic extracts were concentrated under reduced pressure to obtain crude product **15c**, which was used for the next step without purification.

Tert-butyl (S)-(2-((2-(2-((4-bromophenyl) carbamoyl) pyrrolidine-1-carbonyl) thiophen-3-yl) amino)-2-oxoethyl) carbamate 17:

To a solution of trimer acid **15b** (0.3 g, 0.75 mmol) and 4-bromoaniline (0.142 g, 0.83 mmol) in dry DCM (10 mL), EDC.HCl (0.188 g, 0.98 mmol) and HOBT

(0.010 g, 0.07 mmol) were added and the reaction mixture was stirred overnight at room temperature. The reaction mixture was diluted with DCM (20 mL). The organic layer was washed with sat. NaHCO₃, water, sat. KHSO₄, brine and dried over anhydrous Na₂SO₄. The solvent was evaporated under reduced pressure and the crude product was purified by column chromatography (60:40 EtOAc/pet ether, R_f 0.3) to afford **17** as a white crystalline solid (0.328 g, 79%). mp: 126-128 °C; $[\alpha]_D^{25}$: -118.03° (c 0.17, MeOH); IR (CHCl₃) ν (cm⁻¹): 3323, 2980, 1693, 1540, 1404, 1178, 767; ¹H NMR (400 MHz, CDCl₃) δ : 11.29 (s, 1H), 9.34 (s, 1H), 7.68–7.67 (d, *J* = 5.4 Hz, 1H), 7.11–7.05 (m, 2H), 7.00–7.01 (d, *J* = 5.4 Hz, 1H), 6.91–6.88 (m, 2H), 5.99 (s, 1H), 4.33 (s, 1H), 3.55 (s, 1H), 3.45–3.38 (m, 3H), 1.75–1.68 (m, 3H), 1.61–1.57 (m, 1H), 0.91 (s, 9H); ¹³C NMR (100 MHz, CDCl₃) δ : 169.78, 167.42, 163.71, 155.69, 143.43, 137.47, 130.99, 128.48, 121.60, 121.00, 115.39, 112.18, 79.01, 61.89, 48.48, 44.39, 29.03, 27.82, 24.87; HRMS: C₂₃H₂₈O₅N₄BrS: Calcd: 551.0958 Found: 551.0964.

Hexapeptide benzyl ester **18**:

To a solution of trimer acid **15b** (0.5 g, 1.25 mmol) and trimer amine **15c** (0.584 g, 1.51 mmol) in DCM (25 mL), EDC.HCl (0.313 g, 1.63 mmol) and HOBT (0.017 g, 0.12 mmol) were added and the reaction mixture was stirred overnight at room temperature. The reaction mixture was diluted with DCM and then washed with sat. NaHCO₃, sat. KHSO₄ and brine. The organic layer was dried over Na₂SO₄ and concentrated under reduced pressure. The solid residue was purified by column chromatography (80:20 EtOAc/pet ether, R_f 0.3) to yield hexapeptide **18** (0.694 g, 72%) as a white solid; mp: 118-120 °C; $[\alpha]_D^{25}$: -193.18° (c 0.15, CHCl₃); IR (CHCl₃) ν (cm⁻¹): 3296, 2980, 1684, 1555, 1403, 1170, 772; ¹H NMR (400 MHz, CDCl₃) δ : 11.76 (s, 2H), 8.20–8.16 (dd, *J* = 9.3, 5.5 Hz, 2H), 7.80 (s, 1H),

7.47–7.45 (d, $J = 5.1$ Hz, 2H), 7.33 (s, 5H), 5.48 (s, 1H), 5.24–5.16 (m, 2H), 4.90–4.88 (d, $J = 6.9$ Hz, 1H), 4.55 (s, 1H), 4.24–4.17 (m, 1H), 4.12–3.98 (m, 4H), 3.93 (s, 1H), 3.83–3.78 (m, 2H), 2.51–2.49 (m, 1H), 2.27–2.17 (m, 2H), 2.09–1.98 (m, 3H), 1.93–1.84 (m, 2H), 1.47 (s, 9H); ^{13}C NMR (100 MHz, CDCl_3) δ : 171.80, 171.41, 167.51, 166.63, 165.04, 163.86, 155.84, 144.41, 128.95, 128.51, 128.29, 128.01, 122.22, 112.24, 80.06, 66.87, 61.53, 60.63, 49.01, 48.52, 44.84, 43.87, 31.53, 28.30, 22.60, 14.06; HRMS: $\text{C}_{36}\text{H}_{43}\text{O}_9\text{N}_6\text{S}_2$: Calcd: 767.2527 Found: 767.2520; $\text{C}_{36}\text{H}_{42}\text{O}_9\text{N}_6\text{NaS}_2$: Calcd: 789.2347 Found: 789.2337.

Hexapeptide amide 19:

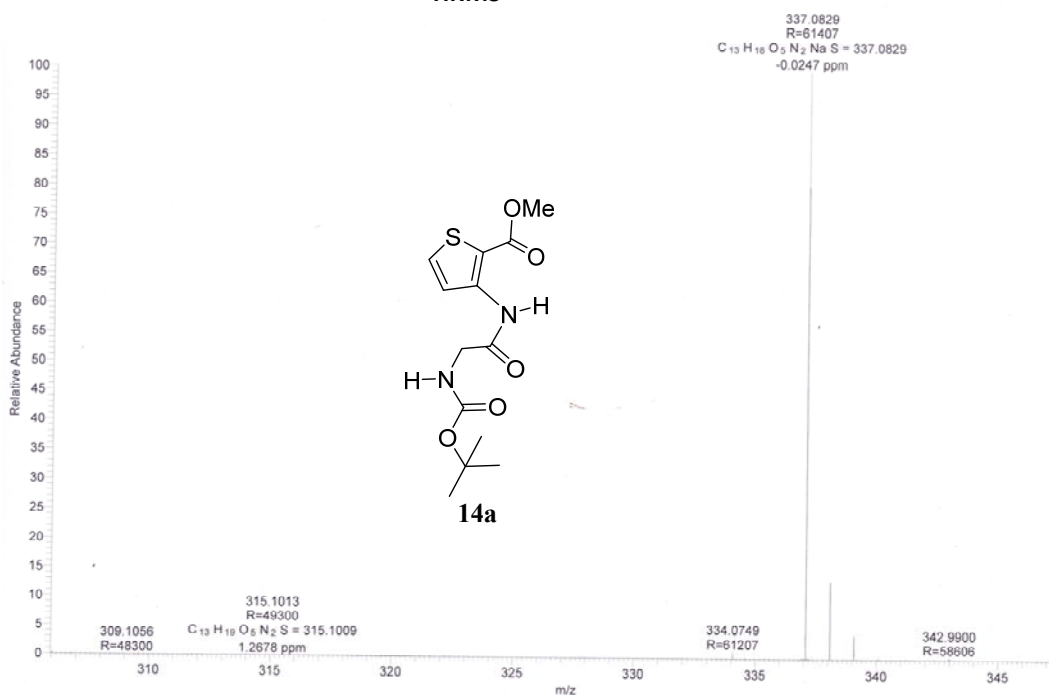
To a stirred solution of hexapeptide **18** (0.350 g, 0.45 mmol) in MeOH (2 mL), sat. solution of methanolic MeNH_2 (10 mL) was added and the reaction mixture was stirred overnight at room temperature. The volume of MeOH was reduced to one fourth by concentrating under reduced pressure and the crude reaction mixture was precipitated with addition of DCM (5 mL). The precipitate was filtered and the residue was washed with DCM (10 mL) to obtain product **1** as a white solid (0.273 g, 87%); mp: 148–151 °C; $[\alpha]_{\text{D}}^{25}$: -161.80° (c 0.11, MeOH); IR (CHCl_3) ν (cm^{-1}): 3143, 2926, 1681, 1556, 1402, 764; ^1H NMR (700 MHz, CDCl_3) δ : 11.64 (s, 2H), 8.13 (s, 2H), 7.85 (s, 1H), 7.45 (s, 2H), 6.64 (s, 1H), 5.47 (s, 1H), 4.91–4.90 (d, $J = 7.0$ Hz, 1H), 4.63 (s, 1H), 4.28–4.23 (m, 1H), 4.09–4.05 (m, 1H), 4.03–3.98 (m, 2H), 3.92–3.87 (m, 2H), 3.81 (bs, 2H), 2.82–2.81 (d, $J = 4.7$ Hz, 3H), 2.49 (s, 1H), 2.33 (s, 1H), 2.25 (s, 1H), 2.17–2.09 (m, 2H), 2.05–1.96 (m, 3H), 1.47 (s, 9H); ^{13}C NMR (176 MHz, CDCl_3) δ : 171.65, 167.53, 166.69, 165.14, 164.90, 155.90, 144.23, 129.35, 128.98, 122.41, 112.41, 80.10, 61.58, 49.13, 48.97, 44.81, 44.02, 28.33, 26.35, 25.60; HRMS: $\text{C}_{30}\text{H}_{40}\text{O}_8\text{N}_7\text{S}_2$: Calcd: 690.2374 Found: 690.2379; $\text{C}_{30}\text{H}_{39}\text{O}_8\text{N}_7\text{NaS}_2$: Calcd: 712.2194 Found: 712.2198.

D:\Data\tuka_21

3/16/2015 1:57:22 PM

tuka_21 #105 RT: 0.47 AV: 1 NL: 2.17E9
T: FTMS + p ESI Full ms [85.40-1281.00]

HRMS

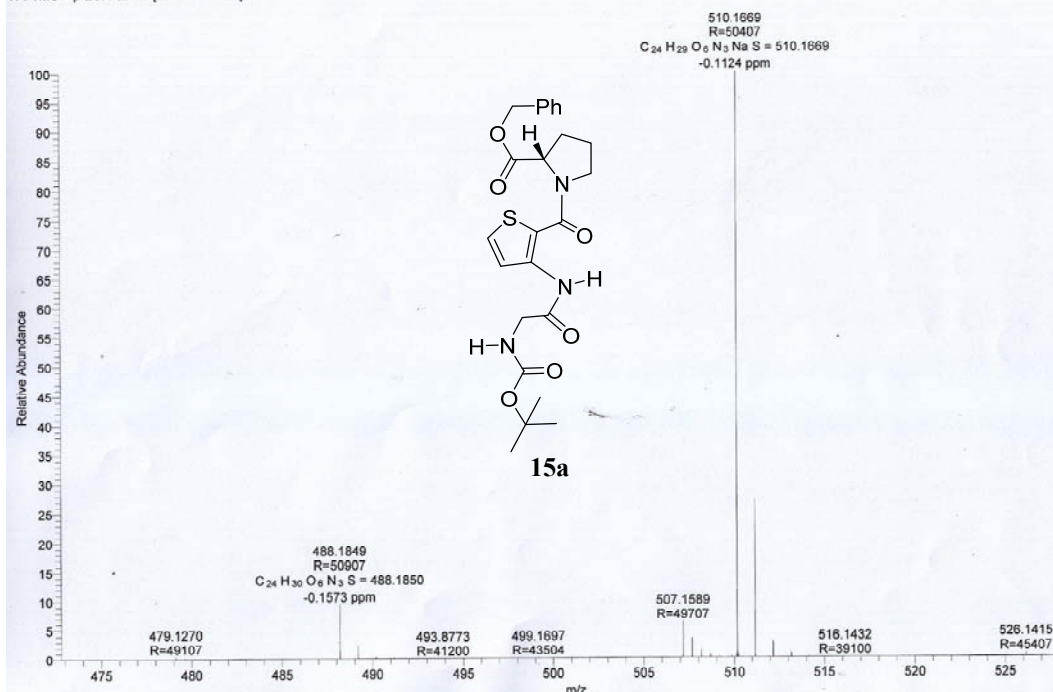


D:\Data\tuka_24

3/16/2015 2:12:46 PM

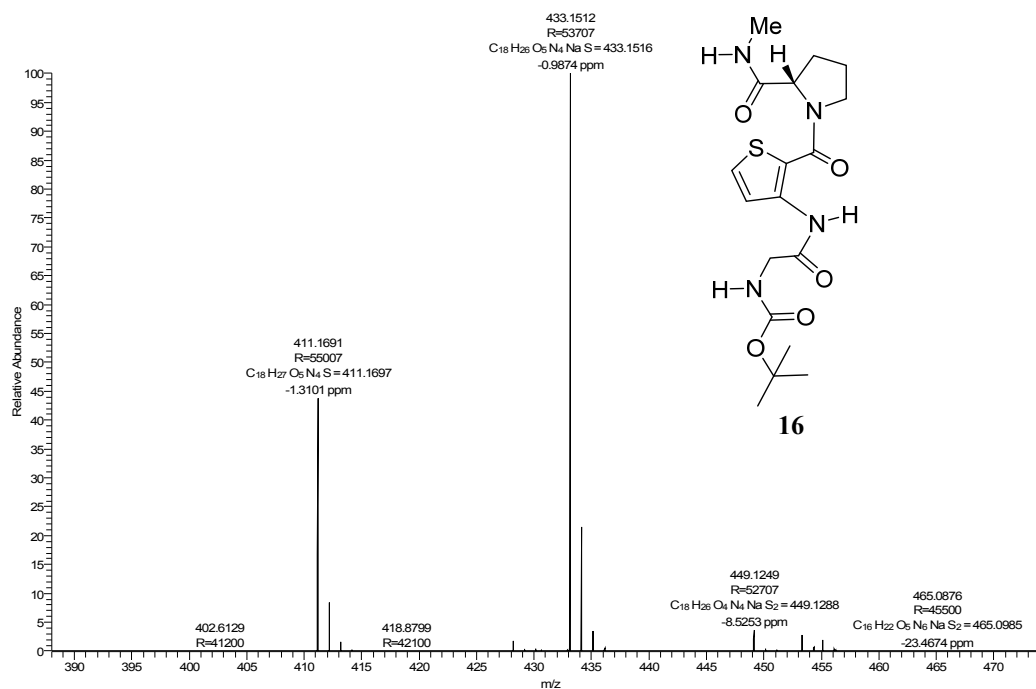
tuka_24 #111 RT: 0.50 AV: 1 NL: 1.12E9
T: FTMS + p ESI Full ms [85.40-1281.00]

HRMS



TUKA-4-TRIN-IME #884 RT: 3.94 AV: 1 NL: 1.14E9
T: FTMS + p ESI Full ms [150.00-2250.00]

HRMS

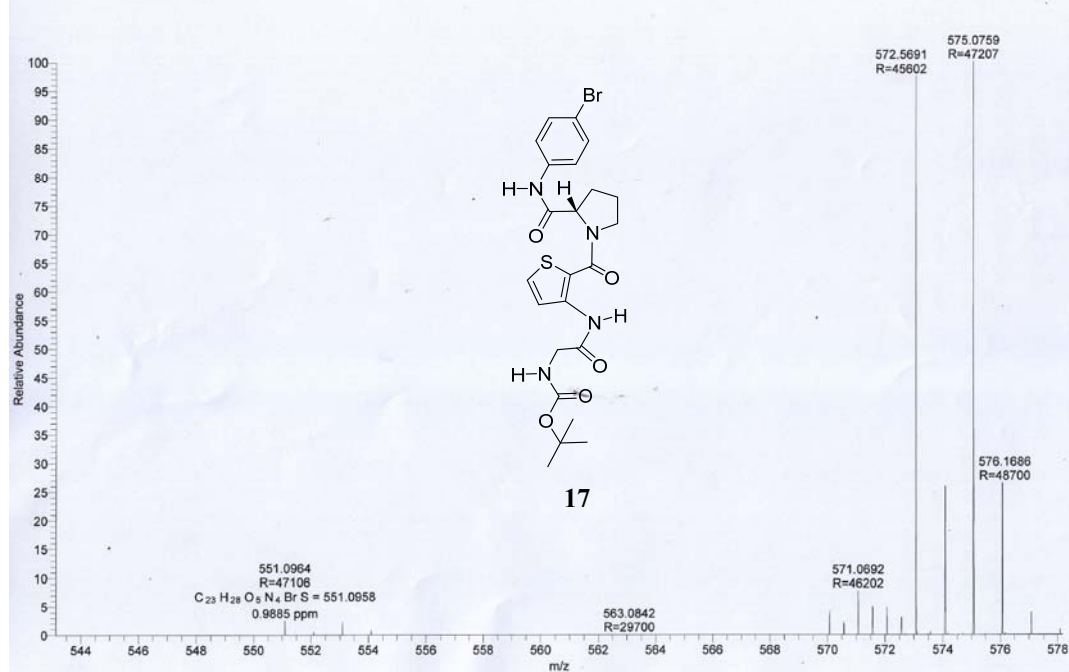


D:\Data\tuka_25

3/16/2015 2:17:53 PM

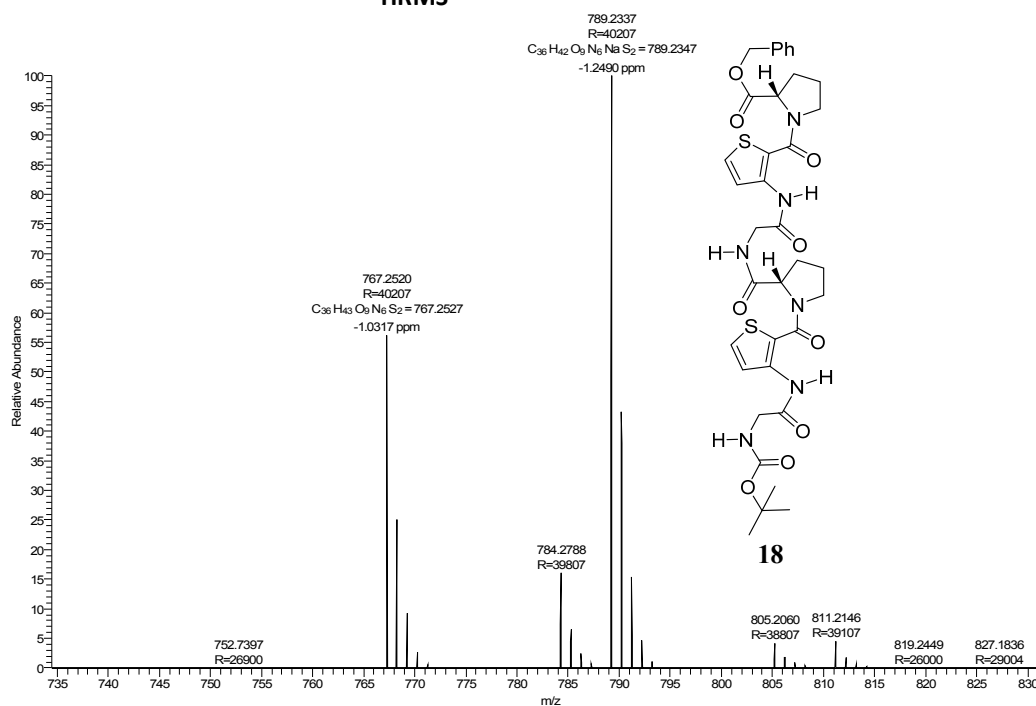
tuka_25 #115 RT: 0.52 AV: 1 NL: 2.76E8
T: FTMS + p ESI Full ms [85.40-1281.00]

HRMS



TUKA-3-HEX-PRV #961 RT: 4.28 AV: 1 NL: 5.53E8
T: FTMS + p ESI Full ms [150.00-2250.00]

HRMS

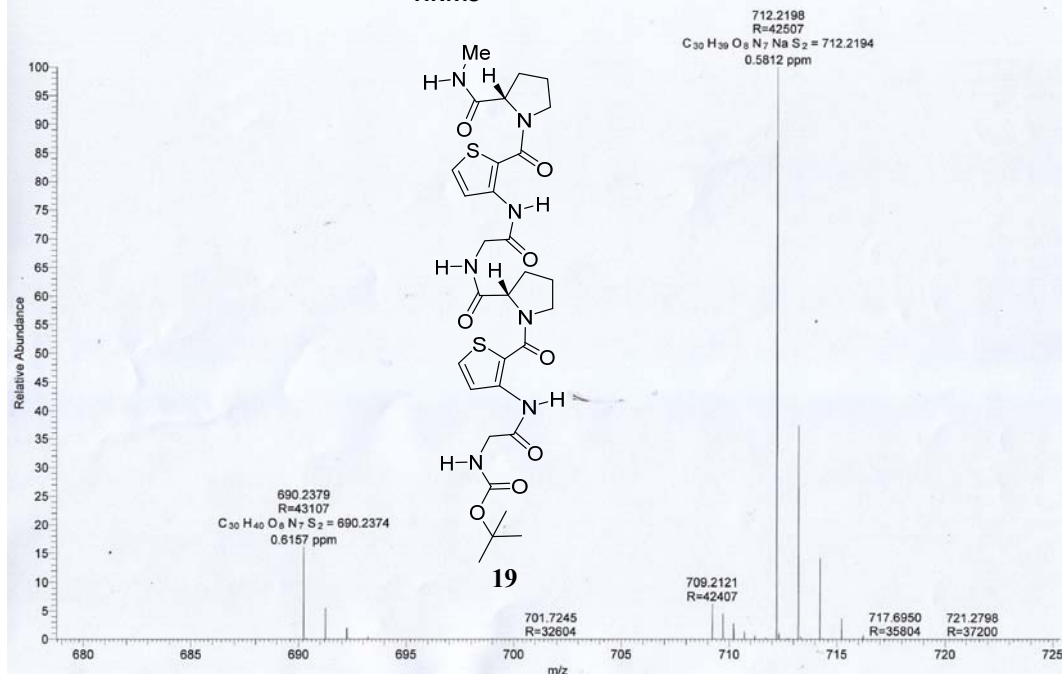


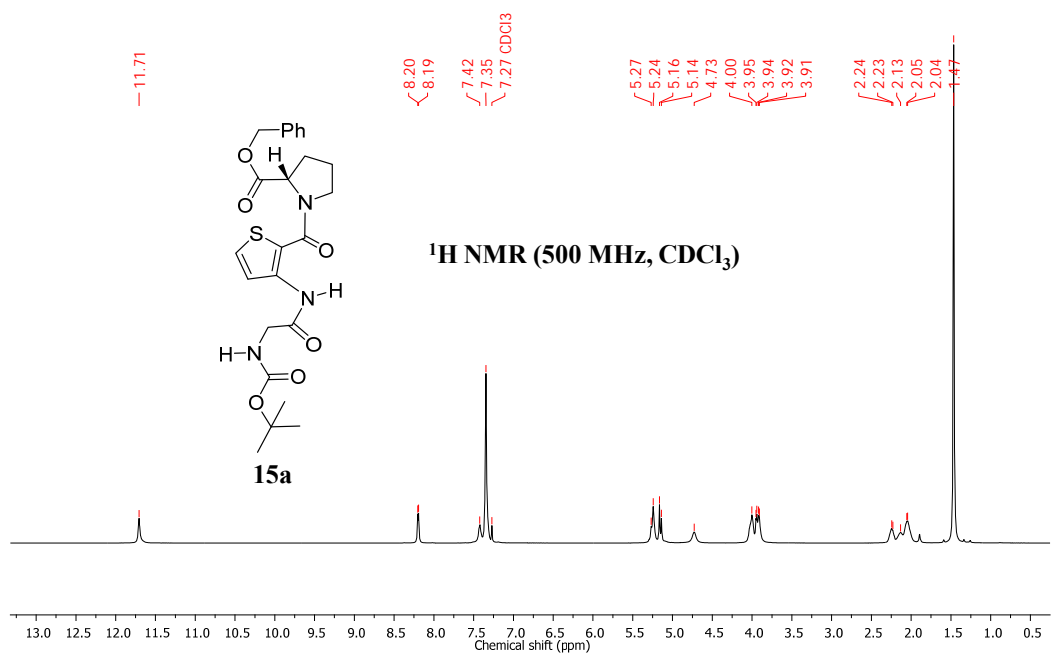
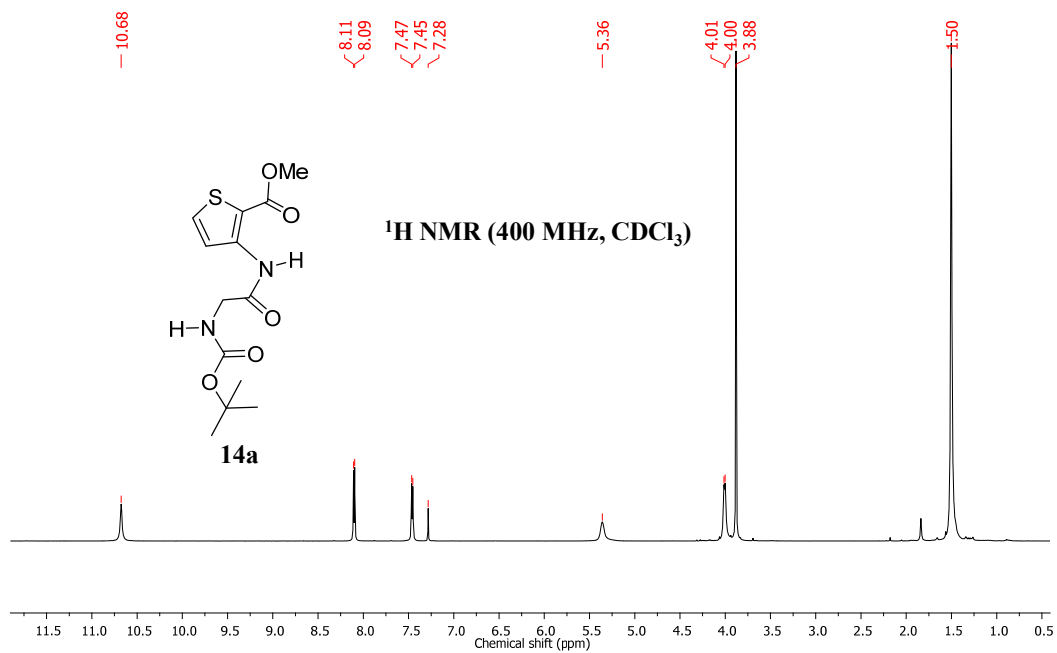
D:\Data\tuka_26

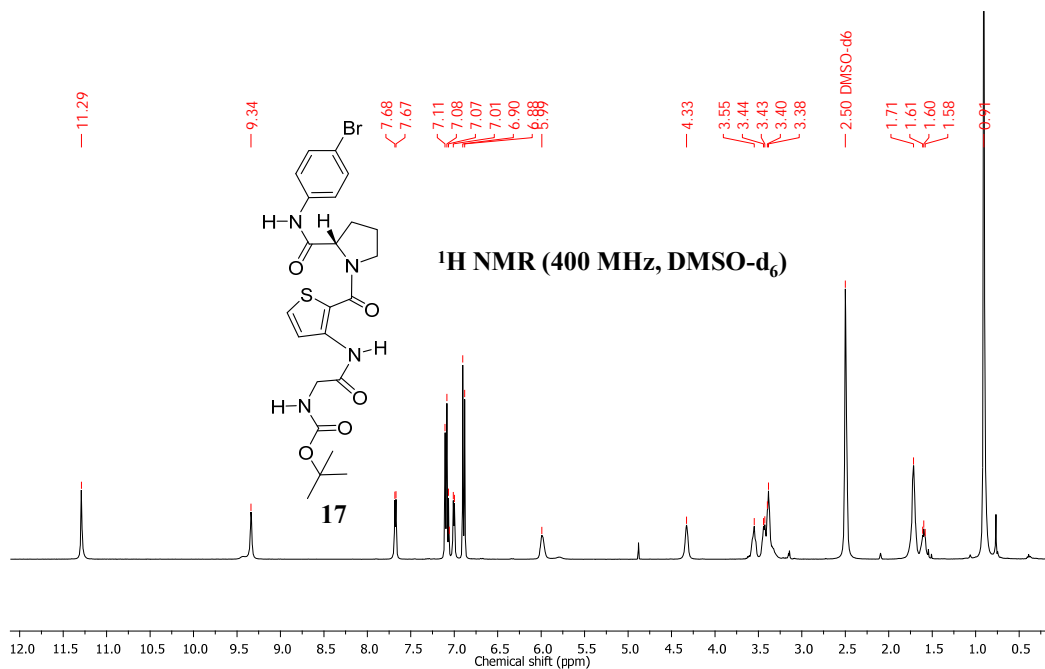
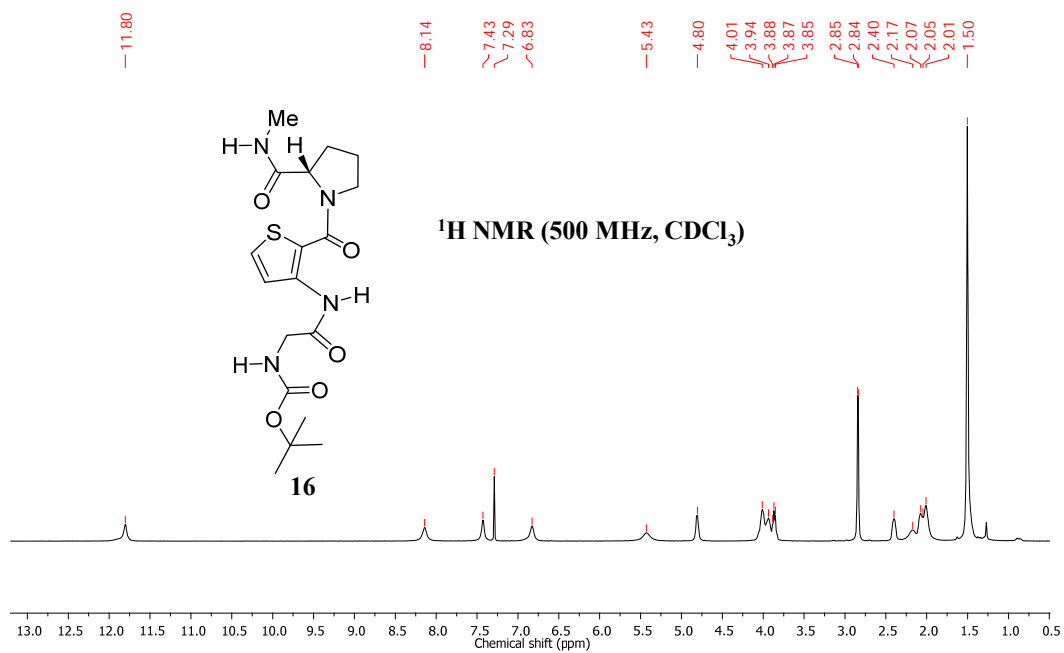
3/16/2015 2:23:01 PM

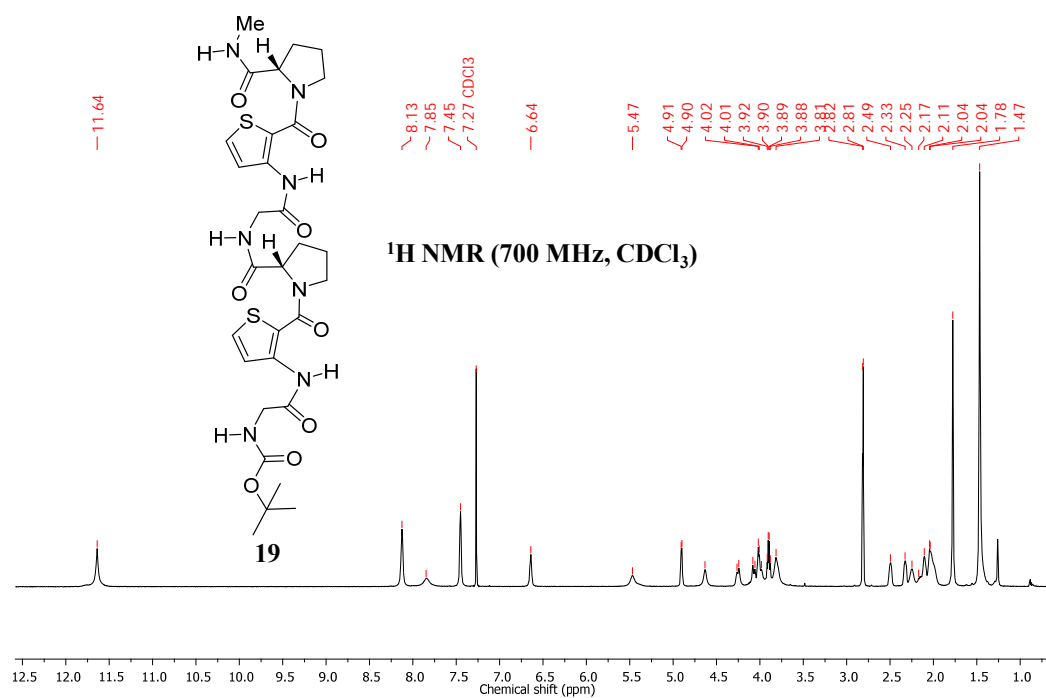
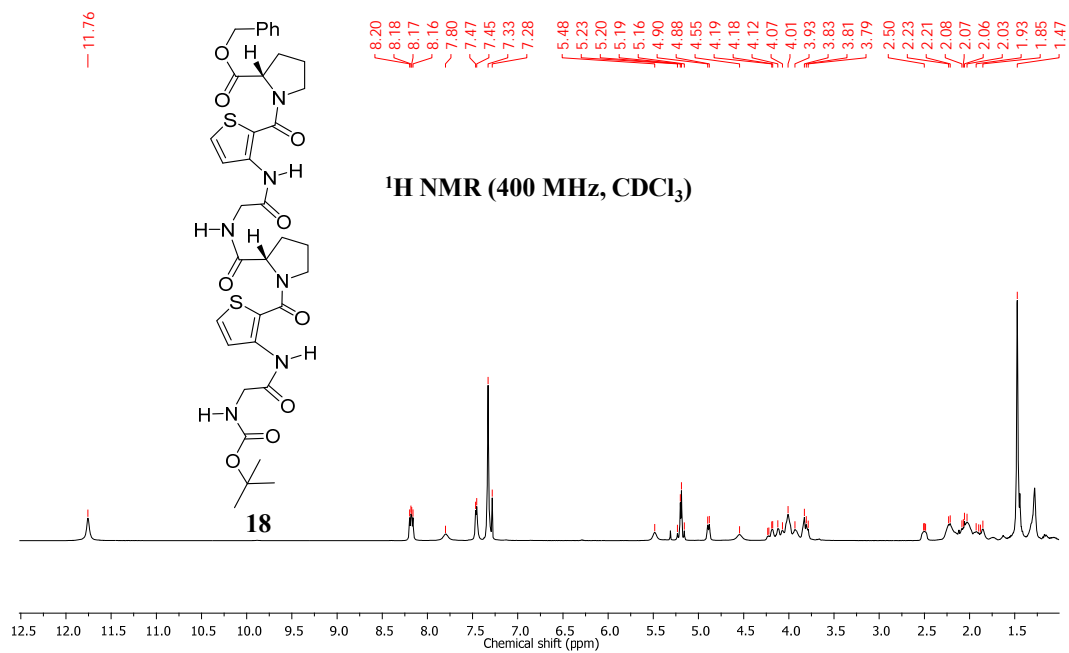
tuka_26 #93 RT: 0.42 AV: 1 NL: 6.54E8
T: FTMS + p ESI Full ms [85.40-1281.00]

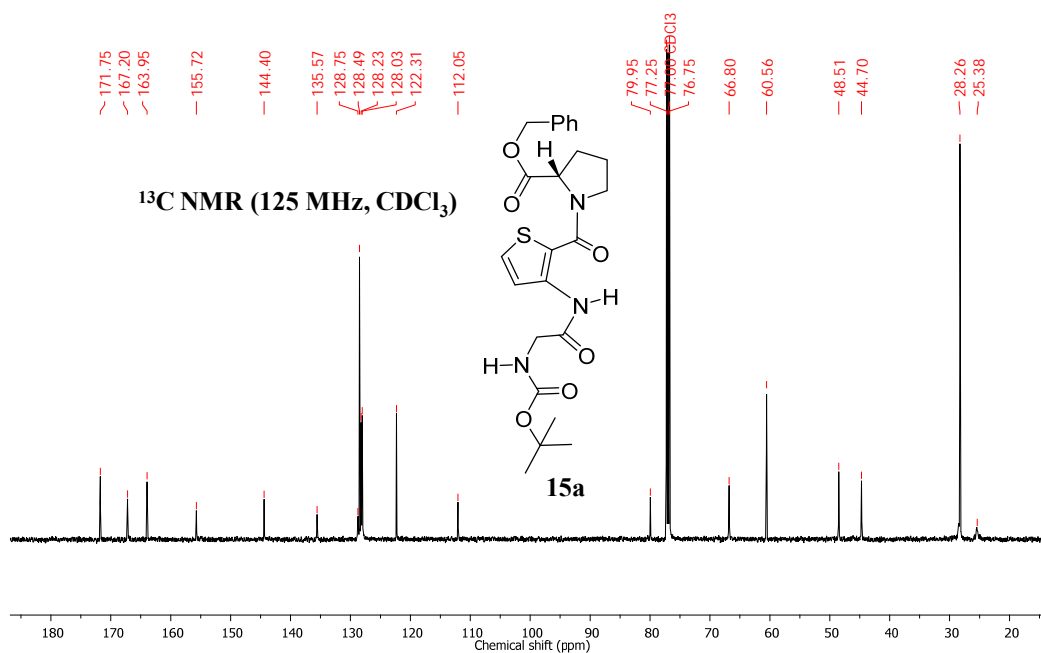
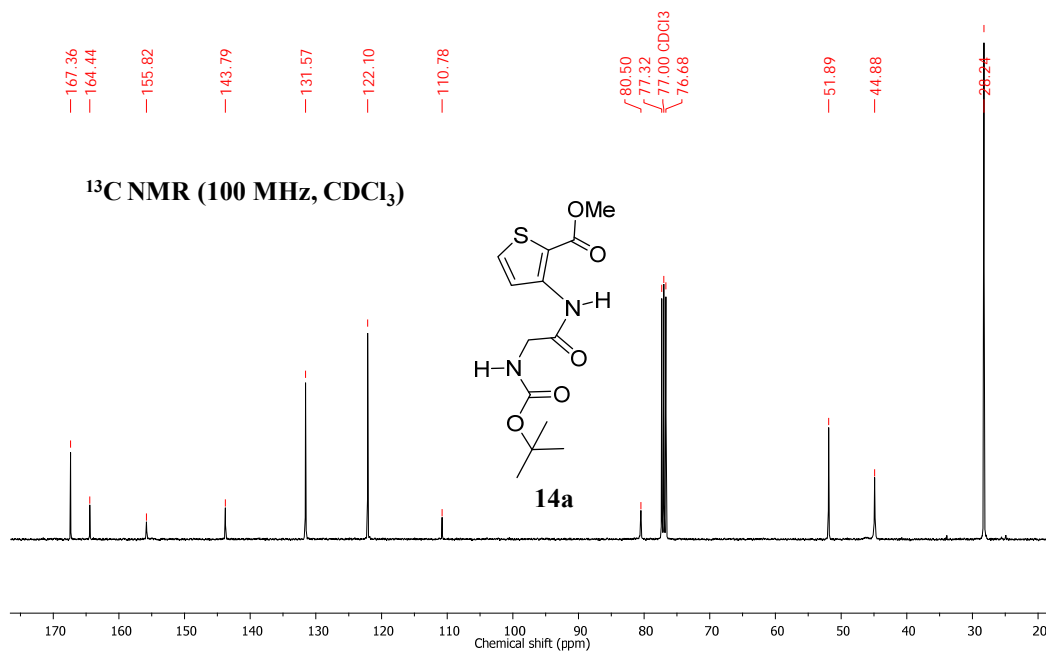
HRMS

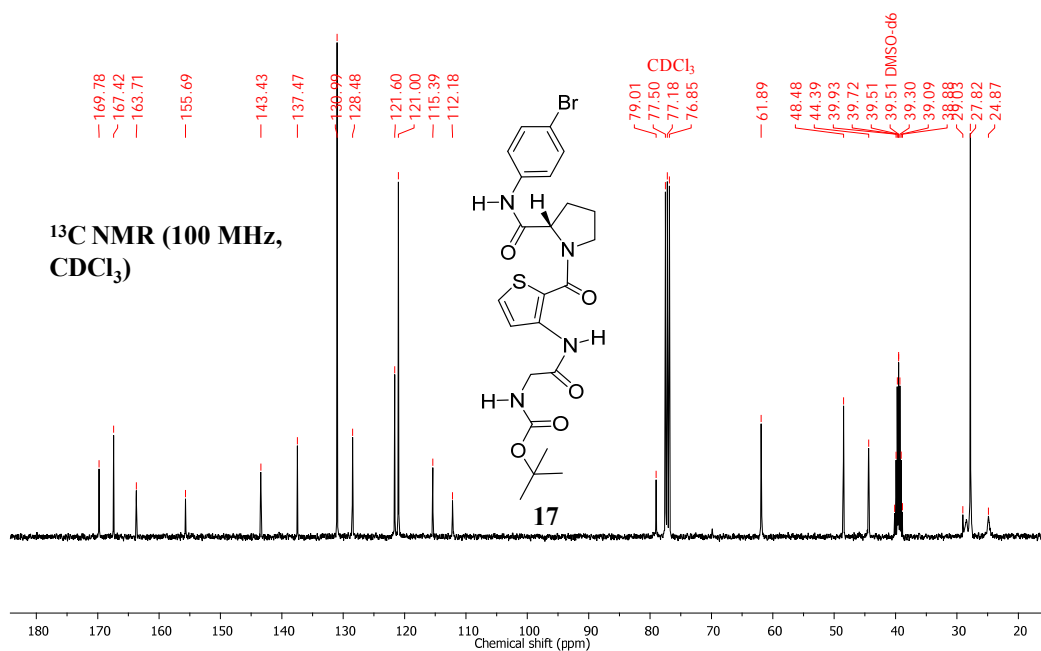
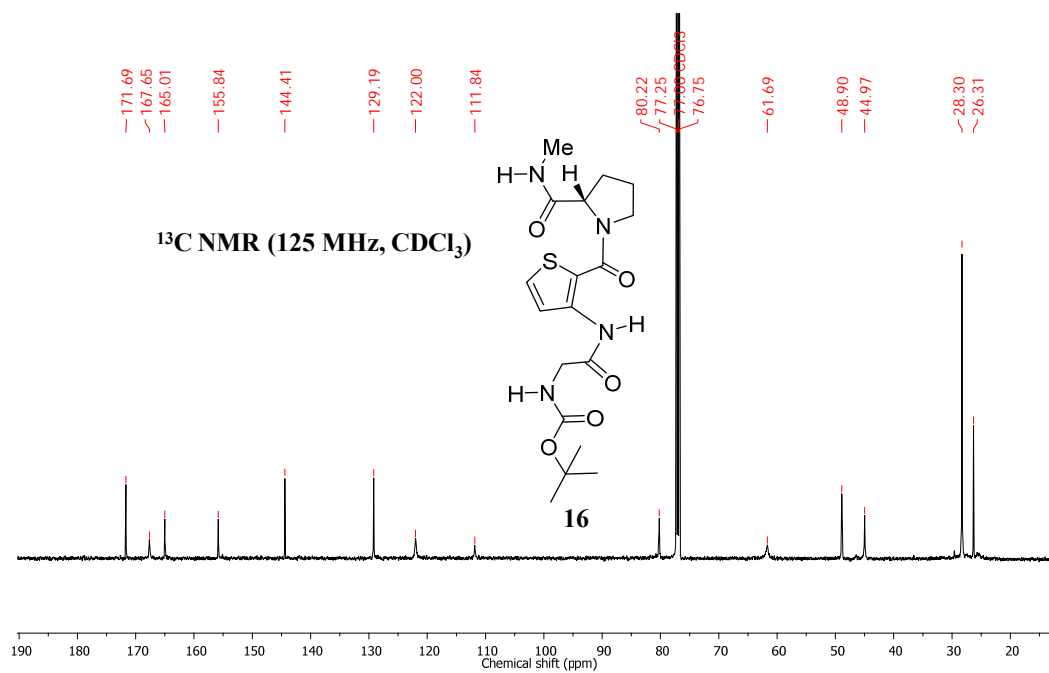












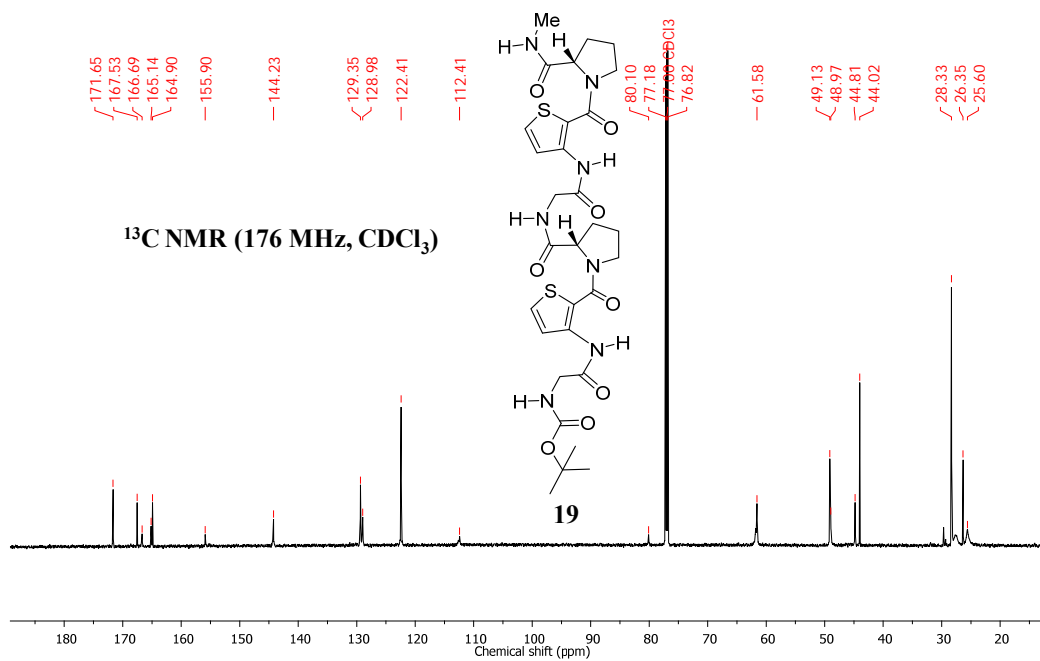
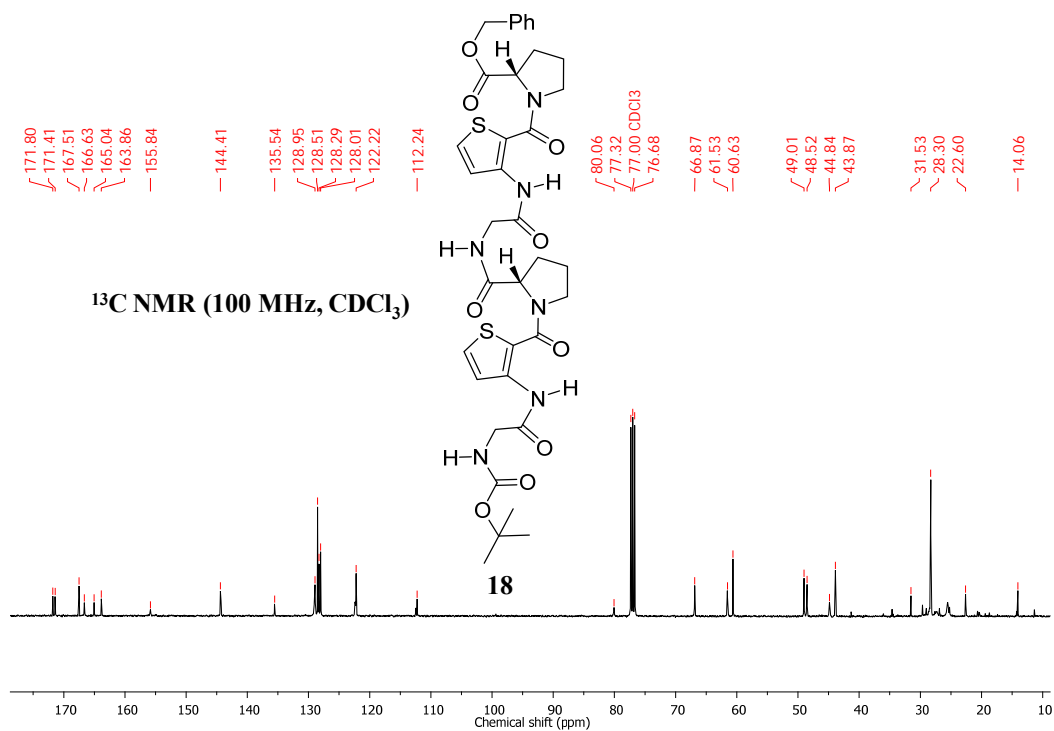


Table 1.5 Titration study of 15a in CDCl₃ (5 mM, 400 MHz) with DMSO-*d*₆ (Volume of DMSO-*d*₆ added at each addition = 5 μL)

No	Volume of DMSO- <i>d</i> ₆ (μL)	Chemical Shift δ (ppm)	
		NH1	NH2
1	0	5.15	11.69
2	5	5.2	11.68
3	10	5.25	11.67
4	15	5.3	11.66
5	20	5.38	11.64
6	25	5.43	11.64
7	30	5.48	11.62
8	35	5.54	11.61
9	40	5.6	11.6
10	45	5.65	11.59
11	50	5.7	11.58

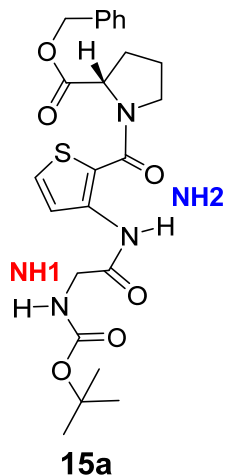


Table 1.6 Titration study of 16 in CDCl₃ (5 mM, 400 MHz) with DMSO-*d*₆ (Volume of DMSO-*d*₆ added at each addition = 5 μL)

No	Volume of DMSO- <i>d</i> ₆ (μL)	Chemical Shift δ (ppm)		
		NH1	NH2	NH3
1	0	5.2	11.77	6.69
2	5	5.27	11.75	6.72
3	10	5.32	11.75	6.75
4	15	5.42	11.73	6.8
5	20	5.48	11.71	6.83
6	25	5.57	11.69	6.87
7	30	5.63	11.68	6.9
8	35	5.7	11.66	6.93
9	40	5.74	11.65	6.95
10	45	5.81	11.63	6.97
11	50	5.84	11.62	6.99

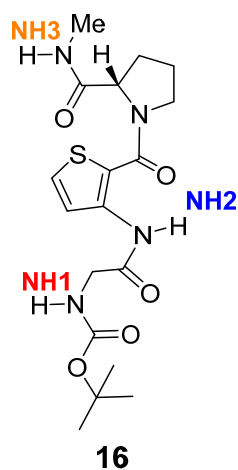


Table 1.7 Titration study of **19** in CDCl_3 (5 mM, 400 MHz) with $\text{DMSO-}d_6$ (Volume of $\text{DMSO-}d_6$ added at each addition = 5 μL)

No	Volume of $\text{DMSO-}d_6$ (μL)	Chemical Shift δ (ppm)				
		NH1	NH2	NH3	NH4	NH5
1	0	5.43	11.69	7.85	11.69	6.58
2	5	5.48	11.66	7.85	11.66	6.66
3	10	5.53	11.63	7.87	11.63	6.72
4	15	5.59	11.6	7.87	11.6	6.78
5	20	5.62	11.59	7.87	11.59	6.82
6	25	5.68	11.56	7.88	11.58	6.86
7	30	5.72	11.54	7.88	11.57	6.89
8	35	5.75	11.52	7.88	11.56	6.93
9	40	5.81	11.5	7.89	11.54	6.95
10	45	5.84	11.49	7.89	11.53	6.98
11	50	5.87	11.47	7.89	11.52	7

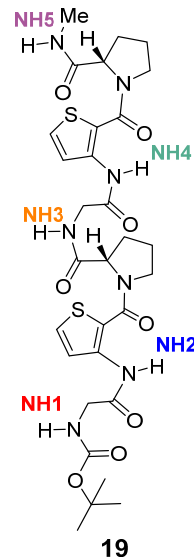


Table 1.8 Variable temperature study of **15a** (5 mM, 400 MHz, CDCl_3)

No	Temperature (K)	Chemical Shift δ in ppm	
		NH1	NH2
1	268	5.19	11.78
2	273	5.18	11.76
3	278	5.17	11.75
4	283	5.16	11.74
5	288	5.15	11.72
6	293	5.15	11.71
7	298	5.14	11.69
8	303	5.13	11.68
9	308	5.13	11.66
10	313	5.12	11.65
11	318	5.1	11.63
12	323	5.09	11.62

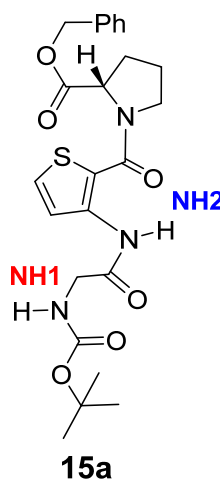
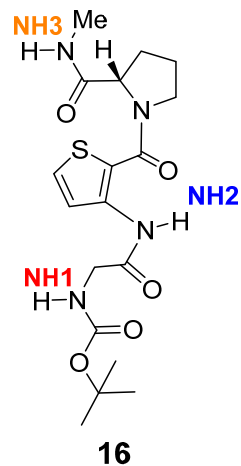
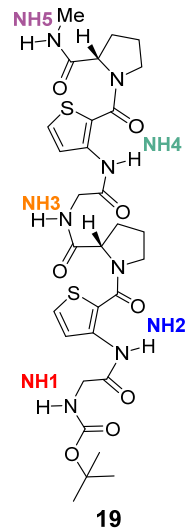


Table 1.9 Variable temperature study of 16 (5 mM, 400 MHz, CDCl₃)

No	Temperature (K)	Chemical Shift δ in ppm		
		NH1	NH2	NH3
1	268	5.25	11.88	6.79
2	273	5.25	11.87	6.78
3	278	5.24	11.85	6.76
4	283	5.24	11.83	6.74
5	288	5.23	11.81	6.72
6	293	5.22	11.8	6.71
7	298	5.2	11.77	6.69
8	303	5.19	11.76	6.67
9	308	5.18	11.74	6.65
10	313	5.18	11.73	6.64
11	318	5.15	11.71	6.63
12	323	5.14	11.69	6.61

Table 1.10 Variable temperature study of 19 (5 mM, 400 MHz, CDCl₃)

No	Temperature (K)	Chemical Shift δ in ppm				
		NH1	NH2	NH3	NH4	NH5
1	268	5.62	11.75	8.01	11.84	6.66
2	273	5.58	11.75	7.98	11.81	6.65
3	278	5.56	11.74	7.96	11.79	6.64
4	283	5.53	11.73	7.94	11.73	6.62
5	288	5.48	11.72	7.92	11.72	6.6
6	293	5.46	11.71	7.88	11.71	6.59
7	298	5.43	11.69	7.85	11.69	6.57
8	303	5.4	11.66	7.82	11.67	6.57
9	308	5.38	11.64	7.79	11.66	6.56
10	313	5.37	11.62	7.77	11.64	6.54
11	318	5.34	11.61	7.74	11.63	6.52
12	323	5.32	11.59	7.71	11.61	6.52



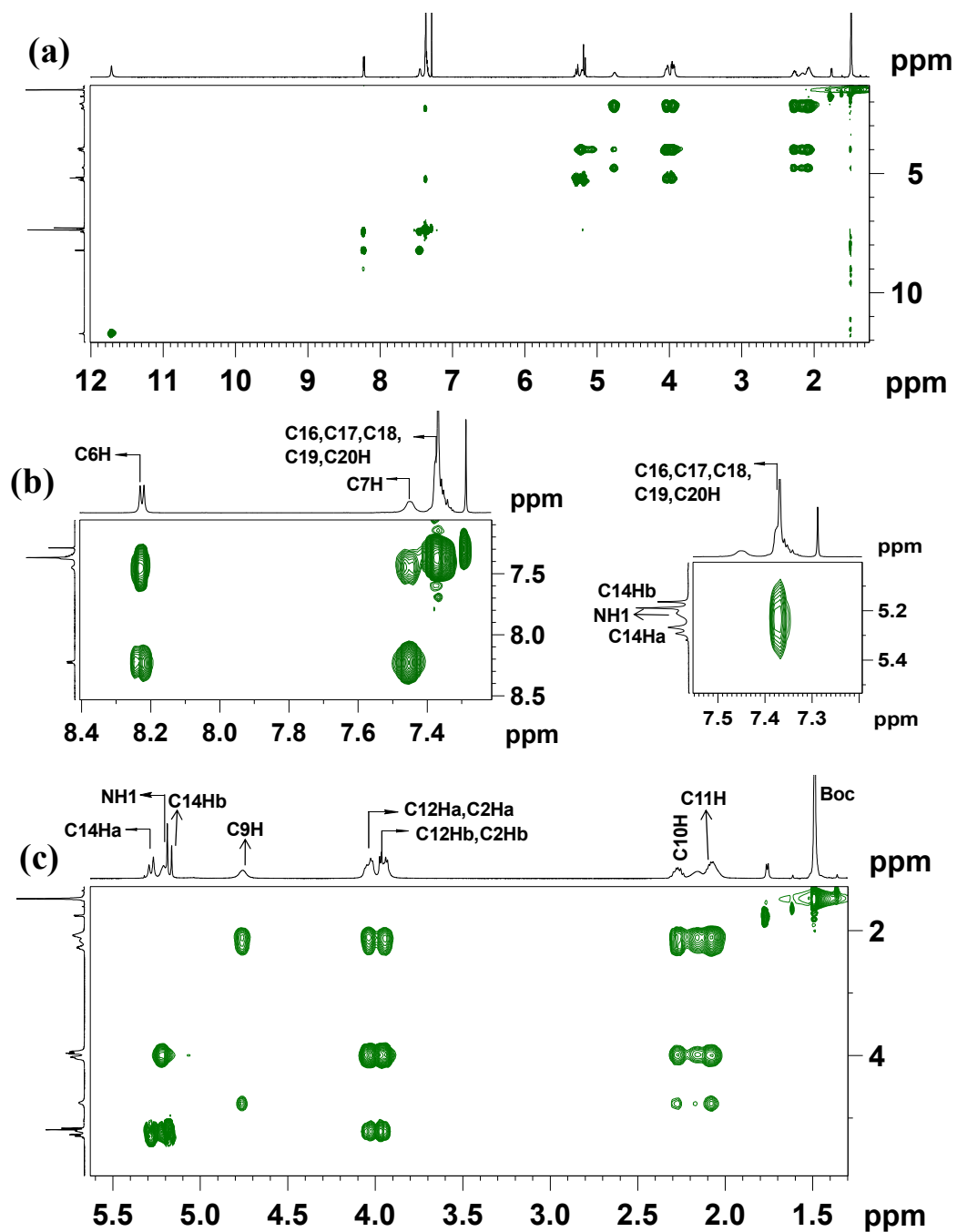


Fig. 1.35 TOCSY full spectrum of **15a** (a) (25 mM, 500 MHz, CDCl_3 , 298 K); aromatic (b) and aliphatic (c) regions shown separately.

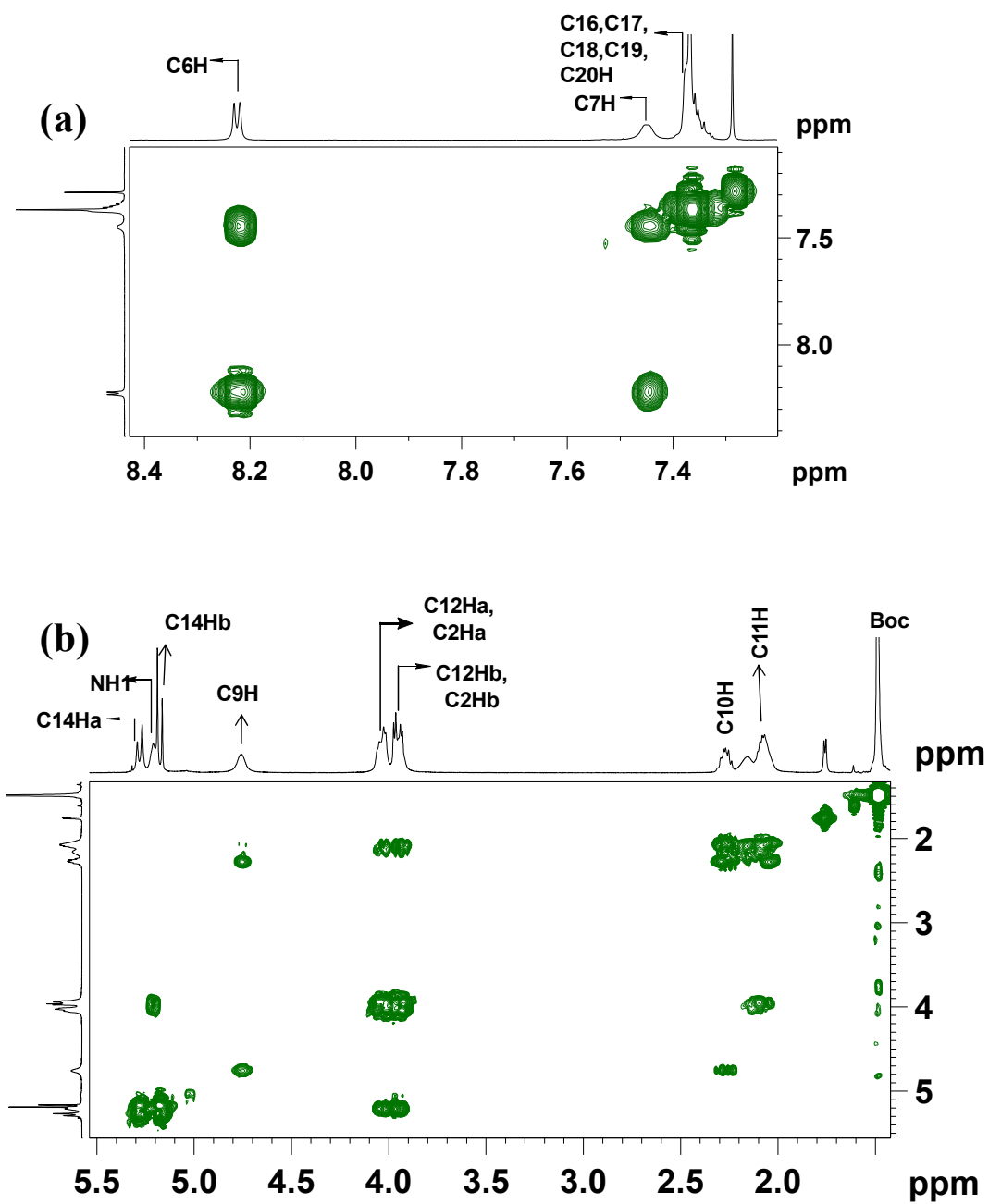


Fig. 1.36 Partial COSY spectra of **15a** (25 mM, 500 MHz, CDCl₃, 298 K); aromatic (a) and aliphatic (b) regions shown separately.

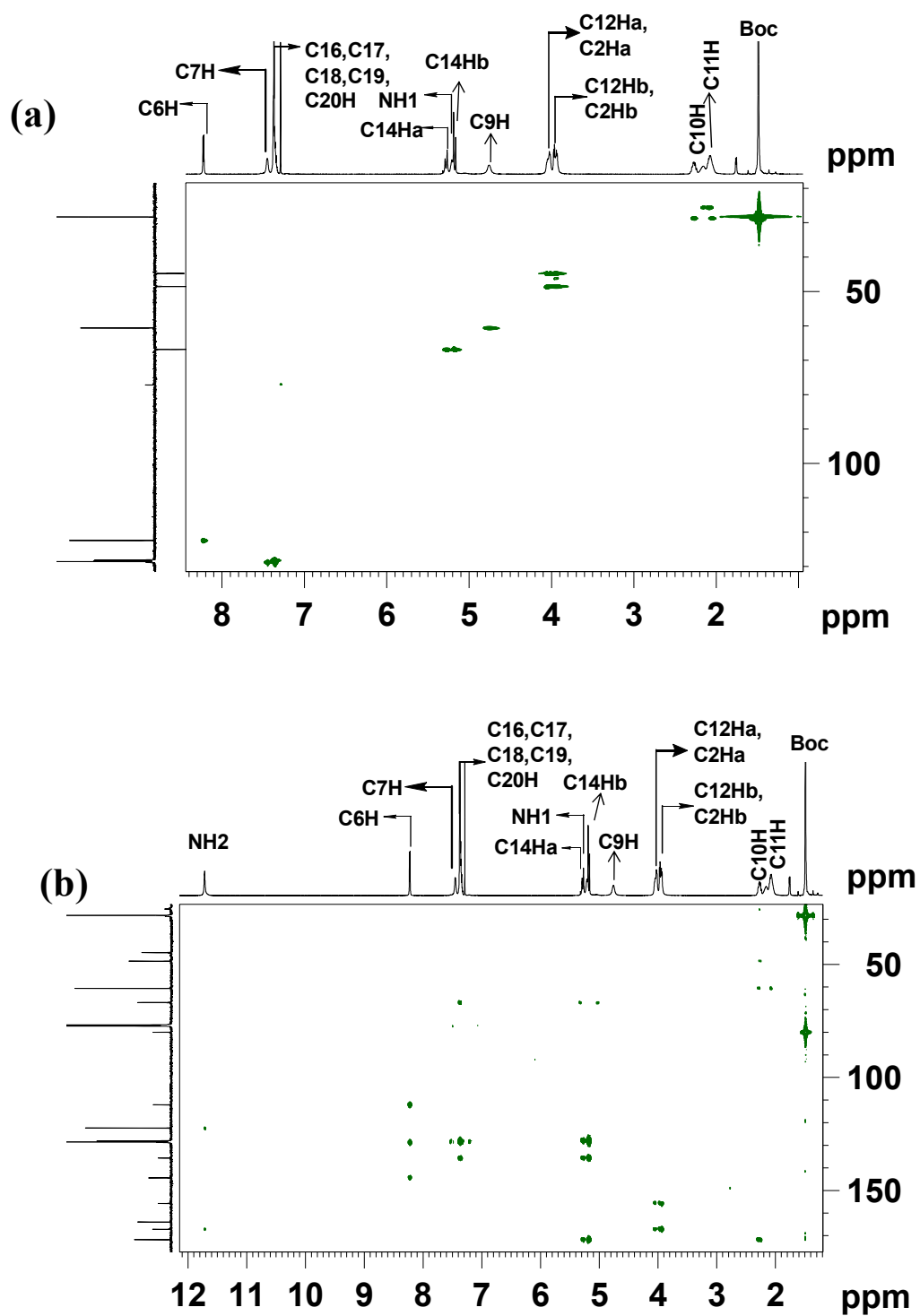


Fig. 1.37 HSQC (a) and HMBC (b) full spectra of **15a** (25 mM, 500 MHz, CDCl₃, 298 K).

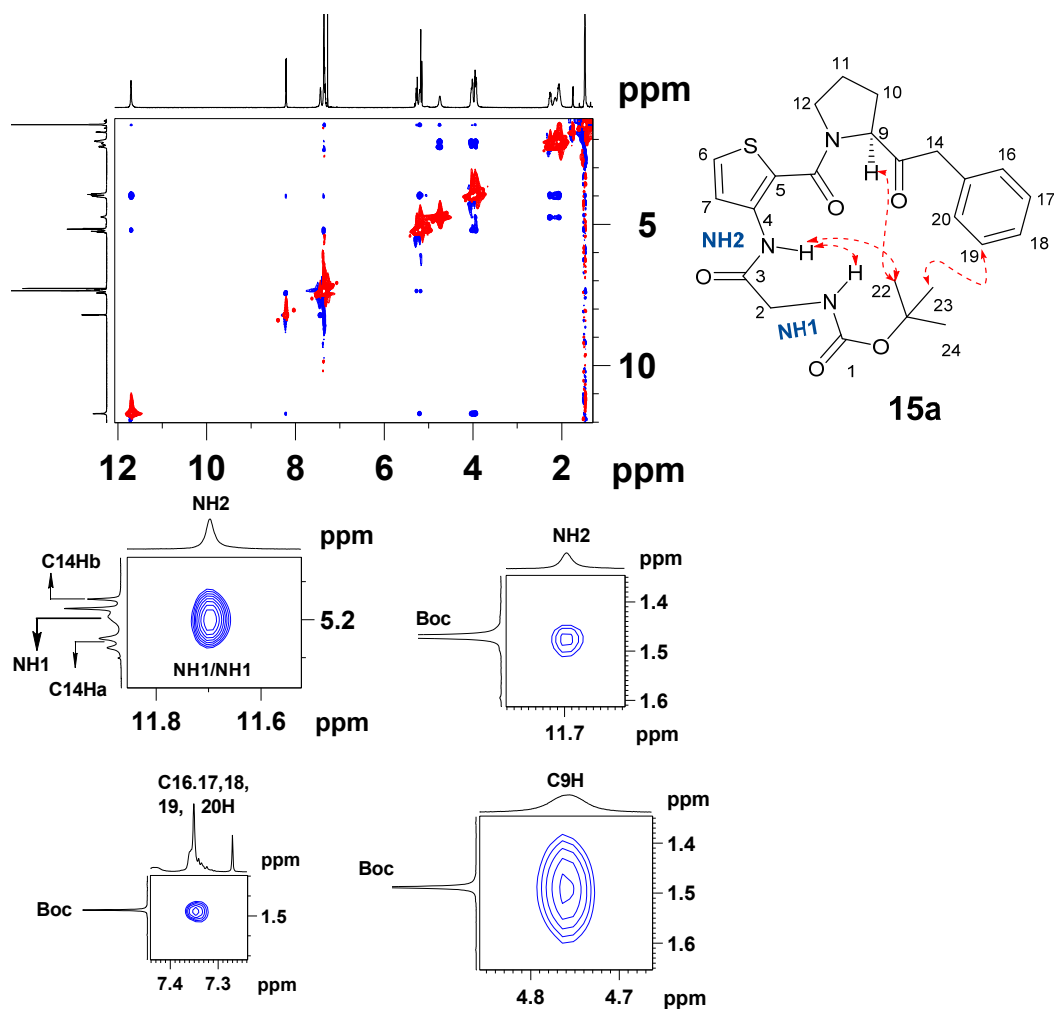


Fig. 1.38 2D NOESY full spectrum and excerpts of **15a** (25 mM, 500 MHz, CDCl_3 , 298 K).

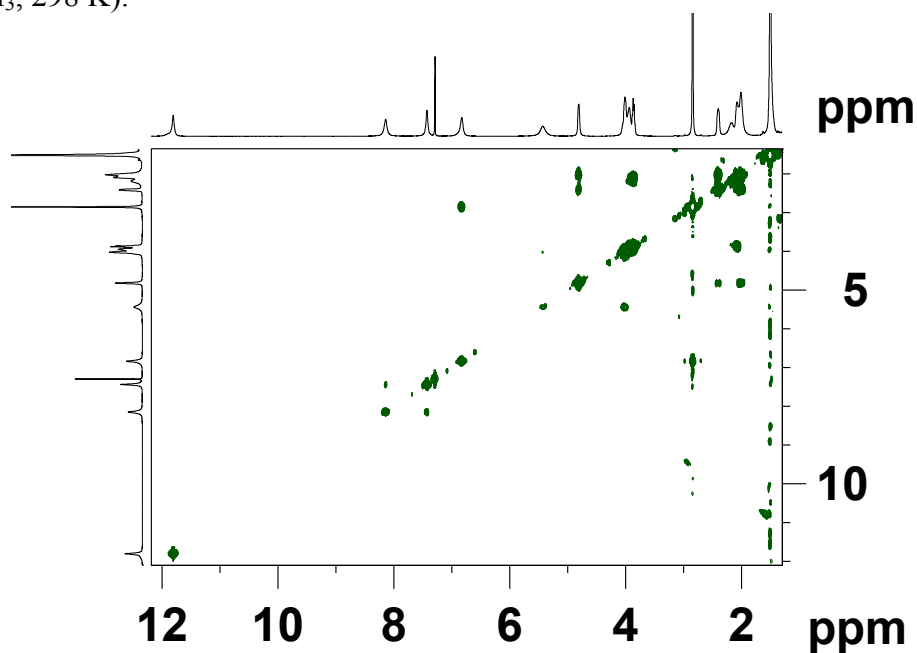


Fig. 1.39 COSY full spectrum of **16** (25 mM, 500 MHz, CDCl_3 , 298 K).

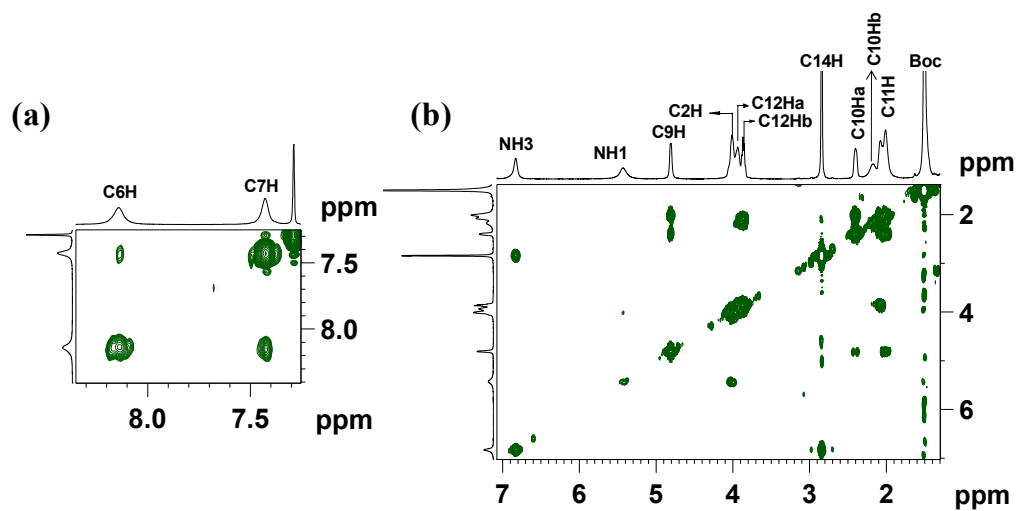


Fig. 1.40 Partial COSY spectra of **16** (25 mM, 500 MHz, CDCl_3 , 298 K); aromatic (a) and aliphatic (b) regions shown separately.

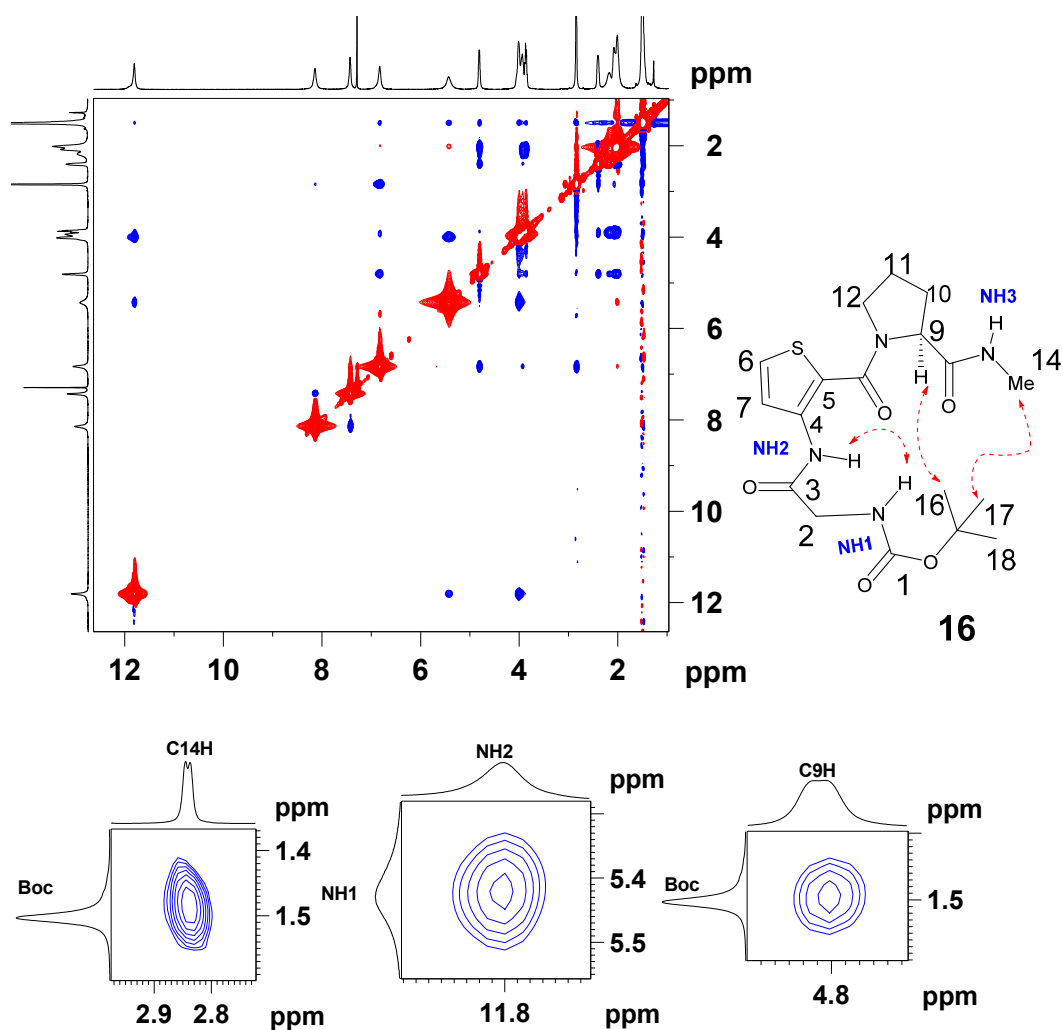


Fig. 1.41 2D NOESY full spectrum and excerpts of **16** (25 mM, 500 MHz, CDCl_3 , 298 K).

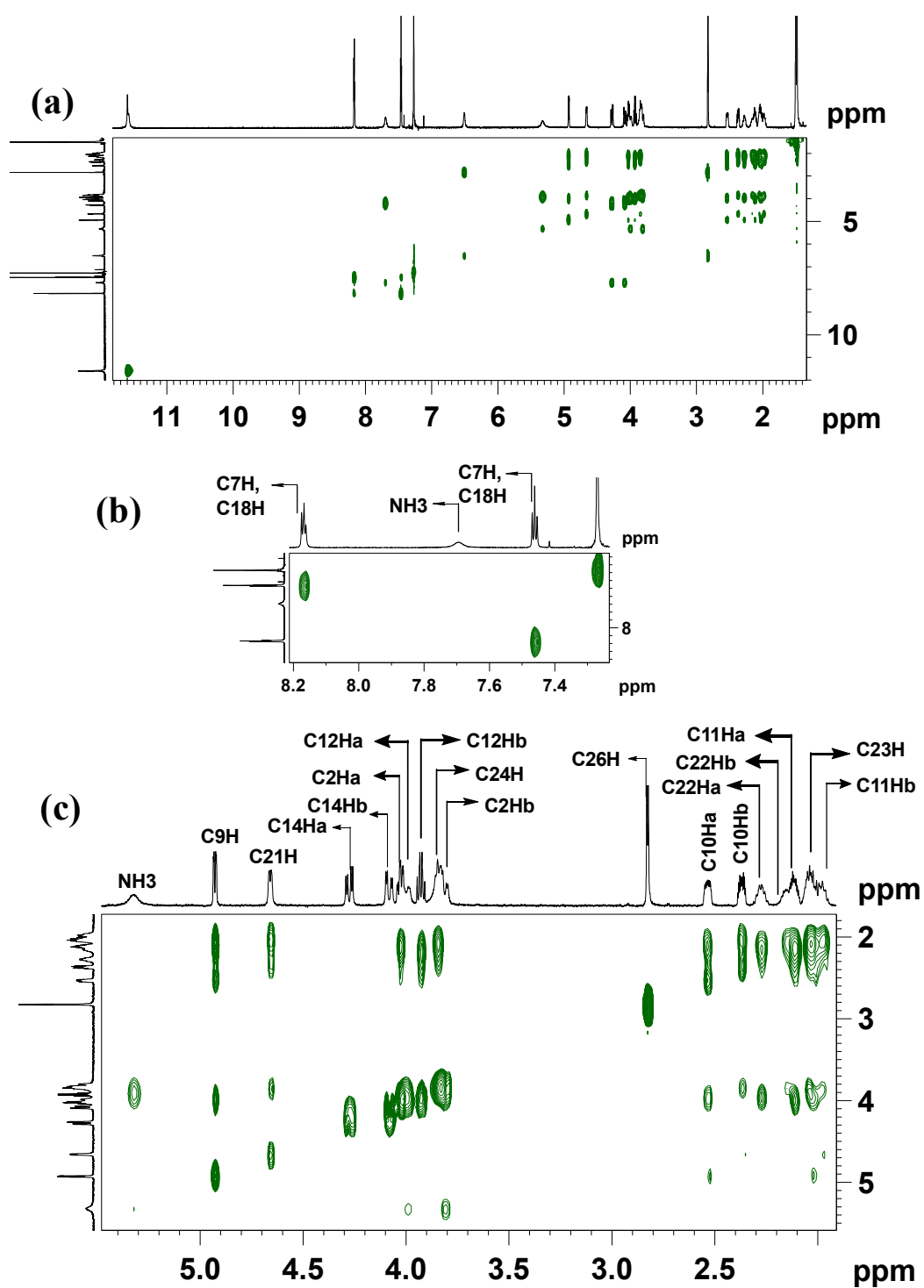


Fig. 1.42 TOCSY full spectrum of **19** (a) (6 mM, 700 MHz, CDCl_3 , 328 K); aromatic (b) and aliphatic (c) regions shown separately.

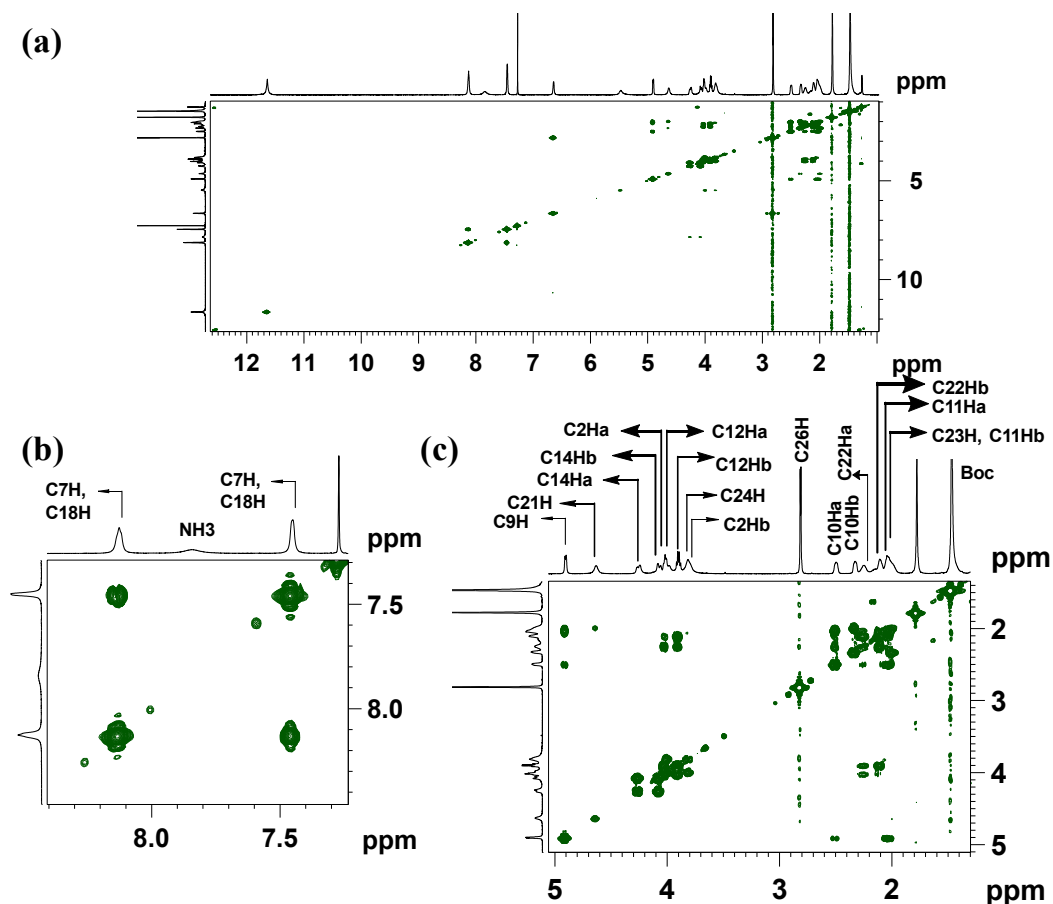


Fig. 1.43 COSY full spectrum of **19** (a) (23 mM, 700 MHz, CDCl₃, 298 K); aromatic (b) and aliphatic (c) regions shown separately.

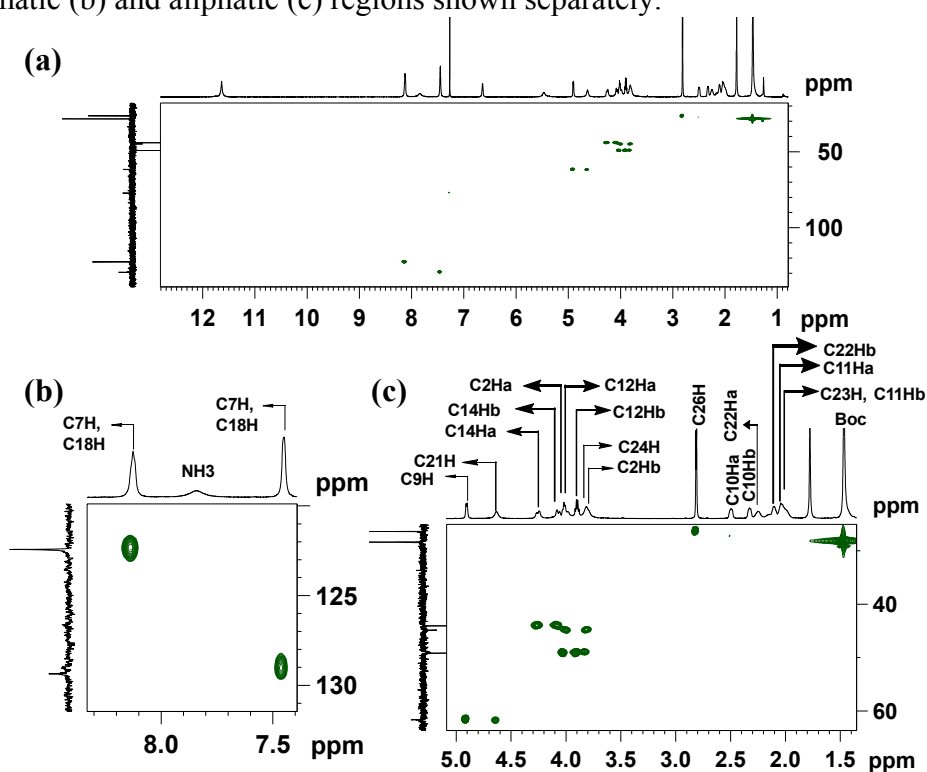


Fig. 1.44 HSQC full spectrum of **19** (a) (23 mM, 700 MHz, CDCl₃, 298 K); aromatic (b) and aliphatic (c) regions shown separately.

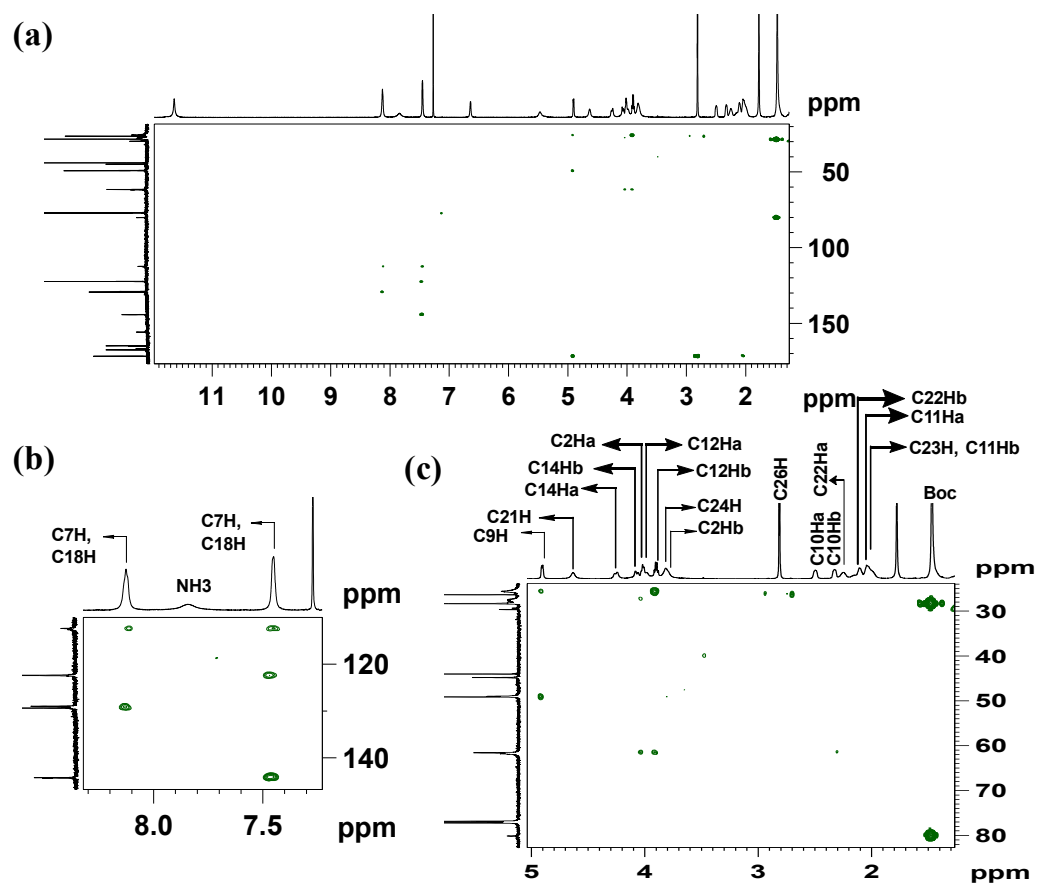


Fig. 1.45 HMBC full spectrum of **19** (23 mM, 700 MHz, CDCl_3 , 298 K); aromatic (b) and aliphatic (c) regions shown separately.

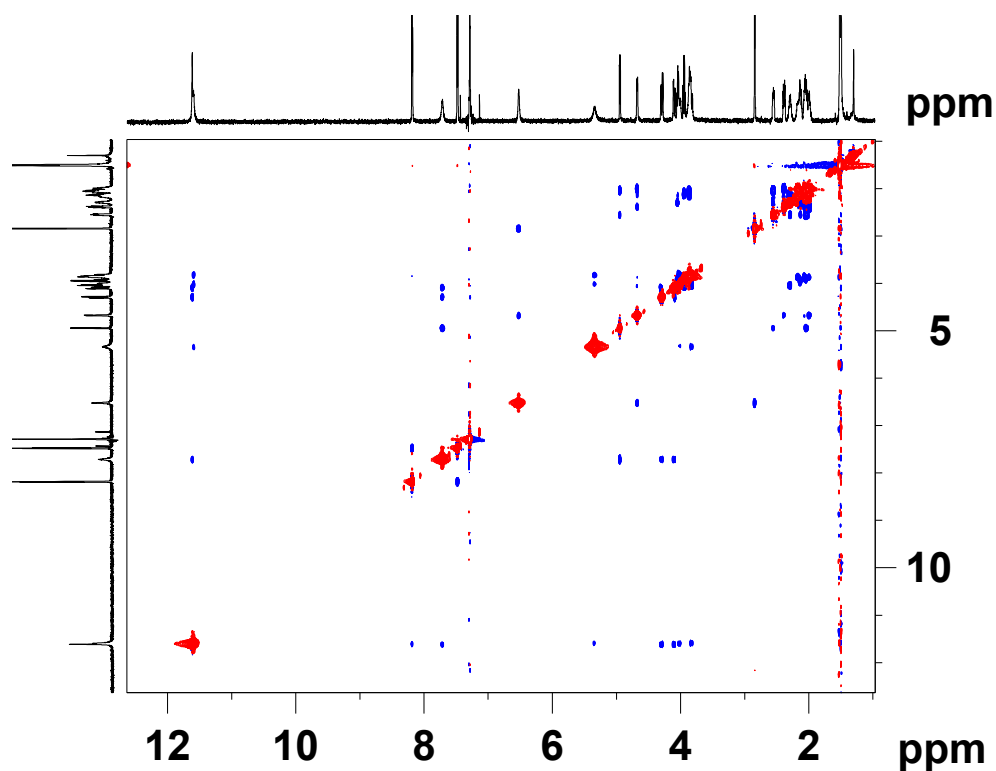


Fig. 1.46 NOESY full spectrum of **19** (6 mM, 700 MHz, CDCl_3 , 328 K).

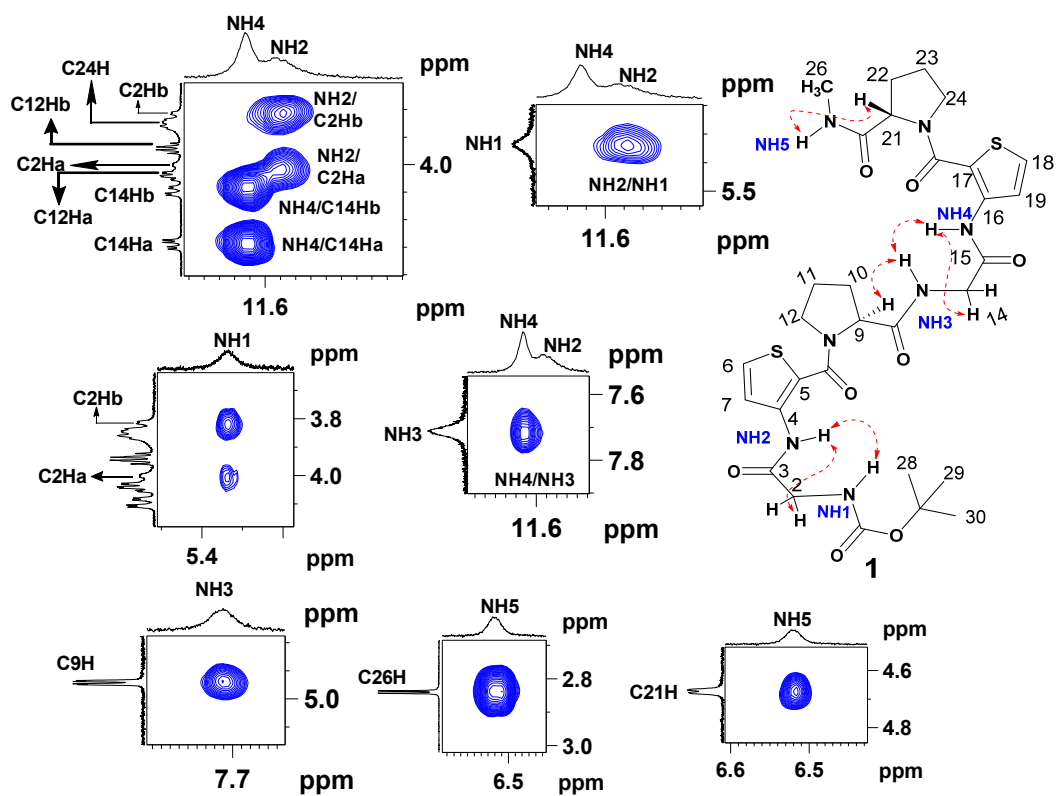


Fig. 1.47 2D NOESY extracts of **19** (6 mM, 700 MHz, CDCl₃, 328 K).

Table 1.11 nOe-derived distance constraints used in molecular modeling for structural elucidation of oligomer **19**.

Atom I	Atom II	Chemical Shift I	Chemical Shift II	Upper Bound	Lower Bound
C19H	NH4	8.178	11.614	3.615	2.958
NH3	NH4	7.721	11.614	3.229	2.642
NH1	NH2	5.327	11.601	3.473	2.842
C14Ha	NH4	4.292	11.614	3.206	2.623
C14Hb	NH4	4.100	11.614	3.264	2.670
C2Ha	NH2	3.987	11.601	3.175	2.598
C2Hb	NH2	3.828	11.601	3.326	2.721
C9H	NH3	4.935	7.721	2.822	2.309
C14Ha	NH3	4.292	7.721	3.433	2.809
C14Hb	NH3	4.100	7.721	3.187	2.607
C21H	NH5	4.663	6.514	3.204	2.622
C2Ha	NH1	3.987	5.327	3.418	2.797
C2Hb	NH1	3.828	5.327	3.227	2.640
C26H	NH5	2.833	6.514	2.787	2.280
C10Ha	C9H	2.541	4.935	3.538	2.895
C23H	C21H	1.991	4.663	3.003	2.457
Boc	NH3	1.487	7.721	4.571	3.740
Boc	NH1	1.487	5.327	4.941	4.042

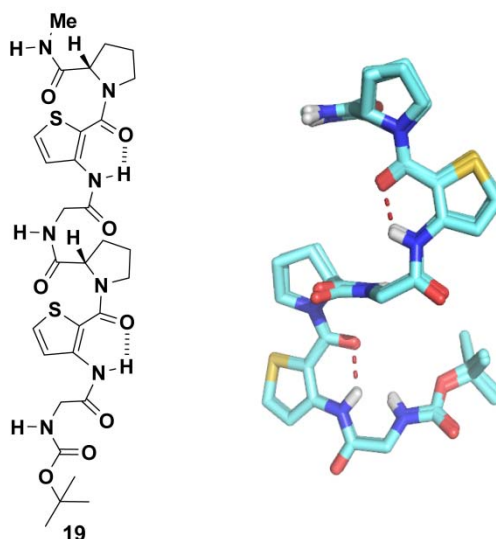


Fig. 1.48 Molecular structure of hexapeptide **19** displaying observed hydrogen bonding and its superimposed 20 energy minimized structures generated by nOe-restrained MD simulation.

1.15 References and notes

- (1) (a) C. B. Anfinsen, *Science*, 1973, **181**, 223; (b) L. M. Salonen, M. Ellermann and F. Diederich, *Angew. Chem. Int. Ed.*, 2011, **50**, 4808; (c) K. U. Linderström-Lang, “*Proteins and Enzymes*”, Lane Medical Lectures, Stanford University Publications, University Series, Medical Sciences, Stanford University Press, 1952, **6**.
- (2) (a) A. Karshikoff, *Non-covalent interactions in proteins*, Imperial College Press, United Kingdom, 2006; (b) J. P. Hendrick and F. U. Hartl, *Annu. Rev. Biochem.*, 1993, **62**, 349; (c) V. Saudek, A. Atkinson and J. T. Pelton, *Biochemistry*, 1991, **30**, 7369; (d) D. Eisenberg, *Annu. Rev. Biochem.*, 1984, **53**, 595.
- (3) (a) L. G. Presta and G. D. Rose, *Nature*, 1988, **240**, 1632; (b) C. Branden and J. Tooze, *Introduction to Protein Structure* edn 2nd Ed. New York, NY: Garland, 1998; (c) M. Fandrich, M. A. Fletcher and C. M. Dobson, *Nature*, 2001, **410**, 165; (d) D. C. Richardson and J. S. Richardson, *Proc. Natl. Acad. Sci. U. S. A.*, 2002, **99**, 2754.
- (4) (a) P. Ball, *Designing the Molecular World*, Princeton Univ. Press, Princeton, 1994; (b) J.-M. Lehn, *Supramolecular Chemistry: Concepts and Perspectives*, Wiley-VCH, Weinheim, Germany, 1995.
- (5) (a) S. H. Gellman, *Acc. Chem. Res.*, 1998, **31**, 173; (b) D. Seebach, A. K. Beck and D. J. Bierbaum, *Chem. Biodiversity*, 2004, **1**, 1111; (c) D. J. Hill; M. J. Mio, R. B. Prince, T. S. Hughes and J. S. Moore, *Chem. Rev.*, 2001, **101**, 3893; (d) C. M Goodman, S. Choi, S. Shandler and W. F DeGrado, *Nat. Chem. Biol.*, 2007, **3**, 252.
- (6) (a) D. Seebach and J. Gardiner, *Acc. Chem. Res.*, 2008, **41**, 1366; (b) P. G. Vasudev, S. Chatterjee, N. Shamala and P. Balaram, *Chem. Rev.*, 2011, **111**, 657; (c) I. Avan, C. D. Hall and A. R. Katritzky, *Chem. Soc. Rev.*, 2014, **43**, 3575; (d) A. Roy, P. Prabhakaran, P. K. Baruah and G. J. Sanjayan, *Chem. Commun.*, 2011, **47**, 11593.
- (7) (a) T. Hintermann and D. Seebach, *Chimia*, 1997, **51**, 244; (b) D. L. Steer, R. A. Lew, P. Perlmutter, A. I. Smith and M. I. Aguilar, *Curr. Med. Chem.*, 2002, **9**, 811.

-
-
- (8) S. H. Choi, I. A. Guzei, L. C. Spencer and S. H. Gellman, *J. Am. Chem. Soc.*, 2009, **131**, 2917.
- (9) J. J. Barchi Jr., X. Huang, D. H. Appella, L. A. Christianson, S. R. Durell and S. H. Gellman, *J. Am. Chem. Soc.*, 2000, **122**, 2711.
- (10) D. H. Appella, L. A. Christianson, I. L. Karle, D. R. Powell and S. H. Gellman, *J. Am. Chem. Soc.*, 1996, **118**, 13071.
- (11) D. H. Appella, L. A. Christianson, D. A. Klein, D. R. Powell, X. Huang, J. J. Barchi, Jr. and S. H. Gellman, *Nature*, 1997, **387**, 381.
- (12) S. H. Choi, I. A. Guzei, L. C. Spencer and S. H. Gellman, *J. Am. Chem. Soc.*, 2009, **131**, 2917.
- (13) C. Fernandes, S. Faure, E. Pereira, V. Thery, V. Declerck, R. Guillot and D. J. Aitken, *Org. Lett.*, 2010, **12**, 3606.
- (14) A. Altmayer-Henzien, V. Declerck, J. Farjon, D. Merlet, R. Guillot and D. J. Aitken, *Angew. Chem. Int. Ed.*, 2015, **54**, 10807.
- (15) S. D. Pol, C. Zorn, C. D. Klein, O. Zerbe and O. Reiser, *Angew. Chem. Int. Ed.*, 2004, **43**, 511.
- (16) P. Prabhakaran, S. S. Kale, V. G. Puranik, P. R. Rajamohanan, O. Chetina, J. A. K. Howard, H. J. Hofmann and G. J. Sanjayan, *J. Am. Chem. Soc.*, 2008, **130**, 17743.
- (17) (a) V. V. E. Ramesh, S. S. Kale, A. S. Kotmale, R. L. Gawade, V. G. Puranik, P. R. Rajamohanan and G. J. Sanjayan, *Org. Lett.*, 2013, **15**, 1504; (b) S. S. Kale, S. M. Kunjir, R. L. Gawade, V. G. Puranik, P. R. Rajamohanan and G. J. Sanjayan, *Chem. Commun.*, 2014, **50**, 2886.
- (18) J. L. Price, W. S. Horne and S. H. Gellman, *J. Am. Chem. Soc.*, 2010, **132**, 12378.
- (19) D. S. Daniels, E. J. Petersson, J. X. Qiu and A. Schepartz, *J. Am. Chem. Soc.*, 2007, **129**, 1532.
- (20) (a) S. Hanessian, X. Luo, R. Schaum and S. Michnick, *J. Am. Chem. Soc.*, 1998, **120**, 8569; (b) S. Hanessian, X. Luo and R. Schaum, *Tetrahedron Lett.*, 1999, **40**, 4925.
- (21) (a) D. Seebach, S. Abele, K. Gademann and B. Jaun, *Angew. Chem. Int. Ed.*, 1999, **38**, 1595; (b) T. Hintermann, K. Gademann, B. Jaun and D. Seebach, *Helv. Chim. Acta*, 1998, **81**, 983; (c) D. Seebach, M. Brenner, M.

- Rueping, B. Schweizer and B. Jaun, *Chem. Commun.*, 2001, 207; (d) D. Seebach, M. Brenner, M. Rueping and B. Jaun, *Chem. - Eur. J.*, 2002, **8**, 573.
- (22) J. Frackenpohl, P. I. Arvidsson, J. V. Schreiber and D. Seebach, *ChemBioChem*, 2001, **2**, 445.
- (23) F. Bouillere, S. Thetiot-Laurent, C. Kouklovsky and V. Alezra, *Amino Acids*, 2011, **41**, 687.
- (24) G. V. M. Sharma, P. Jayaprakash, K. Narsimulu, A. R. Sankar, K. R. Reddy, K. R. Krishna and A. C. Kunwar, *Angew. Chem. Int. Ed.*, 2006, **45**, 2944.
- (25) P. G. Vasudev, N. Shamala, K Ananda and P. Balaram, *Angew. Chem. Int. Ed.*, 2005, **44**, 4972.
- (26) (a) R. W. Hoffmann, *Angew. Chem. Int. Ed.*, 2000, **39**, 2054; (b) R. W. Hoffmann, M. A. Lazaro, F. Caturla and E. Framery, *Tetrahedron Lett.*, 1999, **40**, 5983; (c) M. Brenner and D. Seebach, *Helv. Chim. Acta*, 2001, **84**, 2155.
- (27) J. Farrera-Sinfreu, L. Zaccaro, D. Vidal, X. Salvatella, E. Giralt, M. Pons, F. Albericio and M. Royo, *J. Am. Chem. Soc.*, 2004, **126**, 6048.
- (28) R. Gutierrez-Abad, D. Carbajo, P. Nolis, C. Acosta-Silva, J. A. Cobos, O. Illa, M. Royo and R. M. Ortuno, *Amino Acids*, 2011, **41**, 673.
- (29) A. A. Edwards, G. J. Sanjayan, S. Hachisu, G. E. Tranter and G. W. Fleet, *Tetrahedron*, 2006, **62**, 7718.
- (30) A. Kothari, M. K. N. Qureshi, E. M. Beck and M. D. Smith, *Chem. Commun.*, 2007, 2814.
- (31) M. Brenner and D. Seebach, *Helv. Chim. Acta*, 2001, **84**, 1181.
- (32) M. Hagihara, N. J. Anthony, T. J. Stout, J. Clardy and S. L. Schreiber, *J. Am. Chem. Soc.*, 1992, **114**, 6568.
- (33) M. G. Woll, J. R. Lai, I. A. Guzei, S. J. C. Taylor, M. E. B. Smith and S. H. Gellman, *J. Am. Chem. Soc.*, 2001, **123**, 11077.
- (34) M. K. N. Qureshi and M. D. Smith, *Chem. Commun.*, 2006, 5006.
- (35) C. R. Jones, M. K. N. Qureshi, F. R. Truscott, S. T. D. Hsu, A. J. Morrison and M. D. Smith, *Angew. Chem. Int. Ed.*, 2008, **47**, 7099.
- (37) B. J. Byun and Y. K. Kang, *Biopolymers*, 2014, **101**, 87.

- (38) M. W. Giuliano, S. J. Maynard, A. M. Almeida, A. G. Reidenbach, L. Guo, E. C. Ulrich, I. A. Guzei and S. H. Gellman, *J. Org. Chem.*, 2013, **78**, 12351.
- (39) (a) L. Guo, W. Zhang, I. A. Guzei, L. C. Spencer and S. H. Gellman, *Org. Lett.*, 2012, **14**, 2582; (b) M. W. Giuliano, S. J. Maynard, A. M. Almeida, L. Guo, I. A. Guzei, L. C. Spencer and S. H. Gellman, *J. Am. Chem. Soc.*, 2014, **136**, 15046.
- (40) (a) M. D. Smith and G. W. J. Fleet, *J. Peptide Sci.*, 1999, **5**, 425; (b) M. D. Smith, D. D. Long, D. G. Marquess, T. D. W. Claridge and G. W. J. Fleet, *Chem. Commun.*, 1998, 2039; (c) D. D. Long, N. L. Hungerford, M. D. Smith, D. E. A. Brittain, D. G. Marquess, T. D. W. Claridge and G. W. J. Fleet, *Tetrahedron Lett.*, 1999, **40**, 2195; (d) M. I. Simone, A. A. Edwards, G. E. Tranter, G. W. J. Fleet, *Amino Acids*, 2011, **41**, 643.
- (41) (a) T. K. Chakraborty, S. Ghosh and S. Jayaprakash, *Curr. Med. Chem.*, 2002, **9**, 421; (b) S. A. W. Gruner E. Locardi, E. Lohof and H. Kessler, *Chem. Rev.*, 2002, **102**, 491; (c) F. Schweizer, *Angew. Chem. Int. Ed.*, 2002, **41**, 230; (d) R. Baron, D. Bakowies and W. F. van Gunsteren *Angew. Chem. Int. Ed.*, 2004, **43**, 4055.
- (42) E. R. Gillies, C. Dolain, J.-M. Leger and I. Huc, *J. Org. Chem.*, 2006, **71**, 7931.
- (43) E. R. Gillies, F. Deiss, C. Staedel, J.-M. Schmitter and I. Huc, *Angew. Chem. Int. Ed.*, 2007, **46**, 4081.
- (44) M. Kudo, V. Maurizot, B. Kauffmann, A. Tanatani and I. Huc, *J. Am. Chem. Soc.*, 2013, **135**, 9628.
- (45) N. Chandramouli, Y. Ferrand, G. Lautrette, B. Kauffmann, C. D. Mackereth, M. Laguerre, D. Dubreuil and I. Huc, *Nat. Chem.*, 2015, **7**, 334.
- (46) L. Fischer and G. Guichard, *Org. Biomol. Chem.*, 2010, **8**, 3101.
- (47) V. Semetey, D. Rognan, C. Hemmerlin, R. Graff, J.-P. Briand, M. Marraud and G. Guichard, *Angew. Chem. Int. Ed.*, 2002, **41**, 1893.
- (48) P. Claudon, A. Violette, K. Lamour, M. Decossas, S. Fournel, B. Heurtault, J. Godet, Y. Mely, B. Jamart-Gregoire, M.-C. Averlant-Petit, J.-

- P. Briand, G. Duportail, H. Monteil and G. Guichard, *Angew. Chem. Int. Ed.*, 2010, **49**, 333.
- (49) C. Douat, C. Aisenbrey, S. Antunes, M. Decossas, O. Lambert, B. Bechinger, A. Kichler and G. Guichard, *Angew. Chem. Int. Ed.*, 2015, **54**, 11133.
- (50) G. W. Collie, K. Pulka-Ziach, C. M. Lombardo, J. Fremaux, F. Rosu, M. Decossas, L. Mauran, O. Lambert, V. Gabelica, C. D. Mackereth and G. Guichard, *Nat. Chem.*, 2015, **7**, 871.
- (51) (a) D. Yang, Y. H. Zhang and N. Y. Zhu, *J. Am. Chem. Soc.*, 2002, **124**, 9966; (b) D. Yang, Y. H. Zhang, B. Li, D. W. Zhang, J. C. Y. Chan, N. Y. Zhu, S. W. Luo and Y. D. Wu, *J. Am. Chem. Soc.*, 2004, **126**, 6956; (c) D. Yang, D. W. Zhang, Y. Hao, N. Y. Zhu, S. W. Luo and Y. D. Wu, *Angew. Chem. Int. Ed.*, 2004, **43**, 6719; (d) Y.-H. Zhang, K. Song, N. Y. Zhu and D. Yang, *Chem. –Eur. J.*, 2010, **16**, 577; (e) X. Li, Y.-D. Wu and D. Yang, *Acc. Chem. Res.*, 2008, **41**, 1428; (f) Z.-G. Jiao, X.-W. Chang, W. Ding, G.-J. Liu, K.-S. Song, N.-Y. Zhu, D.-W. Zhang and D. Yang, *Chem. Asian J.*, 2011, **6**, 1791.
- (52) (a) S. Chandrasekhar, C. L. Rao, M. S. Reddy, G. D. Sharma, M. U. Kiran, P. Naresh, G. K. Chaitanya, K. Bhanuprakash and B. Jagadeesh, *J. Org. Chem.*, 2008, **73**, 9443; (b) G. V. M. Sharma, V. Manohar, S. K. Dutta, V. Subash and A. C. Kunwar, *J. Org. Chem.*, 2008, **73**, 3689.
- (53) (a) C. Simo, A. Salaun, C. Arnarez, L. Delemotte, A. Haegy, A. Kachmar, A. D. Laurent, J. Thomas, B. Jamart-Gregoire, P. Le Grel and A. Hocquet, *Themochem*, 2008, **869**, 41; (b) P. Le Grel, A. Salaun, M. Potel, B. Le Grel and F. Lassagne, *J. Org. Chem.*, 2006, **71**, 5638; (c) A. Hetenyi, G. K. Toth, C. Somlai, E. Vass, T. A. Martinek and F. Fulop, *Chem. –Eur. J.*, 2009, **15**, 10736.
- (54) A. Salaun, M. Potel, T. Roisnel, P. Gall and P. Le Grel, *J. Org. Chem.*, 2005, **70**, 6499.
- (55) R. J. Simon, R. S. Kania, R. N. Zuckermann, V. D. Huebner, D. A. Jewell, S. Banville, S. Ng. L. Wang, S. Rosenberg, C. K. Marlowe, D. C. Spellmeyer, R. Tan, A. D. Frankel, D. V. Santi, F. E. Cohen and P. A. Bartlett, *Proc. Natl. Acad. Sci. U. S. A.*, 1992, **89**, 9367.

-
- (56) (a) R. N. Zuckermann, J. M. Kerr, S. B. H. Kent and W. H. Moos, *J. Am. Chem. Soc.*, 1992, **114**, 10646; (b) J. A. Crapster, I. A. Guzei and H. E. Blackwell, *Angew. Chem. Int. Ed.*, 2013, **52**, 5079; (c) S. A. Fowler and H. E. Blackwell, *Org. Biomol. Chem.*, 2009, **7**, 1508.
- (57) S. M. Miller, R. J. Simon, S. Ng. R. N. Zuckermann, J. M. Kerr and W. H. Moos, *Bioorg. Med. Chem. Lett.*, 1994, **4**, 2657.
- (58) (a) P. A. Wender, D. J. Mitchell, K. Pattabiraman, E. T. Pelkey, L. Steinman and J. B. Rothbard, *Proc. Natl. Acad. Sci. U. S. A.*, 2000, **97**, 13003; (b) Y.-U. Kwon and T. Kodadek, *J. Am. Chem. Soc.*, 2007, **129**, 1508.
- (59) T. Hjelmgaard, S. Faure, C. Caumes, E. D. Santis, A. A. Edwards and C. Taillefumier, *Org. Lett.*, 2009, **11**, 4100.
- (60) N. H. Shah, G. L. Butterfoss, K. Nguyen, B. Yoo, R. Bonneau, D. L. Rabenstein and K. Kirshenbaum, *J. Am. Chem. Soc.*, 2008, **130**, 16622.
- (61) J. S. Laursen, P. Harris, P. Fristrup and C. A. Olsen, *Nat. Commun.*, 2015, **6**, 1.
- (62) (a) C. M. Wilmot and J. M. Thornton, *J. Mol. Biol.*, 1988, 203, 221; (b) S. Chatterjee, R. S. Roy and P. Balaram, *J. R. Soc. Interface*, 2007, **4**, 587.
- (63) K. C. Chou, *Anal. Biochem.*, 2000, **286**, 1.
- (64) (a) E. J. Milner-White, *J. Mol. Biol.*, 1990, **216**, 386; (b) D. Frishman and P. Argos, *Proteins*, 1995, **23**, 566; (c) P. K. Baruah, N. K. Sreedevi, R. Gonnade, S. Ravindranathan, K. Damodaran, H.-J. Hofmann and G. J. Sanjayan, *J. Org. Chem.*, 2006, **72**, 636.
- (65) G. D. Rose, L. M. Gierasch, and J. A. Smith, *Adv. Protein Chem.*, 1985, **37**, 1.
- (66) (a) V. Pavone, G. Geata, A. Lombardi, F. Nastri, O. Maglio, C. Isernia and M. Saviano, *Biopolymers*, 1996, **38**, 705; (b) D. V. Nataraj, N. Srinivasan, R. Sowdhamini and C. Ramakrishnan, *Curr. Sci.*, 1995, **69**, 434; (c) L. A. Cavacini, R. L. Stanfield, D. R. Burton and A. I. Wilson, *J. Mol. Biol.*, 2008, **375**, 969.
- (67) R. Hahin, Z. Chen, D. Wang, G. Reddy and L. Mao, *Cell Biochem. Biophys.*, 2002, **37**, 169.

- (68) (a) C. Toniolo, *Crit. Rev. Biochem.*, 1980, **9**, 1; (b) A. M. C. Marcelino and L. M. Gierasch, *Biopolymers*, 2008, **89**, 380.
- (69) (a) H. Yin and A. D. Hamilton, *Angew. Chem. Int. Ed.*, 2005, **44**, 4130; (b) G. N. Tew, R. W. Scott, M. L. Klein and W. F. DeGrado, *Acc. Chem. Res.*, 2010, **43**, 30; (c) C. Cabrele, T. A. Martinek, O. Reiser and L. Berlicki, *J. Med. Chem.*, 2014, **57**, 9718.
- (70) (a) G. Guichard and I. Huc, *Chem. Commun.*, 2011, **47**, 5933; (b) L. Milli, M. Larocca, M. Tedesco, N. Castellucci, E. Ghibaudi, A. Cornia, M. Calvaresi, F. Zerbetto and C. Tomasini, *J. Org. Chem.*, 2014, **79**, 5958; (c) C. Tomasini, G. Angelici and N. Castellucci, *Eur. J. Org. Chem.*, 2011, 3648.
- (71) (a) T. A. Martinek and F. Fulop, *Chem. Soc. Rev.*, 2012, **41**, 687; (b) M. I. Simone, A. A. Edwards, G. E. Tranter and G. W. J. Fleet, *Amino Acids*, 2011, **41**, 643; (c) E. D. Santis, T. Hjelmgaard, C. Caumes, S. Faure, B. D. Alexander, S. J. Holder, G. Siligardi, C. Taillefumier and A. A. Edwards, *Org. Biomol. Chem.*, 2012, **10**, 1108; (d) T. Szekely, O. Roy, S. Faure and C. Taillefumier, *Eur. J. Org. Chem.*, 2014, 5641; (e) J. S. Nowick, K. S. Lam, T. V. Khasanova, W. E. Kemnitzer, S. Maitra, H. T. Mee and R. Liu, *J. Am. Chem. Soc.*, 2002, **124**, 4972; (f) R. V. Nair, S. B. Baravkar, T. S. Ingole and G. J. Sanjayan, *Chem. Commun.*, 2014, **50**, 13874.
- (72) (a) J. T. B. Kueh, K. W. Choi, G. M. Williams, K. Moehle, B. Bacsá, J. A. Robinson and M. A. Brimble, *Chem. – Eur. J.*, 2013, **19**, 3807; (b) Y. J. Chung, L. A. Christianson, H. E. Stanger, D. R. Powell and S. H. Gellman, *J. Am. Chem. Soc.*, 1998, **120**, 10555; (c) K. Oh and Z. Guan, *Chem. Commun.*, 2006, 3069;
- (73) (a) R. V. Nair, S. Kheria, S. Rayavarapu, A. S. Kotmale, B. Jagadeesh, R. G. Gonnade, V. G. Puranik, P. R. Rajamohanan and G. J. Sanjayan, *J. Am. Chem. Soc.*, 2013, **135**, 11477; (c) R. V. Nair, K. N. Vijayadas, A. Roy and G. J. Sanjayan, *Eur. J. Org. Chem.*, 2014, 7763, and refs cited therein.
- (74) R. M. Freidinger, D. S. Perlow and D. F. Veber, *J. Org. Chem.*, 1982, **47**, 104.
- (75) M. Feigel, *J. Am. Chem. Soc.*, 1986, **108**, 181.
- (76) H. Diaz and J. W. Kelly, *Tetrahedron Lett.*, 1991, **32**, 5725.

-
- (77) M. G. Hinds, J. H. Welsh, D. M. Brennand, J. Fisher, M. J. Glennie, N. G. J. Richards, D. L. Turner and J. A. Robinson, *J. Med. Chem.*, 1991, **34**, 1777.
- (78) D. S. Kemp and Z. Q. Li, *Tetrahedron Lett.*, 1995, **36**, 4179.
- (79) J. S. Nowick, S. Mahrus, E. M. Smith and J. W. Ziller, *J. Am. Chem. Soc.*, 1996, **118**, 1066.
- (80) R. R. Gardner, G.-B. Liang and S. H. Gellman, *J. Am. Chem. Soc.*, 1999, **121**, 1806.
- (81) Y. J. Chung, L. A. Christianson, H. E. Stanger, D. R. Powell and S. H. Gellman, *J. Am. Chem. Soc.*, 1998, **120**, 10555.
- (82) (a) W. M. D. Borggraeve, F. J. R. Rombouts, E. V. V. der Eycken, S. M. Toppet and G. J. Hoornaert, *Tetrahedron Lett.*, 2001, **42**, 5693; (b) G. Luppi, D. Lanci, V. Trigari, M. Garavelli, A. Garelli and C. Tomasini, *J. Org. Chem.*, 2003, **68**, 1982.
- (83) G. M. Grotenbreg, M. S. M. Timmer, A. L. Llamas-Saiz, M. Verdoes, G. A. van der Marel, M. J. van Raaij, H. S. Overkleeft and M. Overhand, *J. Am. Chem. Soc.*, 2004, **126**, 3444.
- (84) M. H. V. R. Rao, E. Pinyol and W. D. Lubell, *J. Org. Chem.*, 2007, **72**, 736.
- (85) A. Sacchetti, A. Silvani, G. Lesma and T. Pilati, *J. Org. Chem.*, 2011, **76**, 833.
- (86) C. Andre, B. Legrand, C. Deng, C. Didierjean, G. Pickaert, J. Martinez, M. C. Averlant-Petit, M. Amblard and M. Calmes, *Org. Lett.*, 2012, **14**, 960.
- (87) S. Aravinda, V. V. Harini, N. Shamala, C. Das and P. Balaram, *Biochemistry*, 2004, **43**, 1832.
- (88) T. S. Haque, J. C. Little and S. H. Gellman, *J. Am. Chem. Soc.*, 1994, **116**, 4105.
- (89) (a) J. D. Fisk, D. R. Powell and S. H. Gellman, *J. Am. Chem. Soc.*, 2000, **122**, 5443; (b) M. G. Woll, J. R. Lai, I. A. Guzei, S. J. C. Taylor, M. E. B. Smith and S. H. Gellman, *J. Am. Chem. Soc.*, 2001, **123**, 11077.
- (90) A. K. Medda, C M Park, A Jeon, H. Kim, J.-H. Sohn and H.-S. Lee, *Org. Lett.*, 2011, **13**, 3486.

- (91) V. H. Thorat, T. S. Ingole, K. N. Vijayadas, R. V. Nair, S. S. Kale, V. V. E. Ramesh, H. C. Davis, P. Prabhakaran, R. G. Gonnade, R. L. Gawade, V. G. Puranik, P. R. Rajamohanam and G. J. Sanjayan, *Eur. J. Org. Chem.*, 2013, 3529.
- (92) K. N. Vijayadas, H. C. Davis, A. S. Kotmale, R. L. Gawade, V. G. Puranik, P. R. Rajamohanam and G. J. Sanjayan, *Chem. Commun.*, 2012, **48**, 9747.
- (93) K. Gademann, M. Ernst, D. Hoyer and D. Seebach, *Angew. Chem., Int. Ed.*, 1999, **38**, 1223.
- (94) N. de la Figuera, M. Martin-Martinez, R. Herranz, M. Teresa Garcia-Lopez, M. Latorre, E. Cenarruzabeitia, J. del Rio and R. Gonzalez-Muniz, *Bioorg. Med. Chem. Lett.*, 1999, **9**, 43.
- (95) U. Rosenstrom, C. Skold, G. Lindeberg, M. Botros, F. Nyberg, A. Karlen and A. Hallberg, *J. Med. Chem.*, 2006, **49**, 6133.
- (96) B. Legrand, L. Mathieu, A. Lebrun, S. Andriamanarivo, V. Lisowski, N. Masurier, S. Zirah, Y. K. Kang, J. Martinez and L. T. Maillard, *Chem. – Eur. J.*, 2014, **20**, 1.
- (97) (a) S. J. Miller, *Acc. Chem. Res.*, 2004, **37**, 601; (b) E. A. C. Davie, S. M. Mennen, Y. Xu and S. J. Miller, *Chem. Rev.*, 2007, **107**, 5759; (c) C. M. Rufo, Y. S. Moroz, O. V. Moroz, J. Stohr, T. A. Smith, X. Hu, W. F. DeGrado and I. V. Korendovych, *Nat. Chem.*, 2014, **6**, 303; (d) F. Bachle, J. Duschmale, C. Ebner, A. Pfaltz and H. Wennemers, *Angew. Chem., Int. Ed.*, 2013, **52**, 12619.
- (98) Y. Hamuro, S. J. Geib and A. D. Hamilton, *J. Am. Chem. Soc.*, 1996, **118**, 7529.
- (99) (a) a) M. Chorev and M. Goodman, *Trends Biotechnol.*, 1995, **13**, 438; (b) T. Weeden, J. Stefano, S. Duan, A. Edling, L. Hou, W. L. Chuang, M. A. Perricone, C. Pan and J. L. Dzuris, *J. Pept. Sci.*, 2011, **17**, 47.
- (100) P. K. Baruah, N. K. Sreedevi, B. Majumdar, R. Pasricha, P. Poddar, R. Gonnade, S. Ravindranathan and G. J. Sanjayan, *Chem. Commun.*, 2008, 712.
- (101) N. J. Greenfield, *Nat. Protoc.*, 2006, **1**, 2876.

- (102) (a) A. J. Wilson, *Prog. Biophys. Mol. Biol.*, 2015, **119**, 33; (b) R. M. J. Liskamp, D. T. S. Rijkers, J. A. W. Kruijtzter and J. Kemmink, *ChemBioChem*, 2011, **12**, 1626; (c) K. Estieu-Gionnet and G. Guichard, *Expert Opin. Drug Discovery*, 2011, **6**, 937; (d) H. Yin and A. D. Hamilton, *Angew. Chem. Int. Ed.*, 2005, **44**, 4130; (e) E. Ko, J. Liu, and K. Burgess, *Chem. Soc. Rev.*, 2011, **40**, 4411; (f) A. D. Bautista, J. S. Appelbaum, C. J. Craig, J. Michel and A. Schepartz, *J. Am. Chem. Soc.*, 2010, **132**, 2904.
- (103) (a) A. Wittelsberger, M. Keller, L. Scarpellino, L. Patiny, H. Acha-Orbea and M. Mutter, *Angew. Chem. Int. Ed.*, 2000, **39**, 1111; (b) F. Bernardi, M. Garavelli, M. Scatizzi, C. Tomasini, V. Trigari, M. Crisma, F. Formaggio, C. Peggion and C. Toniolo, *Chem.-Eur. J.*, 2002, **8**, 2516; (c) R. D. Marco, A. Greco, S. Rupiani, A. Tolomelli, C. Tomasini, S. Pieraccini and L. Gentilucci, *Org. Biomol. Chem.*, 2013, **11**, 4316; (d) C. Tomasini, G. Luppi, M. Monari, *J. Am. Chem. Soc.*, 2006, **128**, 2410; (e) C. Tomasini, G. Angelici and N. Castellucci, *Eur. J. Org. Chem.*, 2011, 3648.
- (104) (a) A. R. Viguera and L. Serrano, *Protein Sci.*, 1999, **8**, 1733; (b) E. Cabezas and A. C. Satterthwait, *J. Am. Chem. Soc.*, 1999, **121**, 3862; (c) W. Maison, E. Arce, P. Renold, R. J. Kennedy and D. S. Kemp, *J. Am. Chem. Soc.*, 2001, **123**, 10245; (d) D. Wang, W. Liao and P. S. Arora, *Angew. Chem. Int. Ed.*, 2005, **44**, 6525; (e) R. Rai, S. Aravinda, K. Kanagarajadurai, S. Raghothama, N. Shamala and P. Balaram, *J. Am. Chem. Soc.*, 2006, **128**, 7916; (f) A. Patgiri, A. L. Jochim and P. S. Arora, *Acc. Chem. Res.*, 2008, **41**, 1289.
- (105) (a) B. Gong, *Chem. -Eur. J.* 2001, **7**, 4337; (b) I. Huc, *Eur. J. Org. Chem.*, 2004, 17; (c) Z.-T. Li, J.-L. Hou and C. Li, *Acc. Chem. Res.*, 2008, **41**, 1343.
- (106) (a) P. Wilhelm, B. Lewandowski, N. Trapp and H. Wennemers *J. Am. Chem. Soc.*, 2014, **136**, 15829; (b) B. R. Huck, J. D. Fisk, I. A. Guzei, H. A. Carlson and S. H. Gellman, *J. Am. Chem. Soc.*, 2003, **125**, 9035; (c) G. Priya, A. S. Kotmale, R. L. Gawade, D. Mishra, S. Pal, V. G. Puranik, P. R. Rajamohanam and G. J. Sanjayan, *Chem. Commun.*, 2012, **48**, 8922; (d) C. C. Caumes, O. Roy, S. Faure and C. Taillefumier, *J. Am. Chem. Soc.*,

- 2012, **134**, 9553; (e) F. Bouillere, D. Feytens, D. Gori, R. Guillot, C. Kouklovsky, E. Miclet and V. Alezra, *Chem. Commun.*, 2012, **48**, 1982.
- (107) E. G. Hutchinson and J. M. Thornton, *Protein Sci.*, 1994, **3**, 2207.
- (108) MacroModel, version 10.7, Schrödinger, LLC, New York, NY, 2015.
- (109) M. Buck, *Q. Rev. Biophys.*, 1998, **31**, 297.
- (110) T. Sawada and S. H. Gellman, *J. Am. Chem. Soc.*, 2011, **133**, 7336.

CHAPTER 2

*Conformational preference of^S Ant-Pro reverse
turn scaffold over native β -turn elements – a
competition experiment*

Conformational preference of ^SAnt-Pro reverse turn scaffold over native β -turn elements – a competition experiment

2.1 Introduction

β -Turn structures are the most commonly found secondary structures in proteins and polypeptides and have gained importance due to their participation in the fundamental biological processes since these structures are located at the exterior of proteins. Thus, β -turn secondary structure has attracted the attention of researchers across the globe for developing small molecule therapeutics. Intense research in the area of reverse turn mimetics resulted in the development of novel scaffolds with potential biomedical applications. In this regard, various non-natural amino acids-containing peptidomimetics have been developed with a view to modulate properties such as therapeutic profile and proteolytic stability. Typical β -turn involves the ten-membered hydrogen-bonded network formed between CO of amino acid residue '*i*' and NH of amino acid residue '*i*+3' in the backward direction (4 \leftarrow 1).

Detailed account on peptidomimetics based on β -turn has been discussed earlier in the chapter 1. Herein, this chapter is focused on conformational features of peptides containing amide bond isoster such as sulfonamide, particularly when it is connected to native β -turn scaffolds. Because of the unusual physical and chemical properties, sulfonamide moiety has been the choice of group for isosteric replacement of carboxamide group. Moreover, sulfonamide moiety in the peptide backbone offers high resistance towards proteolytic degradation.¹

The isosteric replacement of carboxamide by sulfonamide resulted in various secondary structural architectures with potential biomedical applications.^{1,2} The sulfonamides show different conformational features

compared to carboxamide (Fig. 2.1) due to following facts: (i) NH group of sulfonamide is more acidic compared to carboxamide NH group, this results in more efficient involvement in the hydrogen bonding; (ii) due to the presence of additional oxygen as hydrogen bonding acceptor sulfonamide moiety has better hydrogen bonding propensity; (iii) the bond length of S-N in sulfonamide is greater than C-N in sulfonamide, and hence, S-N bond has restricted rotation which would lead to formation of particular conformation; and (iv) sulfonamides show unusual ω dihedral angle ($\leq 90^\circ$) which is in contrast to the carboxamide ($\leq 180^\circ$).^{2,3}

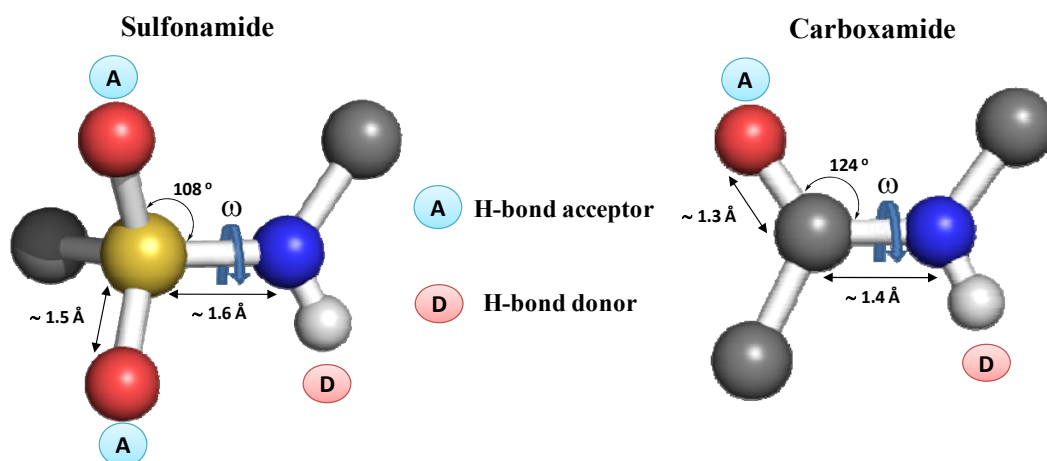


Fig. 2.1 Comparison of dihedral angle and hydrogen bonding parameters between sulfonamide and carboxamide bond.

2.2 Objective and design strategy

Proline, a cyclic constrained amino acid, with its unusual dihedral angles has a strong propensity to induce a turn in the peptide backbone.⁴ Consequently, proline in conjunction with unnatural amino acids has been employed to create various stable secondary structures.^{5,19} Moreover, pseudoproline (ψ Pro) have also been used in the generation of conformationally constrained β -turn mimetics.⁶ ^LPro-Gly motif (Fig. 2.2), a well known turn inducer that can form stable β -turn

structures,⁷ has found use in modulating the biological activity of therapeutic drugs.⁸ Heterochiral ^DPro-^LPro has been extensively used as a strong turn inducer for the creation of stable β -hairpin structures.⁹ Though homochiral diproline (^LPro-^LPro) motif has found application in the generation of helical structures in peptide sequences;¹⁰ it may also adopt stable β -turn conformation in certain heterogeneous peptides, which is dictated by the neighboring residues.¹¹ ^DPro-Aib dipeptide unit has been used to nucleate stable β -hairpin structures.¹² It is noteworthy that Aib-^LPro oligomer assumes β -bent conformation – stabilized by consecutive hydrogen bonding between Aib and ^LPro residues.¹³

Earlier, our group developed the ^SAnt-Pro (orthanilic acid - proline) scaffold, which forms a *pseudo* β -turn, stabilized by 9-membered hydrogen bonding in the forward direction (1 \rightarrow 2) featuring just two amino acid residues (Fig. 2.2F).¹⁴

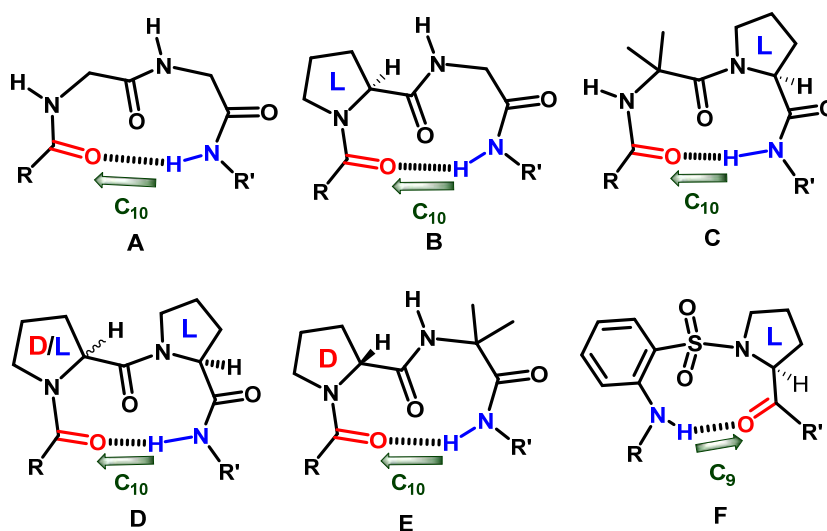


Fig. 2.2 Native β -turn (A), common turn inducers (B-E) and a *pseudo* β -turn featuring orthanilic acid and proline (^SAnt-Pro motif, F).

When possibilities of multiple hydrogen bonding networks exist in a peptide chain, it is often very difficult to predict which hydrogen bonding network will prevail and hence the outcome of the folding competition.^{15,19a,b} While

investigating the conformational propensities and resemblance of native β -turn and S Ant-Pro-based *pseudo* β -turn, we became interested in evaluating their direct folding competition. Thus, we designed peptide sequences containing both turn elements (native 10-membered β -turn and 9-membered S Ant-Pro-based *pseudo* β -turn). Various native 10-membered β -turn motifs such as L Pro- L Pro (in peptide 1), D Pro- L Pro (in peptide 2), Aib- L Pro (in peptide 3), L Pro-Gly (in peptide 4) and D Pro-Aib (in peptide 5) were attached at the N-terminus of S Ant-Pro turn segment (Fig. 2.3) and we investigated their preferred hydrogen bonding pattern using solid, solution-state and nOe-based MD simulation studies. In all the designed peptides, NH of S Ant is in competition with three H-bonding networks i.e. a β -turn (C10 H-bonding between ' i ' and ' $i+3$ ' residue), a *pseudo* β -turn (C9 H-bonding between ' $i+3$ ' and ' $i+4$ ' residue) and a C6 intra-residual hydrogen bonding within ' $i+3$ ' residue (S Ant). Additionally, C14 hydrogen bonding can also be anticipated between C=O of ' $i+1$ ' residue and NH of ' $i+5$ ' residue which is often noticed in β -peptide C14-helices.¹⁶

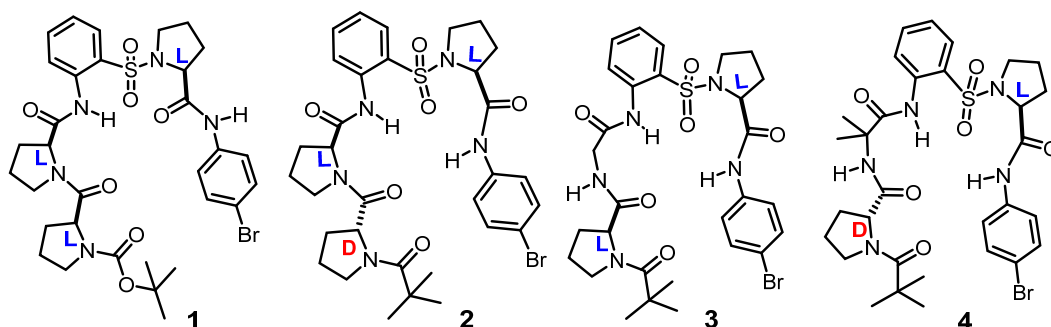


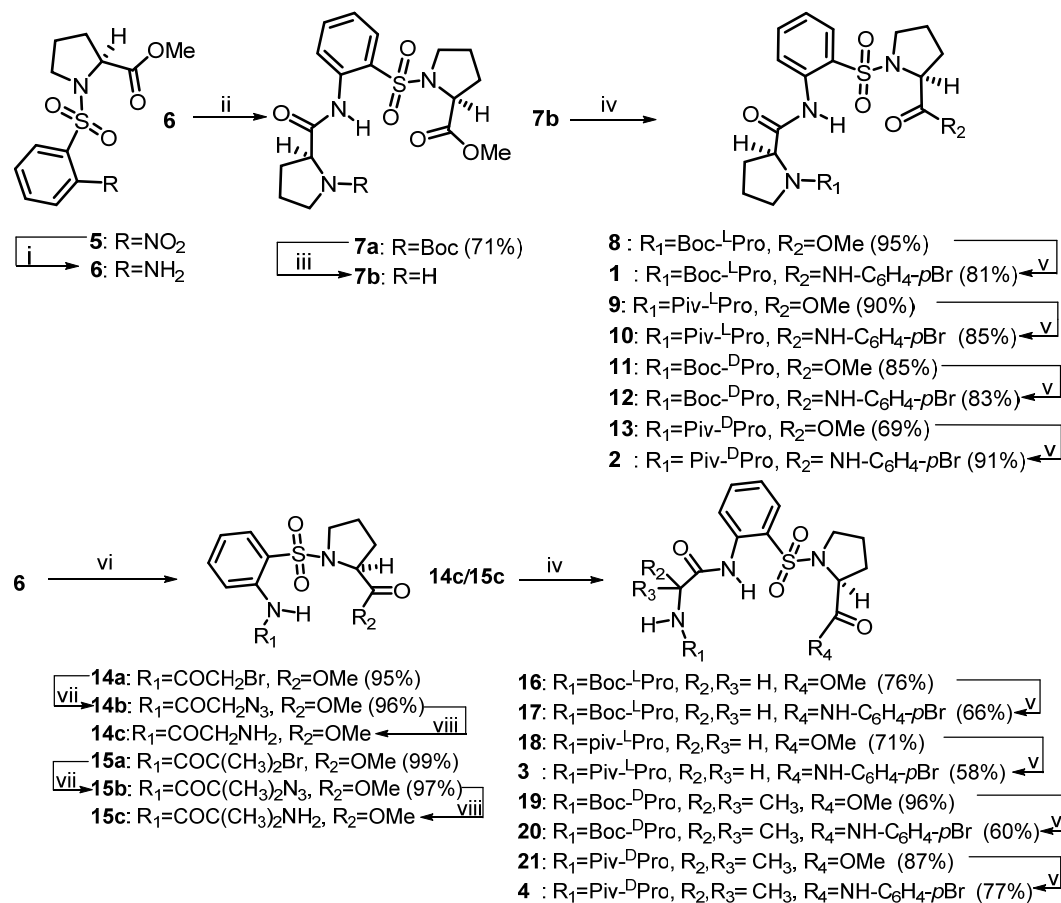
Fig. 2.3 Molecular structures of peptides described in this study, containing native and S Ant-Pro-based *pseudo* β -turns.

2.3 Results and discussion

2.3.1 Synthesis

All the tetrapeptides (**1-4**) were synthesized by conventional solution phase peptide synthesis using standard coupling reaction protocols (Scheme 2.1).

Compounds **7a**^{18a} and **14a-14c**^{18b} were synthesized by reported procedures. Boc group of tripeptide **7a** was removed using trifluoroacetic acid to furnish amine **7b**, which was then reacted with Boc and Piv-Pro-OH (L and D) in presence of EDC.HCl as a coupling reagent to obtain tetrapeptides. The tetrapeptide methyl esters **8**, **9**, **11** and **13** were hydrolyzed under basic condition to obtain the respective carboxylic acids, which were then treated with 4-bromoaniline to obtain their 4-bromoanilide derivatives **1**, **10**, **12** and **2**. Due to less reactivity of amine group of ^SAnt with the Gly and Aib, we have used azide route for the synthesis of tetrapeptides **3** and **4**. Dipeptide **6** was treated with 2-bromoacetyl bromide and 2-bromoisobutyryl bromide to obtain **14a** and **15a**, respectively. These bromo derivatives were converted to respective azides using NaN₃, which were then reduced to respected amines **14c** and **15c** under catalytic hydrogenation conditions. The amine **14c** was reacted with Boc and Piv-^LPro-OH in presence of EDC.HCl as a coupling reagent to obtain tetrapeptides **16** and **18**, respectively. The tetrapeptide esters **16** and **18** were further subjected to hydrolysis and obtained respective carboxylic acids, which were then reacted with 4-bromoaniline to obtain 4-bromoanilide derivatives **17** and **3**. Similarly, tetrapeptides **20** and **4** were obtained from the amine **15c**.

Scheme 2.1 Synthesis of oligomers **1**, **2**, **3** and **4**.

Reagents and conditions: (i) H₂, Pd/C, 60 psi, EtOAc, 8 h; (ii) Boc-L-Pro-OH, EtOCOCl, Et₃N, THF, reflux, 48 h; (iii) TFA, DCM, rt, 2 h; (iv) Boc-L-Pro-OH (for **8**, **16**)/Piv-L-Pro-OH (for **9**, **18**)/Boc-D-Pro-OH (for **11**, **19**)/Piv-D-Pro-OH (for **13**, **21**), EDC.HCl, HOBT, DCM, rt, 12 h; (v) (a) LiOH, MeOH, H₂O, rt, 4 h, and then (b) H₂N-C₆H₄-pBr, EDC.HCl, HOBT, DCM, rt, 12 h; (vi) bromoacetyl bromide (for **14a**)/2-bromo-2-methylpropionyl bromide (for **15a**), Et₃N, DCM, 0 °C, 1 h; (vii) NaN₃, DMF, 50 °C, 1 h; (viii) H₂, Pd/C, 60 psi, EtOAc, 8 h.

2.3.2 Conformational analyses by crystal structure and NMR studies

Conformational analysis of peptides **1** and **4** was carried out in the solid-state (X-ray crystal structure) and solution-state (2D NMR) studies. In case of peptides **2** and **4**, where we could not obtain the crystal structure, their structural elucidation was carried out *via* combination of solution-state 2D NMR and nOe-based MD simulation studies. The results of conformational investigation showed that **1** adopts C9 H-bonding, while **2**, **3** and **4** adopt C14 hydrogen bonding.

Intriguingly, formation of native β -turn was not observed in any of the peptides (Fig. 2.4).

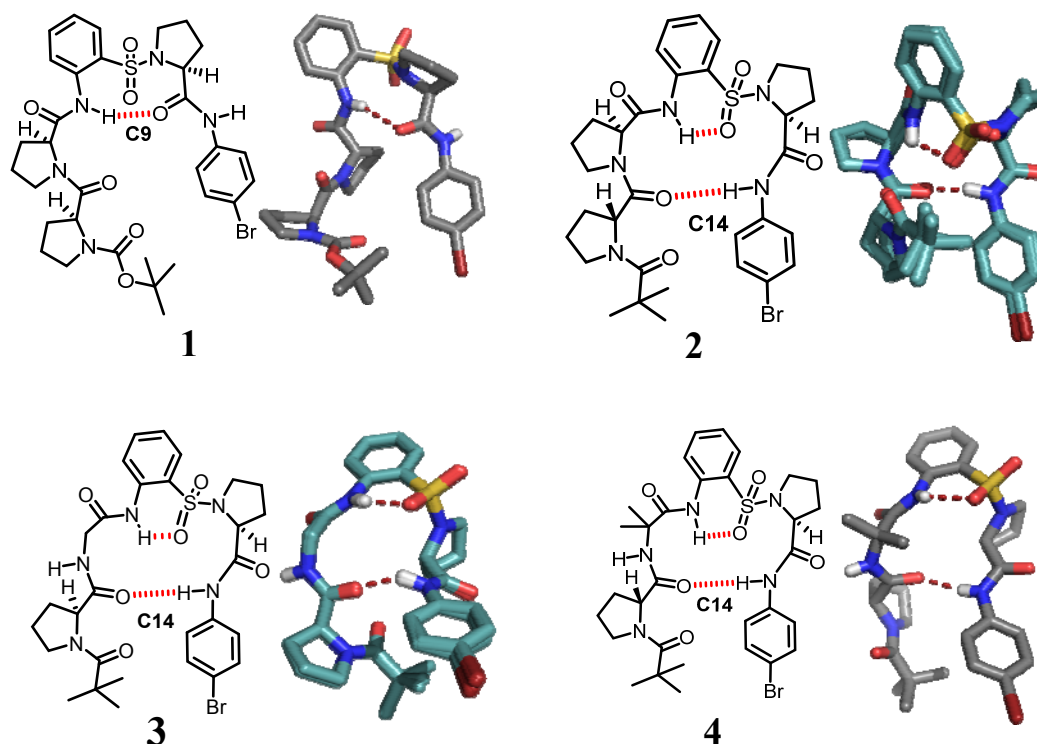


Fig. 2.4 Molecular structures of peptides showing observed hydrogen bonding pattern and their corresponding crystal structures (for **1** and **4**) or nOe-based MD simulated 20 superimposed energy minimized structures (for **2** and **3**).

Careful analysis of torsion angle parameters of the crystal structures **1** and **4** revealed that there is drastic change in the ψ (ψ_2) values of ' $i+2$ ' residues, in comparison with typical native β -turns (Table 2.1). For instance, peptides **1** and **4** featuring L Pro- L Pro and D Pro-Aib dipeptide segments, respectively, ψ_2 adopt a high value: 153.63° (' $i+2$ ' residue of **1**) and -145.80° (' $i+2$ ' residue of **4**) in place of 2.9° and -30.4° ,^{11,12} as observed in the native β -turns. The hydrogen bonding distances [$d(\text{N}-\text{H}\cdots\text{O}=\text{C})$] observed from crystal structure of **1** (C9 H-bonding) and **4** (C14 H-bonding) were found to be 2.35 \AA and 2.04 \AA , respectively. Peptides **1** and **3** accordingly adopted C9 hydrogen bonded network,¹⁴ while **4** showed C14,¹⁶ along with C6^{18b} hydrogen bonded network.

Table 2.1 Torsion angle parameters extracted from the crystal structures of **1** and **4**.

Compounds		1	4
Residue 1	ϕ_1	-66.85	82.87
(<i>i</i> +1)	ψ_1	147.73	-153.00
Residue 2	ϕ_2	-80.06	57.39
(<i>i</i> +2)	ψ_2	153.63	-145.80
Residue 3	ϕ_3	-132.62	-146.75
(<i>i</i> +3)	ψ_3	-63.27	94.32
Residue 4	ϕ_4	-118.12	-108.03
(<i>i</i> +4)	ψ_4	163.83	157.78

To gain insights into their solution-state conformation, extensive NMR conformational analysis of **10** (a close analogue of **1**), **2**, **3** and **20** (a close analogue of **4**) were undertaken. ¹H NMR spectra of **1** and **4** showed multiple signals, which were seen due to free rotation of amide bond connecting Pro residue (rotamer effect)¹¹ and hence their close analogues **10** and **20** were used for NMR studies. Signal assignments were carried out unambiguously using a combination of two-dimensional COSY, TOCSY, HSQC, HMBC and NOESY experiments.

The characteristic inter-residual nOes which supported the C9 H-bonded folded structure of **10** include: NH1 vs C21H (Pro3 δ H), C14H vs C21H (Pro3 δ H), NH2 vs C18H (Pro3 δ H) and C27H vs C30H (Fig. 2.5), indicating the prevalence of C9 folded structure in the solution-state, as observed in its crystal structure.

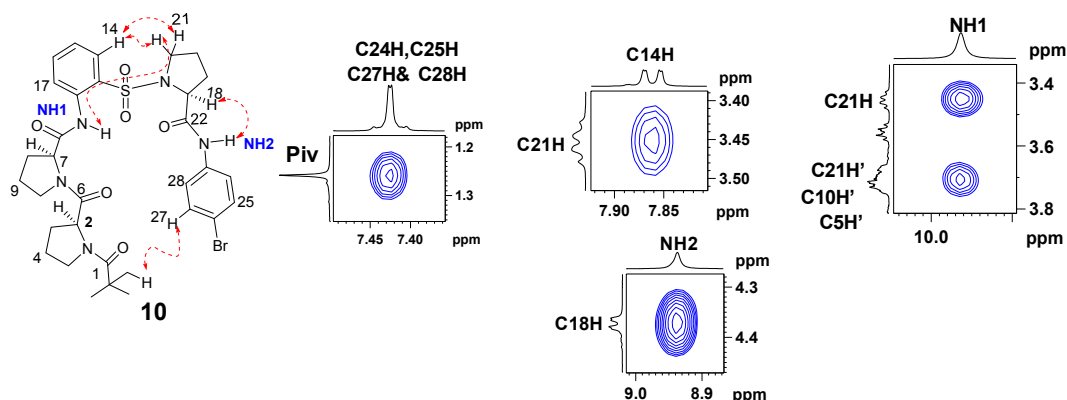


Fig. 2.5 2D NOESY extracts of **10** (28 mM, 500 MHz, CDCl_3).

In order to investigate the strength of hydrogen bonding, we undertook the NMR $\text{DMSO-}d_6$ titration and variable temperature studies for peptide **10** (Fig. 2.6). The outcome of these studies revealed that amide NH1 of **10** is involved in strong 9-membered intramolecular hydrogen bonding, while NH2 is available for intermolecular hydrogen bonding. NH1 group of peptide **10** showed very negligible chemical shift difference [$\Delta\delta(\text{NH}) = 0.12$ ppm] during titration experiment and low temperature coefficient [$\Delta\delta/\Delta T(\text{NH}) = -0.54$ ppb/K] during variable temperature experiment, which indicates its solvent shielded nature. In contrast, NH2 group of **10** showed larger chemical shift difference [$\Delta\delta(\text{NH}) = 0.37$ ppm] and high temperature coefficient [$\Delta\delta/\Delta T(\text{NH}) = -4.5$ ppb/K] suggesting its solvent exposed nature.

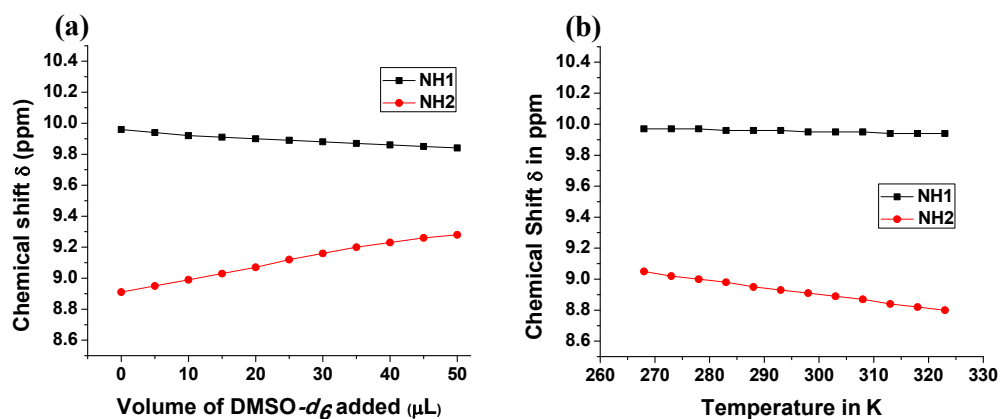


Fig. 2.6 $\text{DMSO-}d_6$ titration (a) and variable temperature (b) studies of **10** (5 mM, 400 MHz, CDCl_3).

In the case of **20** (a close analogue of **4**), critical nOes characteristic of C14 H-bonded conformation were observed. Most notably, nOes between NH3 vs C8H (Aib), NH3 vs NH2 and C24H vs C29H (illustrated in Fig. 2.7) were diagnostic of C14 folded conformation as observed in the crystal structure of its close analogue **4**.

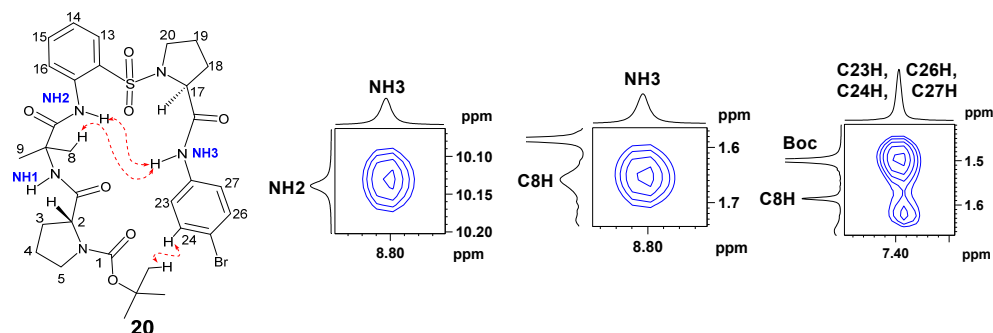


Fig. 2.7 2D NOESY extracts of **20** (48 mM, 500 MHz, CDCl_3).

The solvent shielding nature of NHs of **20** was confirmed by DMSO- d_6 titration and variable temperature studies. The negligible chemical shift of NH2 and NH3 of **20** [$\Delta\delta(\text{NH}_2) = 0.17$ ppm and $\Delta\delta(\text{NH}_3) = 0.14$ ppm] suggest their involvement in the strong intramolecular C6 and C14 H-bonding, respectively, as deduced from the DMSO- d_6 titration experiment (Fig. 2.8a). Moreover, variable temperature experiment of **20** was undertaken to support the intramolecular H-bonding strength and the observations were in agreement with the titration studies:

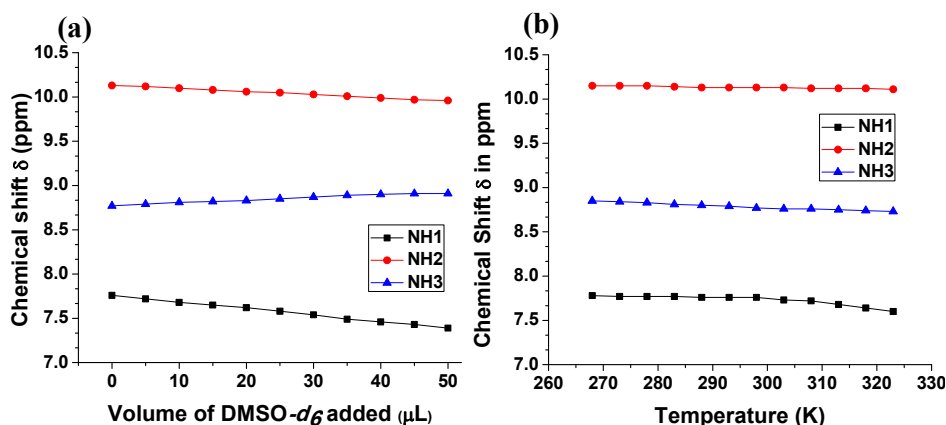


Fig. 2.8 DMSO- d_6 titration (a) and variable temperature (b) studies of **20** (5 mM, 400 MHz, CDCl_3).

$(\Delta\delta/\Delta T)\text{NH2} = -0.72$ ppb/K and $(\Delta\delta/\Delta T)\text{NH3} = -2.1$ ppb/K (Fig. 2.8b).

Similarly, C14 folded structures for **2** and **3** were confirmed by the presence of diagnostic long-range inter-residual nOes. The nOes for **2**: NH2 vs C7H (Pro2 α H), NH2 vs C3H (Pro1 β H) and C27H vs C30H (Fig. 2.9) and for **3**: NH3 vs NH2, NH3 vs C7H (Gly-CH2) and C24H vs C27H (Fig. 2.10) are indicative nOe interactions for C14 folded structure.

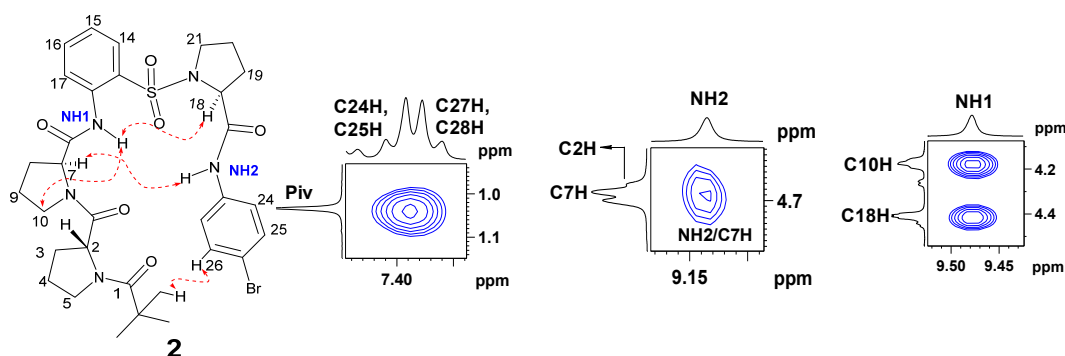


Fig. 2.9 2D NOESY extracts of **2** (30 mM, 500 MHz, CDCl_3).

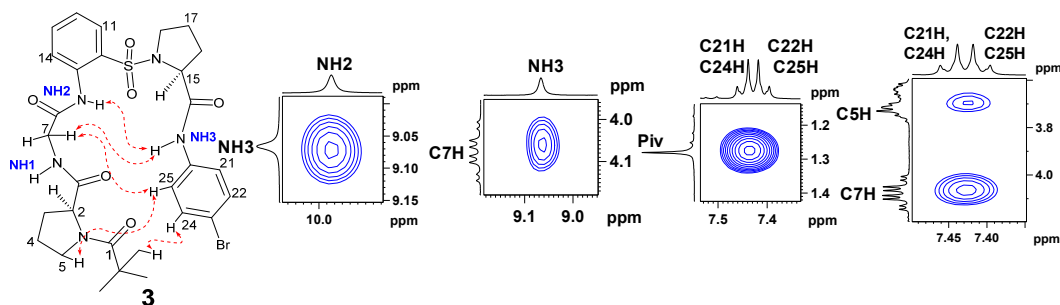


Fig. 2.10 2D NOESY extracts of **3** (63 mM, 400 MHz, CDCl_3).

Small chemical shift difference of NHs in the $\text{DMSO-}d_6$ titration studies (Fig. 2.11) [for **2**: $\Delta\delta(\text{NH1}) = 0.12$ ppm, $\Delta\delta(\text{NH2}) = 0.03$ ppm, and for **3**: $\Delta\delta(\text{NH2}) = 0.13$ ppm, $\Delta\delta(\text{NH3}) = 0.14$ ppm] suggested their involvement in the intramolecular hydrogen bonding.

In addition to $\text{DMSO-}d_6$ titration studies, low temperature coefficients of NHs in variable temperature studies (Fig. 2.12) further supported their involvement in intramolecular hydrogen bonding [for **2** $(\Delta\delta/\Delta T)\text{NH1} = -0.54$

ppb/K, $(\Delta\delta/\Delta T)_{\text{NH2}} = -2.0$ ppb/K, for **3** $(\Delta\delta/\Delta T)_{\text{NH2}} = -1.27$ ppb/K, $(\Delta\delta/\Delta T)_{\text{NH3}} = -2.36$ ppb/K].

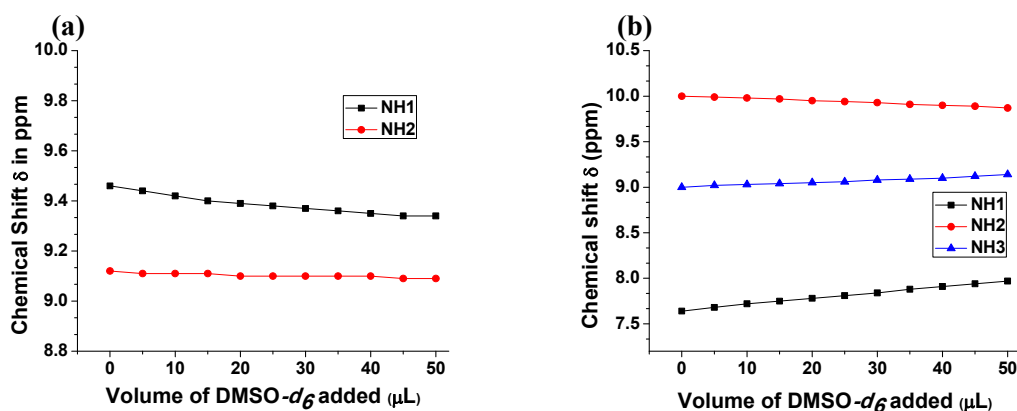


Fig. 2.11 DMSO- d_6 titration plots of **2** (a, 5 mM, 400 MHz, CDCl_3) and **3** (b, 5 mM, 400 MHz, CDCl_3).

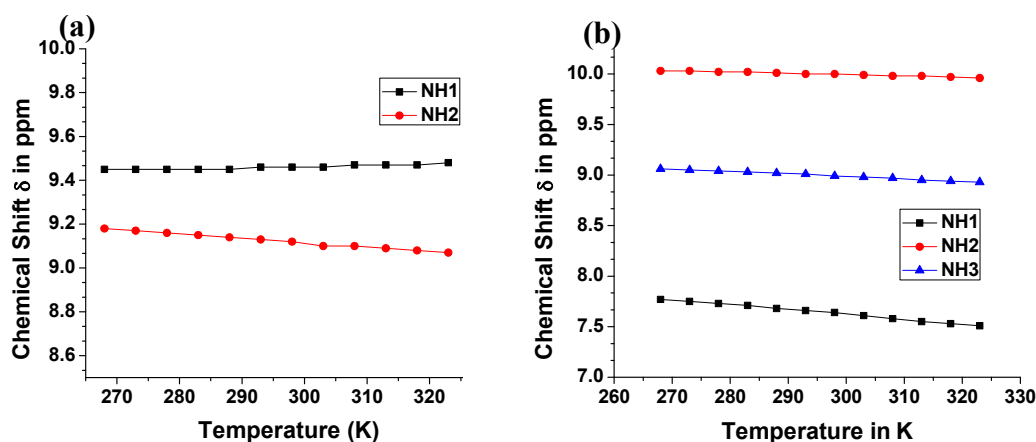


Fig. 2.12 Variable temperature studies of **2** (a, 5 mM, 400 MHz, CDCl_3) and **3** (b, 5 mM, 400 MHz, CDCl_3).

2.3.3 Conformational analysis by FT-IR studies

In addition to the detailed NMR studies, we also carried out IR studies in order to investigate the existence of the intramolecular hydrogen-bonded amide NH groups in the designed peptides. The IR studies of the designed peptides in the solution-state were carried out using Bruker, Alfa FT-IR spectrometer. The IR absorption spectra of compounds **10**, **2**, **3** and **20** were recorded in dry chloroform at the concentration of 6 mM (Fig. 2.13) where intramolecular aggregation is insignificant. The IR spectra of peptides **10** and **20** recorded in the solution-state

show a strong band at about 3340 cm^{-1} and a weak band at about 3390 cm^{-1} indicating the presence of strong intramolecular hydrogen-bonded amide NH, while band $\approx 3450\text{ cm}^{-1}$ indicates non hydrogen-bonded amide NH.^{6d,20} The IR spectra of peptides **2** and **3** show three bands: a weak band $\approx 3330\text{ cm}^{-1}$, a medium band $\approx 3390\text{ cm}^{-1}$ and a strong band $\approx 3460\text{ cm}^{-1}$ suggesting an equilibrium state of amide NH between hydrogen-bonded and non hydrogen-bonded conformation. The involvement of amide NH in the intramolecular hydrogen-bonding is also supported by NMR DMSO- d_6 titration and variable temperature studies.

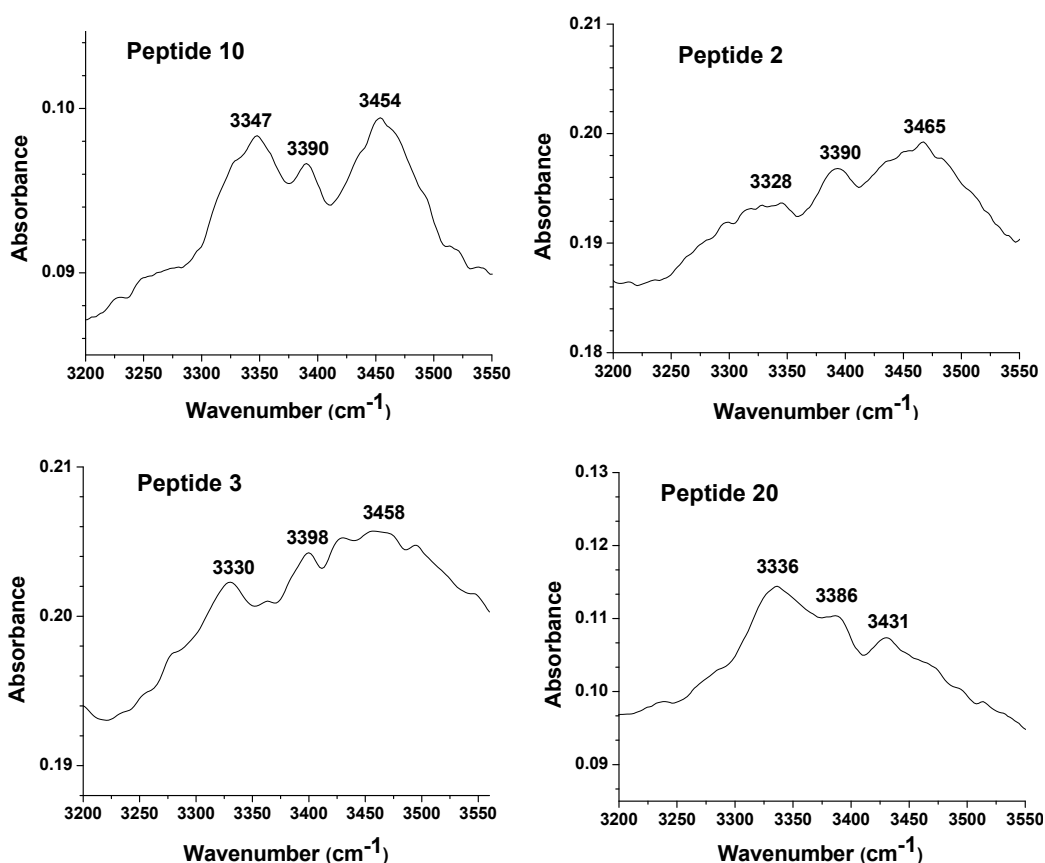


Fig. 2.13 Excerpts of amide NH region in the FT-IR spectra tetrapeptides **10**, **2**, **3** and **4** in CHCl_3 at the concentration of 6 mM.

2.3.4 Structural elucidation of **2** and **3** by nOe-based MD simulation

The difficulty in crystallizing the oligomers **2** and **3** impelled us to carry out their structural elucidation in solution-state by nOe-restrained MD simulation

(Fig. 2.4, *vide supra*). The energy minimized structures of **2** and **3** were obtained by MacroModel, version 10.7 program from Schrödinger¹⁷ and superimposed (RMSD < 0.2 Å). The dynamic ensembled structures of oligomers **2** and **3** revealed the formation of C14 hydrogen bonding between C=O of '*i*+1' and NH of '*i*+5' residue and absence of native β-turn (C10 H-bonding) conformation, which was supported by NMR DMSO-*d*₆ titration and variable temperature studies.

2.4 Conclusion

In summary, investigations of direct folding competition between native 10-membered β-turn-forming elements and a 9-membered pseudo β-turn based on the ^SAnt-Pro motif revealed unexpected folding preferences. Extensive structural investigations by single crystal X-ray crystallography, solution-state NMR and nOe-restrained MD simulation studies revealed the disruption of native β-turn architecture. Notably, differences in the ψ (ψ_2) angle of '*i*+2' residues of native β-turn and designed peptides indicate that the formation of native β-turn structure is not favored. The study has provided useful insights into the stability of native 10-membered β-turns like ^Lpro-^Lpro, ^Dpro-^Lpro, Aib-^LPro, ^Lpro-Gly, ^Dpro-Aib in the presence of other possible turn inducing motifs.^{11,19}

2.5 Experimental section

Table 2.2 Crystal data for peptides 10 and 4.

Crystal Data	B LPLP (10)	PivAIB (4)
Formula	C ₃₂ H ₄₀ BrN ₅ O ₇ S	C ₃₁ H ₄₀ BrN ₅ O ₆ S
M _r	718.66	690.65
Crystal Size, mm	0.32 x 0.12 x 0.09	0.25 x 0.10 x 0.08
Temp. (K)	297(2)	297(2)
Crystallizing solvent	EtOAc-petroleum ether	EtOAc-methanol
Crystal Syst.	Monoclinic	Monoclinic
Space Group	<i>P</i> 2 ₁	<i>P</i> 2 ₁
<i>a</i> /Å	6.7004(12)	6.5980(2)
<i>b</i> /Å	15.440(3)	25.5565(8)
<i>c</i> /Å	16.310(3)	9.6629(3)
α°	90	90
β°	98.363(9)	96.854(2)
γ°	90	90
<i>V</i> /Å ³	1669.5(5)	1617.73(9)
<i>Z</i>	2	2
<i>D</i> _{calc} /g cm ⁻³	1.430	1.418
μ /mm ⁻¹	1.348	1.385
<i>F</i> (000)	748	720
<i>Ab. Correct.</i>	multi-scan	multi-scan
2 θ _{max}	50	50
Total reflns.	12722	13068
unique reflns.	5433	5353
<i>h, k, l</i> (min, max)	(-7,7, -18,18, -19,19)	(-7,6, -30,27, -11,11)
R _{int}	0.0369	0.0430
No. of para	419	403
<i>R</i> 1 [<i>I</i> > 2 σ (<i>I</i>)]	0.0350	0.0502
<i>wR</i> 2 [<i>I</i> > 2 σ (<i>I</i>)]	0.0791	0.0746
<i>R</i> 1 [all data]	0.0402	0.0886
<i>wR</i> 2 [all data]	0.0815	0.0831
goodness-of-fit	0.967	1.112
$\Delta\rho_{\max}, \Delta\rho_{\min}$ (eÅ ⁻³)	0.709, -0.307	0.349, -0.425
CCDC no.	1402837	1402836

General method for the preparation of compounds 8, 9, 11, 13, 16, 18, 19 and 21:**Tert-butyl(S)-2-((S)-2-((2-(((S)-2-(methoxycarbonyl) pyrrolidin-1-yl) sulfonyl) phenyl) carbamoyl) pyrrolidine-1-carbonyl) pyrrolidine-1-carboxylate 8:**

To a stirred solution of **7a**^{18a} (2.0 g, 4.15 mmol) in DCM (20 mL), TFA (5 mL) was added at room temperature. After completion of the reaction (2 h), solvent was evaporated and the reaction mixture was neutralized with sat. NaHCO₃. The product was extracted with DCM (15 mL x 3) and organic layer dried over anhydrous Na₂SO₄. The solvent was evaporated and the crude amine **7b** was carried forward without purification. To a solution of Boc-^LPro-OH (0.67 g, 3.14 mmol) in DCM (30 mL), trimer amine **7b** (1.0 g, 2.62 mmol) and EDC.HCl (0.6 g, 3.14 mmol) were added followed by the addition of catalytic amount of HOBT (0.1 g). The reaction mixture was stirred at room temperature overnight. The solvent was evaporated and the reaction mixture was diluted with EtOAc. The organic layer was washed with sat. NaHCO₃, water, sat. KHSO₄, brine and dried over anhydrous Na₂SO₄. After removal of volatiles in vacuum, the crude product was chromatographed on silica gel (80:20 EtOAc/pet ether, R_f 0.5) to afford **8** as a viscous compound (1.44 g, 95%). $[\alpha]_{\text{D}}^{25}$: -175.30° (c 0.25, CHCl₃); IR (CHCl₃) ν (cm⁻¹): 3320, 3150, 2950, 1745, 1690, 1540, 1507, 1400, 1160, 768; ¹H NMR (400 MHz, CDCl₃) δ : 9.86_{rotamer} (0.4H), 9.83_{rotamer} (0.6H), 8.48-8.45 (dd, *J* = 8.3, 4.2 Hz, 1H), 7.89-7.87 (dd, *J* = 8.0, 1.4 Hz, 1H), 7.57-7.53 (t, *J* = 8.3 Hz, 1H), 7.21-7.16 (q, *J* = 8.0 Hz, 1H), 4.85-4.77 (m, 1H), 4.56-4.53 (m, 1H), 4.44-4.39 (m, 1H), 3.87-3.81 (m, 1H), 3.73 (s, 3H), 3.67 (bs, 1H), 3.57-3.49 (m, 1H), 3.47-3.38 (m, 1H), 3.37-3.28 (m, 2H), 2.29-2.11 (m, 5H), 2.10-2.00 (m, 4H), 1.98-1.91 (m, 1H), 1.90-1.80 (m, 2H), 1.44_{rotamer} (5H), 1.40_{rotamer} (4H); ¹³C NMR (100 MHz, CDCl₃) δ : 172.51, 172.23, 171.90, 171.15, 170.78, 154.61, 153.78, 136.76,

136.61, 134.31, 129.65, 129.57, 125.30, 123.74, 123.61, 123.53, 123.32, 79.43, 61.37, 59.59, 59.42, 57.71, 52.71, 52.52, 48.83, 47.02, 46.89, 46.67, 30.84, 30.09, 29.39, 29.25, 28.46, 28.35, 24.93, 24.74, 24.18, 23.66; HRMS: $C_{27}H_{39}O_8N_4S$, Calcd: 579.2483 Found: 579.2483; $C_{27}H_{38}O_8N_4NaS$, calcd: 601.2303 Found: 601.2296.

General method for the preparation of compounds 1, 10, 12, 2, 17, 3, 20 and 4:

Tert-butyl (S)-2-((S)-2-((2-(((S)-2-((4-bromophenyl) carbamoyl) pyrrolidin-1-yl) sulfonyl) phenyl) carbamoyl) pyrrolidine-1-carbonyl) pyrrolidine-1-carboxylate 1:

To a solution of tetramer ester **8** (0.44 g, 0.76 mmol) in methanol (6 mL), LiOH.H₂O (0.038 g, 0.91 mmol) in water (1 mL) was added at room temperature. The reaction mixture was stirred at room temperature for 4 h. The solvent was evaporated under vacuum and the free carboxylic acid was obtained by treating with sat. KHSO₄; followed by extraction with DCM (2 × 10 mL). The crude free acid obtained after evaporation of the solvent under vacuum was carried forward for the next reaction. To the solution of tetramer acid (0.4 g, 0.7 mmol) and 4-bromoaniline (0.12 g, 0.7 mmol) in DCM (10 mL), EDC.HCl (0.16 g, 0.85 mmol) was added followed by the addition of catalytic amount of HOBT (0.04 g). The reaction mixture was stirred at room temperature overnight. The reaction mixture was diluted with DCM (20 mL). The organic layer was washed with sat. NaHCO₃, water, sat. KHSO₄, brine and dried over anhydrous Na₂SO₄. After removal of volatiles in vacuum, the crude product was chromatographed on silica gel (65:35 EtOAc/pet ether, R_f 0.3) to afford **1** as a white crystalline solid (0.41 g, 81%). mp: 192-193 °C; $[\alpha]_D^{25}$: -178.02° (c 0.1, CHCl₃); IR (CHCl₃) ν (cm⁻¹): 3271, 3118, 2976, 1689, 1593, 1533, 1402, 1322, 1247, 1163, 1078, 827, 755; ¹H NMR (500

MHz, CDCl₃) δ : 9.80 (s, 1H), 9.20_{rotamer} (0.4H), 9.16_{rotamer} (0.6H), 8.30-8.24 (dd, $J = 8.2, 4.2$ Hz, 1H), 7.87-7.85 (t, $J = 7.4$ Hz, 1H), 7.55-7.52 (t, $J = 8.2$ Hz, 1H), 7.48-7.40 (m, 4H), 7.25-7.20 (q, $J = 7.4$ Hz, 1H), 4.72-4.66 (m, 1H), 4.56-4.53 (m, 1H), 4.48-4.41 (m, 1H), 3.93-3.67 (m, 3H), 3.43-3.28 (m, 3H), 2.34 (bs, 1H), 2.25-2.19 (m, 2H), 2.17-2.06 (m, 5H), 2.00-1.93 (m, 2H), 1.83-1.75 (m, 2H), 1.46_{rotamer} (5H), 1.42_{rotamer} (4H); ¹³C NMR (125 MHz, CDCl₃) δ : 173.60, 173.15, 170.82, 170.45, 169.38, 154.56, 153.54, 136.86, 136.08, 135.77, 134.47, 131.68, 130.15, 125.34, 124.38, 123.69, 121.77, 116.90, 79.70, 79.66, 62.30, 62.02, 57.60, 49.40, 47.37, 46.94, 46.71, 30.15, 29.53, 29.34, 28.47, 28.37, 25.10, 24.48, 24.32, 23.82; HRMS: C₃₂H₄₁O₇N₅BrS, Calcd: 718.1905 Found: 718.1902.

Methyl ((2-((S)-1-(pivaloyl-L-prolyl) pyrrolidine-2-carboxamido) phenyl sulfonyl)-L-prolinate) 9:

Compound **9** was prepared by following the procedure for the synthesis of **8**. Purification by column chromatography (80:20 EtOAc/pet ether, R_f 0.3) afforded low melting solid **9** (90%). $[\alpha]_D^{25}$: -188.82° (c 0.1, CHCl₃); IR (CHCl₃) ν (cm⁻¹): 3338, 2985, 1750, 1651, 1517, 1435, 1430, 1145, 765; ¹H NMR (500 MHz, CDCl₃) δ : 9.84 (s, 1H), 8.48-8.47 (d, $J = 8.3$ Hz, 1H), 7.88-7.86 (dd, $J = 8.0, 1.3$ Hz, 1H), 7.56-7.53 (t, $J = 8.3$ Hz, 1H), 7.19-7.16 (t, $J = 8.0$ Hz, 1H), 4.84-4.82 (dd, $J = 8.7, 3.2$ Hz, 1H), 4.74-4.72 (m, 1H), 4.42-4.39 (dd, $J = 8.8, 4.4$ Hz, 1H), 3.93-3.88 (m, 1H), 3.78-3.74 (m, 3H), 3.72 (s, 3H), 3.32-3.29 (t, $J = 6.6$ Hz, 2H), 2.28-2.23 (m, 1H), 2.19-2.11 (m, 4H), 2.09-2.01 (m, 4H), 1.96-1.84 (m, 3H), 1.26 (s, 9H); ¹³C NMR (125 MHz, CDCl₃) δ : 176.66, 172.45, 172.19, 171.19, 136.79, 134.27, 129.57, 125.28, 123.60, 123.52, 61.29, 59.85, 59.52, 52.72, 48.75, 48.52, 47.12, 38.61, 30.83, 29.33, 27.27, 27.18, 26.02, 24.90, 24.71; HRMS:

$C_{27}H_{39}O_7N_4S$, Calcd: 563.2534 Found: 563.2531; $C_{27}H_{38}O_7N_4NaS$, calcd: 585.2353 Found: 585.2347.

(S)-N-(4-bromophenyl)-1-((2-((S)-1-(pivaloyl-L-prolyl) pyrrolidine-2-carboxamido) phenyl) sulfonyl) pyrrolidine-2-carboxamide 10:

Compound **10** was prepared by following the procedure for the synthesis of **1**. Purification by column chromatography (80:20 EtOAc/pet ether, R_f 0.4) afforded white crystalline solid **10** (85%). mp: 118-119 °C; $[\alpha]_D^{25}$: -145.37° (c 0.14, $CHCl_3$); IR ($CHCl_3$) ν (cm^{-1}): 3268, 3117, 2974, 2881, 1689, 1600, 1534, 1320, 1161, 1070, 829, 756; 1H NMR (500 MHz, $CDCl_3$) δ : 9.95 (s, 1H), 8.92 (s, 1H), 8.38-8.36 (d, $J = 8.3$ Hz, 1H), 7.85-7.83 (dd, $J = 8.07, 1.2$ Hz, 1H), 7.54-7.51 (t, $J = 8.3$ Hz, 1H), 7.43-7.39 (m, 4H), 7.22-7.19 (t, $J = 8.07$ Hz, 1H), 4.72-4.69 (m, 1H), 4.67-4.64 (m, 1H), 4.36-4.34 (dd, $J = 8.4, 1.9$ Hz, 1H), 4.02-3.98 (dd, $J = 16.6, 7.7$ Hz, 1H), 3.73-3.66 (m, 3H), 3.56-3.51 (m, 1H), 3.46-3.43 (dd, $J = 17.1, 8.1$ Hz, 1H), 2.2-2.14 (m, 3H), 2.12-2.05 (m, 3H), 2.04-1.95 (m, 2H), 1.88-1.83 (m, 2H), 1.80-1.74 (m, 2H), 1.24 (s, 9H); ^{13}C NMR (125 MHz, $CDCl_3$) δ : 176.74, 172.99, 170.96, 169.16, 136.64, 136.46, 134.65, 131.71, 131.14, 129.94, 124.45, 124.29, 123.24, 121.95, 121.47, 117.14, 62.19, 61.94, 59.75, 49.61, 48.51, 47.42, 38.59, 30.39, 29.40, 27.23, 26.17, 25.19, 24.28; HRMS: $C_{32}H_{41}O_6N_5BrS$, Calcd: 702.1955 Found: 702.1952.

Tert-butyl (R)-2-((S)-2-((2-(((S)-2-(methoxycarbonyl) pyrrolidin-1-yl) sulfonyl) phenyl) carbamoyl) pyrrolidine-1-carbonyl) pyrrolidine-1-carboxylate 11:

Compound **11** was prepared by following the procedure for the synthesis of **8**. Purification by column chromatography (75:25 EtOAc/pet ether, R_f 0.5) afforded **11** as a viscous liquid (85%). $[\alpha]_D^{25}$: -113.32° (c 0.1, $CHCl_3$); IR ($CHCl_3$) ν (cm^{-1}): 3453, 3338, 2973, 2883, 1745, 1695, 1525, 1403, 1163, 1085, 886, 758; 1H

NMR (400 MHz, CDCl₃) δ : 9.82_{rotamer} (0.8H), 9.61_{rotamer} (0.2H), 8.55-8.39 (m, 1H), 8.11_{rotamer} (0.2H), 7.98-7.84_{rotamer} (0.8H), 7.62-7.48 (m, 1H), 7.22-7.16 (t, J = 7.7 Hz, 1H), 4.69-4.65 (dd, J = 10.4, 5.3 Hz, 1H), 4.54-4.43 (m, 1H), 4.39-4.27 (m, 1H), 3.84-3.78 (m, 1H), 3.73 (s, 1H), 3.69 (s, 3H), 3.54-3.45 (m, 2H), 3.41-3.25 (m, 2H), 2.29-2.21 (m, 2H), 2.18-2.12 (m, 2H), 2.09-2.02 (m, 3H), 1.97-1.88 (m, 4H), 1.87-1.82 (m, 1H), 1.42_{rotamer} (7H), 1.18_{rotamer} (2H); ¹³C NMR (100 MHz, CDCl₃) δ : 172.89, 172.65, 172.47, 171.65, 171.02, 170.71, 170.56, 154.31, 153.96, 136.79, 136.26, 134.67, 134.20, 133.62, 130.13, 129.83, 129.73, 129.17, 128.07, 125.99, 125.67, 125.35, 124.50, 124.14, 123.70, 123.58, 123.08, 122.47, 79.80, 79.47, 61.56, 60.06, 59.34, 58.99, 58.34, 57.57, 52.74, 52.59, 52.48, 48.99, 48.59, 48.34, 47.34, 47.03, 46.90, 46.79, 46.38, 32.26, 32.09, 31.21, 30.86, 30.18, 29.60, 29.07, 28.41, 28.04, 24.98, 24.75, 24.56, 23.75, 23.34, 22.37; HRMS: C₂₇H₃₉O₈N₄S, Calcd: 579.2483 Found: 579.2485; C₂₇H₃₈O₈N₄NaS, calcd: 601.2303 Found: 601.2298.

Tert-butyl (R)-2-((S)-2-((2-(((S)-2-((4-bromophenyl) carbamoyl) pyrrolidin-1-yl) sulfonyl) phenyl) carbamoyl) pyrrolidine-1-carbonyl) pyrrolidine-1-carboxylate 12:

Compound **12** was prepared by following the procedure for the synthesis of **1**. Purification by column chromatography (70:30 EtOAc/pet ether, R_f 0.3) afforded **12** as a white solid (83%). mp: 126-128 °C; [α]_D²⁵: -83.5° (c 0.14, CHCl₃); IR (CHCl₃) ν (cm⁻¹): 3286, 2981, 2878, 1697, 1680, 1540, 1400, 1158, 756; ¹H NMR (400 MHz, CDCl₃) δ : 10.08_{rotamer} (0.3H), 9.68_{rotamer} (0.5H), 8.85_{rotamer} (0.7H), 8.50_{rotamer} (0.3H), 7.96-7.86 (dd, J = 7.5, 1.2 Hz, 1H), 7.73-7.55 (m, 1H), 7.50-7.37 (m, 5H), 7.27-7.21 (m, 1H), 4.74-4.50 (m, 1H), 4.48-4.37 (m, 1H), 4.34-4.09 (m, 1H), 3.90-3.70 (m, 1H), 3.67-3.57 (m, 1H), 3.56-3.38 (m, 4H), 2.33-2.16 (m, 4H), 2.14-2.02 (m, 2H), 1.99-1.84 (m, 4H), 1.83-1.79 (m, 2H), 1.39_{rotamer} (4H),

1.20_{rotamer} (5H); ¹³C NMR (100 MHz, CDCl₃) δ : 172.59, 172.36, 171.00, 170.15, 169.33, 169.11, 154.65, 153.82, 136.82, 136.27, 134.73, 134.22, 131.83, 131.60, 129.83, 128.01, 126.63, 125.40, 124.07, 122.97, 121.56, 117.11, 116.76, 79.94, 79.87, 62.59, 62.18, 61.82, 58.56, 58.01, 50.19, 49.34, 47.18, 46.92, 46.53, 41.31, 30.40, 30.22, 29.27, 29.13, 28.80, 28.43, 28.11, 25.30, 24.79, 24.66, 24.58, 24.42, 23.53, 22.58; HRMS: C₃₂H₄₁O₇N₅BrS, Calcd: 718.1905 Found: 718.1901.

Methyl ((2-((S)-1-(pivaloyl-D-prolyl) pyrrolidine-2-carboxamido) phenyl) sulfonyl)-L-prolinate 13:

Compound **13** was prepared by following the procedure for the synthesis of **8**. Purification by column chromatography (95:5 EtOAc/pet ether, R_f 0.3) afforded **13** as a viscous liquid (69%). [α]_D²⁵: -105.89° (c 0.2, CHCl₃); IR (CHCl₃) ν (cm⁻¹): 3414, 2971, 1744, 1649, 1609, 1522, 1428, 1332, 1159, 1086, 760; ¹H NMR (500 MHz, CDCl₃) δ : 9.98_{rotamer} (0.6H), 9.49_{rotamer} (0.4H), 8.57-8.55 (d, *J* = 8.3 Hz, 1H), 7.97-7.86 (m, 1H), 7.60-7.49 (m, 1H), 7.24-7.21 (t, *J* = 7.6 Hz, 1H), 5.17-5.15 (dd, *J* = 9.0, 2.1 Hz, 1H), 4.70-4.63 (m, 1H), 4.47-4.33 (m, 1H), 3.80-3.70 (m, 3H), 3.65 (s, 3H), 3.56-3.53 (dd, *J* = 16.8, 7.8 Hz, 1H), 3.44-3.26 (m, 2H), 2.51-2.29 (m, 1H), 2.26-2.14 (m, 3H), 2.08-2.03 (m, 2H), 1.97-1.90 (m, 4H), 1.88-1.77 (m, 2H), 1.23_{rotamer} (6H), 1.01_{rotamer}(3H); ¹³C NMR (125 MHz, CDCl₃) δ : 176.51, 173.31, 172.28, 171.70, 170.98, 136.44, 134.44, 133.53, 129.76, 129.34, 126.77, 125.78, 123.93, 122.38, 62.10, 61.53, 59.95, 52.70, 48.56, 47.10, 38.50, 32.15, 30.89, 29.10, 28.06, 27.24, 24.74, 22.62; HRMS: C₂₇H₃₉O₇N₄S, Calcd: 563.2534 Found: 563.2533; C₂₇H₃₈O₇N₄NaS, calcd: 585.2353 Found: 585.2349.

(S)-N-(4-bromophenyl)-1-((2-((S)-1-(pivaloyl-D-prolyl) pyrrolidine-2-carboxamido) phenyl) sulfonyl) pyrrolidine-2-carboxamide 2:

Compound **2** was prepared by following the procedure for the synthesis of **1**. Purification by column chromatography (90:10 EtOAc/pet ether, R_f 0.3) afforded **2** as a white solid (91%). mp: 117-118 °C $[\alpha]_D^{25}$: -109.32° (c 0.16, CHCl₃); IR (CHCl₃) ν (cm⁻¹): 3226, 3114, 2978, 2882, 1684, 1607, 1532, 1436, 1322, 1162, 1075, 829, 756; ¹H NMR (500 MHz, CDCl₃) δ : 9.46 (s, 1H), 9.12 (s, 1H), 7.90-7.89 (d, J = 8.1 Hz, 1H), 7.74-7.73 (d, J = 7.8 Hz, 1H), 7.45-7.42 (dd, J = 8.1, 1.4 Hz, 1H), 7.39-7.34 (m, 4H), 7.26-7.23 (t, J = 7.8 Hz, 1H), 4.68-4.66 (m, 2H), 4.43-4.38 (m, 1H), 4.16 (bs, 1H), 3.77-3.71 (m, 2H), 3.65-3.61 (m, 1H), 3.60-3.54 (m, 1H), 3.50-3.44 (m, 1H), 2.33-2.25 (m, 2H), 2.21-2.11 (m, 4H), 2.06-1.98 (m, 2H), 1.92-1.85 (m, 3H), 1.82-1.77 (m, 1H), 1.02 (s, 9H); ¹³C NMR (125 MHz, CDCl₃) δ : 177.23, 172.5, 171.36, 169.53, 136.92, 136.56, 136.03, 134.14, 131.93, 131.45, 130.28, 128.98, 127.18, 125.66, 124.26, 121.48, 116.53, 62.86, 61.68, 60.24, 49.06, 48.55, 47.14, 38.48, 32.07, 30.56, 29.43, 28.05, 27.08, 26.83, 26.20, 24.93, 24.52; HRMS: C₃₂H₄₁O₆N₅BrS, Calcd: 702.1955 Found: 702.1953.

Methyl ((2-(2-azidoacetamido) phenyl) sulfonyl)-L-prolinate 14a:

To a stirred solution of **6** (1 g, 3.52 mmol) in DCM (30 mL), Et₃N (0.98 mL, 7.04 mmol) and bromoacetyl bromide (0.85 g, 4.2 mmol) were added dropwise sequentially at 0 °C. The reaction mixture was stirred at room temperature for 1 h and after completion of reaction; it was diluted with DCM (30 mL). The organic layer was washed with water, sat. NaHCO₃ and brine. The organic layer was dried over Na₂SO₄ and volatiles were evaporated under reduced pressure. Purification by column chromatography (40:60 EtOAc/pet ether, R_f 0.4) afforded **14a** as a viscous liquid (1.34 g, 95%). $[\alpha]_D^{26}$: -60.6° (c 0.3, CHCl₃); IR (CHCl₃) ν (cm⁻¹): 3305, 3020, 2956, 1742, 1698, 1586, 1531, 1466, 1437, 1337, 1216, 1154, 766, 667, 607, 578; ¹H NMR (400 MHz, CDCl₃) δ : 10.13 (s, 1H), 8.51-8.49 (d, J = 8.3

Hz, 1H), 7.96-7.94 (dd, $J = 8.0, 1.5$ Hz, 1H), 7.65-7.60 (m, 1H), 7.29-7.25 (m, 1H), 4.48-4.44 (m, 1H), 4.15-4.11 (d, $J = 4.7$ Hz, 2H), 3.72 (s, 3H), 3.41-3.35 (m, 2H), 2.26-2.19 (m, 1H), 2.09-2.03 (m, 1H), 1.98-1.90 (m, 2H); ^{13}C NMR (100 MHz, CDCl_3) δ : 172.51, 164.96, 136.10, 134.49, 129.98, 125.72, 124.26, 122.83, 59.52, 52.68, 48.67, 30.96, 29.38, 24.68; HRMS: $\text{C}_{14}\text{H}_{18}\text{O}_5\text{N}_2\text{BrS}$, Calcd: 407.0094 Found: 407.0089.

Methyl ((2-(2-azidoacetamido) phenyl) sulfonyl)-L-prolinate 14b:

To a stirred solution of **14a** (0.8 g, 1.97 mmol) in DMF (5 mL), NaN_3 (0.38 g, 5.91 mmol) was added and the reaction mixture was heated at 50 °C for 1 h. The reaction mixture was diluted with EtOAc (30 mL) and washed with water and brine. The organic layer was dried over Na_2SO_4 and evaporated in vacuum. Purification by column chromatography (40:60 EtOAc/pet ether, R_f 0.4) afforded **14b** as a viscous liquid (0.69 g, 96%). $[\alpha]_D^{26}$: -71.79° (c 0.3, CHCl_3); IR (CHCl_3) ν (cm^{-1}): 3305, 3021, 2116, 1704, 1586, 1531, 1437, 1338, 1284, 1218, 1153, 1021, 771, 668, 608; ^1H NMR (400 MHz, CDCl_3) δ : 10.11 (s, 1H), 8.54-8.52 (d, $J = 8.3$ Hz, 1H), 7.94-7.92 (d, $J = 7.8$ Hz, 1H), 7.62-7.58 (t, $J = 7.3$ Hz, 1H), 7.27-7.23 (m, 1H), 4.45-4.41 (m, 1H), 4.18-4.16 (m, 2H), 3.67 (s, 3H), 3.40-3.37 (m, 2H), 2.24-2.18 (m, 1H), 2.08-2.02 (m, 1H), 1.98-1.88 (m, 2H); ^{13}C NMR (100 MHz, CDCl_3) δ : 172.36, 165.87, 135.84, 134.45, 129.90, 125.86, 124.18, 122.77, 59.68, 53.19, 52.60, 48.61, 31.01, 24.62; HRMS: $\text{C}_{14}\text{H}_{18}\text{O}_5\text{N}_5\text{S}$, Calcd: 368.1023 Found: 368.1022; $\text{C}_{14}\text{H}_{17}\text{O}_5\text{N}_5\text{NaS}$, calcd: 390.0843 Found: 390.0838.

Tert-butyl (S)-2-((2-(((S)-2-(methoxycarbonyl) pyrrolidin-1-yl) sulfonyl) phenyl) amino)-2-oxoethyl) carbamoyl) pyrrolidine-1-carboxylate 16:

To a solution of **14b** (0.7 g, 1.9 mmol) in EtOAc (20 mL), 10% Pd/C (0.07 g) was added. The reaction mixture was stirred at 60 psi H_2 atmosphere for 8 h. The

catalyst was filtered through celite and the filtrate was concentrated to obtain crude product **14c**, which was used for the next step without purification. The product **16** was obtained from **14c** following the procedure for **8**. Purification by column chromatography (70:30 EtOAc/pet ether, R_f 0.3) afforded **16** as a viscous liquid (76%). $[\alpha]_D^{25}$: -92.17° (c 0.16, CHCl_3); IR (CHCl_3) ν (cm^{-1}): 3314, 2982, 1747, 1699, 1507, 1507, 1395, 1338, 1154, 760; ^1H NMR (400 MHz, CDCl_3) δ : 9.90 (bs, 1H), 8.45 (bs, 1H), 7.89-7.87 (d, $J = 7.9$ Hz, 1H), 7.70 (bs, 1H), 7.60-7.57 (t, $J = 7.6$ Hz, 1H), 7.24-7.20 (t, $J = 7.9$ Hz, 1H), 4.42 (bs, 1H), 4.32-4.25 (m, 1H), 4.20-4.10 (m, 1H), 3.76-3.68 (m, 3H), 3.48 (s, 2H), 3.36-3.28 (m, 3H), 2.21-2.12 (m, 2H), 2.07-2.00 (m, 2H), 1.97-1.94 (m, 2H), 1.87-1.85 (m, 2H), 1.46 (s, 9H); ^{13}C NMR (100 MHz, CDCl_3) δ : 172.91, 168.09, 136.13, 134.42, 129.83, 125.46, 123.88, 123.05, 80.45, 59.59, 52.79, 48.58, 47.18, 43.82, 30.86, 28.32, 24.66; HRMS: $\text{C}_{24}\text{H}_{35}\text{O}_8\text{N}_4\text{S}$, Calcd: 539.2170 Found: 539.2171; $\text{C}_{24}\text{H}_{34}\text{O}_8\text{N}_4\text{NaS}$, calcd: 561.1990 Found: 561.1989.

Tert-butyl (S)-2-((2-(((S)-2-((4-bromophenyl) carbamoyl) pyrrolidin-1-yl) sulfonyl) phenyl) amino)-2-oxoethyl) carbamoyl) pyrrolidine-1-carboxylate **17:**

Compound **17** was prepared by following the procedure for the synthesis of **1**. Purification by column chromatography (70:30 EtOAc/pet ether, R_f 0.3) afforded **17** as a white crystalline solid (66%). mp: 116-118 $^\circ\text{C}$; $[\alpha]_D^{26}$: -118.28° (c 0.12, CHCl_3); IR (CHCl_3) ν (cm^{-1}): 3318, 3120, 2976, 1681, 1592, 1400, 1332, 1161, 1079, 827, 759; ^1H NMR (500 MHz, CDCl_3) δ : 9.98 (s, 1H), 8.90 (s, 1H), 8.40-8.39 (d, $J = 8.2$ Hz, 1H), 7.92 (bs, 1H), 7.88-7.86 (d, $J = 7.6$ Hz, 1H), 7.60-7.57 (t, $J = 8.2$ Hz, 1H), 7.48-7.41 (m, 4H), 7.26-7.24 (t, $J = 7.6$ Hz, 1H), 4.47 (bs, 1H), 4.38-4.36 (m, 1H), 4.14 (bs, 1H), 4.00 (bs, 1H), 3.64 (s, 1H), 3.43-3.41 (m, 1H), 3.32 (bs, 2H), 2.18-2.15 (m, 1H), 2.00-1.85 (m, 5H), 1.77-1.74 (m, 2H), 1.46 (s,

9H); ^{13}C NMR (125 MHz, CDCl_3) δ : 173.68, 169.31, 167.75, 136.69, 135.79, 134.67, 131.82, 129.97, 125.08, 124.47, 123.35, 121.52, 117.07, 80.83, 62.63, 59.97, 49.24, 47.29, 44.23, 41.31, 30.65, 28.37, 27.63, 24.43, 22.59, 20.4, 19.40; HRMS: $\text{C}_{29}\text{H}_{37}\text{O}_7\text{N}_5\text{BrS}$, Calcd: 678.1592 Found: 678.1594.

Methyl ((2-(2-((S)-1-pivaloylpyrrolidine-2-carboxamido) acetamido) phenyl) sulfonyl)-L-prolinate 18:

Compound **18** was prepared by following the procedure for the synthesis of **8**. Purification by column chromatography (90:10 EtOAc/pet ether, R_f 0.4) afforded **18** as a viscous liquid (71%). $[\alpha]_{\text{D}}^{25}$: -97.7° (c 0.26, CHCl_3); IR (CHCl_3) ν (cm^{-1}): 3320, 2968, 1749, 1695, 1505, 1338, 1150, 760; ^1H NMR (400 MHz, CDCl_3) δ : 9.88 (s, 1H), 8.47-8.45 (d, $J = 8.3$ Hz, 1H), 7.88-7.86 (d, $J = 7.8$ Hz, 1H), 7.59-7.56 (t, $J = 8.3$ Hz, 1H), 7.49 (s, 1H), 7.23-7.19 (t, $J = 7.8$ Hz, 1H), 4.72-4.69 (m, 1H), 4.41 (dd, $J = 8.6, 3.9$ Hz, 1H), 4.29-4.22 (m, 1H), 4.12-4.05 (m, 1H), 3.76-3.73 (m, 2H), 3.72 (s, 3H), 3.35-3.25 (m, 2H), 2.31-2.28 (m, 1H), 2.19-2.11 (m, 2H), 2.07-2.00 (m, 1H), 1.94-1.90 (m, 2H), 1.88-1.85 (m, 2H), 1.28 (s, 9H); ^{13}C NMR (100 MHz, CDCl_3) δ : 178.14, 172.85, 172.54, 168.10, 136.20, 134.39, 129.76, 125.51, 123.84, 123.11, 61.90, 59.58, 52.75, 48.44, 43.86, 39.18, 30.85, 27.43, 26.78, 25.79, 24.62; HRMS: $\text{C}_{24}\text{H}_{35}\text{O}_7\text{N}_4\text{S}$, Calcd: 523.2221 Found: 523.2221; $\text{C}_{24}\text{H}_{34}\text{O}_7\text{N}_4\text{NaS}$, calcd: 545.2040 Found: 545.2038.

(S)-N-(4-bromophenyl)-1-((2-(2-((S)-1-pivaloylpyrrolidine-2-carboxamido) acetamido) phenyl) sulfonyl) pyrrolidine-2-carboxamide 3:

Compound **3** was prepared by following the procedure for the synthesis of **1**. Purification by column chromatography (90:10 EtOAc/pet ether, R_f 0.4) afforded **3** as a white crystalline solid (58%). mp: 109-110 $^\circ\text{C}$; $[\alpha]_{\text{D}}^{26}$: -122.94° (c 0.11, CHCl_3); IR (CHCl_3) ν (cm^{-1}): 3418, 2970, 2970, 1643, 1580, 1418, 1223, 1117, 1088, 770; ^1H NMR (400 MHz, CDCl_3) δ : 9.97 (s, 1H), 9.05 (s, 1H), 8.32-8.30 (d,

$J = 8.2$ Hz, 1H), 7.86-7.84 (dd, $J = 7.9, 1.1$ Hz, 1H), 7.64 (s, 1H), 7.57-7.54 (t, $J = 8.2$ Hz, 1H), 7.45-7.38 (m, 4H), 7.26-7.24 (t, $J = 7.9$ Hz, 1H), 4.74-4.71 (dd, $J = 7.8, 3.9$ Hz, 1H), 4.44-4.41 (dd, $J = 8.2, 2.8$ Hz, 1H), 4.09-4.03 (m, 2H), 3.74-3.68 (m, 2H), 3.66-3.60 (m, 1H), 3.39-3.33 (dd, $J = 16.9, 7.4$ Hz, 1H), 2.28-2.22 (m, 1H), 2.20-2.14 (m, 1H), 2.09-2.04 (m, 1H), 1.97-1.89 (m, 4H), 1.80-1.76 (m, 1H), 1.27 (s, 9H); ^{13}C NMR (100 MHz, CDCl_3) δ : 178.47, 173.47, 169.29, 167.93, 136.75, 135.71, 134.51, 131.75, 129.82, 125.68, 124.56, 123.66, 121.47, 117.00, 62.53, 62.02, 49.31, 48.51, 44.08, 39.19, 30.67, 29.66, 27.41, 26.60, 25.94, 24.44; HRMS: $\text{C}_{29}\text{H}_{37}\text{O}_6\text{N}_5\text{BrS}$, Calcd: 662.1642 Found: 662.1640.

Compounds 15a-c were prepared by the reported procedures.^{18b}

Tert-butyl (R)-2-((1-((2-(((S)-2-(methoxycarbonyl) pyrrolidin-1-yl) sulfonyl) phenyl) amino)-2-methyl-1-oxopropan-2-yl) carbamoyl) pyrrolidine-1-carboxylate 19:

Compound **19** was prepared by following the procedure for the synthesis of **8**. The Purification by column chromatography (60:40 EtOAc/pet ether, R_f 0.3) afforded **19** as a low melting solid (96%). mp: 54 °C; $[\alpha]_D^{25}$: -81.45° (c 0.15, CHCl_3); IR (CHCl_3) $\nu(\text{cm}^{-1})$: 3316, 2981, 1748, 1699, 1518, 1334, 1447, 834, 604; ^1H NMR (400 MHz, CDCl_3) δ : 10.09 (s, 1H), 8.61-8.59 (d, $J = 8.1$ Hz, 1H), 7.82-7.80 (d, $J = 7.9$ Hz, 1H), 7.78 (s, 1H), 7.57-7.53 (t, $J = 8.1$ Hz, 1H), 7.19-7.15 (t, $J = 7.9$ Hz, 1H), 4.34-4.31 (m, 2H), 3.64 (s, 3H), 3.53-3.45 (m, 2H), 3.38-3.31 (m, 2H), 2.07-1.97 (m, 4H), 1.95-1.91 (m, 1H), 1.85-1.81 (m, 3H), 1.59 (s, 6H), 1.48 (s, 9H); ^{13}C NMR (100 MHz, CDCl_3) δ : 173.16, 172.00, 134.28, 129.33, 124.84, 123.34, 122.10, 80.43, 60.27, 57.51, 53.28, 53.01, 52.74, 48.34, 47.10, 30.86, 28.29, 24.51; HRMS: $\text{C}_{26}\text{H}_{39}\text{O}_8\text{N}_4\text{S}$, Calcd: 567.2483 Found: 567.2484; $\text{C}_{26}\text{H}_{38}\text{O}_8\text{N}_4\text{NaS}$, calcd: 589.2303 Found: 589.2300.

Tert-butyl (R)-2-((1-((2-(((S)-2-((4-bromophenyl) carbamoyl) pyrrolidin-1-yl) sulfonyl) phenyl) amino)-2-methyl-1-oxopropan-2-yl) carbamoyl) pyrrolidine-1-carboxylate 20:

Compound **20** was prepared by following the procedure for the synthesis of **1**. Purification by column chromatography (60:40 EtOAc/pet ether, R_f 0.3) afforded **20** as a white solid (94%). mp: 92-93 °C; $[\alpha]_D^{26}$: -135.49° (c 0.17, CHCl_3); IR (CHCl_3) $\nu(\text{cm}^{-1})$: 3388, 2969, 1655, 1590, 1406, 1119, 770; ^1H NMR (500 MHz, CDCl_3) δ : 10.12 (s, 1H), 8.79 (s, 1H), 8.45-8.44 (d, $J = 8.4$ Hz, 1H), 7.86-7.85 (d, $J = 7.9$ Hz, 1H), 7.75 (s, 1H), 7.54-7.51 (t, $J = 8.4$ Hz, 1H), 7.38 (s, 4H), 7.21-7.18 (t, $J = 7.9$ Hz, 1H), 4.39-4.35 (m, 1H), 4.33 (bs, 1H), 3.72-3.68 (m, 1H), 3.49-3.45 (dd, $J = 16.8, 8.1$ Hz, 1H), 3.32 (bs, 2H), 2.21-2.18 (m, 1H), 1.98-1.91 (m, 2H), 1.84-1.75 (m, 4H), 1.72-1.68 (m, 1H), 1.64 (s, 3H), 1.57 (s, 3H), 1.48 (s, 9H); ^{13}C NMR (125 MHz, CDCl_3) δ : 172.69, 172.48, 169.19, 136.86, 136.53, 134.80, 131.63, 129.81, 124.21, 123.98, 122.87, 121.87, 117.03, 80.80, 62.31, 59.97, 57.41, 49.62, 47.16, 41.31, 30.99, 28.33, 24.42, 22.59; HRMS: $\text{C}_{31}\text{H}_{41}\text{O}_7\text{N}_5\text{BrS}$, Calcd: 706.1905 Found: 706.1908.

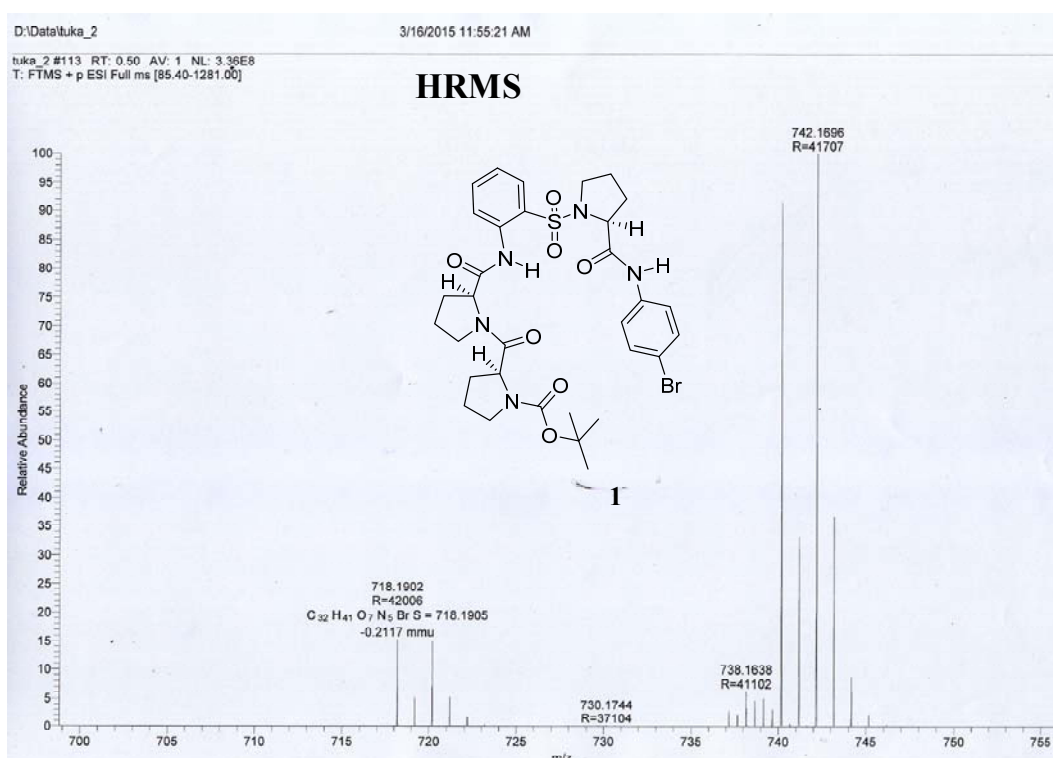
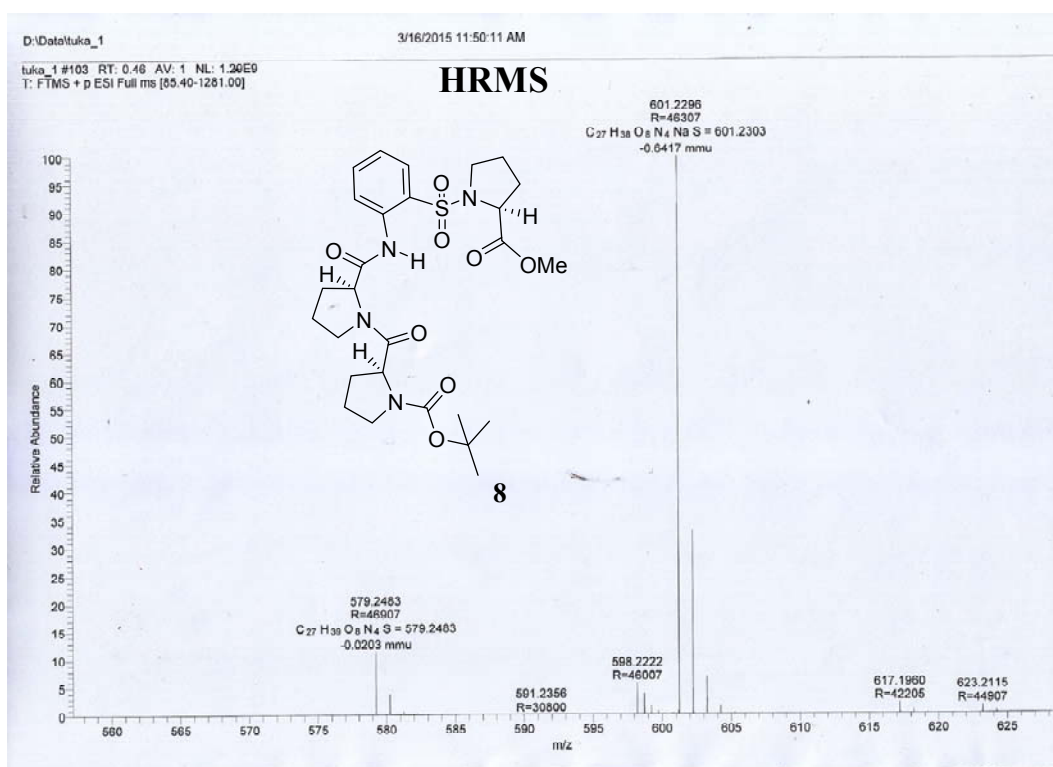
Methyl ((2-(2-methyl-2-((R)-1-pivaloylpyrrolidine-2-carboxamido) propanamido) phenyl) sulfonyl)-L-prolinate 21:

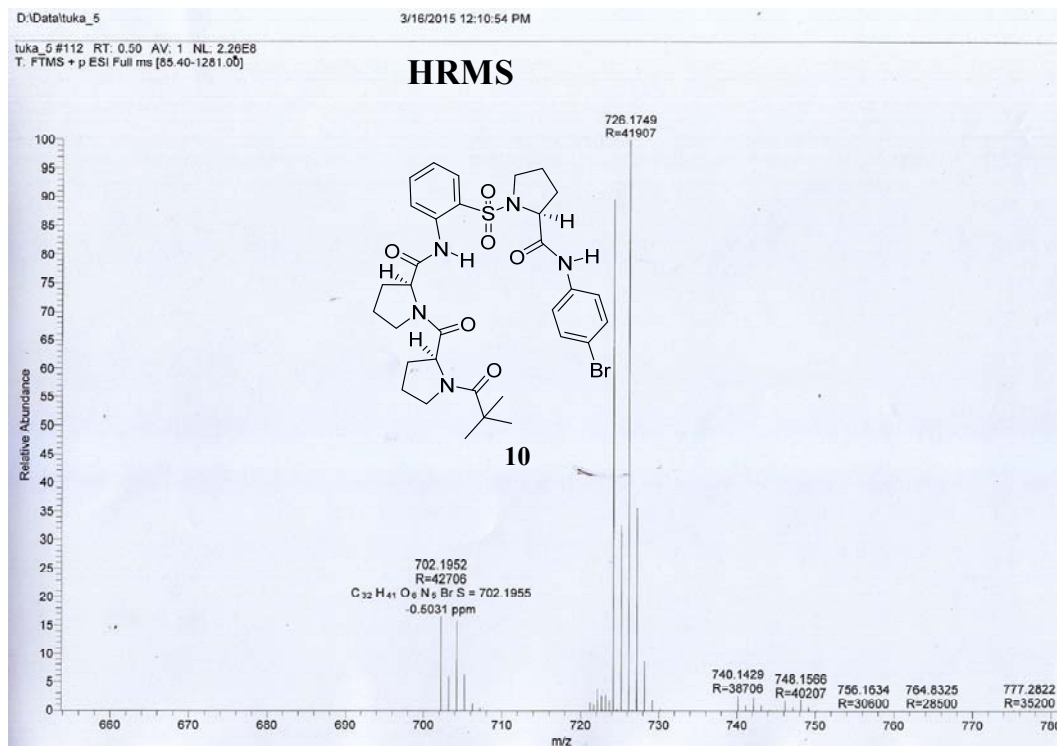
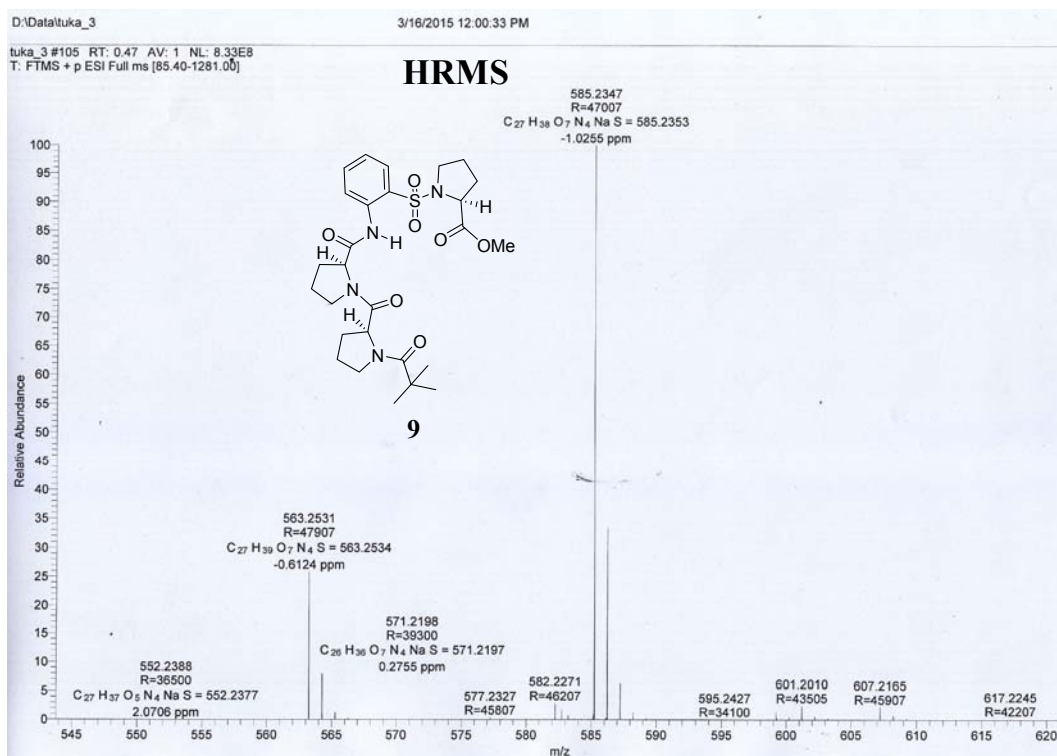
Compound **21** was prepared by following the procedure for the synthesis of **8**. Purification by column chromatography (70:30 EtOAc/pet ether, R_f 0.2) afforded **21** as a low melting solid (87%). mp: 48-49 °C; $[\alpha]_D^{25}$: -91.50° (c 0.12, CHCl_3); IR (CHCl_3) $\nu(\text{cm}^{-1})$: 3315, 2983, 1750, 1697, 1521, 1336, 1148, 761; ^1H NMR (500 MHz, CDCl_3) δ : 10.12 (s, 1H), 8.60-8.58 (d, $J = 8.3$ Hz, 1H), 7.82-7.80 (d, $J = 7.7$ Hz, 1H), 7.58 (bs, 1H), 7.56-7.53 (t, $J = 8.3$ Hz, 1H), 7.18-7.15 (t, $J = 7.7$ Hz, 1H), 4.68-4.66 (m, 1H), 4.34-4.31 (m, 1H), 3.71-3.68 (m, 2H), 3.65 (s, 3H), 3.54-3.50 (m, 1H), 3.35-3.30 (m, 1H), 2.30-2.25 (m, 1H), 2.10-2.03 (m, 2H), 2.02-

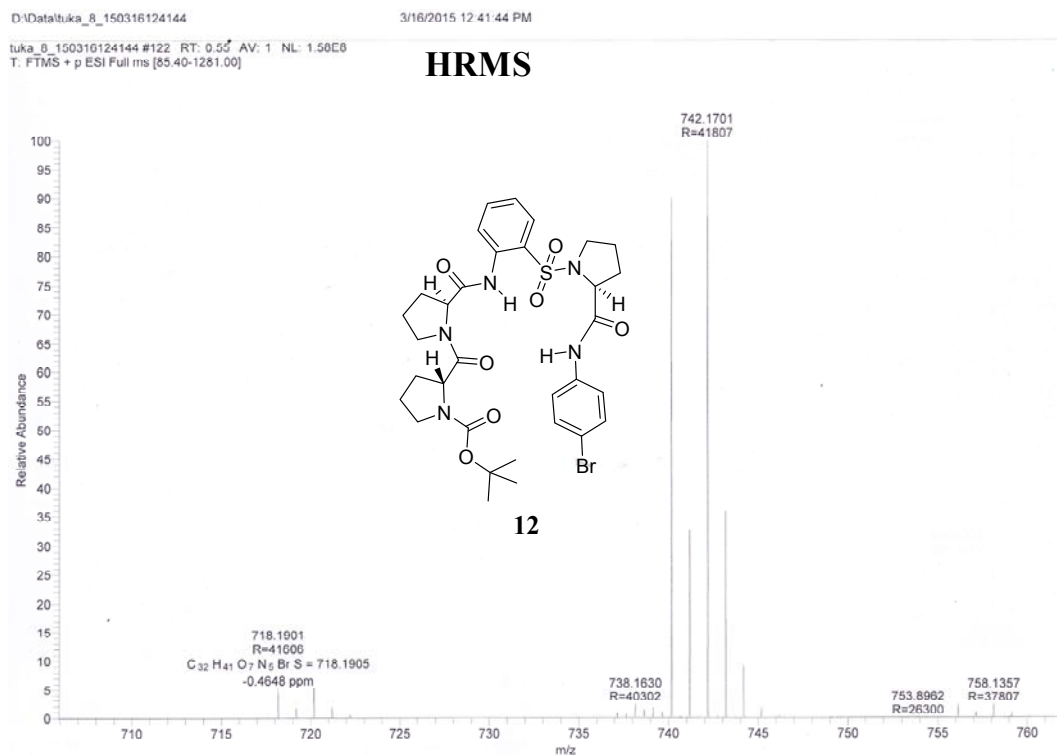
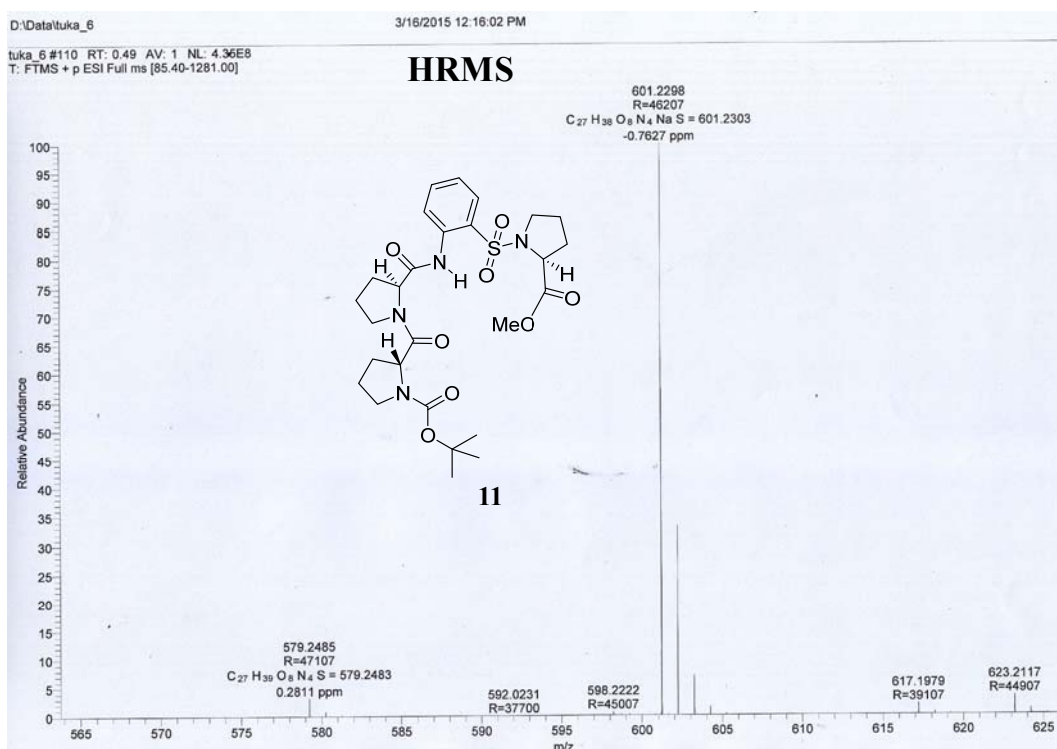
1.96 (m, 2H), 1.91-1.81 (m, 3H), 1.58 (d, 6H), 1.27 (s, 9H); ^{13}C NMR (125 MHz, CDCl_3) δ : 178.24, 173.27, 172.05, 171.81, 137.28, 134.27, 129.31, 124.96, 123.38, 122.32, 122.14, 61.95, 61.77, 60.41, 60.30, 57.54, 52.45, 48.36, 39.23, 30.88, 27.51, 25.94, 25.83, 25.33, 24.66, 24.52, 24.10; HRMS: $\text{C}_{26}\text{H}_{39}\text{O}_7\text{N}_4\text{S}$, Calcd: 551.2534 Found: 551.2536; $\text{C}_{26}\text{H}_{38}\text{O}_7\text{N}_4\text{NaS}$, Calcd: 573.2353 Found: 573.2353.

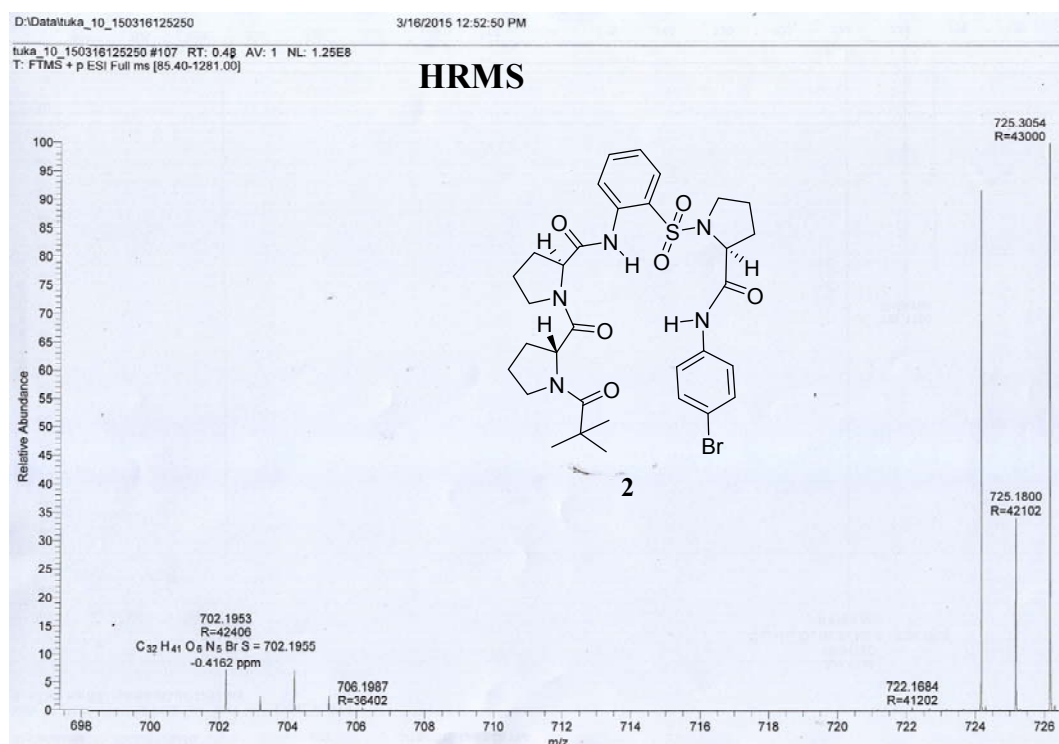
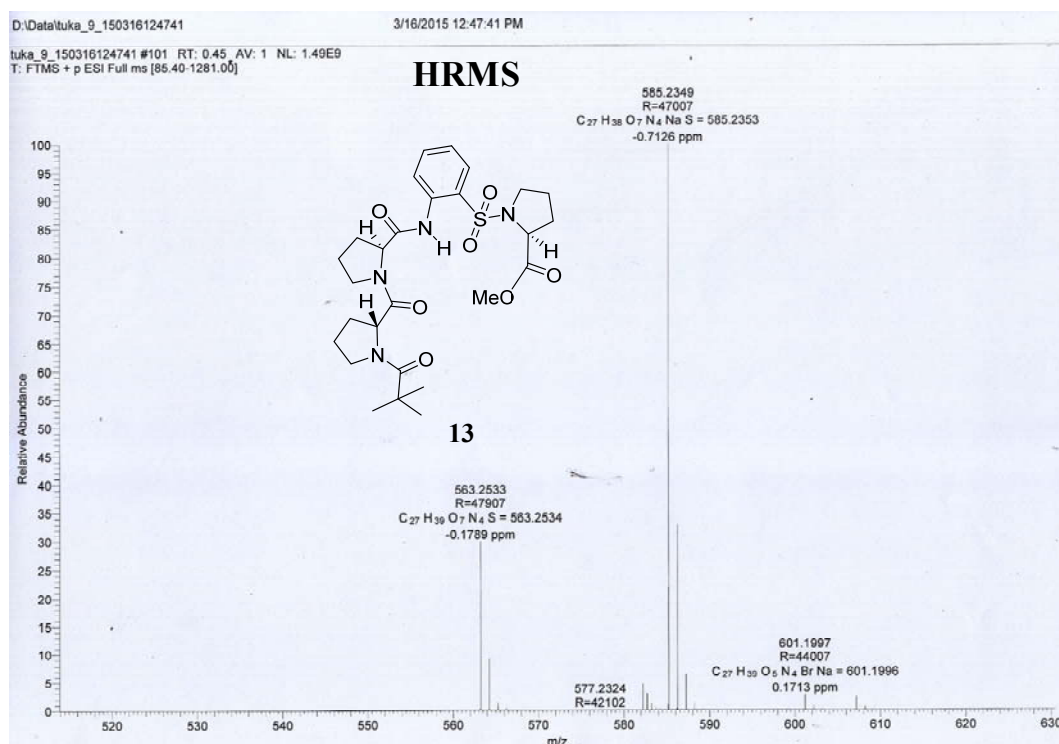
(S)-N-(4-bromophenyl)-1-((2-(2-methyl-2-((R)-1-pivaloylpyrrolidine-2-carboxamido) propanamido) phenyl) sulfonyl) pyrrolidine-2-carboxamide 4:

Compound **4** was prepared by following the procedure for the synthesis of **1**. Purification by column chromatography (70:30 EtOAc/pet ether, R_f 0.2) afforded **4** as a white solid (77%). mp: 101-103 °C; $[\alpha]_D^{26}$: -101.32° (c 0.14, CHCl_3); IR (CHCl_3) ν (cm^{-1}): 3370, 2973, 1671, 1594, 1529, 1424, 1332, 1155, 1076, 826, 766; ^1H NMR (500 MHz, CDCl_3) δ : 10.10_{rotamer} (0.2H), 10.06_{rotamer} (0.8H), 8.82 (s, 1H), 8.39-8.37 (d, $J = 8.3$ Hz, 1H), 7.85-7.83 (dd, $J = 8.0, 1.4$ Hz, 1H), 7.53-7.50 (t, $J = 8.3$ Hz, 1H), 7.43 (s, 1H), 7.41-7.37 (m, 4H), 7.21-7.18 (t, $J = 8.0$ Hz, 1H), 4.66-4.63 (dd, $J = 8.0, 3.6$ Hz, 1H), 4.38-4.35 (m, 1H), 3.71-3.65 (m, 2H), 3.58-3.52 (m, 1H), 3.48-3.42 (m, 1H), 2.24-2.20 (m, 1H), 2.18-2.13 (m, 1H), 1.96-1.88 (m, 3H), 1.86-1.78 (m, 3H), 1.60 (s, 3H), 1.54 (s, 3H), 1.24 (s, 9H); ^{13}C NMR (125 MHz, CDCl_3) δ : 178.39, 172.91, 172.33, 172.17, 169.15, 136.95, 136.54, 134.68, 131.64, 129.73, 129.66, 124.70, 124.11, 124.00, 123.43, 123.07, 121.82, 117.00, 62.33, 61.71, 57.36, 49.71, 49.55, 48.33, 39.19, 30.82, 27.40, 26.16, 25.89, 25.79, 25.49, 24.88, 24.42, 24.25; HRMS: $\text{C}_{31}\text{H}_{41}\text{O}_6\text{N}_5\text{BrS}$, Calcd: 690.1955 Found: 690.1954.







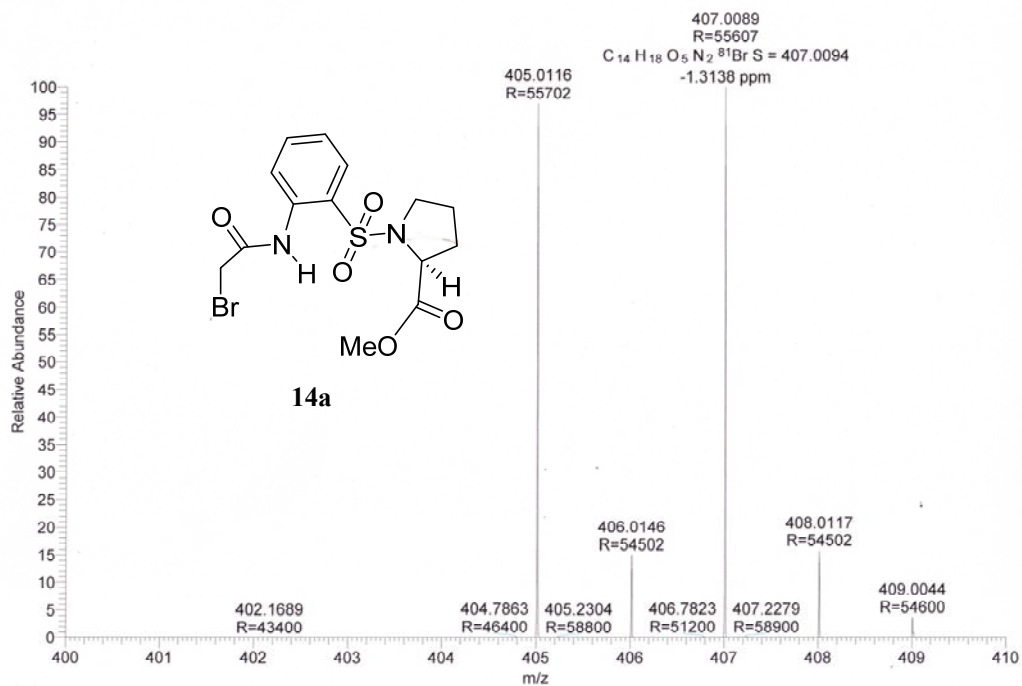


D:\Data\SGP-24

1/7/2013 12:58:34 PM

SGP-24 #893 RT: 3.98 AV: 1 NL: 6.57E8
T: FTMS + p ESI Full ms [100.00-700.00]

HRMS

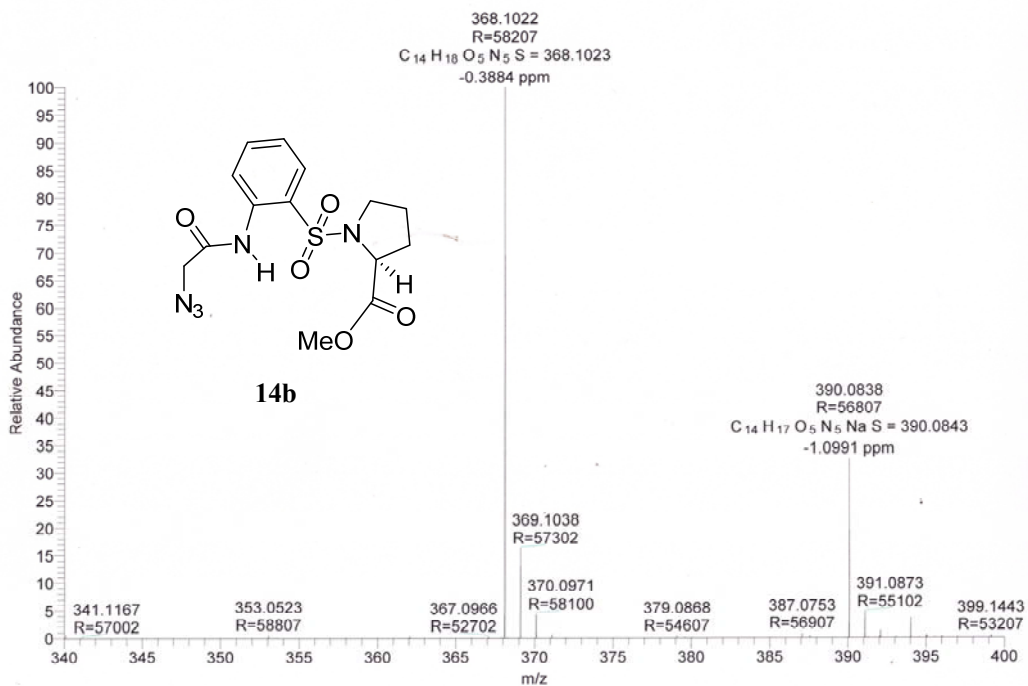


D:\Data\SGP-25

1/7/2013 1:09:46 PM

SGP-25 #883 RT: 3.93 AV: 1 NL: 1.51E9
T: FTMS + p ESI Full ms [100.00-700.00]

HRMS

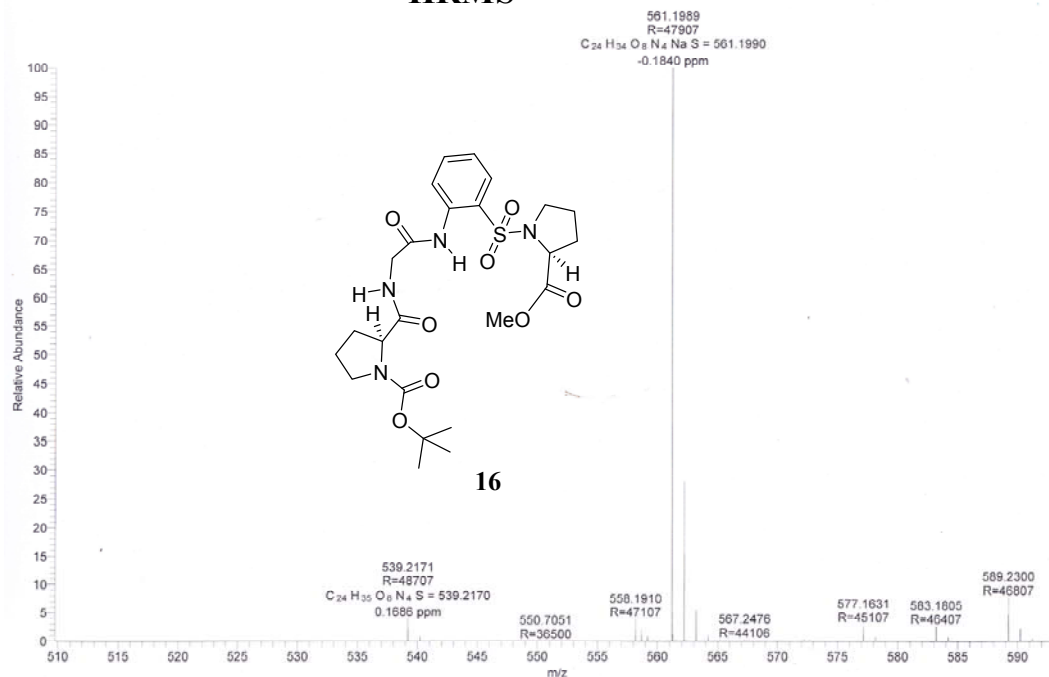


D:\Data\tuka_11_150316125800

3/16/2015 12:58:00 PM

tuka_11_150316125800 #101 RT: 0.45 AV: 1 NL: 9.74E8
T: FTMS + p ESI Full ms [85.40-1281.00]

HRMS

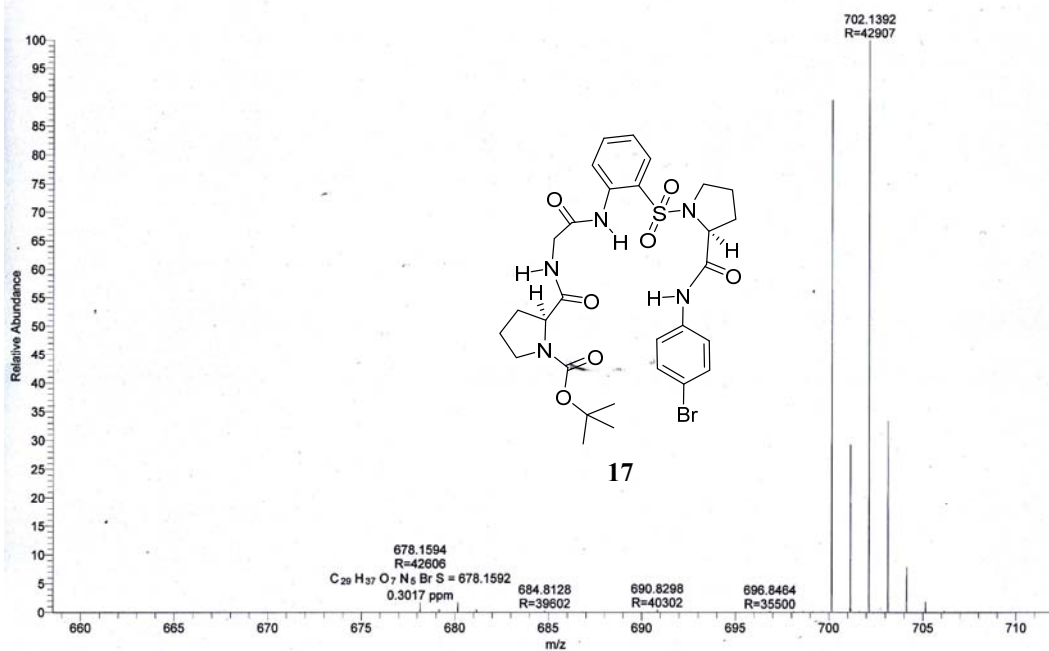


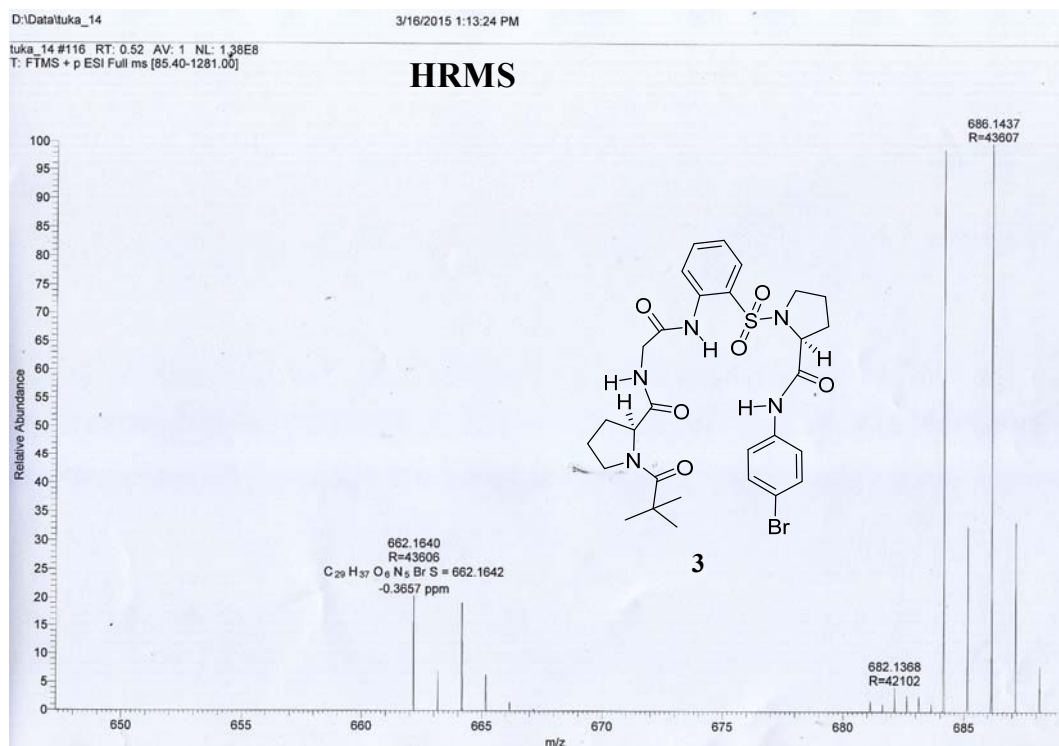
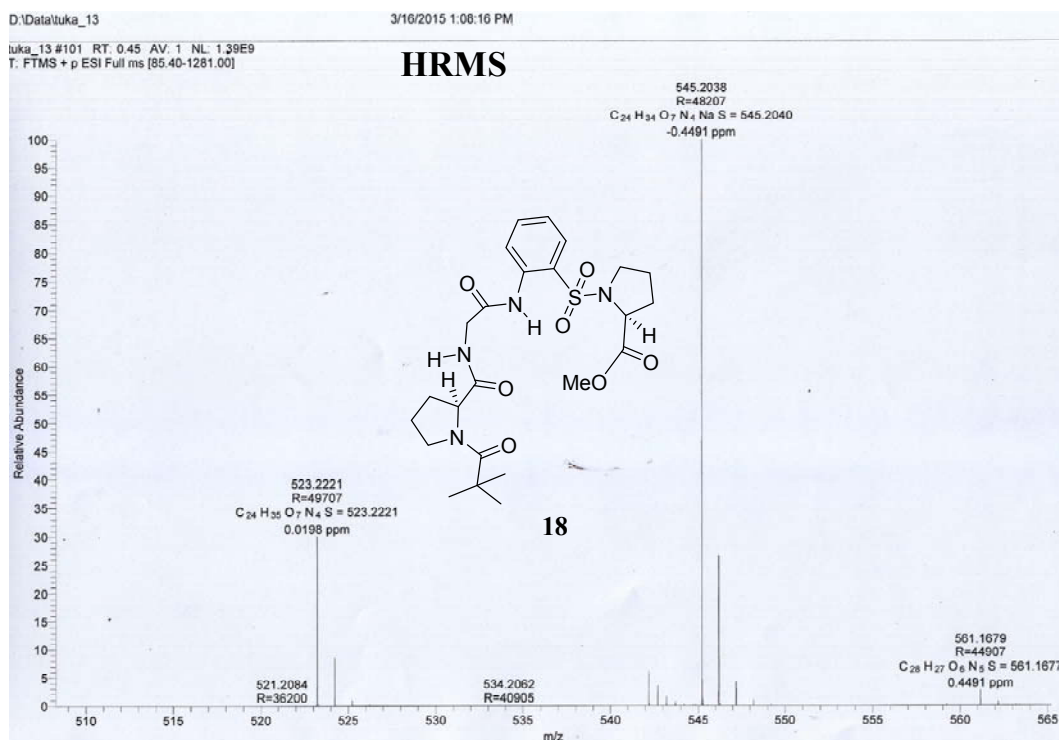
D:\Data\tuka_12_150316130308

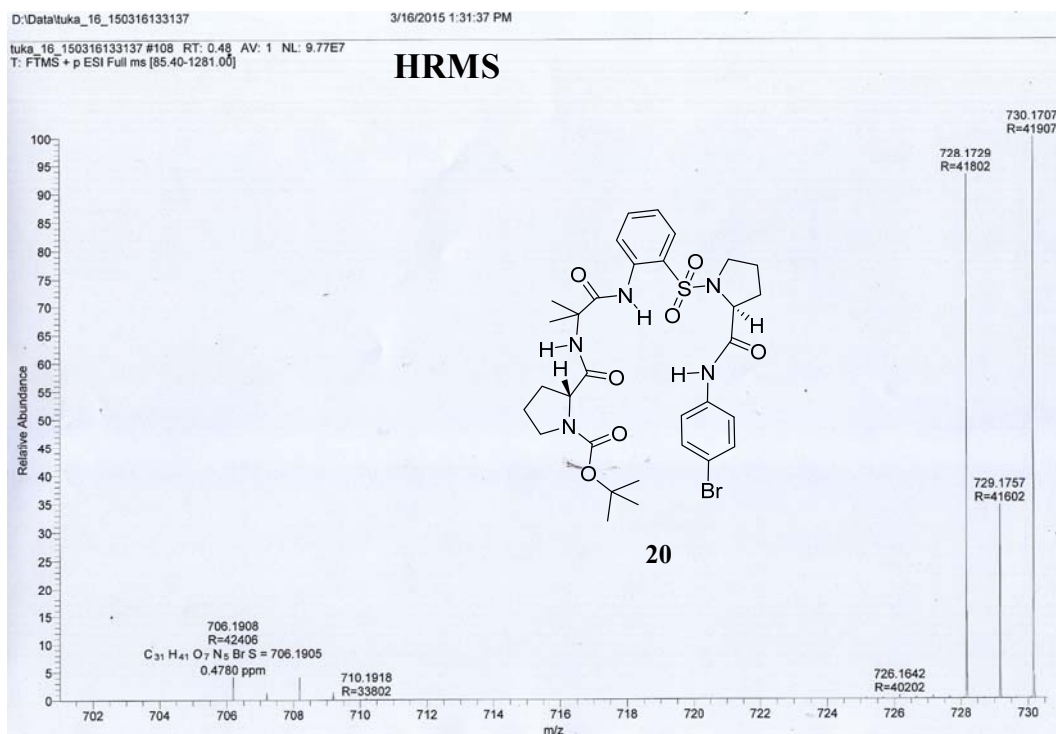
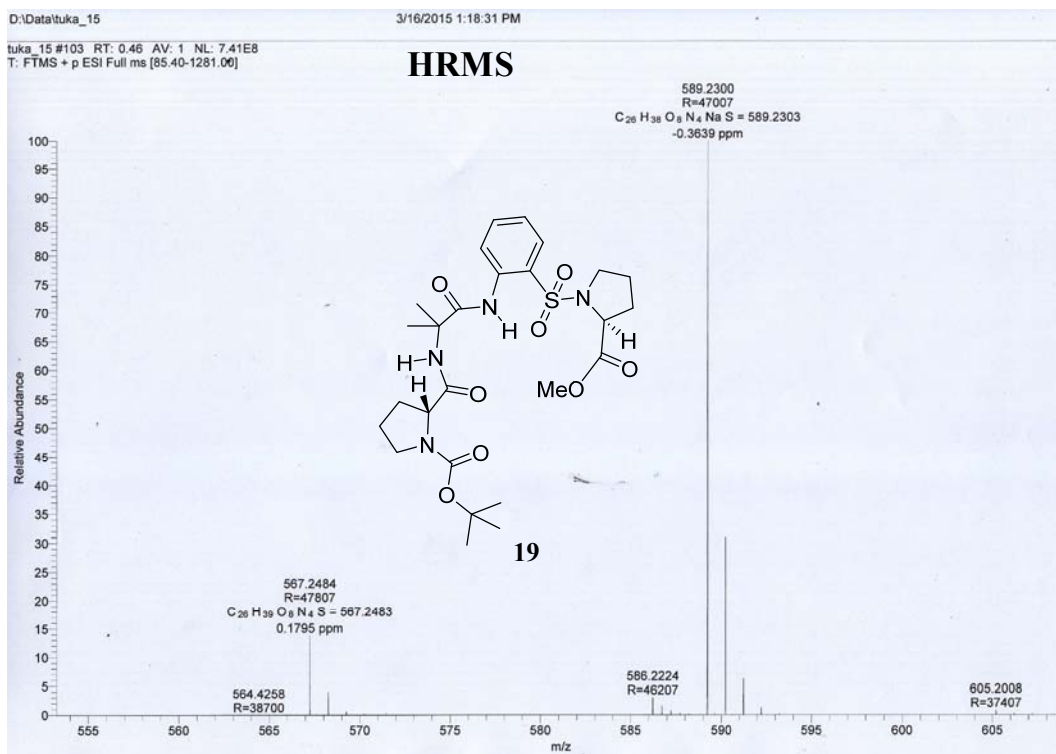
3/16/2015 1:03:08 PM

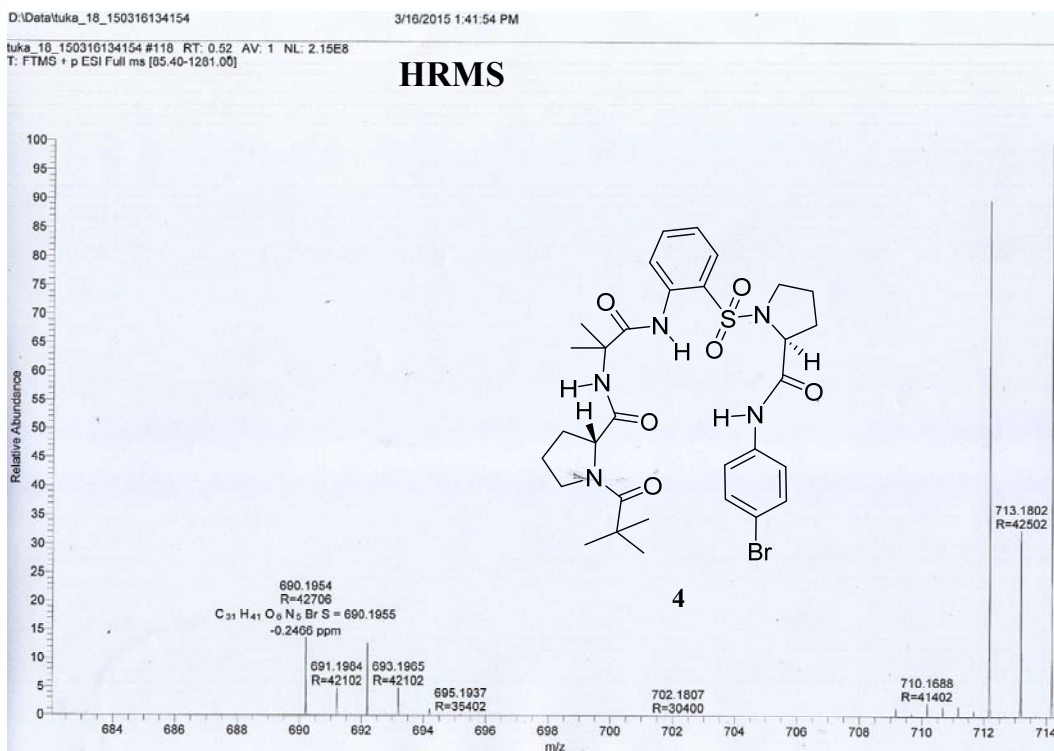
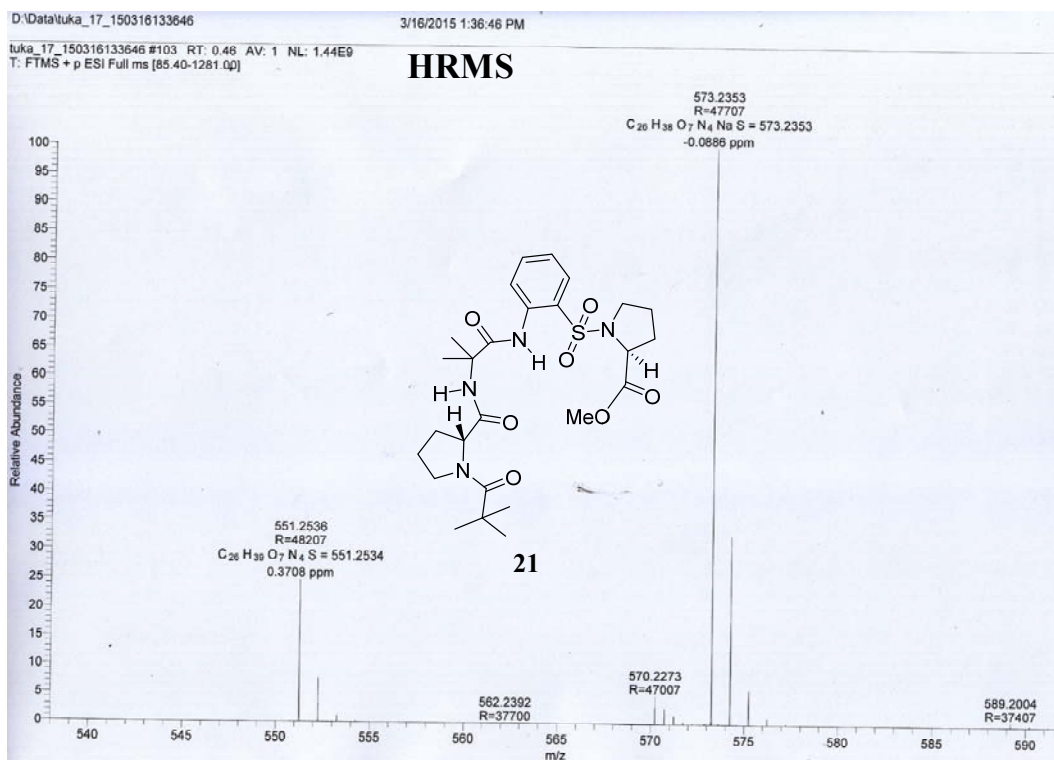
tuka_12_150316130308 #106 RT: 0.47 AV: 1 NL: 5.55E7
T: FTMS + p ESI Full ms [85.40-1281.00]

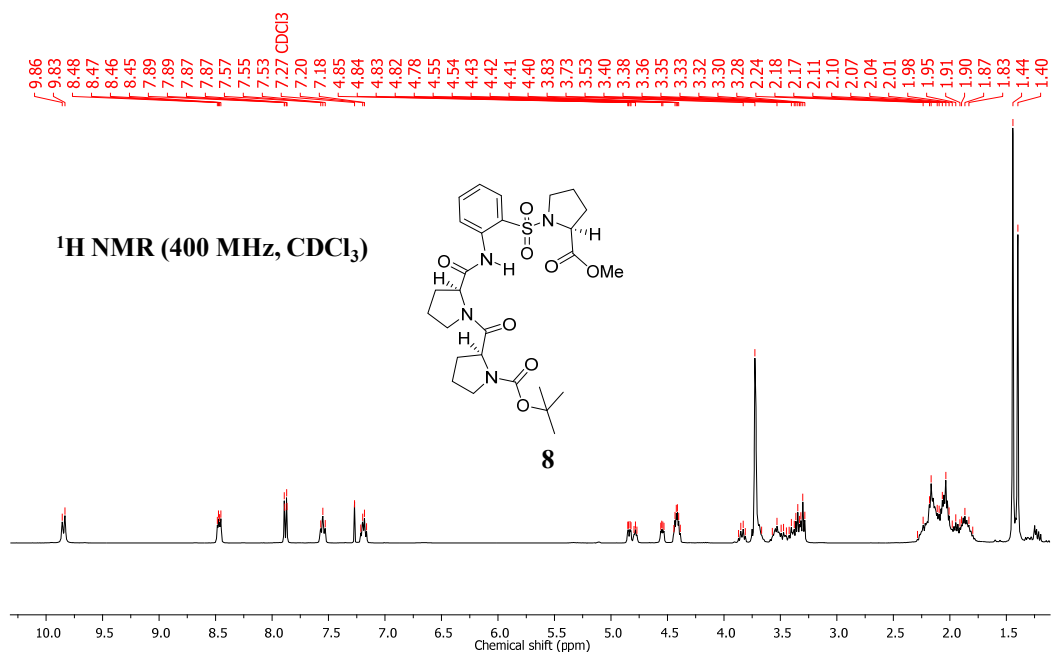
HRMS



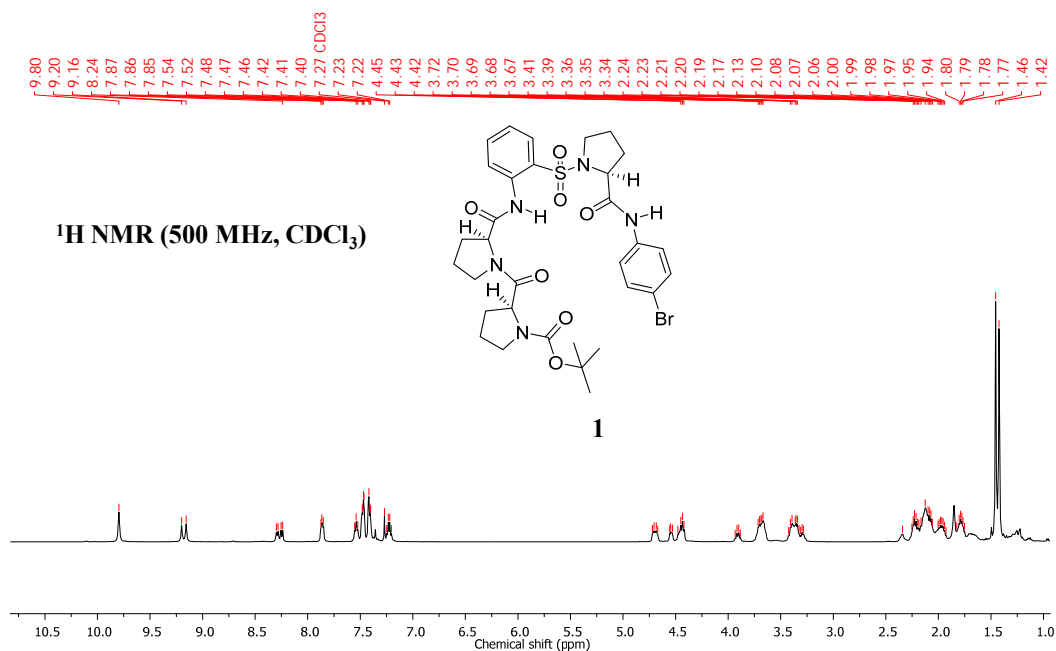




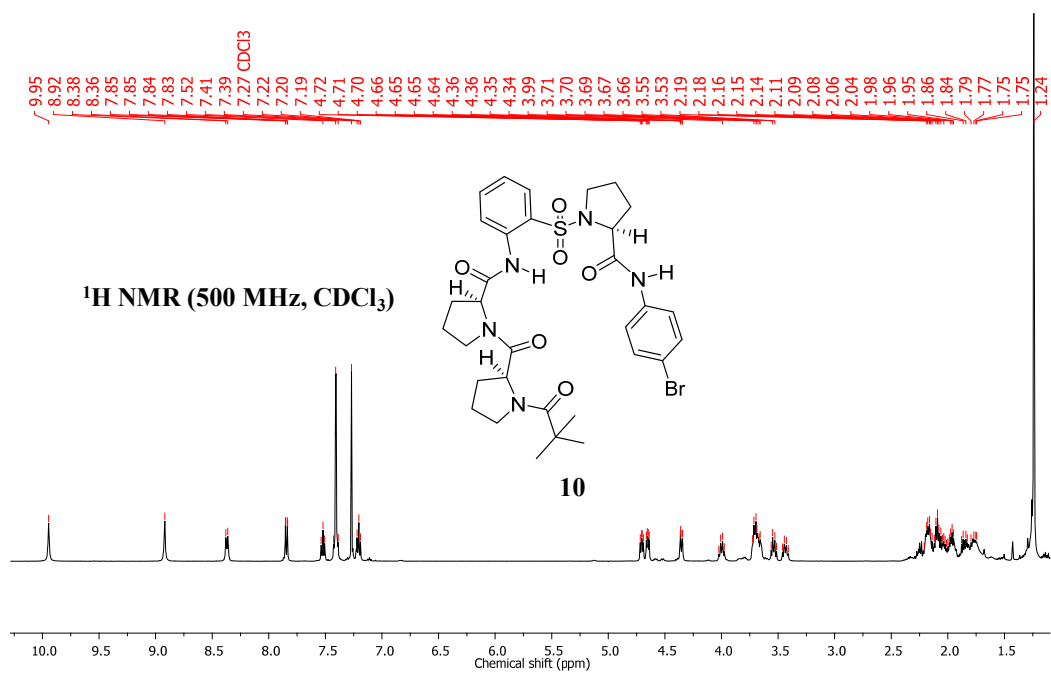
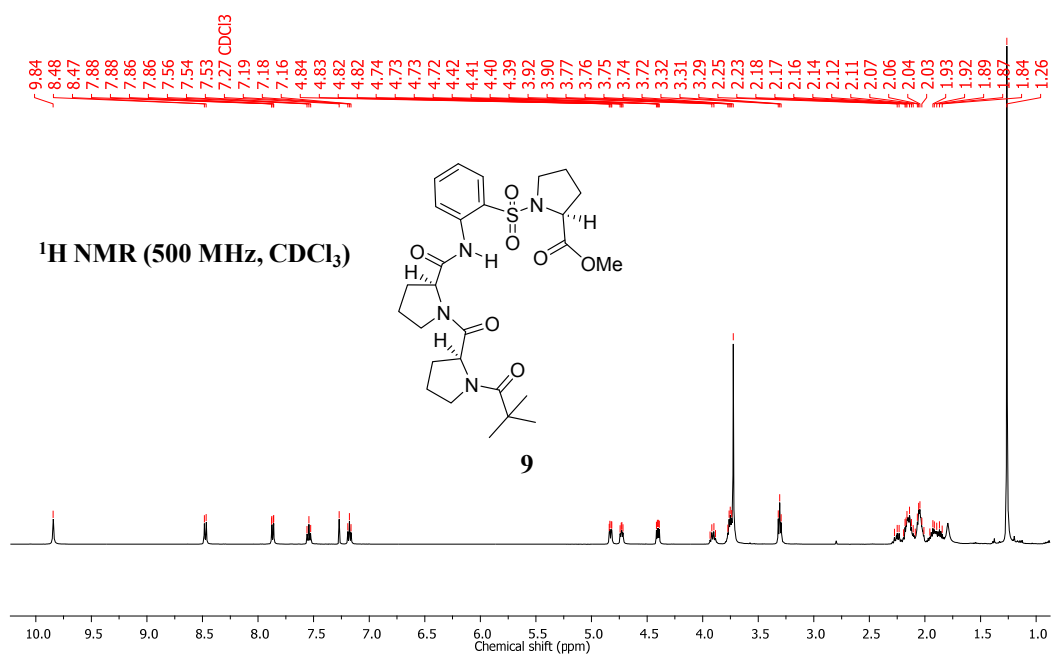


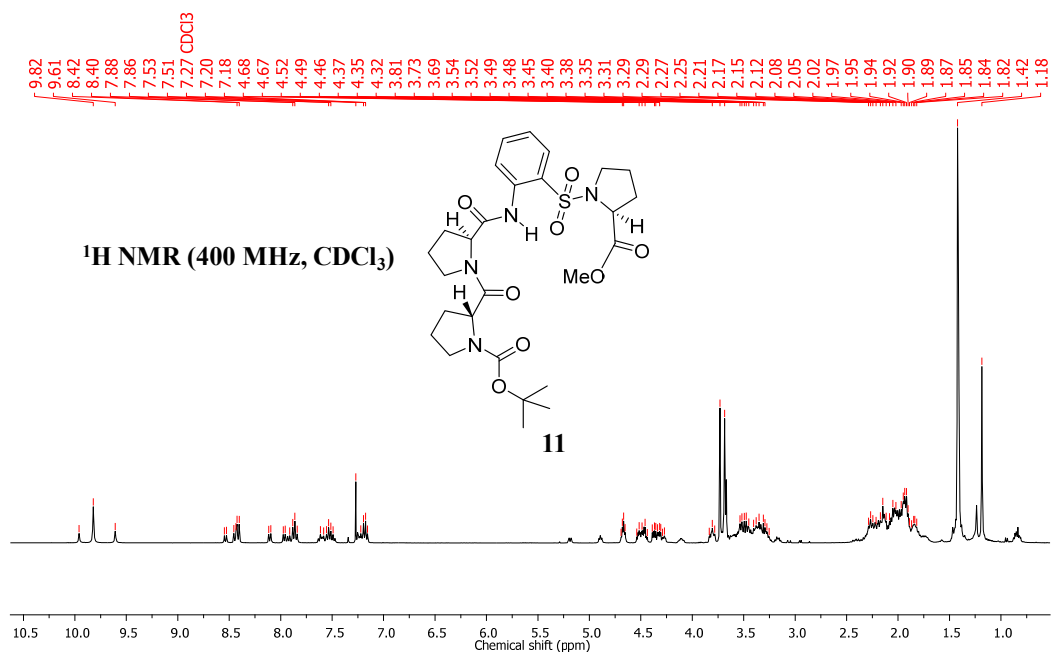


NOTE: Extra signals and / or signal broadening are seen due to rotamer (minor conformer) formation at N-terminus of proline residue (*Chem. Eur. J.* **2008**, *14*, 6192).

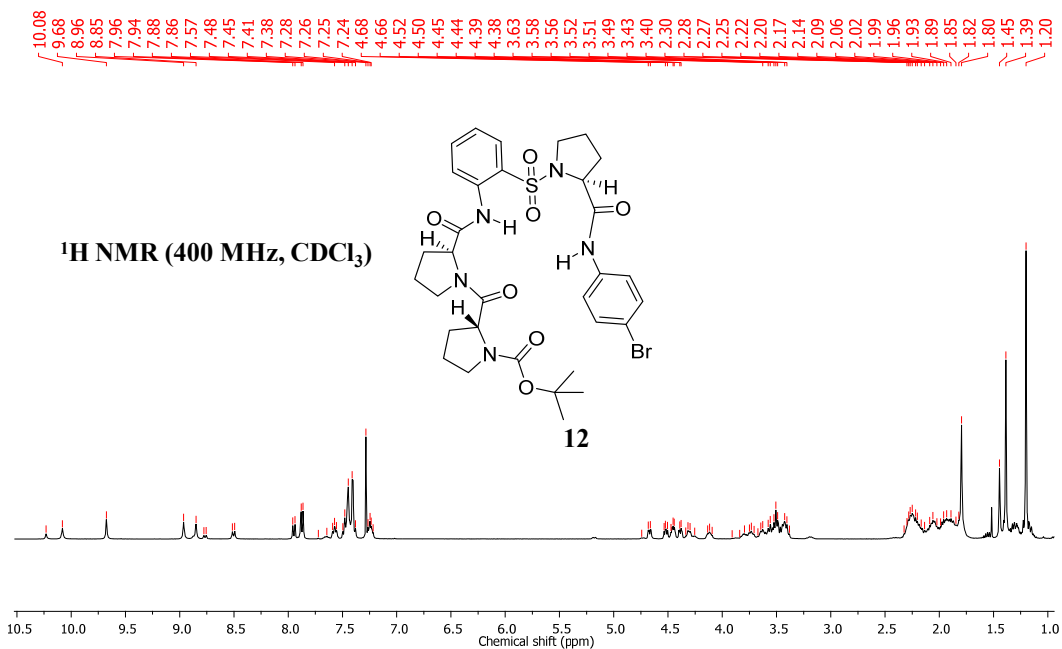


NOTE: Extra signals and / or signal broadening are seen due to rotamer (minor conformer) formation at N-terminus of proline residue (*Chem. Eur. J.* **2008**, *14*, 6192).

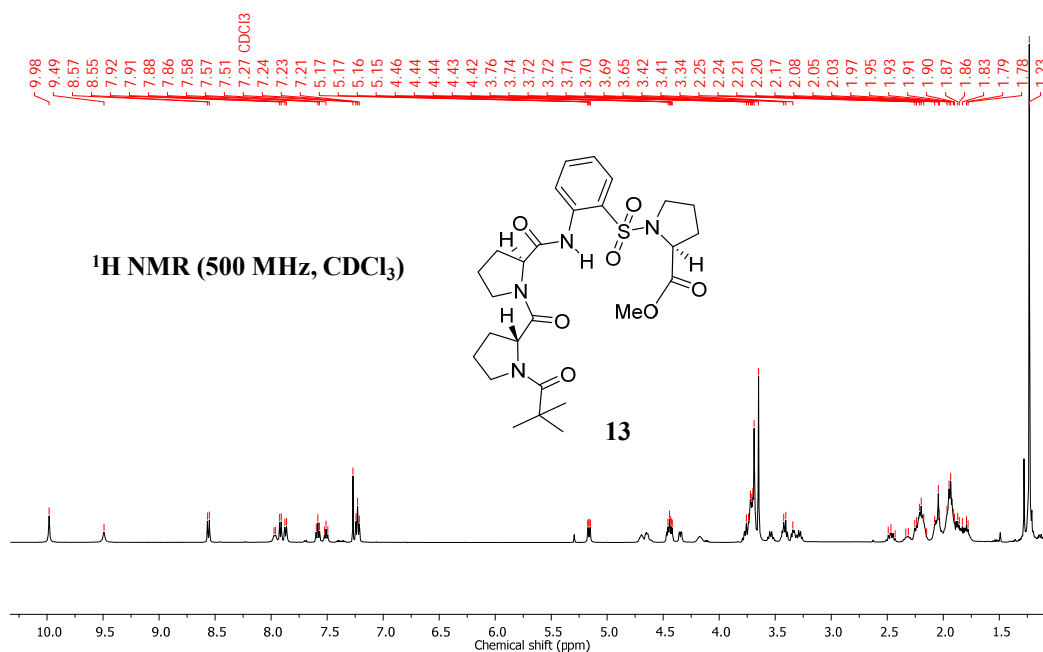




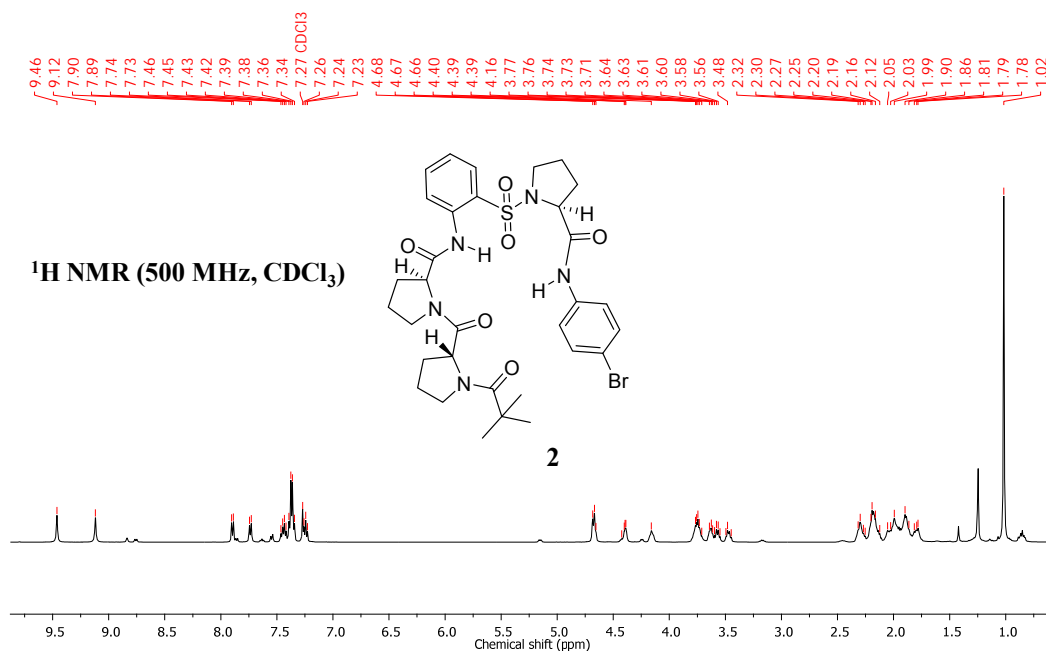
NOTE: Extra signals and / or signal broadening are seen due to rotamer (minor conformer) formation at N-terminus of proline residue (*Chem. Eur. J.* **2008**, *14*, 6192).



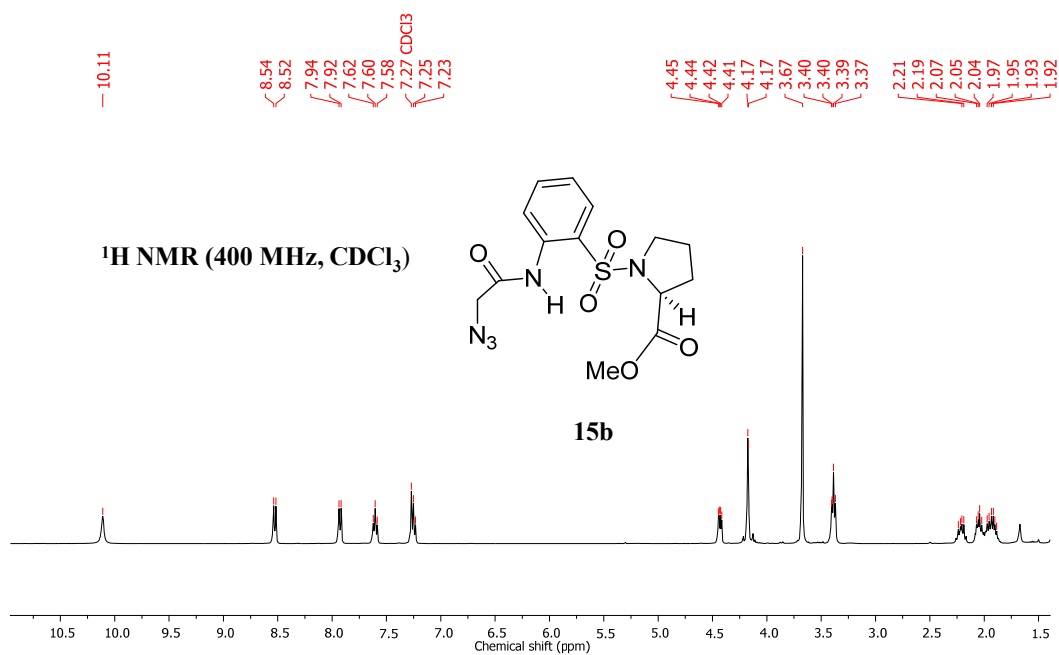
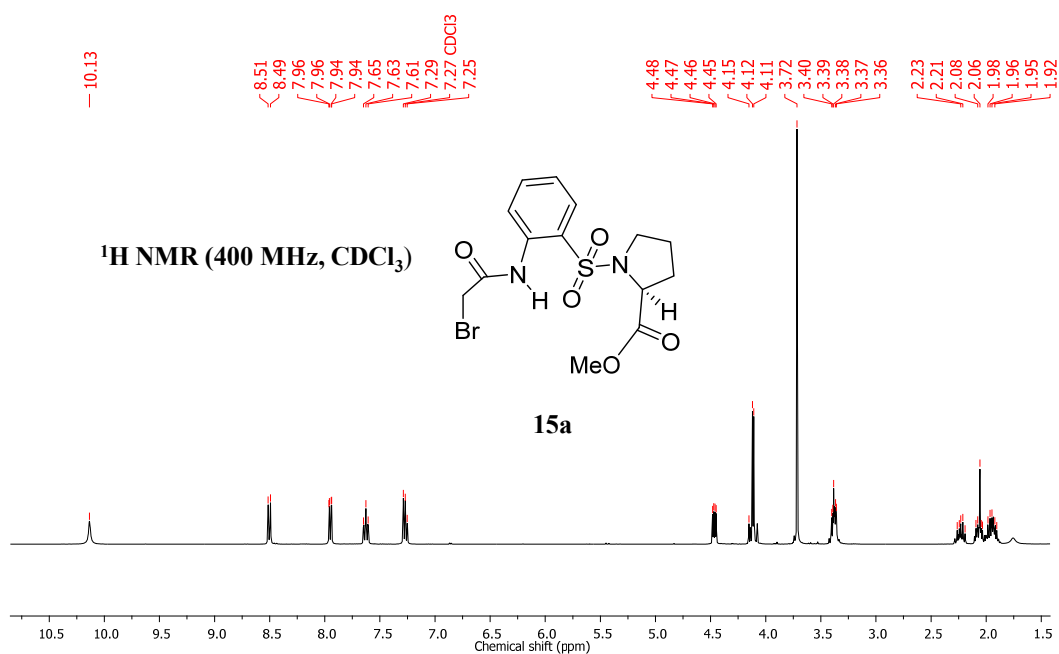
NOTE: Extra signals and / or signal broadening are seen due to rotamer (minor conformer) formation at N-terminus of proline residue (*Chem. Eur. J.* **2008**, *14*, 6192).

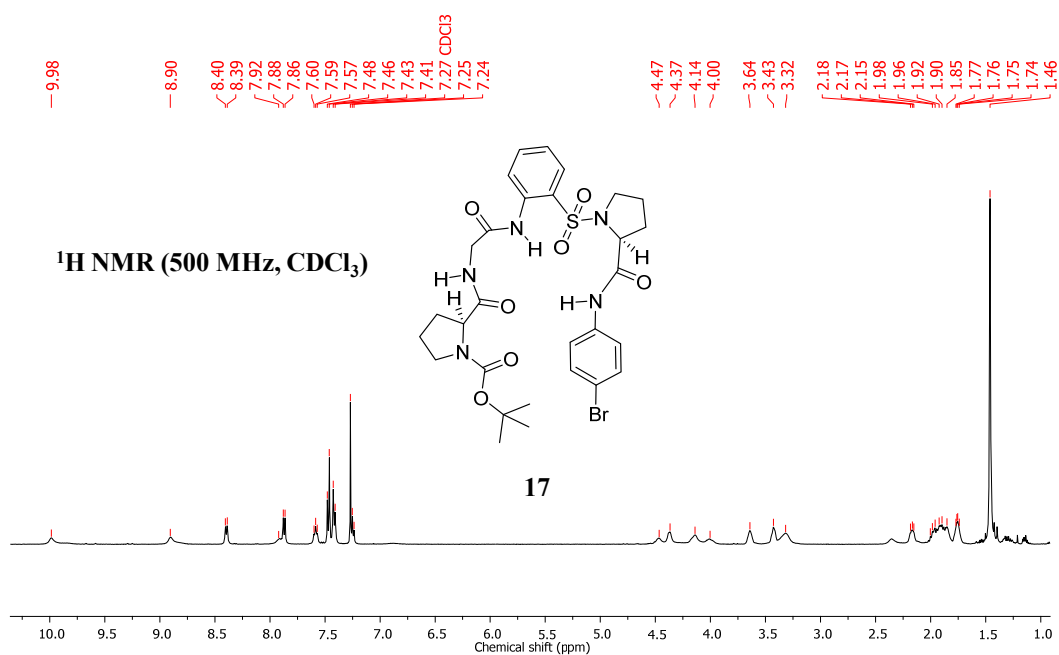
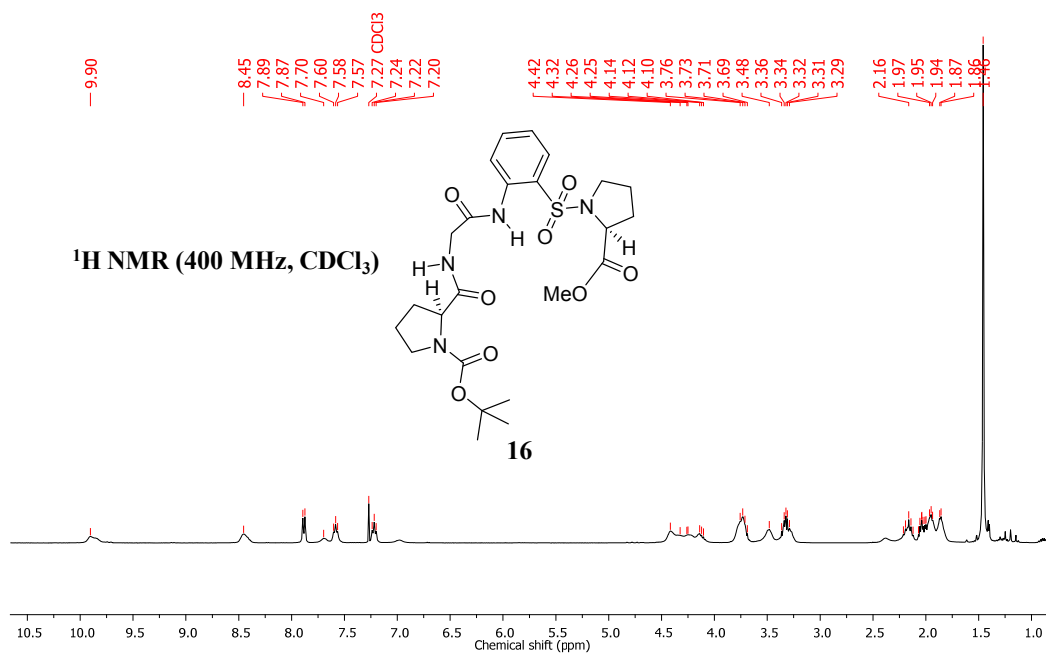


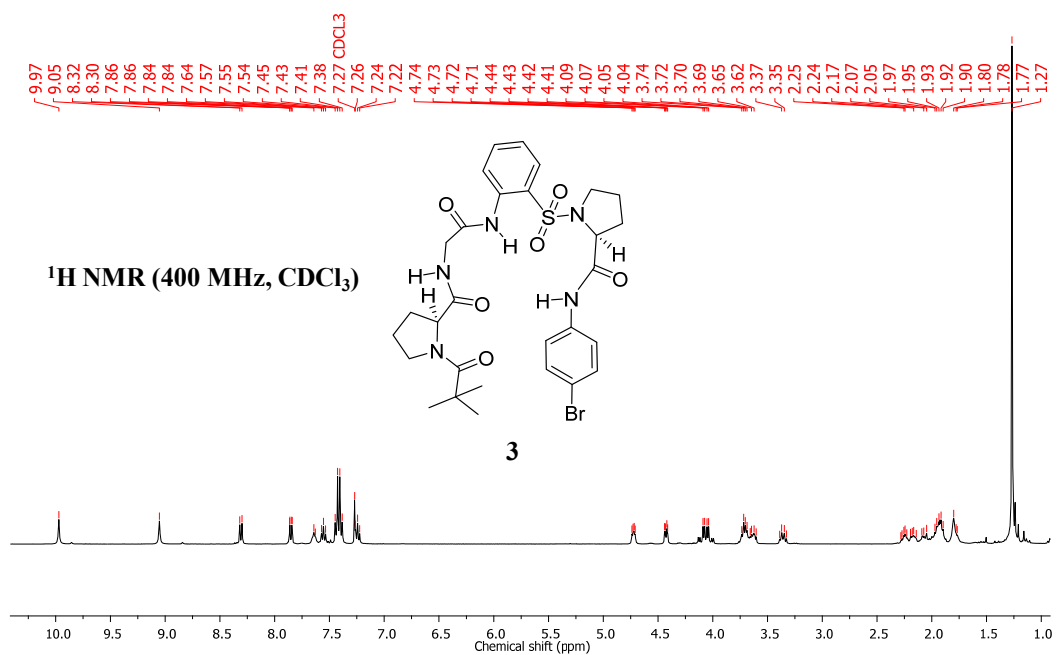
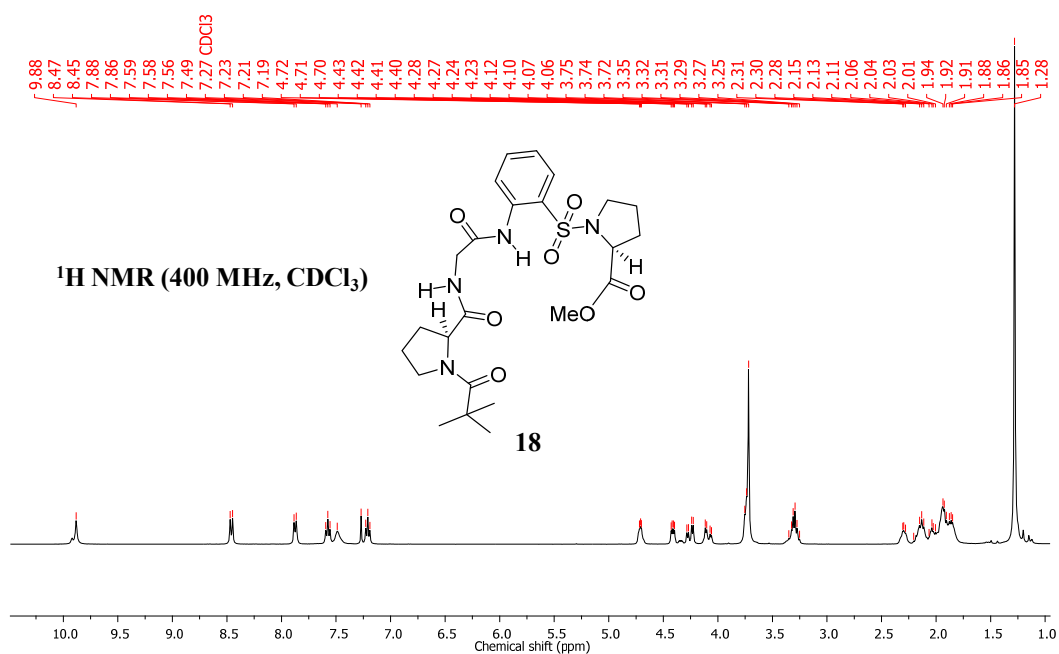
NOTE: Extra signals and / or signal broadening are seen due to rotamer (minor conformer) formation at N-terminus of proline residue (*Chem. Eur. J.* **2008**, *14*, 6192).

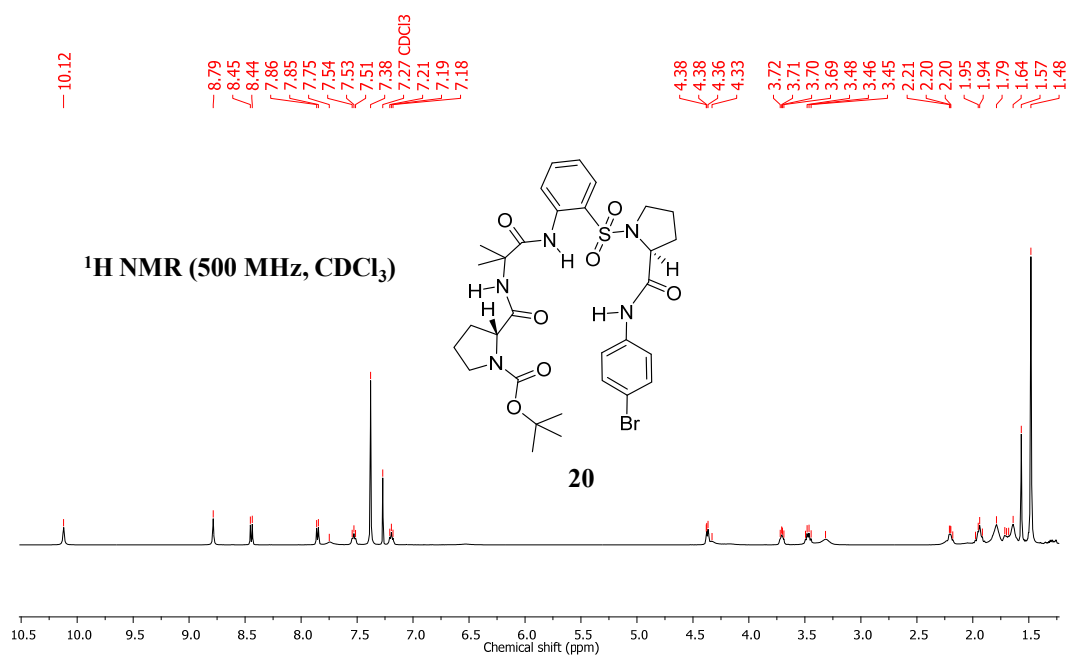
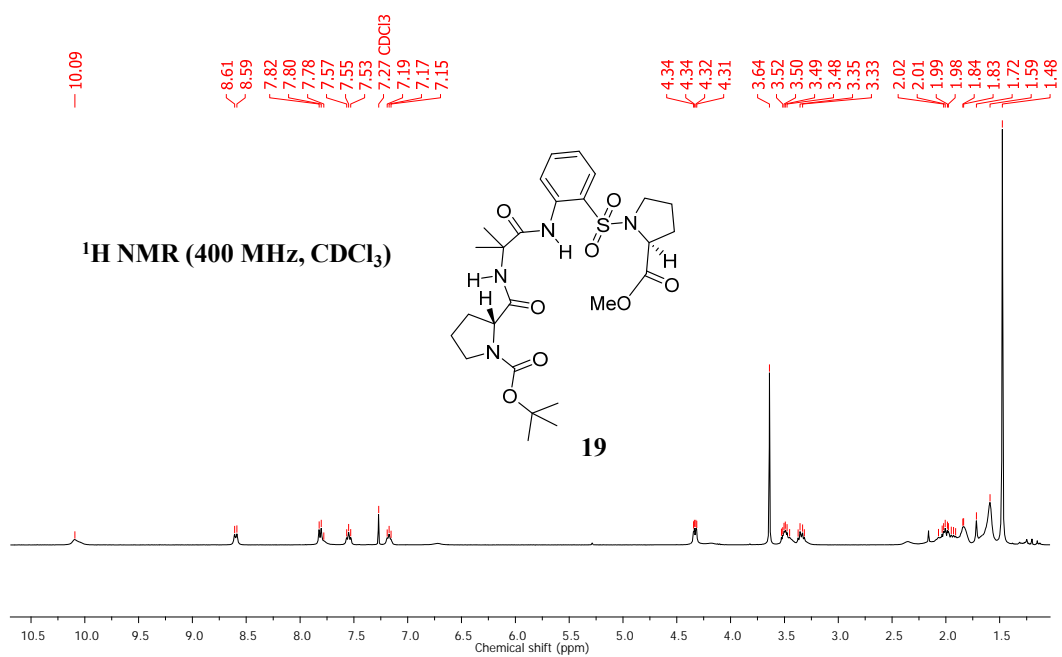


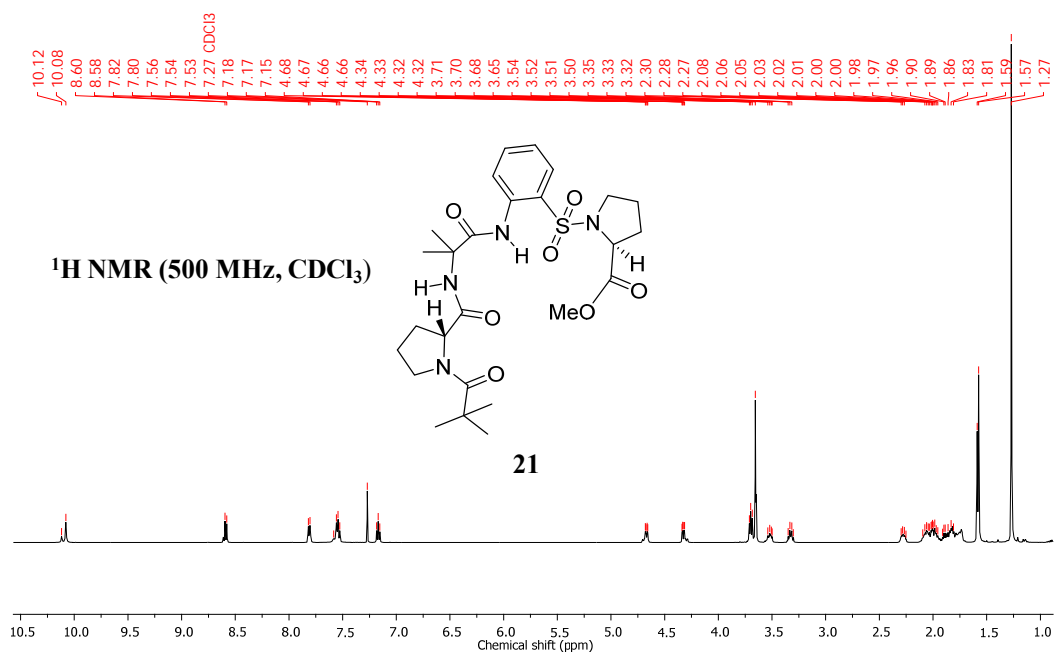
NOTE: Extra signals and / or signal broadening are seen due to rotamer (minor conformer) formation at N-terminus of proline residue (*Chem. Eur. J.* **2008**, *14*, 6192).



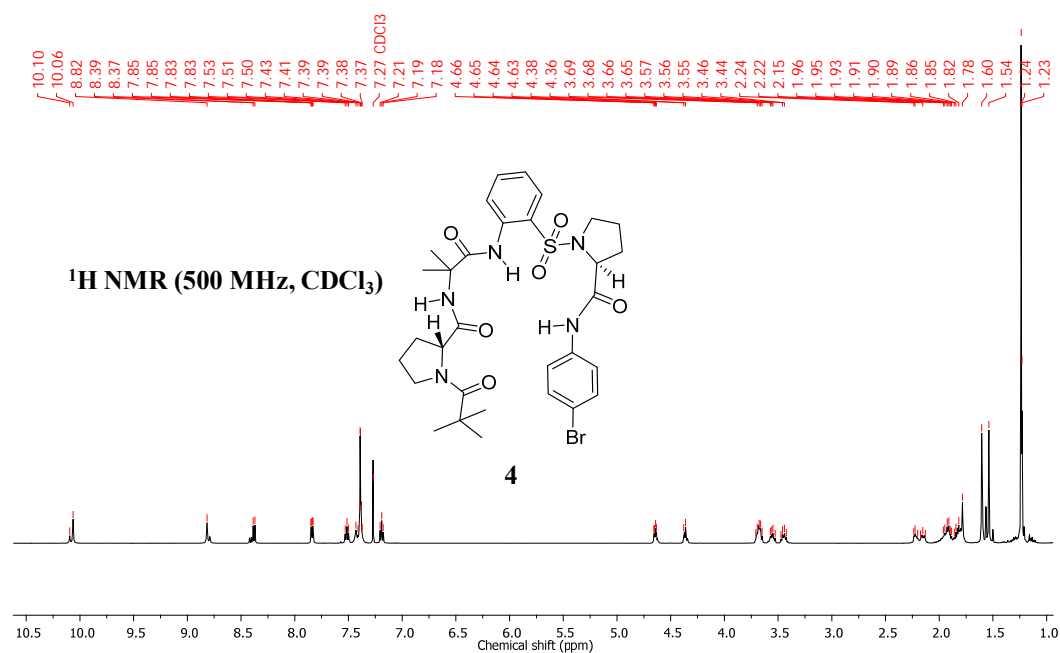




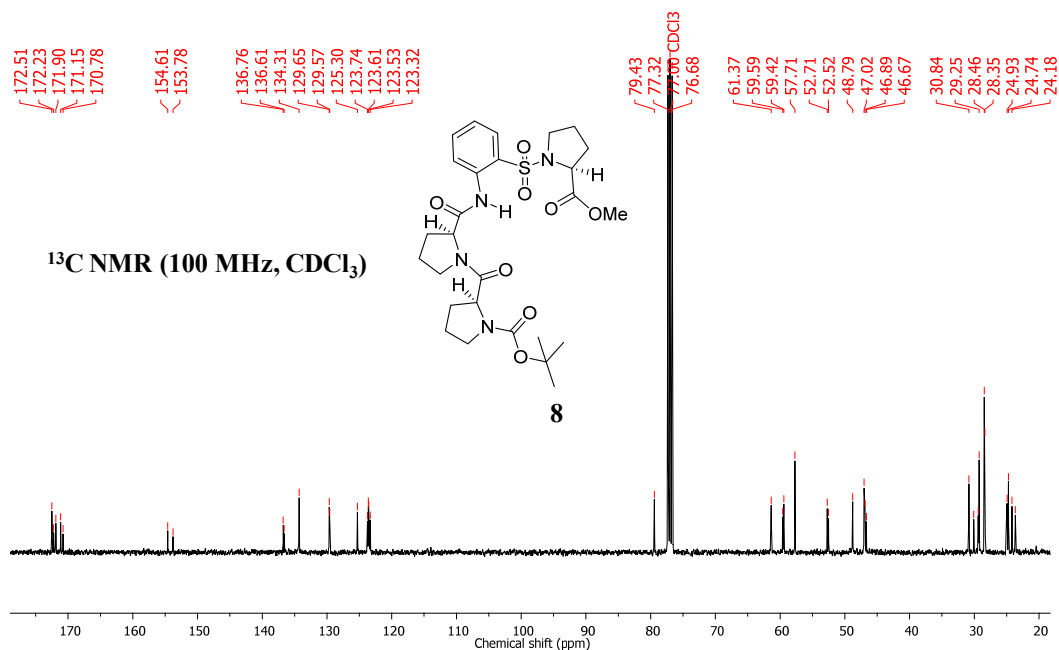




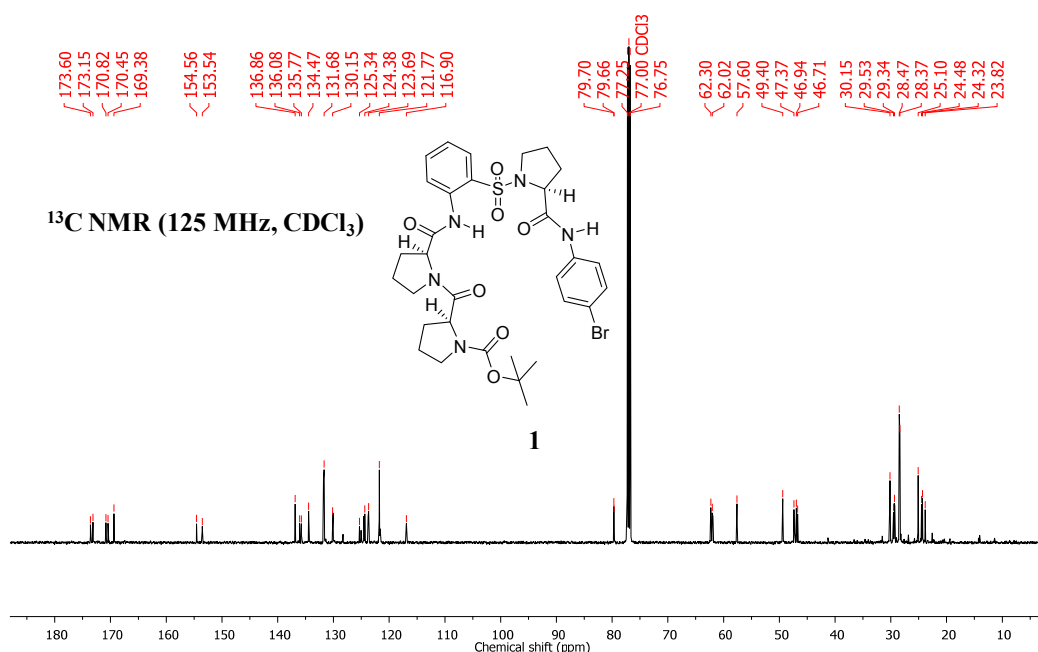
NOTE: Extra signals and / or signal broadening are seen due to rotamer (minor conformer) formation at N-terminus of proline residue (*Chem. Eur. J.* **2008**, *14*, 6192).



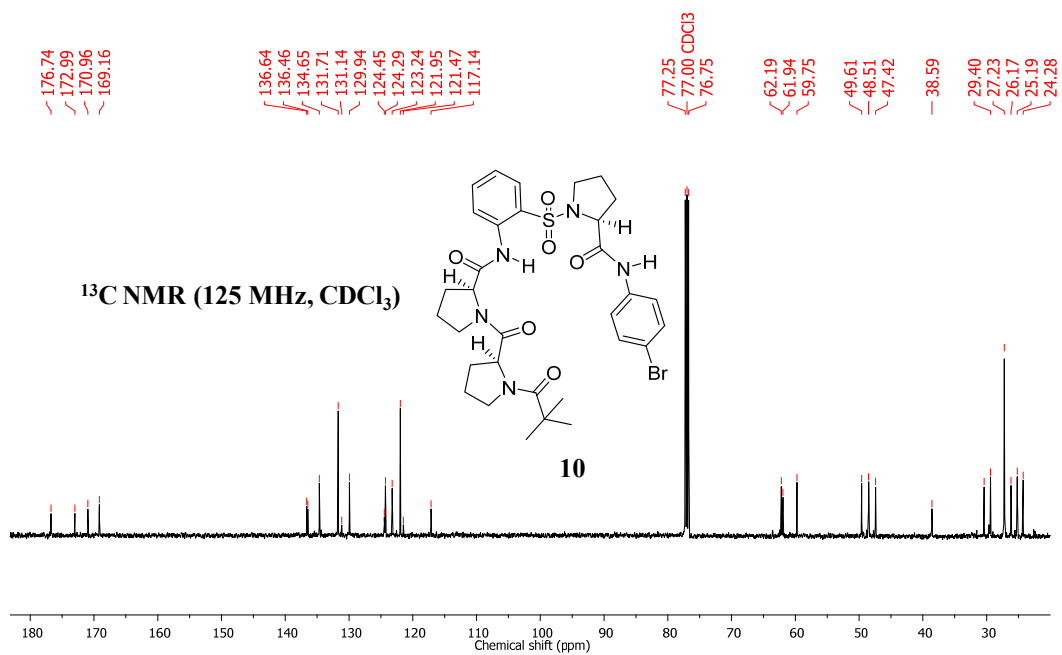
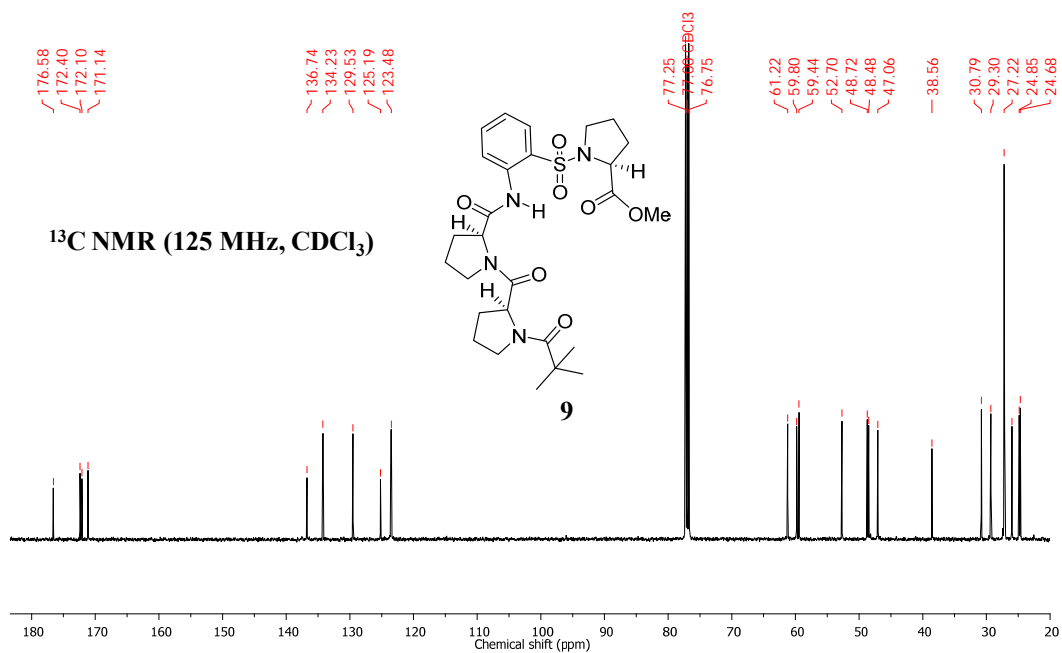
NOTE: Extra signals and / or signal broadening are seen due to rotamer (minor conformer) formation at N-terminus of proline residue (*Chem. Eur. J.* **2008**, *14*, 6192).

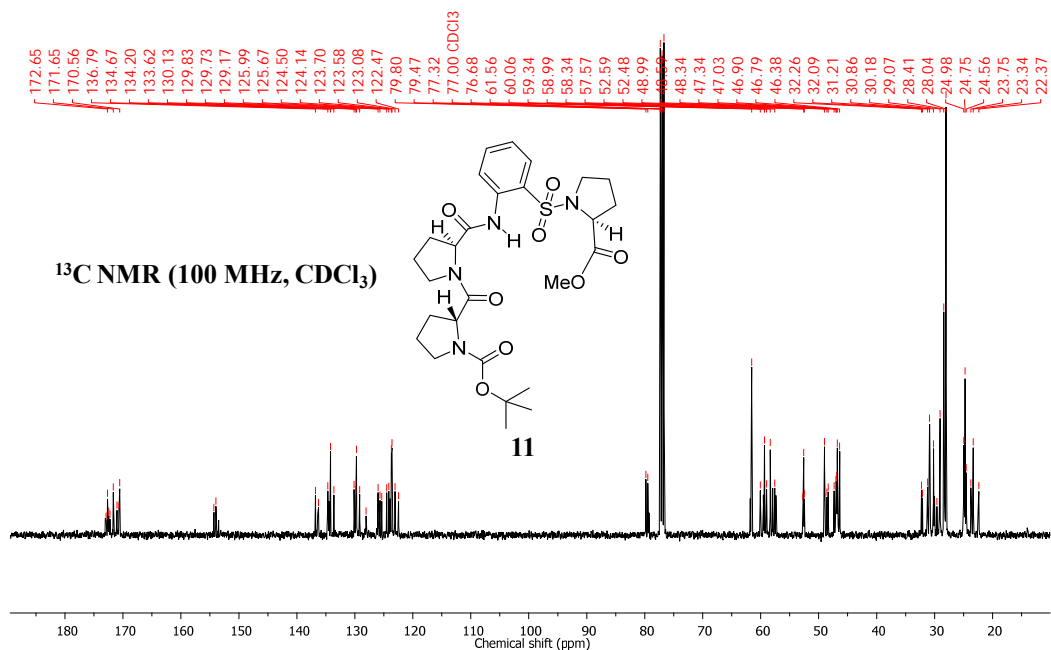


NOTE: Extra signals and / or signal broadening are seen due to rotamer (minor conformer) formation at N-terminus of proline residue (*Chem. Eur. J.* **2008**, *14*, 6192).

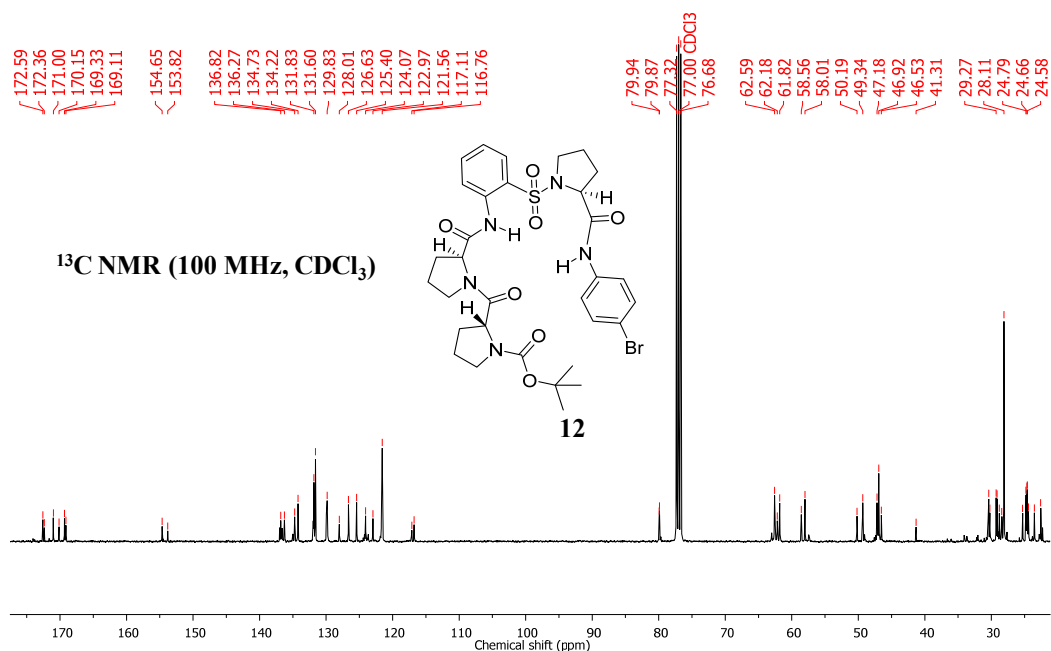


NOTE: Extra signals and / or signal broadening are seen due to rotamer (minor conformer) formation at N-terminus of proline residue (*Chem. Eur. J.* **2008**, *14*, 6192).

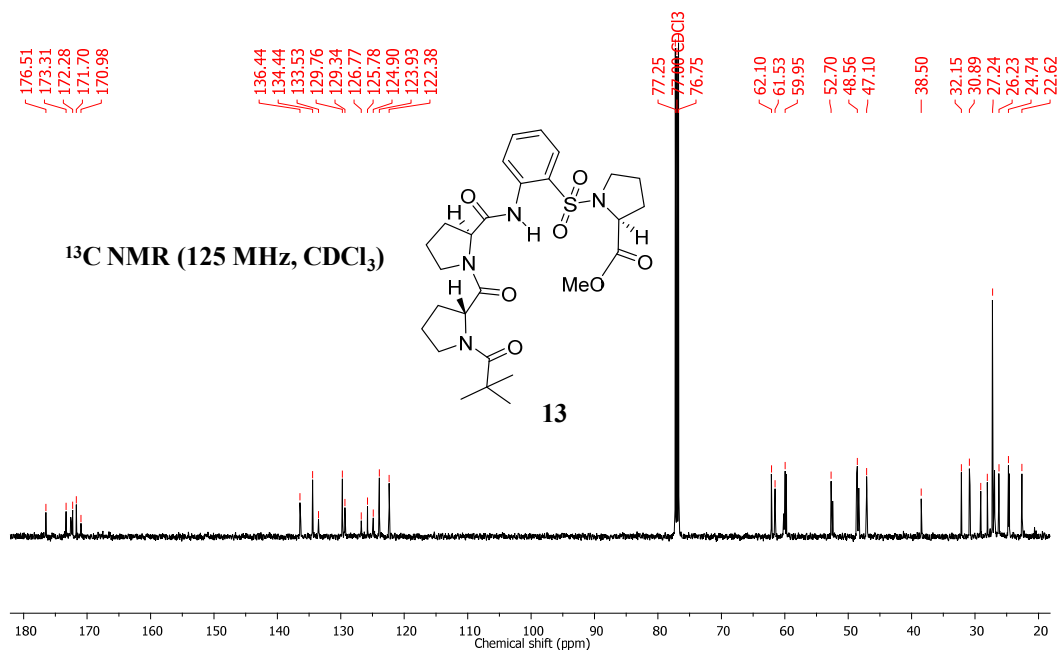




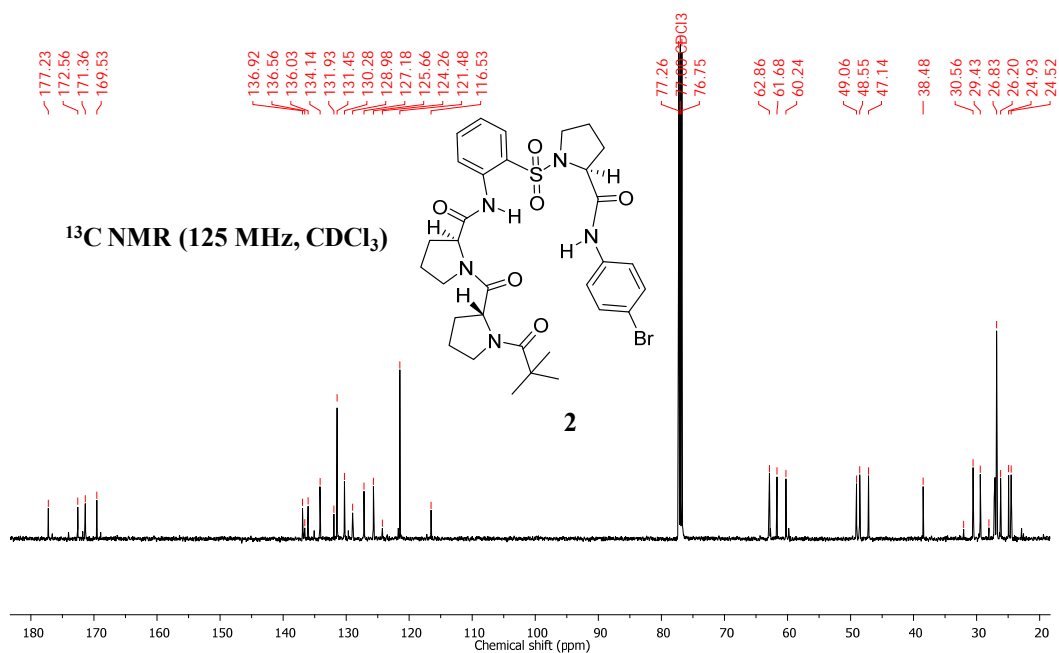
NOTE: Extra signals and / or signal broadening are seen due to rotamer (minor conformer) formation at N-terminus of proline residue (*Chem. Eur. J.* **2008**, *14*, 6192).



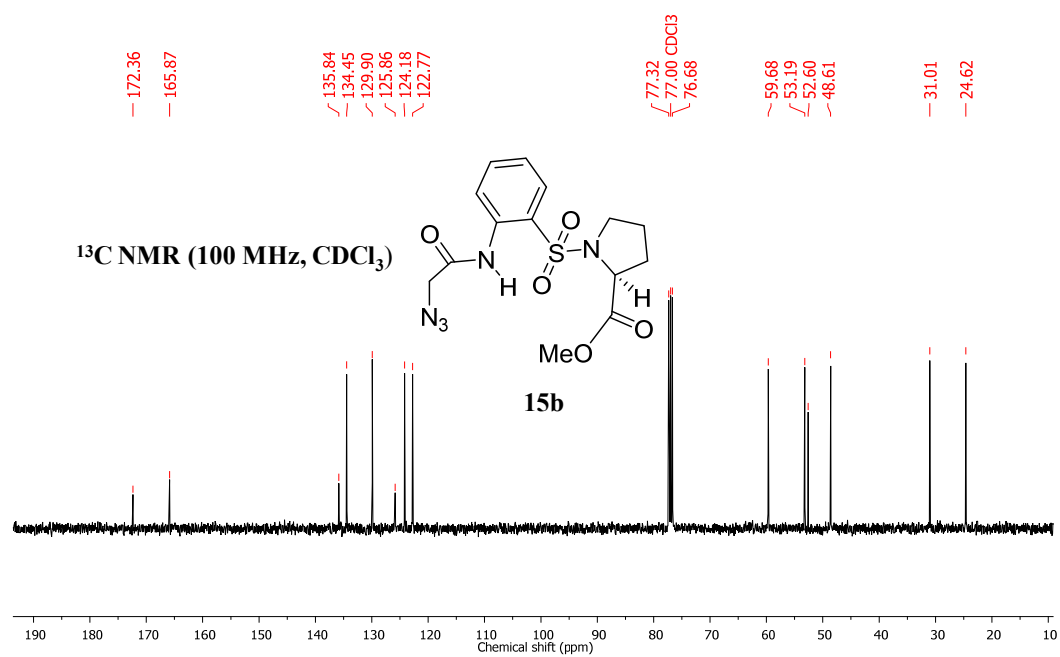
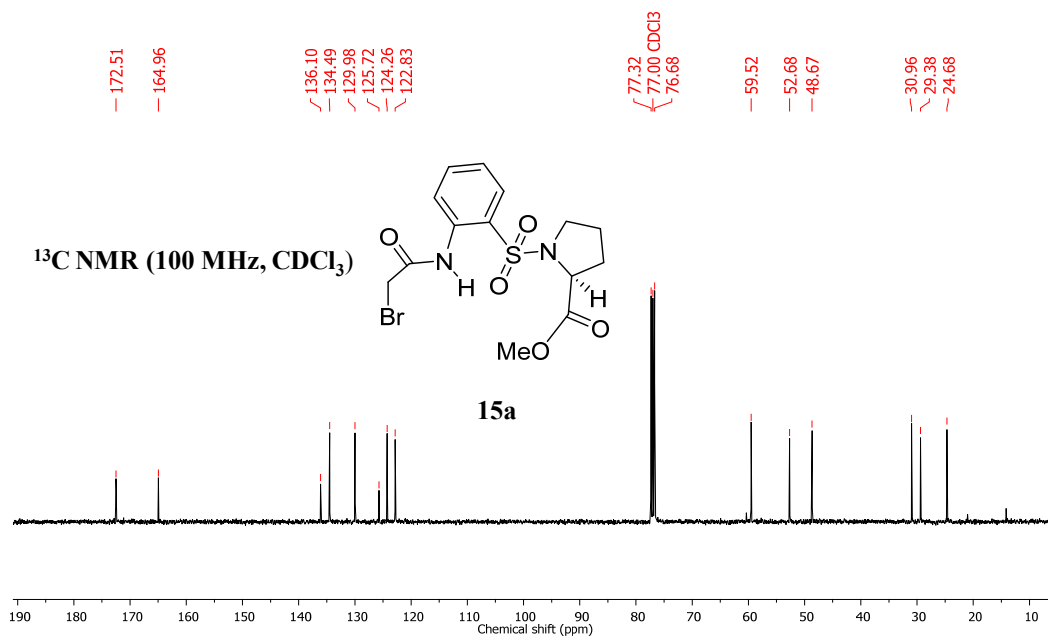
NOTE: Extra signals and / or signal broadening are seen due to rotamer (minor conformer) formation at N-terminus of proline residue (*Chem. Eur. J.* **2008**, *14*, 6192).

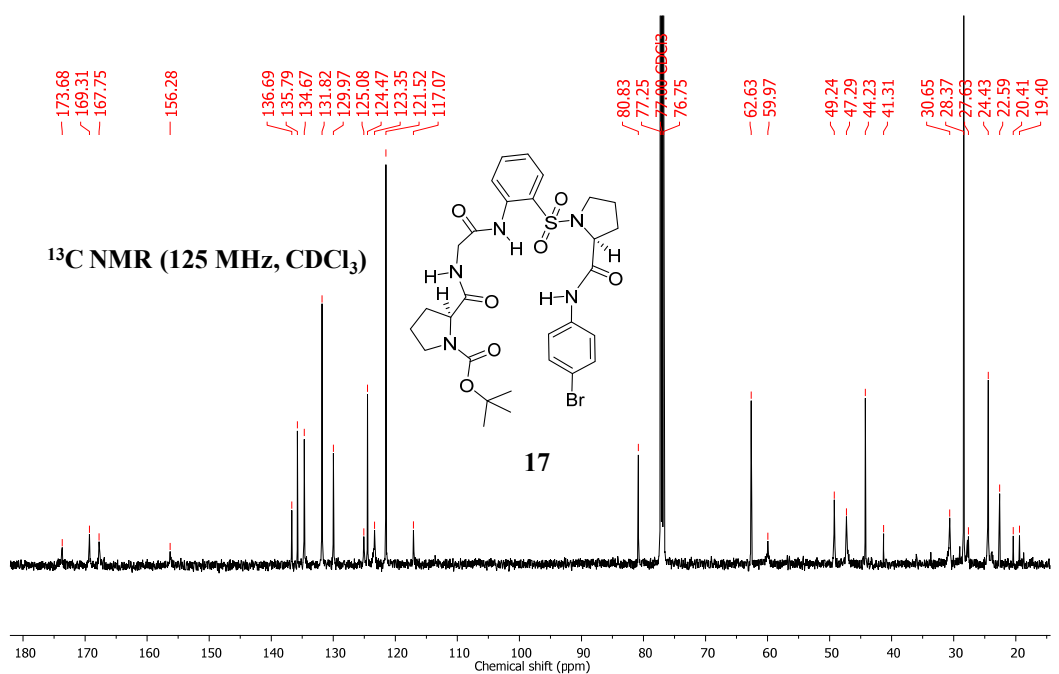
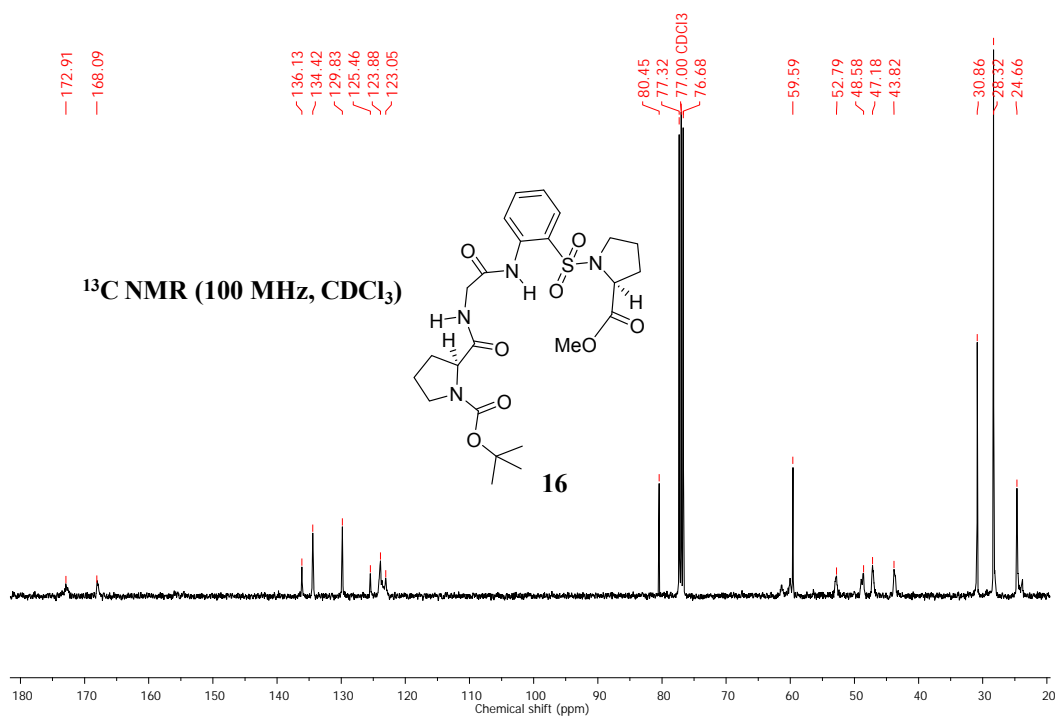


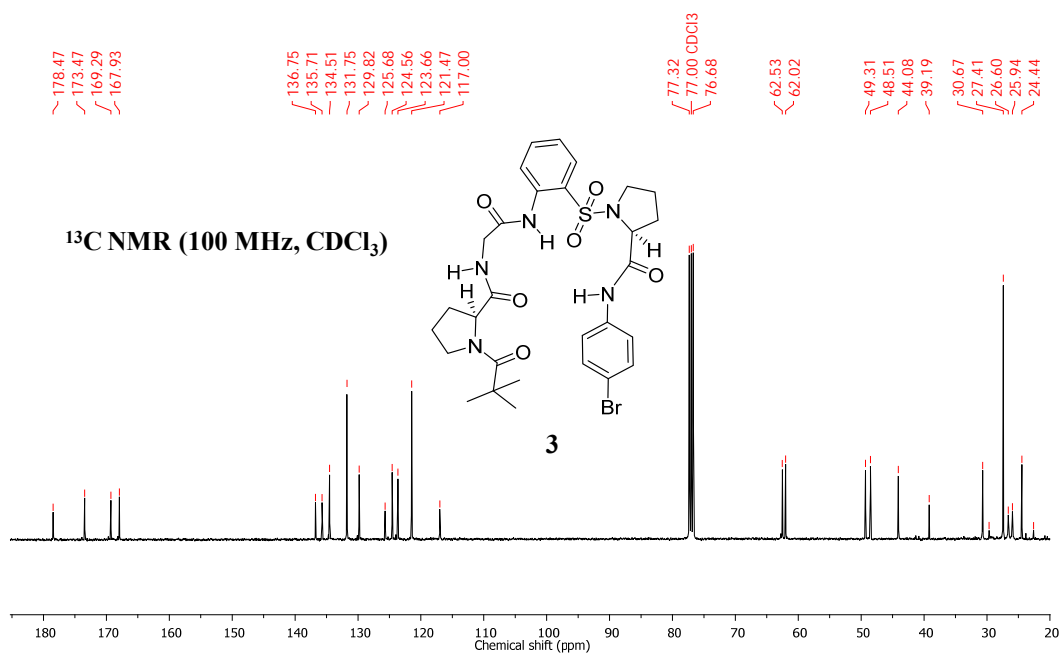
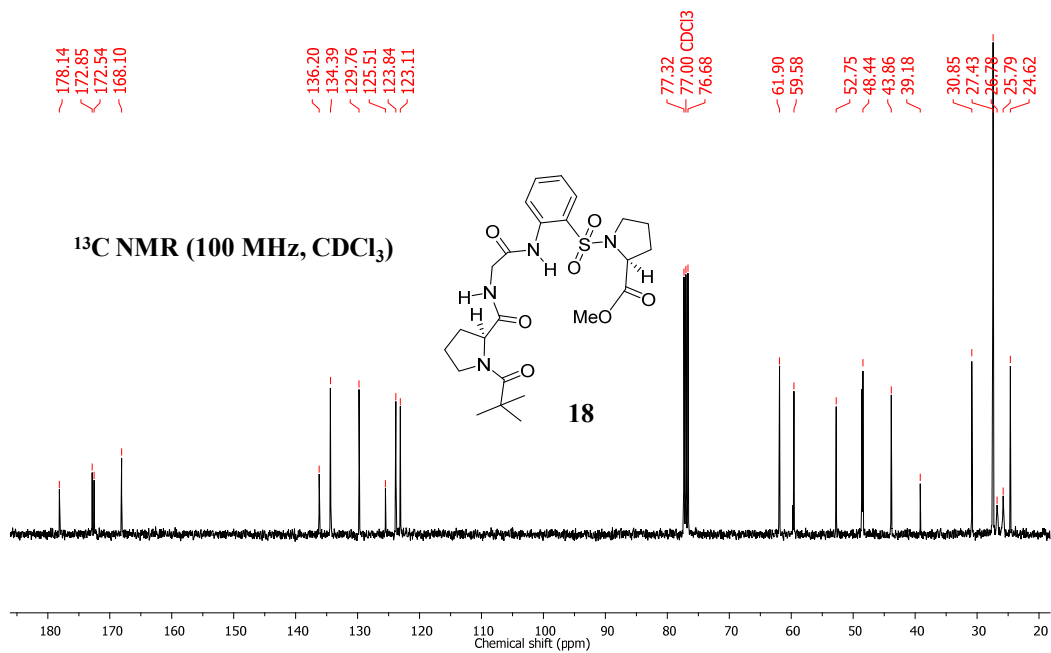
NOTE: Extra signals and / or signal broadening are seen due to rotamer (minor conformer) formation at N-terminus of proline residue (*Chem. Eur. J.* **2008**, *14*, 6192).

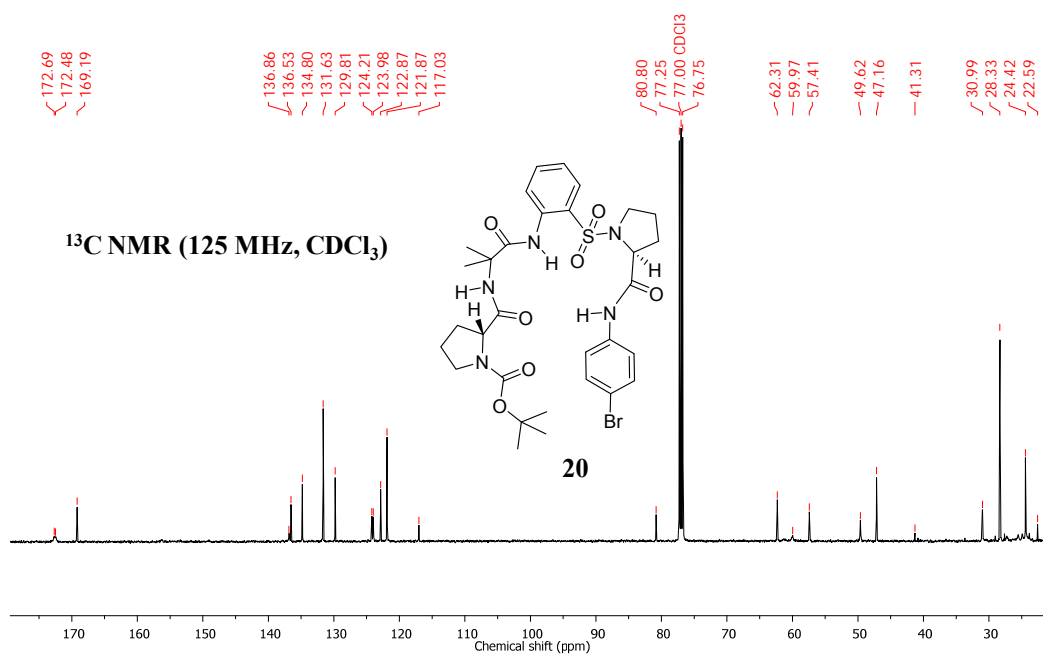
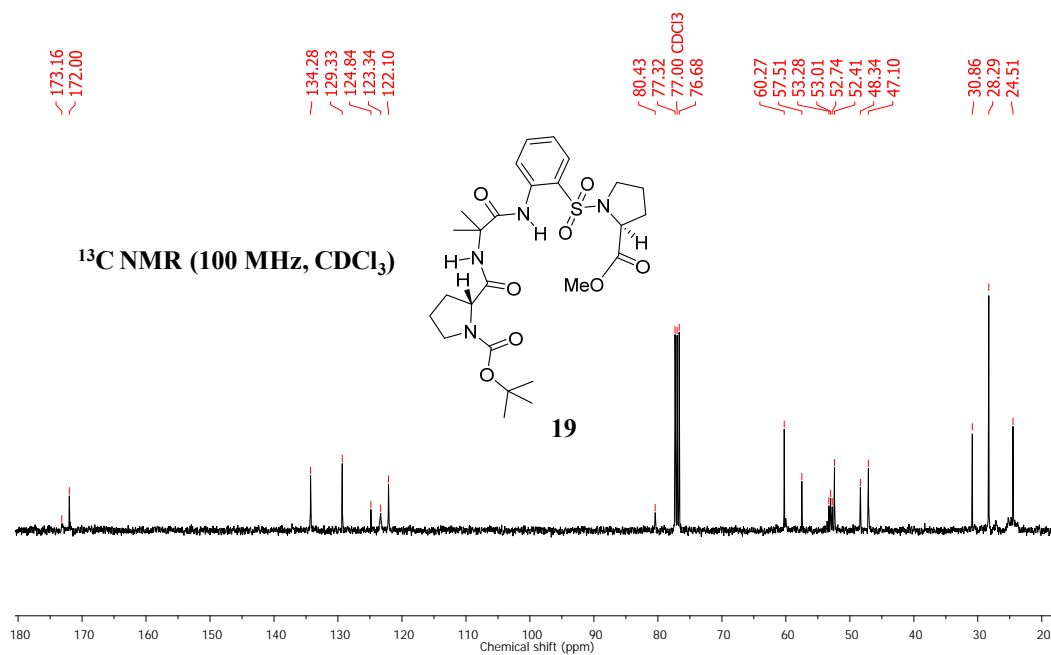


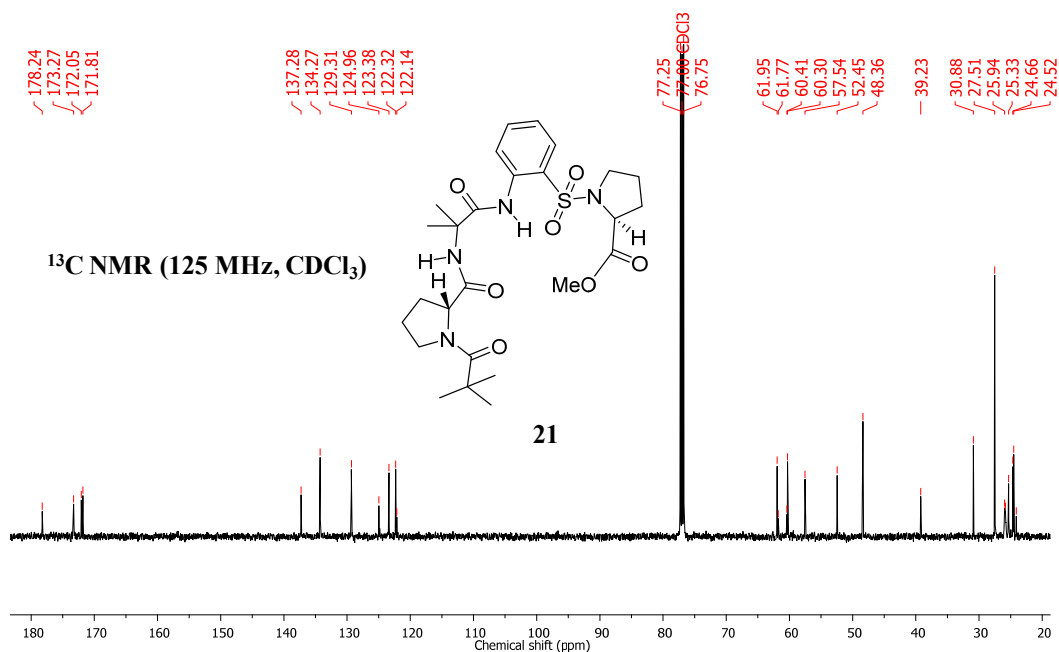
NOTE: Extra signals and / or signal broadening are seen due to rotamer (minor conformer) formation at N-terminus of proline residue (*Chem. Eur. J.* **2008**, *14*, 6192).



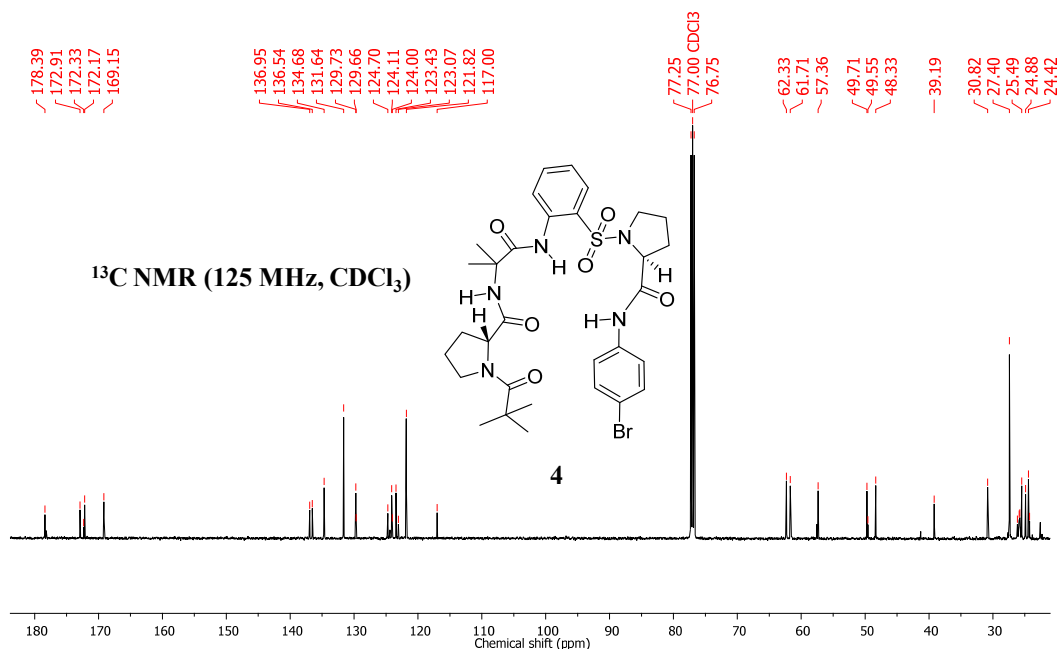








NOTE: Extra signals and / or signal broadening are seen due to rotamer (minor conformer) formation at N-terminus of proline residue (*Chem. Eur. J.* **2008**, *14*, 6192).



NOTE: Extra signals and / or signal broadening are seen due to rotamer (minor conformer) formation at N-terminus of proline residue (*Chem. Eur. J.* **2008**, *14*, 6192).

Table 2.3 Titration study of **10** (a close analogue of **1**) in CDCl_3 (5 mM) with $\text{DMSO-}d_6$ (volume of $\text{DMSO-}d_6$ added at each addition = 5 μL).

No	Volume of $\text{DMSO-}d_6$ (μL)	Chemical Shift δ (ppm)	
		NH1	NH2
1	0	9.96	8.91
2	5	9.94	8.95
3	10	9.92	8.99
4	15	9.91	9.03
5	20	9.9	9.07
6	25	9.89	9.12
7	30	9.88	9.16
8	35	9.87	9.2
9	40	9.86	9.23
10	45	9.85	9.26
11	50	9.84	9.28

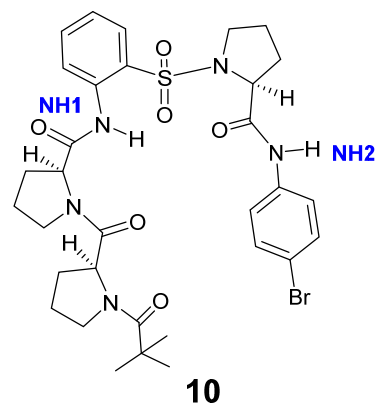


Table 2.4 Titration study of **2** in CDCl_3 (5 mM) with $\text{DMSO-}d_6$ (volume of $\text{DMSO-}d_6$ added at each addition = 5 μL)

No	Volume of $\text{DMSO-}d_6$ (μL)	Chemical Shift δ (ppm)	
		NH1	NH2
1	0	9.46	9.12
2	5	9.44	9.11
3	10	9.42	9.11
4	15	9.4	9.11
5	20	9.39	9.1
6	25	9.38	9.1
7	30	9.37	9.1
8	35	9.36	9.1
9	40	9.35	9.1
10	45	9.34	9.09
11	50	9.34	9.09

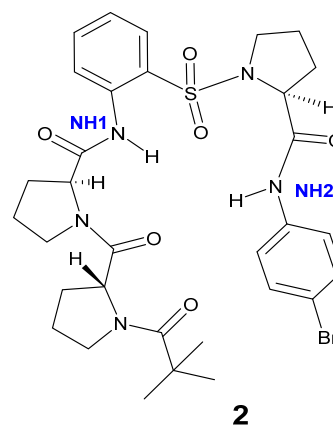


Table 2.5 Titration study of **3** in CDCl_3 (5 mM) with $\text{DMSO-}d_6$ (volume of $\text{DMSO-}d_6$ added at each addition = 5 μL)

No	Volume of $\text{DMSO-}d_6$ (μL)	Chemical Shift δ (ppm)		
		NH1	NH2	NH3
1	0	7.64	10	9
2	5	7.68	9.99	9.02
3	10	7.72	9.98	9.03
4	15	7.75	9.97	9.04
5	20	7.78	9.95	9.05
6	25	7.81	9.94	9.06
7	30	7.84	9.93	9.08
8	35	7.88	9.91	9.09
9	40	7.91	9.9	9.1
10	45	7.94	9.89	9.12
11	50	7.97	9.87	9.14

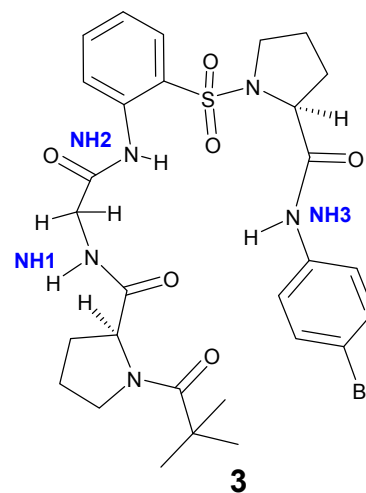


Table 2.6 Titration study of **20** (a close analogue of **4**) in CDCl_3 (5 mM) with $\text{DMSO-}d_6$ (volume of $\text{DMSO-}d_6$ added at each addition = 5 μL)

No	Volume of $\text{DMSO-}d_6$ (μL)	Chemical Shift δ (ppm)		
		NH1	NH2	NH3
1	0	7.76	10.13	8.77
2	5	7.72	10.12	8.79
3	10	7.68	10.1	8.81
4	15	7.65	10.08	8.82
5	20	7.62	10.06	8.83
6	25	7.58	10.05	8.85
7	30	7.54	10.03	8.87
8	35	7.49	10.01	8.89
9	40	7.46	9.99	8.9
10	45	7.43	9.97	8.91
11	50	7.39	9.96	8.91

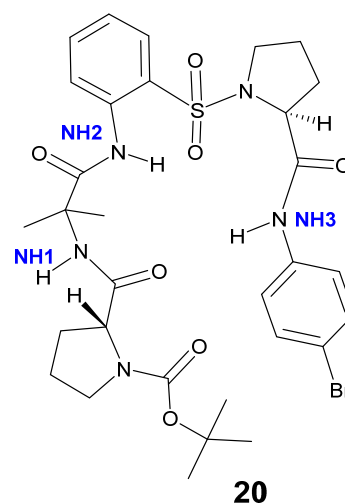


Table 2.7 Variable temperature study of **10** (a close analogue of **1**) (5 mM, 400 MHz, CDCl₃)

No	Temperature (K)	Chemical Shift δ in ppm	
		NH1	NH2
1	268	9.97	9.05
2	273	9.97	9.02
3	278	9.97	9
4	283	9.96	8.98
5	288	9.96	8.95
6	293	9.96	8.93
7	298	9.95	8.91
8	303	9.95	8.89
9	308	9.95	8.87
10	313	9.94	8.84
11	318	9.94	8.82
12	323	9.94	8.8

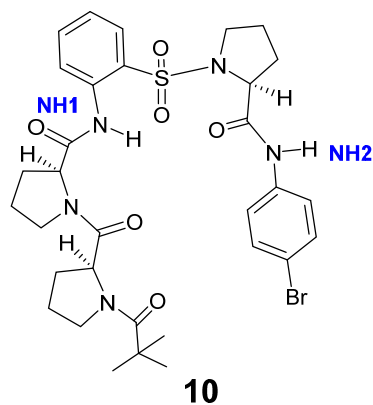


Table 2.8 Variable temperature study of **2** (5 mM, 400 MHz, CDCl₃)

No	Temperature (K)	Chemical Shift δ in ppm	
		NH1	NH2
1	268	9.45	9.18
2	273	9.45	9.17
3	278	9.45	9.16
4	283	9.45	9.15
5	288	9.45	9.14
6	293	9.46	9.13
7	298	9.46	9.12
8	303	9.46	9.1
9	308	9.47	9.1
10	313	9.47	9.09
11	318	9.47	9.08
12	323	9.48	9.07

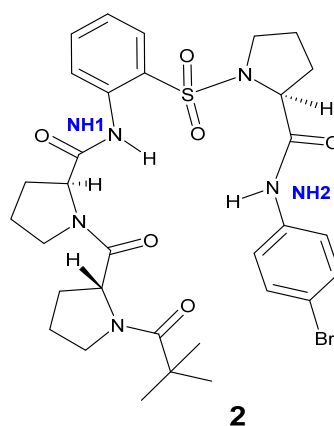
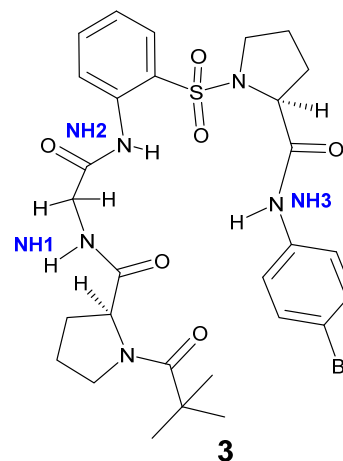
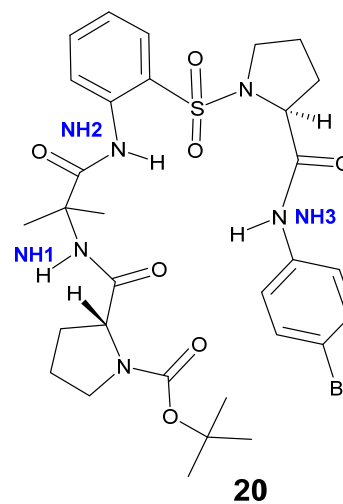


Table 2.9 Variable temperature study of **3** (5 mM, 400 MHz, CDCl₃)

No	Temperature (K)	Chemical Shift δ (ppm)		
		NH1	NH2	NH3
1	268	7.77	10.03	9.06
2	273	7.75	10.03	9.05
3	278	7.73	10.02	9.04
4	283	7.71	10.02	9.03
5	288	7.68	10.01	9.02
6	293	7.66	10	9.01
7	298	7.64	10	8.99
8	303	7.61	9.99	8.98
9	308	7.58	9.98	8.97
10	313	7.55	9.98	8.95
11	318	7.53	9.97	8.94
12	323	7.51	9.96	8.93

Table 2.10 Variable temperature study of **20** (a close analogue of **4**) (5 mM, 400 MHz, CDCl₃)

No	Temperature (K)	Chemical Shift δ (ppm)		
		NH1	NH2	NH3
1	268	7.78	10.15	8.85
2	273	7.77	10.15	8.84
3	278	7.77	10.15	8.83
4	283	7.77	10.14	8.81
5	288	7.76	10.13	8.8
6	293	7.76	10.13	8.79
7	298	7.76	10.13	8.77
8	303	7.73	10.13	8.76
9	308	7.72	10.12	8.76
10	313	7.68	10.12	8.75
11	318	7.64	10.12	8.74
12	323	7.6	10.11	8.73



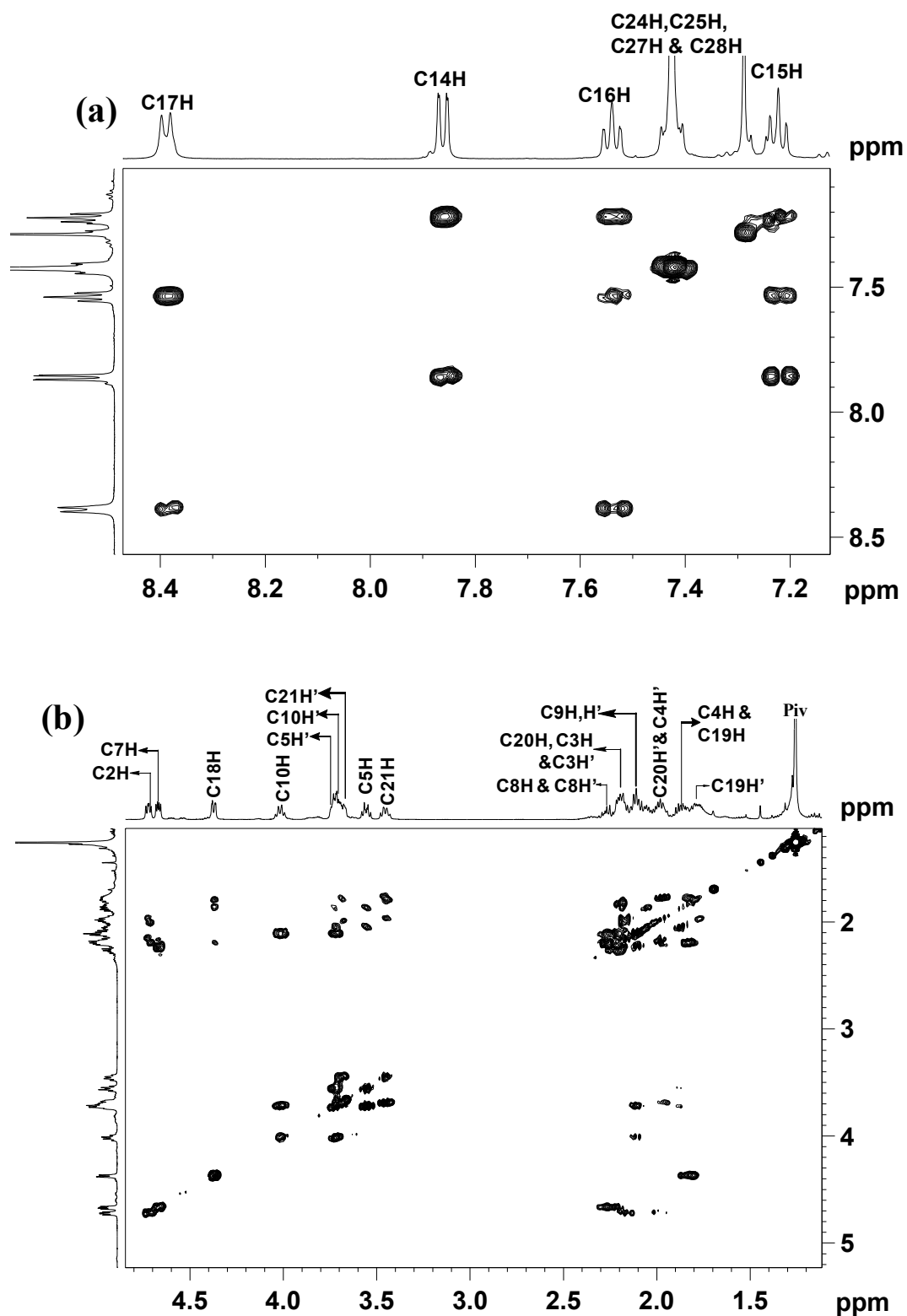


Fig. 2.14 Partial COSY spectra of tetramer 10 (a close analogue of 1) (28 mM, 500MHz, CDCl₃): aromatic (a) and aliphatic regions (b).

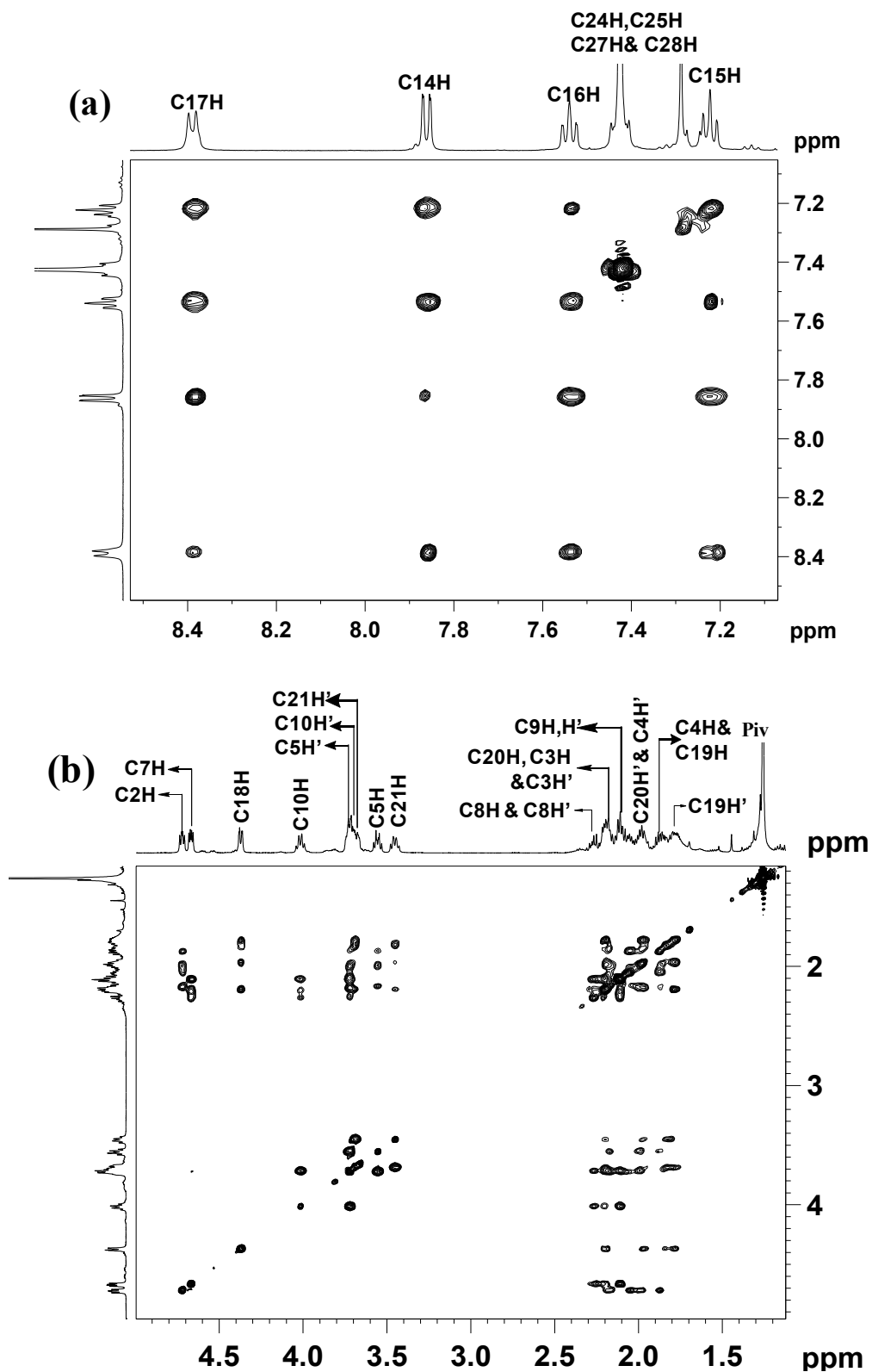


Fig. 2.15 Partial TOCSY spectra of tetramer **10** (a close analogue of **1**) (28 mM, 500MHz, CDCl₃): aromatic (a) and aliphatic regions (b).

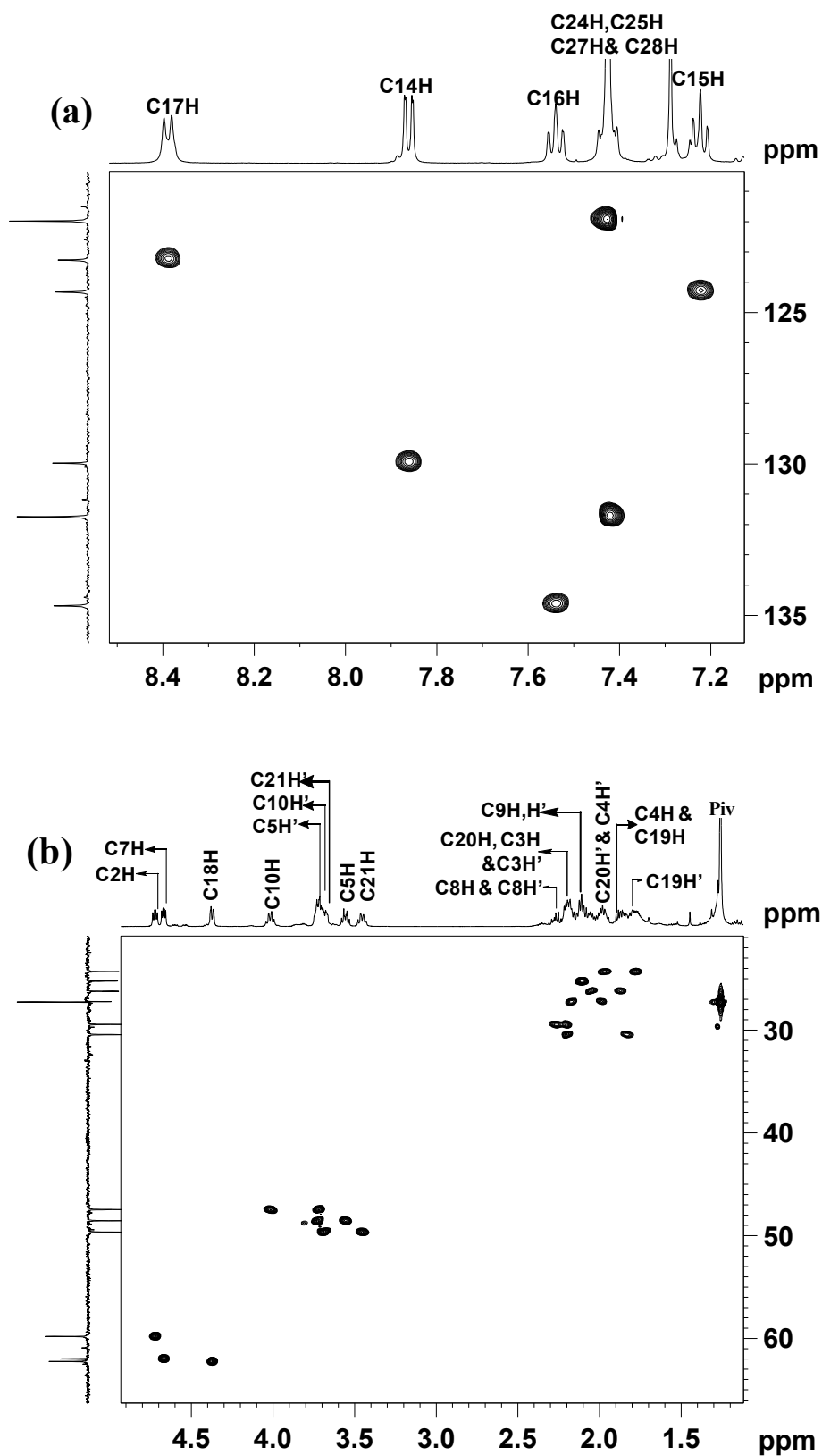


Fig. 2.16 Partial HSQC spectra of tetramer **10** (a close analogue of **1**) (28 mM, 500MHz, CDCl_3): aromatic (a) and aliphatic regions (b).

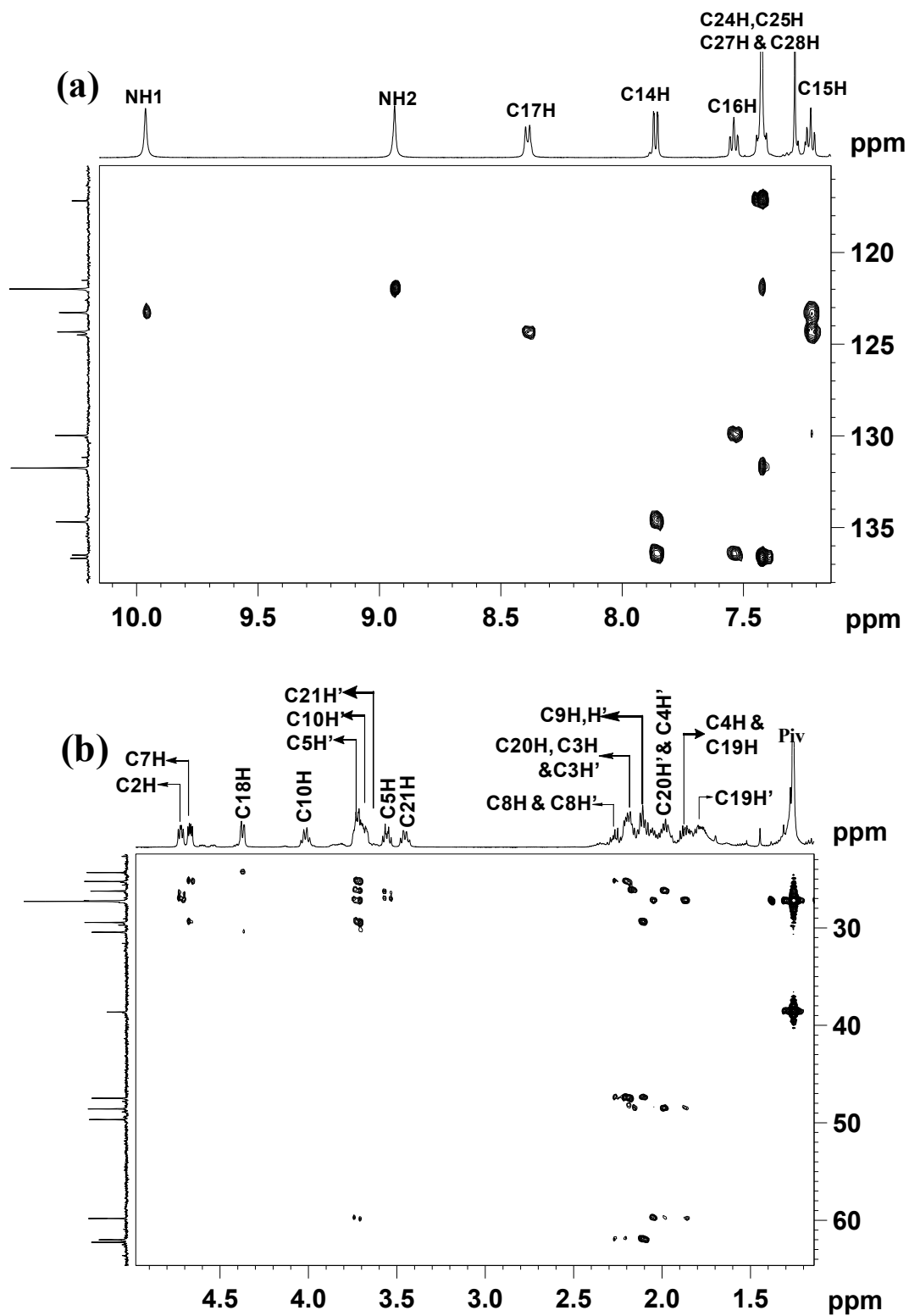


Fig. 2.17 Partial HMBC spectra of tetramer **10** (a close analogue of **1**) (28 mM, 500MHz, CDCl₃): aromatic (a) and aliphatic regions (b).

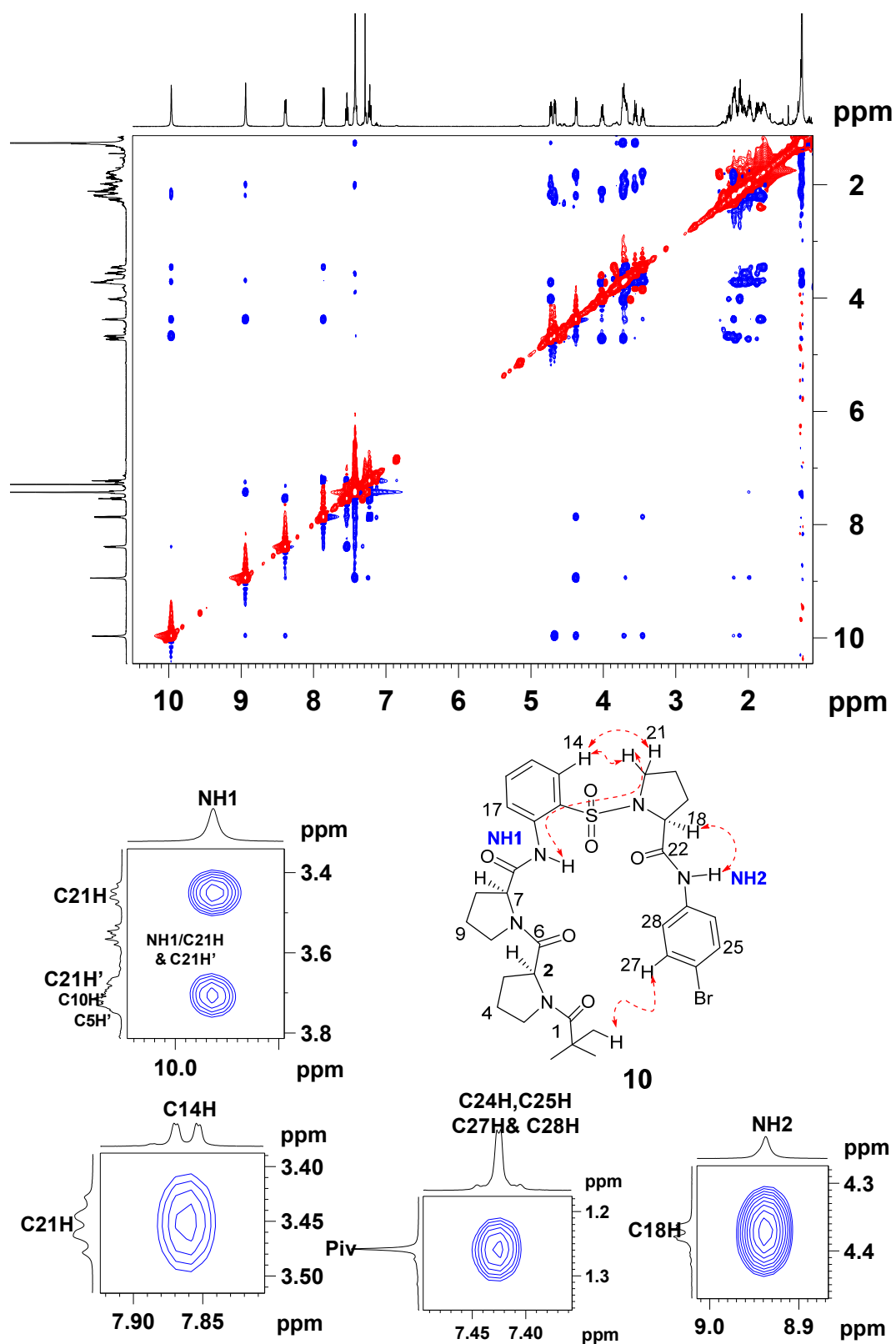


Fig. 2.18 2D NOESY full spectrum and selected nOe extracts of tetramer **11** (a close analogue of **1**) (28 mM, 500 MHz, CDCl_3).

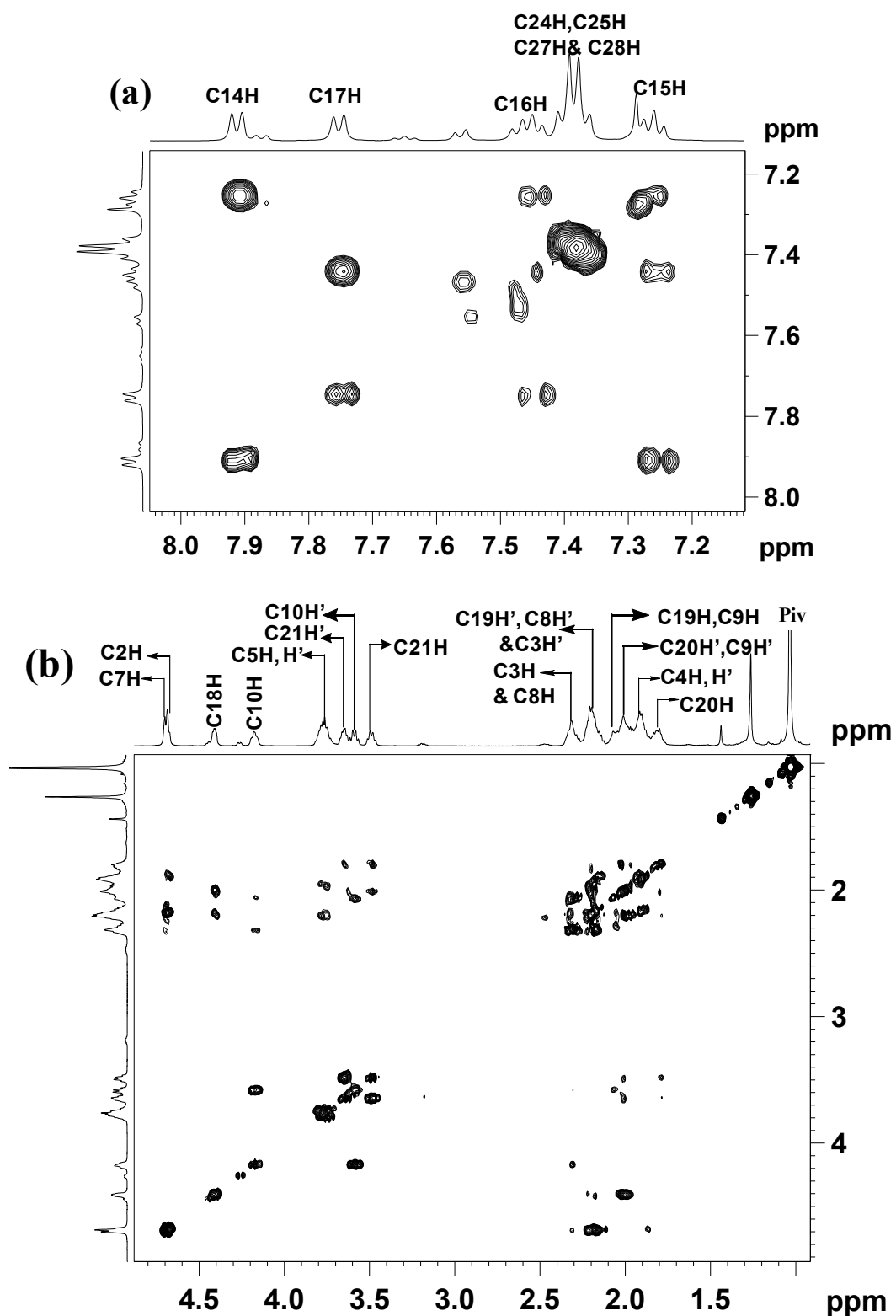


Fig. 2.19 Partial COSY spectra of tetramer 2 (30 mM, 500MHz, CDCl₃): aromatic (a) and aliphatic regions (b).

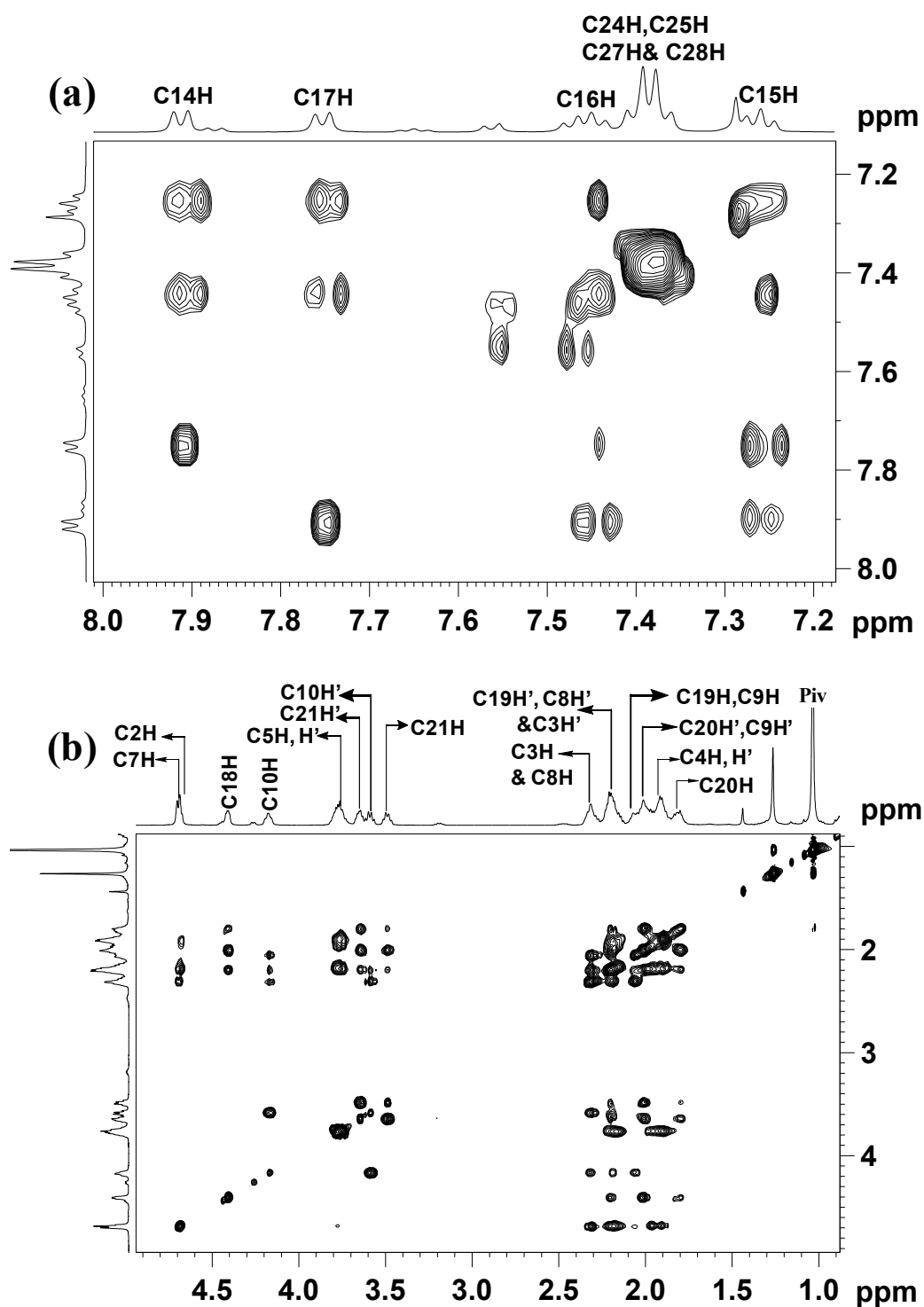


Fig. 2.20 Partial TOCSY spectra of tetramer **2** (30 mM, 500MHz, CDCl₃): aromatic (a) and aliphatic regions (b).

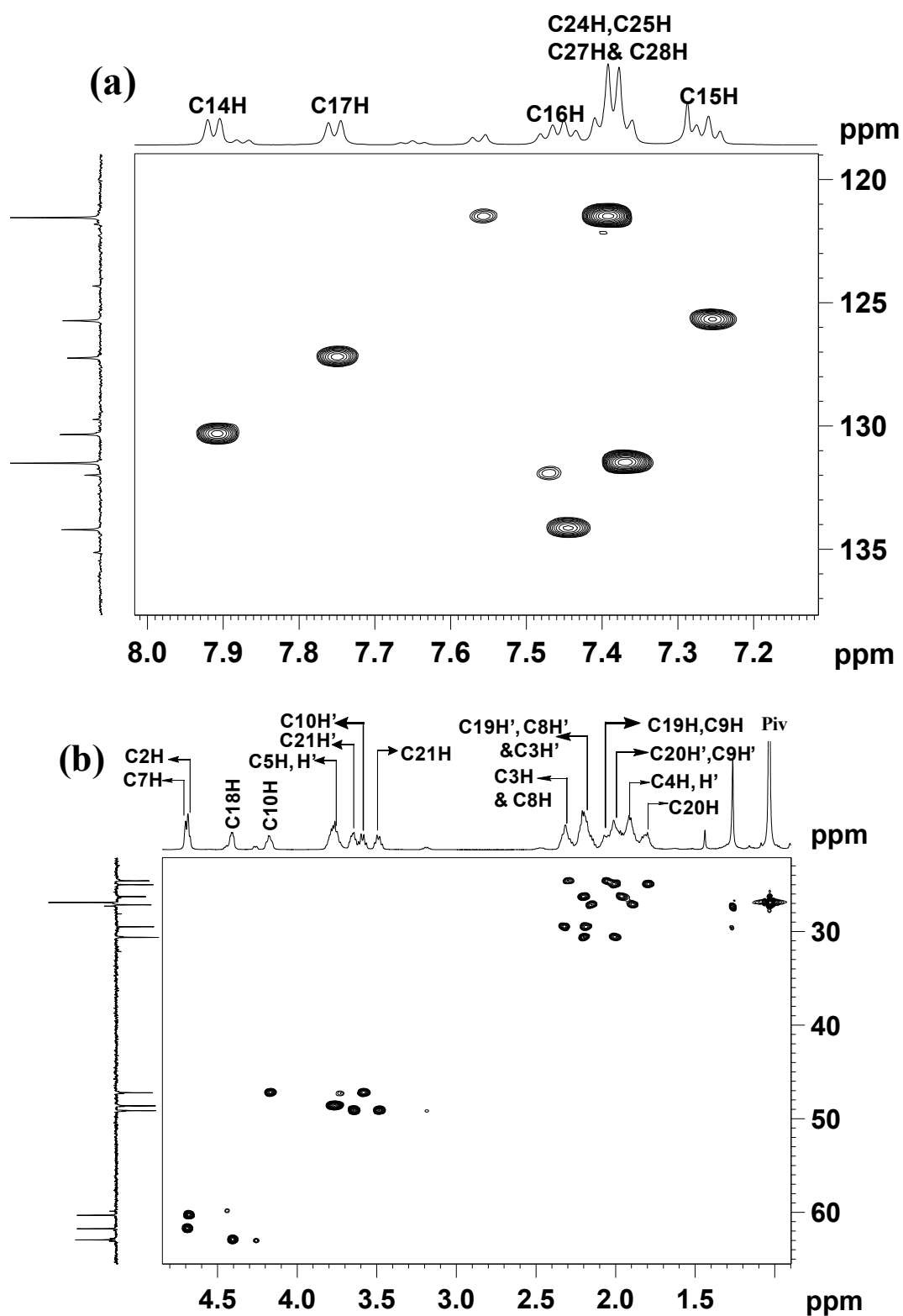


Fig. 2.21 Partial HSQC spectra of tetramer 2 (30 mM, 500MHz, CDCl_3): aromatic (a) and aliphatic regions (b).

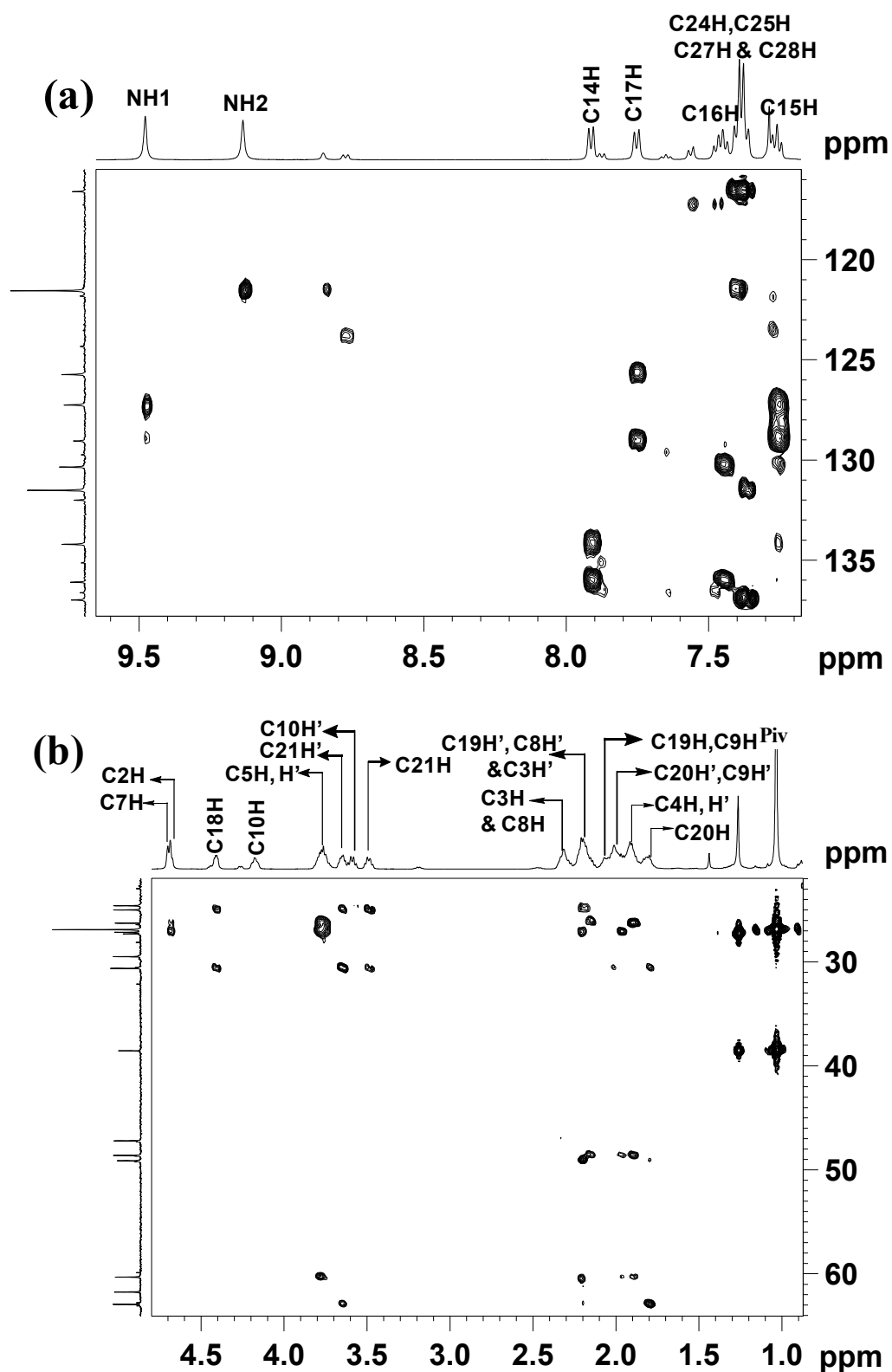


Fig. 2.22 Partial HMBC spectra of tetramer **2** (30 mM, 500MHz, CDCl₃): aromatic (a) and aliphatic regions (b).

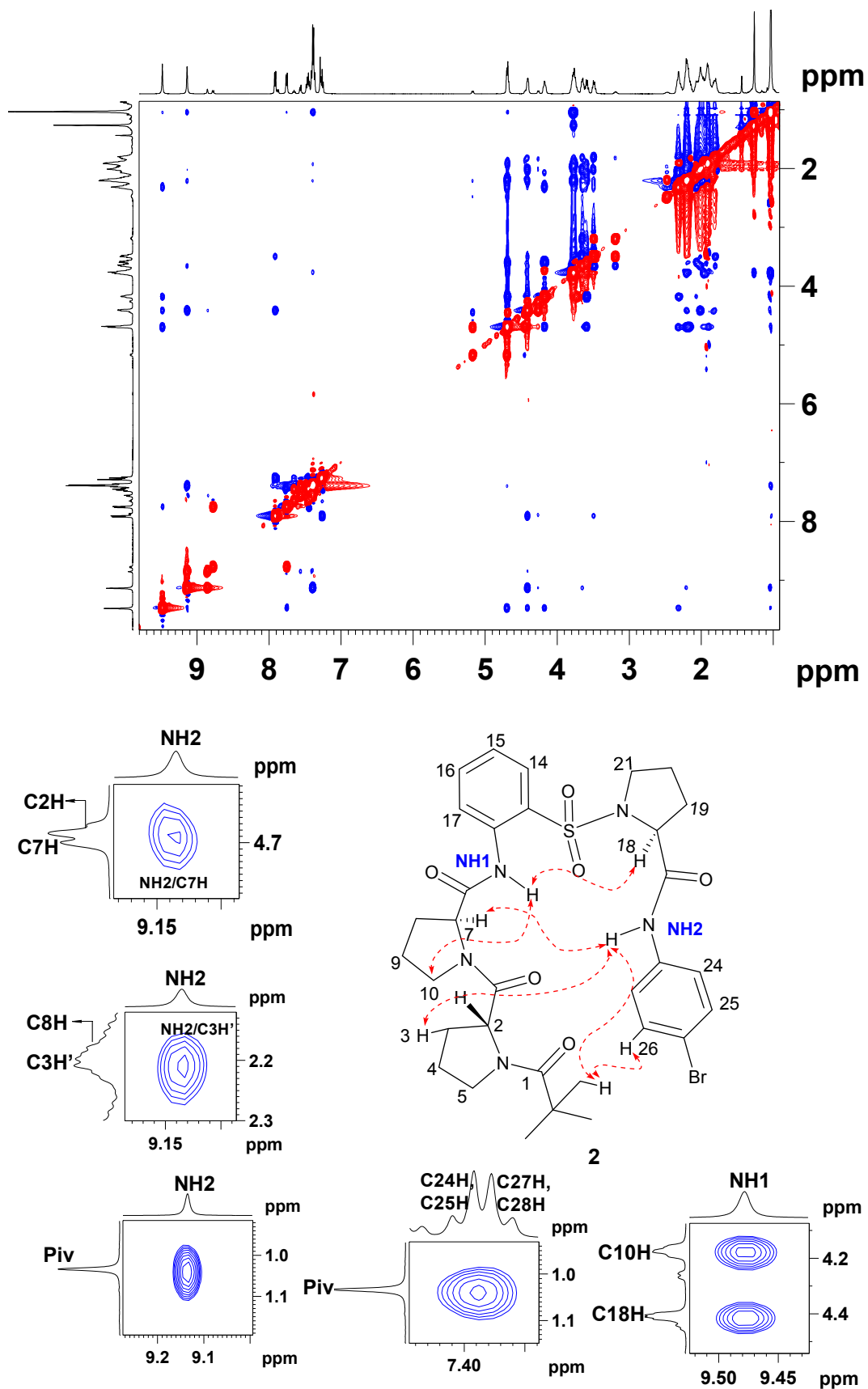


Fig. 2.23 2D NOESY full spectrum and selected nOe extracts of tetramer 2 (30 mM, 500 MHz, CDCl₃).

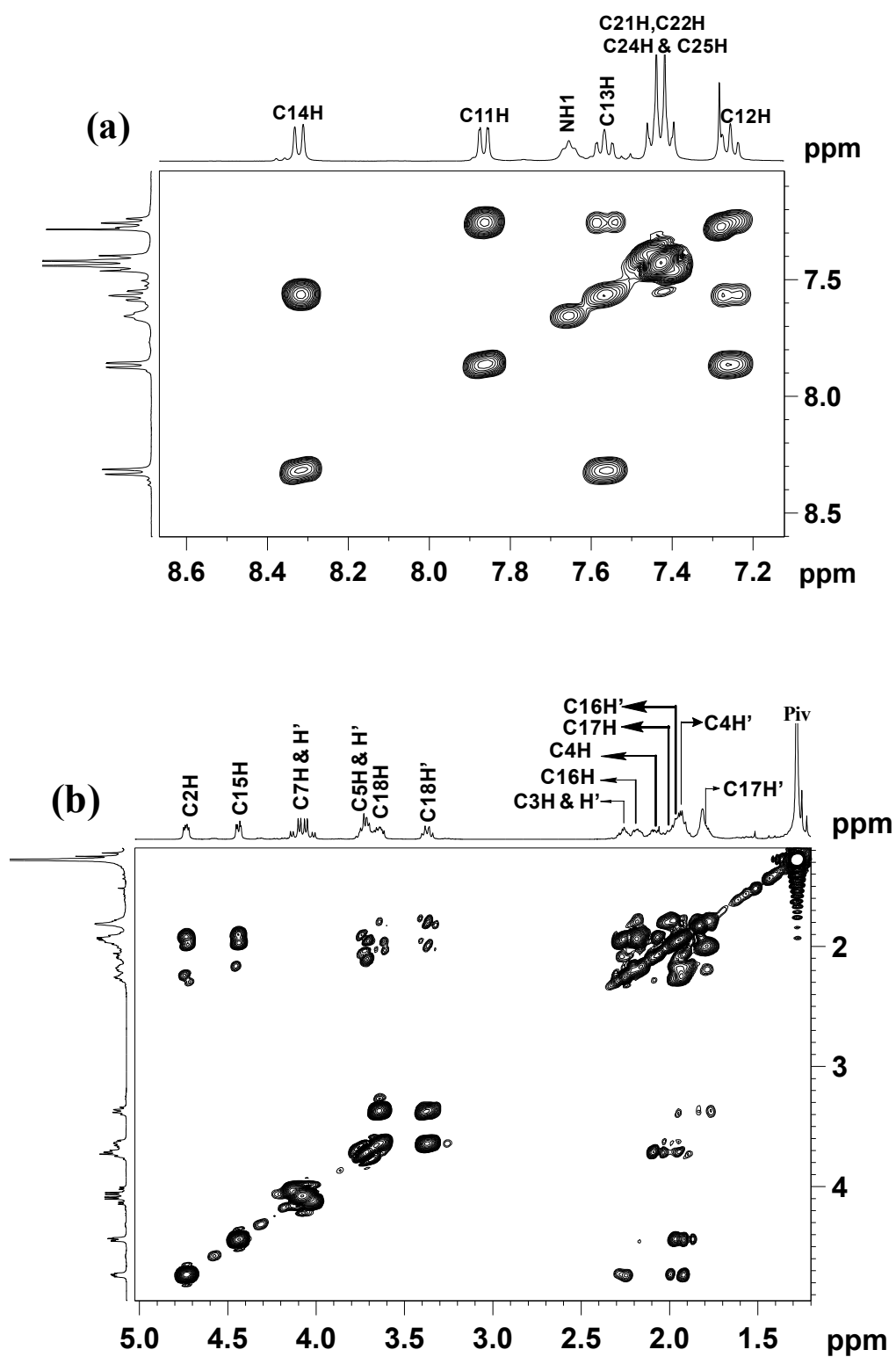


Fig. 2.24 Partial COSY spectra of tetramer **3** (63 mM, 400 MHz, CDCl₃): aromatic (a) and aliphatic regions (b).

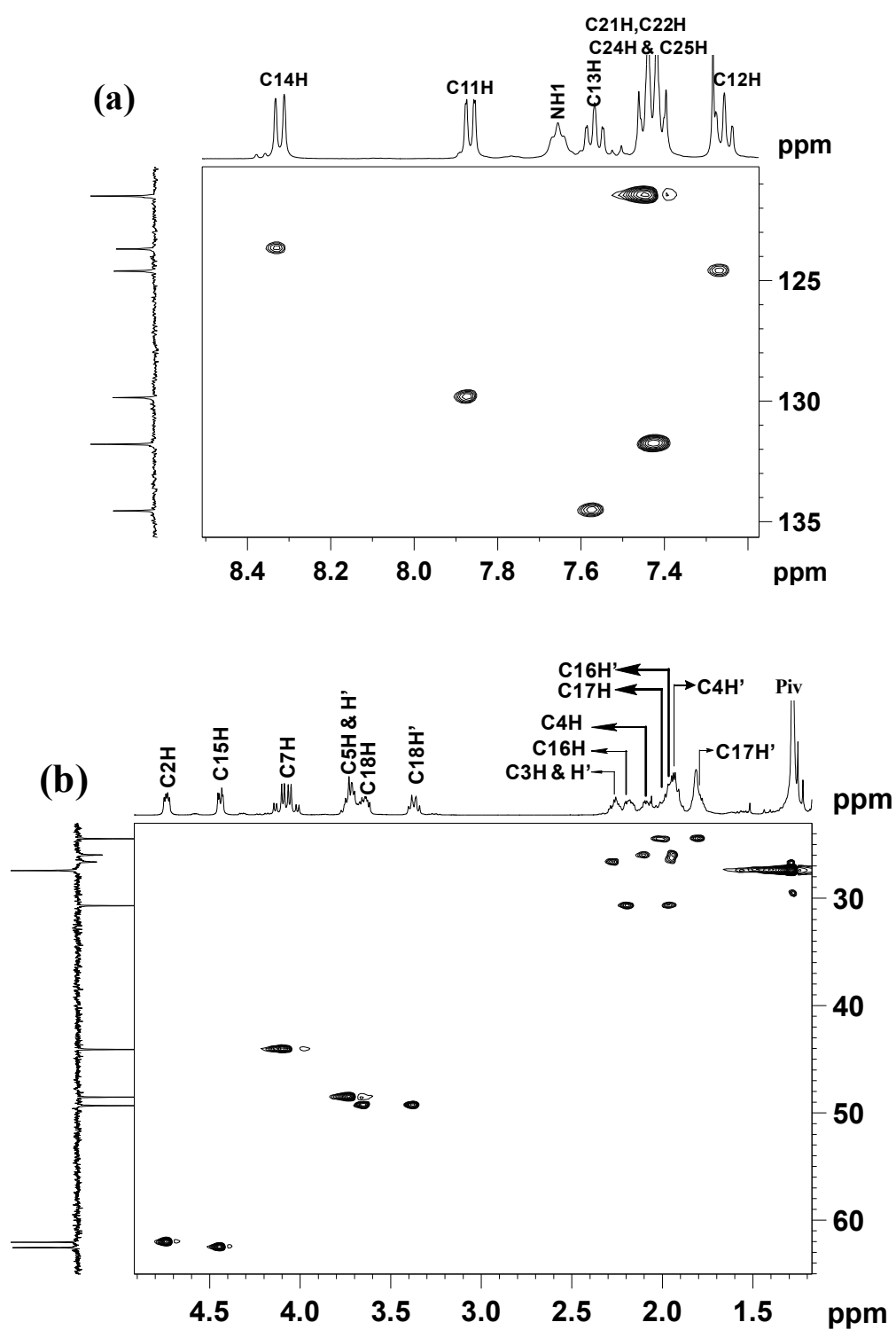


Fig. 2.25 Partial HSQC spectra of tetramer **3** (63 mM, 400 MHz, CDCl_3): aromatic (a) and aliphatic regions (b).

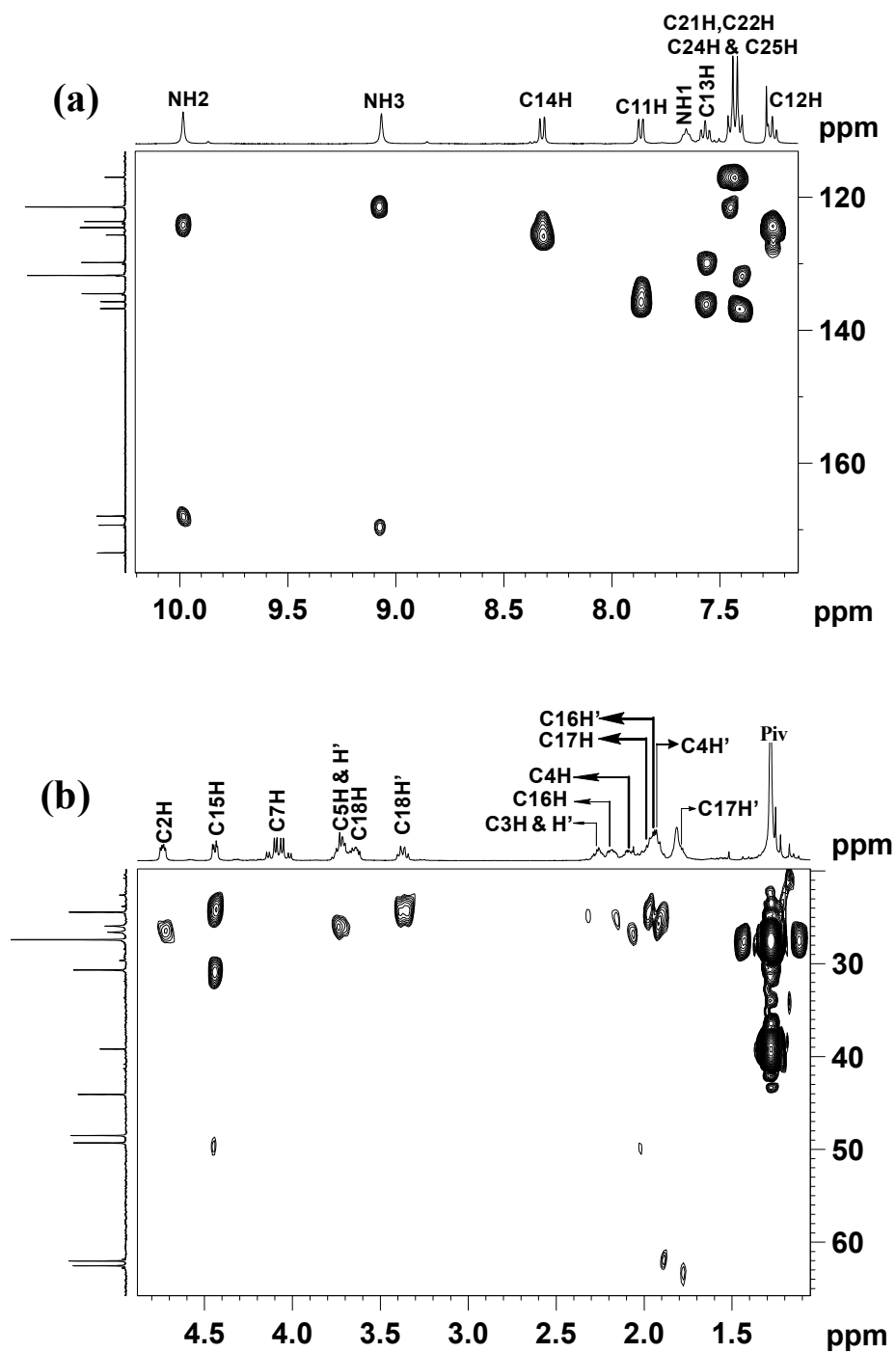


Fig. 2.26 Partial HMBC spectra of tetramer 3 (63 mM, 400 MHz, CDCl_3): aromatic (a) and aliphatic regions (b).

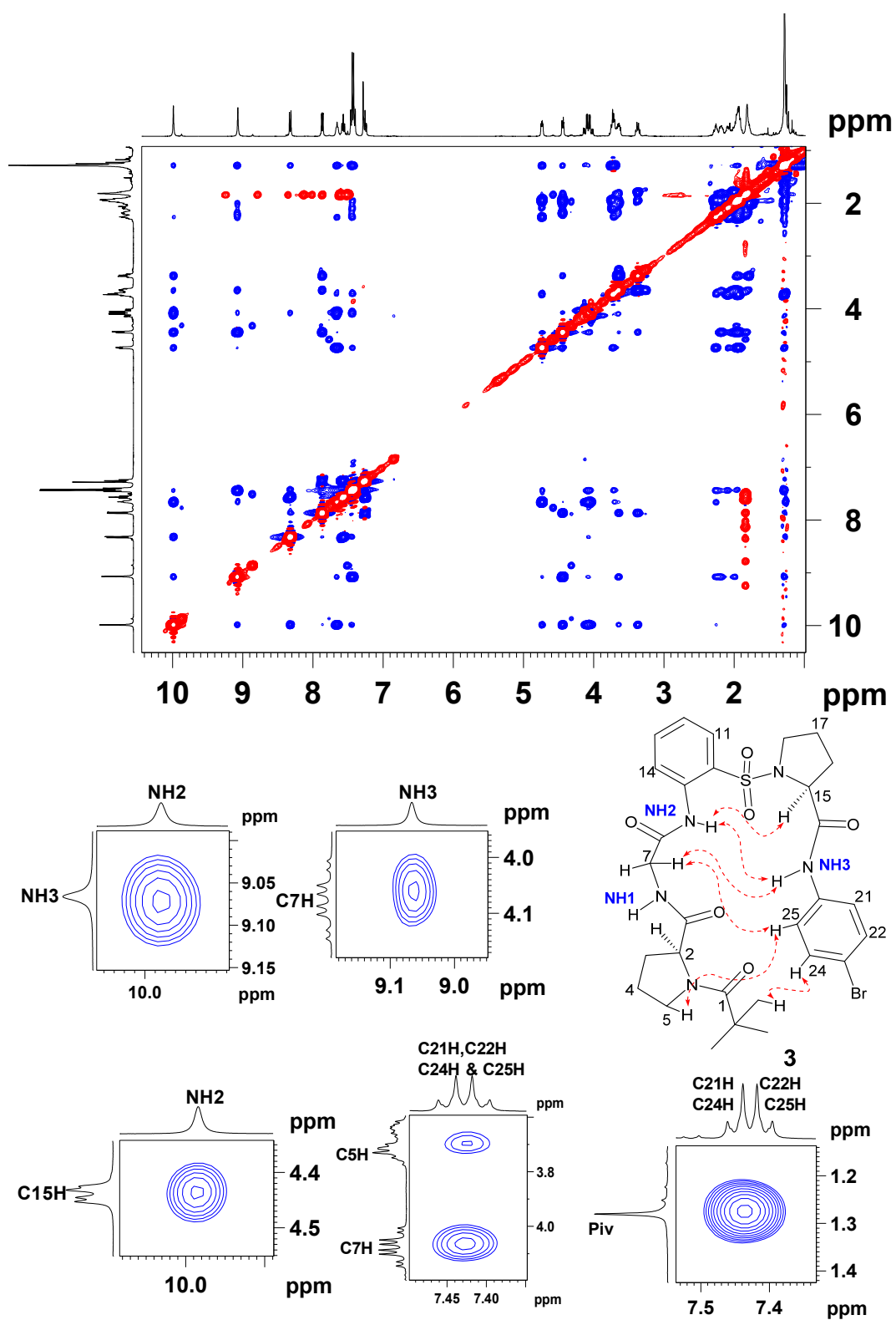


Fig. 2.27 2D NOESY full spectrum and selected nOe extracts of tetramer **3** (63 mM, 400 MHz, CDCl_3).

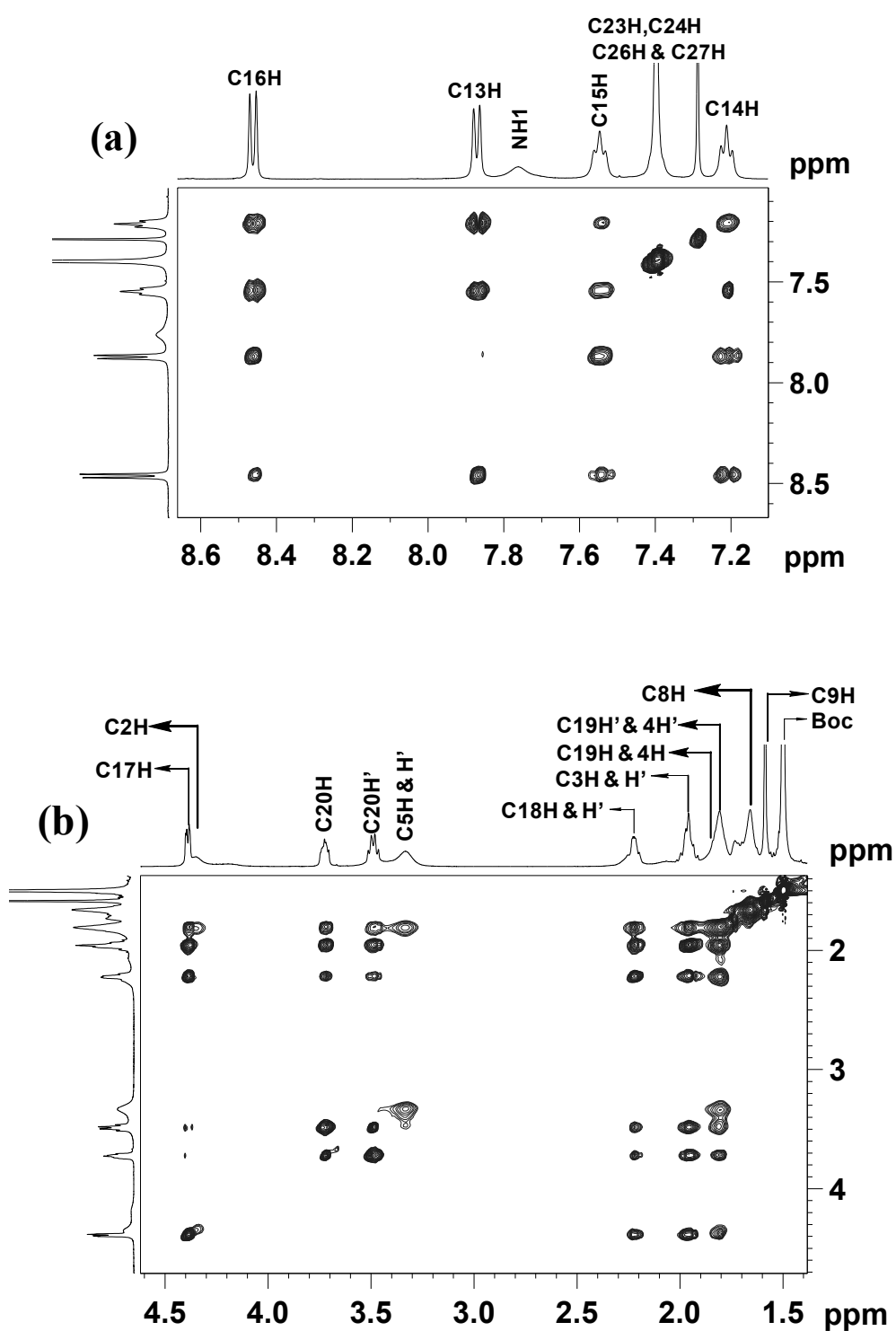


Fig. 2.28 Partial TOCSY spectra of tetramer **20** (a close analogue of **4**) (48 mM, 500 MHz, CDCl_3): aromatic (a) and aliphatic regions (b).

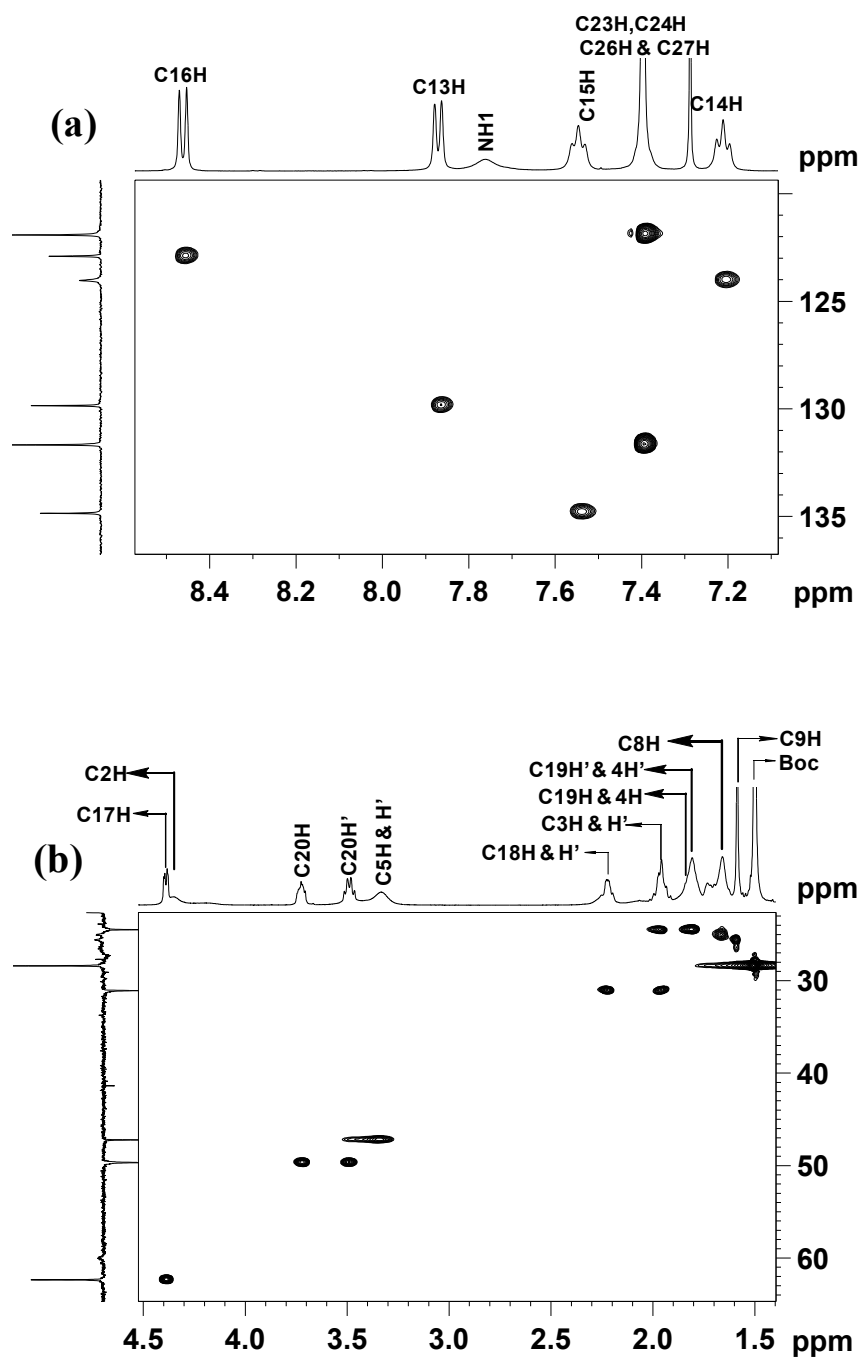


Fig. 2.29 Partial HSQC spectra of tetramer **20** (a close analogue of **4**) (48 mM, 500 MHz, CDCl₃): aromatic (a) and aliphatic regions (b).

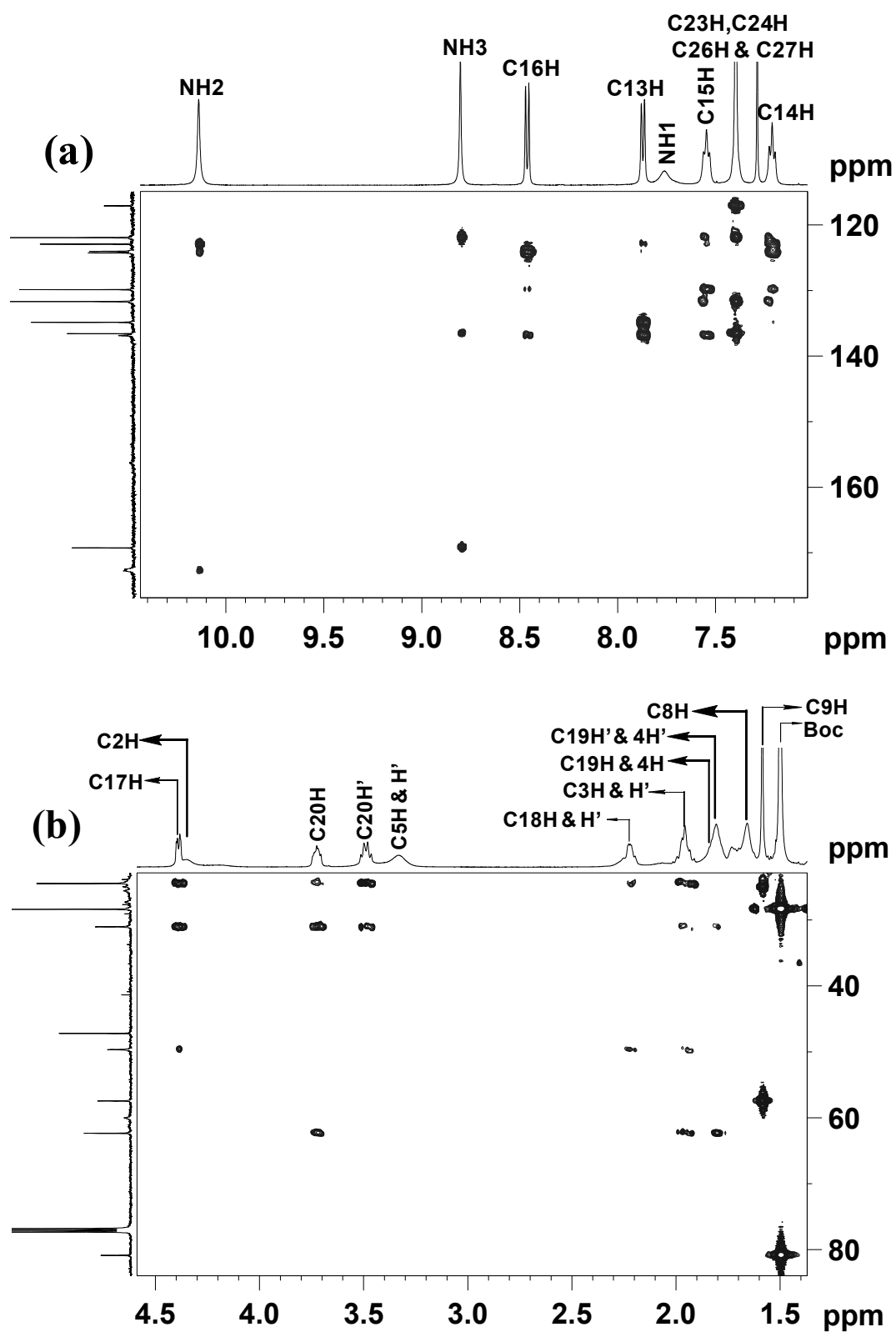


Fig. 2.30 Partial HMBC spectra of tetramer **20** (a close analogue of **4**) (48 mM, 500 MHz, CDCl₃): aromatic (a) and aliphatic regions (b).

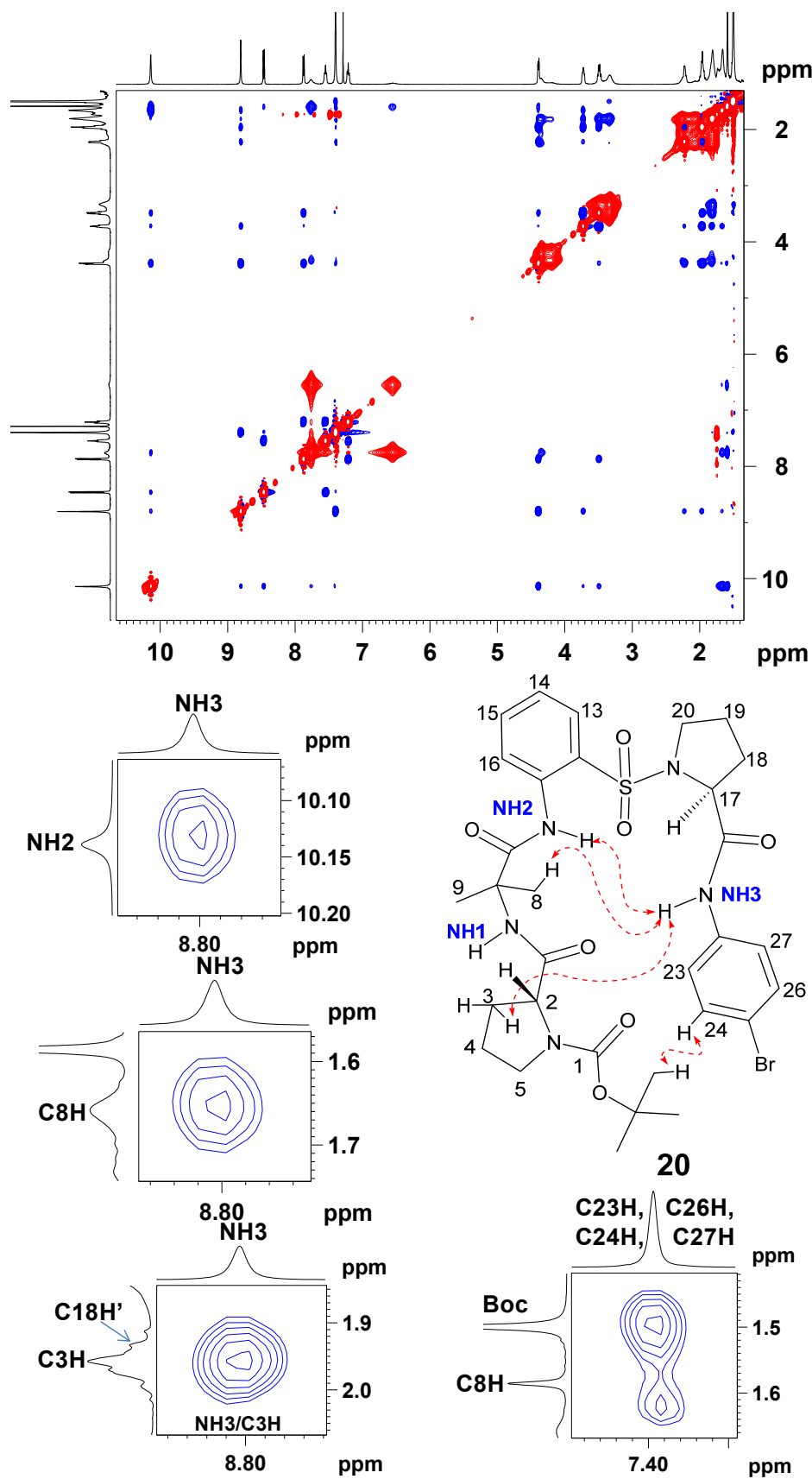


Fig. 2.31 2D NOESY full spectrum and selected nOe extracts of tetramer **20** (a close analogue of **4**) (48 mM, 500 MHz, CDCl₃).

Table 2.11 nOe-derived distance constraints used in molecular modeling for structure elucidation of peptide **2**.

Atom I	Atom II	Chemical Shift I	Chemical Shift II	Upper Bound	Lower Bound
NH1	C17H	9.470	7.738	3.876	3.171
NH1	C7H	9.470	4.686	3.105	2.540
NH1	C18H	9.470	4.407	3.611	2.955
NH1	C10H	9.470	4.177	3.546	2.901
NH1	C21H	9.470	3.650	4.804	3.931
NH1	C8H	9.470	2.287	3.461	2.832
NH1	Piv CH3	9.470	1.040	4.211	3.446
NH2	Piv CH3	9.131	1.034	3.819	3.124
NH2	C19H	9.131	2.009	4.408	3.607
NH2	C3H	9.131	2.215	3.938	3.222
NH2	C18H	9.131	4.401	2.870	2.349
NH2	C7H	9.131	4.686	4.710	3.853
NH2	C28H	9.131	7.387	2.790	2.283
C14H	C18H	7.902	4.407	3.071	2.512
C14H	C21H'	7.902	3.487	3.685	3.015
C14H	C21H	7.902	3.632	4.519	3.697
C17H	C8H	7.750	2.312	4.534	3.710
C27H	C5H	7.381	3.753	3.938	3.222
C28H	C5H	7.387	2.191	4.154	3.398
C28H	C4H	7.387	1.918	4.097	3.352
C27H	Piv CH3	7.381	1.034	3.410	2.790
C5H,H'	Piv CH3	3.771	1.040	2.364	1.934

Table 2.12 nOe-derived distance constraints used in molecular modeling for structure elucidation of peptide 3.

Atom I	Atom II	Chemical Shift I	Chemical Shift II	Upper Bound	Lower Bound
NH2	NH3	9.976	9.068	4.617	3.778
NH2	C14H	9.976	8.318	4.048	3.312
NH2	NH1	9.976	7.645	3.247	2.657
NH2	C15H	9.976	4.436	3.506	2.869
NH2	C7H	9.976	4.059	3.243	2.653
NH2	C18H	9.976	3.643	4.974	4.070
NH2	C18H'	9.976	3.364	4.071	3.331
NH3	PivCH3	9.068	1.270	4.306	3.523
NH3	C4H	9.068	2.000	4.735	3.874
NH3	C16H	9.068	2.205	4.027	3.295
NH3	C7H	9.068	4.064	5.155	4.217
NH3	C15H	9.068	4.436	2.774	2.270
NH3	C25H	9.068	7.427	2.783	2.277
NH3	NH1	9.068	7.645	4.870	3.984
C14H	C7H	8.318	4.075	5.009	4.099
C24H	PivCH3	7.428	1.270	3.560	2.912
C24H	C3H	7.434	2.244	4.291	3.511
C25H	C3H	7.428	2.244	4.412	3.610
C24H	C4H	7.428	2.000	6.005	4.913
C24H	C5H,H'	7.428	3.687	4.585	3.751
C25H	C7H	7.423	4.059	4.109	3.362
NH1	C7H	7.645	4.059	3.024	2.474
NH1	C2H	7.645	4.726	2.806	2.296
C25H	C2H	7.428	4.726	4.978	4.073
C2H	Piv CH3	4.726	1.270	3.991	3.265
C15H	Piv CH3	4.432	1.270	4.892	4.003
C5H,H'	Piv CH3	3.710	1.270	2.593	2.122

2.6 References and notes

- (1) C. T. Supuran, A. Casini and A. Scozzafava, *Med. Res. Rev.*, 2003, **23**, 535.
- (2) (a) S. Turcotte, S. H. B. Gervais and W. D. Lubell, *Org. Lett.*, 2012, **14**, 1318; (b) R. M. J. Liskamp, D. T. S. Rijkers, J. A. W. Kruijtzter and J. Kemmink, *ChemBioChem*, 2011, **12**, 1626; (c) R. M. J. Liskamp and J. A. W. Kruijtzter, *Mol. Diversity*, 2004, **8**, 79; (d) C. Baldauf, R. Gunther and H.-J. Hofmann, *J. Mol. Struct. (Theochem)*, 2004, **675**, 19; (e) J. M. Langenhan, J. D.; Fisk and S. H. Gellman, *Org. Lett.*, 2001, **3**, 2559; (f) C. Gennari, B. Salom, D. Potenza, C. Longari, E. Fioravanzo, O. Carugo and N. Sardone, *Chem. -Eur. J.*, 1996, **2**, 644; (g) C. Gennari, B. Salom, D. Potenza and A. Williams, *Angew. Chem. Int. Ed.*, 1994, **33**, 2067.
- (3) (a) J. L. Radkiewicz, M. A. McAllister, E. Goldstein and K. N. Houk, *J. Org. Chem.*, 1998, **63**, 1419; (b) J. Heyd, W. Thiel and W. Weber, *Theochem*, 1997, **391**, 125.
- (4) (a) C. M. Deber, B. Brodsky and A. Rath, *Proline Residues in Proteins*. In *eLS [Encyclopedia of Life Sciences]*; John Wiley & Sons, Ltd.: Chichester, **2010**, pp. 1-9; b) M. P. Williamson, *Biochem. J.*, 1994, **297**, 249.
- (5) R. V. Nair, S. B. Baravkar, T. S. Ingole and G. J. Sanjayan, *Chem. Commun.*, 2014, **50**, 13874.
- (6) (a) Kantharaju, S. Raghothama, U. S. Raghavender, S. Aravinda, N. Shamala and P. Balaram, *Biopolymers (Peptide Sci)*, 2009, **92**, 405; (b) C. Tomasini, G. Luppi and M. Monari, *J. Am. Chem. Soc.*, 2006, **128**, 2410; (c) G. Jeannotte and W. D. Lubell, *J. Am. Chem. Soc.*, 2004, **126**, 14334; (d) G. Luppi, D. Lanci, V. Trigari, M. Garavelli, A. Garelli and C. Tomasini, *J. Org. Chem.*, 2003, **68**, 1982.
- (7) (a) P. Y. Chou and G. D. Fasman, *J. Mol. Biol.*, 1977, **115**, 135; (b) E. G. Hutchinson and J. M. Thornton, *Protein Sci.*, 1994, **3**, 2207.
- (8) V. Krishnakumari, A. Sharadadevi, S. Singh and R. Nagaraj, *Biochemistry*, 2003, **42**, 9307.
- (9) (a) N. Srinivas, P. Jetter, B. J. Ueberbacher, M. Werneburg, K. Zerbe, J. Steinmann, B. Van der Meijden, F. Bernardini, A. Lederer, R. L. A. Dias, P. E. Misson, H. Henze, J. Zumbunn, F. O. Gombert, D. Obrecht, P.

- Hunziker, S. Schauer, U. Ziegler, A. Kach, L. Eberl, K. Riedel, S. J. DeMarco and J. A. Robinson, *Science*, 2010, **327**, 1010; (b) R. M. Hughes and M. L. Waters, *Curr. Opin. Struct. Biol.*, 2006, **16**, 514; (c) R. Rai, S. Raghothama and P. Balaram, *J. Am. Chem. Soc.*, 2006, 128, 2675.
- (10) (a) R. Rai, S. Aravinda, K. Kanagarajadurai, S. Raghothama, N. Shamala and P. Balaram, *J. Am. Chem. Soc.*, 2006, **128**, 7916.
- (11) B. Chatterjee, I. Saha, S. Raghothama, S. Aravinda, R. Rai, N. Shamala and P. Balaram, *Chem.–Eur. J.*, 2008, **14**, 6192.
- (12) S. Aravinda, V. V. Harini, N. Shamala, C. Das and P. Balaram, *Biochemistry*, 2004, **43**, 1832.
- (13) B. D. Blasio, V. Pavone, M. Saviano, A. Lombardi, F. Nastri, C. Pedone, E. Benedetti, M. Crisma, M. Anzolin and C. Toniolo, *J. Am. Chem. Soc.*, 1992, **114**, 6273.
- (14) K. N. Vijayadas, H. C. Davis, A. S. Kotmale, R. L. Gawade, V. G. Puranik, P. R. Rajamohan and G. J. Sanjayan, *Chem. Commun.*, 2012, **48**, 9747.
- (15) (a) L. Belvisi, C. Gennari, A. Mielgo, D. Potenza and C. Scolastico, *Eur. J. Org. Chem.*, 1999, 389; (b) V. V. E. Ramesh, G. Priya, A. S. Kotmale, R. G. Gonnade, P. R. Rajamohan and G. J. Sanjayan, *Chem. Commun.*, 2012, **48**, 11205.
- (16) (a) W. C. Pomerantz, T. L. R. Grygiel, J. R. Lai and S. H. Gellman, *Org. Lett.*, 2008, **10**, 1799; (b) Basuroy, B. Dinesh, M. B. M. Reddy, S. Chandrappa, S. Raghothama, N. Shamala and P. Balaram, *Org. Lett.*, 2013, **15**, 4866.
- (17) MacroModel, version 10.7, Schrödinger, LLC, New York, NY, 2015.
- (18) (a) K. N. Vijayadas, A. S. Kotmale, S. H. Thorat, R. G. Gonnade, R. V. Nair, P. R. Rajamohan and G. J. Sanjayan, *Org. Biomol. Chem.*, 2015, **13**, 3064; (b) S. S. Kale, S. M. Kunjir, R. L. Gawade, V. G. Puranik, P. R. Rajamohan and G. J. Sanjayan, *Chem. Commun.*, 2014, **50**, 2886.
- (19) (a) P.-Y. Chen, C.-K. Lin, C.-T. Lee, H. Jan and S. I. Chan, *Protein Sci.*, 2001, **10**, 1794; (b) A. I. Jimenez, G. Ballano and C. Cativiela, *Angew. Chem. Int. Ed.*, 2005, **44**, 396; (c) E. D. Alba, M. A. Jimenez and M. Rico, *J. Am. Chem. Soc.*, 1997, **119**, 175.

- (20) (a) C. P. Rao, R. Nagaraj, C. N. R. Rao and P. Balaram, *Biochemistry*, 1980, **19**, 425; (b) J. Yang, L. A. Christianson and S. H. Gellman, *Org. Lett.*, 1999, **1**, 11.

CHAPTER 3

PART A

*H-X-H three-centered hydrogen bonding
promoted nonpeptidic robust reverse turn
mimetics*

PART B

*Synthesis and characterization of novel urea -
(^SAnt-Pro) peptide conjugates for potential
biomedical applications*

PART C

*Vesicular self-assembly of urea-tethered α,β -
hybrid foldamer as a hydrophobic cargo carrier*

H-X-H three-centered hydrogen bonding promoted nonpeptidic robust reverse turn mimetics**3.1 Introduction**

Reverse turn and β -hairpin scaffolds are the smallest part of proteins and polypeptides, which play a vital role in several fundamental biological processes.^{1,2} Because of significant biological properties, the reverse turn and β -hairpin structures have attracted much attention. Several research groups have constructed the model systems by making use of synthetically modified backbones, which mimic intriguing structures and functions of these protein subunits. With intensive research, chemists and biologists have shown that synthetically modified novel peptidomimetic systems possess potential applications in the interdisciplinary fields such as medicinal chemistry,² organocatalysis³ and material chemistry.⁴ In this context, in recent years, researchers have shown that it is possible to prepare stable two-stranded⁵ and three-stranded⁶ antiparallel β -sheets from short peptide sequence that contain 9-16 and 20-24 amino acid residues, respectively. Studies of synthetic β -sheet models have provided fundamental insights into the peptide and protein aggregation phenomenon and also helped us to understand protein topology and protein design.^{2d,e}

β -hairpins (antiparallel β -sheets) can be constructed by attaching two adjacent antiparallel peptide strands to a peptidic or nonpeptidic-based linker, most often, a short loop or turn segment (Fig. 3.1a).⁵ Parallel β -sheets can be constructed using nonpeptidic turn motifs such as diamine (Fig. 3.1b) or diacid (Fig. 3.1c) linker, which can connect adjacent peptide strands through the C-terminus-to-C-terminus or N-terminus-to-N-terminus connection respectively.⁷⁻¹⁷

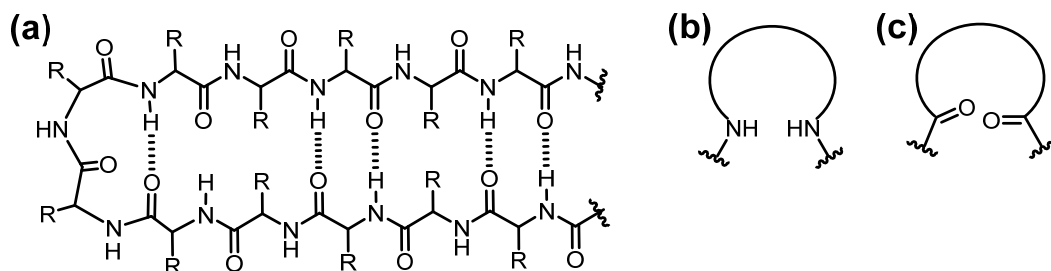


Fig. 3.1 General schematic representation of antiparallel β -sheet (a) and parallel β -sheet promoting linkers: diamine (b) and diacid (c).

Collectively, studies in the development of β -sheet models revealed that in addition to the noncovalent interactions, there are two factors which substantially determine the stability of β -sheet structures: one is the turn scaffold which holds adjacent peptide strands and another is its precise position in the peptide sequence.

In the previous chapters, literature precedents on the development of nonpeptidic-based turn mimetics that can stabilize β -sheet structures have been discussed in detail. Herein, we discuss the turn mimetics, in particular, that finds application in generating parallel β -sheet models. In this context, Kelly group reported a dibenzofuran moiety-based diacid linker that promote parallel β -sheet conformation in peptides.⁷ Feigel group prepared parallel β -sheet macrocycles using central scaffolds such as phenoxathiin-4,6-dicarboxylic acid and 2,8-dimethyl-4,6-bis(aminomethyl)phenoxathiin-10,10-dioxide moieties.⁸ Sogah group studied the parallel β -sheet models that contain 2,8-dimethylphenoxathiin 4,6-dicarboxylic acid motif as a turn inducing scaffold.⁹ Nowick group prepared artificial parallel β -sheet models utilizing urea-based reverse turn mimetics.¹⁰ Karle group developed the norbornene-based reverse turn scaffold to induce parallel β -sheet structures.¹¹ Gellman reported the reverse turn scaffold such as D-prolyl-(1,1-dimethyl)-1,2-diaminoethyl linker (D-Pro-DADME) to induce parallel β -sheet conformation (Fig. 3.2a).¹² Subsequently, Gellman group also utilized diacid linker-based reverse turn mimetics such as *cis*-1,2-cyclohexanedicarboxylic

acid-Gly [(*S,R*)-CHDA-Gly, Fig. 3.2b] to create parallel β -sheet structures, wherein they attached adjacent peptide strands to nonpeptidic reverse turn scaffold *via* N-terminus-to-N-terminus connection.¹³ Similarly, Lee group introduced D-prolyl-*cis*-1,2-diaminocyclohexane (D-Pro-DACH); a conformationally constrained turn scaffold, which can find application in the generation of parallel β -sheet structures (Fig. 3.2c).¹⁴ Kraatz and coworkers developed ferrocene-derived diacid linker which acts as a reverse turn scaffold to induce parallel sheet conformation in peptides.¹⁵ An intriguing example of urea-based nonpeptidic reverse turn scaffold was developed by Smith group, which can promote parallel β -sheet conformation in a cyclopropane-based γ -amino acid-containing peptide (Fig. 3.2d).¹⁶ Smith group further showed that synthetically modified urea-based analogues efficiently catalyze the asymmetric Mukaiyama-Mannich reaction (Fig. 3.2e).¹⁷

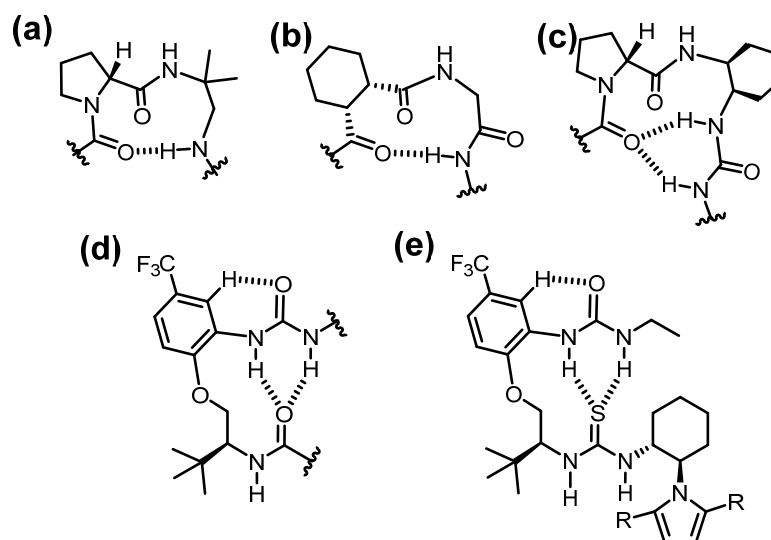


Fig. 3.2 Various templates for the induction of parallel β -sheet structures (a-d) and dual hydrogen-bonded urea-based organocatalyst for Mukaiyama-Mannich reaction (e).

3.2 Objective and design strategy

Herein we have designed the urea-based H-X-H three-centered hydrogen bonding-stabilized reverse turn scaffold containing a ^SAnt-Pro reverse turn and a

urea moiety at the N-terminus of the turn motif (Fig. 3.3). We anticipated that the urea NHs would form intramolecular dual hydrogen bonding with the C=O of proline. In this regard, the urea moiety can be installed at the N-terminus of ^SAnt-Pro reverse turn scaffold¹⁸ by reacting H₂N-^SAnt-Pro with trichloroacetyl chloride to access trichloroacetamide **3** and further reacting it with the amine counterpart. In the present study, trichloroacetamide derivative **3** was used as a common intermediate to generate the unsymmetrical urea analogues (**4-9**) *via* coupling with various amines (Fig. 3.3). This urea-based dual hydrogen-bonded reverse turn scaffold can be linked to the peptide strands *via* N-terminus-to-N-terminus connection and thus can promote parallel-sheet structures in the peptides.

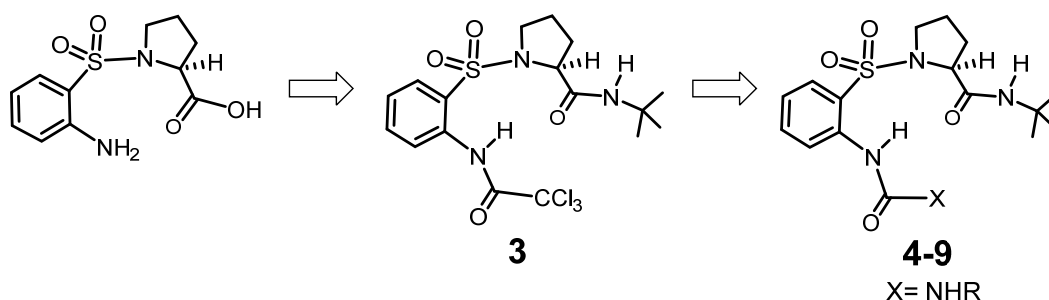


Fig. 3.3 Design strategy for the H-X-H three centered dual hydrogen bonding-stabilized reverse turn scaffold.

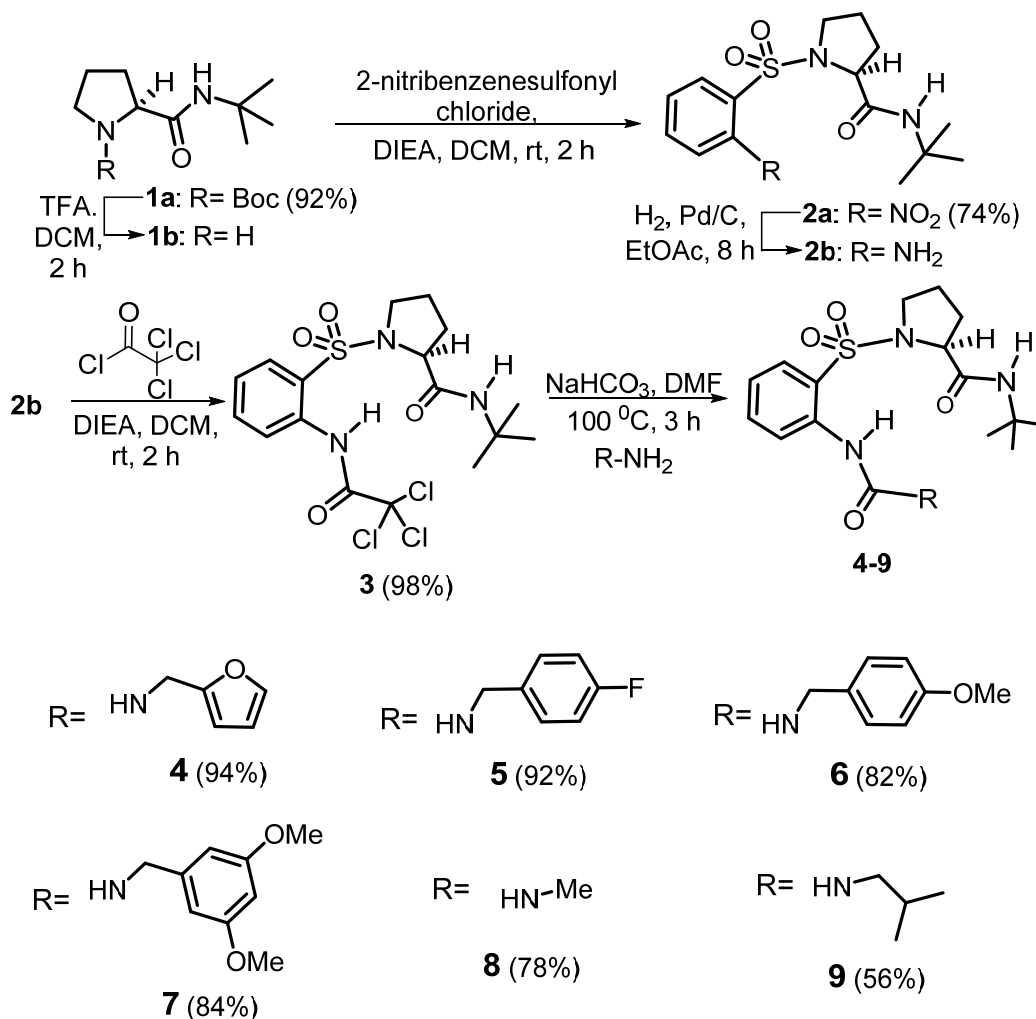
3.3 Results and discussion

3.3.1 Synthesis

The unsymmetrical urea analogues were synthesized from amine NH₂-^SAnt-Pro-^tBu building block as displayed in the scheme 3.1. The synthesis started by coupling of H-Pro-^tBu **1b**¹⁹ with the 2-nitrobenzenesulfonyl chloride in the presence of DIEA to obtain nitro derivative **2a**, which was then reduced under hydrogenation reaction condition using H₂, Pd/C to furnish amine **2b**. The amine **2b** was converted to the trichloroacetamide derivative **3** by reacting **2b** with trichloroacetyl chloride in the presence of DIEA. The trichloroacetamide

derivative **3** was used as a common intermediate, which was further reacted with various primary amines in the presence dry sodium bicarbonate under heating condition to obtain various dual hydrogen-bonded urea derivatives **4-9**.

Scheme 3.1 Synthesis of urea-based dual hydrogen-bonded reverse turn scaffolds.



3.3.2 NMR Studies

We undertook detailed 2D NMR studies to gain insights into solution-state conformation of urea-based scaffolds. The involvement of urea-NHs in an intramolecular hydrogen bonding was confirmed by variable temperature (VT) experiments in a polar solvent such as DMSO-*d*₆ and DMSO-*d*₆ titration studies in CDCl₃. The values of temperature coefficients for urea-NHs of **4** (Fig. 3.4a) were found to be very negligible [$\Delta\delta/\Delta T(\text{NH1}) = -0.12$, $\Delta\delta/\Delta T(\text{NH2}) = -0.12$ ppb/K],

which clearly indicated their participation in strong intramolecular hydrogen bonding. On the contrary, larger value of temperature coefficient for NH3 [$\Delta\delta/\Delta T(\text{NH}_3) = -6.83$ ppb/K] suggested its solvent exposed nature. Similarly, results of the DMSO- d_6 titration studies (Fig. 3.4b) clearly indicated that the urea NHs are involved in strong intramolecular dual hydrogen bonding [$\Delta\delta_{\text{NH1}} = 0.01$, $\Delta\delta_{\text{NH2}} = 0.01$ ppm]. Furthermore, the conformation of compound **4** in the solution-state was investigated by 2D NMR studies.

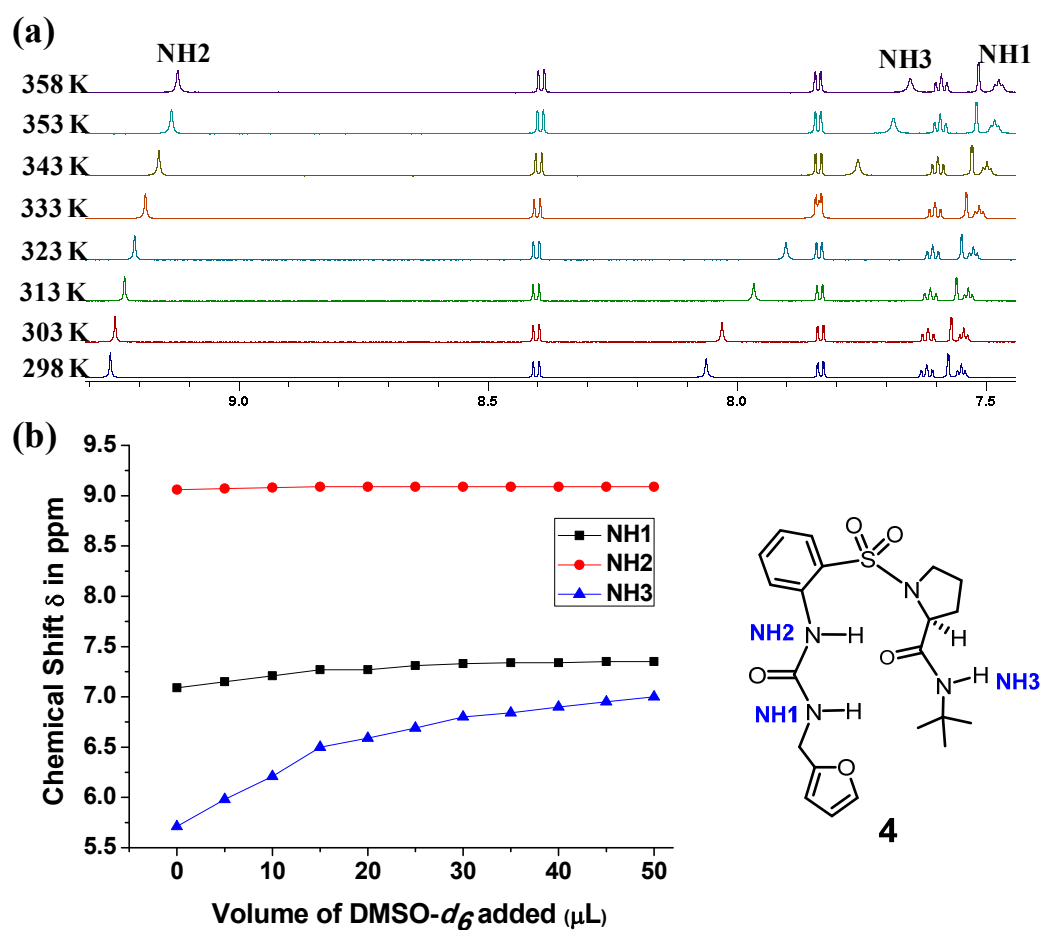


Fig. 3.4 Plots of variable temperature (2 mM, 700 MHz, DMSO- d_6) and DMSO- d_6 titration studies of **4** (2 mM, 400 MHz, CDCl_3).

The noticeable long-range inter-residual nOes were observed in the compound **4**, such as NH2/C11Hb, C4H/C11Ha, C21H/C15H and NH1/C16H (Fig. 3.5), which unequivocally confirmed that compound **4** adopted well-defined

folded conformation. The appropriately positioned C=O group of proline and *trans-trans* conformation of urea can form the dual hydrogen bonding effectively. The significant nOe: C8H/NH3 confirmed projection of C=O group of proline towards urea-NHs while nOe: NH2/NH1 confirmed the *trans-trans* conformation of urea. This proper arrangement of hydrogen bonding sites facilitated participation of C=O in the dual hydrogen bonding with urea-NHs. These observations were strongly supported by its crystal structure analysis.

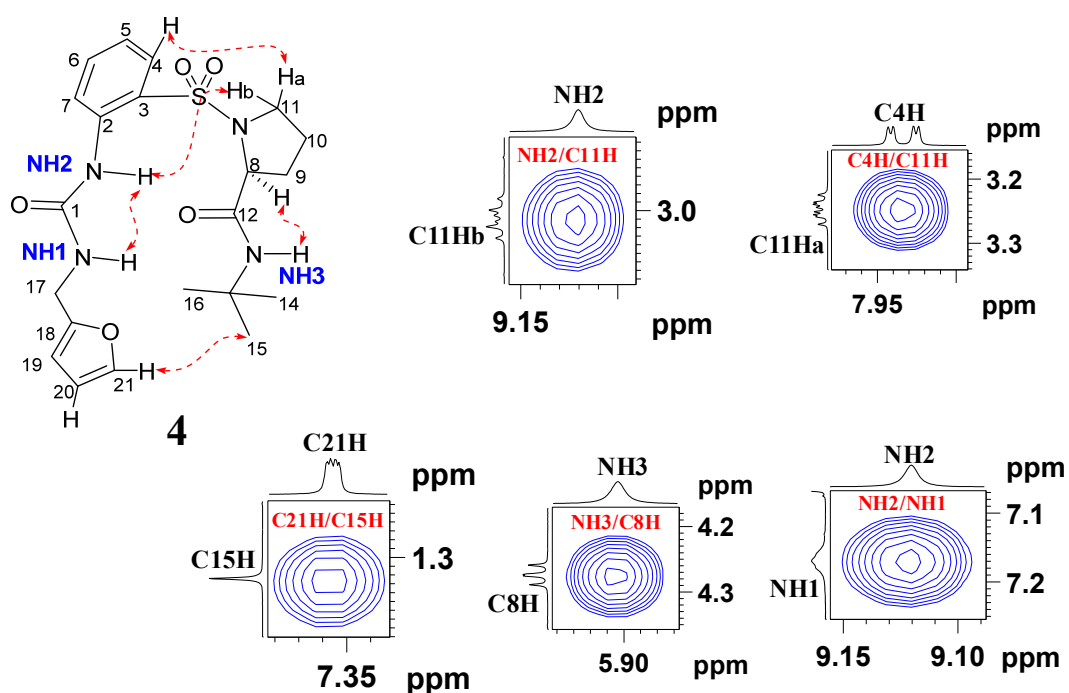


Fig. 3.5 Selected nOe extracts of **4** (20 mM, 500 MHz, CDCl₃).

Compounds **5-9** showed significant nOes as well, which indicated these compounds adopt folded conformation, as observed in case of compound **4**. Moreover, negligible chemical shifts and small temperature coefficients confirmed the solvent shielding nature of urea-NHs in the compounds **5-9** (Table 3.1).

Table 3.1 Temperature coefficients and chemical shifts of compounds **4-9**.

Compd	Temp coefficients ^a			Chemical shifts ^b		
	$\Delta\delta/\Delta T$ (ppb/K)			$\Delta\delta$ (ppm)		
	NH1	NH2	NH3	NH1	NH2	NH3
4	-1.33	-2.33	-6.83	0.26	0.03	1.29
5	-1.00	-2.16	-6.66	0.25	0.03	1.36
6	-1.00	-2.16	-6.66	0.24	0.02	1.18
7	-0.83	-2.33	-6.66	0.28	0.03	1.31
8	-2.33	-2.16	-7.16	0.30	0.02	1.26
9	-2.00	-2.16	-6.83	0.26	0.03	1.20

Note: ^aValues of chemical shifts obtained from DMSO-*d*₆ titration studies (2 mM, 400 MHz, CDCl₃, 298 K). ^bVariable temperature studies carried out in DMSO-*d*₆ (2 mM, 700 MHz).

Furthermore, analysis of ¹H NMR spectra of **4-9** recorded in CDCl₃ at the temperature range from 323 K to 268 K with 10 K gradual increment revealed that chemical shifts of urea-NHs show downfield shift. The results of variable temperature studies in CDCl₃ provided further evidence of well-defined conformations in the urea-based analogues.

3.3.3 Crystal structure analysis

After extensive crystallization trials, we could obtain good quality crystals of an analogue **4**, suitable for X-ray diffraction. Its crystal structure (Fig. 3.6) analysis revealed that the distance between NH1 and NH2 was found to be 2.09 Å which indicated the *trans-trans* configuration of the urea-NHS and *planar* orientation of urea moiety in the solid-state. The hydrogen bonding distances were found to be [$d(\text{NH1} \cdots \text{O}) = 2.01 \text{ \AA}$] and [$d(\text{NH2} \cdots \text{O}) = 2.22 \text{ \AA}$], which clearly suggested participation of urea NHs in strong intramolecular hydrogen bonding. Moreover, an additional stabilization force emanating from the interaction

between NH2 and Pro-N [$d(\text{NH} \cdots \text{N}) = 2.38 \text{ \AA}$] further augmented the stability of the reverse turn scaffold.

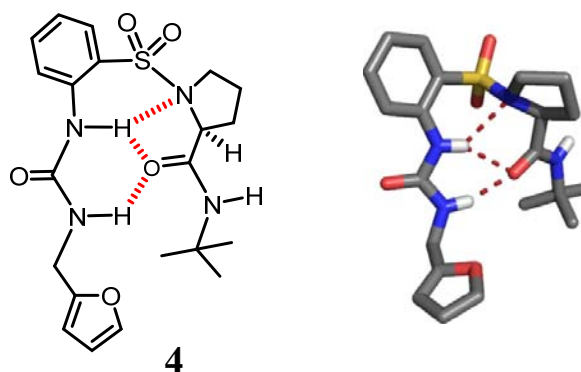


Fig. 3.6 Molecular structure (left) of **4** displaying observed hydrogen bonding and its crystal structure (right).

3.4 Conclusion

Conformational investigations of designed unsymmetrical urea derivatives in the solid and solution-state by single crystal X-ray crystallography and detailed 2D NMR studies, respectively, revealed that these scaffolds adopt well-defined conformation featuring robust urea-based H-X-H three-centered hydrogen bonding. Interestingly, an interaction between ^SAnt-NH and Pro-N was found to be an augmenting force for the stabilization of urea-based reverse turn scaffold. This nonpeptidic reverse turn scaffold can be attached to peptide strands through N-terminus connection, thus it can serve as a template to promote parallel β -sheet structures.

Synthesis and characterization of novel urea - (^SAnt-Pro) peptide conjugates for potential biomedical applications

3.5 Introduction

The sulfonamides are known to be an important class of drug candidates and studies on the development of sulfonamide-based pharmaceutical agents have attracted much attention in recent years. Several compounds containing sulfonamide moiety (Fig. 3.7) are identified as effective drugs possessing anticancer,²⁰ antimicrobial,²¹ anticonic anhydrase,²² hypoglycemic,²³ diuretic,²⁴ antithyroid²⁵ activities or resistance towards proteases.²⁶

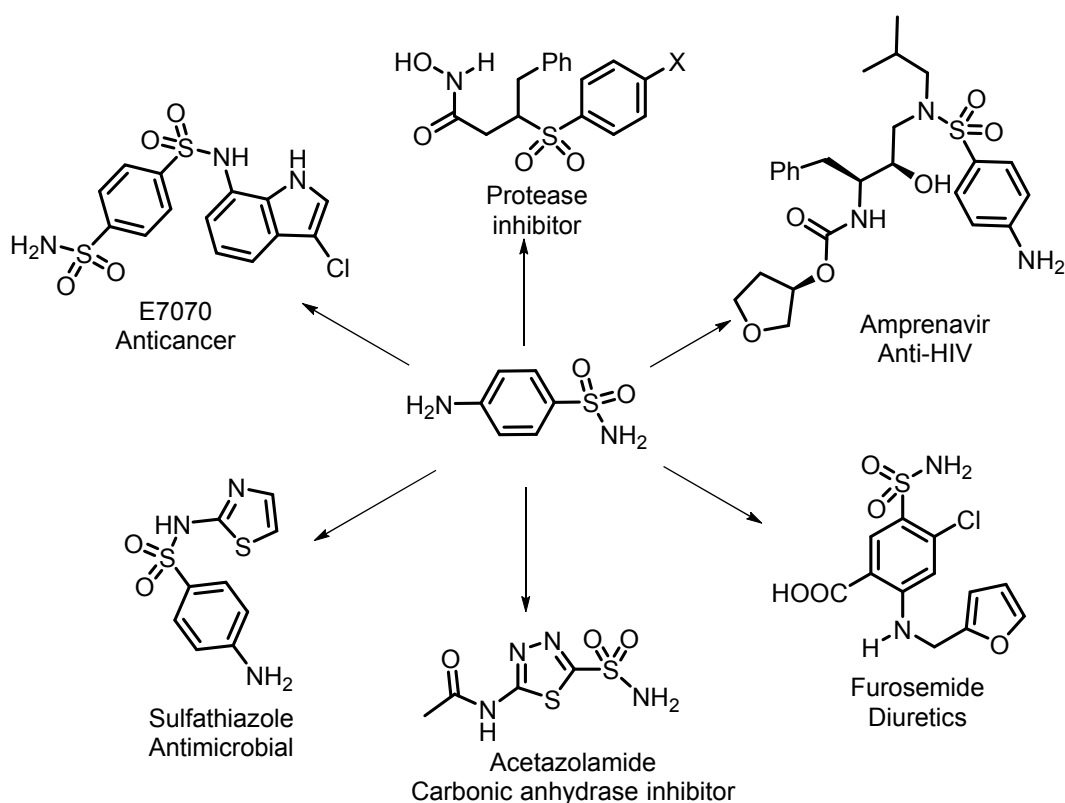


Fig. 3.7 Representative examples of sulfonamide moiety-containing drugs.

In the previous chapters, we already have discussed advantages of sulfonamide moiety over carboxamide moiety and the consequences of isosteric replacement of amide bond by sulfonamide on the conformational preferences of

peptide sequences. Due to exceptional proteolytic resistance sulfonamides, are considered as ideal candidates for the development of pharmaceutical agents.

[1,4]-diazepane moiety has been found in many biologically active compounds as an active pharmacophore. For instance, compound A YM-60828²⁷ contains [1,4]-diazepane moiety, acting as anticoagulant, while compound B having [1,4]-diazepane and urea moieties acting as a CXCR3 antagonist.²⁸ Compound C containing benzothiazole and benzoyl group attached to [1,4]-diazepane unit exhibits CNS-penetrant orexin receptor antagonist activity²⁹ and compound D containing units such as morpholine, [1,4]-diazepane and isoxazole exhibit cannabinoid receptor 2 (CB2) agonist activity with high selectivity (Fig. 3.8).³⁰

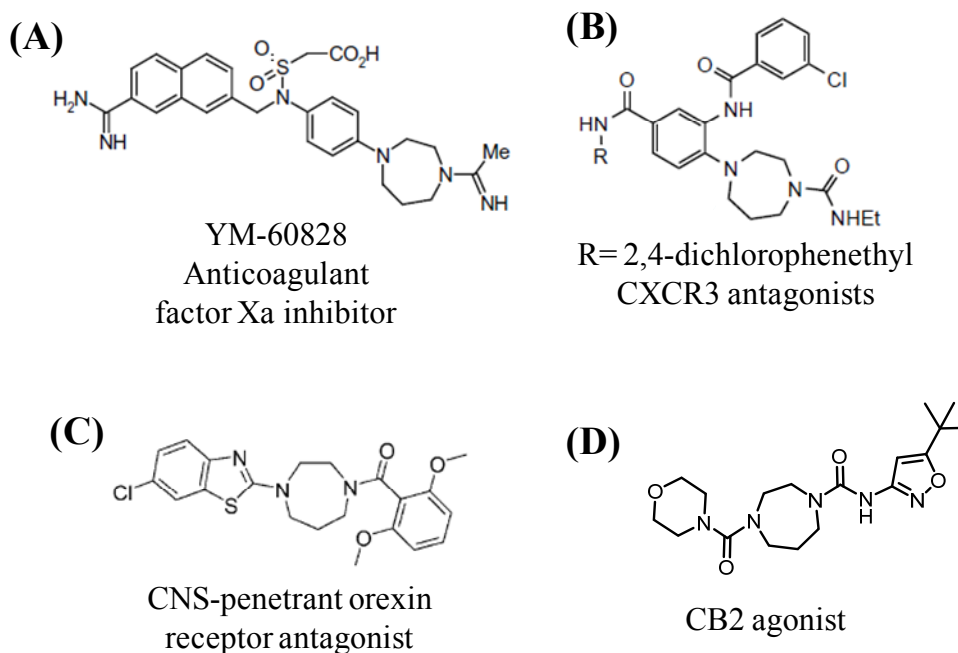


Fig. 3.8 Representative examples of biologically active compounds containing [1,4]-diazepane moiety.

3.6 Objective of the work and design strategy

Herein, we describe the design and synthesis of novel [1,4]-diazepane urea-^SAnt-Pro peptide conjugates. We have designed a series of hybrid analogues

featuring [1,4]-diazepane moiety linked to ^SAnt-Pro reverse turn scaffold through the urea linkage (**10-14**, Fig. 3.9). One of the prominent features of this system is [1,4]-diazepane scaffold,²⁷⁻³⁰ which is found in many drugs; e.g. orexin receptor antagonists, CXCR3 antagonists, cannabinoid receptor 2 agonists and factor Xa inhibitors for anticoagulation. Another important feature of designed system is ^SAnt-Pro reverse turn scaffold,^{18a} which is anticipated to rigidify the peptide backbone. Moreover, the incorporation of ^SAnt (β -aminobenzenesulfonic acid) - an unnatural β -amino acid, may rectify the proteolytic degradation issue. Additionally, we also have prepared analogues that contain pyrrolidine, piperidine and morpholine urea moieties attached to ^SAnt-Pro reverse turn scaffold (**15-17**, Fig. 3.9). Many of folded peptides are biologically active since they provide molecular recognition sites for numerous biological processes.

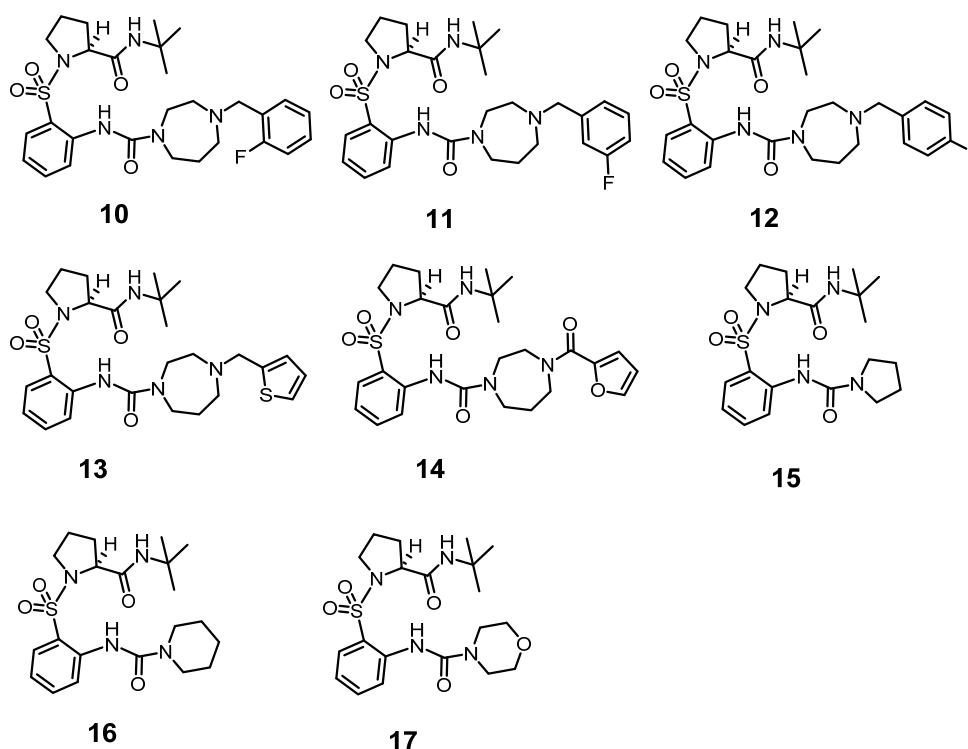


Fig. 3.9 Molecular structures of urea-(^SAnt-Pro) peptide conjugates.

3.7.2 Conformational analysis

Careful analysis of ^1H NMR spectrum of all designed analogues (**10-17**) showed that the chemical shift of $^{\text{S}}\text{Ant-NH}$ was found to be around 9-9.25 ppm, which is a typical chemical shift of 9-membered hydrogen bonding.^{18b} Thus, these analogues show folded conformation similar to compounds **4-9** (chapter 3, section A). On the contrary, ^1H NMR of compound **3** showed the chemical shift of $^{\text{S}}\text{Ant-NH}$ at 11.07 ppm spectrum, which indicated the involvement of NH in the 6-membered hydrogen bonding.

3.8 Conclusion

In summary, we have successfully synthesized a series of urea-($^{\text{S}}\text{Ant-Pro}$) peptide conjugates. These compounds show characteristics of 9-membered hydrogen bonding folded conformation. These scaffolds containing $^{\text{S}}\text{Ant-Pro}$ C9 folded core and urea moiety may find application in drug development programme.

Vesicular self-assembly of urea-tethered α,β -hybrid foldamer as a hydrophobic cargo carrier**3.9 Introduction**

Inspired from the Nature, researchers have developed self-assembled nanometer-, micrometer- and macrometer-sized novel materials using bottom-up approach. The biologically originated building blocks such as nucleic acids, amino acids, carbohydrates and lipids have been utilized to design and fabricate a myriad of supramolecular architectures.³¹ The bottom-up approach features small building blocks undergoing self-association in a specific manner to form well-defined nano-sized or micro-sized supramolecular structural architectures. In this process of association of building blocks, noncovalent interactions such as hydrogen bonds, ionic, hydrophobic and pi-stacking play an important role.

Peptide molecules have the ability to undergo self-assembly to form well-defined supramolecular structures of nano, micro and macro-size. Peptides are considered as a choice of material in studying self-assembly owing to their numerous versatile properties such as intrinsic folding secondary structure, stability, structural diversity, ease in structural modification (or functional group modulation), biocompatibility and participation in molecular recognition events. Numerous applications of peptide-based materials have been reported such as targeted drug delivery scaffolds, antibacterial agents, regenerative medicines, biomedical imaging, biosensors, tissue engineering, nanoelectronics, and catalysts *etc.*^{31,32} Peptide-based compounds like amphiphilic peptides, surfactant-like peptides, cyclic peptides, and peptide oligomers (foldamers) have been shown to undergo self-assembly to form supramolecular structures such as nanotubes, nanovesicles, nanorods, nanofibrils, nanotapes and gels (Fig. 3.10) depending up

on condition applied.^{31,32} Various factors determine the formation of specific morphology, including pH, solvent polarity, light, temperature, metal ions and enzymes.^{31e,h,33}

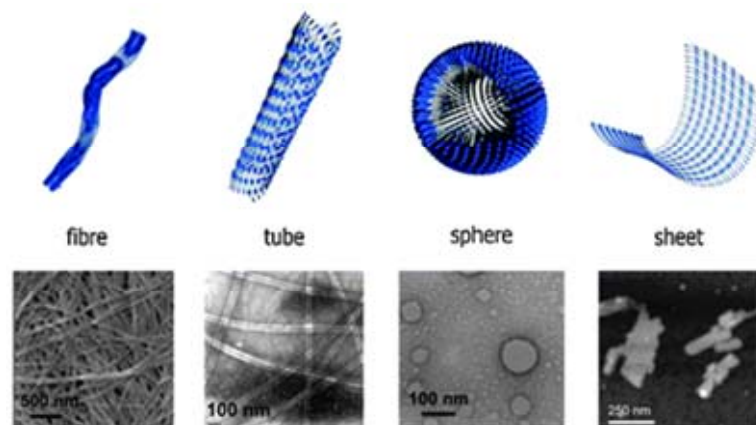


Fig. 3.10 Peptide-based supramolecular architectures prepared *via* self-assembly.³⁴

Vesicles are one of the important self-assemblies owing to their wide applications in a variety of interdisciplinary fields such as nanomaterials, biomimetics, guest encapsulation and drug and gene delivery.³¹⁻³⁵ It is well-known that vesicular self-assembly is commonly exhibited by compounds which are amphiphilic in nature; for example phospholipids.³⁶ With intensive research in the area of self-assembly, chemists have shown that amphiphilic polymers are able to form vesicular structures.³⁷ Additionally, other compounds such as amphiphilic calixarene,³⁸ fullerene,³⁹ dendrimers⁴⁰ and cyclodextrin⁴¹ have been shown to exhibit spherular self-assembly. But, the preparation of vesicular morphology from nonamphiphilic compounds has been a challenging task for researchers.⁴² Recently, it has been shown that nonamphiphilic opioid peptide enkephalin mimetic forms micro-sized vesicular morphology in organic solvent which can encapsulate drug such as curcumin.^{32a} Ghosh group illustrated the formation of variable-sized vesicular structures from oligo-(phenylene-ethylene) in organic

solvent.⁴² Chauhan and coworkers reported that a dipeptide (methionine-dehydrophenylalanine) forms vesicles in methanol and these vesicles have been shown to exhibit the enhanced cellular uptake and release of an antitumor drug curcumin.⁴³

3.10 Objective of the work and design strategy

Because of properties like intrinsic folding, self-organization, biocompatibility, versatility, and ease of synthetic modification, peptide molecules have been considered as an attractive new choice of materials for developing supramolecular materials using molecular self-assembly process.³¹ Earlier, our group reported that Ant-Pro oligomers bearing iodo substitution on phenyl ring assume helical folding.⁴⁴ We envisioned that substitution of iodo group by functional group like urea would induce the intermolecular interactions between molecules. In the present study, a urea moiety was chosen, which can be installed on phenyl group through an alkyne spacer using Sonogashira reaction (Fig. 3.11).⁴⁵ The characteristic feature of this system is that unsymmetrical urea moieties were appended on Ant (anthranilic acid) units of Ant-Pro oligomer which

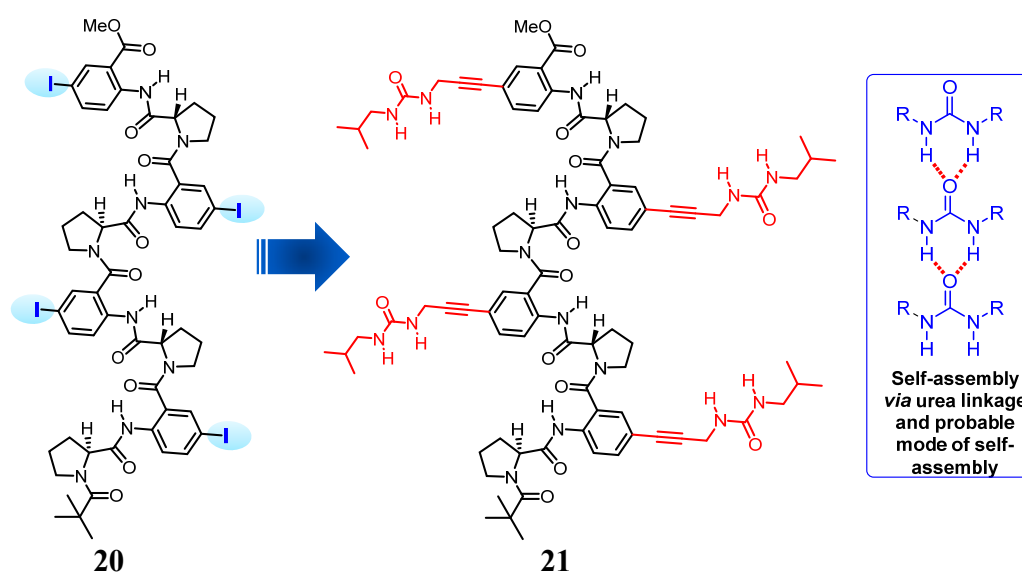


Fig. 3.11 Design of urea-tethered Ant-Pro octapeptide **21** and schematic presentation of probable mode of urea-mediated self-assembly.

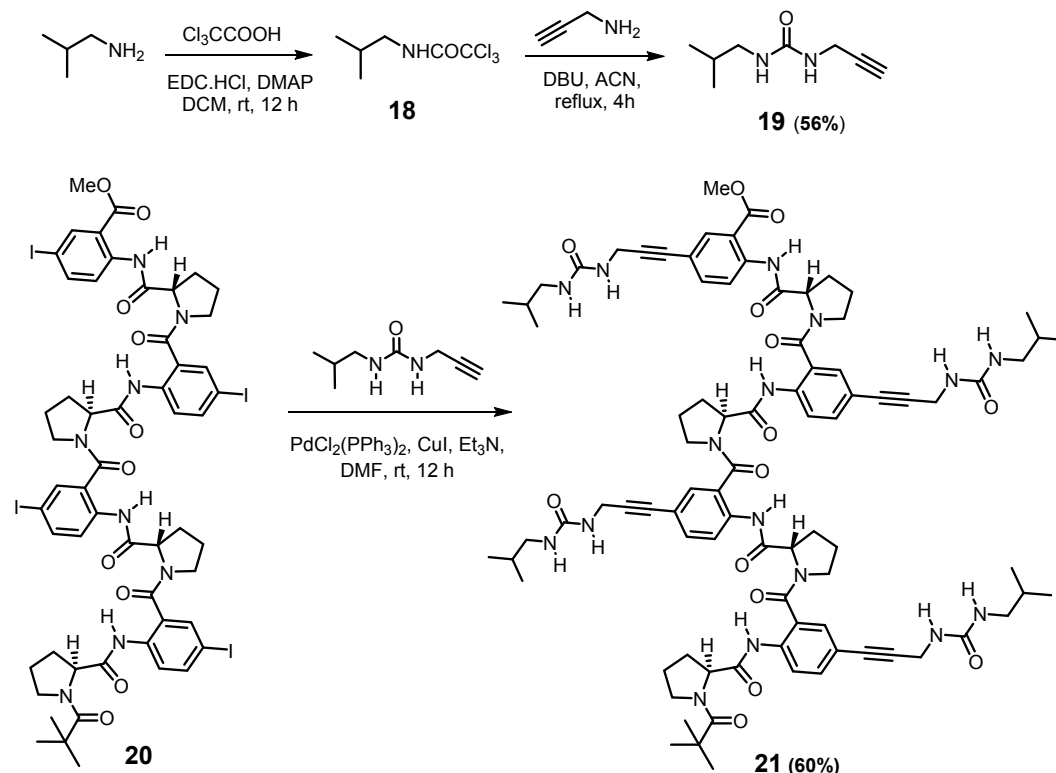
would boost intermolecular association through the urea-mediated intermolecular H-bonding.

3.11 Results and discussion

3.11.1 Synthesis

The synthesis of urea-tethered Ant-Pro octapeptide (Scheme 3.3) was started by coupling of isobutylamine with trichloroacetic acid using EDC.HCl as a coupling reagent to furnish trichloroacetamide derivative **18**, which was used for the next step, without purification. The urea formation was achieved by reacting propargylamine with trichloroacetamide intermediate **18** using DBU as a base to furnish unsymmetrical urea **19** in 56% yield, which was further coupled with *para*-iodo substituted Ant-Pro octapeptide **20**⁴⁴ using Sonogashira reaction protocol [$\text{PdCl}_2(\text{PPh}_3)_2$, CuI and Et_3N]⁴⁵ to obtain urea-appended Ant-Pro octapeptide **21** in 60% yield.

Scheme 3.3 Synthesis of urea-tethered Ant-Pro hybrid octapeptide **21**.



3.11.2 Microscopic analyses

The morphological studies of self-assembled octapeptide **21** have been investigated by scanning electron microscope (SEM), transmission electron microscopy (TEM) and atomic force microscopy (AFM). The peptide concentrations used in the microscopic analyses were 1.25 mM (1 mg/0.5 mL) and 0.62 mM (1 mg/1 mL). SEM measurements were performed on a FEI, QUANTA 200 3D scanning electron microscope with tungsten filament as electron source. For SEM analysis, solution of octapeptide **21** at concentration of 1.25 mM (1 mg/0.5 mL) was prepared in organic solvent (or binary solvent mixture). Freshly prepared each of transparent solutions was drop-casted on silicon surface and allowed to dry at room temperature for 12 h. Before recording of morphology, a gold film was applied by sputtering method. SEM analysis revealed that octapeptide **21** forms sphericular morphologies of micro-size in methanolic solution (Fig. 3.12a). SEM analysis also revealed the aggregation of spheres to form twins, triplets and multiplets which in turn form larger sphericular self-assembled structures *via* fusion process.⁴⁶ Furthermore, in order to explore the solvent-modulated self-assembly, we have examined the self-assembly of octapeptide **21** in a binary solvent mixture such as methanol-toluene. We have incubated the octapeptide **21** at the concentration of 1.25 mM (1 mg/0.5 mL) in the different combination of methanol-toluene solvent mixtures (v/v) such as 9:1, 8:2, 6:4, 5:5, 2:8 and 1:9 (Fig. 3.12c-h). Freshly prepared samples of octapeptide **21** were drop-casted on silicon material and dried at room temperature for 12 h. The morphology analyses by SEM revealed that gradual decrease of methanol content in the solution led to the formation of vesicular morphology with pores. The morphology obtained by evaporation of its 1:9 methanol-toluene solutions

was found to be pot-like self-assembly of diameter approximately ranging from 0.4 to 1 μm with pore diameter ranging from 0.08 to 0.3 μm which is uniformly distributed (Fig. 3.12g).

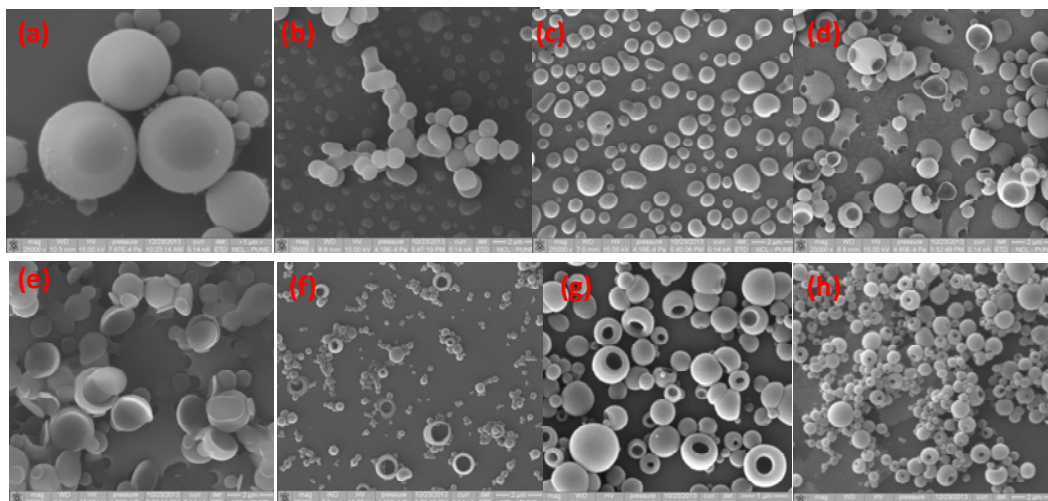


Fig. 3.12 Microscopic analyses of self-assembly of octapeptide **21**. SEM images of vesicles at the concentration of 1 mg/0.5 mL obtained by evaporation of its methanol-toluene solutions, solvent ratio and scale bar are: a) methanol, 10 μm ; b) 9:1 methanol-toluene, 2 μm ; c) 8:2 methanol-toluene, 2 μm ; d) 6:4 methanol-toluene, 2 μm ; e) 5:5 methanol-toluene, 2 μm ; f) 2:8 methanol-toluene, 2 μm ; g) 1:9 methanol-toluene, 1 μm ; h) 0.8:9.2 methanol-toluene, 2 μm .

Furthermore, the vesicular morphology was studied by TEM. TEM measurements were performed on a JEOL-JEM-3010 instrument at 80 kV. For TEM analysis, freshly prepared 1:9 methanol-toluene solution of octapeptide **21** (0.62 mM) was drop-casted directly on a carbon coated copper grid and dried at room temperature for 12 h. TEM analysis revealed the hollow nature of vesicles having diameter ranging from 0.2 to 0.5 μm and pore diameter ranging from 0.02 to 0.08 μm (Fig. 3.13a, b). TEM study also suggested that the smaller vesicles associate through fusion to form larger vesicle. At the peptide concentration < 0.62 mM we could not find any well-defined morphology, which indicated that morphology of octapeptide **21** is concentration-dependant.^{41,47} We also carried out AFM analysis to investigate the self-assembly of octapeptide **21**. The AFM

measurements were performed on a Multimode scanning probe microscope equipped with a Nanoscope IV controller from Veeco Instrument Inc., Santa Barbara, CA. The imaging was done under ambient conditions in tapping-mode, using the Tap190Al probe purchased from Budget Sensors®. The 10 μm x 10 μm areas were scanned at resolution of 512 X 512 pixels. For AFM analysis, freshly prepared transparent 1:9 methanol-toluene solution of octapeptide **21** was drop-casted on silicon surface and allowed to dry at room temperature for 12 h. Similarly, AFM analysis revealed the hollow nature of vesicular self-assembly of octapeptide **21** (Fig. 3.13c).

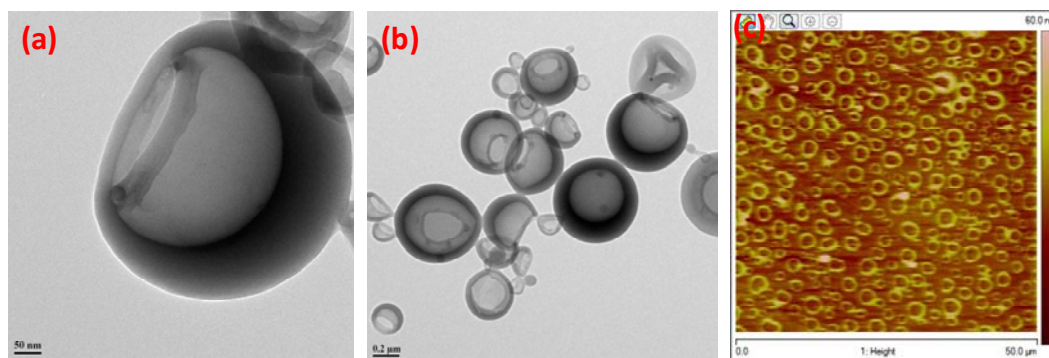


Fig. 3.13 Self-assembly of octapeptide **21** at the concentration of 1 mg/mL obtained by evaporation of its 1:9 methanol-toluene solvent mixture. a,b) TEM images showing hollow nature of vesicles [scale bars are 50 nm for (a) and 0.2 μm for (b)] and c) tapping-mode AFM image.

We have also checked the morphology in other solvents or binary solvent mixtures. Microscopic analyses by SEM revealed that octapeptide **21** at the peptide concentration of 1 mg/0.5 mL forms sphericular self-assembly in trifluoroethanol (Fig. 3.14a) and 5:5 methanol-chloroform (v/v) (Fig. 3.14b) and 1:9 DMSO-trifluoroethanol (v/v) (Fig. 3.14c).

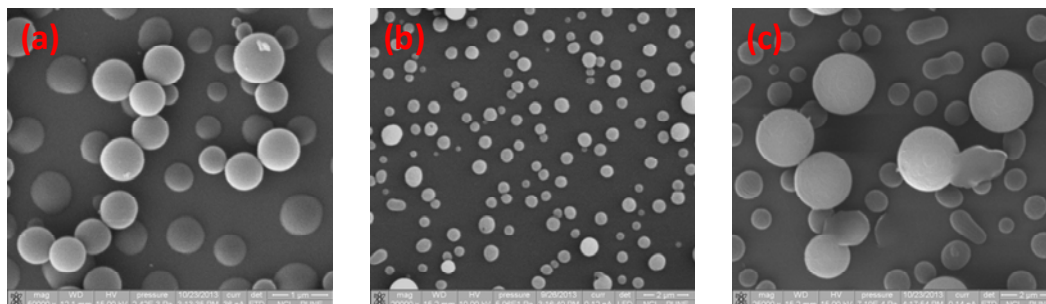


Fig. 3.14 Self-assembly of octapeptide **21** at the concentration of 1 mg/0.5 mL SEM images and scale bars are: a) trifluoroethanol, 1 μm ; b) 5:5 methanol-chloroform, 2 μm ; c) 1:9 DMSO-TFE, 2 μm .

3.11.3 Encapsulation study

The medicinal applications of drugs are restricted due to issues like poor cellular uptake, low bioavailability, poor solubility, intestinal degradation and instant elimination from body.⁴⁸ For example, curcumin is commonly known as a drug with wide range of pharmacological properties such as antitumor, antioxidant, antimicrobial and anti-inflammatory.⁴⁹ Several studies have shown that curcumin inhibit the proliferation of many cancer cell lines such as cervical, breast, ovarian, colon, hepatic, pancreatic, gastric and prostate tumors.⁵⁰ But due to its hydrophobic nature it has low water solubility which makes it less suitable candidate for clinical use. In this regard, several studies have shown that the nanoparticles of polymers, liposomes, lipids, cyclodextrin and hydrogels⁵¹ can act as carrier for effective cellular uptake and delivery of curcumin drug.

In the present work, we utilized urea-tethered spherular self-assembly of the α,β -hybrid octapeptide **21** as a hydrophobic drug carrier. The SEM, TEM and AFM analyses confirmed the hollow nature of vesicles. It was worthwhile to utilize the hollow nature of vesicles by loading vesicles with the hydrophobic or hydrophilic cargo molecules. In this context, we have chosen curcumin- a hydrophobic drug. Curcumin is a well-known drug used in the cancer therapy but

due to the low water solubility its medicinal use is limited. It has been demonstrated that cellular uptake of curcumin can be enhanced using nanoparticle-mediated delivery. The cellular uptake by curcumin-loaded nanoparticles deliver the curcumin almost twice compared to free curcumin.⁴³ In order to encapsulate hydrophobic drug like curcumin, we have incubated the methanolic solution of curcumin with the vesicular solution of octapeptide **21** in 1:9 methanol-toluene for 18 h. The solution was the dialyzed against methanol. The resultant solution was drop-casted on glass slide and analyzed under fluorescence microscope. The bright green fluorescence in the vesicles confirmed the curcumin encapsulation by the vesicles (Fig. 3.15).

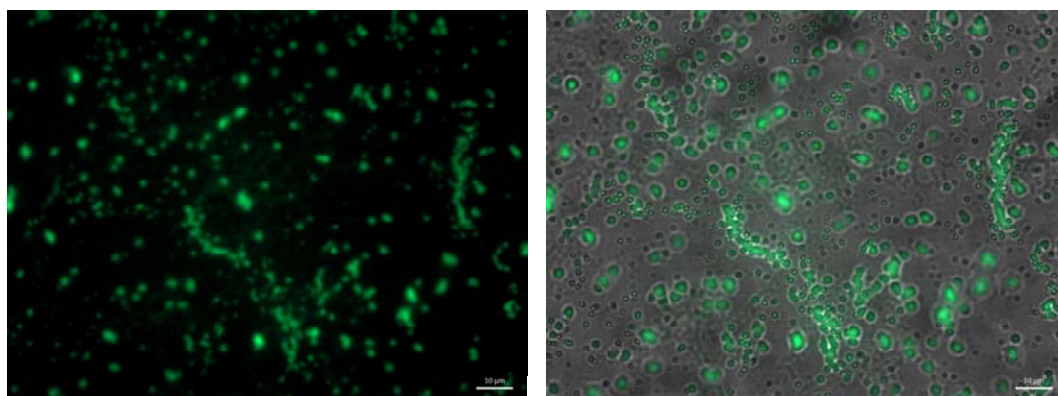


Fig. 3.15 Fluorescence microscopic images showing bright green fluorescence of curcumin encapsulated vesicles of octapeptide **21** (scale bar 10 μm and peptide concentration: 1 mg/0.5 ml).

3.12 Conclusion

Microscopic analyses confirmed that the urea-appended octapeptide **21** undergoes self-assembly through the urea-mediated intermolecular interactions forming vesicular structures from methanolic solution. Up on decreasing the concentration of methanol from binary solvent mixture, octapeptide **21** forms hollow pot-like self-assembled vesicles. These vesicles are able to encapsulate the hydrophobic drug like curcumin efficiently which was confirmed by bright green

fluorescence in the vesicles under fluorescence microscope. On further development, these α,β -hybrid peptide vesicles may find application in drug delivery.

3.13 Experimental section (Part A)

Crystal Data for 4:

Table 3.2 X-ray crystallographic data of trimer 4.

Crystal Data	dhfur_1
Formula	C ₂₁ H ₂₈ N ₄ O ₅ S
M _r	448.53
Crystal Size, mm	0.35 x 0.25 x 0.12
Temp. (K)	150(2)
Crystallizing solvent	Ethyl acetate-petroleum ether
Crystal Syst.	Orthorhombic
Space Group	<i>P</i> 2 ₁ 2 ₁ 2 ₁
<i>a</i> /Å	11.4420(4)
<i>b</i> /Å	13.9086(5)
<i>c</i> /Å	14.2643(5)
α ⁰	90
β ⁰	90
γ ⁰	90
<i>V</i> /Å ³	2270.05(14)
<i>Z</i>	4
<i>D</i> _{calc} /g cm ⁻³	1.312
μ /mm ⁻¹	0.182
<i>F</i> (000)	952
<i>Ab. Correct.</i>	multi-scan
2 θ _{max}	50
Total reflns.	35731
unique reflns.	4003
<i>h, k, l</i> (min, max)	(-13, 13),(-16, 16),(-16, 16)
<i>R</i> _{int}	0.0255
No. of para	283
<i>R</i> 1 [<i>I</i> > 2 σ (<i>I</i>)]	0.0315
<i>wR</i> 2 [<i>I</i> > 2 σ (<i>I</i>)]	0.0692
<i>R</i> 1 [all data]	0.0333
<i>wR</i> 2 [all data]	0.0702
goodness-of-fit	1.011
$\Delta\rho$ _{max} , $\Delta\rho$ _{min} (eÅ ⁻³)	0.262,-0.237
CCDC no.	1419216

N-(tert-butyl)-1-((2-nitrophenyl) sulfonyl) pyrrolidine-2-carboxamide 2a:

Trifluoroacetic acid (5 mL) was added to a solution of **1a**¹⁹ (1 g, 3.7 mmol) in DCM and the reaction mixture was stirred for 2 h at room temperature. The reaction mixture was neutralized with saturated solution of NaHCO₃ and extracted with DCM (3×20 mL). The combined organic extracts were dried over Na₂SO₄ and the solvent was removed under reduced pressure. The crude product **1b** was used for the next step without purification. To a solution of amine **1b** (0.62 g, 3.64 mmol) in DCM (10 mL), DIEA (0.612 g, 4.74 mmol) and 2-nitrobenzenesulfonyl chloride (0.97 g, 4.37 mmol) solution in DCM (15 mL) were added dropwise at 0 °C under N₂, and then the reaction mixture was stirred at room temperature for 2 h. The reaction mixture was diluted with DCM (10 mL) and washed with water, the saturated solution of NaHCO₃, the saturated solution of KHSO₄ and then with brine. The organic layer was dried over Na₂SO₄ and concentrated under vacuum. The crude product was purified by column chromatography (35:65 EtOAc/pet ether, R_f 0.5) to obtain **2a** (0.96g, 74%) as a white solid; mp: 165-167 °C; [α]_D²⁵: -255.96° (c 0.28, CHCl₃); IR (CHCl₃) ν (cm⁻¹): 2965, 2734, 1682, 1540, 1365, 1156, 855; ¹H NMR (500 MHz, CDCl₃) δ : 8.08-8.06 (d, *J* = 7.7 Hz, 1H), 7.78-7.75 (t, *J* = 7.2 Hz, 1H), 7.73-7.71 (t, *J* = 7.2 Hz, 1H), 7.68-7.67 (d, *J* = 7.7 Hz, 1H), 6.39 (s, 1H), 4.32-4.30 (dd, *J* = 8.6, 2.4 Hz, 1H), 3.65-3.59 (m, 2H), 2.26-2.21 (m, 1H), 2.12-2.07 (m, 1H), 1.94-1.89 (m, 2H), 1.15 (s, 9H); ¹³C NMR (125 MHz, CDCl₃) δ : 169.79, 148.21, 134.21, 132.04, 131.69, 131.41, 124.12, 62.73, 51.07, 49.55, 31.27, 28.34, 24.40; HRMS: C₁₅H₂₂O₅N₃S, Calcd: 356.1275 Found: 356.1275; C₁₅H₂₁O₅N₃NaS, calcd: 378.1094 Found: 378.1094.

N-(tert-butyl)-1-((2-(2, 2, 2-trichloroacetamido) phenyl) sulfonyl) pyrrolidine-2-carboxamide 3:

10% pd/C (0.050 g) was added to the solution of **2a** (0.5 g, 1.4 mmol) in EtOAc (20 mL) and the reaction mixture was stirred at 60 psi under H₂ atmosphere for 8 h. Pd catalyst was filtered through celite and the filtrate was evaporated to obtain amine **2b**, which was used for the next step without purification. To a solution of **2b** (2 g, 6.15 mmol) in DCM (60 mL), DIEA (1.59 g, 12.3 mmol) and trichloroacetyl chloride (1.34 g, 7.38 mmol) were added dropwise at 0 °C under N₂. After stirring at room temperature for 2 h, the reaction mixture was diluted with DCM (30 mL) and washed with water, the saturated solution of NaHCO₃ and then brine. The solvent was evaporated and the crude product was column chromatographed (30:70 EtOAc/pet ether, R_f 0.5) to get pure compound **3** as pale yellow colored solid (2.83 g, 98%); mp: 133-135 °C; $[\alpha]_D^{25}$: -78.58° (c 0.24, CHCl₃); IR (CHCl₃) ν (cm⁻¹): 3274, 2966, 1728, 1682, 1534, 1340, 1152, 815, 610; ¹H NMR (500 MHz, CDCl₃) δ : 11.07 (s, 1H), 8.63-8.61 (d, *J* = 8.4 Hz, 1H), 7.91-7.90 (d, *J* = 7.9 Hz, 1H), 7.73-7.70 (t, *J* = 8.4 Hz, 1H), 7.38-7.35 (t, *J* = 7.9 Hz, 1H), 6.40 (s, 1H), 4.04-4.03 (d, *J* = 8.5 Hz, 1H), 3.62-3.60 (t, *J* = 6.9 Hz, 1H), 3.29-3.24 (m, 1H), 2.24-2.20 (m, 1H), 1.84-1.70 (m, 3H), 1.33 (s, 9H); ¹³C NMR (125 MHz, CDCl₃) δ : 169.30, 159.69, 135.47, 135.11, 130.04, 125.53, 124.49, 122.04, 92.59, 62.84, 51.36, 49.78, 30.35, 28.52, 24.33; HRMS: C₁₇H₂₃O₄N₃Cl₃S, Calcd: 470.0469 Found: 470.0475.

Representative procedure for urea preparation, 4-9:**(S)-N-(tert-butyl)-1-((2-(3-(furan-3-ylmethyl) ureido) phenyl) sulfonyl) pyrrolidine-2-carboxamide 4:**

To a solution of **3** (0.2 g, 0.42 mmol) in DMF (3 mL), furfurylamine (0.045 g, 0.46 mmol) and NaHCO₃ (0.107 g, 1.27 mmol, powdered and dried in furnace

prior to use) were added sequentially. The reaction mixture was heated at 100 °C for 3 h. The reaction mixture was cooled to room temperature and diluted with EtOAc (20 mL). The organic layer was washed with water, the saturated solution of KHSO₄ and then brine. The organic layer was dried over Na₂SO₄ and concentrated under vacuum. The crude product was purified over a neutral alumina column (40:60 EtOAc/pet ether, R_f 0.5) to afford **4** as a white solid (0.180 g, 94%); mp: 177-179 °C; $[\alpha]_D^{25}$: -81.0° (c 0.15, CHCl₃); IR (CHCl₃) ν (cm⁻¹): 3354, 3016, 2973, 2930, 2883, 1702, 1662, 1546, 1363, 1304, 1218, 1151, 1066, 759; ¹H NMR (500 MHz, CDCl₃) δ : 9.10 (s, 1H), 8.66–8.64 (d, *J* = 8.4 Hz, 1H), 7.92–7.91 (d, *J* = 8.0 Hz, 1H), 7.57–7.54 (t, *J* = 8.4 Hz, 1H), 7.34 (s, 1H), 7.15 (s, 1H), 7.05–7.02 (t, *J* = 8.0 Hz, 1H), 6.31–6.27 (m, 2H), 5.88 (s, 1H), 4.50–4.48 (t, *J* = 5.0 Hz, 2H), 4.27–4.24 (m, 1H), 3.26–3.20 (m, 1H), 3.02–2.97 (m, 1H), 2.31–2.24 (m, 1H), 2.04–1.97 (m, 1H), 1.96–1.87 (m, 2H), 1.31 (s, 9H); ¹³C NMR (125 MHz, CDCl₃) δ : 171.69, 154.87, 152.27, 141.89, 139.60, 135.09, 130.26, 122.03, 121.53, 120.79, 110.26, 107.20, 60.57, 52.05, 48.90, 37.06, 31.79, 28.48, 25.24; HRMS: C₂₁H₂₈O₅N₄NaS, Calcd: 471.1673 Found: 471.1670.

(S)-N-(tert-butyl)-1-((2-(3-(4-fluorobenzyl) ureido) phenyl) sulfonyl) pyrrolidine-2-carboxamide 5:

Compound **5** was prepared by following the procedure for the synthesis of **4**. The crude product was purified over a neutral alumina column (30:70 EtOAc/pet ether, R_f 0.4) to afford **5** as a low melting solid (92%); mp: 64-66 °C; $[\alpha]_D^{26}$: -103.12° (c 0.1, CHCl₃); IR (CHCl₃) ν (cm⁻¹): 3348, 3094, 2967, 2928, 2871, 2398, 1702, 1659, 1549, 1464, 1374, 1307, 1255, 1153, 1063, 767; ¹H NMR (400 MHz, CDCl₃) δ : 9.10 (s, 1H), 8.67–8.65 (d, *J* = 8.5 Hz, 1H), 7.93–7.91 (d, *J* = 8.0 Hz, 1H), 7.58–7.54 (d, *J* = 8.5 Hz, 1H), 7.37–7.33 (m, 2H), 7.18 (s, 1H), 7.06–6.98

(m, 3H), 5.85 (s, 1H), 4.53–4.37 (m, 2H), 4.26–4.23 (t, $J = 7.3$ Hz, 1H), 3.26–3.20 (m, 1H), 3.02–2.95 (m, 1H), 2.33–2.24 (m, 1H), 2.02–1.96 (m, 1H), 1.95–1.88 (m, 2H), 1.20 (s, 9H); ^{13}C NMR (125 MHz, CDCl_3) δ : 171.69, 154.87, 152.27, 141.89, 139.60, 135.09, 130.26, 122.03, 121.53, 120.79; HRMS: $\text{C}_{23}\text{H}_{29}\text{O}_4\text{N}_4\text{NaFS}$, Calcd: 499.1786 Found: 499.1778.

(S)-N-(tert-butyl)-1-((2-(3-(4-methoxybenzyl) ureido) phenyl) sulfonyl) pyrrolidine-2-carboxamide 6:

Compound **6** was prepared by following the procedure for the synthesis of **4**. The crude product was purified over a neutral alumina column (40:60 EtOAc/pet ether, R_f 0.5) to afford **6** as a low melting solid (82%); mp: 62-64 °C; $[\alpha]_D^{26}$: -132.20° (c 0.12, CHCl_3); IR (CHCl_3) ν (cm^{-1}): 3350, 3095, 2967, 2932, 2881, 1700, 1659, 1548, 1463, 1373, 1306, 1245, 1153, 1040, 762; ^1H NMR (400 MHz, CDCl_3) δ : 9.07 (s, 1H), 8.68–8.66 (d, $J = 8.5$ Hz, 1H), 7.92–7.90 (d, $J = 8.0$ Hz, 1H), 7.57–7.53 (t, $J = 8.5$ Hz, 1H), 7.32–7.29 (d, $J = 8.4$ Hz, 2H), 7.08–7.01 (m, 2H), 6.86–6.84 (d, $J = 8.5$ Hz, 2H), 5.84 (s, 1H), 4.48–4.35 (m, 2H), 4.25–4.21 (t, $J = 7.4$ Hz, 1H), 3.79 (s, 3H), 3.25–3.19 (m, 1H), 3.03–2.97 (m, 1H), 2.30–2.21 (m, 1H), 2.02–1.96 (m, 1H), 1.95–1.88 (m, 2H), 1.21 (s, 9H); ^{13}C NMR (125 MHz, CDCl_3) δ : 171.69, 154.87, 152.27, 141.89, 139.60, 135.09, 130.26, 122.03, 121.53, 120.79; HRMS: $\text{C}_{24}\text{H}_{32}\text{O}_5\text{N}_4\text{NaS}$, Calcd: 511.1986 Found: 511.1978.

(S)-N-(tert-butyl)-1-((2-(3-(3, 5-dimethoxybenzyl) ureido) phenyl) sulfonyl) pyrrolidine-2-carboxamide 7:

Compound **7** was prepared by following the procedure for the synthesis of **4**. The crude product was purified over a neutral alumina column (45:55 EtOAc/pet ether, R_f 0.4) to afford **7** as a white solid (84%); mp: 73-75 °C; $[\alpha]_D^{26}$: -79.35° (c 0.13, CHCl_3); IR (CHCl_3) ν (cm^{-1}): 3348, 3094, 2968, 1701, 1660, 1548, 1461, 1364, 1312, 1257, 1224, 1149, 1063, 1030, 756; ^1H NMR (400 MHz, CDCl_3) δ : 9.08 (s,

1H), 8.68–8.66 (d, $J = 8.5$ Hz, 1H), 7.93–7.90 (dd, $J = 8.0, 1.4$ Hz, 1H), 7.58–7.54 (m, 1H), 7.09–7.01 (m, 2H), 6.94–6.91 (m, 2H), 6.82–6.80 (d, $J = 8.7$ Hz, 1H), 5.82 (s, 1H), 4.50–4.35 (m, 2H), 4.25–4.20 (m, 1H), 3.87–3.86 (d, $J = 1.6$ Hz, 6H), 3.26–3.19 (m, 1H), 3.03–2.96 (m, 1H), 2.31–2.21 (m, 1H), 2.01–1.95 (m, 1H), 1.95–1.85 (m, 2H), 1.19 (s, 9H); ^{13}C NMR (100 MHz, CDCl_3) δ : 171.61, 155.02, 148.98, 148.16, 139.72, 135.11, 131.69, 130.28, 121.89, 121.42, 120.70, 120.28, 111.36, 111.08, 60.53, 55.94, 55.80, 51.90, 48.91, 44.07, 31.79, 28.37, 25.20; HRMS: $\text{C}_{25}\text{H}_{34}\text{O}_6\text{N}_4\text{NaS}$, Calcd: 541.2091 Found: 541.2081.

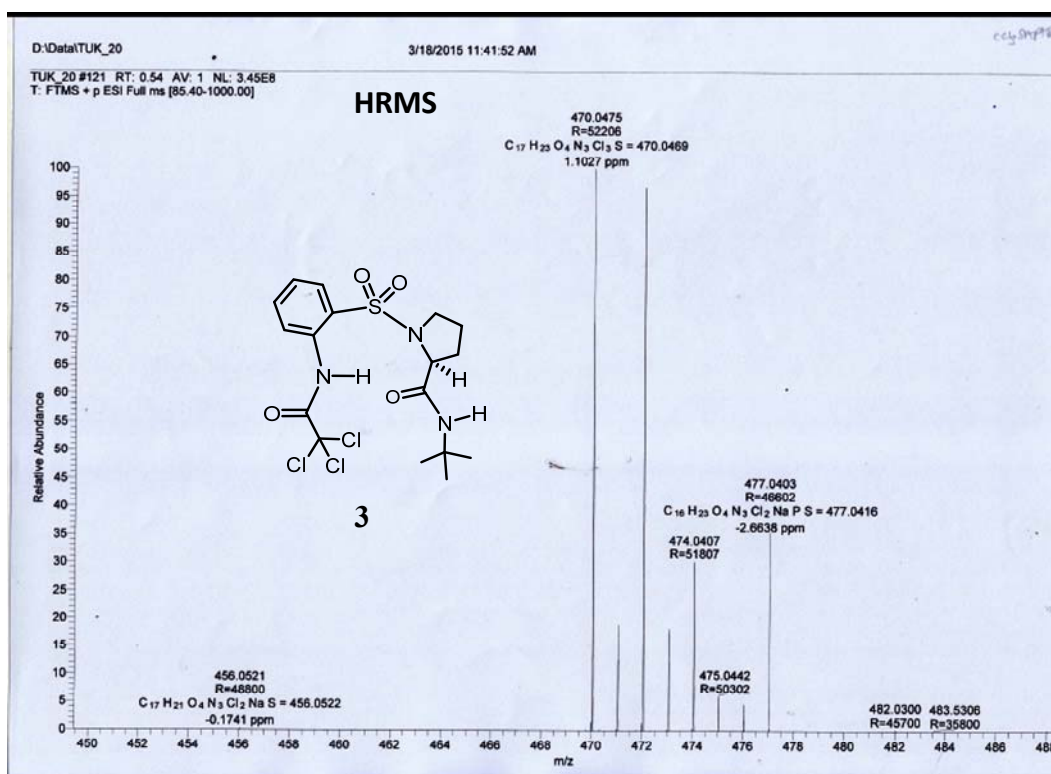
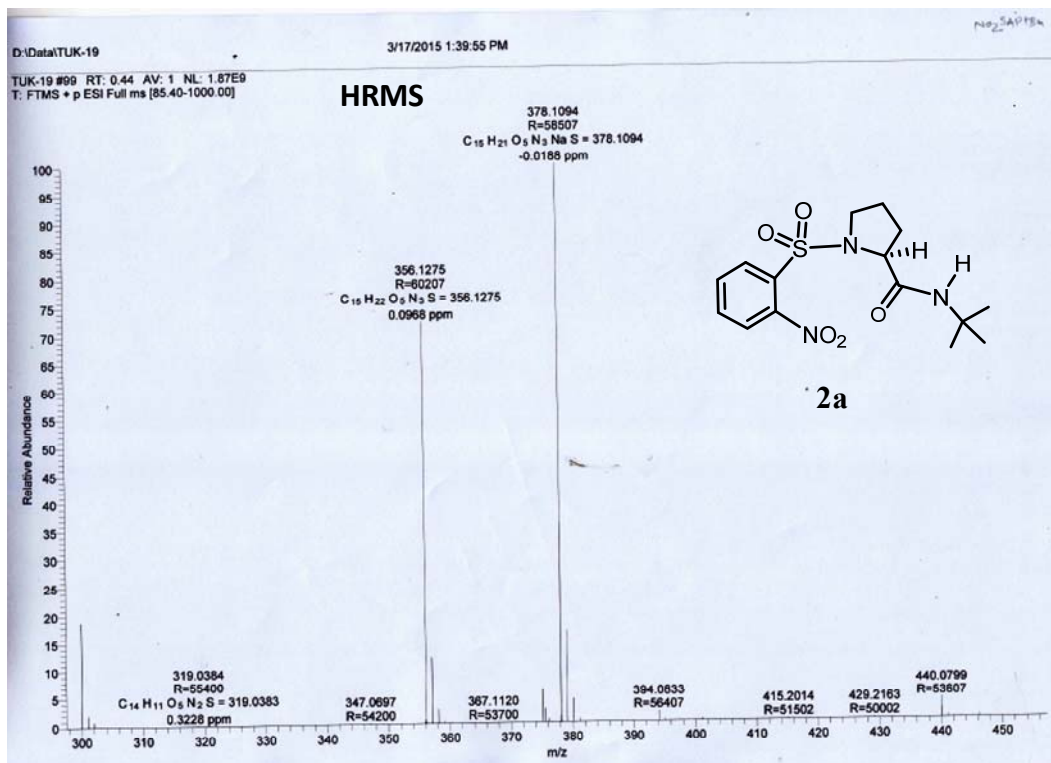
(S)-N-(tert-butyl)-1-((2-(3-methylureido) phenyl) sulfonyl) pyrrolidine-2-carboxamide 8:

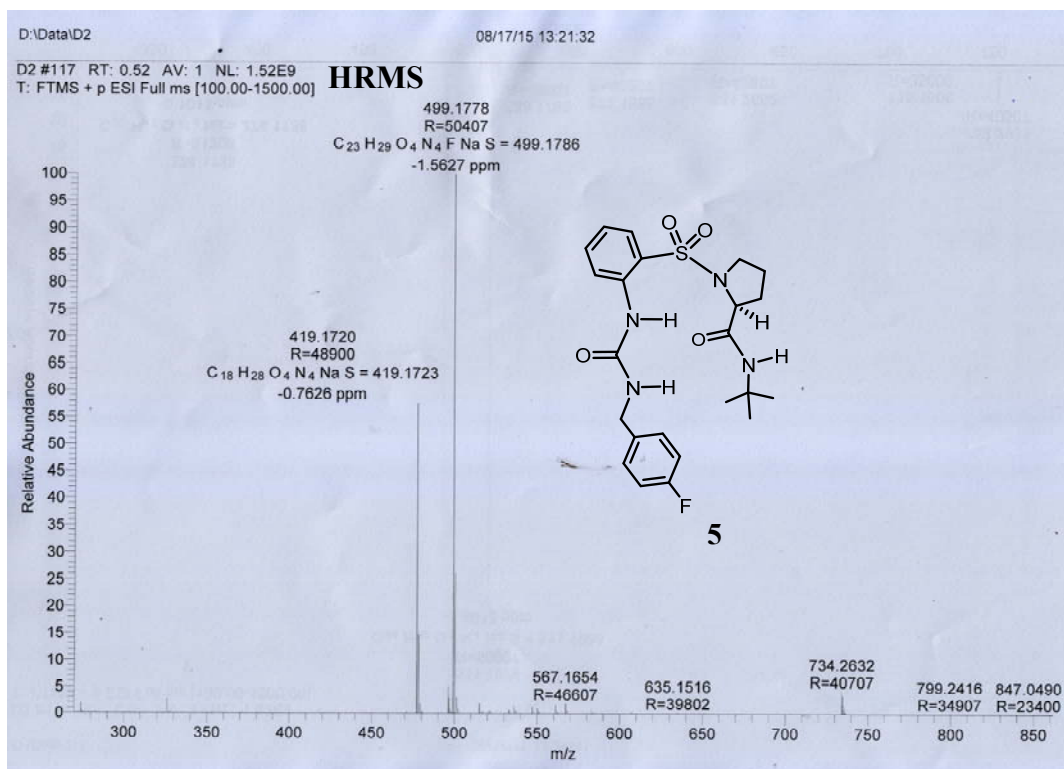
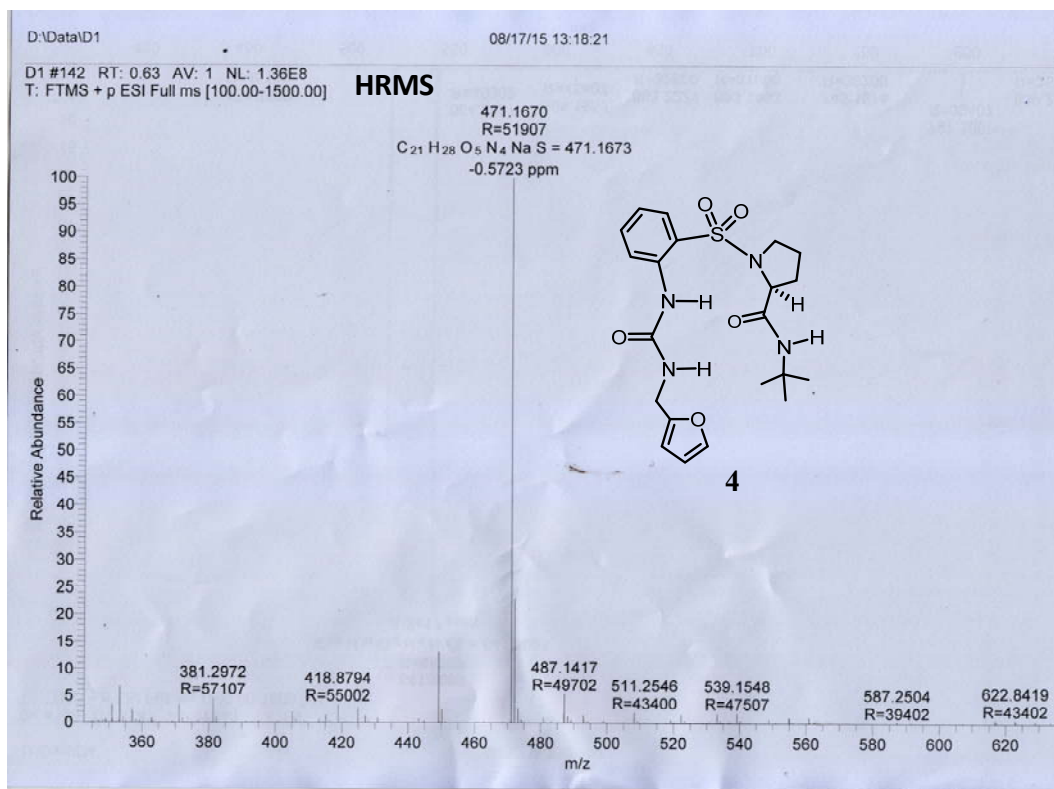
Compound **8** was prepared by following the procedure for the synthesis of **4**. The crude product was purified over a neutral alumina column (50:50 EtOAc/pet ether, R_f 0.5) to afford **8** as a white solid (78%); mp: 140–143 °C; $[\alpha]_D^{26}$: -105.25° (c 0.18, CHCl_3); IR (CHCl_3) ν (cm^{-1}): 3362, 3290, 3096, 2973, 2887, 1701, 1660, 1563, 1464, 1362, 1307, 1258, 1225, 1152, 1062, 757; ^1H NMR (400 MHz, CDCl_3) δ : 8.97 (s, 1H), 8.58–8.56 (d, $J = 8.5$ Hz, 1H), 7.90–7.88 (d, $J = 7.9$ Hz, 1H), 7.57–7.53 (t, $J = 8.5$ Hz, 1H), 7.04–7.00 (t, $J = 7.9$ Hz, 1H), 6.71 (s, 1H), 6.33 (s, 1H), 4.37–4.33 (t, $J = 7.1$ Hz, 1H), 3.27–3.19 (m, 1H), 3.03–2.99 (m, 1H), 2.87–2.87 (d, $J = 4.5$ Hz, 3H), 2.32–2.27 (m, 1H), 2.04–1.89 (m, 3H), 1.36 (s, 9H); ^{13}C NMR (100 MHz, CDCl_3) δ : 171.98, 155.82, 139.73, 135.06, 130.12, 122.05, 121.65, 120.67, 60.53, 51.92, 49.01, 31.81, 28.58, 26.54, 25.25; HRMS: $\text{C}_{17}\text{H}_{26}\text{O}_4\text{N}_4\text{NaS}$, Calcd: 405.1567 Found: 405.1567.

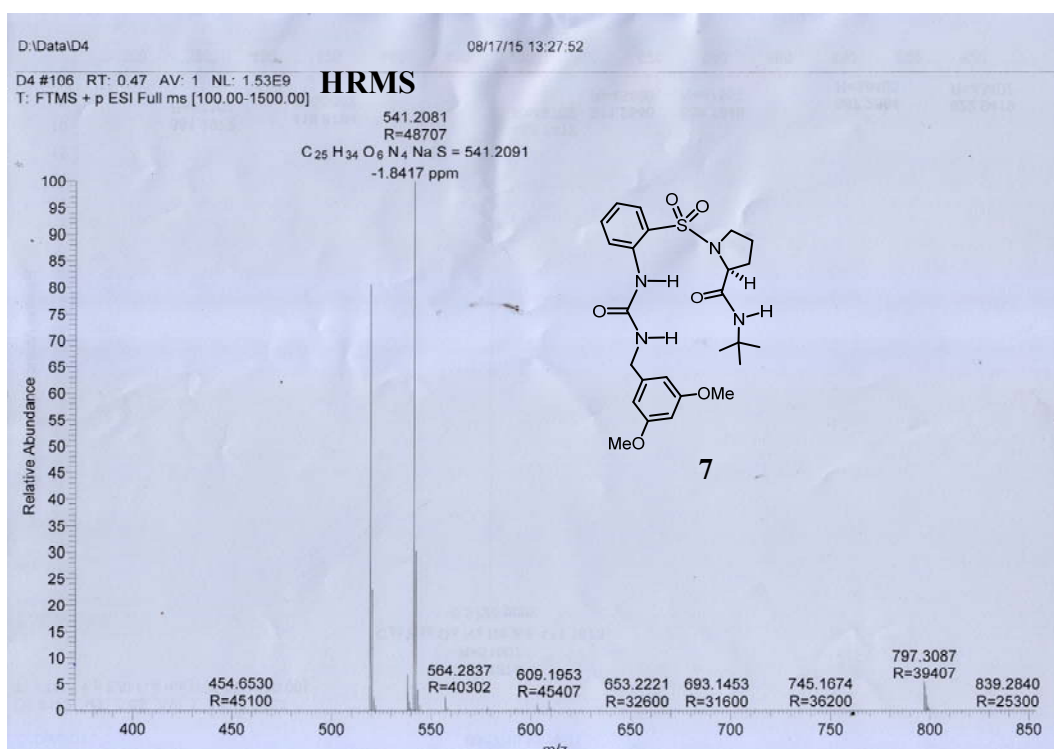
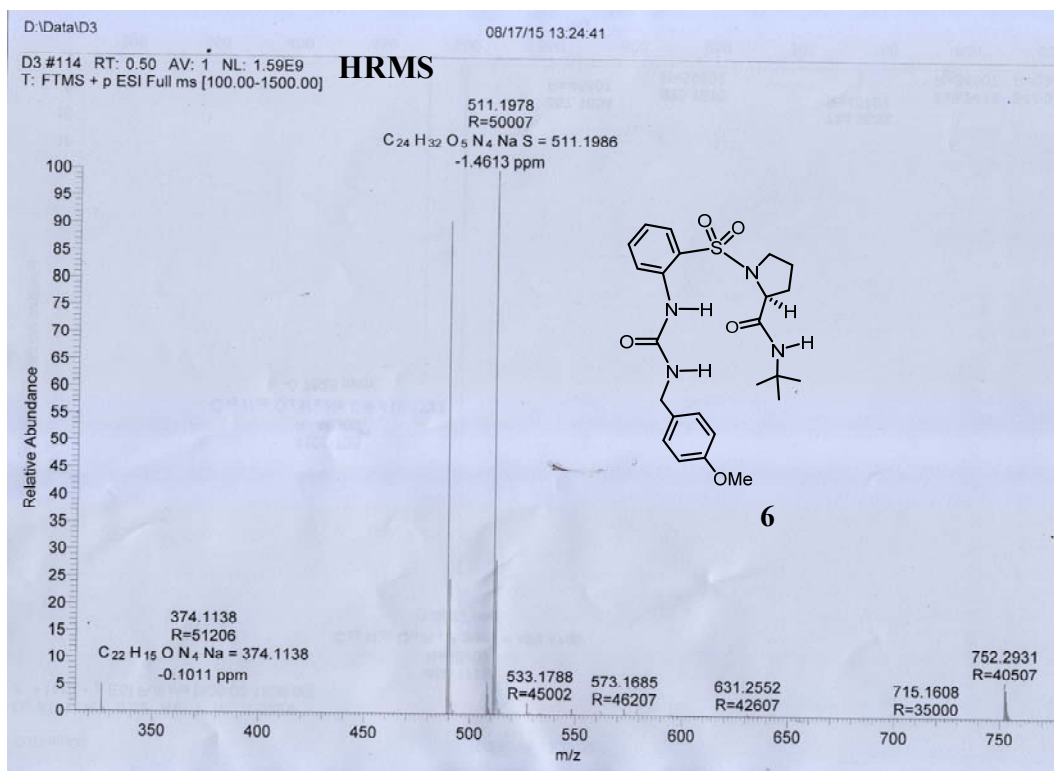
(S)-N-(tert-butyl)-1-((2-(3-isobutylureido) phenyl) sulfonyl) pyrrolidine-2-carboxamide 9:

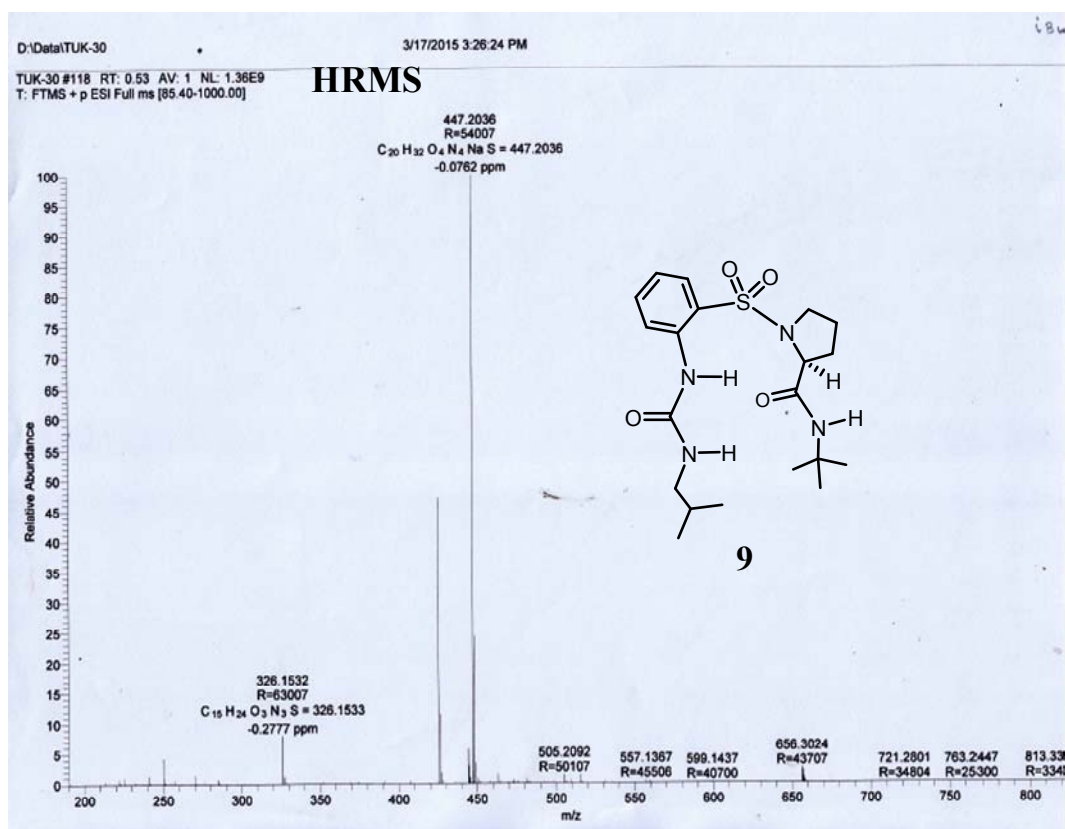
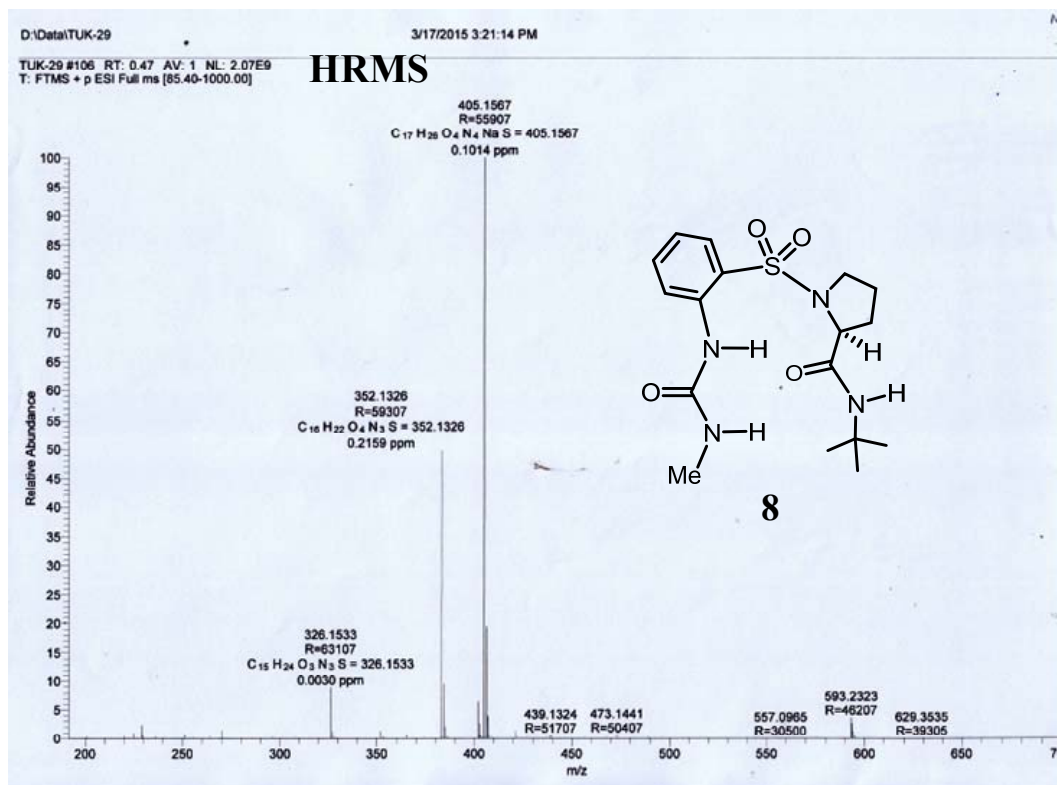
Compound **9** was prepared by following the procedure for the synthesis of **4**. The crude product was purified over a neutral alumina column (40:60 EtOAc/pet ether,

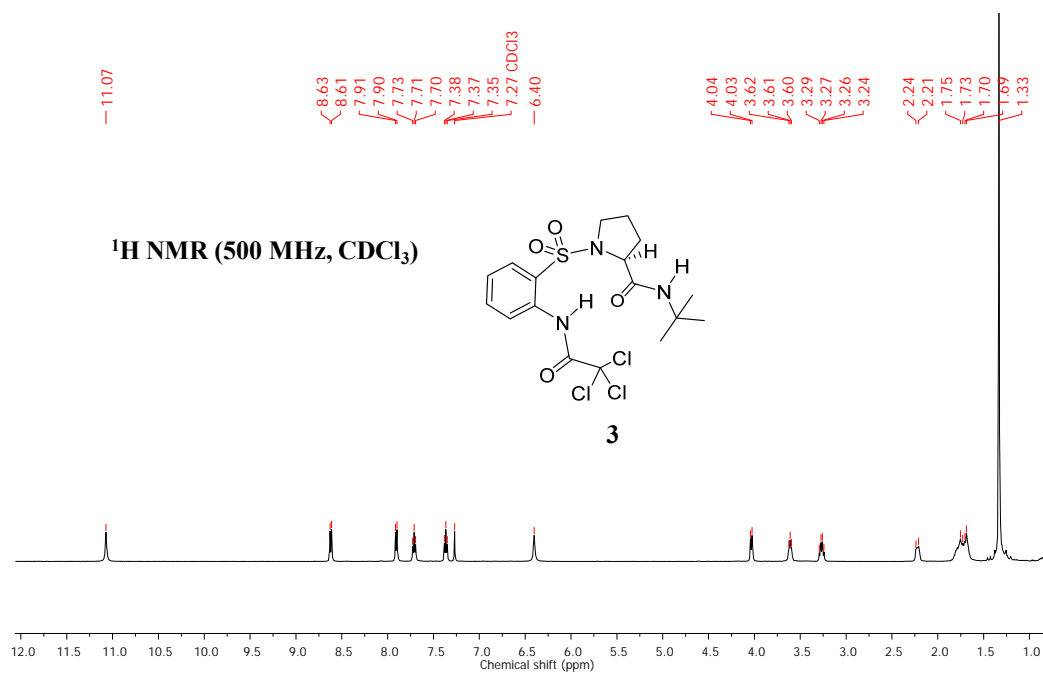
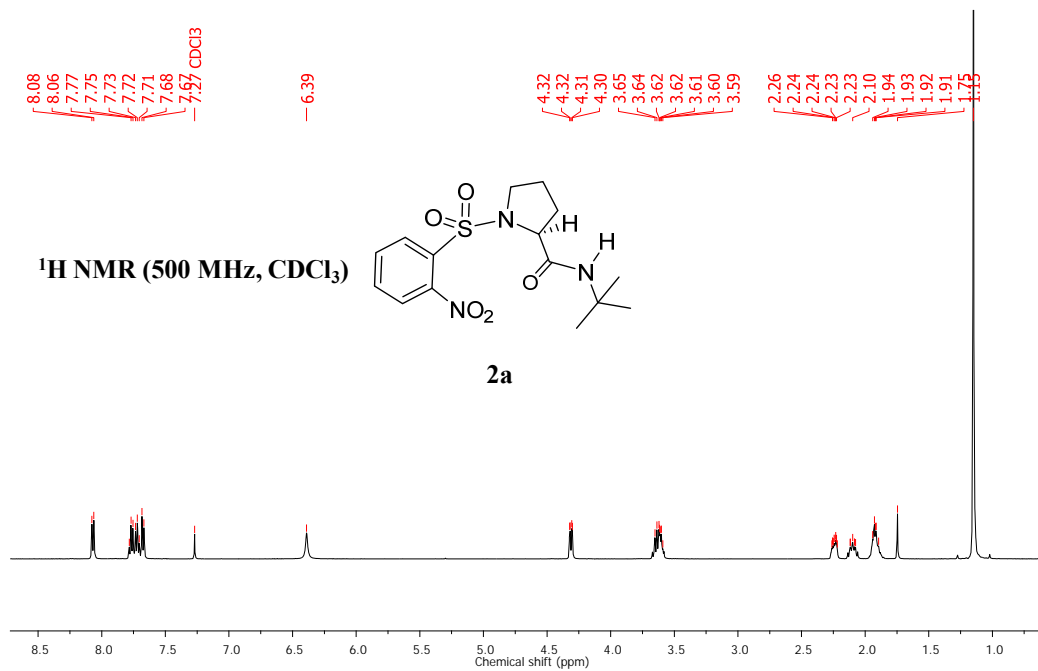
R_f 0.5) to afford **9** as a viscous liquid (56%); $[\alpha]_D^{26} : -73.54^\circ$ (c 0.1, CHCl₃); IR (CHCl₃) $\nu(\text{cm}^{-1})$: 3358, 3125, 2925, 1705, 1652, 1557, 1403, 1155, 1060, 763; ¹H NMR (400 MHz, CDCl₃) δ : 8.95 (s, 1H), 8.69–8.66 (d, $J = 8.6$ Hz, 1H), 7.91–7.89 (dd, $J = 8.0, 1.5$ Hz, 1H), 7.56–7.52 (t, $J = 8.6$ Hz, 1H), 7.03–7.00 (t, $J = 8.0$ Hz, 1H), 6.71 (s, 1H), 5.87 (s, 1H), 4.24–4.20 (m, 1H), 3.26–3.14 (m, 2H), 3.11–3.03 (m, 2H), 2.27–2.19 (m, 1H), 2.08–2.01 (m, 1H), 1.96–1.88 (m, 3H), 1.40 (s, 9H), 0.99–0.97 (d, $J = 6.7$ Hz, 6H); ¹³C NMR (100 MHz, CDCl₃) δ : 171.62, 155.27, 139.87, 135.08, 130.19, 121.51, 121.19, 120.54, 60.88, 52.00, 48.93, 47.67, 36.62, 31.72, 29.68, 28.84, 28.58, 25.12, 20.30, 20.26; HRMS: C₂₀H₃₂O₄N₄NaS, Calcd: 447.2036 Found: 447.2036.

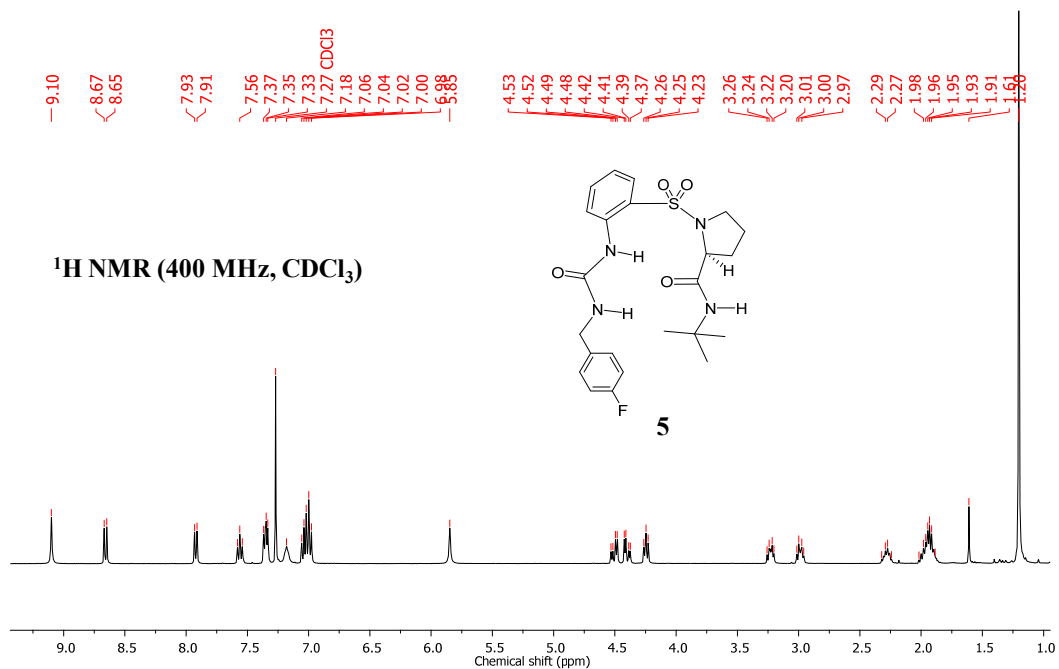
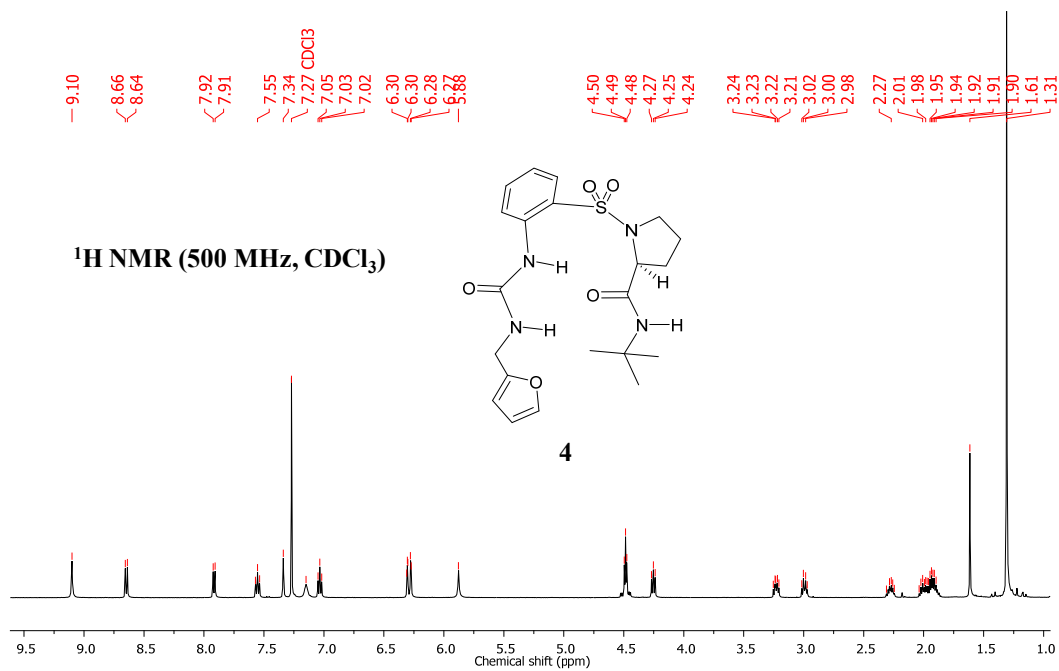


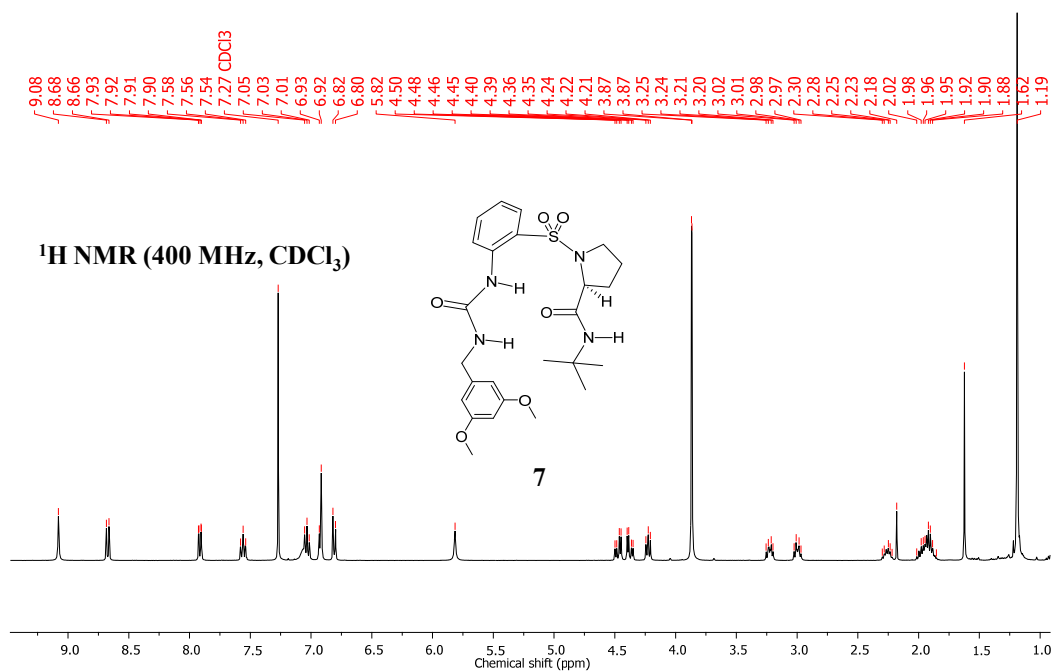
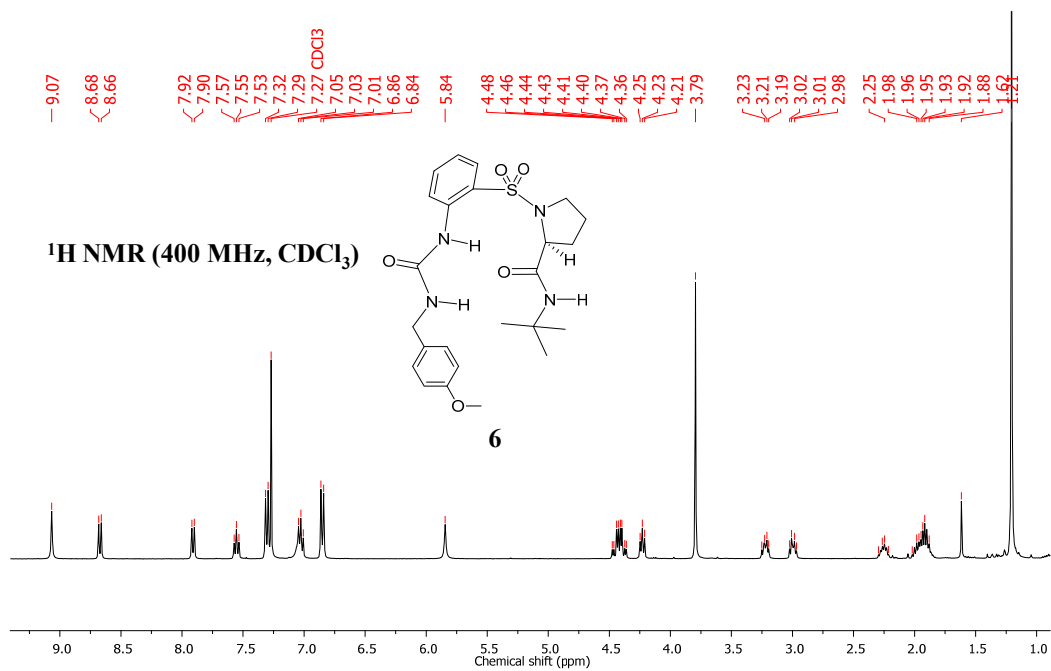


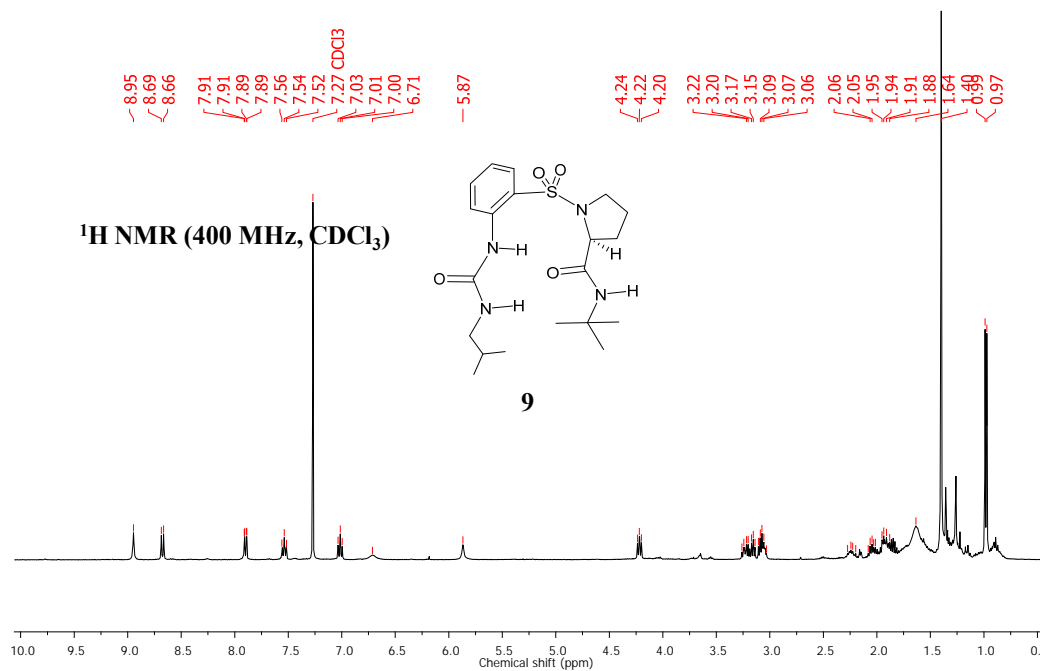
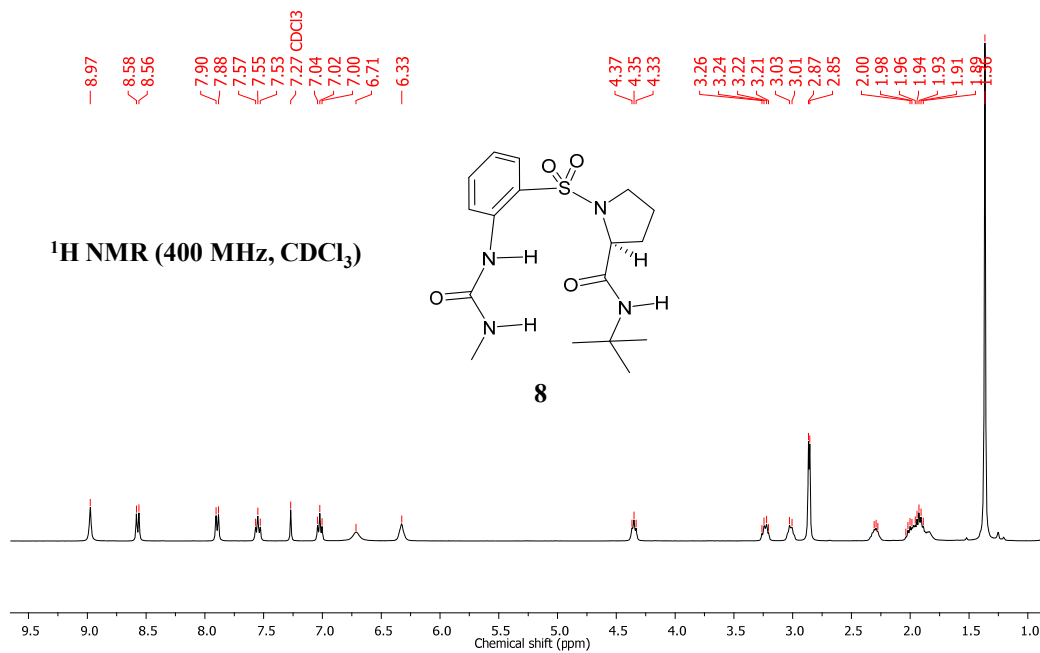


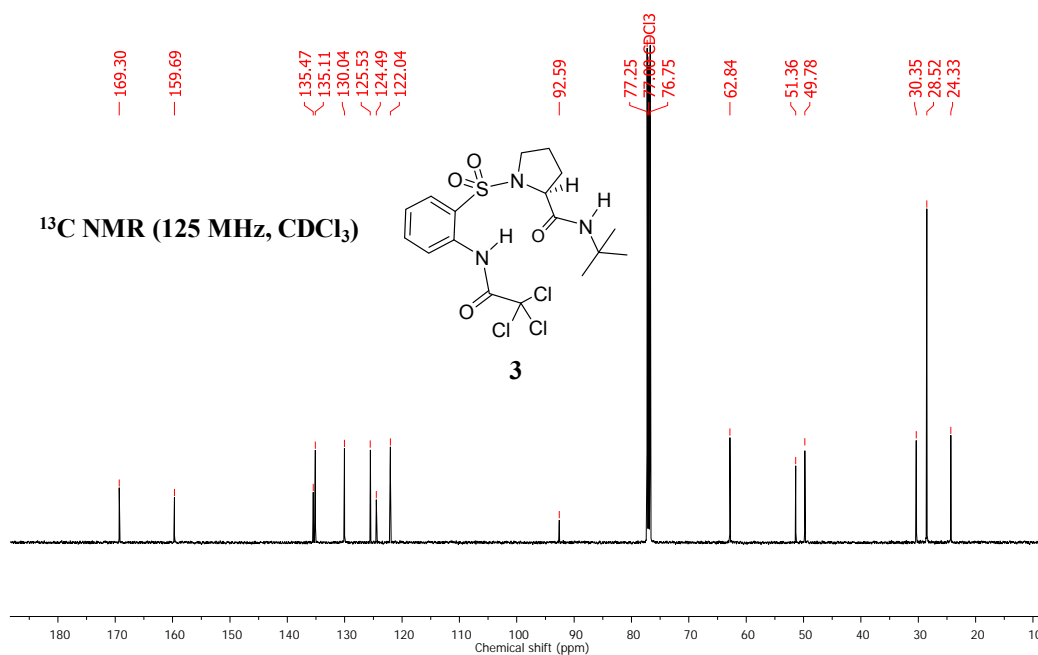
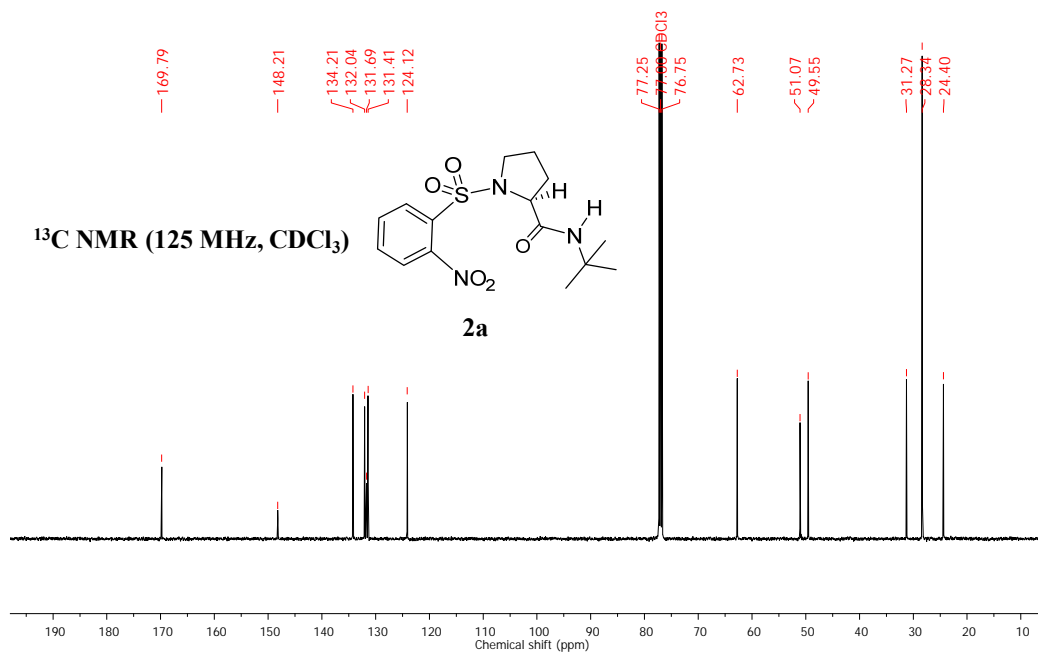


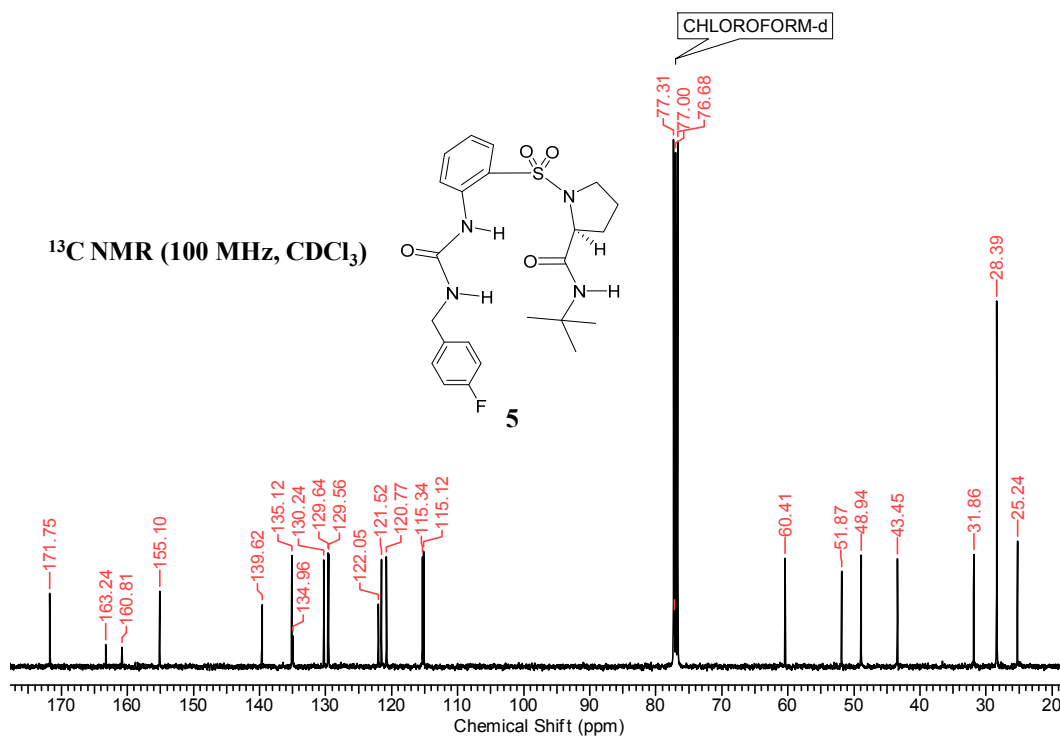
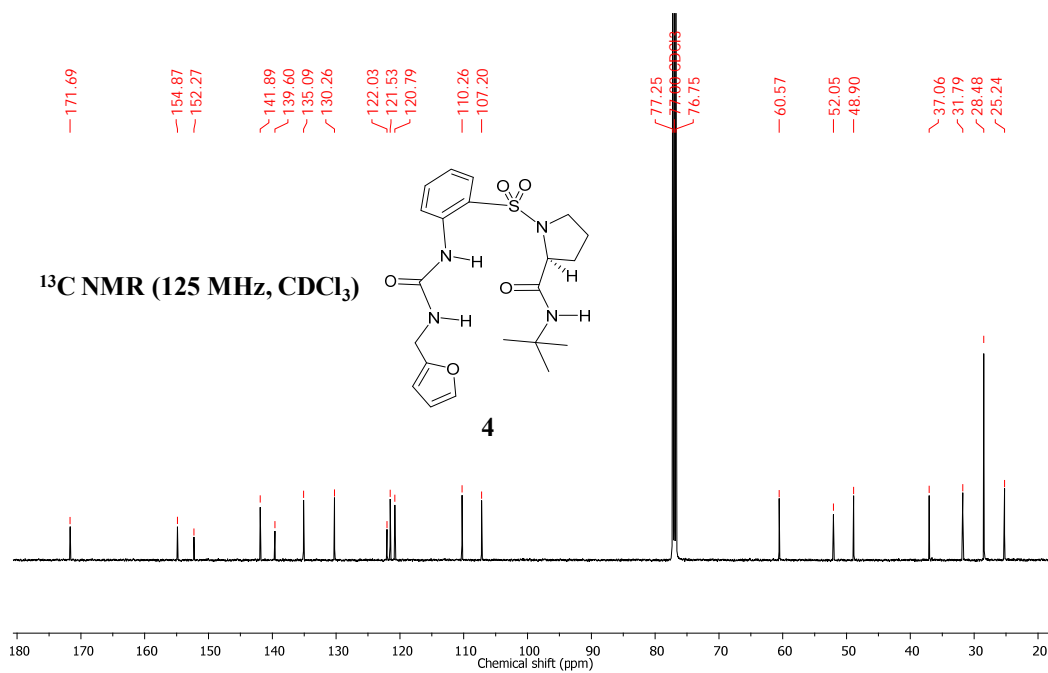


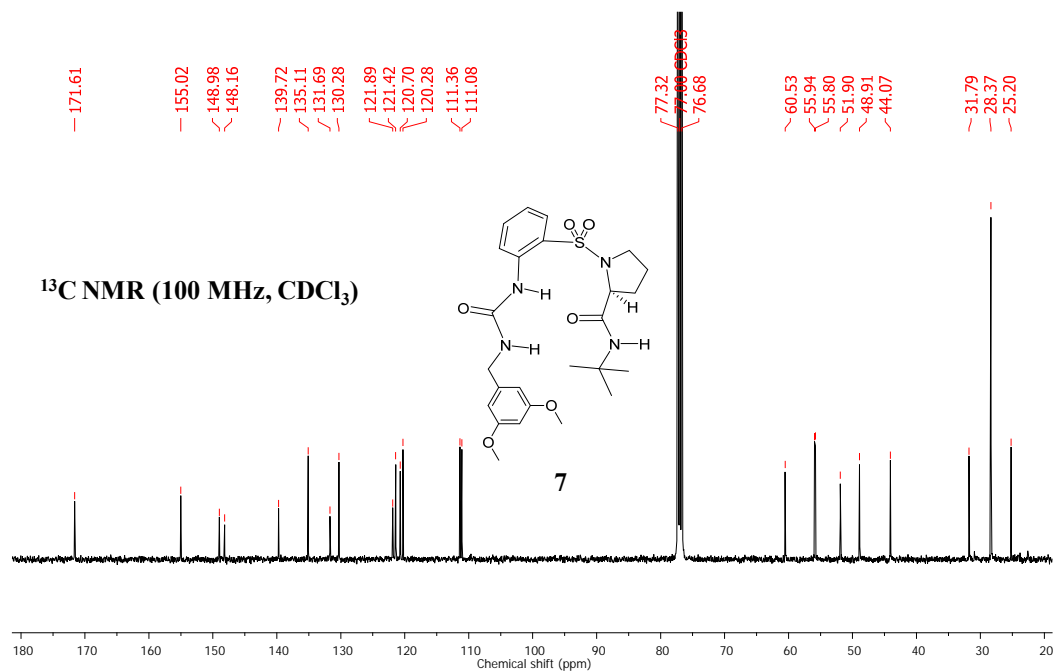
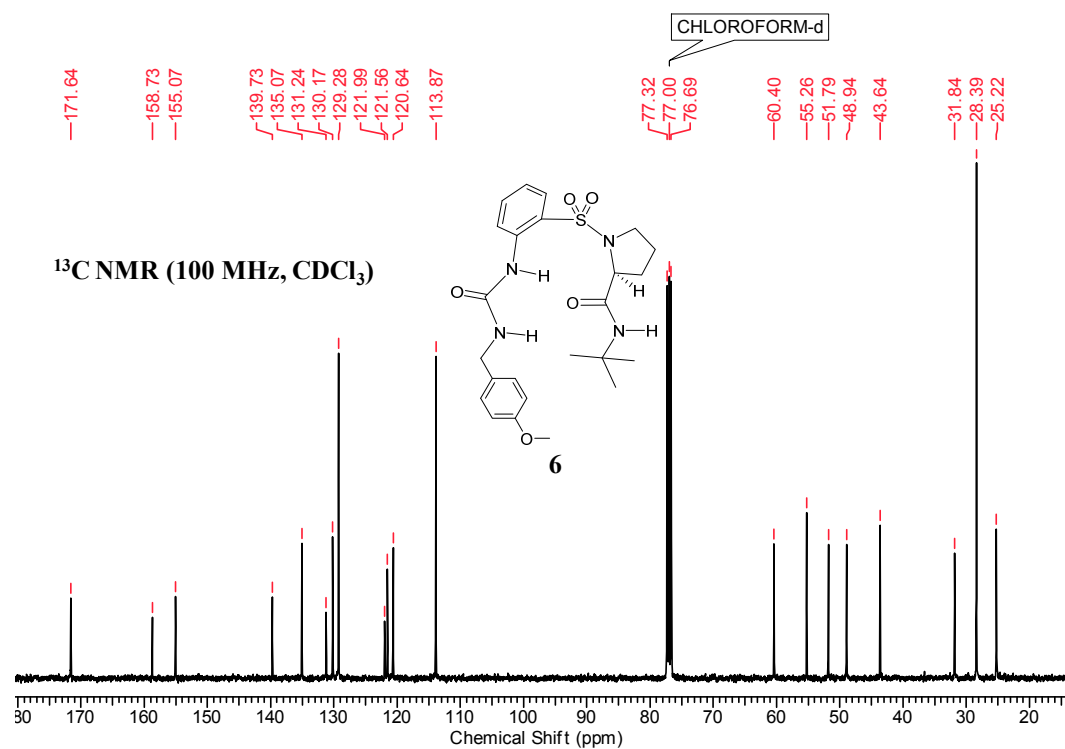












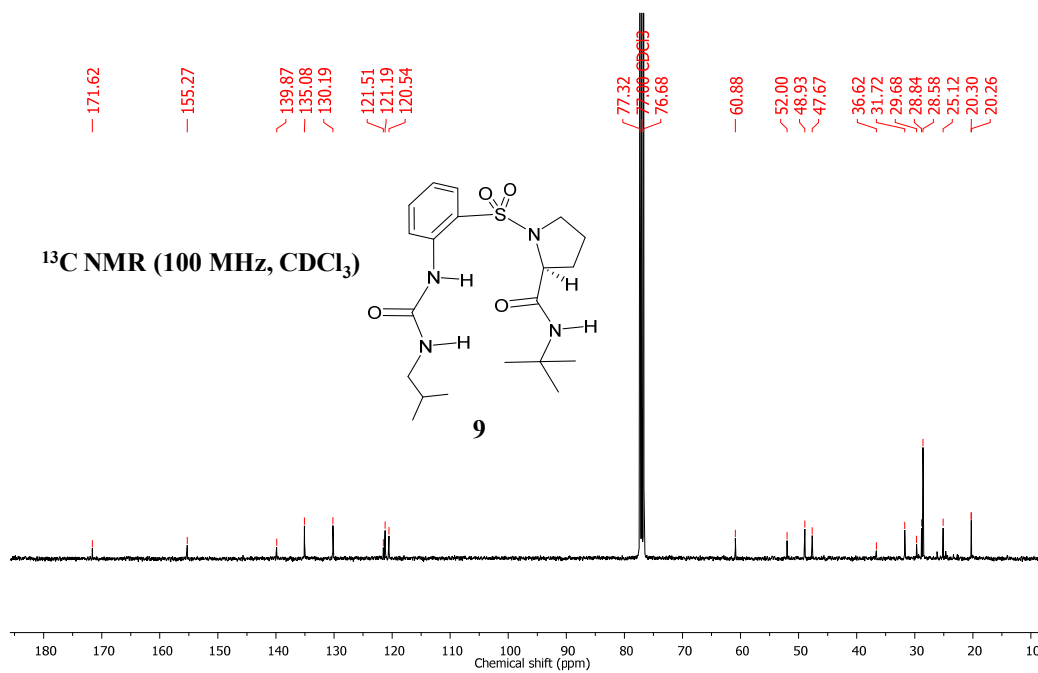
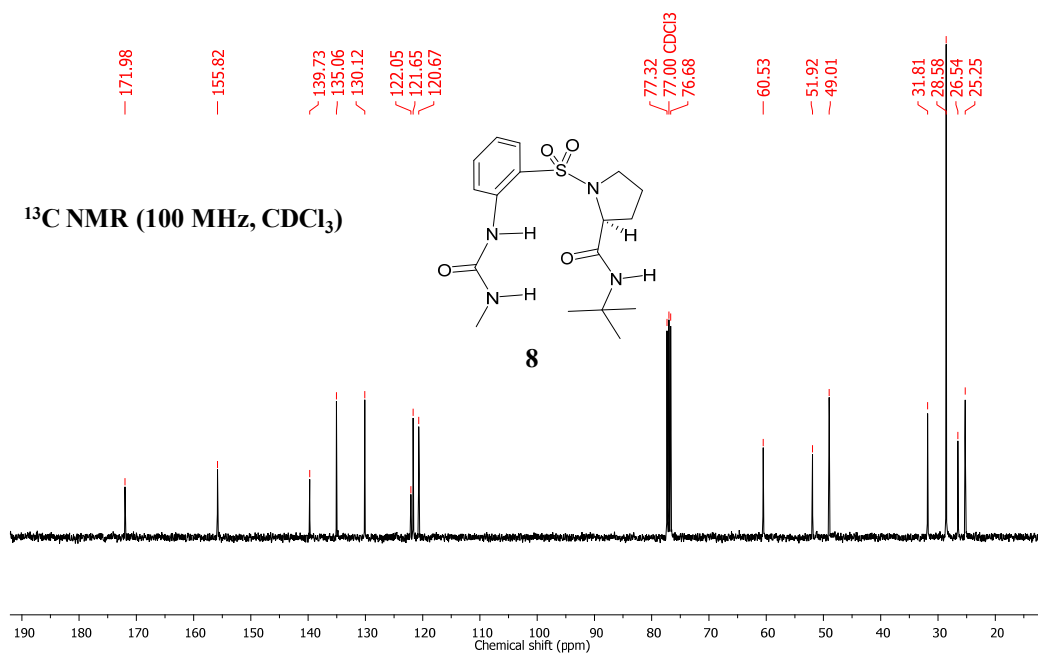


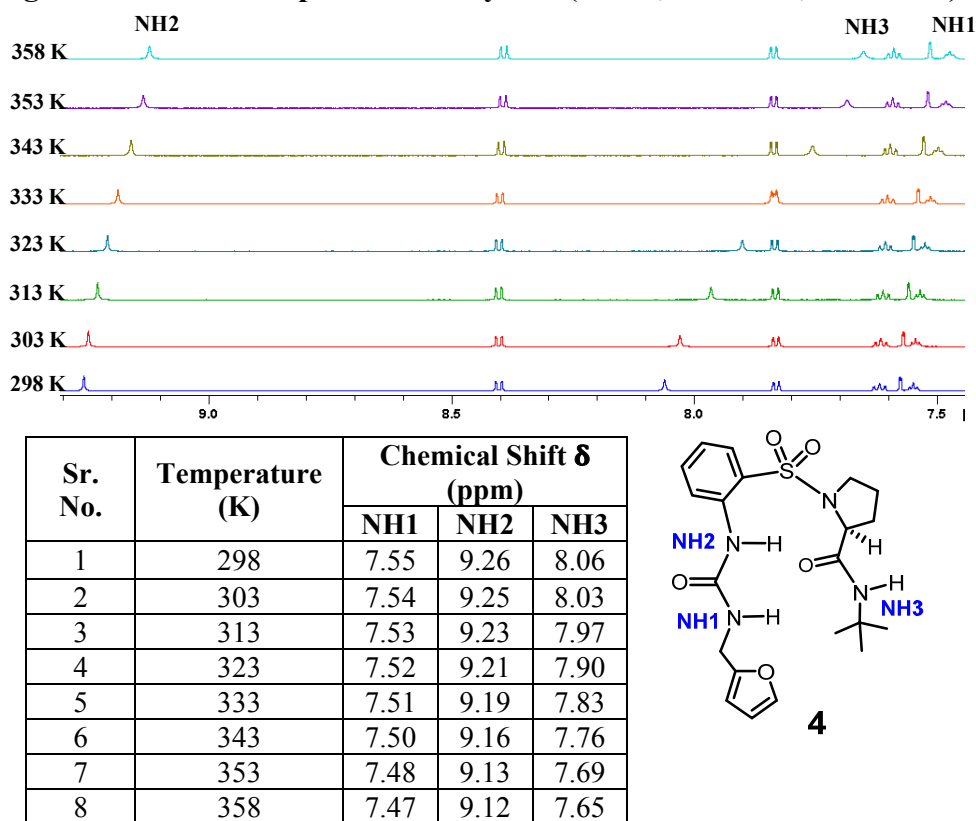
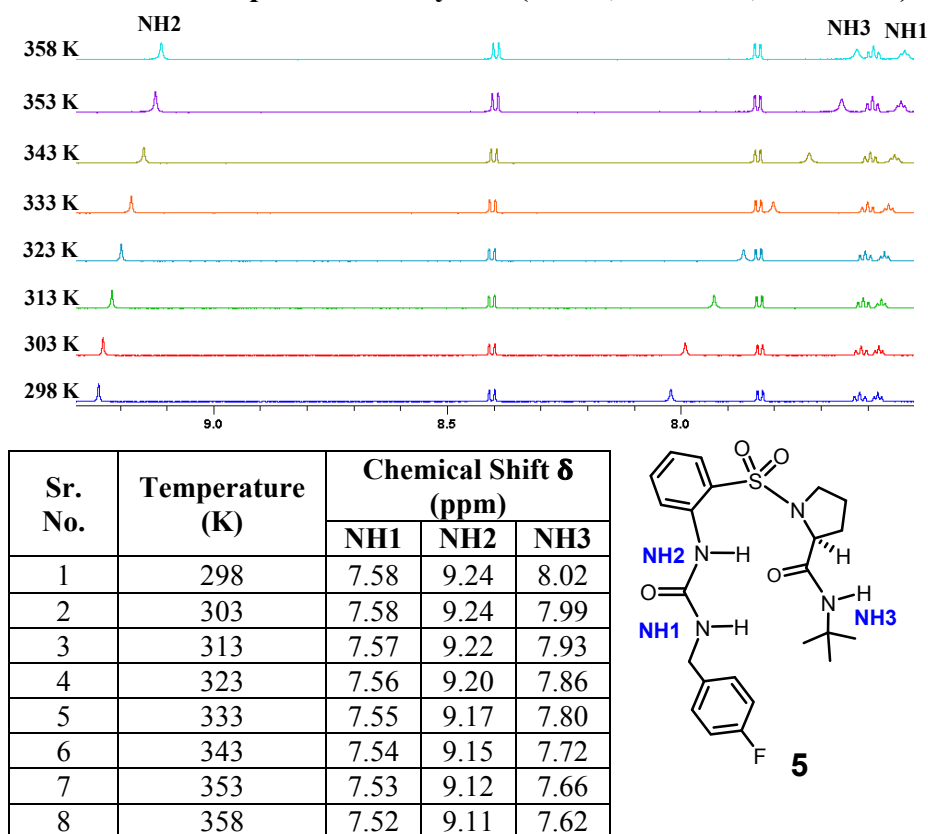
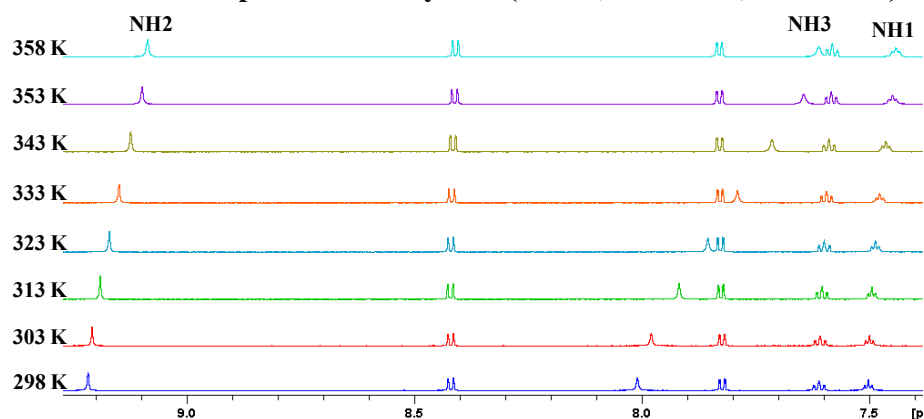
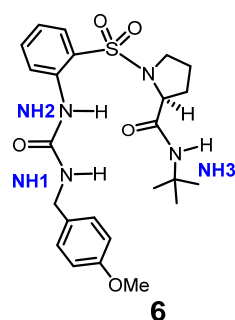
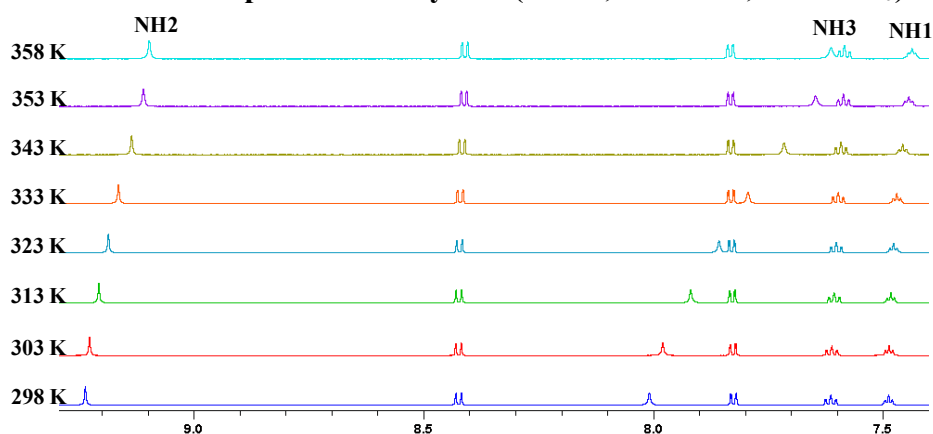
Fig. 3.16 Variable temperature study of 4 (2 mM, 700 MHz, DMSO-*d*₆).Fig. 3.17 Variable temperature study of 5 (2 mM, 700 MHz, DMSO-*d*₆).

Fig. 3.18 Variable temperature study of **6** (2 mM, 700 MHz, DMSO-*d*₆).

Sr. No.	Temperature (K)	Chemical Shift δ (ppm)		
		NH1	NH2	NH3
1	298	7.50	9.22	8.01
2	303	7.50	9.21	7.98
3	313	7.49	9.19	7.92
4	323	7.49	9.17	7.86
5	333	7.48	9.15	7.79
6	343	7.46	9.12	7.71
7	353	7.45	9.10	7.64
8	358	7.44	9.09	7.61

**Fig. 3.19** Variable temperature study of **7** (2 mM, 700 MHz, DMSO-*d*₆).

Sr. No.	Temperature (K)	Chemical Shift δ (ppm)		
		NH1	NH2	NH3
1	298	7.49	9.24	8.01
2	303	7.49	9.23	7.98
3	313	7.48	9.21	7.92
4	323	7.48	9.19	7.86
5	333	7.47	9.16	7.79
6	343	7.46	9.14	7.72
7	353	7.45	9.11	7.65
8	358	7.44	9.10	7.61

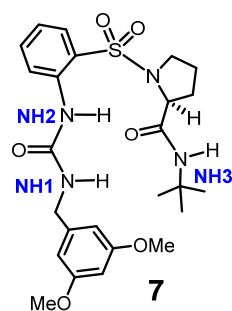
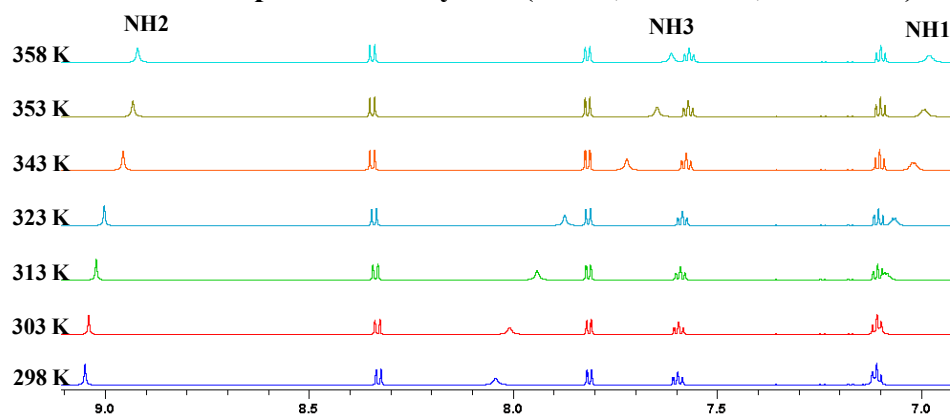
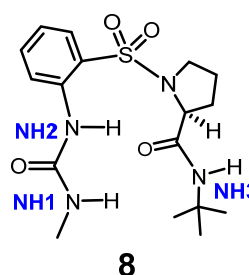
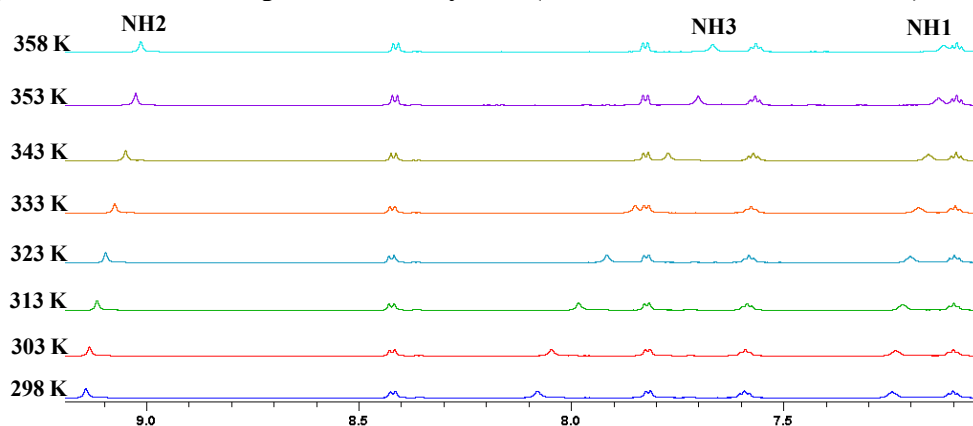


Fig. 3.20 Variable temperature study of **8** (2 mM, 700 MHz, DMSO-*d*₆).

Sr. No.	Temperature (K)	Chemical Shift δ (ppm)		
		NH1	NH2	NH3
1	298	7.12	9.05	8.04
2	303	7.11	9.04	8.01
3	313	7.09	9.02	7.94
4	323	7.07	9.00	7.87
5	343	7.02	8.96	7.72
6	353	7.00	8.93	7.65
7	358	6.98	8.92	7.61

Fig. 3.21 Variable temperature study of **9** (2 mM, 700 MHz, DMSO-*d*₆).

Sr. No.	Temperature (K)	Chemical Shift δ (ppm)		
		NH1	NH2	NH3
1	298	7.24	9.14	8.08
2	303	7.24	9.13	8.05
3	313	7.22	9.12	7.98
4	323	7.20	9.10	7.92
5	333	7.18	9.08	7.85
6	343	7.16	9.05	7.77
7	353	7.14	9.03	7.70
8	358	7.12	9.01	7.67

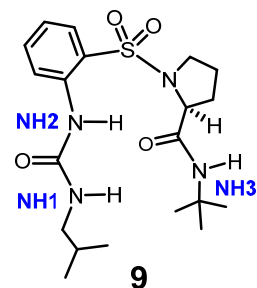


Table 3.3 Titration study of **4** in CDCl_3 (2 mM, 400 MHz) with $\text{DMSO-}d_6$ (volume of $\text{DMSO-}d_6$ added at each addition = 5 μL).

Sr. No.	Volume of $\text{DMSO-}d_6$ (μL)	Chemical Shift δ (ppm)		
		NH1	NH2	NH3
1	0	7.09	9.06	5.71
2	5	7.15	9.07	5.98
3	10	7.21	9.08	6.21
4	15	7.27	9.09	6.50
5	20	7.27	9.09	6.59
6	25	7.31	9.09	6.69
7	30	7.33	9.09	6.80
8	35	7.34	9.09	6.84
9	40	7.34	9.09	6.90
10	45	7.35	9.09	6.95
11	50	7.35	9.09	7.00

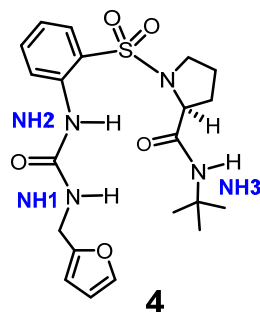


Table 3.4 Titration study of **5** in CDCl_3 (2 mM, 400 MHz) with $\text{DMSO-}d_6$ (volume of $\text{DMSO-}d_6$ added at each addition = 5 μL).

Sr. No.	Volume of $\text{DMSO-}d_6$ (μL)	Chemical Shift δ (ppm)		
		NH1	NH2	NH3
1	0	7.11	9.06	5.66
2	5	7.19	9.07	6.11
3	10	7.25	9.09	6.30
4	15	7.28	9.09	6.46
5	20	7.31	9.09	6.60
6	25	7.33	9.10	6.71
7	30	7.35	9.10	6.80
8	35	7.35	9.10	6.87
9	40	7.36	9.10	6.94
10	45	7.36	9.09	6.98
11	50	7.36	9.09	7.02

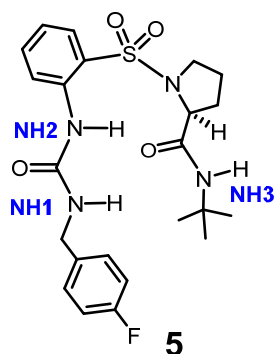


Table 3.5 Titration study of **6** in CDCl_3 (2 mM, 400 MHz) with $\text{DMSO-}d_6$ (volume of $\text{DMSO-}d_6$ added at each addition = 5 μL).

Sr. No.	Volume of $\text{DMSO-}d_6$ (μL)	Chemical Shift δ (ppm)		
		NH1	NH2	NH3
1	0	6.98	9.03	5.72
2	5	7.10	9.04	6.04
3	10	7.14	9.05	6.28
4	15	7.17	9.06	6.42
5	20	7.20	9.06	6.51
6	25	7.22	9.06	6.60
7	30	7.23	9.06	6.67
8	35	7.24	9.06	6.76
9	40	7.24	9.06	6.81
10	45	7.22	9.06	6.85
11	50	7.22	9.05	6.90

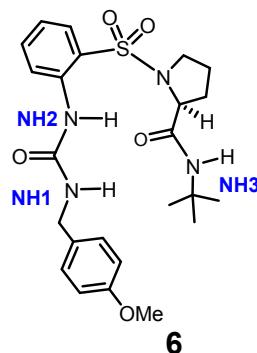


Table 3.6 Titration study of **7** in CDCl_3 (2 mM, 400 MHz) with $\text{DMSO-}d_6$ (volume of $\text{DMSO-}d_6$ added at each addition = 5 μL).

Sr. No.	Volume of $\text{DMSO-}d_6$ (μL)	Chemical Shift δ (ppm)		
		NH1	NH2	NH3
1	0	7.00	9.04	5.67
2	5	7.09	9.06	6.03
3	10	7.14	9.07	6.30
4	15	7.18	9.08	6.46
5	20	7.22	9.08	6.58
6	25	7.24	9.08	6.68
7	30	7.26	9.08	6.78
8	35	7.27	9.08	6.83
9	40	7.27	9.08	6.91
10	45	7.27	9.08	6.96
11	50	7.28	9.07	6.98

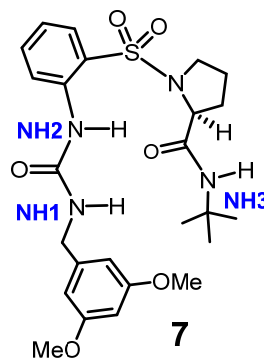


Table 3.7 Titration study of **8** in CDCl_3 (2 mM, 400 MHz) with $\text{DMSO-}d_6$ (volume of $\text{DMSO-}d_6$ added at each addition = 5 μL).

Sr. No.	Volume of $\text{DMSO-}d_6$ (μL)	Chemical Shift δ (ppm)		
		NH1	NH2	NH3
1	0	6.55	8.90	5.88
2	5	6.67	8.90	6.30
3	10	6.74	8.90	6.57
4	15	6.77	8.91	6.69
5	20	6.80	8.91	6.80
6	25	6.83	8.91	6.89
7	30	6.84	8.92	6.97
8	35	6.85	8.92	7.03
9	40	6.85	8.92	7.07
10	45	6.85	8.92	7.11
11	50	6.85	8.92	7.14

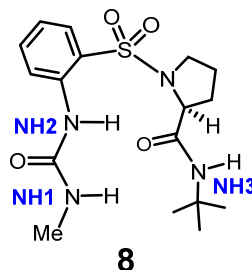


Table 3.8 Titration study of **9** in CDCl_3 (2 mM, 400 MHz) with $\text{DMSO-}d_6$ (volume of $\text{DMSO-}d_6$ added at each addition = 5 μL).

Sr. No.	Volume of $\text{DMSO-}d_6$ (μL)	Chemical Shift δ (ppm)		
		NH1	NH2	NH3
1	0	6.69	8.94	5.80
2	5	6.78	8.95	6.07
3	10	6.83	8.96	6.29
4	15	6.87	8.96	6.44
5	20	6.90	8.97	6.56
6	25	6.92	8.97	6.65
7	30	6.93	8.97	6.75
8	35	6.95	8.97	6.81
9	40	6.96	8.97	6.88
10	45	6.97	8.96	6.93
11	50	6.97	8.96	7.00

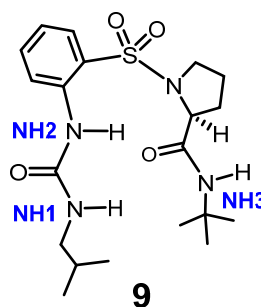
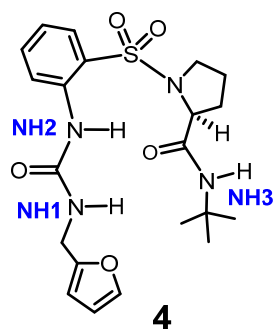


Table 3.9 Variable temperature study of 4 (2 mM, 700 MHz, CDCl₃).

Sr. No.	Temperature (K)	Chemical Shift δ (ppm)		
		NH1	NH2	NH3
1	268	7.25	9.11	5.74
2	273	7.23	9.1	5.73
3	278	7.2	9.09	5.72
4	283	7.17	9.09	5.71
5	288	7.14	9.08	5.70
6	293	7.11	9.07	5.70
7	298	7.08	9.06	5.69
8	303	7.05	9.06	5.69
9	308	7.02	9.05	5.69
10	313	6.99	9.04	5.68
11	318	6.96	9.03	5.68
12	323	6.93	9.02	5.68

Table 3.10 Variable temperature study of 5 (2 mM, 700 MHz, CDCl₃).

Sr. No.	Temperature (K)	Chemical Shift δ (ppm)		
		NH1	NH2	NH3
1	268	7.23	9.10	5.68
2	273	7.22	9.09	5.68
3	278	7.2	9.09	5.67
4	283	7.18	9.08	5.66
5	288	7.16	9.07	5.65
6	293	7.13	9.07	5.65
7	298	7.11	9.06	5.64
8	303	7.09	9.05	5.65
9	308	7.06	9.04	5.64
10	313	7.04	9.04	5.64
11	318	7.00	9.03	5.64
12	323	6.98	9.02	5.64

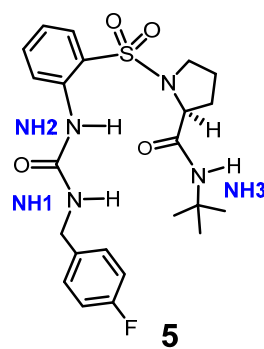
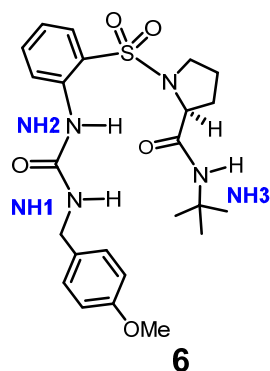


Table 3.11 Variable temperature study of **6** (2 mM, 700 MHz, CDCl₃).

Sr. No.	Temperature (K)	Chemical Shift δ (ppm)		
		NH1	NH2	NH3
1	268	7.15	9.08	5.77
2	273	7.13	9.08	5.76
3	278	7.10	9.07	5.75
4	283	7.08	9.06	5.73
5	288	7.05	9.05	5.73
6	293	7.02	9.04	5.72
7	298	6.98	9.03	5.71
8	303	6.94	9.02	5.70
9	308	6.92	9.02	5.70
10	313	6.87	9.01	5.70
11	318	6.85	9.00	5.69
12	323	6.82	8.99	5.69

Table 3.12 Variable temperature study of **7** (2 mM, 700 MHz, CDCl₃).

Sr. No.	Temperature (K)	Chemical Shift δ (ppm)		
		NH1	NH2	NH3
1	268	7.16	9.09	5.69
2	273	7.14	9.08	5.68
3	278	7.11	9.08	5.67
4	283	7.09	9.07	5.66
5	288	7.06	9.06	5.66
6	293	7.04	9.05	5.66
7	298	7.00	9.04	5.65
8	303	6.96	9.04	5.65
9	308	6.93	9.03	5.65
10	313	6.90	9.02	5.65
11	318	6.87	9.01	5.65
12	323	6.84	9.00	5.65

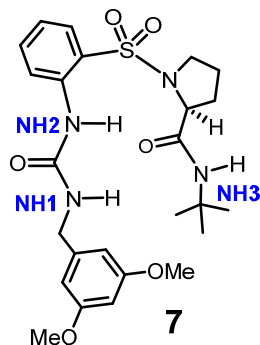
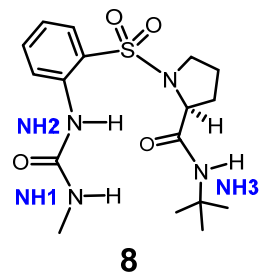
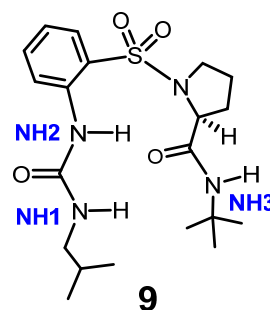


Table 3.13 Variable temperature study of **8** (2 mM, 700 MHz, CDCl₃).

Sr. No.	Temperature (K)	Chemical Shift δ (ppm)		
		NH1	NH2	NH3
1	268	6.76	8.93	5.93
2	273	6.73	8.92	5.91
3	278	6.69	8.91	5.89
4	283	6.65	8.91	5.88
5	288	6.61	8.9	5.87
6	293	6.56	8.89	5.87
7	298	6.53	8.89	5.86
8	303	6.47	8.88	5.85
9	308	6.44	8.88	5.85
10	313	6.4	8.87	5.84
11	318	6.36	8.86	5.84
12	323	6.32	8.86	5.84

Table 3.14 Variable temperature study of **9** (2 mM, 700 MHz, CDCl₃).

Sr. No.	Temperature (K)	Chemical Shift δ (ppm)		
		NH1	NH2	NH3
1	268	6.91	8.98	5.82
2	273	6.88	8.98	5.80
3	278	6.85	8.97	5.79
4	283	6.82	8.96	5.79
5	288	6.78	8.95	5.78
6	293	6.75	8.94	5.78
7	298	6.70	8.93	5.78
8	303	6.66	8.93	5.78
9	308	6.61	8.92	5.78
10	313	6.57	8.91	5.78
11	318	6.53	8.90	5.78
12	323	6.49	8.89	5.78



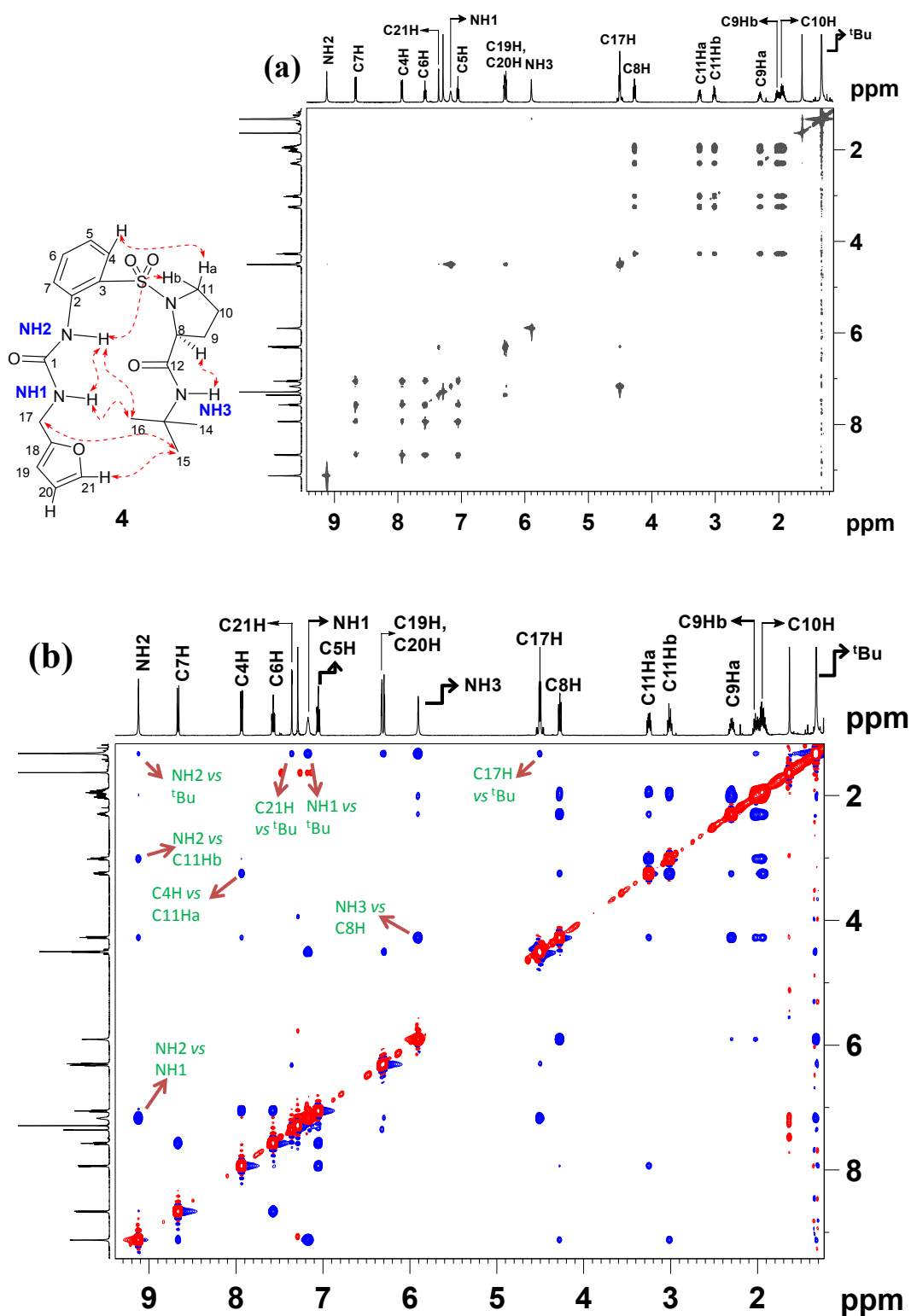


Fig. 3.22 Molecular structure of **4** showing key nOe interactions; full TOCSY (a) and NOESY (b) spectra (20 mM, 500 MHz, CDCl₃). *Note:* In NOESY spectrum positive cross peaks are originating from exchange between NH and trace amount of water.

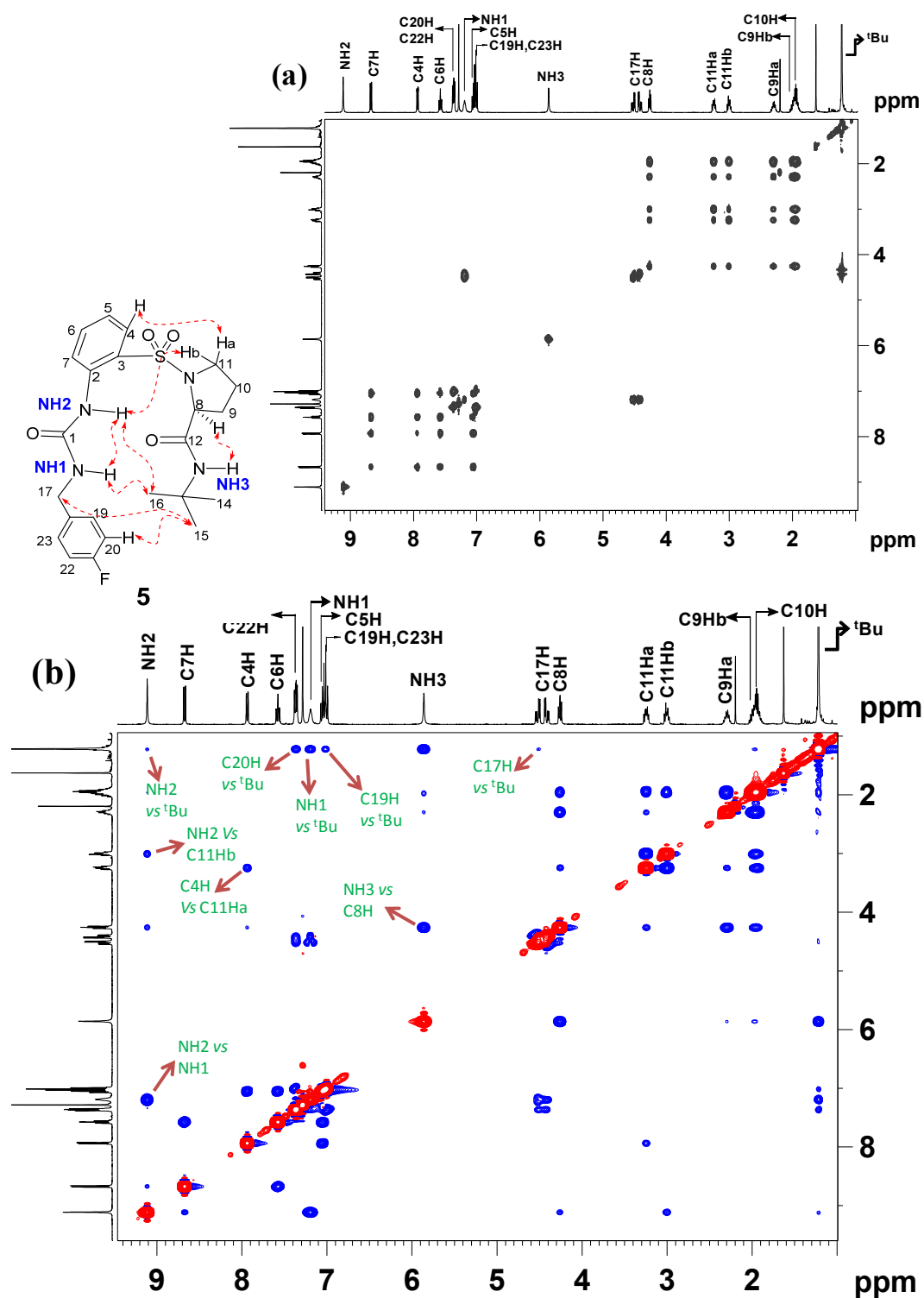


Fig. 3.23 Molecular structure of **5** showing key nOe interactions; full TOCSY (a) and NOESY (b) spectra (20 mM, 400 MHz, CDCl₃).

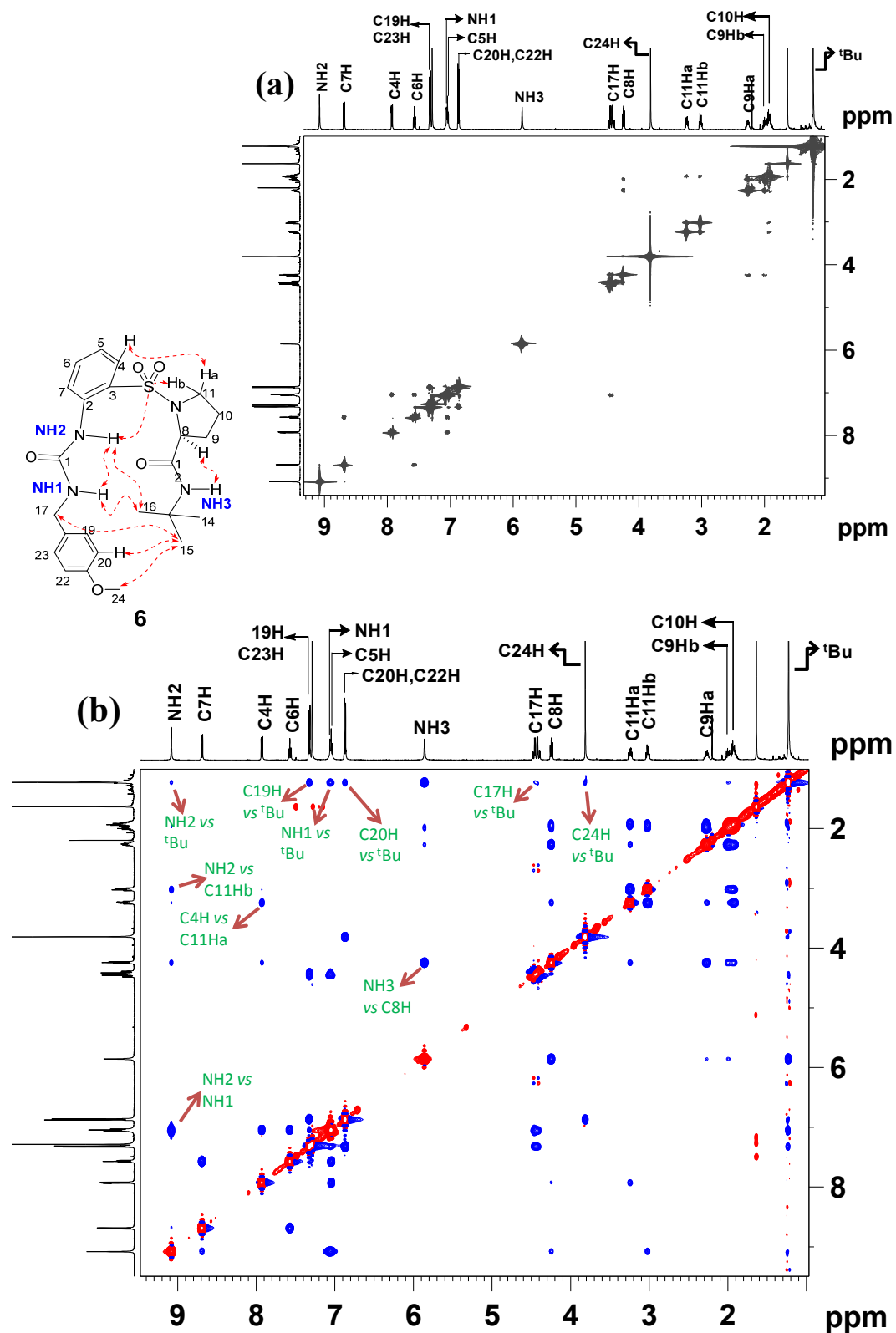


Fig. 3.24 Molecular structure of **6** showing key nOe interactions; full TOCSY (a) and NOESY (b) spectra (20 mM, 500 MHz, CDCl₃). *Note:* In NOESY spectrum positive cross peaks are originating from exchange between NH and trace amount of water.

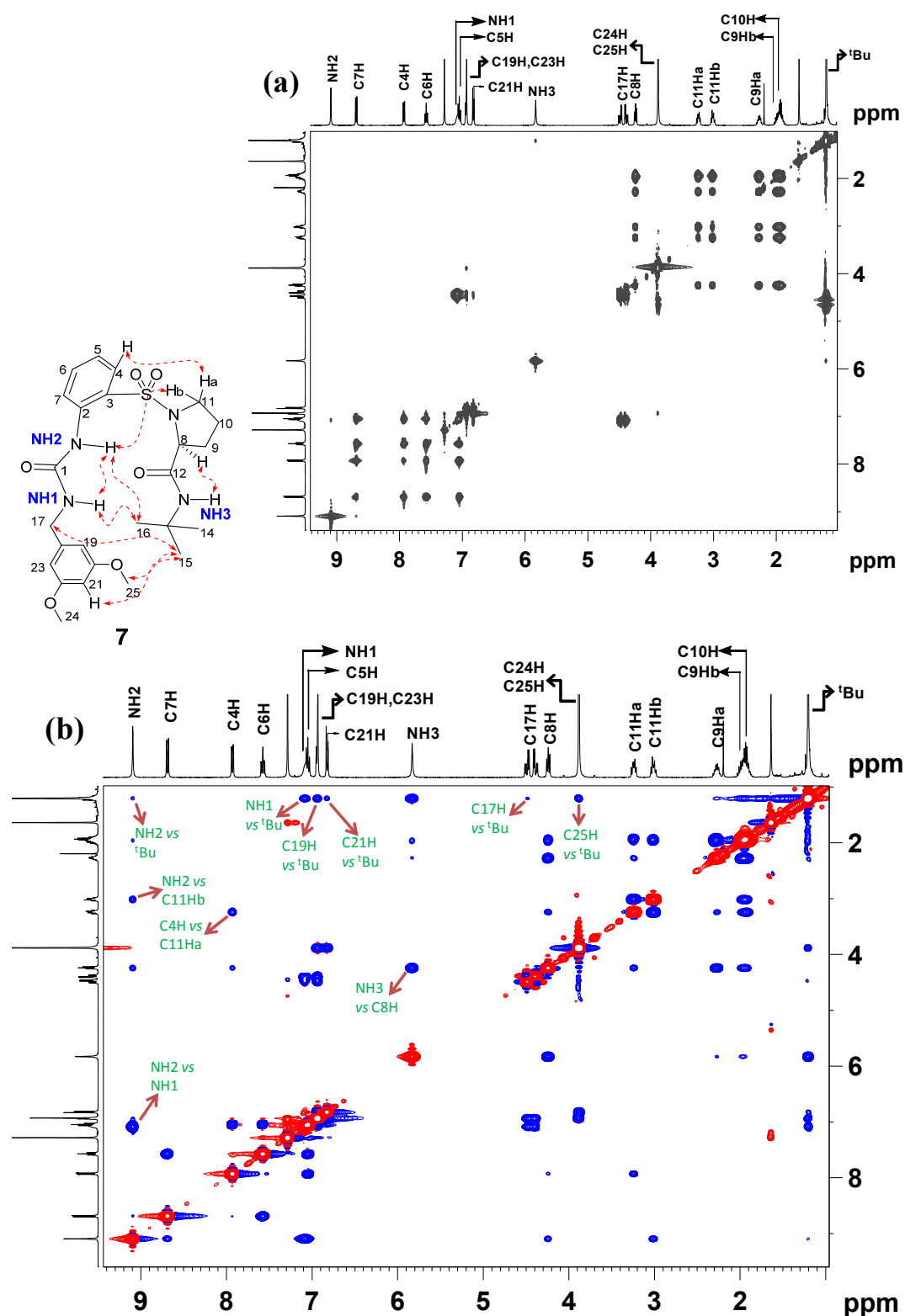


Fig. 3.25 Molecular structure of **7** showing key nOe interactions; full TOCSY (a) and NOESY (b) spectra (20 mM, 400 MHz, CDCl₃). *Note:* In NOESY spectrum positive cross peaks are originating from exchange between NH and trace amount of water.

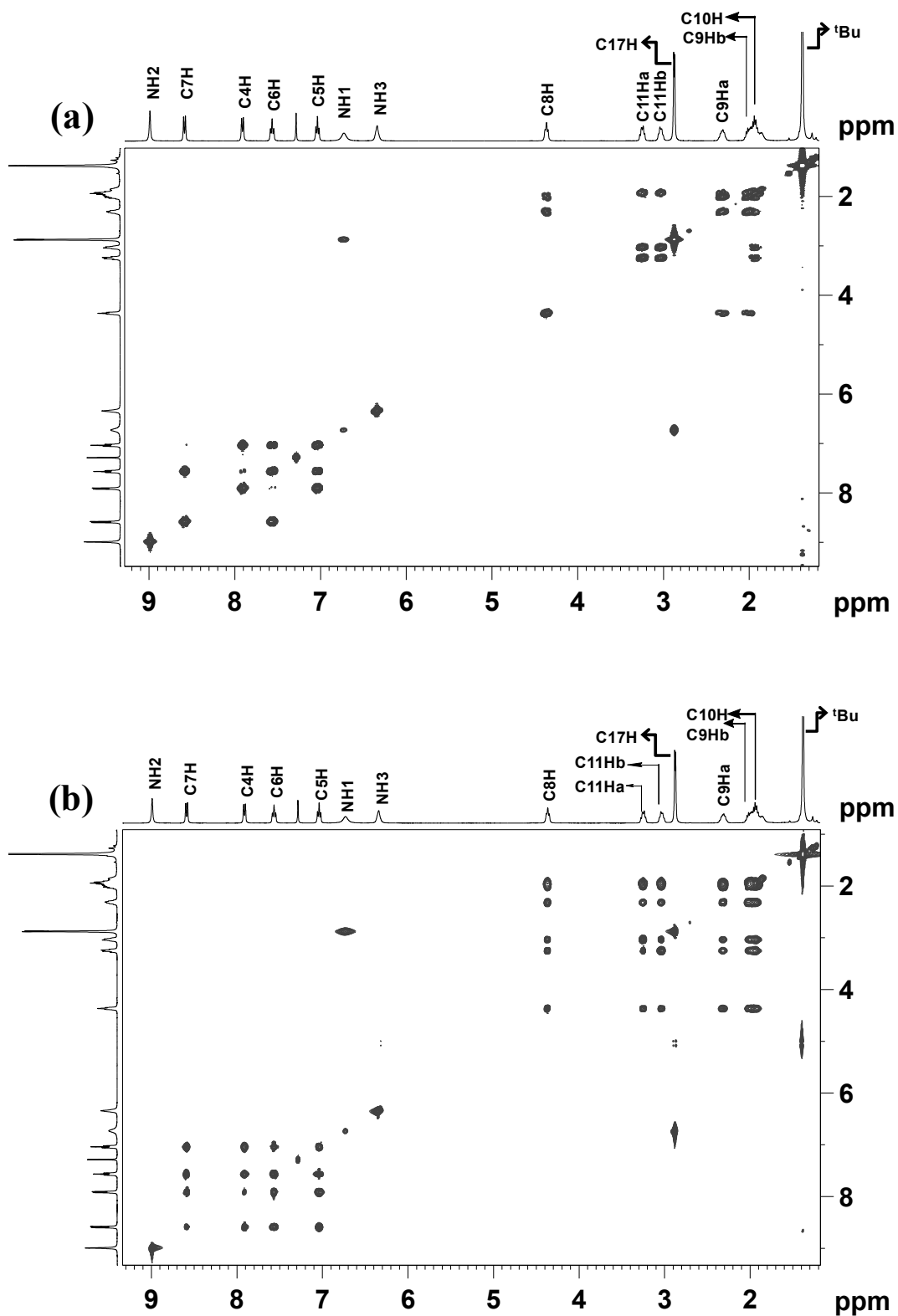


Fig. 3.26 Full COSY (a) and TOCSY (b) spectra of **8** (20 mM, 400 MHz, CDCl_3).

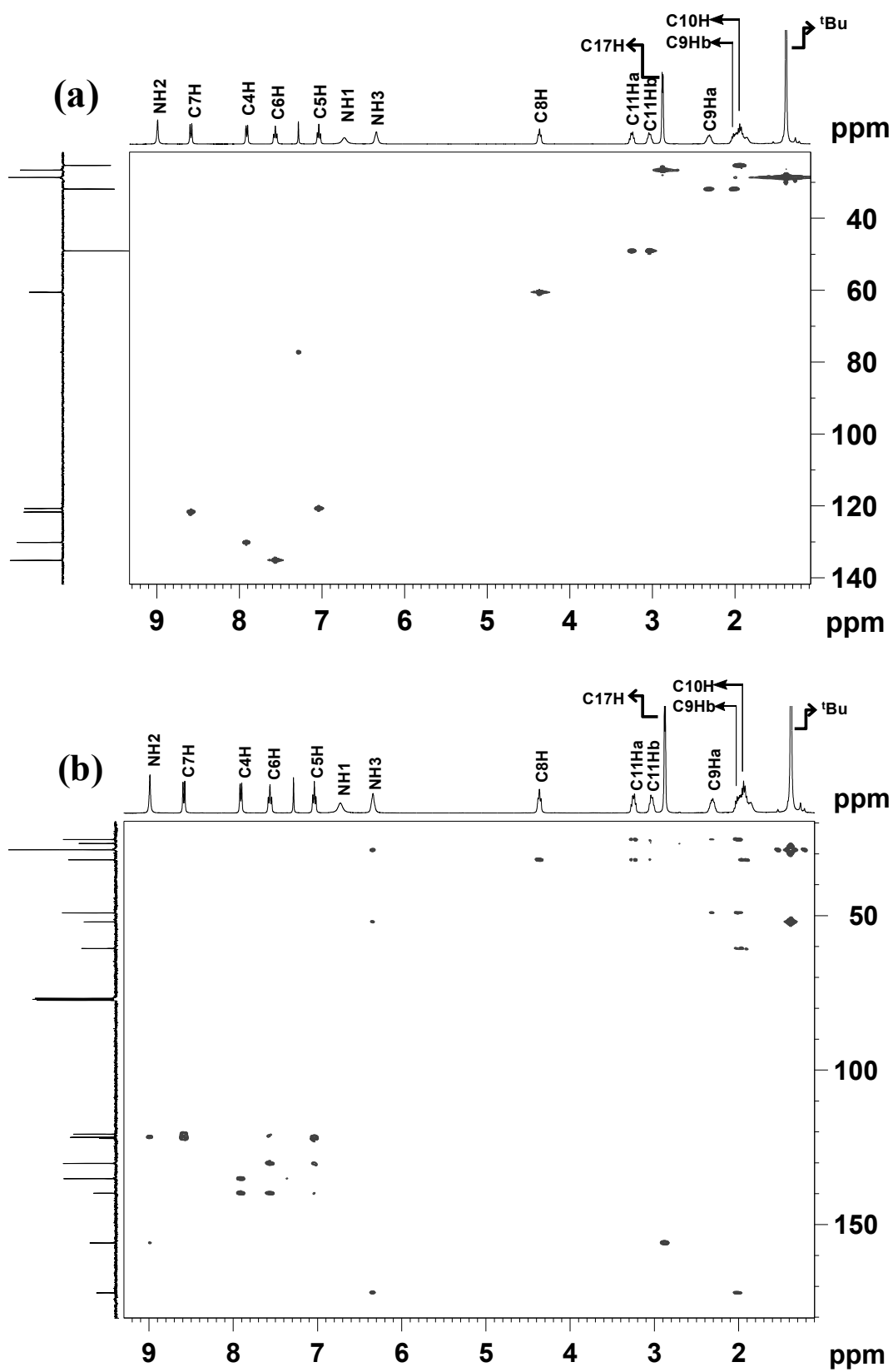


Fig. 3.27 Full HSQC (a) and HMBC (b) spectra of **8** (20 mM, 400 MHz, CDCl_3).

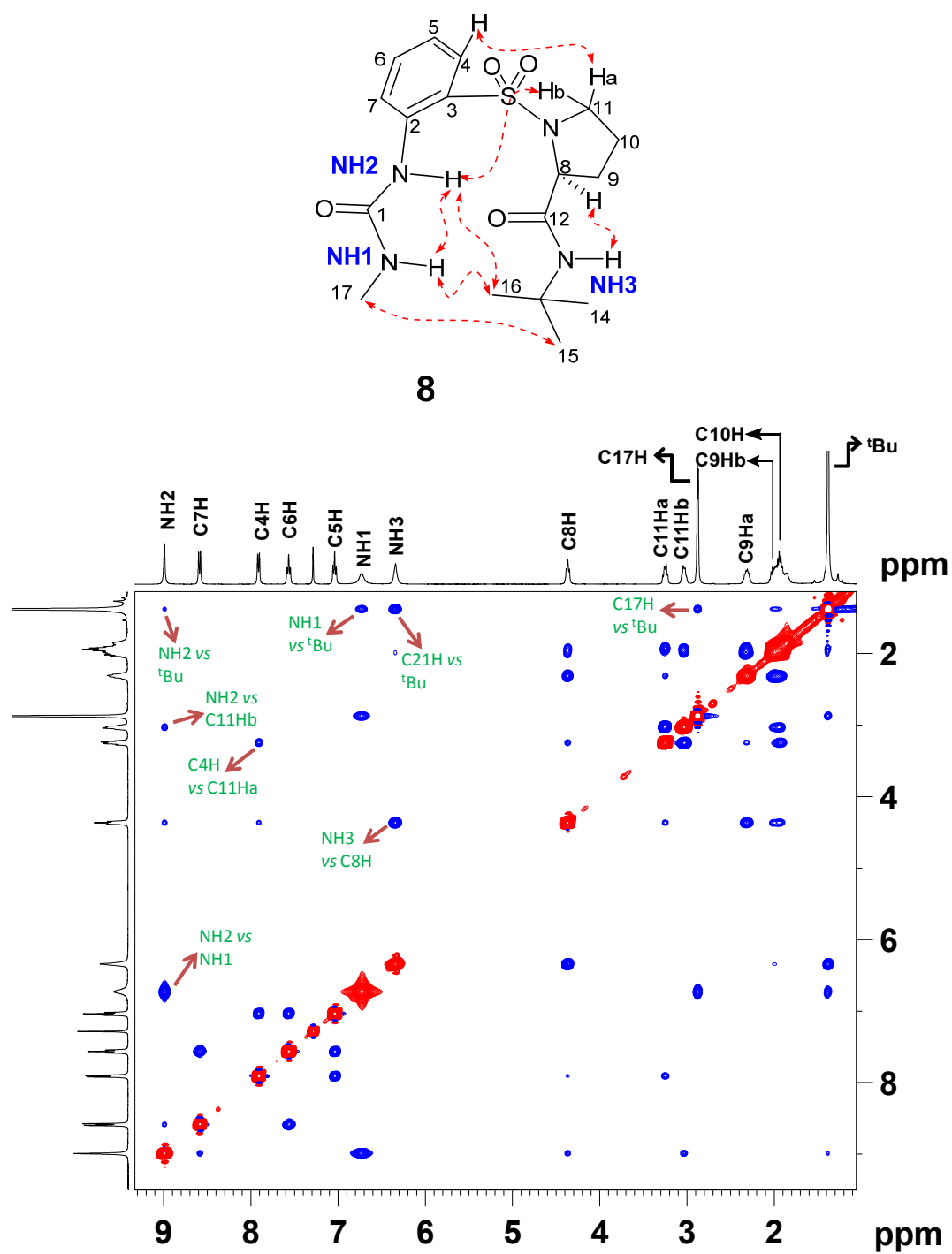


Fig. 3.28 Molecular structure of **8** showing key nOe interactions and full NOESY spectrum (20 mM, 400 MHz, CDCl₃).

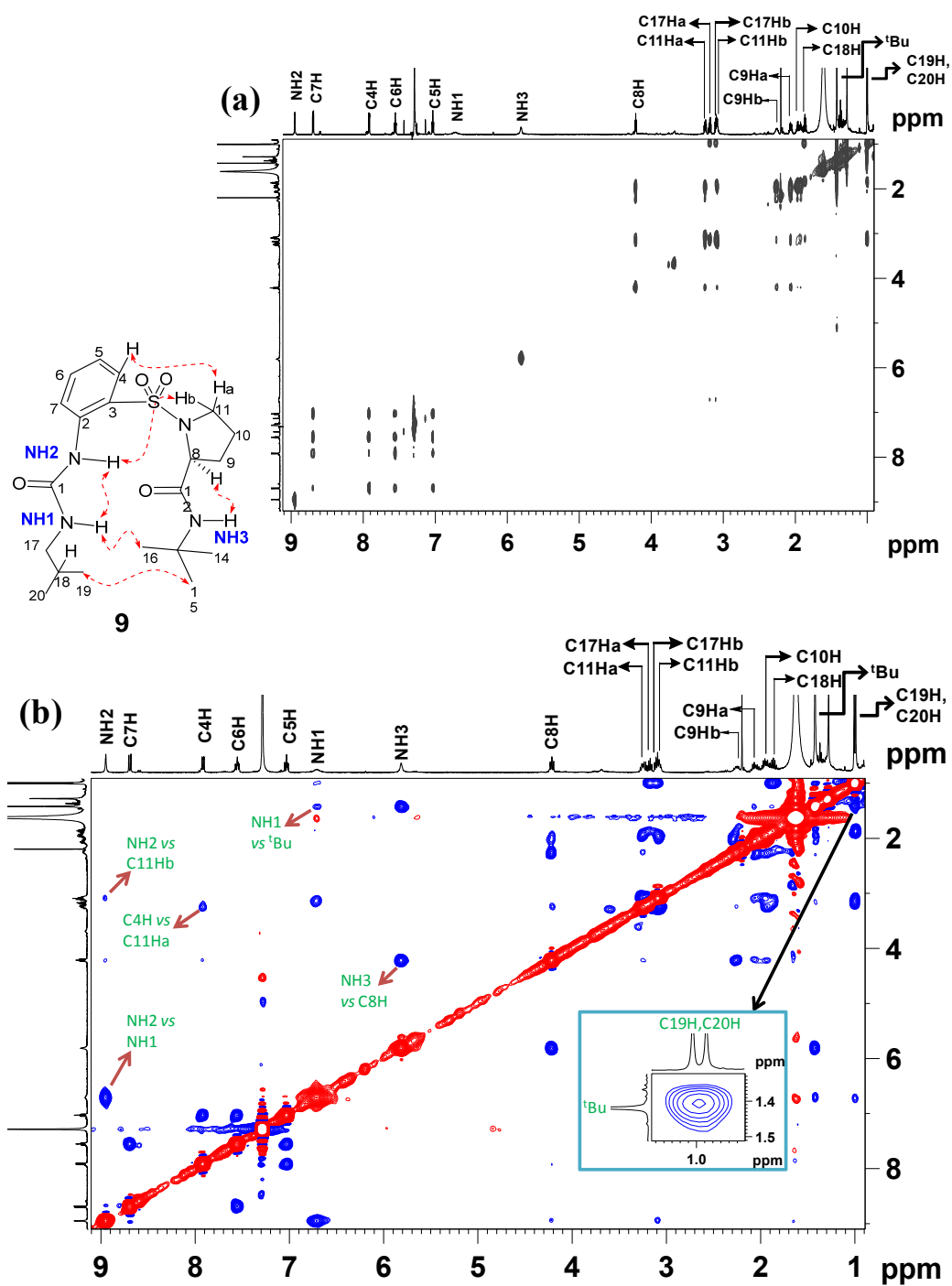


Fig. 3.29 Molecular structure of **9** showing key nOe interactions and full NOESY spectrum (2 mM, 400 MHz, CDCl_3).

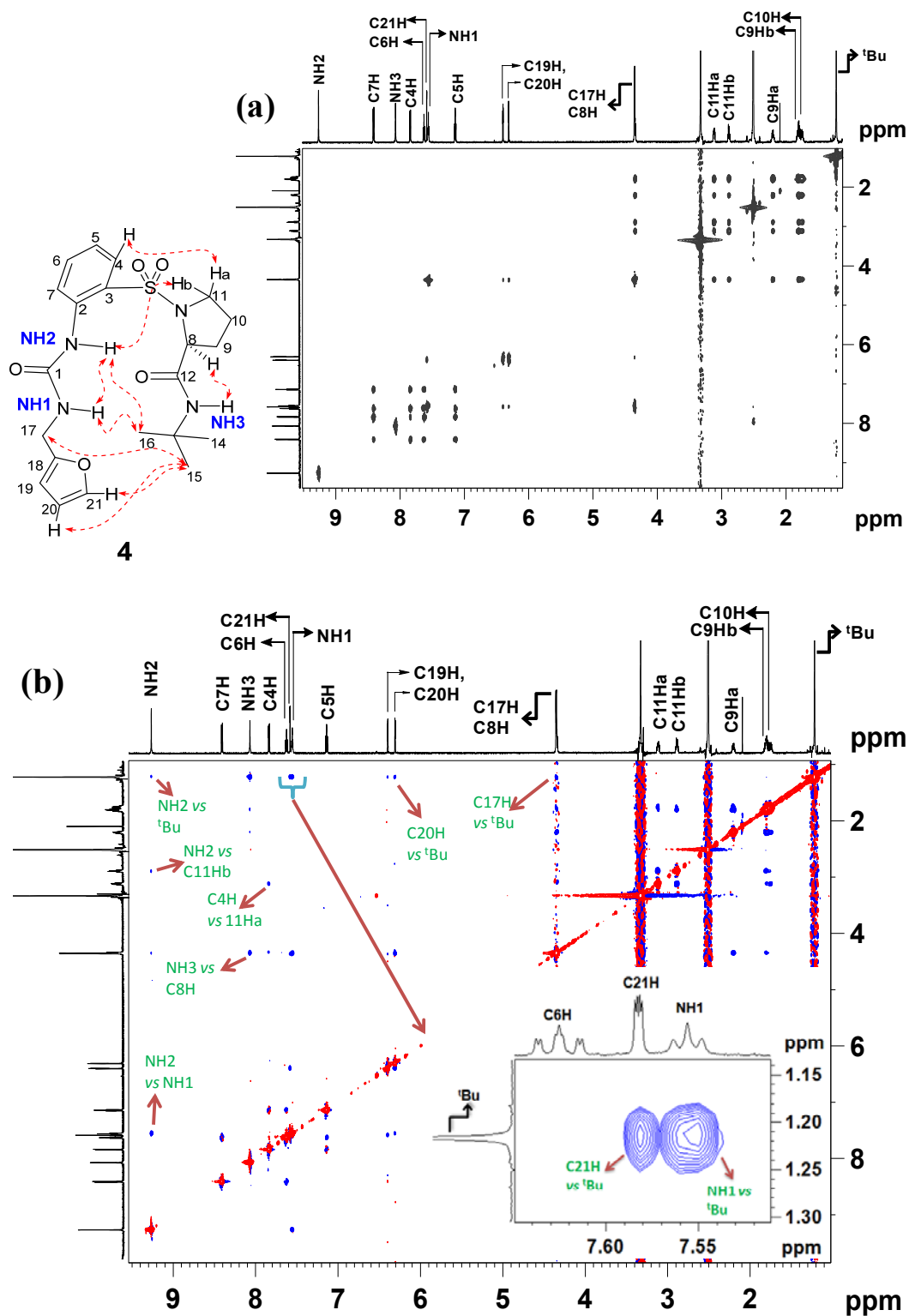


Fig. 3.30 Molecular structure of **4** showing key nOe interactions; full TOCSY (a) and NOESY (b) spectra and inset shows nOes of ^tBu with NH1 and C21H (2 mM, 700 MHz, DMSO-*d*₆).

3.14 Experimental section (Part B)

Procedure for the preparation of common intermediate **3** has been provided in the experimental section of part A. The designed urea-(^SAnt-Pro) peptide conjugates **10-17** were prepared from compound **3**.

Representative procedure for the preparation of urea derivatives **10-17**:

(S)-N-(2-((2-(tert-butylcarbamoyl) pyrrolidin-1-yl) sulfonyl) phenyl)-4-(2-fluorobenzyl)-1,4-diazepane-1-carboxamide **10**:

To a solution of **3** (0.2 g, 0.42 mmol) in DMF (3 mL), 1-(2-fluorobenzyl)-1,4-diazepane hydrochloride salt (0.127 g, 0.42 mmol) and NaHCO₃ (0.143 g, 1.7 mmol, powdered and dried in furnace prior to use) were added sequentially. The reaction mixture was heated at 100 °C for 3 h. The reaction mixture was cooled to room temperature and diluted with EtOAc (20 mL). The organic layer was washed with water, sat. KHSO₄ and then brine. The organic layer was dried over Na₂SO₄ and concentrated under vacuum. The crude product was purified over a neutral alumina column (70:30 EtOAc/pet ether, R_f 0.5) to afford **10** as a viscous liquid (0.195 g, 82%); [α]_D²⁵ : -50.70° (c 0.21, CHCl₃); IR (CHCl₃) ν (cm⁻¹): 3368, 2926, 1679, 1532, 1339, 1146, 760, 609; ¹H NMR (400 MHz, CDCl₃) δ : 9.15 (s, 1H), 8.54-8.52 (d, *J* = 7.9 Hz, 1H), 7.77-7.74 (d, *J* = 9.1 Hz, 1H), 7.57-7.52 (t, *J* = 8.7 Hz, 1H), 7.42-7.38 (t, *J* = 7.5 Hz, 1H), 7.24-7.20 (m, 1H), 7.12-7.06 (m, 2H), 7.04-6.99 (t, *J* = 9.1 Hz, 1H), 6.47 (s, 1H), 4.04-4.00 (m, 1H), 3.72 (s, 2H), 3.68-3.56 (m, 4H), 3.49-3.46 (m, 1H), 3.26-3.19 (m, 1H), 2.80-2.75 (m, 2H), 2.72-2.68 (m, 2H), 2.15-2.12 (m, 1H), 1.96 (bs, 2H), 1.74-1.68 (m, 3H), 1.33 (s, 9H); ¹³C NMR (100 MHz, CDCl₃) δ : 169.87, 162.46, 160.02, 154.27, 139.40, 134.77, 131.19, 131.14, 129.53, 128.76, 128.68, 125.26, 125.12, 123.89, 121.83, 121.62,

115.35, 115.13, 62.80, 56.05, 54.73, 51.18, 49.66, 45.83, 30.43, 29.63, 28.50, 27.85, 24.36; HRMS: C₂₈H₃₉O₄N₅FS, Calcd: 560.2701 Found: 560.2708.

(S)-N-(2-((2-(tert-butylcarbamoyl) pyrrolidin-1-yl) sulfonyl) phenyl)-4-(3-fluorobenzyl)-1, 4-diazepane-1-carboxamide 11:

Compound **11** was prepared by following the procedure for the synthesis of **10**. The crude product was purified over a neutral alumina column (70:30 EtOAc/pet ether, R_f 0.5) to afford **11** as a viscous liquid (98%); $[\alpha]_D^{25}$: -41.18° (c 0.23, CHCl₃); IR (CHCl₃) ν (cm⁻¹): 3355, 2967, 1677, 1526, 1340, 1147, 756, 605; ¹H NMR (500 MHz, CDCl₃) δ : 9.17 (s, 1H), 8.56-8.54 (d, *J* = 8.5 Hz, 1H), 7.77-7.75 (d, *J* = 7.8 Hz, 1H), 7.57-7.54 (t, *J* = 7.7 Hz, 1H), 7.27-7.23 (m, 1H), 7.11-7.07 (m, 3H), 6.95 (s, 1H), 6.47 (s, 1H), 4.04-4.01 (m, 1H), 3.72-3.59 (m, 6H), 3.50 (bs, 1H), 3.26-3.21 (m, 1H), 2.74 (bs, 2H), 2.66 (bs, 2H), 2.14 (bs, 1H), 1.95 (s, 2H), 1.76-1.69 (m, 3H), 1.33 (s, 9H); ¹³C NMR (125 MHz, CDCl₃) δ : 169.86, 163.92, 161.97, 154.26, 141.70, 139.41, 134.80, 129.69, 129.55, 124.14, 121.83, 121.75, 121.56, 115.41, 115.24, 114.02, 113.85, 62.78, 61.91, 54.82, 51.18, 49.70, 45.85, 30.46, 28.51, 27.95, 24.36; HRMS: C₂₈H₃₉O₄N₅FS, Calcd: 560.2701 Found: 560.2704.

(S)-N-(2-((2-(tert-butylcarbamoyl) pyrrolidin-1-yl) sulfonyl) phenyl)-4-(4-fluorobenzyl)-1, 4-diazepane-1-carboxamide 12:

Compound **12** was prepared by following the procedure for the synthesis of **10**. The crude product was purified over a neutral alumina column (70:30 EtOAc/pet ether, R_f 0.5) to afford **12** as a viscous liquid (84%); $[\alpha]_D^{25}$: -39.57° (c 0.16, CHCl₃); IR (CHCl₃) ν (cm⁻¹): 3361, 2924, 1677, 1510, 1336, 1147, 759, 608; ¹H NMR (400 MHz, CDCl₃) δ : 9.15 (s, 1H), 8.55-8.53 (d, *J* = 9.3 Hz, 1H), 7.77-7.75 (d, *J* = 9.6 Hz, 1H), 7.57-7.53 (t, *J* = 8.7 Hz, 1H), 7.31-7.26 (m, 2H), 7.11-7.07 (t, *J* = 8.2 Hz, 1H), 6.01-6.96 (t, *J* = 8.7 Hz, 2H), 6.47 (s, 1H), 4.04-3.99 (m, 1H),

3.65–3.58 (m, 6H), 3.50–3.46 (m, 1H), 3.27–3.20 (m, 1H), 2.74–2.70 (m, 2H), 2.66–2.62 (m, 2H), 2.15–2.12 (m, 1H), 1.93 (bs, 2H), 1.76–1.69 (m, 3H), 1.33 (s, 9H); ^{13}C NMR (100 MHz, CDCl_3) δ : 169.89, 163.16, 160.73, 154.28, 139.40, 134.78, 134.41, 130.29, 130.21, 129.55, 121.83, 121.76, 121.58, 115.14, 114.92, 62.76, 61.60, 56.02, 54.69, 51.18, 49.71, 45.92, 30.48, 29.63, 28.50, 27.86, 24.35; HRMS: $\text{C}_{28}\text{H}_{39}\text{O}_4\text{N}_5\text{FS}$, Calcd: 560.2701 Found: 560.2704.

(S)-N-(2-((2-(tert-butylcarbamoyl) pyrrolidin-1-yl) sulfonyl) phenyl)-4-(thiophen-2-ylmethyl)-1, 4-diazepane-1-carboxamide 13:

Compound **13** was prepared by following the procedure for the synthesis of **10**. The crude product was purified over a neutral alumina column (60:40 EtOAc/pet ether, R_f 0.5) to afford **13** as a viscous liquid (78%); $[\alpha]_D^{25}$: -52.42° (c 0.14, CHCl_3); IR (CHCl_3) ν (cm^{-1}): 3356, 2923, 1674, 1534, 1399, 1148, 755, 609; ^1H NMR (500 MHz, CDCl_3) δ : 9.16 (s, 1H), 8.54–8.53 (d, $J = 8.5$ Hz, 1H), 7.78–7.76 (d, $J = 7.8$ Hz, 1H), 7.57–7.54 (t, $J = 7.5$ Hz, 1H), 7.24–7.23 (d, $J = 4.7$ Hz, 1H), 7.11–7.08 (t, $J = 7.5$ Hz, 1H), 6.96–6.93 (dd, $J = 9.5, 4.7$ Hz, 2H), 6.48 (s, 1H), 4.03–4.02 (d, $J = 1.8$ Hz, 1H), 3.90 (s, 1H), 3.68–3.60 (m, 5H), 3.52–3.48 (m, 1H), 3.27–3.21 (m, 1H), 2.81 (bs, 2H), 2.73 (bs, 2H), 2.18–2.12 (m, 1H), 1.98 (bs, 2H), 1.75–1.70 (m, 3H), 1.34 (s, 9H); ^{13}C NMR (125 MHz, CDCl_3) δ : 169.91, 154.28, 139.41, 134.82, 129.59, 126.52, 125.06, 121.89, 121.67, 62.84, 56.99, 54.51, 51.23, 49.73, 30.49, 29.68, 28.56, 24.41; HRMS: $\text{C}_{26}\text{H}_{38}\text{O}_4\text{N}_5\text{S}_2$, Calcd: 548.2360 Found: 548.2368.

(S)-N-(2-((2-(tert-butylcarbamoyl) pyrrolidin-1-yl) sulfonyl) phenyl)-4-(furan-2-carbonyl)-1, 4-diazepane-1-carboxamide 14:

Compound **14** was prepared by following the procedure for the synthesis of **10**. The crude product was purified over a neutral alumina column (70:30 EtOAc/pet ether, R_f 0.5) to afford **14** as a viscous liquid (69%); $[\alpha]_D^{25}$: -43.52° (c 0.22,

CHCl₃); IR (CHCl₃) ν (cm⁻¹): 3359, 2926, 1679, 1531, 1332, 1145, 756, 610; ¹H NMR (400 MHz, CDCl₃) δ : 9.24 (s, 1H), 8.47 (bs, 1H), 7.76-7.74 (d, J = 9.4 Hz, 1H), 7.56-7.52 (t, J = 8.6 Hz, 1H), 7.47 (s, 1H), 7.12-7.04 (m, 2H), 6.46 (s, 2H), 4.00-3.99 (d, J = 5.9 Hz, 1H), 3.86 (bs, 3H), 3.76 (bs, 3H), 3.60 (bs, 2H), 3.51 (bs, 1H), 3.19 (s, 1H), 2.12-2.05 (m, 3H), 1.77-1.65 (m, 3H), 1.32 (s, 9H); ¹³C NMR (100 MHz, CDCl₃) δ : 169.89, 159.71, 153.70, 148.02, 143.91, 138.98, 134.78, 129.53, 122.09, 121.70, 116.92, 111.43, 62.79, 51.20, 49.67, 36.57, 30.55, 29.60, 28.46, 24.32; HRMS: C₂₆H₃₆O₆N₅S, Calcd: 546.2381 Found: 546.2387; C₂₆H₃₅O₆N₅NaS, Calcd: 568.2200 Found: 568.2205.

(S)-N-(2-((2-(tert-butylcarbamoyl) pyrrolidin-1-yl) sulfonyl) phenyl) pyrrolidine-1-carboxamide 15:

Compound **15** was prepared by following the procedure for the synthesis of **10**. The crude product was purified over a neutral alumina column (60:40 EtOAc/pet ether, R_f 0.5) to afford **15** as a viscous liquid (96%); $[\alpha]_D^{25}$: -54.37° (c 0.16, CHCl₃); IR (CHCl₃) ν (cm⁻¹): 3355, 2964, 1680, 1538, 1371, 1146, 757, 608; ¹H NMR (400 MHz, CDCl₃) δ : 9.06 (s, 1H), 8.64-8.62 (d, J = 8.5 Hz, 1H), 7.76-7.74 (d, J = 8.0 Hz, 1H), 7.56-7.52 (t, J = 8.5 Hz, 1H), 7.09-7.05 (t, J = 8.0 Hz, 1H), 6.50 (s, 1H), 4.05-4.02 (m, 1H), 3.54-3.46 (m, 5H), 3.28-3.21 (m, 1H), 2.15-2.12 (m, 1H), 1.96 (s, 4H), 1.78-1.67 (m, 3H), 1.34 (s, 9H); ¹³C NMR (100 MHz, CDCl₃) δ : 169.92, 152.94, 139.43, 134.86, 129.53, 121.58, 121.24, 62.62, 51.16, 49.87, 45.71, 36.31, 30.53, 28.48, 25.49, 24.33; HRMS: C₂₀H₃₁O₄N₄S, Calcd: 423.2061 Found: 423.2063; C₂₀H₃₀O₄N₄NaS, calcd: 445.1880 Found: 445.1882.

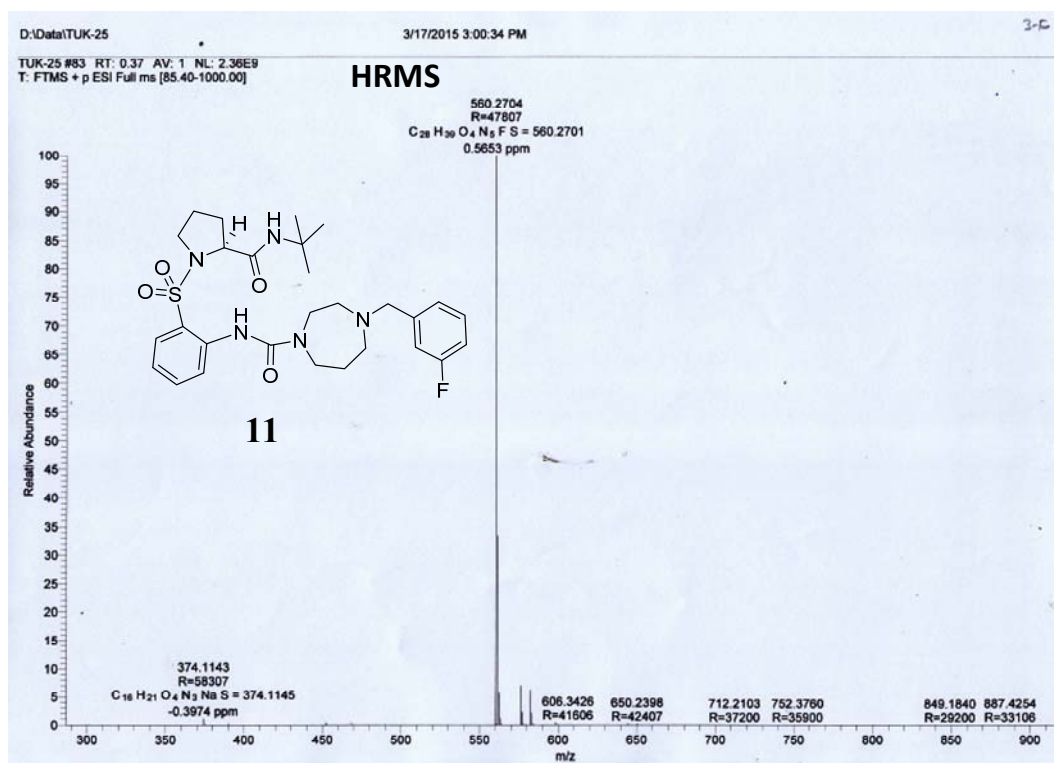
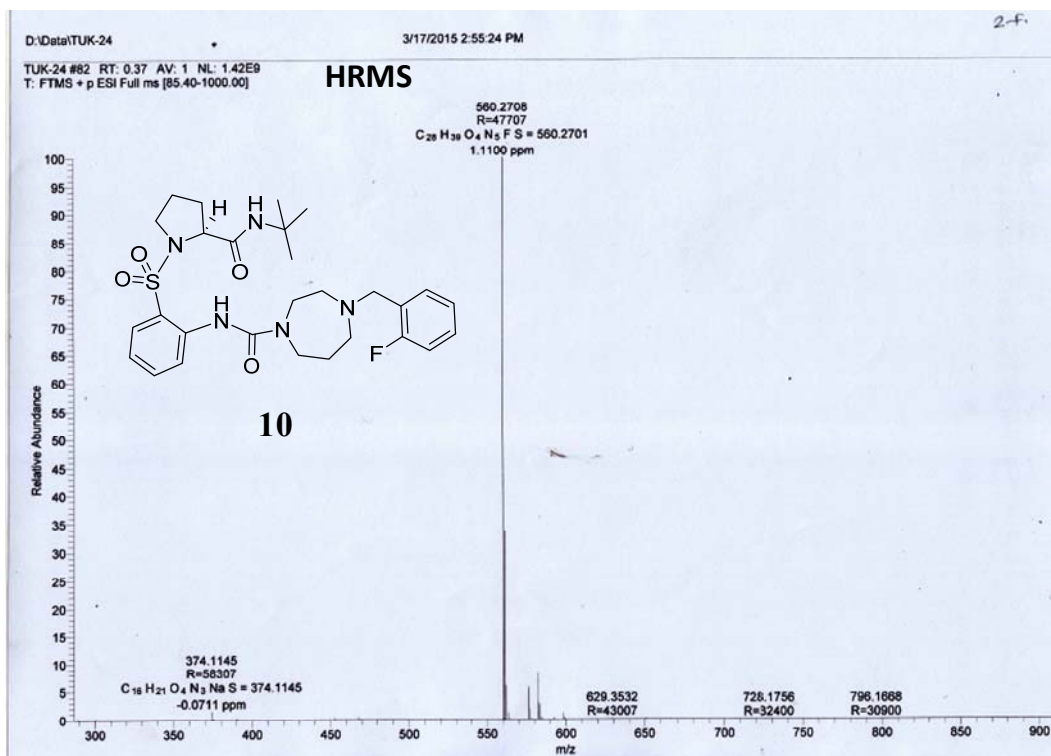
(S)-N-(2-((2-(tert-butylcarbamoyl) pyrrolidin-1-yl) sulfonyl) phenyl) piperidine-1-carboxamide 16:

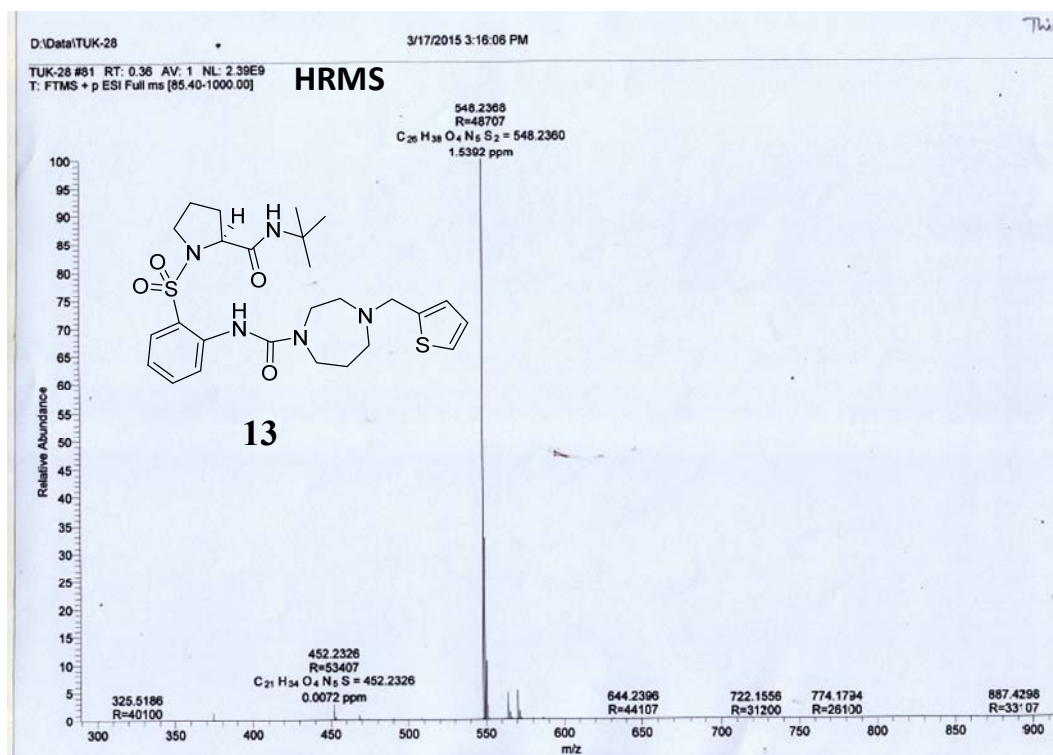
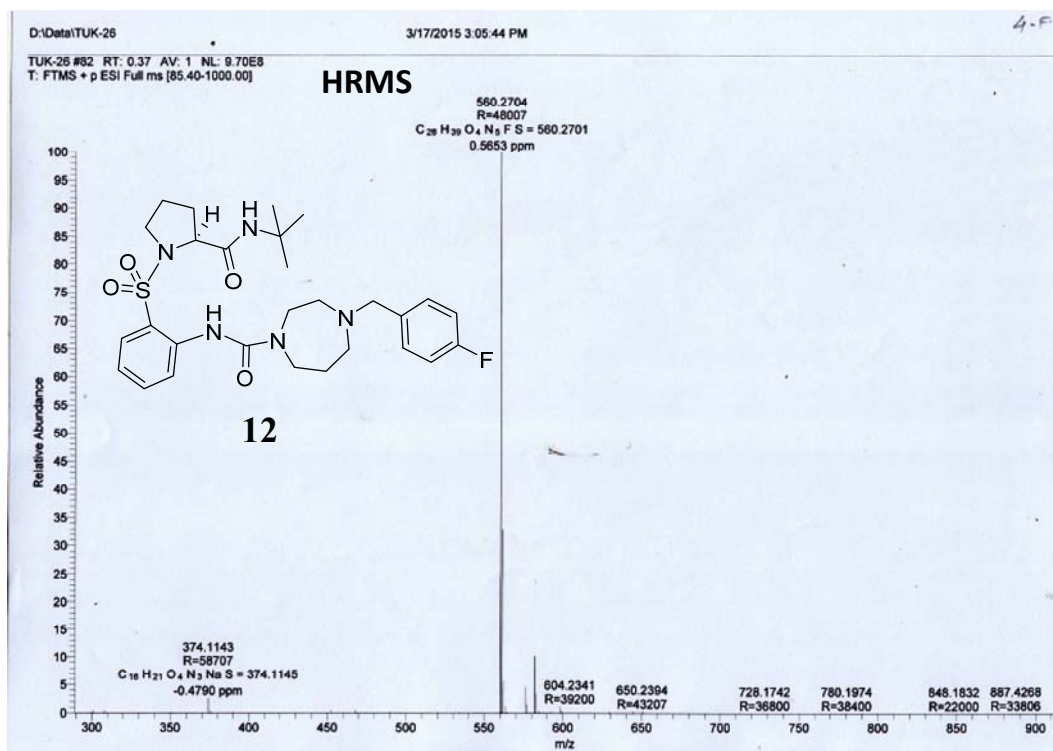
Compound **16** was prepared by following the procedure for the synthesis of **10**. The crude product was purified over a neutral alumina column (60:40 EtOAc/pet

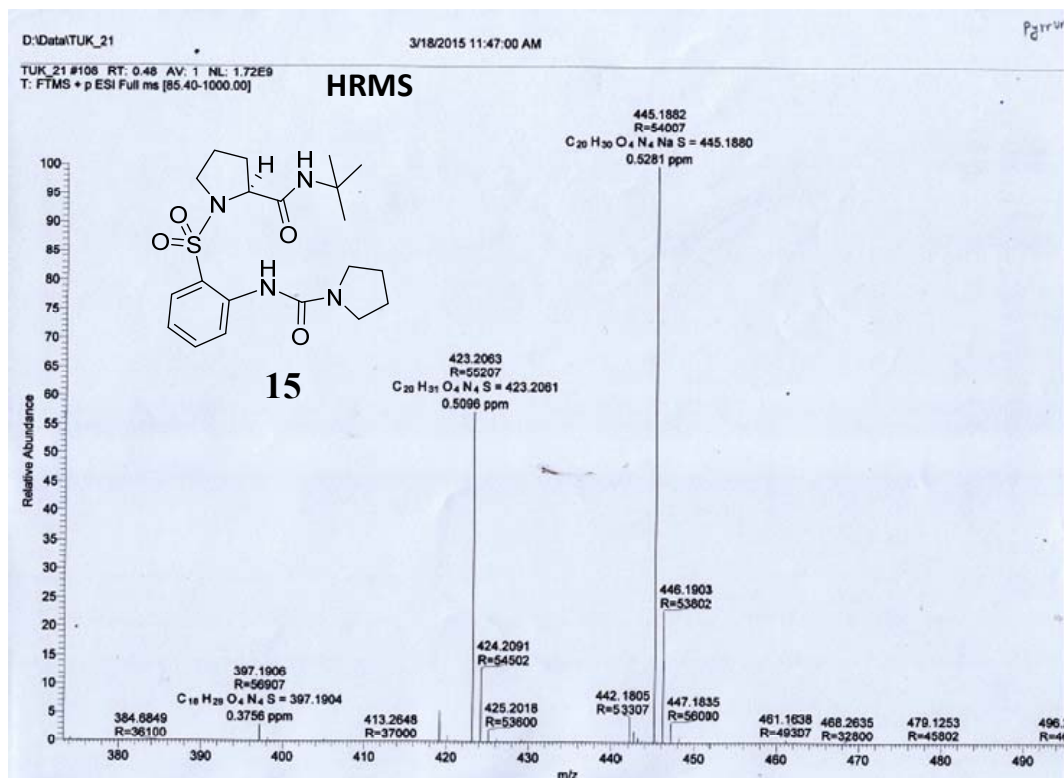
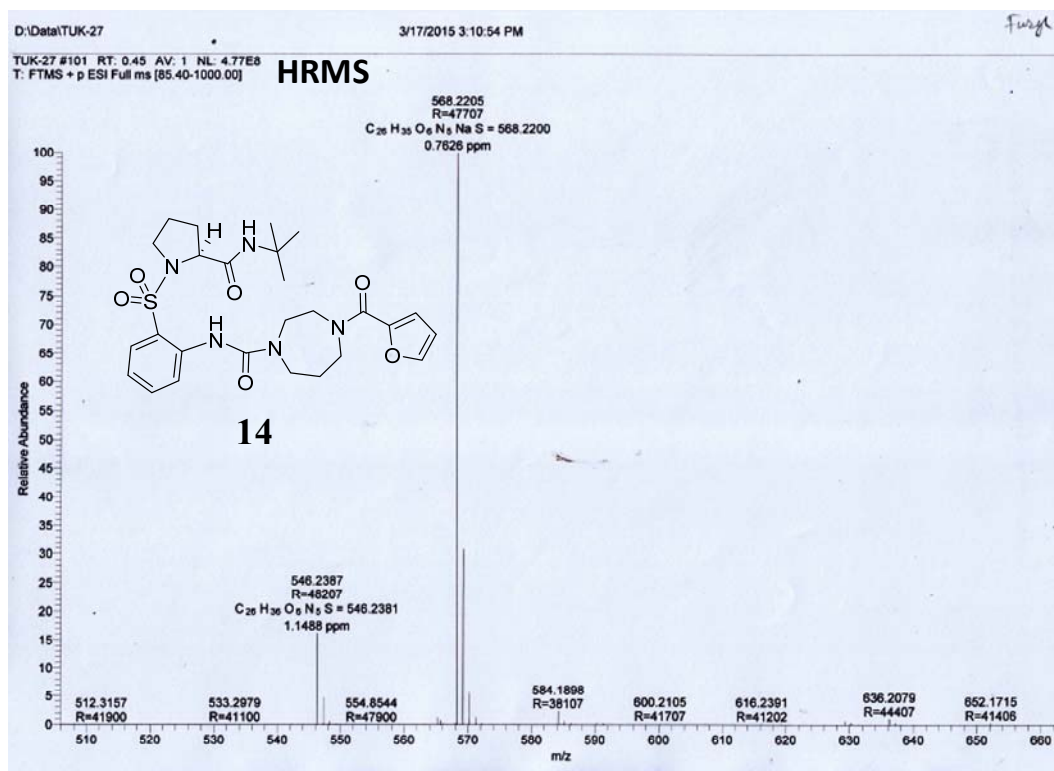
ether, R_f 0.3) to afford **16** as a viscous liquid (85%); $[\alpha]_D^{25}$: -52.98° (c 0.33, CHCl_3); IR (CHCl_3) ν (cm^{-1}): 3371, 2932, 2853, 1681, 1519, 1434, 1335, 1145, 607; ^1H NMR (400 MHz, CDCl_3) δ : 9.16 (s, 1H), 8.47-8.45 (d, $J = 8.5$ Hz, 1H), 7.77-7.75 (d, $J = 9.0$ Hz, 1H), 7.57-7.53 (t, $J = 8.5$ Hz, 1H), 7.11-7.07 (t, $J = 7.6$ Hz, 1H), 6.49 (s, 1H), 4.04-4.02 (m, 1H), 3.53-3.48 (m, 5H), 3.27-3.20 (m, 1H), 2.17-2.14 (m, 1H), 1.77-1.69 (m, 4H), 1.65-1.62 (m, 5H), 1.35 (s, 9H); HRMS: $\text{C}_{21}\text{H}_{33}\text{O}_4\text{N}_4\text{S}$, Calcd: 437.2217 Found: 437.2220.

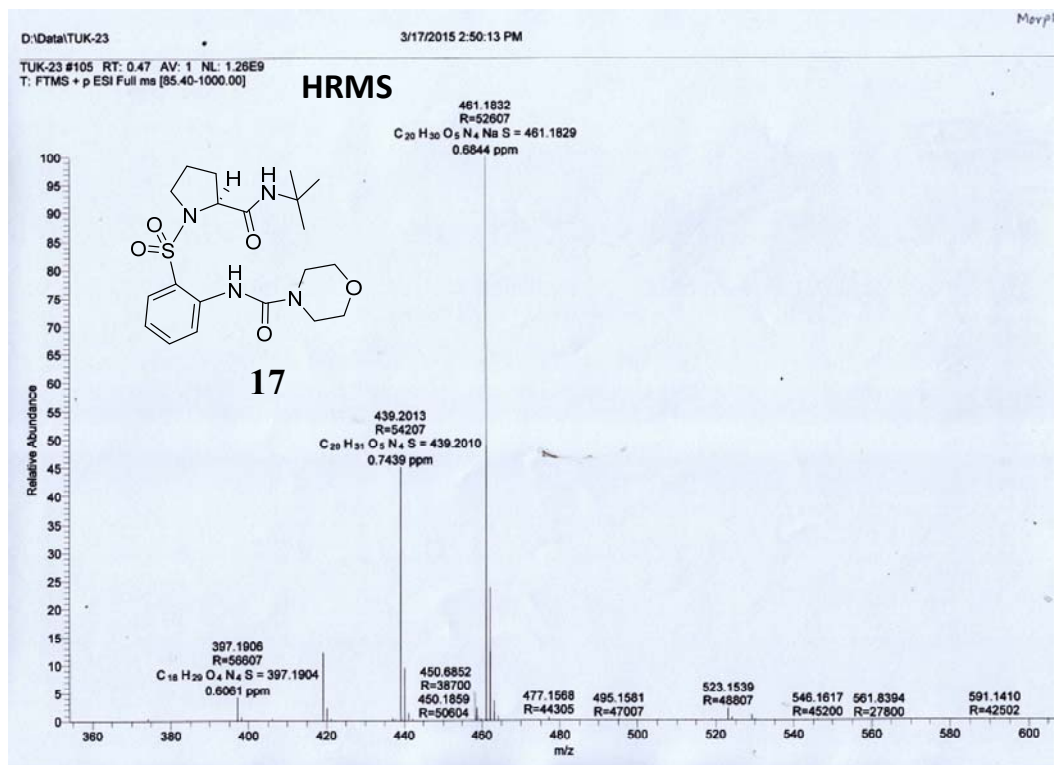
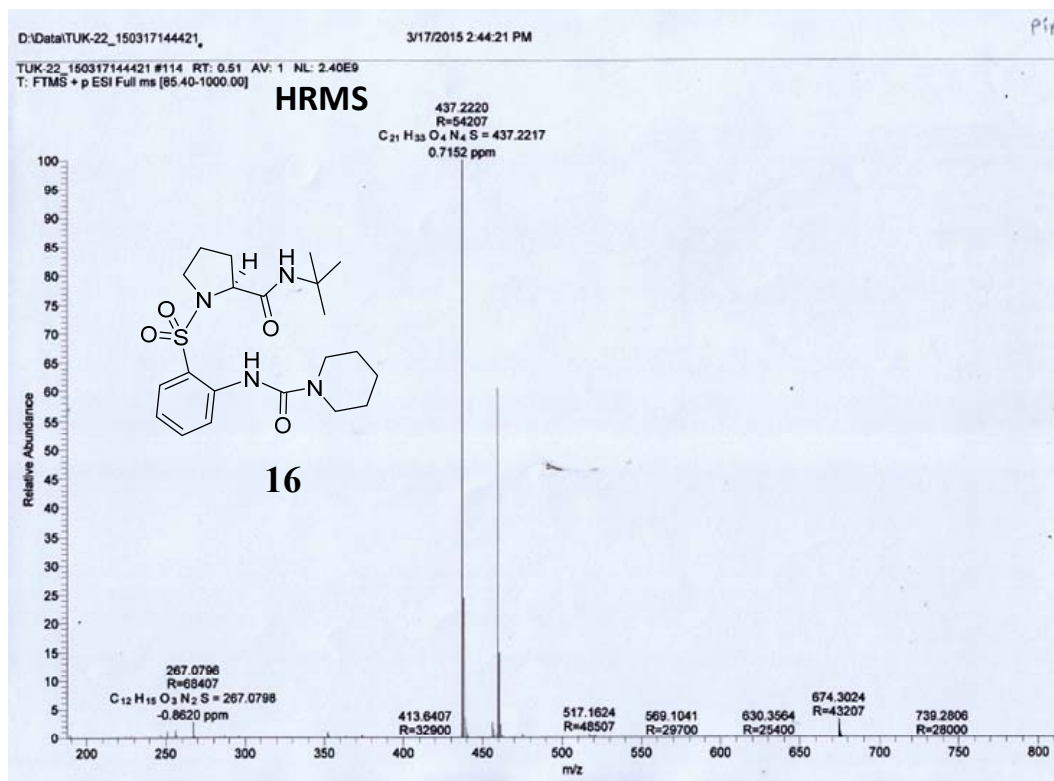
(S)-N-(2-((2-(tert-butylcarbamoyl) pyrrolidin-1-yl) sulfonyl) phenyl) morpholine-4-carboxamide 17:

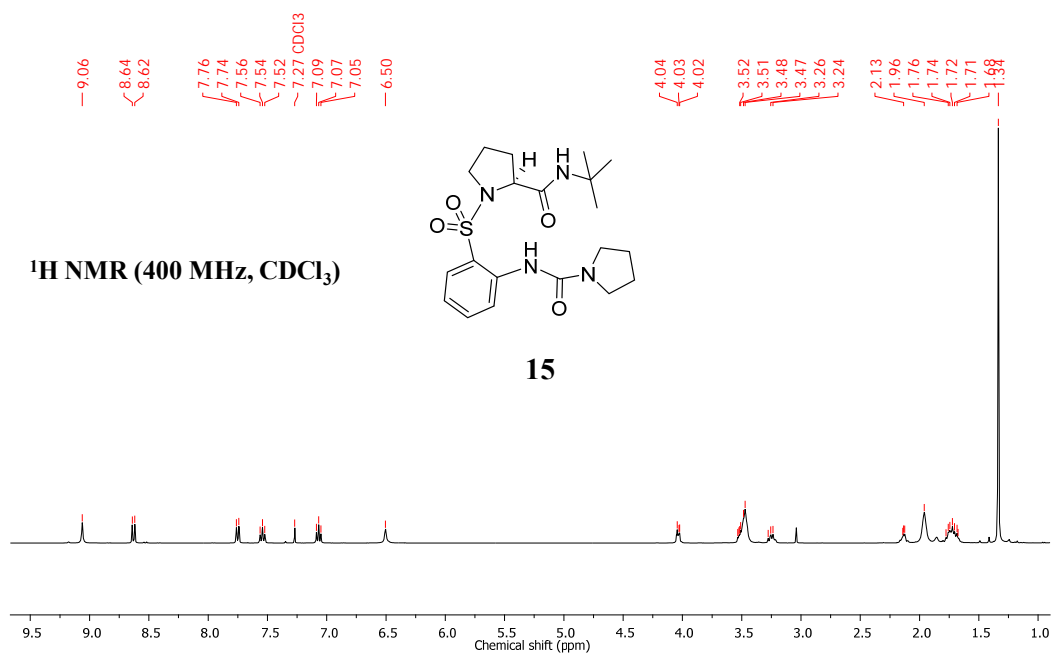
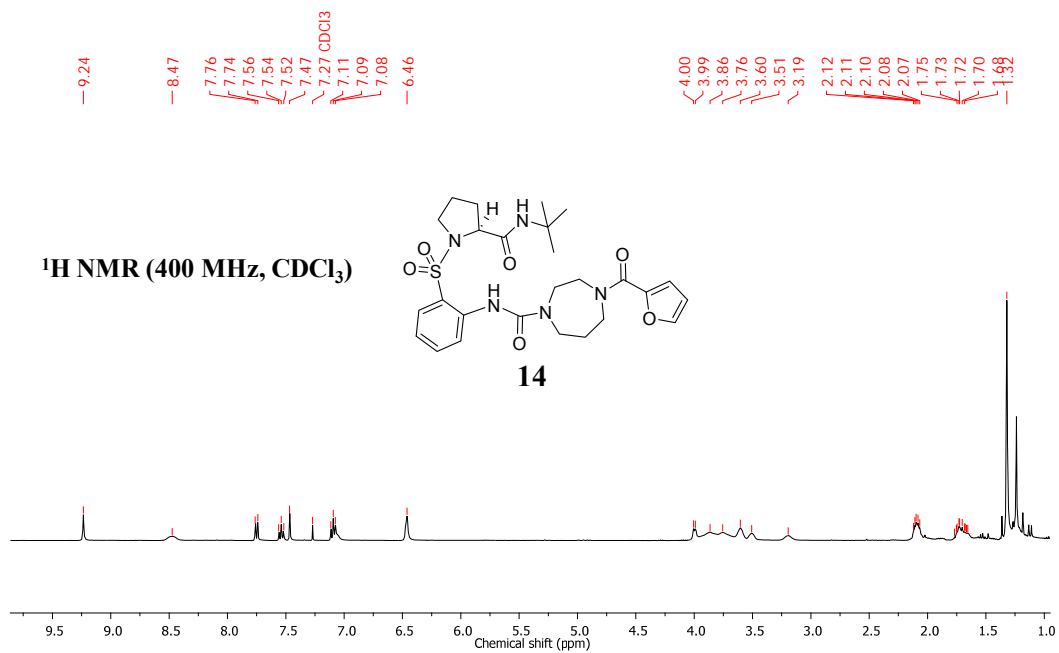
Compound **17** was prepared by following the procedure for the synthesis of **10**. The crude product was purified over a neutral alumina column (70:30 EtOAc/pet ether, R_f 0.3) to afford **17** as a viscous liquid (72%); $[\alpha]_D^{25}$: -42.86° (c 0.1, CHCl_3); IR (CHCl_3) ν (cm^{-1}): 3360, 2963, 2860, 1683, 1530, 1433, 1332, 1118, 761, 609; ^1H NMR (500 MHz, CDCl_3) δ : 9.22 (s, 1H), 8.49-8.47 (d, $J = 8.5$ Hz, 1H), 7.77-7.75 (d, $J = 9.1$ Hz, 1H), 7.58-7.55 (t, $J = 8.5$ Hz, 1H), 7.13-7.10 (t, $J = 7.6$ Hz, 1H), 6.44 (s, 1H), 4.00-3.97 (m, 1H), 3.74-3.72 (t, $J = 4.8$ Hz, 4H), 3.54-3.48 (m, 5H), 3.23-3.18 (m, 1H), 2.13-2.11 (m, 1H), 1.82 (bs, 1H), 1.79-1.74 (m, 2H), 1.70-1.66 (m, 1H), 1.35 (s, 9H); ^{13}C NMR (125 MHz, CDCl_3) δ : 169.88, 153.86, 138.92, 134.85, 129.57, 122.21, 121.85, 121.75, 66.42, 62.71, 51.23, 49.82, 43.94, 30.65, 28.52, 24.34; HRMS: $\text{C}_{20}\text{H}_{31}\text{O}_5\text{N}_4\text{S}$, Calcd: 439.2010 Found: 439.2013; $\text{C}_{20}\text{H}_{30}\text{O}_5\text{N}_4\text{NaS}$, calcd: 461.1829 Found: 461.1832.

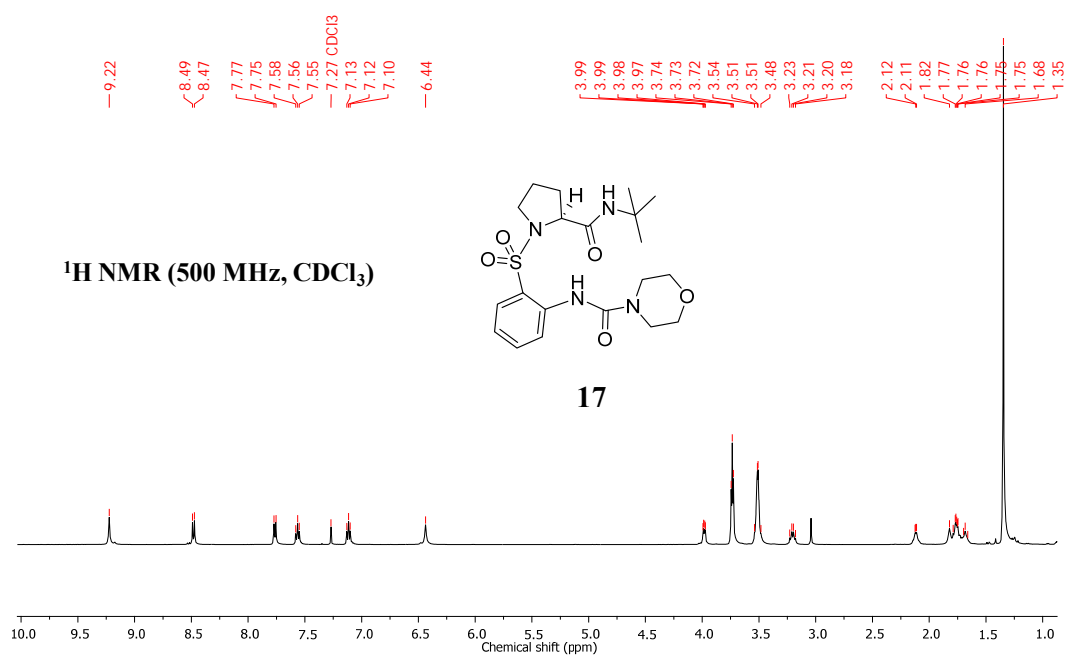
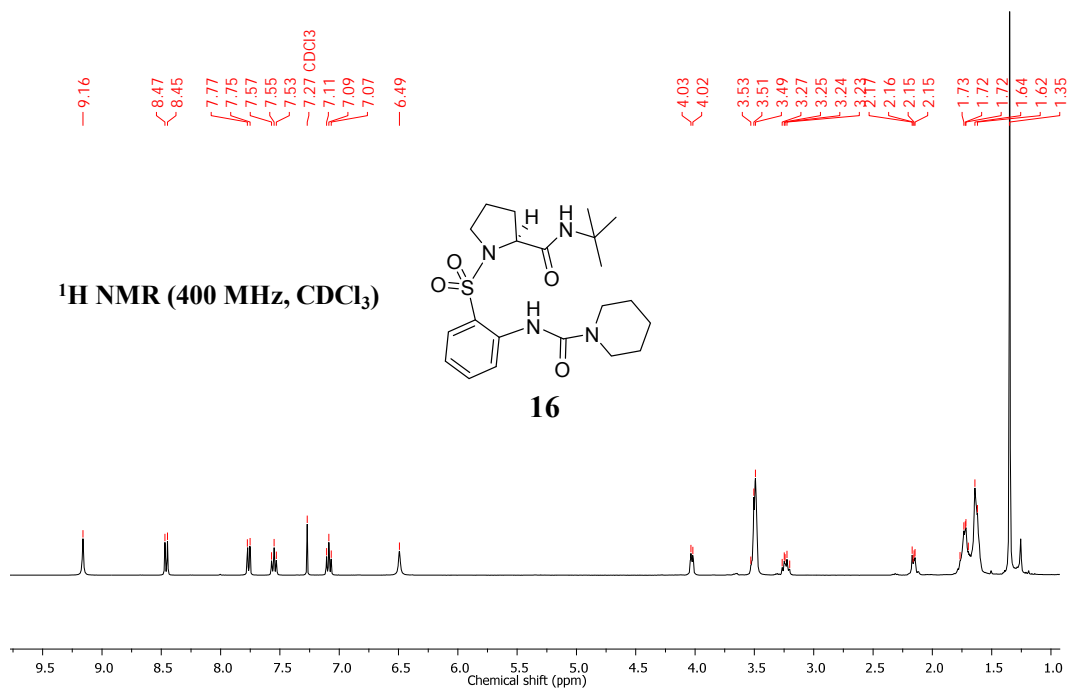


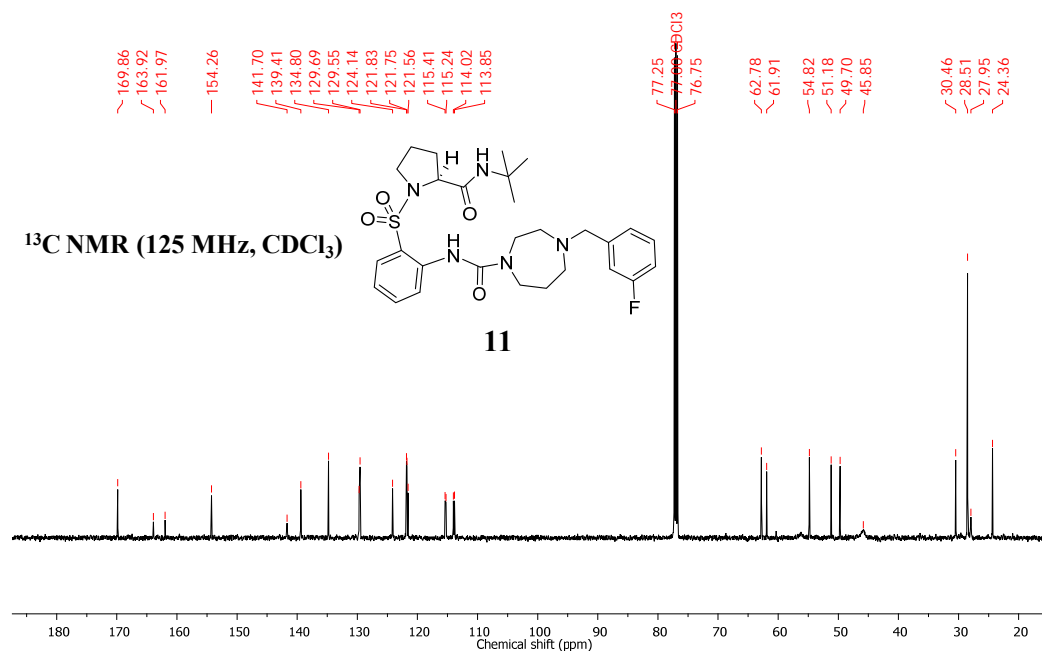
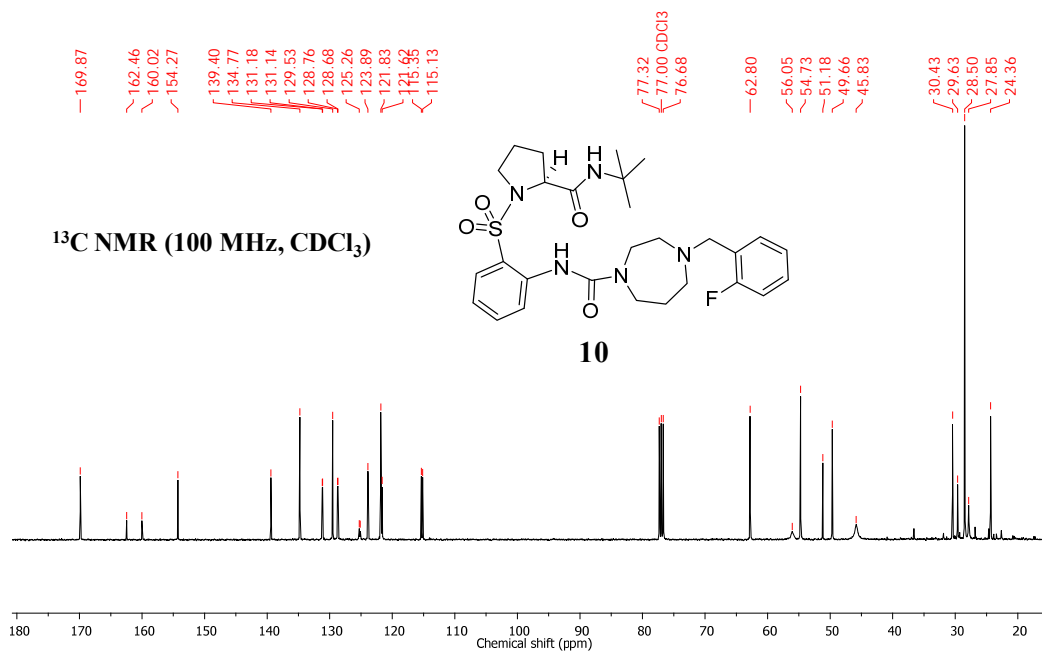


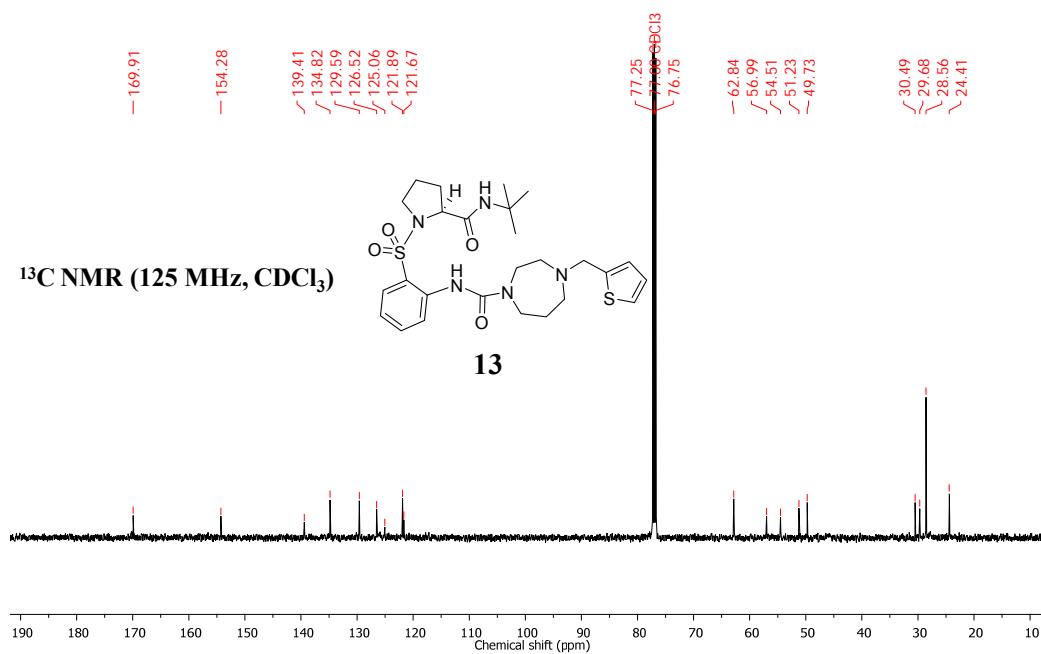
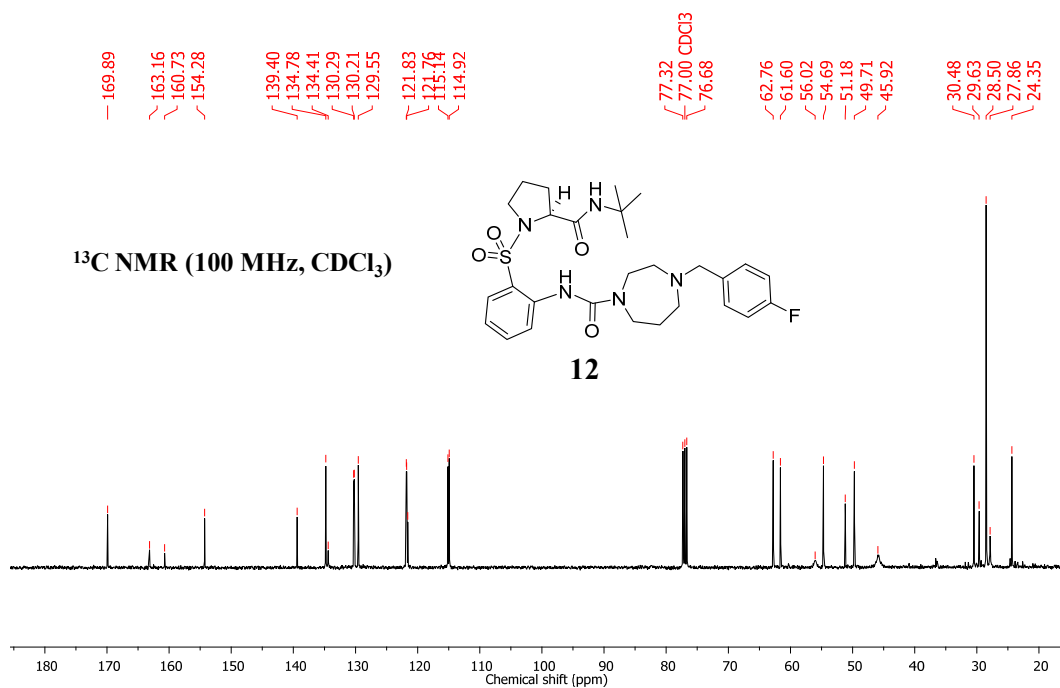


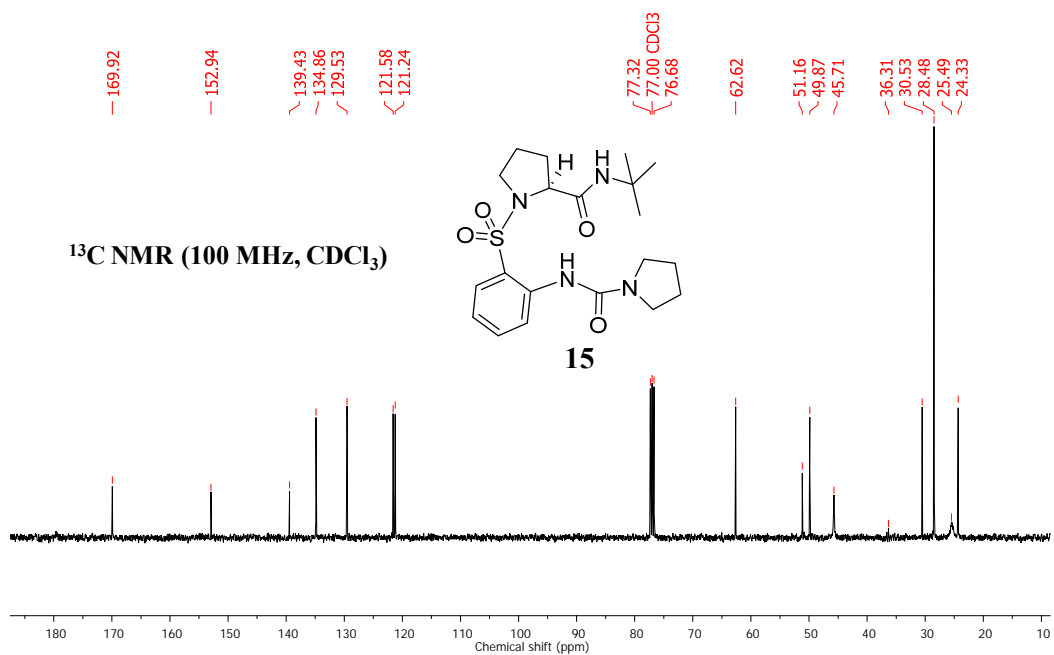
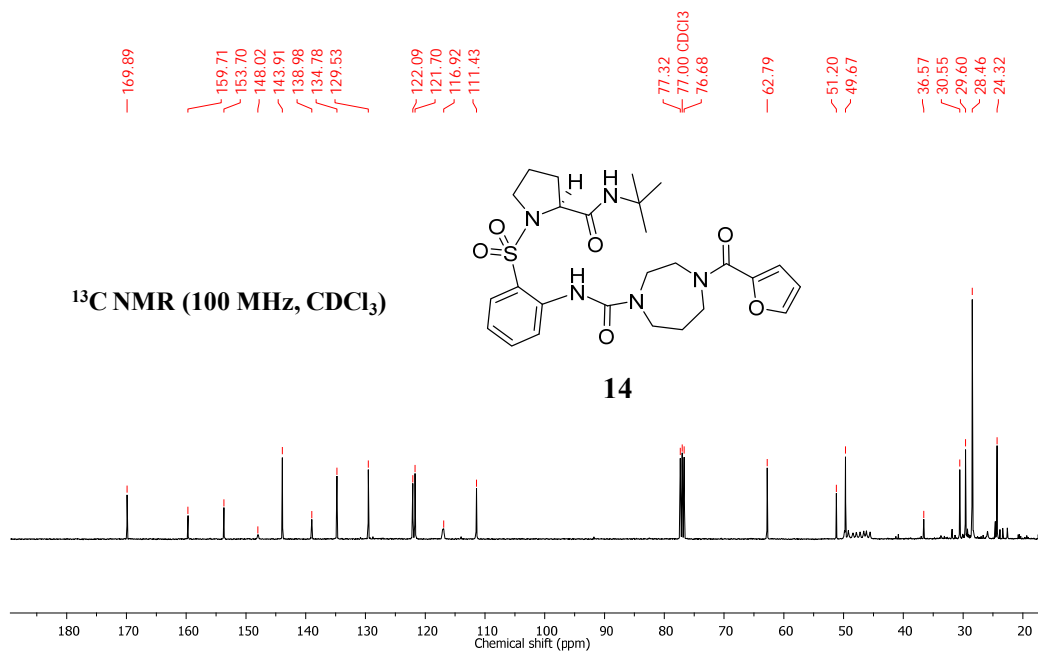


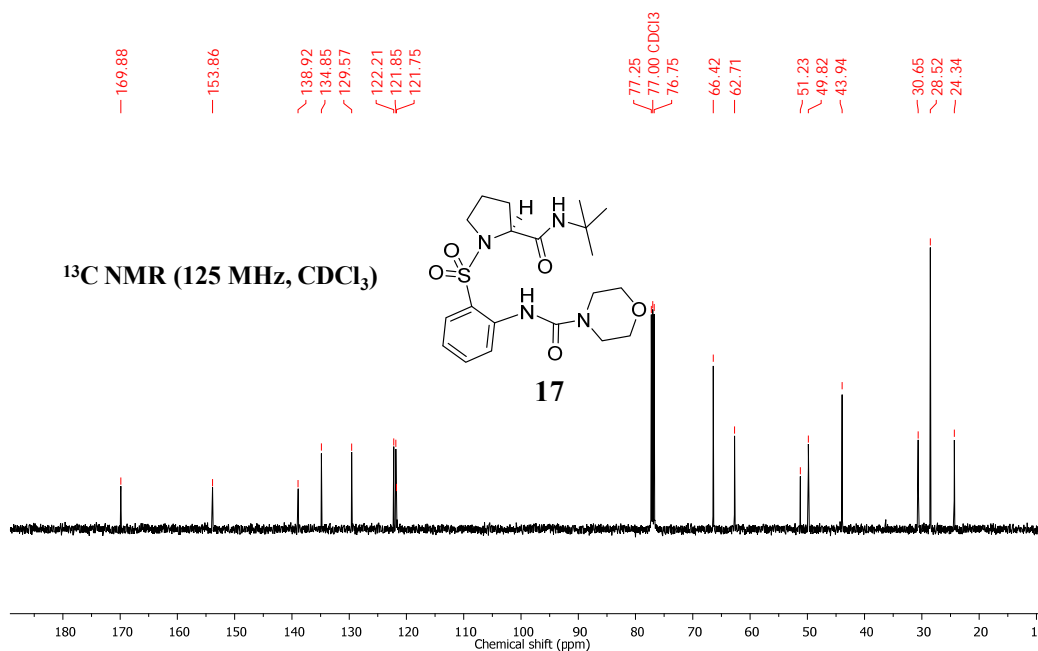
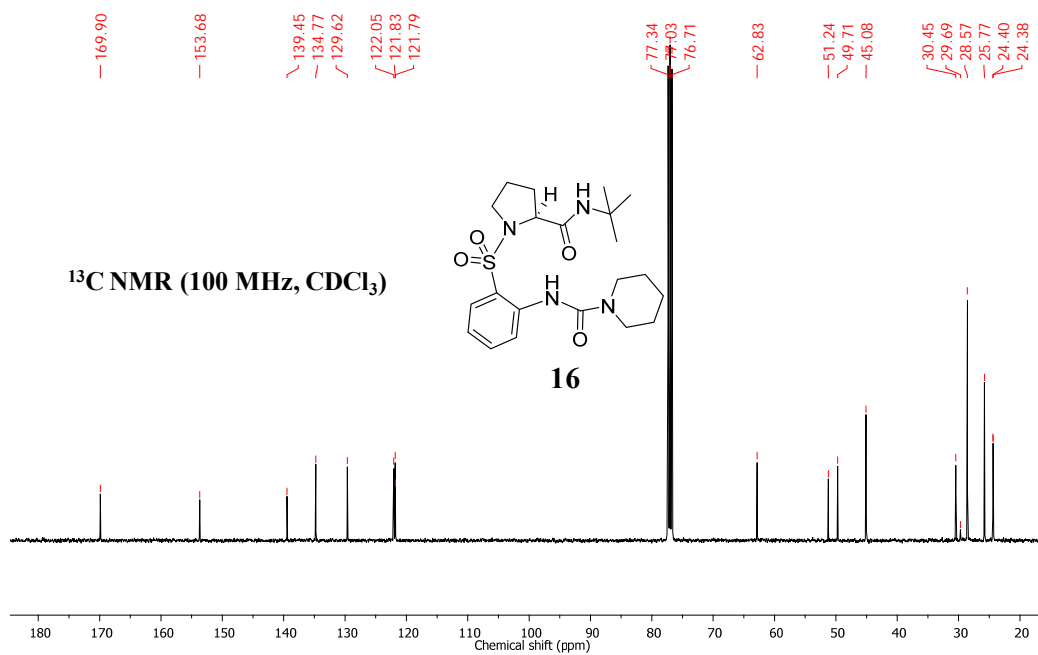












3.15 Experimental section (Part C)

1-isobutyl-3-(prop-2-yn-1-yl) urea **19**:

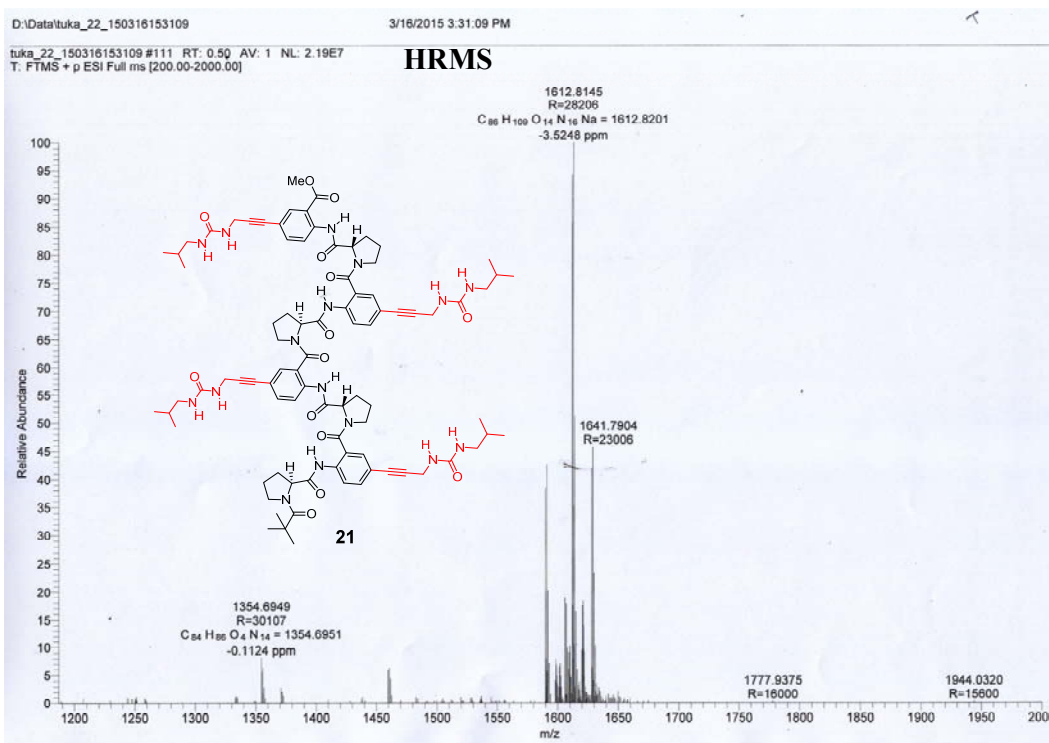
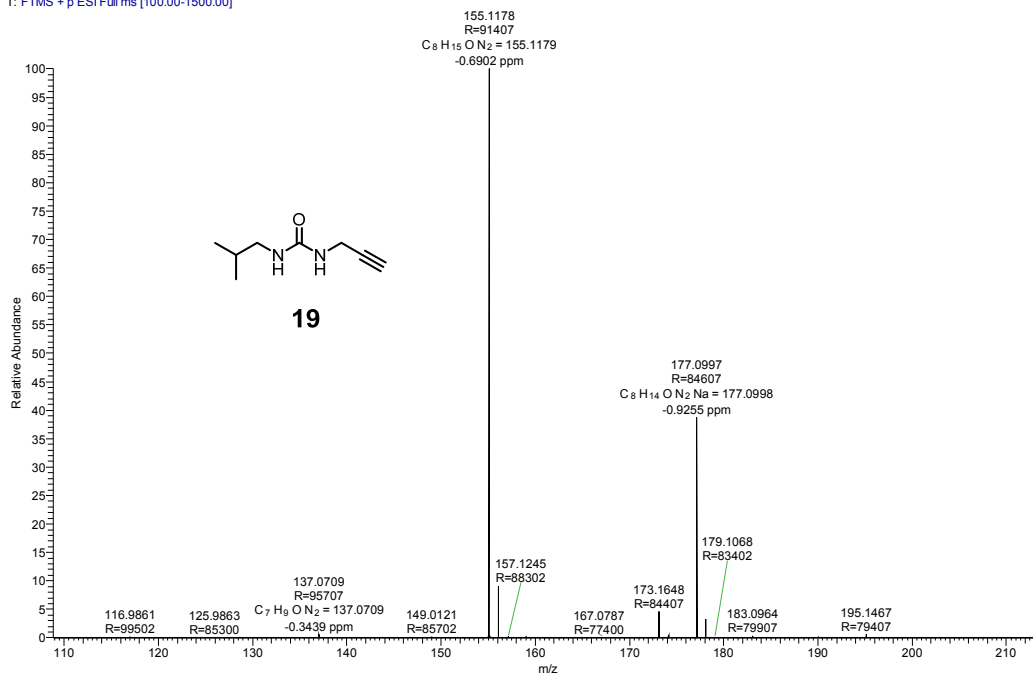
To a solution of trichloroacetic acid (1.58 g, 9.14 mmol) and isobutyl amine (0.736 g, 10 mmol) in dry DCM (50 mL), EDC.HCl (2.63 g, 13.7 mmol) and DMAP (0.57 g, 4.57 mmol) were added. The reaction mixture was stirred overnight at room temperature. The reaction mixture was diluted with DCM (50 mL). The organic layer was washed with water, saturated solution of KHSO₄ and then with brine. The organic layer was dried over Na₂SO₄ and concentrated under vacuum. The crude product **18** was used for the next step without purification. To a solution of **18** (1.58 g, 9.14 mmol) and propargyl amine (0.736 g, 10 mmol) in dry acetonitrile (50 mL), DBU (2.63 g, 13.7 mmol) was added. The reaction mixture was refluxed for 4 h. Then the reaction mixture was cooled and diluted with EtOAc (50 mL). The organic layer was washed with water, saturated solution of KHSO₄ and then with brine. The organic layer was dried over Na₂SO₄ and concentrated under vacuum. The crude product was purified by column chromatography (40:60 EtOAc/pet ether, R_f 0.5) to afford **19** as a white solid (0.86 g, 56%); mp: 48-50 °C; IR (CHCl₃) ν (cm⁻¹): 3343, 3310, 3143, 3040, 1960, 2877, 1631, 1586, 1463, 1430, 1354, 1271, 1052, 917, 654; ¹H NMR (400 MHz, CDCl₃) δ : 5.93 (bs, 1 H), 5.73 (bs, 1 H), 3.95 (dd, *J* = 2.4, 5.4 Hz, 2 H), 3.01-2.92 (m, 2 H), 2.19-2.13 (m, 1 H), 1.77-1.65 (m, 1 H), 0.90 (d, *J* = 6.8 Hz, 6 H); ¹³C NMR (100 MHz, CDCl₃) δ : 158.74, 81.12, 70.60, 47.79, 29.986, 28.94, 20.07; HRMS: C₈H₁₅ON₂, Calcd: 154.1106 Found: 154.1108.

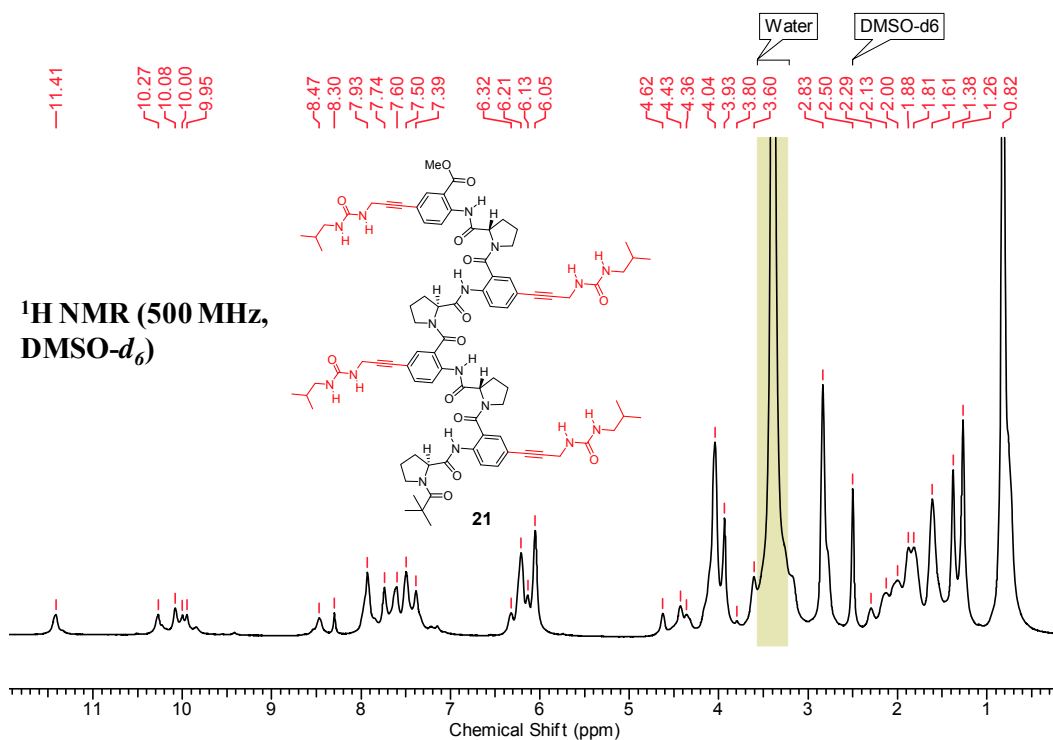
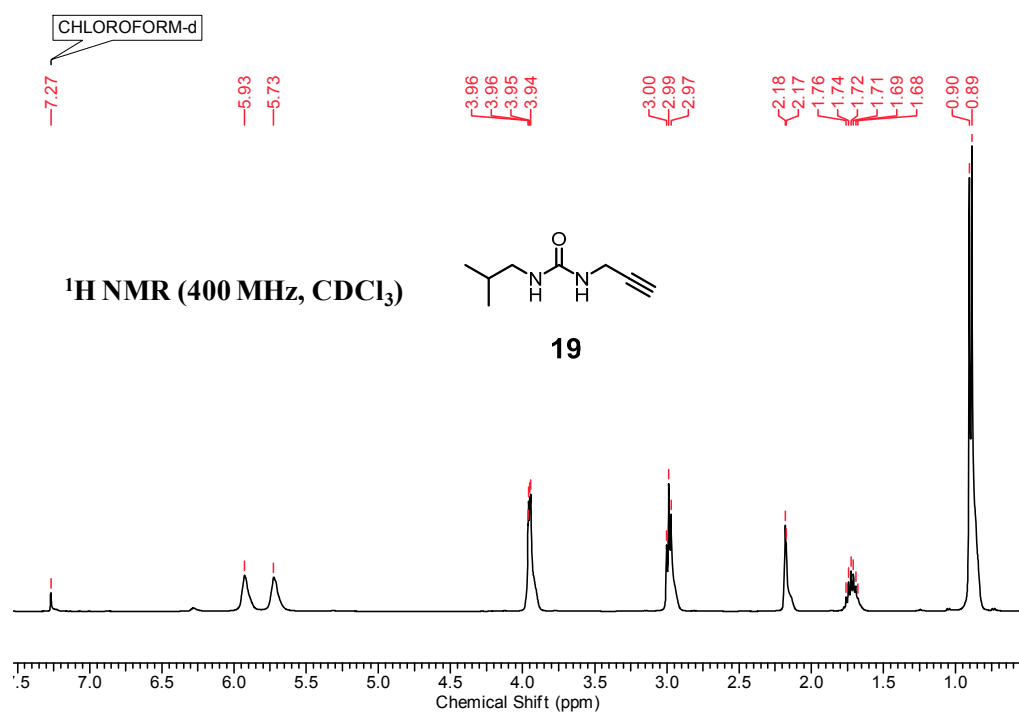
Urea-tethered octapeptide **21**:

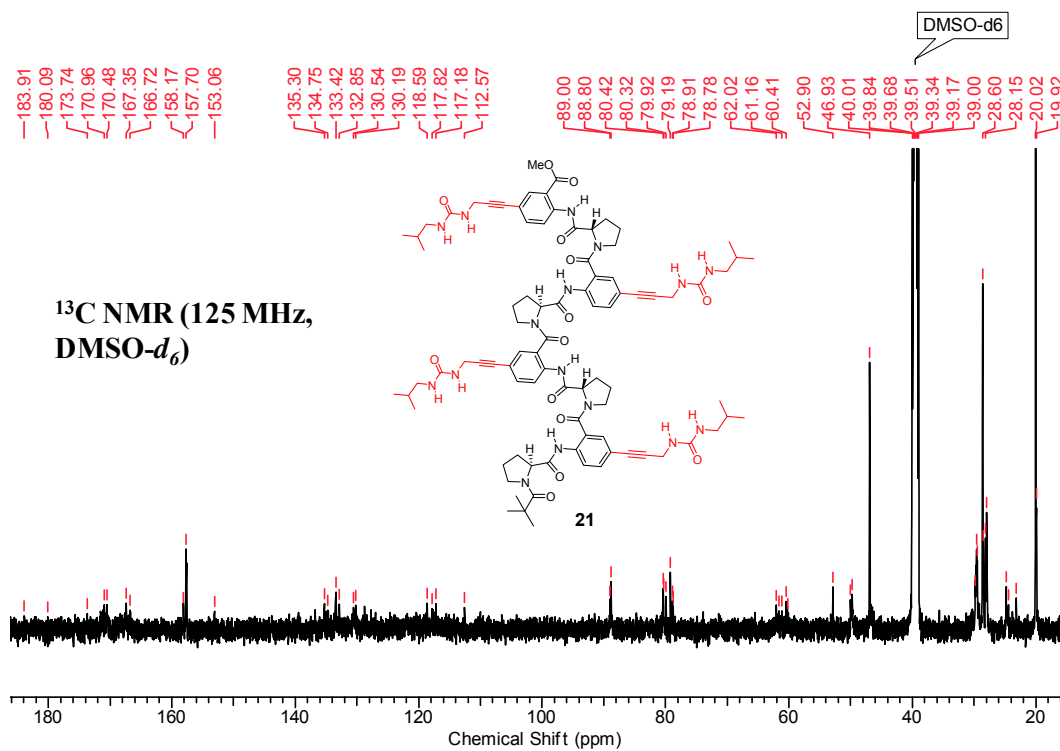
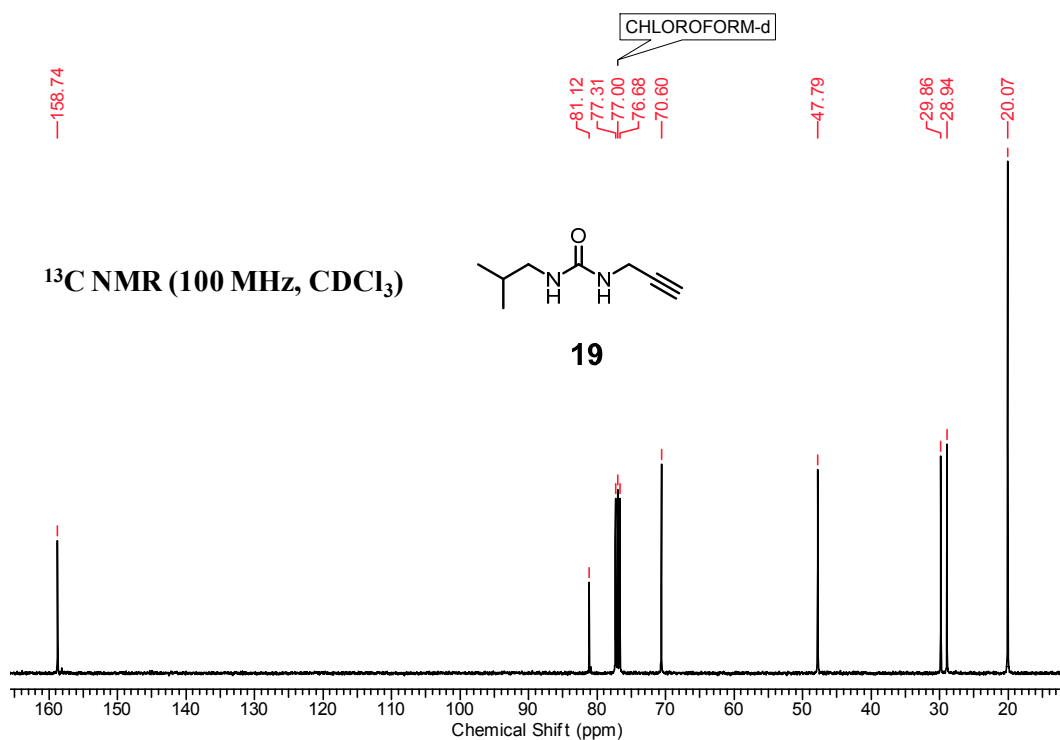
To a solution of **20**⁴⁴ (0.150 g, 0.1 mmol) and **19** (0.09 g, 0.6 mmol) in DMF (2 mL), Et₃N (4 mL) was added under an inert atmosphere. The reaction mixture was

cooled using liquid N₂ and argon was purged. Then the reaction mixture was warmed to room temperature and again purged with argon. The reaction mixture was stirred overnight at room temperature. The reaction mixture was diluted with ethyl acetate (20 mL). The organic layer was washed with water, saturated solution of KHSO₄ and then with brine. The organic layer was dried over Na₂SO₄ and concentrated under vacuum. The crude product was purified by column chromatography (0.8:92 MeOH/EtOAc, R_f 0.4) to afford **21** as a yellow solid (0.096 g, 60%); mp: 182-185 °C; [α]_D²⁶: -35.18° (c 0.1, MeOH); IR (nujol) ν (cm⁻¹): 3390, 2840, 1704, 1641, 1624, 1577, 1462, 1374, 1160, 680; ¹H NMR (500 MHz, DMSO-*d*₆) δ : 11.41 (bs, 1 H), 10.27 (bs, 1 H), 10.26-9.84 (m, 3 H), 8.47-8.30 (m, 1 H), 7.93-7.85 (m, 3 H), 7.74-7.15 (m, 8 H), 6.32-6.05 (m, 8 H), 4.62 (bs, 1 H), 4.43-4.36 (m, 2 H), 4.10-3.93 (m, 9 H), 2.83-2.78 (m, 8 H), 2.32-1.96 (m, 7 H), 1.93-1.74 (m, 7 H), 1.61 (bs, 7 H), 1.38 (bs, 3H), 1.26 (s, 9H), 0.82-0.75 (m, 28 H); ¹³C NMR (125 MHz, DMSO-*d*₆) δ : 183.91, 180.09, 173.74, 170.96, 167.35, 166.72, 158.17, 157.70, 153.06, 135.30, 134.75, 132.85, 130.54, 130.19, 118.59, 117.18, 112.57, 89.00, 88.80, 80.42, 80.32, 79.92, 79.19, 78.91, 78.78, 62.02, 61.16, 60.41, 60.14, 52.90, 50.00, 49.74, 46.93, 29.83, 29.61, 29.49, 28.60, 28.47, 28.15, 27.93, 24.78, 24.45, 23.14, 20.02, 19.92; HRMS: C₈₆H₁₀₉O₁₄N₁₆Na, Calcd: 1612.8201 Found: 1612.8145.

UREA #97 RT: 0.43 AV: 1 NL: 4.76E9
T: FTMS + p ESI Full ms [100.00-1500.00]







3.16 References and notes

- (1) (a) A. M. C. Marcelino and L. M. Gierasch, *Biopolymers*, 2008, **89**, 380; (b) P. Prabakaran, J. Gan, Y.-Q. Wu, M.-Y. Zhang, D. S. Dimitrov and X. Ji, *J. Mol. Biol.*, 2006, **357**, 82; (c) J. D. Puglisi, L. Chyen, S. Blanchard and A. D. Frankel, *Science*, 1995, **270**, 1200; (d) W. S. Somers and S. E. Phillips, *Nature*, 1992, **359**, 387; (e) J. L. Crawford, W. N. Lipscomb and C. G. Schellman, *Proc. Natl. Acad. Sci. U. S. A.*, 1973, **70**, 538.
- (2) (a) D. Obrecht, E. Chevalier, K. Moehle and J. A. Robinson, *Drug Discovery Today: Technol.*, 2012, **9**, e63; (b) R. M Hughes and M. L Waters, *Curr. Opin. Struct. Biol.*, 2006, **16**, 514; (c) C. E. Stotz and E. M. Topp, *J. Pharm. Sci.*, 2004, **93**, 2881; (d) C. Ritter, M-L. Maddelein, A. B. Siemer, T. Luhrs, M. Ernst, B. H. Meier, S. J. Saupe and R. Riek, *Nature*, 2005, **435**, 844; (e) T. A. Petkova, Y. Ishii, J. J. Balbach, O. N. Antzutkin, R. D. Leapman, F. Delaglio and R. Tycko, *Proc. Natl. Acad. Sci. U.S.A.*, 2002, **99**, 16742.
- (3) (a) F. Bachle, J. Duschmale, C. Ebner, A. Pfaltz and H. Wennemers, *Angew. Chem. Int. Ed.*, 2013, **52**, 12619; (b) K. W. Fiori, A. L. A. Puchlopek and S. J. Miller, *Nat. Chem.*, 2009, **1**, 630; (c) E. A. C. Davie, S. M. Mennen, Y. Xu and S. J. Miller, *Chem. Rev.*, 2007, **107**, 5759; (d) C. M. Rufo, Y. S. Moroz, O. V. Moroz, J. Stohr, T. A. Smith, X. Hu, W. F. DeGrado and I. V. Korendovych, *Nat. Chem.*, 2014, **6**, 303; (e) D. R. Kelly and S. M. Roberts, *Biopolymers (Pept. Sci.)*, 2006, **84**, 74; (f) A. Berkessel, B. Koch, C. Toniolo, M. Rainaldi, Q. B. Broxterman and B. Kaptein, *Biopolymers (Pept. Sci.)*, 2006, **84**, 90; (g) (a) Scott J. Miller, *Acc. Chem. Res.*, 2004, **37**, 601.
- (4) (a) C. M. Micklitsch, S. H. Medina, T. Yucel, K. J. Nagy-Smith, D. J. Pochan and J. P. Schneider, *Macromolecules*, 2015, **48**, 1281; (b) P. J. Knerr, M. C. Branco, R. Nagarkar, D. J. Pochan and J. P. Schneider, *J. Mater. Chem.*, 2012, **22**, 1352.
- (5) (a) S. H. Gellman, *Curr. Opin. Chem. Biol.*, 1998, **2**, 717; (b) E. Lacroix, T. Kortemme, M. L. de la Paz and L. Serrano, *Curr. Opin. Struct. Biol.*, 1999, **9**, 487.

-
- (6) (a) G. J. Sharman and M. S. Searle, *J. Am. Chem. Soc.*, 1998, **120**, 5291;
(b) H. L. Schenck and S. H. Gellman, *J. Am. Chem. Soc.*, 1998, **120**, 4869;
(c) T. Kortemme, J. Ramirez-Alvarado and L. Serrano, *Science*, 1998, **281**, 253; (d) C. Das, S. Raghothama and P. Balaram, *J. Am. Chem. Soc.*, 1998, **120**, 5812.
- (7) H. Diaz and J. W. Kelly, *Tetrahedron Lett.*, 1991, **32**, 5725.
- (8) G. Wagner and M. Feigel, *Tetrahedron*, 1993, **49**, 10831.
- (9) M. J. Winningham and D. Y. Sogah, *J. Am. Chem. Soc.*, 1994, **116**, 11173.
- (10) (a) J. S. Nowick, E. M. Smith and G. Noronha, *J. Org. Chem.*, 1995, **60**, 7386; (b) J. S. Nowick and S. Insaf, *J. Am. Chem. Soc.*, 1997, **119**, 10903; (c) J. S. Nowick, *Acc. Chem. Res.*, 1999, **32**, 287.
- (11) D. Ranganathan, V. Haridas, S. Kurur, A. Thomas, K. P. Madhusudanan, R. Nagaraj, A. C. Kunwar, A. V. S. Sarma and I. L. Karle, *J. Am. Chem. Soc.*, 1998, **120**, 8448.
- (12) (a) M. G. Woll, J. R. Lai, I. A. Guzei, S. J. C. Taylor, M. E. B. Smith and S. H. Gellman, *J. Am. Chem. Soc.*, 2001, **123**, 11077; (b) J. M. Langenhan, I. A. Guzei and S. H. Gellman, *Angew. Chem. Int. Ed.*, 2003, **42**, 2402.
- (13) F. Freire, J. D. Fisk, A. J. Peoples, M. Ivancic, I. A. Guzei and S. H. Gellman, *J. Am. Chem. Soc.*, 2008, **130**, 7839.
- (14) A. K. Medda, C. M. Park, A. Jeon, H. Kim, J.-H. Sohn and H.-S. Lee, *Org. Lett.*, 2011, **13**, 3486.
- (15) S. Chowdhury, G. Schatte, H.-B. Kraatz, *Angew. Chem. Int. Ed.*, 2008, **47**, 7056.
- (16) C. R. Jones, M. K. N. Qureshi, F. R. Truscott, S. T. D. Hsu, A. J. Morrison and M. D. Smith, *Angew. Chem. Int. Ed.*, 2008, **47**, 7099.
- (17) C. R. Jones, G. D. Pantos, A. J. Morrison and M. D. Smith, *Angew. Chem. Int. Ed.*, 2009, **48**, 7391.
- (18) (a) K. N. Vijayadas, H. C. Davis, A. S. Kotmale, R. L. Gawade, V. G. Puranik, P. R. Rajamohan and G. J. Sanjayan, *Chem. Commun.*, 2012, **48**, 9747; (b) P. Prabhakaran, S. S. Kale, V. G. Puranik, P. R. Rajamohan, O. Chetina, J. A. K. Howard, H. J. Hofmann and G. J. Sanjayan, *J. Am. Chem. Soc.*, 2008, **130**, 17743.
- (19) D. Gryko and R. Lipinski, *Eur. J. Org. Chem.*, 2006, 3864.
-

-
- (20) C. T. Supuran, *I. Drugs*, 2002, **5**, 1075.
- (21) J. Drew, *Science*, 2000, **287**, 1960.
- (22) (a) C. T. Supuran and A. Scozzafava, *Curr. Med. Chem.- Imm. Endoc. Metab. Agents*, 2001, **1**, 61; (b) C. T. Supuran and A. Scozzafava, *Exp. Opin. Ther. Patents*, 2002, **12**, 217; (c) C. T. Supuran, A. Scozzafava and A. Casini, *Med. Res. Rev.*, 2003, **23**, 146.
- (23) A. E. Boyd, *Diabetes*, 1988, **37**, 847.
- (24) (a) C. T. Supuran, C. W. Conroy and T. H. Maren, *Eur. J. Med. Chem.*, 1996, **31**, 843; (b) T. H. Maren, *Annu. Rev. Pharmacol. Toxicol.*, 1976, **16**, 309.
- (25) C. W. Thornber, *Chem. Soc. Rev.*, 1979, **8**, 563.
- (26) (a) A. Scozzafava and C. T. Supuran, *J. Med. Chem.*, 2000, **43**, 3677; (b) C. T. Supuran, A. Scozzafava and B. W. Clare, *Med. Res. Rev.*, 2002, **22**, 329.
- (27) H. Koshio, F. Hirayama, T. Ishihara, H. Kaizawa, T. Shigenaga, Y. Taniuchi, K. Sato, Y. Moritani, Y. Iwatsuki, T. Uemura, S. Kaku, T. Kawasaki, Y. Matsumoto, S. Sakamoto and S.-I Tsukamoto, *Bioorg. Med. Chem.*, 2004, **12**, 5415.
- (28) A. G. Cole, I. L. Stroke, M.-R. Brescia, S. Simhadri, J. J. Zhang, Z. Hussain, M. Snider, C. Haskell, S. Ribeiro, K. C. Appell, I. Henderson and M. L. Webb, *Bioorg. Med. Chem. Lett.*, 2006, **16**, 200.
- (29) D. B. Whitman, C. D. Cox, M. J. Breslin, K. M. Brashear, J. D. Schreier, M. J. Bogusky, R. A. Bednar, W. Lemaire, J. G. Bruno, G. D. Hartman, D. R. Reiss, C. M. Harrell, R. L. Kraus, Y. Li, S. L. Garson, S. M. Doran, T. Prueksaritanont, C. Li, C. J. Winrow, K. S. Koblan, J. J. Renger and P. J. Coleman, *ChemMedChem*, 2009, **4**, 1069.
- (30) D. Riether, L. Wu, P. F. Cirillo, A. Berry, E. R. Walker, M. Ermann, B. Noya-Marino, J. E. Jenkins, D. Albaugh, C. Albrecht, M. Fisher, M. J. Gemkow, H. Grbic, S. Lobbe, C. Moller, K. O'Shea, A. Sauer, D.-T. Shih and D. S. Thomson, *Bioorg. Med. Chem. Lett.*, 2011, **21**, 2011.
- (31) (a) Shuguang Zhang, *Nat. Biotechnol.*, 2003, **21**, 1171; (b) E. Gazit, *Chem. Soc. Rev.*, 2007, **36**, 1263; (c) S. Kim and C. B. Park, *Adv. Funct. Mater.*, 2013, **23**, 10; (d) I. W. Hamley, *Angew. Chem. Int. Ed.*, 2014, **53**, 2; (e) X.

- Yan, P. Zhua and J. Li, *Chem. Soc. Rev.*, 2010, **39**, 1877; (f) S. Fleming and R. V. Ulijn, *Chem. Soc. Rev.*, 2014, **43**, 8150; (g) X. Zhao, S. Zhang, *Chem. Soc. Rev.*, 2006, **35**, 1105; (h) R. V. Ulijn and A. M. Smith, *Chem. Soc. Rev.*, 2008, **37**, 664.
- (32) (a) P. Koley, A. Gayen, M. G. B. Drew, C. Mukhopadhyay and A. Pramanik, *Small*, 2012, **8**, 984; (b) J. Naskar, A. Banerjee, *Chem. Asian. J.*, 2009, **4**, 1817; (c) X. Yan, Y. Cui, W. Qi, Y. Su, Y. Yang, Q. He, J. Li, *Small*, 2008, **4**, 1687.
- (33) (a) E. Gazit, *Nat. Chem.*, 2010, **2**, 1010; (b) R. J. Williams, A. M. Smith, R. Collins, N. Hodson, A. K. Das and R. V. Ulijn, *Nat. Nanotechnol.*, 2009, **4**, 19; (c) D. W. P. M. Lowik, E. H. P. Leunissen, M. van den Heuvel, M. B. Hansen and J. C. M. van Hest, *Chem. Soc. Rev.*, 2010, **39**, 3394; (d) M. Reches and E. Gazit, *Nano Lett.*, 2004, **4**, 581.
- (34) M. Zelzer and R. V. Ulijn, *Chem. Soc. Rev.*, 2010, **39**, 3351; M. Reches and E. Gazit, *Nano Lett.*, 2004, **4**, 581; R. J. Williams, A. M. Smith, R. Collins, N. Hodson, A. K. Das and R. V. Ulijn, *Nat. Nanotechnol.*, 2009, **4**, 19; H. X. Xu, A. K. Das, M. Horie, M. S. Shaik, A. M. Smith, Y. Luo, X. F. Lu, R. Collins, S. Y. Liem, A. M. Song, P. L. A. Popelier, M. L. Turner, P. Xiao, I. A. Kinloch and R. V. Ulijn, *Nanoscale*, 2010, **2**, 960.
- (35) (a) L.-Y. You, G.-T. Wang, X.-K. Jiang, Z.-T. Li, *Tetrahedron*, 2009, **65**, 9494; (b) J. Dua and R. K. O'Reilly, *Soft Matter*, 2009, **5**, 3544.
- (36) I. W. Hamley and V. Castelletto, *Angew. Chem. Int. Ed.*, 2007, **46**, 4442.
- (37) (a) T. M. Allen and P. R. Cullis, *Science*, 2004, **303**, 1818; (b) D. E. Discher and A. Eisenberg, *Science*, 2002, **297**, 967.
- (38) M. Lee, S.-J. Lee and L.-H. Jiang, *J. Am. Chem. Soc.*, 2004, **126**, 12724.
- (39) S. Zhou, C. Burger, B. Chu, M. Sawamura, N. Nagahama, M. Toganoh, U. E. Hackler, H. Isobe and E. Nakamura, *Science*, 2001, 291, 1944.
- (40) Y. Zhou and D. Yan, *Angew. Chem. Int. Ed.*, 2004, **43**, 4896.
- (41) C. W. Lim, O. Crespo-Biel, M. C. A. Stuart, D. N. Reinhoudt, J. Huskens and B. J. Ravoo, *Proc. Natl. Acad. Sci. U.S.A.*, 2007, **104**, 6986.
- (42) A. Ajayaghosh, R. Varghese, V. K. Praveen, S. Mahesh, *Angew. Chem. Int. Ed.*, 2006, **45**, 3261.
- (43) S. Alam, J. J. Panda and V. S Chauhan, *Int. J. Nanomed.*, 2012, **7**, 4207.

-
- (44) S. S. Kale, A. S. Kotmale, A. K. Dutta, S. Pal, P. R. Rajamohanam and G. J. Sanjayan, *Org. Biomol. Chem.*, 2012, **10**, 8426.
- (45) R. Chinchilla and C. Najera, *Chem. Soc. Rev.*, 2011, **40**, 5084.
- (46) W. Cai, G.-T. Wang, Y.-X. Xu, X.-K. Jiang, Z.-T. Li, *J. Am. Chem. Soc.*, 2008, **130**, 6936.
- (47) P. Koley and A. Pramanik, *Adv. Funct. Mater.*, 2011, **21**, 4126.
- (48) M. Nagpal and S. Sood, *J. Nat. Sci. Biol. Med.*, 2013, **4**, 3.
- (49) (a) F. Xu, S. H. Lin, Y. Z. Yang, R. Guo, J. Cao and Q. Liu, *Int. Immunopharmacol.* 2013, **16**, 1; (b) R. K. Maheshwari, A. K. Singh, J. Gaddipati and R. C. Srimal, *Life Sci.*, 2006, **78**, 2081; (c) I. Brouet and H. Ohshima, *Biochem. Biophys. Res. Commun.*, 1995, **206**, 533; (d) H. P. Ammon and M. A. Wahl, *Planta. Med.*, 1991, **57**, 1.
- (50) (a) L. Moragoda, R. Jaszewski and A. P. Majumdar, *Anticancer Res.*, 2001, **21**, 873; (b) K. Mehta, P. Pantazis, T. McQueen and B. B. Aggarwal, *Anticancer Drugs*, 1997, **8**, 470; (c) C. V. Rao, A. Rivenson, B. Simi and B. S. Reddy, *Cancer Res.*, 1995, **55**, 259; (d) R. Kuttan, P. Bhanumathy, K. Nirmala and M. C. George, *Cancer Lett.*, 1985, **29**, 197.
- (51) (a) K. Sou, S. Inenaga, S. Takeoka and E. Tsuchida, *Int. J. Pharm.*, 2008, **352**, 287; (b) W. Tiyaboonchai, W. Tungpradit and P. Plianbangchang, *Int. J. Pharm.*, 2007, **337**, 299; (c) A. Kunwar, A. Barik, R. Pandey and K. I. Priyadarsini, *Biochim. Biophys. Acta*, 2006, **1760**, 1513; (d) V. Kumar, S. A. Lewis, S. Mutalik, D. B. Shenoy, Venkatesh and N. Udupa, *Indian J. Physiol. Pharmacol.*, 2002, **46**, 209.

Erratum